Investigating Placental MicroRNAs in Preeclampsia and Optimising a Gene Therapy Strategy for Targeting the Placenta

Sonya Elena Frazier

BSc (Hons), MSc

Submitted in fulfilment of the requirements for the degree of Doctor of Philosophy (PhD)

Institute of Cardiovascular and Medical Sciences
College of Medical, Veterinary, and Life Sciences
University of Glasgow

September 2020

Author's declaration

I declare that this thesis has been written by myself and is a record of research performed by myself with the exception of the following experiments. Dr Angela Bradshaw assisted with initial tail vein injections, and Dr Delyth Graham assisted with tail vein injections and ultrasound imaging. MicroRNA sequencing and the associated analysis was performed by Glasgow Polyomics. The heatmap and volcano plot were produced together with Simon Fisher. Any contribution from others has been clearly referenced and reproduced with permission. This work has not been submitted previously for any other degree at the University of Glasgow or any other institution and was supervised by Dr Delyth Graham and Dr Helen Mulvana.

Acknowledgements

First and foremost, I'd like to thank my primary supervisor Dr Delyth Graham for her unwavering support these past years – not only for her help with the animal work and all the science side of things but also for her moral support, positive outlook, perseverance, and understanding. I can't express my gratitude enough - she got me through this PhD and made this work possible. I'd also like to thank my secondary supervisor Dr Helen Mulvana for her technical insights into the world of engineering and for encouraging me to engage with it. Finally, I'd also like to thank my 'honorary' supervisor Dr Martin W. McBride for helping me get through every plasmid prep and qPCR experiment with plenty of laughter instead of tears and for always being happy to answer my never-ending list of questions.

A huge thank you to Dr Hannah Morgan, who provided the rat placental tissue that was indispensable to this PhD and who always took the time to help me. Another big thanks to Dr Carolina Motta-Mejia for the human placenta samples and unforgettable conference experiences. In turn, I'd like to acknowledge all the patients who donated their tissue samples, and all the rodents whose lives went towards this research. Thank you to Dr Dilys Freeman and Mrs Fiona Jordan for gifting the trophoblast cells and for supporting pregnancy research in Glasgow. Thank you to the Wellcome Institutional Strategic Support Fund for funding the sequencing experiment and Glasgow Polyomics for running it. I'd also like to extend my thanks towards Dr Angela Bradshaw for help with tail vein injections and several protocols; Dr Lorraine Work for miRNA probes (and all the quiz shenanigans); Dr John McClure for his stats advice; Dr Fiona Lieper for her plasmid prep tips; and Dr Alyson Miller and Dr John Mercer for their encouragement.

Thank you to all the staff and students from Thursday morning meetings for patiently listening to me and always offering your ideas and help. Simon, thank you for helping with the microRNA sequencing data as well as making lab times fun, and Amrita, thank you for the lab support (liquid nitrogen much?) and office support (all my highs and lows): team … Also, huge shout-out to Tuuli and Ashton for cheering me up and on along the way as well as Aisling, Julian, and Laura for all your help with work-related stuff but also making life outside work more enjoyable. Also, thanks to all my other work pals, especially Arun, Sammy,

Lauren, Kayley, Daniel, Antoniya, Eleni, Erin, and Ahmad, for all your help and good times. Thank you to the lab techs (Nic, Elaine, and Andy), lab workers (Jim and Marie), biological services (Stuart, Shona, and Charlie), and security (Steven) and every individual in the BHF GCRC who has been there for me during this PhD.

I'd also like to thank Emily and Lucie for their friendship and support throughout this PhD (all the way from day 1 until submission and until this day). Thank you to my bachelor's and master's lab buddies, Emma and Maria, who have continued to root for me till this day. Also, thank you to Meike, Sarah, Luiza, and Kathy for their lifelong friendships and being shoulders to lean on. Thank you to my other 'Glasgow' family members whom I've not yet mentioned (Rafi, Justin, Kim, Medi, Aaron, and James) for making Glasgow feel like home, and my 'real' family for their never-ending love and support from all around the globe. Finally, I have to thank Paco for not only being there for me every single day but also believing in me every single day.

Published work, awards, and prizes

Journal article

Frazier, S., McBride, M. W., Mulvana, H., Graham, D. 2020. From animal models to patients: the role of placental microRNAs, miR-210, miR-126, and miR-148a/152 in preeclampsia. *Clinical Science*, 134 (8): 1001–1025. Available at: 10.1042/CS20200023

Abstracts

Frazier, S. 2019. Ultrasound and Microbubble Gene Delivery for Targeting Altered Placental MicroRNAs in Preeclampsia. *Placenta [online]*, 83, e56-e57. Available at: 10.1016/j.placenta.2019.06.186

Frazier, S., Morgan, H., McBride, M.W., Bradshaw, A., Mulvana, H., Graham, D. 2019. Ultrasound and Microbubble Gene Delivery for Targeting Altered Placental MicroRNAs in Preeclampsia. *IEEE International Ultrasonics Symposium (IUS)*, Glasgow, United Kingdom, 1551-1555. Available at: 10.1109/ULTSYM.2019.8926052.

Frazier, S., Morgan, H., McBride, M.W., Bradshaw, A., Mulvana, H., Graham, D. 2019. Oral Communications: Ultrasound and Microbubble Gene Delivery for Targeting Altered Placental MicroRNAs in Preeclampsia. *Proc Physiol Soc*, 43, PC262.

Awards

University of Glasgow Medical, Veterinary, and Life Sciences Conference Support Award. Sep 2019.

Physiology Society Travel Grant. Aug 2019.

YW Loke New Investigator Travel Award. May 2019.

Wellcome Trust Institutional Strategic Support Fund. Feb 2019.

Prizes

Scottish Ultrasound 2nd Annual Scientific Meeting poster prize: highly commended. Feb 2020.

Glasgow Paediatric Research Day short oral communications prize: runner-up. Nov 2019.

Glasgow Paediatric Research Day poster prize: first prize. Nov 2018.

Abstract

Improvements in the diagnosis and management of preeclampsia (PE) have contributed to a reduction in maternal mortality in parts of the world. However, current treatments still carry safety and efficacy issues, and perinatal morbidity and mortality remains prevalent. Research into the pathology of PE and new treatment strategies are therefore warranted. Gene therapy represents a potential treatment strategy since PE is now recognised as a complex genetic disorder. Despite the clinical progress of gene therapy in foetal growth restriction, less invasive and non-viral delivery systems targeting the placenta are required to mitigate safety concerns and extend research to other pregnancy disorders, such as PE. Identifying a therapeutic gene target in PE remains a challenge since a lack of replication in gene association studies suggests rare variants with small effect sizes likely contribute to the development of PE. Alternatively, a growing body of evidence suggests placental microRNAs (miRNAs) play a key role in the pathology of PE and may therefore represent therapeutic targets. Preclinical studies however remain limited, and inconsistencies between clinical studies make it difficult to discern placental miRNA profiles characteristic of PE. Therefore, in addition to investigating non-invasive and non-viral delivery systems for gene therapy purposes in PE, there is a need for further preclinical and clinical studies to examine the role of placental miRNAs in PE and evaluate their therapeutic potential.

Ultrasound-mediated gene delivery (UMGD) can be utilised for non-viral and non-invasive gene transfer, a method in which ultrasound (US) stimulates vector uptake through its mechanical effects following interaction with US contrast agents known as microbubbles. Although the technique has been investigated in a variety of tissues, research into targeting the placenta is limited, with a single UMGD study in baboons published to date. Chapter 3 sought to develop and optimise an *in vivo* UMGD protocol in rodents that stimulates targeted transfer of a reporter gene to a surrogate organ which could then be applied to the placenta, given the difficulty in targeting a specific placenta in litter-bearing species. These optimisation studies allowed issues to be identified and logical modifications to be made to the protocol, including the type and size of vector employed, the plasmid DNA and MB dose, and the organ targeted. Through these

studies, a protocol was established showing evidence of gene transfer of a luciferase plasmid to mouse hearts, allowing progression to a proof-of-concept study.

Chapter 4 sought to demonstrate proof-of-concept that UMGD can achieve tissue-specific transfer of an expression vector and is therefore suitable for targeting placenta. UMGD of a luciferase plasmid to mouse hearts showed luciferase activity was significantly greater in the ventricles compared to non-target organs (liver, lungs, and spleen) ($p<0.05$), providing evidence of tissue-specific transfer. Although there was a trend towards greater luciferase activity in the ventricles compared with the remaining non-target organs (skeletal muscle, left kidney, and right kidney), this was non-significant. Due to small n-numbers, significance testing was not performed comparing tissue from the negative control mice with UMGD treatment mice. The protocol was subsequently applied to pregnant mice to target the placenta. Low levels of luciferase gene transfer were evident in the placenta positioned closest to the cervix on the targeted left uterine horn. Non-target tissues were not evaluated for gene transfer due to time constraints, meaning this aspect of safety could not be confirmed. Placental-specific delivery of an expression vector with UMGD therefore remains to be demonstrated in order to support the clinical translatability of this technique.

Identifying a placental miRNA dysregulated in preeclamptic patients or a subset of patients remains essential to identifying miRNAs that represent a clinically relevant therapeutic target. Animal models on the other hand provide a means of exploring the role and therapeutic potential of miRNAs in PE. In Chapter 5, a literature review was conducted to collate evidence from patient studies and identify clinically relevant miRNAs of interest for therapeutic targeting. Subsequently, the expression of candidate miRNAs was evaluated in whole placental tissue and individual placental layers of a rat model of superimposed PE (SPE) previously established by our group. The literature review identified placental miRNAs consistently detected as significantly differentially expressed by miRNA expression profiling studies in third trimester preeclamptic patients. Clinical studies were either in agreement or discordant in the direction of expression of the miRNAs in PE. Evaluation of candidate miRNAs in the placenta

of the SPE rat model contributed to the growing body of evidence that placental miRNAs differ between PE subtypes and placental layers, also providing novel evidence of dysregulation of miRNAs within placental layers in rats, a finding previously only shown in humans. Furthermore, four miRNAs (miR-210-3p, miR-223-3p, miR-181a-5p, and miR-363-3p) were identified as potential therapeutic targets given their consistent dysregulation in PE.

MiRNA expression profiling allows identification of differentially expressed placental miRNAs in a hypothesis free manner. In Chapter 6, miRNA sequencing was performed to identify differentially expressed placental miRNAs in the rat model of SPE, representing the first study to conduct miRNA sequencing in the placenta of an animal model of PE. Furthermore, the dysregulation of select miRNAs and predicted gene targets was examined by RT-qPCR in placental tissue from the SPE rat model as well as preeclamptic patients to evaluate the clinical relevance of the findings. Expression of miR-210-3p and its predicted gene target, fibroblast growth factor receptor-like 1 (FGFRL1), demonstrated an inverse relationship in the placentas of the SPE rat model and preeclamptic patients as well as in a BeWo trophoblast cell line. This is in agreement with published data that show miR-210-3p is upregulated in PE and provides novel evidence of altered FGFRL1 expression in the placentas of preeclamptic patients. This adds to the existing literature that suggests miR-210-3p plays a pathological role in PE and is a promising therapeutic target.

This thesis has provided information on a non-viral and non-invasive gene therapy technique for targeting the placenta as well as miRNAs dysregulated in the placenta in PE and potential therapeutic targets. The development of safe and efficient delivery systems that target the placenta and the identification of suitable targets represent key aspects to establishing placental gene therapy as a treatment strategy in PE. The work in this thesis has provided means to further investigate UMGD for targeting the placenta in pregnant mice, important preclinical models in pregnancy research. Furthermore, the work in this thesis has identified aspects of placental miRNAs that should be considered in future work seeking to investigate the role of and/or target placental miRNAs. Finally, the work in this thesis has identified several miRNAs that are potentially therapeutic targets in PE.

Table of contents

List of tables

List of figures

Abbreviations

°C	Degrees Celsius
µg/µL	Micrograms per microlitre
µg/mL	Micrograms per millilitre
µL	Microlitres
µM	Micromolar
µm	Micrometres
ß-gal	ß-galactosidase
ACOG	The American College of Obstetricians and Gynaecologists
ACTB	ß-actin
ACVR2A	Activin a receptor type 2A
Ad-VEGF	Adenoviral VEGF
Ad-LacZ	Adenoviral LacZ
Ad-RGD	Adenoviral Arg-Gly-Asp
ADA-SCID	Adenosine deaminase severe combined immunodeficiency
Ago	Argonaute
Ang II	Angiotensin II
ARM	Alliance for Regenerative Medicine
AUC	Area under the curve
B2M	ß-2-microglobulin
BNDF	Brain-derived neurotrophic factor
BMI	Body mass index
BMI1	BMI1 proto-oncogene, polycomb ring finger
BMUS	British Medical Ultrasound Society
bp	Base pairs
BSA	Bovine serum albumin
C14MC	Chromosome 15 microRNA cluster
C19MC	Chromosome 19 microRNA cluster
C2MC	Chromosome 2 microRNA cluster
Ca^{2+}	Calcium
cDNA	Complementary DNA
cells/mL	Cells per millilitre
cm	Centimetres
CO_2	Carbon dioxide
CPEB2	Cytoplasmic polyadenylation element-binding 2
CPS	Counts per second

CRP	C-reactive protein
CSF1	Colony stimulating factor 1
Ct	Cycle threshold
CVD	Cardiovascular disease
CYR61	Cysteine-rich angiogenic inducer 61
d	Days
dB/cm/MHz	Decibels per centimetre per megahertz
Dec	Decidua
dH_2O	Distilled H_2O
dMSC	Decidua derived mesenchymal stem cell
DNA	Deoxyribonucleic acid
DNMT1	DNA methyl-transferase 1
dNTP	Deoxyribose nucleotide triphosphate
dpf	Days post fertilisation
E	Embryonic day
E. coli	Escherichia coli
EFNA3	Ephrin-A3
eIF4	Eukaryotic translation initiation factor 4
EMA	European Medicines Agency
eNOS	Endothelial nitric oxide synthase
EO	Early-onset
ESGT	European Society of Gene Therapy
ETOH	Ethanol
EV	Extracellular vesicle
EVT	Extravillous trophoblast
FABP4	Fatty acid-binding protein 4
FBS	Foetal bovine serum
FC	Fold change
FDA	Food and Drug Administration
FDR	False discovery rate
FGF	Fibroblast growth factor
FGFR	Fibroblast growth factor receptor
FGFRL1	Fibroblast growth factor receptor-like 1
FGR	Foetal growth restriction
FLT1	Fms related receptor tyrosine kinase 1
FOXRED1	FAD-dependent oxidoreductase domain-containing 1
G	Gauge

g	Gravitational force
g	Grams
g/L	Grams per litre
GD	Gestational day
GH	Gestational hypertension
GOI	Gene of interest
GWAS	Genome-wide association studies
GWLS	Genome-wide linkage studies
h	Hours
HELLP	Haemolysis, elevated liver enzyme levels, and low platelets
HIF-1 α	Hypoxia-inducible factor 1 α
HLA	Human leukocyte antigen
HOXA9	Homeobox-A9
Hsa	Homo sapien
HUVEC	Human umbilical vein endothelial cell
IGF-1	Insulin-like growth factor 1
IL	Interleukin
INF-γ	Interferon γ
INHBB	Inhibin, beta B
IM	Intramuscular
IPA	Ingenuity Pathway Analysis
IQR	Interquartile range
ISCU	Iron-sulphur cluster assembly scaffold
IsomiR	MicroRNA isoform
ISSHP	International Society for the Study of Hypertension in Pregnancy
ITGAM	Integrin subunit $alpha_M$
IU/mL	International units per millilitre
IV	Intravenous
JHU	Johns Hopkins University
Jx	Junctional zone
kb	Kilobase pairs
kg/m^2	Kilograms per metre squared
KCMF1	Potassium channel modulatory factor 1
kHz	Kilohertz
KIR	Killer cell immunoglobulin-like receptor
KO	Knockout
L	Litres

L/min	Litres per minute
L-NAME	N(γ)-nitro-L-arginine methyl ester
Lab	Labyrinth
LB	Luria-Bertani
LDH	Lactate dehydrogenase
LGA	Large for gestational age
LO	Late-onset
PE	Preeclampsia
M	Molar
m^7G	7-methylguanosine
MB	Microbubble
mbar	Millibars
mg	Milligrams
mg/day	Milligrams per day
mg/dL	Milligrams per decilitre
mg/mg	Milligrams per milligram
mg/mL	Milligrams per millilitre
mg/mmol	Milligrams per millimole
$MgCl_2$	Magnesium chloride
MHz	Megahertz
min	Minutes
miRISC	MicroRNA-induced silencing complex
miRNA	MicroRNA
MI	Mechanical index
mL	Millilitres
mL/kg	Millilitres per kilogram
MM	Mastermix
mM	Millimolar
mm	Millimetres
mmHG	Millimetres of mercury
MPa	Megapascals
mRNA	Messenger RNA
MSC	Mesenchymal stem cell
mV	Millivolts
mW/cm^2	Milliwatts per centimetre squared
NaCl	Sodium chloride
NaDC	Sodium deoxycholate

NaOH	Sodium hydroxide
NDUFA4	NDUFA4, mitochondrial complex associated
NF-κB	Nuclear factor-κB
NFW	Nuclease free water
ng	Nanograms
ng/µL	Nanograms per microlitre
ng/kg/min	Nanograms per kilogram per minute
NICU	Neonatal intensive care unit
NIH	National Institutes of Health
NK	Natural killer cell
nM	Nanomolar
nm	Nanometres
NO	Nitric oxide
nt	Nucleotides
OCT	Optimum cutting temperature
PBS	Phosphate buffered saline
PCA	Principal component analysis
PCR	Polymerase chain reaction
PDPR	Pyruvate dehydrogenase phosphatase regulatory subunit
pg	Picograms
pH	Potential of hydrogen
PlGF	Placental growth factor
PNP	Peak negative pressure
pre-miRNA	Precursor microRNA
PRF1	Perforin 1
pri-miRNA	Primary microRNA
qPCR	Quantitative real-time PCR
RAS	Renin-angiotensin system
RCT	Randomised controlled trial
RGD	Arg-Gly-Asp
RIN	RNA integrity number
RISC	RNA-induced silencing complex
RNA	Ribonucleic acid
Rno	Rattus norvegicus
RPM	Revolutions per minute
RT	Reverse transcriptase

RT-qPCR	Reverse transcription quantitative real-time polymerase chain reaction
s	Seconds
SD	Standard deviation
SEM	Standard error of mean
sEng	Soluble endoglin
sFlt-1	Soluble fms-like tyrosine kinase-1
SGA	Small for gestational age
SHRSP	Stroke-prone spontaneously hypertensive rats
SLC6A1	Solute carrier family 6 member 1
SNAT	Sodium-coupled neutral amino acid transporter
SNP	Single nucleotide polymorphism
SPE	Superimposed preeclampsia
STAT3	Signal transducer and activator of transcription 3
STAT6	Signal transducer and activator of transcription 6
TBE	Tris-Borate EDTA
TBS	Tris-buffered saline
TBST	Tris-buffered saline, 0.05% Tween20
TE	Tris-EDTA
TGC	Trophoblast giant cell
TGF-β	Transforming growth factor β
Th1	T-helper type 1
Th2	T-helper type 2
THSD7A	Thrombospondin type I domain containing 7A
TI	Thermal index
TNF-α	Tumour necrosis factor α
TRBP	Transactivation response element RNA-binding protein
T reg cells	Regulatory T cells
U/μL	Units per microlitre
U/mL	Units per millilitre
UCL	University College London
UMGD	Ultrasound-mediated gene delivery
uNK	Uterine natural killer cells
US	Ultrasound
UTR	Untranslated region
v/v	Volume per volume
VEGF	Vascular endothelial growth factor

W/cm^2	Watts per centimetre squared
w/v	Weight per volume
WHO	World Health Organisation
WKY	Wistar Kyoto
WT	Wild type

Chapter 1 Introduction

1.1 Preeclampsia (PE)

1.1.1 Definition of PE

Preeclampsia (PE) is a multisystem hypertensive disorder of pregnancy defined as new-onset hypertension (systolic blood pressure ≥140 mmHg and/or diastolic blood pressure ≥90 mmHg) occurring at or after 20 weeks of gestation accompanied by proteinuria (spot urine protein/creatinine ≥30 mg/mmol or ≥300 mg in 24 h or ≥ 1 g/L ['2+'] on dipstick testing) or uteroplacental/maternal organ dysfunction, according to guidelines recently published by the International Society for the Study of Hypertension in Pregnancy (ISSHP) (Brown et al., 2018). Uteroplacental dysfunction encompasses complications, such as foetal growth restriction (FGR), abnormal umbilical artery Doppler waveform, and/or stillbirth. Maternal organ dysfunction includes acute kidney injury, liver involvement and/or haematological complications, most notably haemolysis, elevated liver enzyme levels, and low platelets (HELLP) syndrome, and neurological complications, such as seizures or 'eclampsia'. The ISSH guidelines seek to address a shift in PE diagnosis, with revised criteria from international obstetric and gynaecological societies stating proteinuria may be absent from diagnosis if alongside hypertension an adverse or severe event is present (ACOG, 2013, Magee et al., 2014, Lowe et al., 2015). The variable clinical manifestations of PE highlight the diverse nature of this multisystem disorder.

1.1.2 Subtypes of PE

The revised diagnostic criteria of PE were published by the ISSH to address a lack of consensus regarding the definition of PE; similar discordance exists in classifying PE into subtypes. Several classification systems have been proposed relating to the severity and timing of onset of symptoms: mild and severe (primarily determined by blood pressure levels and the presence/absence of proteinuria , HELLP syndrome, and eclampsia), early-onset (EO) and late-onset (LO) (generally referring to a diagnosis before or after 34 weeks of gestation), and preterm and term PE (occurring before or after 37 weeks of gestation) (Tranquilli et al., 2013). Although classifying preeclamptic patients with distinct profiles seeks to improve management, rapid changes to their condition can hinder the clinical utility of classifications. In turn, the ISSH recommends that PE

be classified as *de novo* or superimposed on chronic hypertension (high blood pressure prior to pregnancy or <20 weeks of gestation) with or without severe features (Brown et al., 2018). Superimposed PE (SPE) is defined as patients with chronic hypertension that develop new-onset proteinuria and/or maternal organ dysfunction at or after 20 weeks of gestation (Brown et al., 2018). The recent ISSH recommendations seek to support high-quality and collaborative research into hypertensive pregnancy disorders and promote good clinical practice.

1.1.3 Epidemiology of PE

In the most recent World Health Organisation (WHO) systematic review of global causes of maternal death, hypertensive disorders of pregnancy were the second leading cause of maternal mortality worldwide, accounting for 14% of maternal deaths during 2003-2009 (Say et al., 2014). On its own, PE complicates approximately 3-8% of pregnancies worldwide (Abalos et al., 2013). A systematic review of 74 studies across 40 countries estimated the incidence of PE and eclampsia at 4.6% and 1.4%, respectively (Abalos et al., 2013). PE and eclampsia increase the risk of maternal and perinatal death as well as serious adverse outcomes, representing a leading cause of maternal and perinatal morbidity and mortality worldwide (Vogel et al., 2014, Abalos et al., 2014). The incidence of PE and eclampsia and the risk of adverse outcomes shows disparity between countries. Regions with the highest rates of hypertensive disorders of pregnancy, PE, and eclampsia include Africa, Latin America, and the Caribbean, although substantial heterogeneity appears within regions (Say et al., 2014, Abalos et al., 2013, Abalos et al., 2014). The extent to which environmental and genetic factors contribute to these variations remains inconclusive. However, reduced access to quality care has consistently shown to contribute to higher rates of eclampsia and maternal morbidity and mortality (Giordano et al., 2014, Vousden et al., 2019, Goldenberg et al., 2011).

In the UK, the incidence of eclampsia dropped from 74.1/10000 in the 1930s to 7.2/10000 in the 1980s, and maternal deaths from eclampsia decreased from 15.1% to less than 1% over the same time period (Leitch et al., 1997). These reductions have been attributed to the introduction of anticonvulsants in the 1950s and antihypertensives in the 1970s (Leitch et al., 1997) as well as improvements in the overall standard of maternal care in Britain since the mid-

1930s (Loudon, 2000). Between 2012-2014 in the UK, only two women died from PE (MBRRACE-UK, 2018), and in 2013, PE and eclampsia incidence estimates were 2.5% and 0.0%, respectively (Abalos et al., 2013). Improvements in surveillance, diagnosis, and management, most notably implementation of magnesium sulphate (Altman et al., 2002, Knight and Ukoss, 2007) and routine blood pressure monitoring and treatment (Cantwell et al., 2011), further contribute to the low rates of adverse maternal outcomes in the UK since the turn of the 21st century. However, perinatal mortality rates in preeclamptic pregnancies remain largely unchanged in the UK (Knight and Ukoss, 2007). Although PE interventions have shown to reduce the risk of eclampsia and maternal death, it is less clear whether they have a beneficial effect on perinatal outcomes (Altman et al., 2002).

An analysis of the WHO Multicountry Survey on Maternal and Newborn Health conducted in 2010/11 reported hypertensive disorders of pregnancy were a leading cause of late foetal and early neonatal deaths, and PE and eclampsia were associated with a significant increase in the risk of perinatal deaths (Vogel et al., 2014). PE and eclampsia are also associated with an increased risk of small for gestational age (SGA), stillbirth, and preterm birth, further contributing to perinatal morbidity and mortality (Abalos et al., 2014, Roberts et al., 2005, Ngoc et al., 2006). Preterm birth is the leading cause of newborn deaths and second leading cause of death in children under the age of 5 (Who, 2012). It can cause severe morbidity, ranging from short-term complications to life-long impairments (Teune et al., 2011, D'onofrio et al., 2013, Ancel et al., 2015, Stoll et al., 2015). The increased risk of preterm birth with PE reflects planned early deliveries, now a routine intervention implemented in PE management (Brown et al., 2018). Planned early deliveries are evaluated on a case-by-case basis since the condition of mother and child must be taken into consideration.

The substantial reduction in PE-related maternal mortality in the UK has led to a description of maternal PE deaths as 'avoidable' (Shennan et al., 2017). However, epidemiological data demonstrating the prevalent perinatal morbidity and mortality arising from PE show management of the hypertensive disorder still requires improvement.

1.1.4 Management of PE

Delivery of the foetus and placenta ultimately resolves the maternal complications of PE. However, preterm deliveries are associated with a higher risk of foetal morbidity and mortality (Teune et al., 2011, D'onofrio et al., 2013, Ancel et al., 2015, Stoll et al., 2015). Managing PE therefore represents a balance between inducing delivery to reduce maternal risks and prolonging pregnancy to reduce foetal risks. The gestational age of the mother and the severity of her symptoms dictate the course of treatment since the mother is considered the primary patient.

In patients that develop PE at or after 37 weeks of gestation, delivery is recommended since this is a term pregnancy, which carries a low risk of adverse neonatal outcomes (Brown et al., 2018). In patients that develop PE before 37 weeks of gestation, planned early deliveries are considered on an individual basis. A Cochrane review of hypertensive disorders reported planned early delivery from 34 weeks of gestation was associated with a significantly lower risk of maternal morbidity and mortality compared to expectant management (Cluver et al., 2017). Although a lack of evidence prevented the study from drawing any conclusions on infant morbidity and mortality, planned early delivery was associated with a greater risk of respiratory distress syndrome and neonatal intensive care unit (NICU) admissions (Cluver et al., 2017). Similarly, in a recent large randomised controlled trial (RCT) in late preterm PE patients, early planned delivery led to a significant reduction in maternal adverse outcomes but greater number of NICU admissions, primarily due to prematurity (Chappell et al., 2019). Prolonging pregnancy to 37 weeks is therefore currently recommended as it allows foetal maturation and improves perinatal outcomes (Brown et al., 2018). If maternal or foetal conditions worsen prior to 37 weeks of gestation, delivery is deemed necessary, and antenatal corticosteroids and magnesium sulphate are recommended to promote foetal lung maturation and neuroprotection, respectively (Brown et al., 2018).

Managing maternal complications to delay delivery primarily involves the use of antihypertensives to control blood pressure levels at least below 160/85 mmHg (135/85 mmHg in the UK (NICE, 2019)) (Brown et al., 2018). A Cochrane review of mild to moderate hypertension in pregnancy showed that antihypertensives

approximately halve the risk of severe hypertension, although a lack of high-quality large RCTs made it difficult to discern whether antihypertensives produce beneficial or harmful effects in other clinical outcomes (Abalos et al., 2018). Inconclusive data is similarly evident when comparing antihypertensives, and thus the selection of antihypertensive agent is driven by side-effect profiles, clinician's familiarity with the drug, and the woman's preference (Duley et al., 2013, Abalos et al., 2018). Reported side effects include: headache, flushing, light head, nausea, and palpitations (hydralazine); flushing, light head, palpitations, and scalp tingling (labetalol); flushing, nausea, and vomiting (nifedipine); and somnolence (methyldopa) (Duley et al., 2013).

Alongside blood pressure monitoring and control, management includes routine assessments of whole blood counts, liver and renal function, and foetal status (Brown et al., 2018). During expectant management, magnesium sulphate may be recommended for the prophylaxis of eclampsia (Brown et al., 2018). A Cochrane review reported magnesium sulphate halves the risk of eclampsia and reduces risk of placental abruption, although no significant differences were seen in maternal morbidity and mortality as well as stillbirth and neonatal death (Duley et al., 2010). While toxicity was uncommon, magnesium sulphate increased the risk of any side-effect, including respiratory depression and most commonly flushing (Duley et al., 2010).

At earlier stages of pregnancy, other prophylactic strategies are recommended. If PE occurs before 24 weeks of gestation, when the foetus is at the limits of viability, termination of pregnancy may be recommended to protect the mother (Brown et al., 2018). For mothers at high risk of developing PE, as determined by clinical risk factors, low dose aspirin is recommended (Brown et al., 2018). Systematic reviews have found aspirin reduces the risk of PE as well as adverse perinatal outcomes, including infant deaths, preterm birth, and SGA babies (Henderson et al., 2014, Duley et al., 2007). While this may prevent the risk of preterm PE, a separate systematic review found it does not reduce the risk of term PE (Roberge et al., 2018).

Finally, management of PE extends to postpartum care. Although delivery ultimately resolves maternal complications, women are still at an increased risk of developing complications, such as eclampsia and hypertension, in the early

postpartum period (Kayem et al., 2011, Chames et al., 2002, Smith et al., 2013). Women who have had PE are also at an increased risk of kidney disease (Mcdonald et al., 2010, Dai et al., 2018) and cardiovascular conditions, including hypertension, venous thromboembolism, heart failure, coronary heart disease, stroke, and cardiovascular disease (CVD)-related death later in life (Wu et al., 2017, Bellamy et al., 2007). Underlying cardiovascular risk factors have shown to predispose women to PE (Magnussen et al., 2007), and prepregnancy cardiovascular risk may contribute to the elevated risk post PE (Ghossein-Doha et al., 2017). In contrast, studies have demonstrated CVD risk persists in PE patients when adjusting for potential confounders, suggesting PE may also contribute to the development of CVDs (Berks et al., 2013, Wu et al., 2017). Children born to PE mothers also appear to be at an increased risk of CVD later in life, although it remains unclear the degree to which the intrauterine environment and genetic factors contribute to the heightened risk (Alsnes et al., 2017, Vatten et al., 2003, Tenhola et al., 2006, Davis et al., 2012).

While developments in the management of PE have contributed to fewer PE-related maternal deaths, safety and efficacy issues still persist, particularly in relation to perinatal morbidity and mortality. In turn, different interventions for preventing and treating PE continue to be investigated (Grimes et al., 2019, Esteve-Valverde et al., 2018). Furthermore, due to the complications that can arise in preeclamptic mothers and their children later in life, research into the pathology and new treatments remains key to improve the management of PE.

1.1.5 Pathology of PE

1.1.5.1 Development of the human placenta

The placenta is a maternofoetal organ that provides an interface for nutrient, blood gas, hormone, and waste exchange to support the developing foetus and ensure a healthy pregnancy. One of the initial steps of human pregnancy is implantation of the blastocyst to the mucosal lining of the uterus, known as the endometrium, which occurs 6-7 days post fertilisation (dpf) (Figure 1-1A) (Turco and Moffett, 2019). The blastocyst comprises of an inner layer, the inner cell mass from which the embryo develops, and an outer layer, the trophectoderm, which develops into the placenta. After initial attachment, the trophectoderm

fuses with the surface epithelium to form a multinucleated syncytium which invades into the endometrium (Figure 1-1B). During this process, the maternal endometrium is undergoing decidualization, which is characterised by the transformation of endometrial stromal cells to decidual cells. By around 14 dpf, the blastocyst is fully encapsulated within the decidua and the trophectoderm has differentiated into cytotrophoblasts that lie beneath the syncytium (Turco and Moffett, 2019) (Figure 1-1B). During the subsequent lacunar stage, the syncytium further embeds into the decidua, forming regions known as lacunae, which are initially filled with tissue fluids and uterine gland secretions and eventually become the intervillous space (Figure 1-1C). The next stage is the primary villous stage, in which proliferating cytotrophoblasts project through the syncytium to form primary villi, comprising of an inner cytotrophoblastic core and outer syncytiotrophoblastic lining (Figure 1-1D). By day 18 dpf, cells from the extraembryonic mesoderm have invaded the core of the villi to form secondary villi, and foetal capillaries have emerged in the core to form tertiary villi (Turco and Moffett, 2019). Cytotrophoblasts continue to proliferate and invade, forming a cytotrophoblastic shell that surrounds the villi and lies in contact with the decidua. At around 8 weeks of gestation, the cytotrophoblastic shell gives rise to extravillous trophoblasts (EVTs) that migrate through the decidua towards the maternal spiral arteries (interstitial EVTs) as well as down along the lumen of the maternal spiral arteries (endovascular EVTs) (Figure 1-2 upper panel). Trophoblast invasion leads to the breakdown of trophoblast plugs and remodelling of maternal spiral arteries (Saghian et al., 2019, James et al., 2018, Roberts et al., 2017), key events that enhance maternal blood flow into the intervillous space to accommodate the growing foetus (Figure 1-2 upper panel). This process is largely complete by 12 weeks of gestation and the fundamental structure and function of the placenta is established; significant increases in uterine artery diameter (Palmer et al., 1992), perfusion rate (Roberts et al., 2017), and oxygen tension (Jauniaux et al., 2000) reflect transformation of the arteries to high-capacitance low-resistance vessels, with flow steadily increasing and resistance steadily decreasing throughout pregnancy (Palmer et al., 1992, Gómez et al., 2008). To maintain adequate blood supply to the placenta and ensure the metabolic demands of both mother and foetus are met, the mother undergoes substantial cardiovascular adaptations during pregnancy. Blood volume and heart rate steadily rise throughout pregnancy,

reaching an approximate 45% and 25% increase respectively at term compared to prepregnancy levels (Sanghavi and Rutherford, 2014). Cardiac output and stroke volume also significantly increase until the second trimester, after which it remains unclear whether levels increase, decrease, or stabilise (Sanghavi and Rutherford, 2014). These elevations are mirrored by significant reductions in systemic vascular resistance and blood pressure, which slowly begin to rise again after the second trimester (Sanghavi and Rutherford, 2014). Overall, the development of the placenta is crucial to a successful pregnancy, as the maternofoetal interface enables the exchange of molecules to ensure the demands of mother and foetus are met.

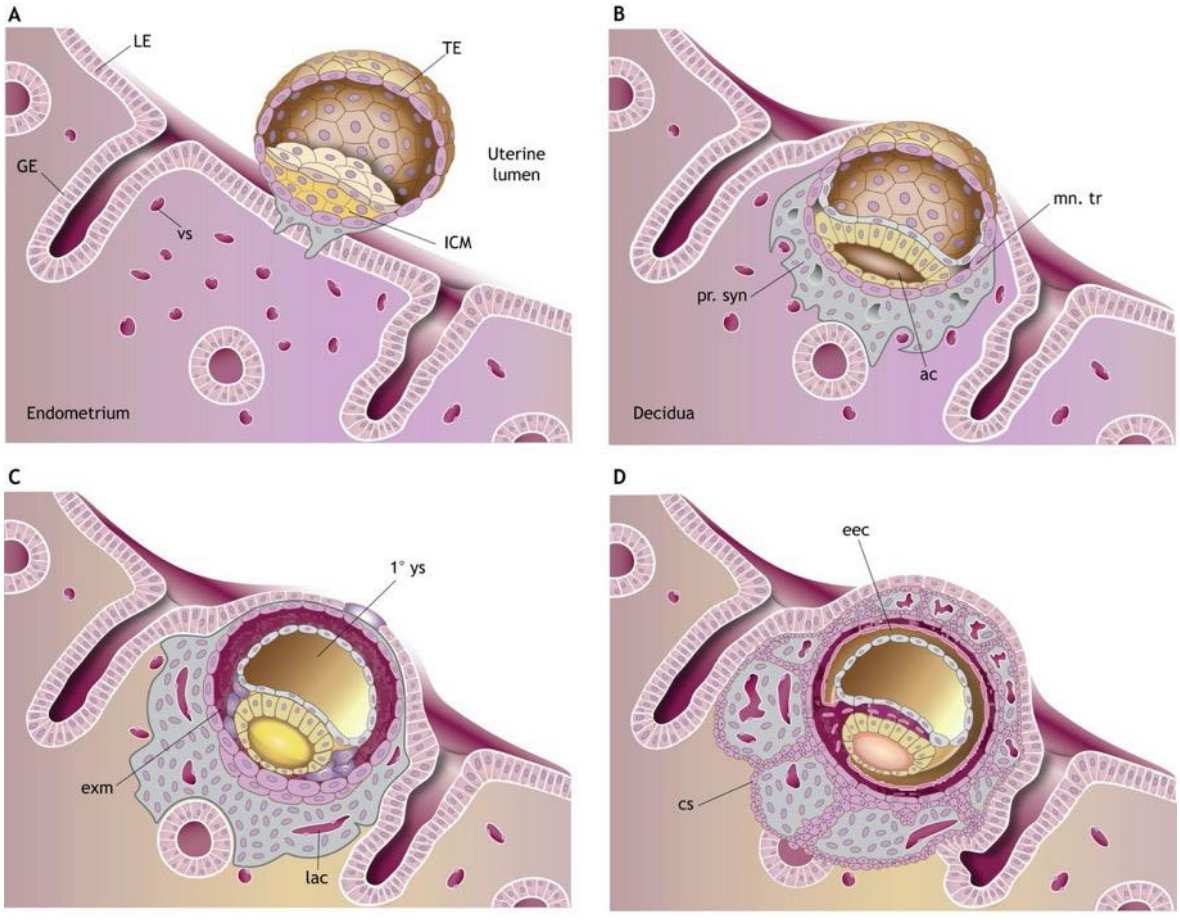

Figure 1-1 The early stages of human placental development.

Diagram depicting the early steps in placenta formation following blastocyst implantation: **(A, B)** pre-lacunar stages, **(C)** lacunar stage, and **(D)** primary villous stage. 1° ys, primary yolk sac; ac, amniotic cavity; cs, cytotrophoblastic shell; eec, extra-embryonic coelom; exm, extra-embryonic mesoderm; GE, glandular epithelium; ICM, inner cell mass; lac, lacunae; LE, luminal epithelium; mn. tr, mononuclear trophoblast; pr. syn, primary syncytium; TE, trophectoderm; vs, blood vessels. Figure taken from (Turco and Moffett, 2019) under Creative Commons Attribution 4.0 International (CC BY 4.0).

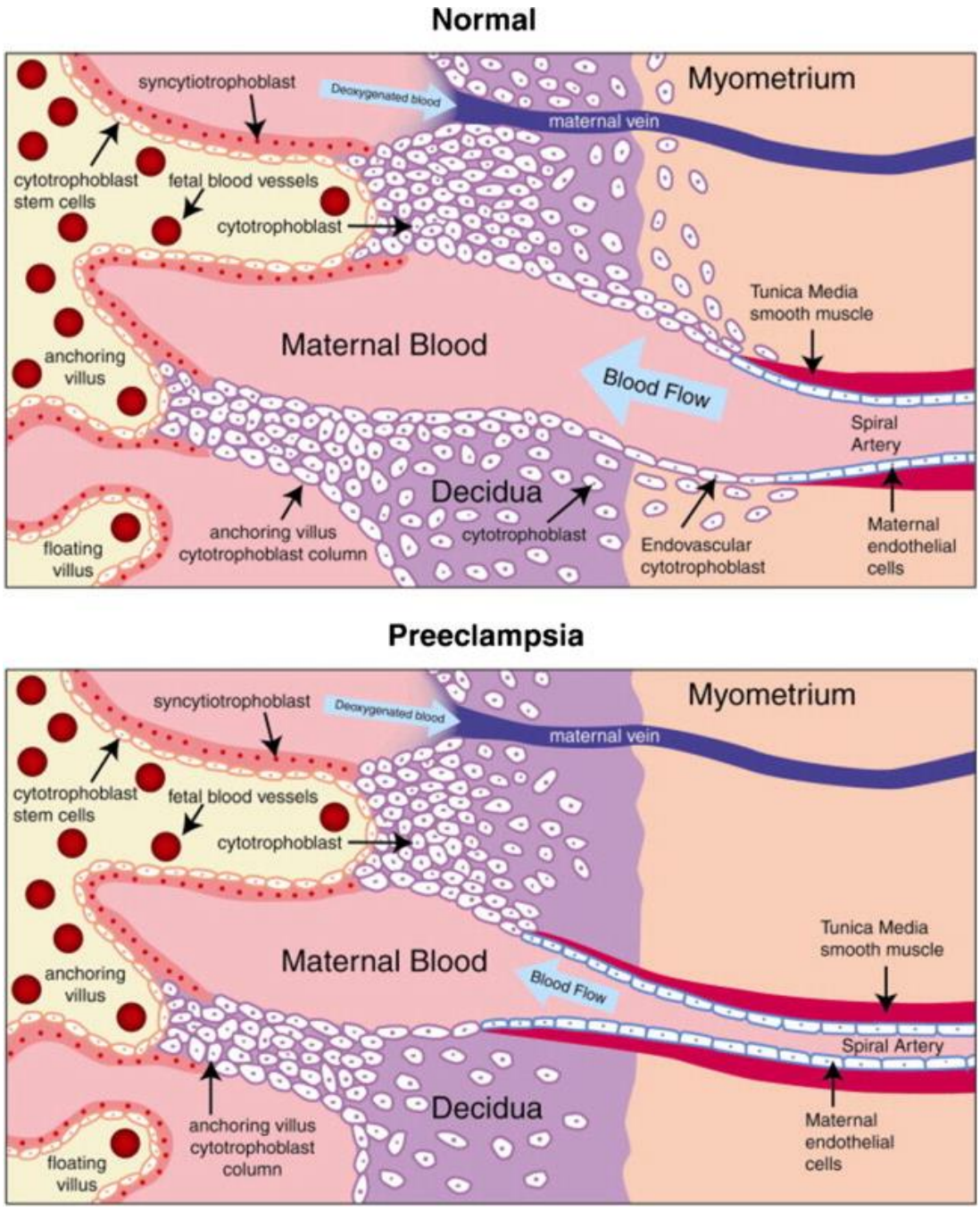

Figure 1-2 Placentation in a normal and preeclamptic placenta.

Schematic of placental vascular remodelling in normal healthy placenta **(upper panel)** and preeclampsia **(lower panel)**. **(Upper panel)** In normal placental development, invasive cytotrophoblasts of foetal origin invade the maternal spiral arteries, transforming them from small-calibre resistance vessels to high-calibre capacitance vessels capable of providing placental perfusion adequate to sustain the growing foetus. **(Lower panel)** In preeclampsia, cytotrophoblasts fail to invade. Instead, invasion of the spiral arteries is shallow, and they remain small calibre, resistance vessels. This may result in placental ischemia. Figure taken from (Karumanchi et al., 2009) with permission from Elsevier.

1.1.5.2 Placental origin of PE

The placenta as the origin of PE was first introduced by Redman in 1991, coined the 'Two Stage Model' (Redman, 1991). The long-standing hypothesis states that poor placental perfusion (stage 1), characterised by maternal spiral artery defects, namely failed trophoblast invasion and acute atherosis, leads to the maternal syndrome (stage 2), the clinical symptoms characteristic of the disorder (Redman, 1991) (Figure 1-3). In 1992, Redman proposed that abnormal placentation in PE was immunologically mediated based on PE being more common in first pregnancies, new paternity increasing PE risk, and placentation involving a maternofoetal interaction (Redman, 1992). In 1993, systemic endothelial dysfunction due to the release of factors from the underperfused placenta was proposed as the link between stage 1 and 2 (Roberts and Redman, 1993) (Figure 1-3).

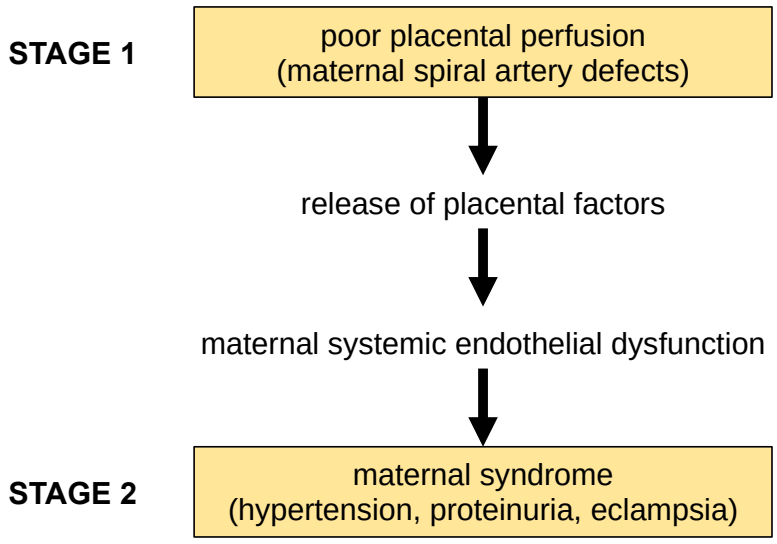

Figure 1-3 The Two Stage Model proposed by Redman and Roberts.

In stage 1, poor placentation arising from maternal spiral artery defects leads to the release of placental factors into the maternal circulation. Circulating factors induce widespread endothelial dysfunction in the mother. This leads to the clinical stage 2. Stage 2 is characterised by the maternal syndrome, namely the clinical symptoms of PE (e.g. hypertension, proteinuria, and eclampsia).

Inadequate spiral artery remodelling in PE patients was first described in the 1970s (Brosens et al., 1970, Brosens et al., 1972) (Figure 1-2 lower panel). Since then, studies of human placental explants have attributed this defect to limited endovascular rather than interstitial EVT invasion (Lyall et al., 2013), although studies have also shown limited interstitial EVT invasion (Kadyrov et al., 2003) (Figure 1-2 lower panel). Inadequate spiral artery remodelling contributes to impaired placental perfusion (Pijnenborg et al., 1991, Matijevic and Johnston, 1999, Aardema et al., 2001). Placental ischaemia and hypoxia induce oxidative and endoplasmic reticulum stress, leading to the release of placental factors, including pro-inflammatory cytokines, anti-angiogenic factors, and trophoblast debris, into the maternal circulation (Burton et al., 2009). An imbalance in maternal circulating factors induces widespread endothelial dysfunction. Elevated levels of soluble fms-like tyrosine kinase-1 (sFlt-1) (a circulating antagonist of vascular endothelial growth factor (VEGF) and placental growth factor (PlGF)) and soluble endoglin (sEng) (a circulating antagonist of transforming growth factor ß (TGF-ß)) and reduced levels of PlGF have consistently been found in PE patients (Powers et al., 2010, Masuyama et al., 2007, Aggarwal et al., 2012). Systematic reviews have shown the ratio of sFlt-1:PlGF has some utility in predicting PE (Agrawal et al., 2018, Yusuf et al., 2018) and is currently recommended to help diagnose suspected PE (NICE, 2019). Endothelial dysfunction is characterised by an increase in vascular reactivity and resistance and loss of vascular integrity, which impacts the cardiovascular system and contributes to the symptoms of PE (Boeldt and Bird, 2017).

However, several key findings do not fit in with the Two Stage Model and placental origin hypothesis. FGR does not occur in all cases of PE, and some infants are born large for gestational age (LGA) (Rasmussen and Irgens, 2003, Xiong et al., 2000, Powe et al., 2011). Impaired spiral artery remodelling and reduced uterine blood flow also do not occur in all cases of PE but can occur in other pregnancy disorders, including FGR, SGA, gestational hypertension (GH), and maternal anaemia, as well as normal pregnancies, although subtle differences in the extent of invasion may differentiate pathological events (Lyall et al., 2013, Aardema et al., 2001, Kadyrov et al., 2003, Olofsson et al., 1993). Lastly, changes in the levels in maternal circulating factors have been reported prior to 12 weeks of gestation, suggesting that pathological insults occur before

trophoblast invasion and establishment of maternal blood flow in the placenta (Akolekar et al., 2011, Salomon et al., 2017).

Limitations of the model were acknowledged at the time, and the Two Stage Model has since been refined and expanded. In 1996, a maternal origin of PE was added to the model, which supported the concept that prepregnancy maternal disorders could contribute to systemic endothelial dysfunction and account for pathological and clinical heterogeneity (Ness and Roberts, 1996). More recently in 2019, the model has been extended to incorporate maternal and placental factors potentially contributing to the development of the disorder at both stages (Staff, 2019) (Figure 1-4). Furthermore, two distinct pathways (extrinsic and intrinsic) have been proposed that precede the development of stage 1 and stage 2 (Figure 1-4). In the extrinsic pathway, factors extrinsic to the placenta cause abnormal placentation, which is linked to an earlier onset of PE and more severe phenotype (Staff, 2019) (Figure 1-4). In the intrinsic pathway, placentation is normal; however, due to the placenta outgrowing the uterine capacity (an intrinsic placental problem), uteroplacental malperfusion occurs, leading to less severe and later onset PE (Staff, 2019) (Figure 1-4).

However, the placental origin of PE remains a highly contested subject. A host of theories, notably abnormal differentiation of the trophoblast lineage (Huppertz, 2008); poor maternal cardiac reserve (Thilaganathan and Kalafat, 2019); maternofoetal immune incompatibility (Moffett-King, 2002); a T-helper type 1 (Th1)/T-helper type 2 (Th2) imbalance (Saito and Sakai, 2003); placental oxidative stress, maternal hypoxia, and abnormalities in oxygen sensing (Zamudio, 2007); dysregulation of the renin-angiotensin system (RAS) (Lumbers et al., 2019), and pathological effects of placenta derived extracellular vesicles (EVs) (Gilani et al., 2016), have been proposed that support the concept that PE can arise from foetal, placental, and/or maternal maladaptations and independent from impaired trophoblast invasion. Nonetheless, a common thread amongst theories is the placenta as a component to the pathogenesis of PE and abnormalities in circulating factors contributing to endothelial dysfunction. Most theories also support the concept that PE can be broadly divided into two subtypes: a more severe EO form with clear placental dysfunction and a more mild LO form with fewer signs of placental dysfunction (Burton et al., 2019).

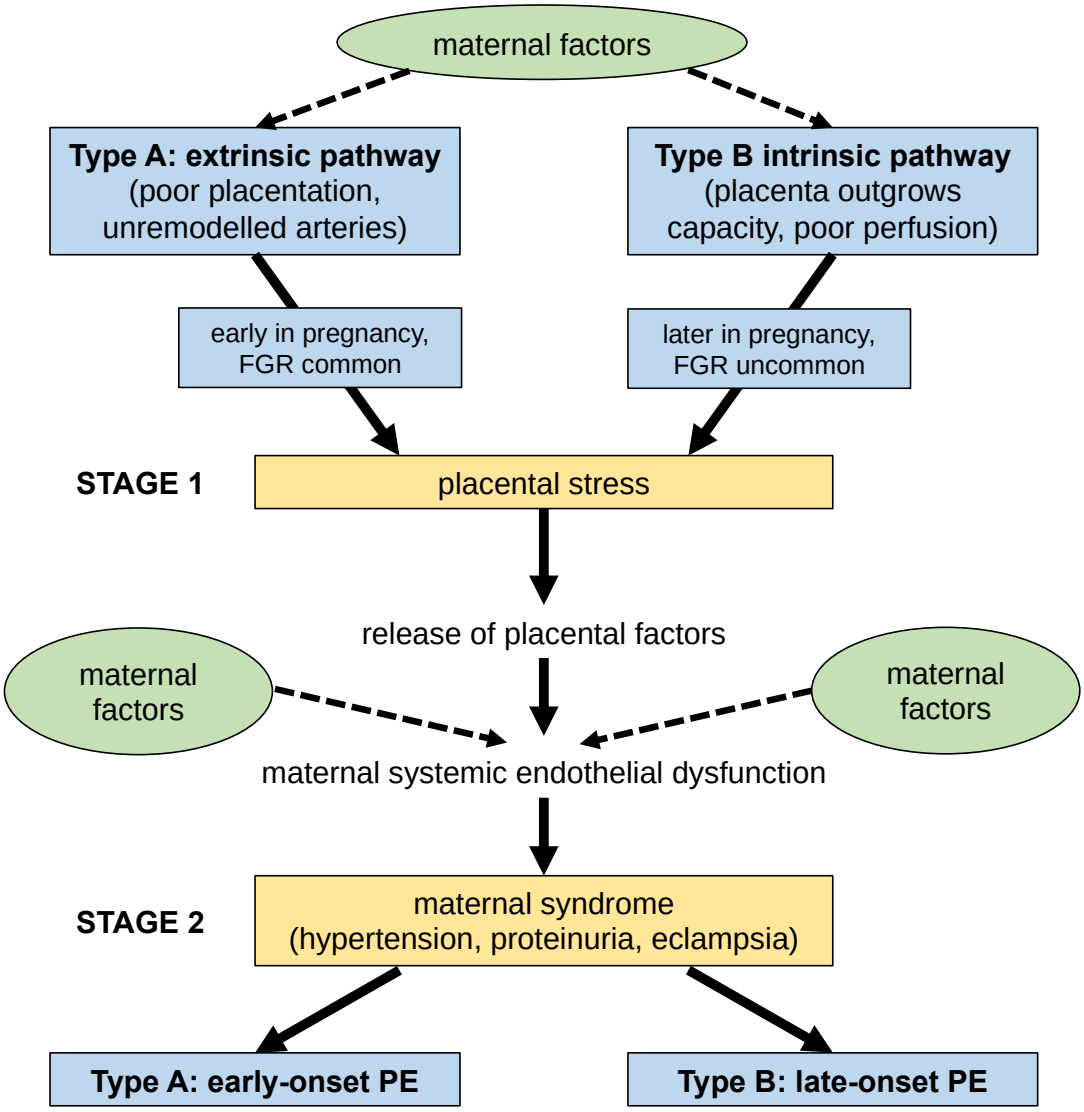

Figure 1-4 The revised Two Stage Model of PE.

Preeclampsia can follow two pathways: the extrinsic (type A) and intrinsic (type B) pathway. Type A: In the extrinsic pathway, factors extrinsic to the placenta cause poor placentation. This occurs earlier in pregnancy and FGR is more common. This pathology leads to early-onset PE. Type B: In the intrinsic pathway, factors intrinsic to the placenta cause the placenta to outgrow its capacity, leading to poor placental perfusion. This occurs later in pregnancy and FGR is less common. This pathology leads to late-onset PE. Type A and Type B: Both pathways induce placental stress, causing the placenta to release of factors into the maternal circulation, which in turn leads to the maternal syndrome characterised by the clinical symptoms of PE. Maternal factors contribute to the pathology of PE prior to or after placental stress occurs.

1.1.6 Animal models of PE

Animal models are essential to our understanding of PE since the disorder is almost exclusive to humans, although several cases have been reported in non-human primates (Thornton and Onwude, 1992, Palmer et al., 1979, Krugner-Higby et al., 2009). The spontaneous development of PE is attributed to the distinct placentation of primates, which involves extensive trophoblast invasion and spiral artery remodelling (Pijnenborg et al., 2011b, Pijnenborg et al., 2011a). However, trophoblast invasion is not unique to primates but rather a feature of haemochorial placentas. Haemochorial is used to describe placentas in which maternal blood is in direct contact with foetal chorionic villi, the type of placenta common to mammals such as primates, lagomorphs, and rodents. One of the distinguishing placental characteristics between species is the depth of trophoblast invasion, with most extensive invasion seen in humans followed by rabbits, guinea pigs, rats, and then mice (Swanson and David, 2015). The number of trophoblast layers also differs between species, with one layer present in primates and guinea pigs (haemomonochorial), two layers in rabbits (haemodichorial), and three layers in rats and mice (haemotrichorial) (Furukawa et al., 2014). Although placentation in rabbits and guinea pigs more closely mirrors that of humans, rats and mice are more commonly used as PE models due to their shorter gestation, larger litter size, and cheaper housing costs.

1.1.6.1 Rodent models of PE

Rodents are valuable models for studying the human placenta since they share commonalities in placental development, structure, function, and genetic make-up (Rai and Cross, 2014, Georgiades et al., 2002, Soncin et al., 2018). Analogous layers consisting of varying portions of maternal and foetal tissue make comparisons between the placenta of rodents and humans possible (Rai and Cross, 2014). Rodent pregnancies also display cardiovascular adaptations similar to those seen in humans, including increased glomerular filtration rate and renal plasma flow (Conrad, 2004); impaired vascular response (Paller, 1984); decreased vascular tone and vasomotion (Meyer et al., 1993); and elevated cardiac output, stroke volume, and heart rate (Wong et al., 2002). Hence, rodent models of PE are vital to preclinical investigations since abnormal placental development and cardiovascular dysfunction are characteristic of PE.

However, key morphological differences persist that are important to consider and highlight the limitations of comparing the placenta.

The rodent placenta is divided into the decidua, junctional zone, and labyrinth. Similarly, the human placenta is divided into the decidua, basal plate, and placenta villi (Figure 1-5). The decidua is the maternal layer of the placenta through which maternal blood passes via spiral arteries. In both rodents and primates, the decidua is derived from endometrial stromal cells (Rai and Cross, 2014). In rodents, trophoblast giant cells (TGCs) line the decidua and maternal spiral arteries, while in humans, it is EVTs that invade maternal spiral arteries (Rai and Cross, 2014). Adjacent to the decidua, the junctional zone in rodents and basal plate in humans is the region in which maternal arteries are further lined by different foetal cells: spongiotrophoblasts, glycogen cells, and TGCs in rodents and cytotrophoblasts and syncytiotrophoblasts in humans (Rai and Cross, 2014). Finally, the labyrinth in rodents and placenta villi in humans is the layer in which gas and nutrient exchange occurs, comprising of the maternal and foetal blood supplies. While in humans, foetal blood vessels lined by villous cytotrophoblasts and syncytiotrophoblasts bathe in maternal blood, in rodents, maternal vessels lined by TGCs and syncytiotrophoblasts form a branch-like structure that is in contact with foetal blood vessels (Rai and Cross, 2014) (Figure 1-5). Despite differences in cellular and structural features, similarities in the placenta and its anatomical layers make comparisons between rodent models of PE and patients with PE possible.

Since rodents do not spontaneously develop PE, pharmacological, surgical, or genetic manipulation is required (Table 1-1). Recapitulating the disorder in rodents therefore carries limitations and extrapolating findings to humans must be carefully considered. In addition, depending on the research question being asked, certain models are more or less suitable and must therefore be appropriately selected (Table 1-1). Nonetheless, numerous rodent models exhibit the hallmark symptoms of PE, hypertension and proteinuria, and other PE-like symptoms, including endothelial dysfunction, placental abnormalities, and foetal demise/growth restriction. Given the ethical implications of conducting research in human pregnancy and the inadequacy of obtaining information from post-delivery examinations, rodents represent a valuable

model system for investigating the pathological mechanisms underlying PE and potential therapeutic interventions.

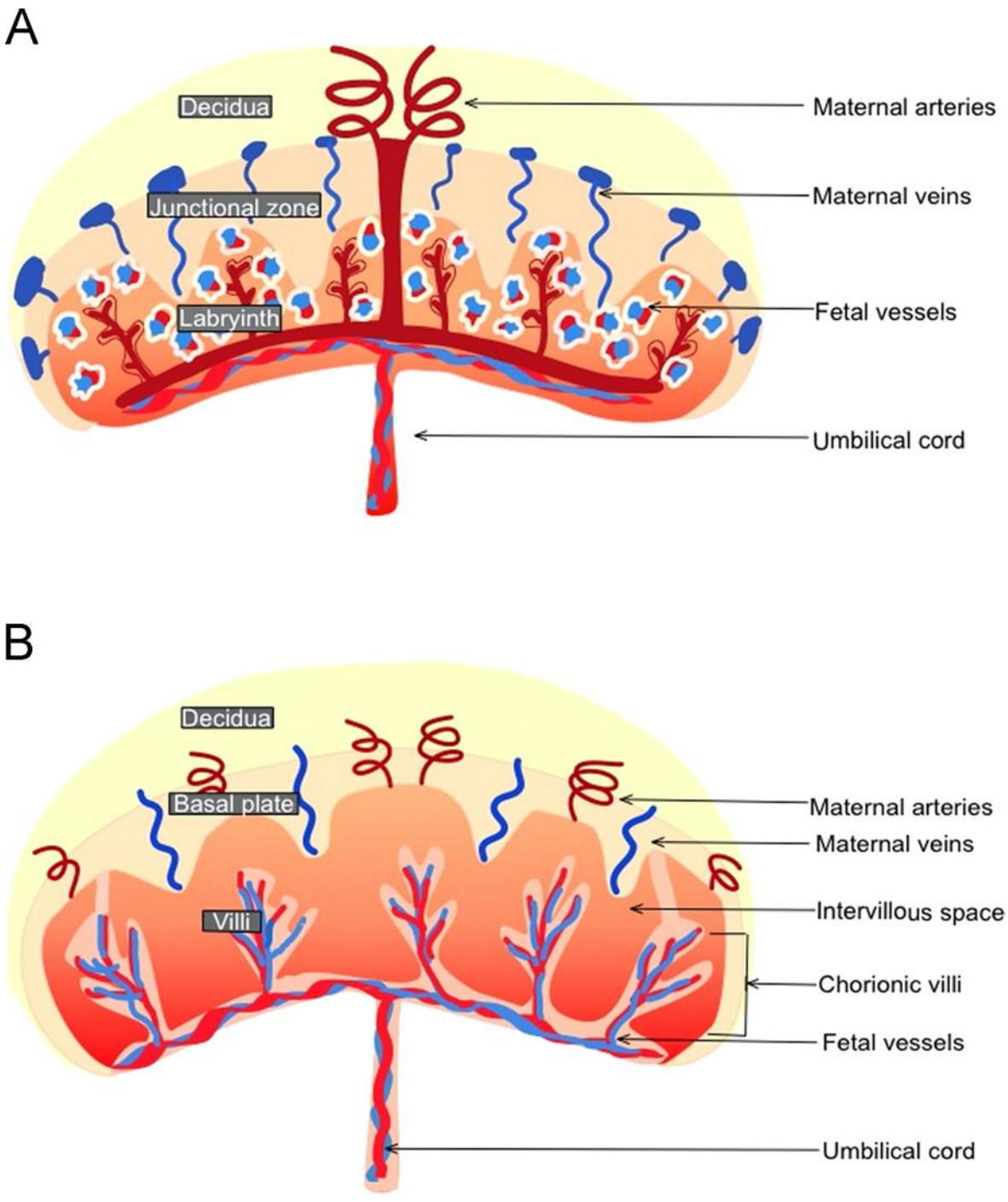

Figure 1-5 Comparative anatomy of the placenta in the (A) mouse and (B) human.

Figure taken from (Rai and Cross, 2014) with permission from Elsevier.

Table 1-1 Key examples of rodent models of PE and their advantages and disadvantages.

Model	Intervention	Advantages	Disadvantages	References
Surgical (RUPP)	Clipping of aorta and ovarian arteries in Sprague Dawley rats on GD 14 / ovarian and/or uterine arteries in CD-1 mice on GD 14.5	- Displays maternal and foetal symptoms - Can be used to study uteroplacental ischaemia - Consistently reproduced across studies	- No impaired trophoblast invasion - Onset of symptoms late in pregnancy	(1) (2) (3) (4)
Genetic	BPH/5 mice	- Displays maternal and foetal symptoms - Onset of foetal symptoms early in pregnancy	- No impaired trophoblast invasion - Mildly elevated blood pressure prepregnancy - Better model for GH or SPE	(5) (6)
	COMT -/- mice	- Displays maternal symptoms - Onset of some symptoms mid-pregnancy	- Displays some foetal symptoms - No impaired trophoblast invasion - No abnormal uterine artery blood flow - No evidence of endothelial dysfunction - Conflicting evidence of COMT in PE patients	(7) (8) (9)
	Ad-sFLT1 injection in Sprague Dawley rats mid-gestation / Lentiviral transduced blastocyst implanted in CD-1 mice	- Displays maternal symptoms - Ability to modify dose – can be used to study more and less severe phenotypes	- Displays some foetal symptoms - Non-pregnant rats also develop hypertension and proteinuria – onset of symptoms independent of pregnancy	(10) (11)
Pharmacological	L-NAME infusion in Sprague Dawley rats mid-gestation	- Displays maternal and foetal symptoms	- No impaired trophoblast invasion - Conflicting evidence of NO in PE patients - Onset of symptoms late in pregnancy	(12) (13) (14) (15)
	AT1-AA infusion in Sprague Dawley rats mid-gestation / injection in C57BL/6J mice on GD13	- Displays maternal symptoms	- No impaired trophoblast invasion - Displays some foetal symptoms - Onset of symptoms late in pregnancy	(16) (17)
	Poly I:C injection in Sprague Dawley rats from GD 10 / in C57BL/6J mice from GD 13	- Displays maternal symptoms	- No impaired trophoblast invasion - Displays some foetal symptoms - Onset of symptoms late in pregnancy	(18) (19)

(1) (Alexander et al., 2001) (2) (Sholook et al., 2007) (3) (Banek et al., 2012) (4) (Fushima et al., 2016) (5) (Davisson et al., 2002) (6) (Dokras et al., 2006) (7) (Kanasaki et al., 2008) (8) (Stanley et al., 2012) (9) (Palmer et al., 2011) (10) (Maynard et al., 2003)(11) (Kumasawa et al., 2011)(12) (Molnár et al., 1994) (13) (Shu et al., 2018) (14) (Seligman et al., 1994) (15) (Smárason et al., 1997) (16) (Lamarca et al., 2009) (17) (Zhou et al., 2008) (18) (Tinsley et al., 2009) (19) (Chatterjee et al., 2012). RUPP, reduced uterine perfusion pressure; GD, gestational day; GH, gestational hypertension; SPE, superimposed preeclampsia; COMT, catechol-O-methyltransferase; PE, preeclampsia; Ad-sFLT1, adenovirus soluble fms-like tyrosine kinase-1; L-NAME, N(γ)-nitro-L-arginine methyl ester; NO, nitric oxide; AT1-AA, angiotensin II type 1-receptor autoantibody.

1.1.7 Genetic and environmental factors in PE

Publications in the 1960s were the first to report familial aggregation of PE, providing evidence of an underlying genetic basis (Chesley et al., 1968, Chelsey et al., 1962). However, elucidating the genetic component of PE has proven challenging, with studies from the 1980s and 1990s producing conflicting models concerning its mode of inheritance and magnitude of effects (Chesley and Cooper, 1986, Arngrimsson et al., 1990). This is due to the role of both maternal and foetal genotypes, which includes maternal and paternal genes and their independent and interactive effects not only with each other but also the environment in determining PE risk. Although some families exhibit a Mendelian pattern of inheritance (Chesley and Cooper, 1986), PE is now recognised as a complex disorder involving multiple genetic and environmental factors. Population-based twin studies from the early 2000s estimate genetic factors contribute approximately 50%, the majority of which is attributed to maternal genetic effects and to a lesser extent foetal (maternal and paternal) genetic effects (Cnattingius et al., 2004, Salonen Ros et al., 2000). PE is twice as likely in women whose mother had PE during their pregnancy and in women born to uncomplicated pregnancies but whose sibling (man or woman) had a child born to a preeclamptic pregnancy (Skjærven et al., 2005). Men born to pregnancies complicated by PE are also at an increased risk of fathering a preeclamptic pregnancy by approximately 1.5-fold (Skjærven et al., 2005). Maternal and paternal ethnicity have also shown to confer genetic susceptibility. Highest rates of PE have been reported in women from black ethnic groups (Bramham et al., 2011, Caughey et al., 2005, Sibai et al., 1997) and lowest rates have been reported in women from Asian ethnic groups (Jian et al., 2012, Nakagawa et al., 2016, Caughey et al., 2005, Anderson et al., 2012) as well as in pregnancies with Asian paternity (Caughey et al., 2005). In contrast, a UK-based study reported highest rates in women with Asian ethnicity (Bramham et al., 2011), and multiple studies show substantial variations between countries from the same region (Nakagawa et al., 2016, Bilano et al., 2014, Abalos et al., 2013), indicating ethnicity is not a strong predictive risk factor. Current research ascertains the involvement of both maternal, foetal, and in turn paternal genotypes as well as environmental factors in the development of PE.

1.1.7.1 Maternal risk factors

Identifying genetic components that determine PE susceptibility remains a challenge. In addition to the involvement of two genotypes, PE presents as a heterogenous disorder, with distinct phenotypes likely corresponding to differing degrees of maternal and foetal contributions to the genetic influence on its pathology (Triche et al., 2014). Candidate gene studies in women with PE have implicated hundreds of genetic variants involved in various biological pathways related to PE, including thrombophilia, blood pressure control, fluid balance, endothelial function, inflammation, lipid metabolism, and oxidative stress (Staines-Urias et al., 2012, Buurma et al., 2013) (Table 1-2). A major issue is a lack of replication between studies due to small sample sizes and poor quality reporting (Staines-Urias et al., 2012). Despite these issues, two metanalyses of candidate gene studies identified genetic variants reproducibly and significantly associated with PE risk (Staines-Urias et al., 2012, Buurma et al., 2013) (Table 1-2). However, a lack of replication is similarly observed with genome-wide linkage studies (GWLS) and genome-wide association studies (GWAS) (Williams and Broughton Pipkin, 2011). Three relatively small-scale GWAS in preeclamptic patients have been conducted to date (Johnson et al., 2012, Zhao et al., 2012, Zhao et al., 2013). Only one study identified single nucleotide polymorphisms (SNPs) that reached genome-wide significance: two SNPs (rs7579169, $p=3.58\times10-7$, odds ratio (OR)=1.57 and rs12711941 $p=4.26\times10-7$, OR=1.56) in the intergenic region downstream of the Inhibin, beta B (INHBB) gene on chromosome 2q14 (Johnson et al., 2012). They were found to be in linkage disequilibrium with one another but not any other genotyped SNP within 250 kilobase pairs (kb), suggesting potential linkage with a rare risk variant (Zhao et al., 2013). The SNP associations were not replicated in case-control cohorts. Larger sample sizes with sufficient power to detect or replicate associations are needed. The heterogenous nature of PE may also contribute to a lack of significance in studies, with placental miRNA expression found to differ between timing of disease onset and delivery (Lykoudi et al., 2018, Weedon-Fekjær et al., 2014, Anton et al., 2015) as well as presenting symptoms (Pineles et al., 2007, Awamleh et al., 2019). Although stratifying patients by subtype could address this issue, obtaining adequate sample sizes is of foremost importance. Overall, a lack of detection and replication amongst genetic studies supports the involvement of rare variants with effects in determining PE risk.

Table 1-2 Results from two meta-analyses of genetic variants reproducibly and significantly associated with PE risk.

Biological pathway	Gene	Gene name	Genetic variant	Studies (n)	Cases (n)	Controls (n)	OR (CI)*	*P* value	Study
RAS	*ACE*	Angiotensin converting enzyme	rs4646994	30	3101	5134	1.17 (0.99,1.40)	0.017	(1)
				20	2855	4582	1.20 (1.08,1.34)	Sig.	(2)
	AGT	Angiotensinogen	rs699	27	2329	4896	1.26 (1.00,1.59)	0.009	(1)
				21	2104	4530	1.23 (0.98,1.54)	Sig.	(2)
	AGTR1	Angiotensin II receptor type 1	rs5186	10	894	1379	1.22 (0.96,1.56)	0.036	(1)
Inflammation	*CTLA4*	Cytotoxic T-lymphocyte-associated protein 4	rs231775	4	353	536	1.24 (1.01,1.52)	Sig.	(2)
Lipid metabolism	*LPL*	Lipoprotein lipase	rs268	3	395	579	2.27 (0.62,8.24)	Sig.	(2)
Thrombophilia	*F5*	Coagulation factor V (factor V Leiden)	rs6025	41	4499	15188	1.74 (1.43,2.12)	<0.001	(1)
				40	4373	6446	1.95 (1.56,2.45	Sig.	(2)
			rs6020	2	266	336	1.94 (1.05,3.60)	Sig.	(2)
	F2	Coagulation factor II (prothrombin)	rs1799963	30	3546	11712	1.72 (1.31,2.26)	<0.001	(1)
				30	3329	4878	1.95 (1.43,2.66)	Sig.	(2)
	SERPINE1	Serpin peptidase inhibitor (plasminogen activator inhibitor type 1)	rs1799889	11	1283	1661	1.17 (1.03,1.33)	Sig.	(2)

*99% CI for (1) and 95% CI for (2). (1) (Staines-Urias et al., 2012) and (2) (Buurma et al., 2013). RAS, renin-angiotensin system; OR, odds ratio; CI, confidence interval.

In addition to specific genetic variants, several other maternal factors are associated with PE risk, although the proportion of environmental and genetic effects contributing to these factors as well as the biological mechanisms underpinning the relationship remain unclear. Women with a history of PE or GH (Nzelu et al., 2018, Duckitt and Harrington, 2005), advanced maternal age (35 years or older) (Khalil et al., 2013, Ogawa et al., 2017), shorter stature (Lee and Magnus, 2018, Sohlberg et al., 2012), higher body mass index (BMI) (Giannakou et al., 2018, Duckitt and Harrington, 2005), and lighter weight or earlier gestational age at birth (Dempsey et al., 2003, Á Rogvi et al., 2012) are at an increased risk of developing PE. Multiple gestations (Laine et al., 2019, Duckitt and Harrington, 2005) and use of assisted reproductive technologies (Almasi-Hashiani et al., 2019), particularly oocyte donation (Giannakou et al., 2018), also put women at an increased risk of PE. In addition, poor mental health (Kurki et al., 2000, Qiu et al., 2007), micro/macronutrient deficiency (Purswani et al., 2017, Qiu et al., 2008), and pre-existing medical conditions (including diabetes, chronic hypertension, obesity, antiphospholipid antibody syndrome, and kidney disease) (Duckitt and Harrington, 2005, Giannakou et al., 2018) are associated with increased PE risk. Finally, several key environmental exposures during pregnancy have shown to influence PE risk. While smoking and physical activity are associated with a reduced risk of PE (England and Zhang, 2007, Aune et al., 2014), high altitude and environmental contaminants are associated with an elevated risk of PE (Keyes et al., 2003, Palmer et al., 1999, Bailey et al., 2020, Rosen et al., 2018). These factors highlight the key role of environmental factors in contributing to the development of PE.

1.1.7.2 Paternal and foetal risk factors

The role of the father in contributing to the development of PE is further supported by a change in paternity altering the risk of PE (Robillard et al., 1993, Li and Wi, 2000) and greater vaginal exposure to paternal sperm reducing the risk of PE (Di Mascio et al., 2020, Wang et al., 2002). These findings support the immune maladaptation theory, which proposes that PE arises from dysregulation of the maternal immune response to ‘paternal antigens’, with research primarily focussing on the interaction between maternal uterine natural killer (uNK) cells and trophoblast cells expressing human leukocyte antigen (HLA)-C and HLA-G (Moffett-King, 2002). Two candidate gene studies found that paternally derived

HLA-G polymorphisms in the foetus significantly increased the risk of PE (Table 1-3). Another candidate gene study reported that the combination of foetal HLA-C2 and maternal killer cell immunoglobulin-like receptor (KIR) AA genotype was significantly associated with PE (Table 1-3). In contrast, a number of studies report no significant association between primipaternity and PE (Verwoerd et al., 2002, Trogstad et al., 2001), and a systematic review found no association between paternal sperm exposure and PE risk (Ness et al., 2004), challenging the immune maladaptation theory.

Table 1-3 Candidate gene studies implicating paternal and foetal genotypes in PE risk.

Biological pathway	Gene	Gene name	Genotype	Genetic variant	OR (CI 95%)	P value	Study
Vasoactive peptide	*END1*	Endothelin 1	Paternal	rs5370	0.42 (0.18,0.94)	0.034	(1)
Oxidative stress	*SOD2*	Superoxide dismutase 2	Paternal	rs4880	2.77 (1.32,5.81)	0.007	(2)
Immune tolerance	*HLA-G*	Human leukocyte antigen G	Foetal	G*0106	10.10 (2.20,6.80)	0.003	(3)
			Foetal/maternal mismatch	Foetal G*0106-positive Maternal G*0106-negative	9.60 (2.40,38.70)	0.001	(3)
			Foetal	Exon 8 +14 bp/+14 bp (transmitted from father)	5.57 (1.79,17.31)	0.002 (0.006)	(4)
	HLA-C and *KIR*	Human leukocyte antigen C and killer cell immunoglobulin-like receptor	Foetal/maternal mismatch	Foetal HLA-C2 Maternal KIR AA	2.38 (1.45,3.90)	0.001	(5)
Metabolic pathways	*COMT* and *MTHFR*	Catechol-O-methyltransferase and methylenetetrahydrofolate reductase	Foetal	ATCA haplotype (*COMT*) and rs1801133 (*MTHFR)*	1.37 (1.05,1.79)	0.022	(6)
Immune response and blood pressure control	*ERAP2*	Endoplasmic reticulum aminopeptidase 2	Foetal	rs2549782	1.53 (1.10, 2.13)	0.012	(7)

(1) (Galaviz-Hernandez et al., 2016) (2) (Luo et al., 2018) (3) (Tan et al., 2008) (4) (Hylenius et al., 2004) (5) (Hiby et al., 2004) (6) (Hill et al., 2011b) (7) (Hill et al., 2011a). OR, odds ratio; CI, confidence interval.

Other paternal factors that have shown to increase the risk of PE include increased weight and advanced age (Harlap et al., 2002, Lee and Magnus, 2018), although it remains unclear whether weight- or age-related gene variants underlie this association. Nonetheless, several candidate gene studies examining genetic variants in foetal and paternal genotypes provide supporting evidence of paternal and foetal genetic effects in determining PE risk (Table 1-3). The first GWAS in offspring of PE patients, identified a SNP that reached genome-wide significance (rs4769613; $P = 5.4 \times 10^{-11}$) located within the enhancer region of the fms related receptor tyrosine kinase 1 (FLT1) gene on chromosome 13 (Mcginnis et al., 2017). Further examination revealed no association between the foetal rs4769613 genotype and Flt-1 and sFlt-1 protein expression in the placenta and no association with maternal serum sFlt-1 levels (Mcginnis et al., 2017). Hence, it remains to be seen whether the foetal rs4769613 genotype impacts FLT1 in a pathological manner. In a recent study, the association of the placental FLT1 variant with PE risk was replicated in a meta-analysis of two independent cohorts (rs4769613; $P = 4 \times 10^{-3}$) (Kikas et al., 2020). Furthermore, placental FLT1 gene expression and maternal serum sFlt-1 were significantly higher in PE patients with CC and CT genotypes versus controls, suggesting the C allele of rs4769613 may promote FLT1 expression and be directly involved in the pathology of PE (Kikas et al., 2020). These studies highlight the role of the placental genome in contributing to PE risk.

1.1.7.3 Epigenetic risk factors

Another component of genetic risk in PE involves epigenetic factors, namely DNA methylation, imprinting, and non-coding RNA. Previous candidate genes associated with PE risk have shown to exhibit altered methylation levels in PE (Kim et al., 2017, White et al., 2016). DNA methylation of polymorphisms associated with PE has also shown to alter the risk of developing PE (Harati-Sadegh et al., 2019). Polymorphisms in the long non-coding imprinted gene H19 have found to influence PE susceptibility (Harati-Sadegh et al., 2018), and polymorphisms in foetal imprinted genes have shown to be associated with maternal blood pressure (Petry et al., 2016). MicroRNAs (miRNAs), a form of non-coding RNA, have also been identified as risk factors in PE. Polymorphisms in miRNA biogenesis machinery (Rezaei et al., 2019, Eskandari et al., 2018), placental and maternal miR-146a (Salimi et al., 2019), and the maternal miR-26

gene influenced PE risk (Eskandari et al., 2019). Collectively, these studies further highlight the complexity of PE aetiology, as epigenetic factors in both the mother and foetus contribute to PE susceptibility.

1.2 MicroRNAs (miRNAs)

1.2.1 MiRNA biogenesis

MiRNAs are a class of short, non-coding RNA molecules that regulate gene expression post-transcriptionally (Bartel, 2009). Since the discovery of miRNA in 1993 (Lee et al., 1993), there are now approximately 2000 miRNAs annotated in the human genome (miRBase v22). It is estimated that 30-60% of protein coding genes may be subject to miRNA regulation (Lewis et al., 2005, Friedman et al., 2009). In order to form functional mature miRNA, miRNAs undergo stepwise processing either via the canonical or non-canonical pathways (Figure 1-6).

In the canonical pathway, miRNA genes are transcribed by RNA polymerase II binding to promoter elements of the gene to produce primary miRNA (pri-miRNA) stem loop structures (Lee et al., 2004). A microprocessor complex consisting of DGCR8 (an RNA binding protein) and Drosha (a nuclear RNase III enzyme) recognises and cleaves the pri-miRNA transcript at the base of the stem loop to release precursor miRNA (pre-miRNA), a hair-pin structure approximately 70 nucleotides (nts) in length characterised by a ~2 nt 3′ overhang (Han et al., 2004, Lee et al., 2002). Pre-miRNA is transported out of the nucleus via exportin 5, a nucleocytoplasmic transport factor (Bohnsack et al., 2004). RanGTP binds to exportin 5 which recognises the ~2 nt 3′ overhang of pre-miRNA and the complex migrates through the nuclear pore complex (Wang et al., 2011). In the cytoplasm, pre-miRNA is released from the complex by hydrolysis of RanGTP to RanGDP. Free pre-miRNA is cleaved by Dicer (a cytoplasmic RNase III enzyme) in complex with transactivation response element RNA-binding protein (TRBP), leading to removal of the terminal loop and production of a ~22 nt miRNA duplex (Chendrimada et al., 2005). TRBP mediates loading of the duplex into an Argonaute (Ago) protein, a core component of the RNA-induced silencing complex (RISC) (Su et al., 2009). Ago proteins unwind the duplex, and a single strand is retained (the guide strand) while the other is degraded (the passenger strand) (Matranga et al., 2005), with selection favouring the strand that exhibits

lower thermostability of the 5' end (Khvorova et al., 2003). Incorporation of the guide strand into an Ago protein forms a mature RISC and guides the miRNA-induced silencing complex (miRISC) to target mRNA and inhibit gene expression (Kwak and Tomari, 2012).

Non-canonical pathways refer to the biogenesis of miRNAs in the absence of components of the canonical pathway, generally grouped into Drosha/DGCR8-independent and Dicer-independent pathways (Figure 1-6). Drosha/DGCR8-independent pathways include mirtrons (pre-miRNAs generated from introns during mRNA splicing (Ruby et al., 2007)) and 7-methylguanosine (m^7G) capped pre-miRNAs, pre-miRNAs generated directly by RNA polymerase II transcription (Xie et al., 2013). The dicer-independent pathway involves Drosha cleavage of transcripts that generate short pre-miRNAs cleaved directly by Ago proteins rather than Dicer due to the mature sequence spanning the pre-miRNA stem loop (Cheloufi et al., 2010). Despite processing differences, all pathways converge at the miRISC to induce posttranscriptional silencing of target genes.

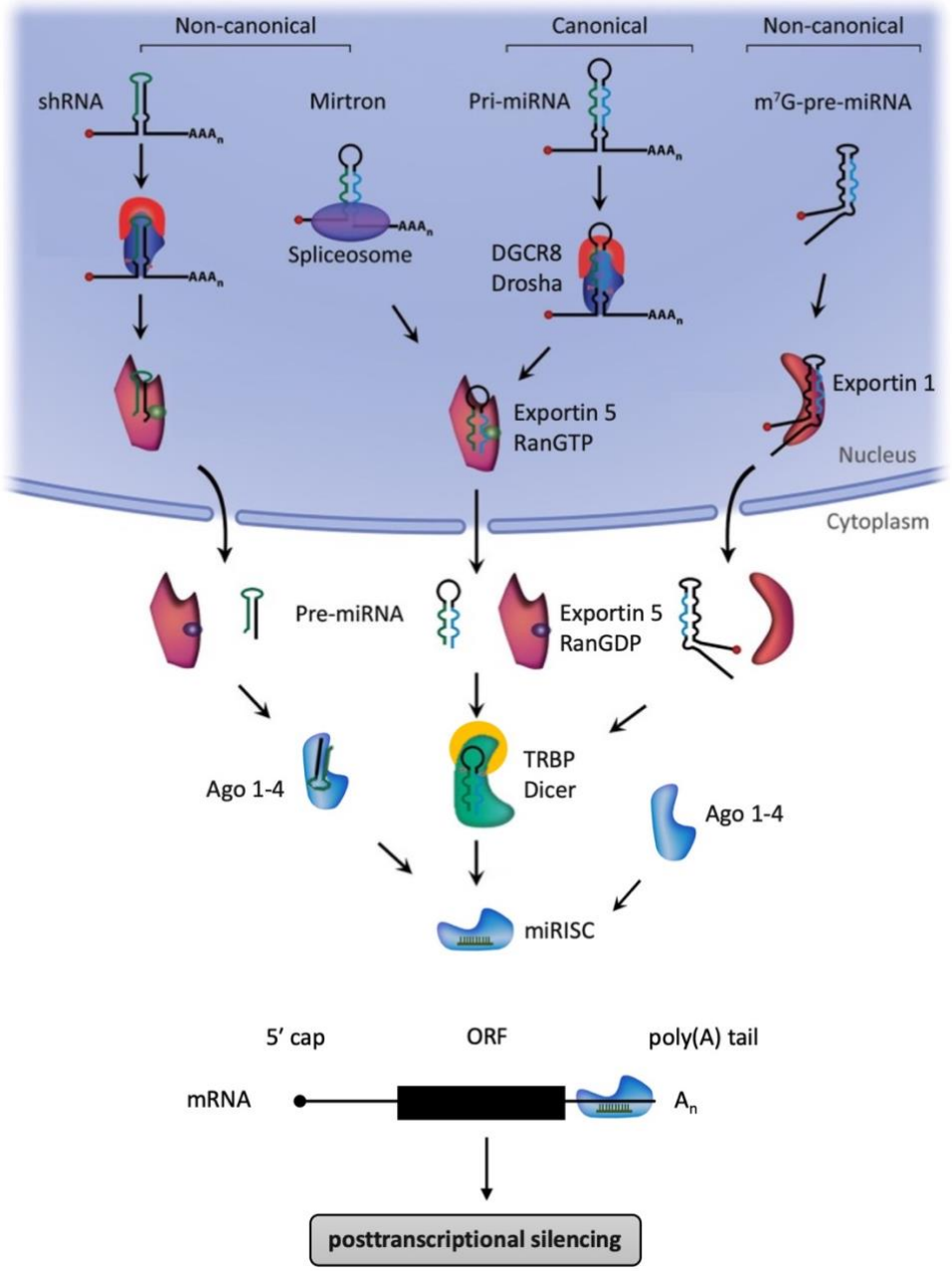

Figure 1-6 Canonical and non-canonical miRNA biogenesis pathways.

In the canonical pathway, miRNA genes are transcribed by RNA polymerase II binding to promoter elements of the gene to produce primary miRNA (pri-miRNA). A microprocessor complex consisting of DGCR8 and Drosha cleaves the pri-miRNA transcript at the base of the stem loop to release precursor miRNA (pre-miRNA). Pre-miRNA is transported out of the nucleus via exportin 5 and RanGTP and released by hydrolysis of RanGTP to RanGDP. Free pre-miRNA is cleaved by Dicer in complex with transactivation response element RNA-binding protein (TRBP) to produce a miRNA duplex. The duplex is loaded into an Argonaute (Ago) protein, a core component of the RNA-induced silencing complex (RISC), which unwinds the duplex. A single strand is retained forming a mature RISC (miRNA-induced silencing complex (miRISC). In non-canonical pathways, miRNAs are processed in the absence of either Drosha/DGCR8 or Dicer. Drosha/DGCR8-independent pathways include mirtrons (pre-miRNAs generated from spliceosomes) and m^7G-capped pre-miRNAs (exported via exportin 1). The dicer-independent pathway involves Drosha cleavage of small hairpin RNA (shRNA) cleaved directly by Ago proteins. All pathways converge at the miRISC to induce posttranscriptional silencing of target genes. Pri-miRNA, primary miRNA; pre-miRNA, precursor miRNA; m^7G, 7-methylguanosine; TRBP, transactivation response element RNA-binding protein, Ago, argonaute; RISC, RNA-induced silencing complex; miRISC, miRNA-induced silencing complex; shRNA, small hairpin RNA. Figure adapted from (O'brien et al., 2018) under Creative Commons Attribution License (CC BY).

Besides the Drosha/DGCR8 complex and Dicer/TRBP complex, the involvement of other RNA binding proteins during biogenesis can further regulate miRNA maturation. For example, RNA binding protein Lin-28 was shown to bind to the loop region of pri-miRNA let-7 family members, and Lin-28 overexpression and knockdown repressed and stimulated miRNA expression respectively, demonstrating the inhibitory effects of Lin-28 prior to Drosha processing (Newman et al., 2008). In contrast, heterogeneous nuclear ribonucleoprotein complex A1 was found to bind to the stem region of pri-miR-18a and promote subsequent Drosha/DGCR8 processing (Guil and Cáceres, 2007). Other RNA binding proteins, such as KH-type splicing regulatory protein and TAR DNA-binding protein-43, have shown to interact directly with Drosha and Dicer complexes and bind to the loop region of pri-miRNA and pre-miRNA to promote miRNA maturation (Trabucchi et al., 2009, Kawahara and Mieda-Sato, 2012). In addition to RNA binding proteins, a host of other accessory proteins, including enzymes, hormones, and cytokines, as well as non-protein factors have shown to regulate miRNA processing (reviewed by (Newman and Hammond, 2010, Kurzynska-Kokorniak et al., 2015). Although the biochemical basis and role of these interactions remains largely unclear, the vast regulatory network of miRNA biogenesis demonstrates how miRNA expression and in turn mRNA expression is a carefully regulated process.

The spatial and temporal regulation of miRNA expression is also subject to modulation at both the transcriptional and posttranscriptional level. The basic mechanisms of transcriptional regulation of miRNA genes are comparable to that of protein-coding genes; transcriptional units consist of promoters, terminators, transcription factors, and other regulatory elements, and transcription is driven by RNA polymerase II (De Rie et al., 2017, Lee et al., 2004). Approximately half of miRNA genes are intergenic and transcribed by their own transcriptional unit (Lee et al., 2002, De Rie et al., 2017). The other half are intronic, where they can be transcribed from the same promoter as their host gene or transcription can also occur independently and involve RNA polymerase III (De Rie et al., 2017, Monteys et al., 2010). Transcriptional units determine the expression of miRNA in specific cells/tissues or in response to certain stimuli, thereby regulating their expression in both health and disease (Sweetman et al., 2008, Bhatt et al., 2015). At the posttranscriptional level, cell-specific expression is primarily

mediated by the existence of alternative 3' untranslated region (UTR) isoforms in mRNAs, which determine the presence or absence of miRNA binding sites (Nam et al., 2014). Besides molecules involved in the biogenesis pathways, transcriptional and posttranscriptional mediators further highlight how the expression and in turn function of miRNAs is subject to extensive regulation.

1.2.2 MiRNA mechanism of action

MiRNAs are responsible for the mRNA targeting specificity of the miRISC, and Ago proteins (Ago 1-4 in mammals) are essential to the mRNA silencing ability of the miRISC (Su et al., 2009). Single stranded mature miRNAs harbour a highly conserved sequence, known as the seed region, which consists of nts 2-8 at the 5' end (Lewis et al., 2005). Via full or partial complementary base pairing, the miRNA seed region binds to miRNA response elements primarily located within the 3' UTR of target mRNA (Lewis et al., 2005). MiRNA:mRNA interaction efficiency is enhanced by positioning of the target site within close proximity to other target sites for coexpressed miRNAs, outside of the first 15 nts of the 3' UTR, and near both ends of the 3' UTR (Grimson et al., 2007). Recent studies have also predicted target sites exist outside of the 3' UTR of mRNA, namely within the 5' UTR and coding regions of mRNA, and shown miRNAs retain their ability to inhibit posttranscriptional gene expression at these sites (Xu et al., 2014b, Lytle et al., 2007, Hausser et al., 2013). Furthermore, studies have identified sites outside the seed region at the 5' end of miRNAs that enhance interaction efficiency, including base pairing at the 3' end of miRNAs, base pairing at miRNA nts 13-16, and mRNA AU-rich nt composition near the target site (Grimson et al., 2007, Broughton et al., 2016, Zhang et al., 2018). These factors underpin the ability of miRNAs to target up to hundreds of genes and the ability of miRNAs with identical seed sequences to target different genes.

In the presence of perfect complementary base pairing, the catalytically active Ago 2 can induce cleavage of target mRNA, leading to mRNA degradation and gene silencing (Jo et al., 2015). In contrast, Ago 1, 3, and 4 do not exhibit independent cleavage activity (Su et al., 2009). During partial complementary base pairing, Ago proteins therefore recruit additional proteins to mediate gene silencing. The GW182 protein family, which interacts with Ago proteins via an Ago-binding domain have been identified as an essential requirement for gene

silencing in animals (reviewed by (Jonas and Izaurralde, 2015)). They act as scaffolds, bridging the interaction between Ago proteins and downstream proteins required for gene silencing. Posttranscriptional gene silencing by miRNAs occurs via two key mechanisms: mRNA degradation, which includes deadenylation, 3'-to-5' decay, decapping, and 5'-to-3' decay, and translational repression (Jonas and Izaurralde, 2015) (Figure 1-7).

Deadenylation refers to shortening or removal of the poly(A) tail of mRNA by poly(A)-specific 3′ exonucleases (deadenylases) (Charenton and Graille, 2018). PAN2-PAN3 and CCR4-NOT deadenylase complexes catalyse deadenylation (Figure 1-7). Deadenylated mRNAs can be directly degraded in a 3'-to-5' direction by RNA exosome complexes or decapped (Charenton and Graille, 2018) (Figure 1-7). Decapping refers to removal of the 5′ m^7G cap by the decapping enzyme, decapping protein 2 (Figure 1-7). Decapped mRNAs undergo 5'-to-3' decay via exoribonuclease 1, leading to mRNA degradation (Charenton and Graille, 2018) (Figure 1-7). Translation is promoted by the poly(A) tail and 5'-cap structure of mRNA (Figure 1-7). The poly(A)-binding protein of the poly(A) tail and cap-binding protein, eukaryotic translation initiation factor 4E (eIF4E), of the 5'-cap structure interact via the scaffolding protein eIF4G, which together with eIF4E and eIF4A forms eIF4F complex (Jonas and Izaurralde, 2015). It is proposed that miRNAs interfere with the activity and/or assembly of the eIF4F complex to induce translational repression (Jonas and Izaurralde, 2015) (Figure 1-7).

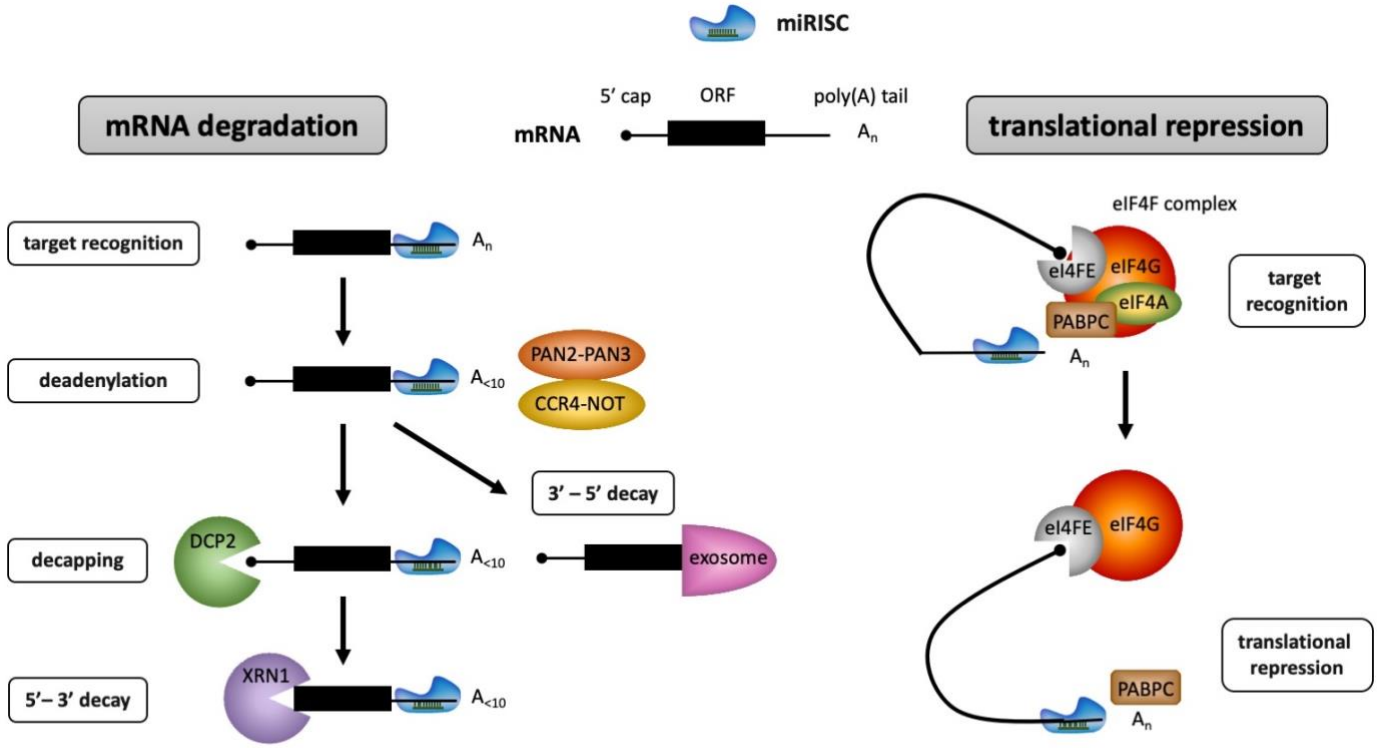

Figure 1-7 Mechanism of action of miRNAs in posttranscriptional silencing of gene targets.

Posttranscriptional gene silencing by miRNAs occurs via two key mechanisms: mRNA degradation (which includes deadenylation, 3'-to-5' decay, decapping, and 5'-to-3' decay) and translational repression. In mRNA degradation, the miRNA-induced silencing complex (miRISC) binds to the 3' UTR of target genes. PAN2-PAN3 and CCR4-NOT deadenylase complexes catalyse deadenylation, which leads to shortening or removal of the poly(A) tail of mRNA. Deadenylated mRNAs can be directly degraded in a 3'-to-5' direction by RNA exosome complexes or decapped. In decapping, the 5′ cap of mRNA is removed by the decapping enzyme, decapping protein 2 (DCPC2). Decapped mRNAs undergo 5'-to-3' decay via exoribonuclease 1 (XRN1), leading to mRNA degradation. In translational repression, miRNA-induced silencing complex (miRISC) binds to the 3' UTR of target genes during translation initiation. Translation is promoted by the poly(A)-binding protein (PABC) of the poly(A) tail and eukaryotic translation initiation factor 4E (eIF4E) of the 5'-cap structure interacting via the scaffolding protein eIF4G, which together with eIF4E and eIF4A forms eIF4F complex. MiRNAs interfere with the activity and/or assembly of the eIF4F complex to induce translational repression. ORF, open reading frame. miRISC, miRNA-induced silencing complex; DCP2, decapping protein 2; XRN1, exoribonuclease 1; eIF4, eukaryotic initiation factor 4; PABC, poly(A)-binding protein.

Besides mRNA degradation and translational repression, miRNAs have shown to exhibit alternative functions under certain conditions. For example, translational activation of mRNA has been observed when Ago 2 associates with fragile-X-mental-retardation-related protein 1 rather than GW182 proteins (Truesdell et al., 2012) and when miRNA binds to the 5' UTR rather than the 3'UTR of mRNA (Ørom et al., 2008). MiRNAs have also shown to act in the nucleus, where they can inhibit transcription via non-seed region binding (Benhamed et al., 2012, Miao et al., 2016).

In addition to regulating intracellular gene targets, miRNAs can be released from cells and act in a paracrine and endocrine manner. Circulating miRNAs have been detected in various extracellular fluids, including plasma (Mitchell et al., 2008), serum (Lawrie et al., 2008), urine (Weber et al., 2010), and saliva (Weber et al., 2010). MiRNAs are stable in biofluids as they are either found in EVs or bound to other proteins, most notably Ago 2, protecting them from RNA degradation and potentially trafficking them to specific cells (Gallo et al., 2012, Arroyo et al., 2011). Although it was initially thought miRNAs were passively released from dying or injured cells, evidence from profiling studies in numerous diseases and *in vitro* characterisation of circulating miRNAs suggests they exert biological and in turn pathological functions, acting as an intercellular communication network (reviewed by (Sohel, 2016)).

1.2.3 MiRNAs in the placenta

MiRNAs and their mRNA targets are well conserved across species (Friedman et al., 2009, Li et al., 2010), highlighting their involvement in critical cellular processes. The importance of miRNAs in prenatal development is demonstrated by knockout (KO) of Dicer and Ago 2 in mice inducing embryo lethal phenotypes (Bernstein et al., 2003, Liu et al., 2004). Embryo and perinatal lethality is also observed in mice with global targeted deletion of several miRNAs, including miR-106b~25 and miR-17~92 (Ventura et al., 2008), miR-1-2 (Zhao et al., 2007), miR-290~295 (Medeiros et al., 2011), miR-126 (Wang et al., 2008), and miR-205 (Wang et al., 2013). In addition to the essential role of miRNAs in embryonic development, knockdown of Ago 2 in mice induces placental and embryo malformation, demonstrating the critical role miRNAs play in placental development (Cheloufi et al., 2010). In *ex vivo* placental explants, primary

trophoblasts, and trophoblast cell lines, knockdown of Dicer has shown to impair the proliferation, invasion, and angiogenic properties of trophoblasts (Forbes et al., 2012, Tang et al., 2020). Moreover, polymorphisms in placental DROSHA and DICER have found to be associated with an increased risk of pregnancy-related disorders such as PE (Rezaei et al., 2019, Eskandari et al., 2018). Collectively, these preclinical and clinical studies support the crucial role of miRNAs in the development of the placenta.

Barad et al. were the first to detect miRNA expression in the human placenta, identifying several miRNAs, miR-141, miR-23A, and miR-136, that were highly enriched in the placenta compared to other tissues (Barad et al., 2004). Subsequently, a miRNA cluster located on chromosome 19 (C19MC) was identified and found to be conserved across primate genomes (Bentwich et al., 2005). The C19MC is preferentially expressed in the placenta, where it has been detected as early as 5 weeks of pregnancy, and comprises of 46 miRNA genes that encode 58 mature miRNAs (Donker et al., 2012). The cluster is imprinted in the placenta, with only the paternally inherited allele being expressed (Noguer-Dance et al., 2010). Similar imprinted miRNA clusters expressed almost exclusively in the placenta have been detected specific to rodents, a paternally expressed chromosome 2 miRNA cluster (C2MC), and to eutherians, a maternally expressed chromosome 14 miRNA cluster (C14MC) (Malnou et al., 2018). KO studies in mice highlight the critical function of these miRNA clusters in the placenta. KO of the C2MC in mice induced severe impaired placental development, embryolethality, and foetal defects (Inoue et al., 2017). KO of one or more miRNAs from the C14MC in mice led to placentomegaly with severe abnormalities in the labyrinth zone and neonatal lethality (Ito et al., 2015, Yoichi et al., 2008). *In-vitro* studies further support their essential role in the placenta, with evidence demonstrating their involvement in trophoblast and endothelial cell development and function as well as cell-to-cell communication (reviewed by (Malnou et al., 2018)). In trophoblast cell lines, overexpression of several members, including miR-520c-3p, miR-520g, and miR-519d-3p, inhibited migration and invasion (Takahashi et al., 2017, Jiang et al., 2017, Ding et al., 2015). Another group showed exosomes isolated from primary human trophoblasts conferred antiviral effects on a range of recipient cells, including human umbilical vein endothelial cells (HUVECs), human uterine microvascular

endothelial cells, and human placental fibroblasts (Delorme-Axford et al., 2013). This effect was attributed to the C19MC since overexpression in cells not naturally expressing the cluster similarly displayed resistance to viral infection (Delorme-Axford et al., 2013). Characterisation of the C19MC in primary trophoblasts and four trophoblast cells lines showed that the cluster accounted for the majority of miRNAs expressed in term trophoblasts as well as in exosomal fractions (Donker et al., 2012). *In vitro* differentiation and hypoxia largely had no effect on the expression of C19MC miRNAs, suggesting the cluster may exert their effects regardless of differentiation status but unlikely modulate the trophoblast response to hypoxic conditions (Donker et al., 2012). Nonetheless, their robust expression and involvement in other pathways support a key role for the cluster in aspects of placentation.

MiRNAs conserved across species have also shown to regulate placental development and function, with the majority of research into their role in trophoblasts. Morales-Prieto et al. conducted microarray expression profiling in first trimester and term primary human trophoblasts as well as four trophoblast cell lines (Morales-Prieto et al., 2012). Of the 762 miRNAs screened, approximately 50% were detected in any of the cell types, demonstrating the vast number of miRNAs potentially involved in mediating trophoblast development and function (Morales-Prieto et al., 2012). In addition to changes in miRNAs from conserved clusters, 27 miRNAs were differentially expressed more than 100-fold between first and third trimester trophoblasts, indicating miRNAs exhibit temporal regulation across pregnancy (Morales-Prieto et al., 2012). This is further supported by a study that examined miRNA expression profiles in villous tissue from the first and third trimester and identified 191 significantly differentially expressed miRNAs between trimesters (Gu et al., 2013). MiRNAs associated with oncogenic and immunosuppressive properties showed higher expression in the first trimester while miRNAs associated with differentiation and tumour suppressive characteristics exhibited higher expression in the third trimester, reflecting the dynamic changes occurring in the placenta (Gu et al., 2013). Placental miRNAs have shown to be altered in response to stimuli characteristic of the intrauterine environment. In trophoblasts exposed to hypoxia and oxidative stress, miRNAs and their gene targets were found to be differentially expressed (Mouillet et al., 2010, Cross et al., 2015). In addition to

impacting gene expression, candidate studies have shown miRNAs modulate an array of trophoblast properties, including migration, invasion, proliferation, differentiation, mitochondrial function, survival, and signalling (Luo et al., 2012, Liu et al., 2019a, Dai et al., 2012, Brkic et al., 2018, Wang et al., 2018a, Gysler et al., 2016, Ospina-Prieto et al., 2016).

In addition to trophoblasts, *in vitro* and *in vivo* studies have examined the intra- and extracellular roles of miRNAs in other placental cell types. In decidua derived mesenchymal stem cells (dMSCs), overexpression of miR-136 inhibited cell viability and proliferation and promoted apoptosis (Ji et al., 2017) and overexpression of miR-494 inhibited cell growth (Chen et al., 2015), with the miRNAs exerting their effects in part via inhibiting VEGF. Both studies collected supernatants from the dMSCs overexpressing the miRNAs and found that co-culture incubation inhibited HUVEC capillary formation and trophoblast invasion and migration (Ji et al., 2017, Chen et al., 2015) . Hence, in addition to regulating dMSCs properties, miRNAs expressed in dMSCs may regulate the angiogenic and invasive properties of other placental cell types. Another study reported supernatant from miR-494-overexpressed dMSCs inhibited macrophage polarisation toward the immunosuppressive M2 macrophages and favoured the formation of proinflammatory M1 macrophages, indicating a further regulatory mechanism of dMSC miRNAs in immune cells (Zhao et al., 2016). MiRNAs have also shown to modulate the properties of placental immune cells directly. For example, in decidual NK cells, suppressing miR-30e promoted cytotoxicity while overexpressing miR-30e inhibited cytotoxicity via targeting perforin 1 (PRF1) (Huang et al., 2019). Elevating miR-30e and in turn suppressing PRF1 led to downregulation of the Th1 proinflammatory cytokines, interferon γ (IFN-γ) and tumour necrosis factor α (TNF-α), and upregulation of the Th2 cytokines (interleukin (IL)-4 and IL-10) and angiogenic factors (VEGF, angiotensin II (Ang II), and PlGF) suggesting miR-30e in NK cells may be involved in the maternofoetal immune response and placental angiogenic signalling (Huang et al., 2019). Several miRNAs have also been implicated in regulating endothelial cell function in the placenta. KO of miR-126 in mice, a miRNA abundantly expressed in endothelial cells, led to embryolethality in approximately 40% of cases and surviving embryos showed severe systemic oedema, multifocal haemorrhages, and ruptured blood vessels due to impaired angiogenesis of

endothelial cells (Wang et al., 2008). A separate group showed miR-126 stimulated endothelial progenitor cell proliferation, differentiation, and migration *in vitro* and subsequently examined the effects of altering placental miR-126 expression in pregnant rats by intraplacental administration of chemically modified oligonucleotides specific to miR-126 (Yan et al., 2013). Agomir-126 administration significantly increased placental microvessel density and the size and weight of placentas and foetuses, while antagomir-126 induced the opposite effects, demonstrating a key role of the miRNA in endothelial cells and in turn placental development and function (Yan et al., 2013). MiR-203 and miR-31-5p have also been implicated in regulating endothelial cell function in the placenta. Examination of placental miR-203 expression in early, term, and late-term human placentas, showed expression decreased with higher gestational age alongside an increase in VEGFA and VEGF receptor 2 expression (Liu et al., 2018a). In HUVECS, overexpression of miR-203 inhibited proliferation, migration, invasion, and tube formation via modulating VEGF levels (Liu et al., 2018b). In an *ex vivo* model of human placenta arteries, miR-31-5p induced endothelial dysfunction by impairing angiogenesis, trophoblast invasion, and vasorelaxation (Kim et al., 2018). Finally, several miRNAs have also shown to be involved in the decidualization of endometrial stromal cells (Qian et al., 2009, Sirohi et al., 2019, Zhang et al., 2015c). For example, miR-145 overexpression inhibited the decidualization of stromal cells and suppressed the migration and invasion of HUVECs (Sirohi et al., 2019). The altered expression of a miRNA in different placental cell types can also produce concerted effects. MiR-15b, miR-155, and miR-320a have shown to inhibit the invasive properties of trophoblasts and angiogenic properties of endothelial cells, demonstrating the involvement of miRNAs in coordinating cellular responses in the placenta during pregnancy (Dai et al., 2012, Yang et al., 2016b, Cheng et al., 2011, Liu et al., 2018c).

MiRNAs may also regulate placentation as cargo of EVs, a heterogenous group of lipid bilayer particles that are released from cells and contain various proteins, nucleic acid, and lipids (Tannetta et al., 2017a) (Figure 1-8). The number of placenta derived EVs, including exosomes, microvesicles, and apoptotic bodies, increase throughout pregnancy and have found to be dysregulated in pregnancy disorders (Tannetta et al., 2017a, Sarker et al., 2014, Redman et al., 2012). EVs derived from the placenta are released into the maternal circulation, where

they can transfer cargo into recipient cells (Figure 1-8). MiRNAs from placenta derived EVs have shown to regulate systemic endothelial function and immune responses by transfer into maternal cells, such as endothelial cells (Cronqvist et al., 2017, Wei et al., 2017) and peripheral blood mononuclear cells (Holder et al., 2012). Locally derived EVs have also shown to exhibit paracrine communication between cell types of the placenta via miRNAs. Exosomal miR-520c-3p derived from chorionic villous trophoblasts inhibited the invasion of EVTs *in vitro* (Takahashi et al., 2017). Exosomal miR-146a-5p and miR-548e-5p derived from amniotic fluid MSCs reduced trophoblast migration and invasion (Yang et al., 2019a). EVs therefore represent another mechanism by which miRNAs can communicate between cells to mediate placental development and function.

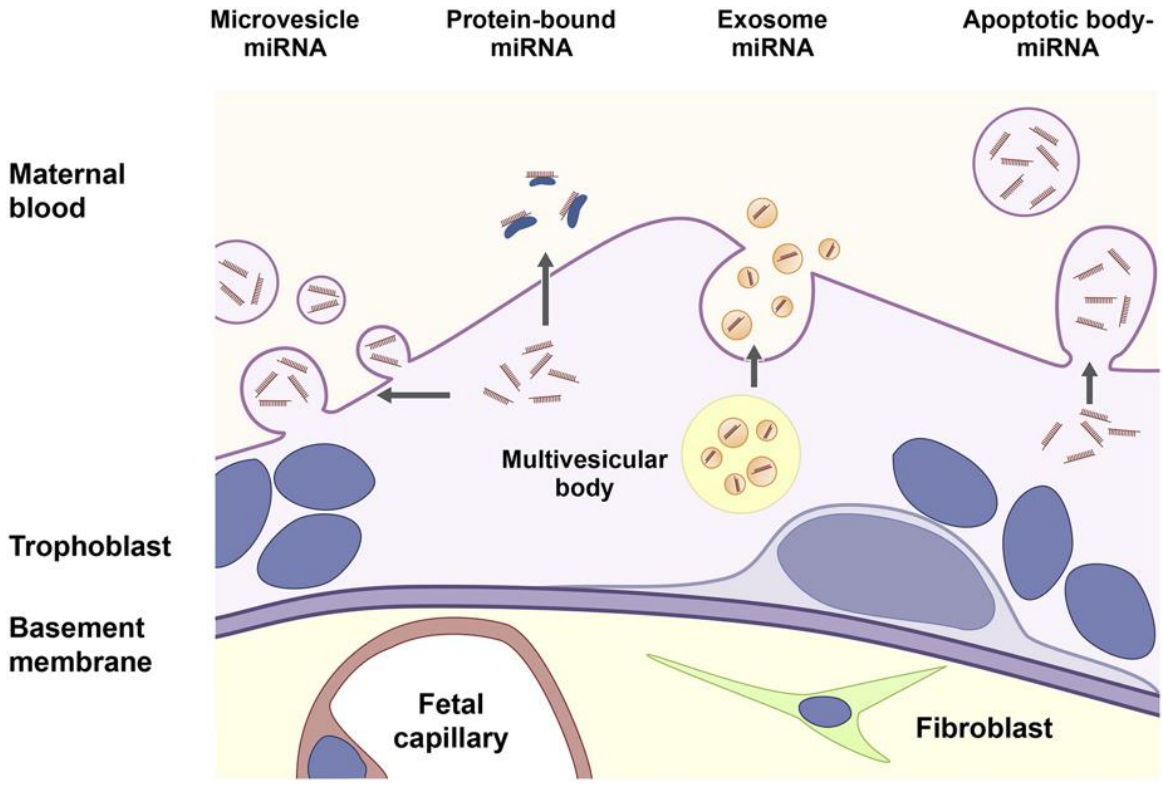

Figure 1-8 Schematic of extracellular miRNAs derived from human trophoblasts.

MiRNAs can be released from trophoblasts in microvesicles, protein-bound, exosomes, and apoptotic bodies. Figure taken from (Ouyang et al., 2014) with permission from Elsevier.

1.2.4 MiRNAs in pregnancy disorders

In 2007, Pineles et al. were the first to report miRNAs were significantly differentially expressed in the placentas of preeclamptic patients with and without SGA infants (Pineles et al., 2007). Since then, studies have found significantly differentially expressed placental miRNAs in a number of other pathological pregnancy conditions, including GH (Hromadnikova et al., 2015a), FGR (Higashijima et al., 2013), SGA and LGA infants (Thamotharan et al., 2017, Guo et al., 2018), gestational diabetes mellitus (Li et al., 2015b), gestational obesity (Carreras-Badosa et al., 2017), placenta accreta (Umemura et al., 2013), and preterm birth (Mayor-Lynn et al., 2011). Studies examining placental miRNA expression across multiple pregnancy disorders have found that disorders show unique as well as overlapping dysregulated miRNA profiles (Hromadnikova et al., 2015a, Mayor-Lynn et al., 2011, Hromadnikova et al., 2015b). Hromadnikova et al. reported four members of the C19MC (miR-517-5p, miR-519d, miR-520a-5p, and miR-525) were downregulated in placental tissue across pregnancies complicated by GH, FGR, and PE, a further two members (miR-518f-5p and miR-519a) were downregulated in both FGR and PE, and an additional five members were downregulated only in PE (miR-515-5p, miR-518b, miR-520h, miR-524-5p, and miR-526a) compared to normal pregnancies (Hromadnikova et al., 2015b). Whether the shared differences in miRNA expression reflect pathological processes common amongst pregnancy disorders remains unclear. Furthermore, it remains a challenge to elucidate whether dysregulated placental miRNAs represent a cause or consequence of pathological processes. Due to ethical reasons, clinical studies are generally limited to placental tissue collected at the time of delivery, preventing investigations at earlier time points in pregnancy. None of the significantly differentially expressed C19 members were associated with abnormal blood flow parameters present in the complicated pregnancies (Hromadnikova et al., 2015b). In addition, more miRNAs were significantly downregulated in complicated pregnancies with later delivery dates (Hromadnikova et al., 2015b). These findings suggest differential expression of these placental miRNAs may be a consequence rather than a cause of pathology. In a separate study, Hromadnikova et al. evaluated the expression of non-clustered miRNAs previously implicated in cardiovascular and cerebrovascular diseases in placental tissue from GH, FGR, and PE pregnancies (Hromadnikova et

al., 2015a). Besides identifying overlapping (miR-499a-5p in GH, FGR, and PE) and unique (miR-122-5p, miR-125b-5p, and miR-195-5p in FGR) miRNAs, three miRNAs (miR-26a-5p, miR-103a-3p, and miR-145-5p) were found to be significantly downregulated in PE and FGR in cases where delivery occurred prior to 34 weeks of pregnancy (Hromadnikova et al., 2015a). *In vitro* studies demonstrate the involvement of the three miRNAs in trophoblast and endothelial cell proliferation and migration, providing evidence that dysregulated placental miRNAs may drive pathological processes (Brooks and Fry, 2017, Lv et al., 2019, Wu et al., 2020, Huang et al., 2016). *In vitro* studies provide a means of investigating the impact of altered miRNA expression on target gene expression and functional properties of cells. However, a major issue in deciphering the role of placental miRNAs in pregnancy disorders lies in the inconsistent findings between clinical studies regarding the direction of miRNA expression (Hu and Zhang, 2019, Frazier et al., 2020). The discordance between studies in part arises from placental miRNA expression being influenced by disease severity, presenting symptoms, gestational age, and labour status (Pineles et al., 2007, Hromadnikova et al., 2015a, Hromadnikova et al., 2015b, Mayor-Lynn et al., 2011). Placental miRNA signatures are therefore more likely to be present in a subset of patients rather than characteristic of a pregnancy disorder as a whole. In addition, it should be noted that methodological aspects of study design, such as sample size, confounding variables, sampling technique, and platform-dependent sensitivity and specificity, likely contribute to inconsistencies between studies as well.

Differences in miRNA expression in serum (Ura et al., 2014), plasma (Fallen et al., 2018), and urine (Gan et al., 2017) have also been reported in pregnancy disorders. In turn, numerous studies have explored the utility of circulating miRNAs as non-invasive biomarkers for adverse pregnancy outcomes (Tsochandaridis et al., 2015). Placenta derived miRNAs are detectable as early as 6 weeks of pregnancy and have shown to act as markers of placental function (Sarker et al., 2014, Whitehead et al., 2013, Hromadnikova et al., 2015a). Biomarkers have the potential to facilitate earlier diagnosis and improve management by predicting maternal and foetal outcomes. Given that maternal history and risk factors alone are generally poor predictors of adverse pregnancy outcomes, biomarkers are important tools for monitoring pregnancies (Kane et

al., 2014). However, there are only a limited number of blood-based biomarkers routinely used in clinical practice due to a lack of sensitivity and/or specificity (Kane et al., 2014). It remains to be seen whether circulating miRNAs can achieve adequate sensitivity and specificity for pregnancy-related disorders in order to be adopted clinically. In patients with macrosomia, one study found miR-376a had a sensitivity of 96.7% and specificity of 40.0% (Hu et al., 2014), and another reported the miR-17-92 cluster had a sensitivity of 82.61% and specificity of 69.57% (Li et al., 2015a). In preterm birth, the predictive performance of miR-150-5p (as measured by area under the curve (AUC)) increased from 0.87 to 0.91 when combined with six other miRNAs (Cook et al., 2019). Similarly, a combination of C19MC miRNAs had a stronger predictive performance then individual C19MC miRNAs in GH (66.1% sensitivity for miR-520a-5p and miR-525-5p versus 48.2% sensitivity for miR-517-5p alone) and PE (44.19% sensitivity for miR-517-5p, miR-520a-5p, and miR-525-5p versus 27.9%, 41.9%, and 39.5% for each miRNA alone respectively) (Hromadnikova et al., 2019). Hence, a combination of circulating miRNAs rather than an individual miRNA may show to be a more accurate biomarker. However, findings to date should be interpreted with caution due to the relatively small sample sizes of studies. Validation in larger cohorts is particularly important given the inconsistencies in circulating miRNA expression between studies. Nonetheless, investigations into differentially expressed circulating miRNAs provides a means of investigating the role of miRNAs at an earlier timepoint in pregnancy disorders. Furthermore, with some miRNAs displaying a correlation between placental and circulating levels in healthy and complicated pregnancies, circulating miRNAs can provide a unique way to explore the role of placental miRNAs in humans (Xu et al., 2014a, Williams et al., 2013).

1.2.5 MiRNAs in PE

MiRNA expression profiling and candidate studies in cells and tissues from the placenta and blood of preeclamptic patients have identified hundreds of miRNAs dysregulated in PE (Sheikh et al., 2016). A change in the concentration, composition, and bioactivity of placenta and non-placental derived EVs has been reported as early as the first trimester in preeclamptic pregnancies (Truong et al., 2017, Salomon et al., 2017). Besides the involvement in placental dysfunction, studies have implicated EVs in promoting the systemic inflammatory

response, endothelial dysfunction, and hypercoagulation in PE through their interaction with immune cells, endothelial cells, and platelets (reviewed by (Tannetta et al., 2017b)). Both clustered miRNAs, such as members from the C19MC, and non-clustered miRNAs in EVs have found to be differentially expressed across the different trimesters of preeclamptic pregnancies, prompting studies to investigate their potential as biomarkers (Hromadnikova et al., 2019, Devor et al., 2020). A systematic review pooled the results from three articles, estimating circulating miRNAs had a sensitivity of 0.61% and specificity of 0.78% for predicting PE (Yin et al., 2020). Studies have shown differences in the concentration and miRNA content of EVs between PE subtypes (Pillay et al., 2016, Pillay et al., 2019), suggesting stratifying preeclamptic patients into subtypes may improve the predictive power of circulating miRNAs as biomarkers. Distinct miRNA profiles in PE subtypes have similarly been reported in the placenta (Lykoudi et al., 2018, Zhu et al., 2009), lending weight to the concept that subtypes show unique miRNA signatures. This may in turn account for the inconsistencies between clinical studies in terms of the direction of expression of dysregulated placental miRNAs, although other patient characteristics (such as ethnicity, age, and the timing of delivery) and study design parameters (sample size, sampling technique, and experimental methodology) also likely contribute.

Characterisation of differentially expressed placental miRNAs has been conducted in an array of placental cell types, such as trophoblasts (Lee et al., 2011, Muralimanoharan et al., 2012, Luo et al., 2012, Wang et al., 2017, Xiao et al., 2017, Wang et al., 2018c, Yang et al., 2019c, Liu et al., 2018a, Zhang et al., 2019, Wang et al., 2019a, Yang and Guo, 2019), immune cells (Wang et al., 2019b), endothelial cells (Cheng et al., 2011, Zhou et al., 2017), MSCs (Liu et al., 2012, Wang et al., 2012c, Hu et al., 2015), and co-cultures of these cells (Chen et al., 2015, Zhao et al., 2016, Ji et al., 2017). *In vitro* characterisation by corroborating gene targets and conducting functional assays supports the involvement of miRNAs in regulating key pathological processes associated with PE, namely impaired trophoblast and endothelial function, angiogenesis, and immune tolerance. The role of differentially expressed miRNAs has been studied most extensively in trophoblasts since placental dysfunction is one of the main pathological features of PE. Figure 1-9 presents miRNAs for which studies have

evaluated the expression of the miRNA and gene target in preeclamptic patients, validated the gene as a target through reporter constructs *in vitro*, and demonstrated overexpression/knockdown of the miRNA impairs trophoblast function.

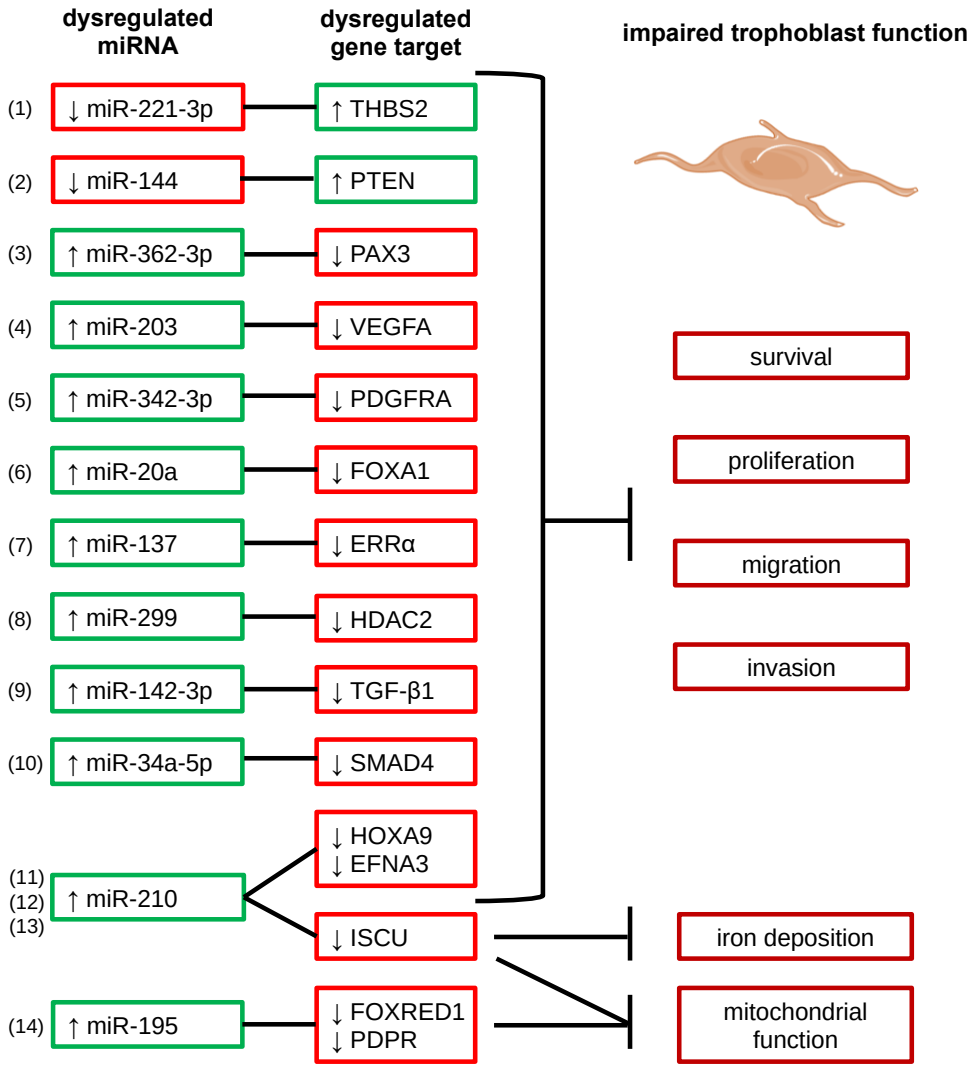

Figure 1-9 MiRNAs and validated gene targets dysregulated in PE implicated in impairing trophoblast function.

MiRNAs for which studies have found dysregulation of the miRNA and gene target in preeclamptic patients, validated the gene as a target through reporter constructs *in vitro*, and demonstrated overexpression/knockdown of the miRNA impairs trophoblast function. (1) (Yang et al., 2019c) (2) (Xiao et al., 2017) (3) (Wang et al., 2018c) (4) (Liu et al., 2018a) (5) (Yang and Guo, 2019) (6) (Wang et al., 2014b) (7) (Lu et al., 2017) (8) (Gao et al., 2018) (9) (Liu et al., 2019a) (10) (Xue et al., 2019) (11) (Zhang et al., 2012) (12) (Lee et al., 2011) (13) (Muralimanoharan et al., 2012) and (14) (Wang et al., 2018a). THBS2, thrombospondin-2; PTEN, phosphatase and tensin homolog; PAX3, paired box gene 3; VEGFA, vascular endothelial growth factor A; PDGFRA, platelet-derived growth factor receptor α; FOXA1, forkhead box protein A1; ERRα, oestrogen-related receptor α; HDAC2, histone deacetylase 2; TGF-β1, transforming growth factor-β1; SMAD4, Smad family member 4; HOXA9, homeobox-A9; EFNA3, ephrin-A3; ISCU, iron-sulphur cluster scaffold; FOXRED1, FAD-dependent oxidoreductase domain-containing 1; PDPR, pyruvate dehydrogenase phosphatase regulatory subunit. Figure was created using images from Servier Medical Art under Attribution 3.0 Unported (CC BY 3.0).

In addition to altering trophoblast function, significantly upregulated placental miRNAs have shown to inhibit the expression of various angiogenic factors that are downregulated in PE, such as VEGFA and endothelial nitric oxide synthase (eNOS), indicating their role in contributing to the imbalance in angiogenic signalling in PE (Li et al., 2013, Jiang et al., 2015). As an example, in trophoblasts, miR-155 inhibited cysteine-rich angiogenic inducer 61 (CYR61), an extracellular matrix-associated signalling protein, and eNOS, key enzyme involved in production of nitric oxide (NO), matching the observed upregulation of the miRNA and downregulation of CYR61 and eNOS in preeclamptic placentas (Zhang et al., 2010, Li et al., 2014). Besides trophoblasts, dysregulation of miRNAs in other cell types in PE has further shown to impair angiogenic signalling. In HUVECs isolated from preeclamptic patients, miR-155 expression was decreased and its gene target Ang II type 1 receptor was increased, leading to excessive Ang II-induced signalling (Cheng et al., 2011). MiR-29a/c-3p were downregulated in HUVECs isolated from preeclamptic patients, and knockdown of the miRNAs in HUVECs from normotensive pregnancies blocked VEGFA- and fibroblast growth factor 2-stimulated endothelial cell migration (Zhou et al., 2017). Overexpression of miR-15b in HUVECs reduced cell proliferation and tube formation via targeting AGO2, in line with the increased expression of miR-15b and decreased expression of AGO2 in preeclamptic placentas (Yang et al., 2016b). In MSCs isolated from patients with PE, miR-136, miR-495, and miR-16 were upregulated and inhibited cell growth and promoted apoptosis (Ji et al., 2017, Li et al., 2017, Wang et al., 2012c). Moreover, supernatants collected from the preeclamptic MSCs overexpressing the miRNAs inhibited trophoblast invasion and HUVEC tube formation by targeting VEGF and BMI1 (Ji et al., 2017, Li et al., 2017, Wang et al., 2012c). The involvement of miRNAs in endothelial dysfunction has also been shown through investigations into maternal blood and vessels. In plasma from preeclamptic patients, elevated sFlt-1 levels showed a positive correlation with circulating miR-195-5p expression (Sandrim et al., 2016a). In a separate study, incubating HUVECs with plasma from preeclamptic patients stimulated miR-195-5p and reduced VEGF expression (Sandrim et al., 2016b). In maternal vessel endothelium from subcutaneous fat tissue from preeclamptic patients, miR-203 was increased and its predicted gene target, suppressor of cytokine signalling 3, was decreased (Wang et al., 2016). Overexpression of miR-203 in HUVECs promoted the expression and production of

IL-6 and IL-8, and intercellular adhesion molecule 1, suggesting involvement of the miRNA in the endothelial inflammatory response (Wang et al., 2016). Other miRNAs dysregulated in the placentas of preeclamptic patients, namely, miR-520c-3p, miR-125b, and miR-181a, have also shown to stimulate the production of inflammatory cytokines in trophoblasts and MSCs, further supporting the role of miRNAs in modulating the immune response in a range of cell types in PE (Liu et al., 2019b, Yang et al., 2016c, Liu et al., 2012). MiRNAs may also be involved in modulating maternofoetal immune compatibility. MiRNAs previously reported as upregulated in PE, miR-152 (Zhu et al., 2009) and miR-365 (Zhou et al., 2016), inhibited HLA-G expression in trophoblasts (Zhu et al., 2010, Mori et al., 2016). Moreover, overexpression of miR-152 increased trophoblast susceptibility to NK cell-mediated cytolysis, providing functional evidence of the consequences of dysregulated miRNAs and their gene targets in immune processes in PE.

In contrast to the extensive *in vitro* experiments, only a handful of studies investigating dysregulated miRNAs have been conducted in animal models of PE (Kopriva et al., 2013, Yan et al., 2014, Yang et al., 2016a, Wang et al., 2020c). In poly I:C induced PE mice, miR-210 was significantly upregulated in the placenta compared to wild type (WT) mice (Kopriva et al., 2013). This finding is in line with the 22 studies that have reported its upregulation in the placenta and blood of preeclamptic patients (Frazier et al., 2020), although one study to date reported it was significantly downregulated in patients with mild PE (Zhu et al., 2009). MiR-210 has been described as the master 'hypoxamir' (a hypoxia-inducible miRNA) (Chan et al., 2012), and multiple *in vitro* studies have shown involvement of miR-210 in mediating trophoblast function (Muralimanoharan et al., 2012, Wang et al., 2019a, Li et al., 2019). In the poly I:C induced PE mice, hypoxia-inducible factor 1 α (HIF-1 α) was significantly upregulated in the placenta, providing supporting evidence of miR-210 as a key mediator of the hypoxia response (Kopriva et al., 2013). In addition, the miR-210 gene target signal transducer and activator of transcription 6 (STAT6) and IL-4, both mediators of the anti-inflammatory Th2 cytokines, were found significantly downregulated, suggesting miR-210 may also play a role in mediating the immune response in PE (Kopriva et al., 2013). In N(γ)-nitro-L-arginine methyl ester (L-NAME) induced PE rats, miR-148a and miR-152 (members of the miR-148/152 family) were upregulated in the placenta, coinciding with a

downregulation of DNA methyl-transferase 1 (DNMT1), a gene target of miR-148/152, and fatty acid-binding protein 4 (FABP4), a gene target of DNMT1 (Yang et al., 2016a). Through altering the expression of the methylation enzyme, DNMT1, miR-148/152 may in turn modulate methylation patterns of various genes and pathways, such as FABP4 which mediates inflammatory and metabolic pathways. *In vitro* studies have also shown miR-152 inhibits HLA-G expression in trophoblasts, suggesting miR-148/152 may be involved in immune tolerance in PE (Zhu et al., 2010). While three studies in preeclamptic patients have reported upregulation of miR-148/152 members (Zhou et al., 2016, Zhu et al., 2009, Jiang et al., 2015), one study found miR-148a was downregulated (Zhao et al., 2014) highlighting a discordance between clinical studies regarding the direction of miRNA expression as seen with miR-210 (Frazier et al., 2020). In another study of L-NAME induced PE rats, miR-576-5p was decreased and its gene target, transcription factor AP-2α, was increased in placenta (Wang et al., 2020c). Investigations in HTR8/SVneo trophoblasts showed inhibition of miR-576-5p suppressed cell proliferation and invasion (Wang et al., 2020c). No published clinical study in preeclamptic patients could be identified that examined or detected differential miR-576-5p expression. Finally, following investigations in pregnant rats, where intraplacental administration of chemically modified oligonucleotides specific to miR-126 altered placental microvessel density and the size and weight of placentas and foetuses (Yan et al., 2013), Yan et al. evaluated the effects of intraplacental agomir-126 administration in L-NAME induced PE rats (Yan et al., 2014). Elevating placental miR-126 expression led to greater placental and foetal weight, enhanced microvessel density, and a higher proportion of live pups (Yan et al., 2014). While increasing placental miR-126 expression may therefore represent a therapeutic strategy in PE, clinical studies provide conflicting results as to the direction of miR-126 expression in the placenta in preeclamptic patients. Three clinical studies have reported decreased miR-126 expression in preeclamptic placentas (Yan et al., 2013, Hong et al., 2014, Jiang et al., 2015), while two have reported increased expression (Yang et al., 2015, Hu et al., 2009). Nonetheless, this study is the first to provide evidence that altering placental miRNA expression may represent a therapeutic strategy in PE. Since animal models provide the opportunity to study the role and therapeutic potential of miRNAs in PE in an *in vivo* setting,

preclinical investigations are essential to our understanding of how miRNAs are involved in a pregnancy disorder almost unique to humans.

1.2.6 MiRNAs as a therapeutic strategy

As research into the role of miRNAs in diseases and disorders has expanded so has the field of miRNA-based therapeutics, with phase I and phase II clinical trials currently underway (Chakraborty et al., 2017). Their use is being explored in a range of conditions, such as cancer, viral infections, and neurological, metabolic, inflammatory, and cardiovascular disorders (Chakraborty et al., 2017). MiRNAs (in the absence of EVs or binding proteins) are unstable in the circulation and unable to penetrate cell membranes. Therapeutic targeting of miRNAs therefore traditionally involves utilizing chemically synthesized oligonucleotides that either inhibit (antagomirs) or mimic (agomirs) the miRNA of interest. Antagomirs are complementary to the target miRNA to inhibit it, while agomirs are double-stranded RNA molecules that mimic the sequence and in turn function of miRNAs. Due to low intestinal absorption following oral administration, antagomirs and agomirs are typically administered by intravenous or subcutaneous injections (Chakraborty et al., 2017). However, these agents are still susceptible to nuclease degradation, off-target binding, and low cellular membrane permeability (Ling, 2016). Various alternatives, such as miRNA expression vectors and miR sponges, as well as delivery systems, most commonly lipid nanoparticles, have in turn been developed to protect against nuclease degradation, promote targeted delivery, and avoid immune responses (Ling, 2016). Results from early clinical trials have provided mixed results in terms of safety and efficacy. While some therapeutics have shown to be safe and improve disease-related measures (Janssen et al., 2013), other therapeutics have shown limited clinical activity and been discontinued due to safety reasons (Hong et al., 2020). One of the major advantages of miRNA-based therapeutics is the ability of miRNAs to target more than one gene, potentially modulating multiple components of a single biological pathway or multiple biological pathways. For example, in a rat model of heart failure, subcutaneous delivery of MGN-9103 (an inhibitor of miR-208a) prevented pathological cardiac remodelling and improved cardiac function, overall health, and survival (Montgomery et al., 2011). Subsequent microarray analysis of heart tissue revealed that 131 genes were differentially expressed of which 31 were predicted gene targets, and the

expression of 28 of these was increased corresponding with decreased expression of miR-203 (Montgomery et al., 2011) . These findings highlight the pleiotropic nature of miRNAs. While this may confer therapeutic benefit, off-target effects due to inhibition of multiple genes is a potential safety issue with miRNA-based therapeutics. In addition to identifying suitable miRNAs to target, developing efficient and safe delivery systems remains key to ensuring the translational success of miRNA-based therapeutics.

1.3 Gene therapy

Gene therapy is the introduction of foreign genetic material (DNA or RNA) into host cells to prevent, treat, or cure a disease. It can be divided into two main categories: somatic and germline. Somatic gene therapy involves transfer of genetic material into non-reproductive or 'somatic' cells. Introduction into somatic cells means any genetic changes occur only in the patient and cannot be inherited by their offspring. In germline gene therapy, genetic material is transferred into germline cells (sperm or egg cells) and can therefore be passed down to subsequent generations. Germline gene therapy remains largely banned or restricted (Araki and Ishii, 2014). Conventional approaches to somatic gene therapy include introducing genetic material to confer therapeutic benefit or to compensate for a missing or defective gene. A fundamental requirement of gene therapy is delivery of foreign genetic material into the cell nucleus. This can be achieved *in vivo,* in which gene transfer occurs inside the body, or *ex vivo*, in which cells from a patient are removed, genetically modified, and reintroduced back into the patient. Its successful application also requires transfer in target cells, with the genetic material expressed at therapeutic levels for a clinically relevant length of time. To address these conditions and due to the rapid degradation of genetic material *in vivo*, different viral and non-viral gene carriers or 'vectors' have been developed, each harbouring advantages and disadvantages (Nayerossadat et al., 2012).

1.3.1 Viral gene therapy

Viral systems take advantage of the innate ability of viruses to infect host cells and access the nucleus. Viruses are genetically modified by deleting components of their genome, which alters their ability to replicate and suppresses their

virulence while maintaining their ability to infect host cells (Nayerossadat et al., 2012). Viral vectors exhibit high transgene efficiency and expression, contributing to their popular use as vectors in more than two thirds of gene therapy clinical trials (Ginn et al., 2018). However, attenuated viruses still carry a risk of immunogenicity, insertional mutagenesis, and toxicity (Nayerossadat et al., 2012). In addition, they have limits in their transgene packaging capacity and can be difficult to manufacture (Van Der Loo and Wright, 2016). Despite their limitations, viruses have shown to be suitable in certain diseases, dependent on their tissue and cell tropism, transgene capacity, integration profile, duration of transgene expression, and immune profile (Table 1-4).

Table 1-4 Profiles of commonly used viral vectors in gene therapy.

Virus	Tissue tropism	Integration profile	Capacity	Expression	Immune response potential	Neutralizing antibodies	Cellular tropism	Clinical applications
Adenovirus	Broad	Episomal	8 kb (38 kb)*	Transient (stable)*	High (low)*	Common	Dividing and non-dividing	• Cancer (brain, pancreatic, ovarian, prostate, breast, skin, liver, bladder, eye, blood, lungs, colorectal, oral, neck) • Cardiovascular diseases (CAD, CHD, CHF) • Rare inherited disorders (cystic fibrosis) • Other conditions (hearing loss, varicose ulcer)
Adeno-associated virus	Broad (individual serotypes: limited)	Episomal / chromosomal	5 kb	Stable	Low	Common	Dividing and non-dividing	• Cancer (neck, gastric) • Blood clotting disorders (haemophilia A/B) • Vision disorders (LHON, LCA, macular degeneration, achromatopsia, choroideremia) • Neurodegenerative disorders (NCL, AD, PD, HD) • Neuromuscular disorders (MD, x-linked myotubular myopathy, SMA) • Inflammatory disorders (arthritis) • Other rare inherited disorders (Danon disease, Pompe disease, AAT deficiency, phenylketonuria, AADC deficiency, mucopolysaccharidosis, OTC deficiency, Crigler-Najjar syndrome, glycogen storage type disease, familial LPL deficiency)
Herpes simplex virus	Nervous tissue	Episomal	50 kb	Transient	High	Common	Dividing and non-dividing	• Skin disease (TGM-1 related ARCI, dystrophic epidermolysis bullosa) • Cancer (brain, liver, skin) • Cancer pain
Retrovirus	Broad	Chromosomal	8 kb	Stable	Low	Uncommon	Dividing	• Cancer (brain, CNS, breast, skin, eye, vaginal, cervical, anal, penile, oral, neck, kidney, blood) • Immune conditions (HIV, X-linked lymphoproliferative disease, EBV infection, hemophagocytic lymphohistiocytosis, arthritis, SCID, Wiskott-Aldrich syndrome, CGD) • Other rare inherited conditions (Gaucher's disease, Fabry's disease, Fanconi anaemia, mucopolysaccharidosis, junctional epidermolysis bullosa, gyrate atrophy)
Lentivirus	Broad	Chromosomal	8 kb	Stable	Low	Uncommon	Dividing and non-dividing	• Immune conditions (HIV, AIDS-related lymphoma, severe combined immunodeficiency, Wiskott-Aldrich syndrome, CGD) • Blood conditions (haemophilia A, Beta-thalassemia, sickle cell disease, Fanconi anaemia) • Other rare inherited conditions (X-linked adrenoleukodystrophy, Fabry's disease, mucopolysaccharidosis, metachromatic leukodystrophy, cystinosis)

*denotes third generation vectors. CAD, coronary artery disease; CHD, coronary heart disease; CHF, congestive heart failure; LHON, Leber's hereditary optic neuropathy; LCA, Leber congenital amaurosis; NCL, neuronal ceroid lipofuscinosis; AD, Alzheimer's disease; PD, Parkinson's disease; HD, Huntington's disease; MD, muscular dystrophy; SMA, spinal muscular atrophy; AAT, alpha-1-antitrypsin; AADC, aromatic l-amino acid decarboxylase; OTC, ornithine transcarbamylase; LPL, lipoprotein lipase; ARCI, autosomal recessive congenital ichthyosis; CNS, central nervous system; HIV, human immunodeficiency virus; EBV, Epstein-barr virus; SCID, severe combined immunodeficiency; CGD, chronic granulomatous disease; AIDS, acquired immunodeficiency. Table was created using the ClinicalTrial.gov database and adapted from (Lundstrom, 2018) under the Creative Commons Attribution 4.0 International (CC BY 4.0).

1.3.2 Non-viral gene therapy

Non-viral systems encompass all methods used to transfer genetic material into host cells that do not employ viral vectors. Although generally less efficient than viral systems, their favourable safety profile, transgene capacity, and ease and cost-effectiveness of production support their continued development (Nayerossadat et al., 2012). 'Naked' plasmid DNA is the third most popular vector used in gene therapy clinical trials (Ginn et al., 2018). It has shown to be a safe and effective method for achieving therapeutic transgene expression in multiple conditions, including cancer (Lavie et al., 2017, Mahvi et al., 2007), cardiovascular diseases (Penn et al., 2013, Kukuła et al., 2019, Deev et al., 2018, Gu et al., 2019), diabetic neuropathy (Ajroud-Driss et al., 2013, Ropper et al., 2009), and amyotrophic lateral sclerosis (Sufit et al., 2017). However, several clinical trials have failed to show lack of a therapeutic effect (Belch et al., 2011, Stewart et al., 2009, Shishehbor et al., 2019, Chung et al., 2015). To promote targeted and efficient gene expression, naked RNA or DNA is routinely delivered in conjunction with chemical and/or physical methods in preclinical studies. The main chemical methods are cationic lipids, cationic polymers, and/or nanoparticles, and physical methods include gene gun, electroporation, hydroporation, magnetofection, and sonoporation.

1.3.2.1 Chemical methods

Chemical methods involve carriers, namely cationic lipids, cationic polymers and/or nanoparticles, that protect genetic material against degradation and deliver genetic material into target cells via endocytosis. The major advantages of chemical methods are low immunogenicity and toxicity, while low transfer efficiency persists as the main disadvantage (Nayerossadat et al., 2012). As a result, targeting moieties, such as proteins (Wolschek et al., 2002), antibodies (Meissner et al., 2015), and peptides (Ren et al., 2015), have shown to promote higher transgene expression levels in preclinical models *in vivo* to achieve therapeutically relevant levels. Clinical trials have demonstrated the feasibility of chemical methods for gene therapy in several diseases, including cancer (Siefker-Radtke et al., 2016, Thaker et al., 2017, Lu et al., 2012), cystic fibrosis (Alton et al., 2015), and coronary artery disease (Hedman et al., 2009). Several clinical trials have however reported lack of a therapeutic effect and low

transfer efficiencies (Grossman et al., 2007, Alvarez et al., 2014). In turn, chemical methods have been employed in conjunction with physical methods, which has shown to achieve safe and effective gene delivery in several preclinical and clinical studies (Lin et al., 2018, Devulapally et al., 2018, Nicol et al., 2002).

1.3.2.2 Physical methods

In the gene gun approach, biocompatible heavy metal particles coated with plasmid DNA are propelled at high velocity via discharge from a 'gun' to induce gene transfer (Figure 1-10). Early preclinical studies demonstrated feasibility of the non-invasive and targeted gene therapy technique for superficial organs (Sun et al., 1995, Rakhmilevich et al., 2000, Lu et al., 2002). However, low transfer efficiency, transient transgene expression, restricted treatment area in terms of depth and surface, and the requirement of invasive procedures for non-superficial organs have limited the development of the tool for gene therapy purposes in humans (Kitagawa et al., 2003, Sato et al., 2000, Chuang et al., 2003). Rather, research has focused on the utility of the device for gene transfer in plants (Acanda et al., 2019) and DNA vaccinations in humans (Hopkins, 2016).

With electroporation, electrodes are placed on either side of the target tissue, and electrical pulses are delivered generating an electric field that leads to reversible breakdown of the cell membrane, permitting transfer of genetic material (Figure 1-10). Efficient delivery of therapeutic genes to skeletal muscle and tumours in preclinical studies has led to application of electroporation in clinical trials (Lucas and Heller, 2003, Ugen et al., 2006, Guha et al., 2019). In a clinical trial, intramuscular electrotransfer of an antiangiogenic plasmid to patients with solid tumours caused local pain and oedema and systemic toxicity in some patients (Spanggaard et al., 2017). Furthermore, low and transient transgene expression coincided with no clinical response (Spanggaard et al., 2017). In contrast, clinical trials of intratumoural plasmid IL-12 electrotransfer to patients with subcutaneous or cutaneous melanoma have shown to produce long-term clinical benefit without systemic toxicity, although local pain was listed as the main side-effect (Daud et al., 2008, Greaney et al., 2020, Daud et al., 2015). While local pain and tissue damage remain a concern, electroporation

as a non-invasive and non-viral gene therapy technique holds potential for targeting superficial organs.

Hydrodynamic gene therapy involves rapid intravenous administration of a large volume to induce gene delivery via pressure, a process known as hydroporation (Figure 1-10). The method is primarily used for targeting the liver since transfer occurs almost exclusively in organs linked within close proximity to the inferior vena cava. Preclinical studies have demonstrated the ability of the technique to produce stable and therapeutic levels of transgene expression in the liver and in turn circulating factors in various diseases, including diabetes (He et al., 2004), growth hormone deficiency (Sondergaard et al., 2003), liver fibrosis (Kobayashi et al., 2016), haemophilia (Ye et al., 2003), metabolic diseases (Meyer-Kovac et al., 2017, Holm et al., 2003), and rare inherited conditions (Grisch-Chan et al., 2017, Zhang et al., 2000, Aliño et al., 2003). While hydroporation research has extended to large animal studies and a clinical trial (Kumbhari et al., 2018, Khorsandi et al., 2008), low transfer efficiency and cardiovascular safety concerns due to volume overload have hindered its translational progress (Sawyer et al., 2008, Sawyer et al., 2007). However, advancements in the delivery method, such as computer-assisted devices (Suda et al., 2008) and image-guided techniques (Kumbhari et al., 2018, Khorsandi et al., 2008), may help the development of hydrodynamic gene therapy as a safe and effective delivery system.

In magnetofection, a magnetic field is applied to target tissue which attracts magnetic nanoparticles coated with genetic material, and the particles are taken up by non-specific endocytosis (Figure 1-10). The gene delivery system has been primarily investigated *in vitro* for transfection in cell culture experiments, cell models (Krötz et al., 2003, Lee et al., 2017, Buerli et al., 2007), and stem cell therapy (Park et al., 2012, Pickard et al., 2017, Fernandes and Chari, 2016). In turn, magnetofection *in vivo* as a gene therapy method remains in the proof-of-concept stage, with reporter gene transfer demonstrated in superficial targets, namely the skin (Holzbach et al., 2010), spinal cord (Song et al., 2010), and brain (Soto-Sánchez et al., 2015). Although safety analyses were not performed in these proof-of-concept studies, in an oncological veterinary study delivering a granulocyte-macrophage colony-stimulating factor plasmid with

magnetofection to cats with fibrosarcoma, low doses were well-tolerated, with only mild adverse events and no major toxicity reported (Hüttinger et al., 2008). Further investigations are required to evaluate the safety and efficacy of magnetofection as a gene therapy strategy for targeting superficial organs.

Ultrasound-mediated gene delivery (UMGD) represents a physical method for enhancing gene transfer via sonoporation (Figure 1-10). In UMGD, viral or non-viral vectors are co-administered with microbubbles (MBs) (systemically or locally) followed by exposure of the target tissue to ultrasound (US). This stimulates uptake of the genetic material in the insonified region via the generation of transient pores (Newman and Bettinger, 2007). This method can augment transgene expression and improve spatial targeting, leading to more efficient delivery of genetic material with both viral (Müller et al., 2008) and non-viral vectors (Lan et al., 2003). Preclinical studies have provided evidence of site-specific gene transfer in a variety of tissue, including the heart (Chen et al., 2003), kidneys (Ishida et al., 2016), liver (Anderson et al., 2013), pancreas (Chen et al., 2006), brain (Thévenot et al., 2012), eyes (Sonoda et al., 2006), skeletal muscle (Pislaru et al., 2003), and tumours (Howard et al., 2006). In addition, safe and efficient transfer of genetic material has been demonstrated in preclinical studies for numerous conditions, such as cancer (Carson et al., 2011), CVD (Yuan et al., 2012), blood clotting disorders (Ye et al., 2003), renal disease (Wu et al., 2014), and neurodegenerative disease (Wang et al., 2014a). With the ability to theoretically target any organ in a non-invasive manner, UMGD represents a promising gene therapy technique, supported by its recent clinical application to deliver therapeutic drugs in cancer patients (Dimcevski et al., 2016, Wang et al., 2018d).

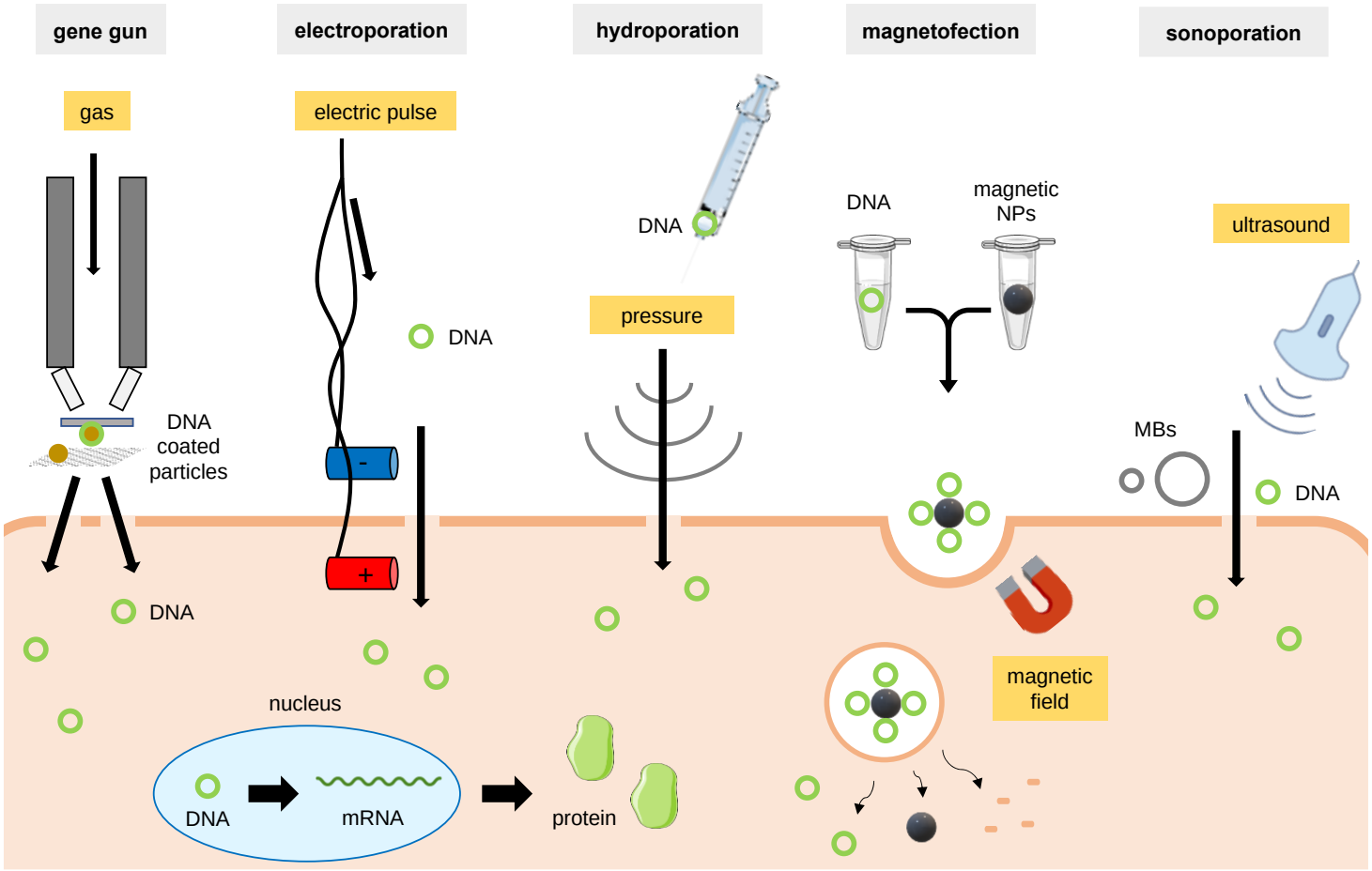

Figure 1-10 Diagram of mechanisms of common physical methods (gene gun, electroporation, hydroporation, magnetofection, and sonoporation) for enhancing transfer of genetic material.

Peach area represents a cell. NPs, nanoparticles; MB, microbubbles. Figure was created using images from Servier Medical Art under Attribution 3.0 Unported (CC BY 3.0).

1.3.3 History of gene therapy

In 1990, the first in-human gene therapy trial demonstrated the feasibility and safety of the technique (Rosenberg et al., 1990). In the trial, tumour-infiltrating lymphocytes were genetically modified *ex vivo* utilizing a retroviral vector and reintroduced into patients with metastatic cancer. The therapy conferred anti-tumour effects in some patients and was well-tolerated by all patients; no side-effects relating to the viral vector were reported (Rosenberg et al., 1990). These results prompted initiation of gene therapy clinical trials, including a lymphocyte-directed gene therapy trial for adenosine deaminase severe combined immunodeficiency (ADA-SCID), a monogenic disorder that if left untreated can be fatal within the first 2 years of life (Blaese et al., 1995). In 1990, a 4-year-old child who lacked a lymphocyte antigen-matched related donor and did not sufficiently respond to traditional treatment entered the trial, receiving lymphocytes transduced *ex vivo* with a retroviral vector containing the ADA gene (Blaese et al., 1995). To date, she requires low-dose enzyme replacement therapy, which has left some questioning the effectiveness of the gene therapy, but she has lived to become a healthy adult and is often described as the first patient cured by gene therapy (Philippidis, 2016). Despite some of the early successes of gene therapy, fatal outcomes in subsequent gene therapy trials highlight the consequences of scientific developments outpacing human understanding, mirrored by concerns expressed in a seminal paper published in 1972 (Friedmann and Roblin, 1972):

> ‘For the foreseeable future, however, we oppose any further attempts at gene therapy in human patients because (i) our understanding of such basic processes as gene regulation and genetic recombination in human cells is inadequate; (ii) our understanding of the details of the relation between the molecular defect and the disease state is rudimentary for essentially all genetic diseases; and (iii) we have no information on the short-range and long-term side effects of gene therapy.’

In 1999, 18-year-old Jesse Gelsinger, who suffered from ornithine transcarbamylase deficiency, was the first person to die in a gene therapy trial (Raper et al., 2003). Administration of an adenoviral vector triggered activation of his innate immune system; systemic inflammation and multiple organ system failure led to his death (Raper et al., 2003). The Food and Drug Administration

(FDA) halted the trial, and the principle investigator was charged with violating federal regulations pertaining to clinical trials, including failure to conduct the trial in accordance with the protocol; failure to protect the rights, safety, and welfare of subjects; failure to submit accurate safety reports; failure to identify changes to research activity; and failure to obtain informed consent (Baker, 2020). In recognition of insufficient monitoring, the FDA and National Institutes of Health (NIH) established the Gene Therapy Clinical Trial Monitoring Plan and the Gene Transfer Safety Symposia the following year (Sibbald, 2001). Although a lack of oversight contributed to the fatal event, the trial demonstrated for the first time the life-threatening capability of viral vectors. Another theoretical safety risk of viral vectors was subsequently confirmed in an *ex vivo* retrovirus-mediated gene therapy trial for X-linked SCID (Hacein-Bey-Abina et al., 2002). Several years after treatment, four out of ten children developed leukaemia due to insertional mutagenesis of the vector near proto-oncogenes (Hacein-Bey-Abina et al., 2008, Hacein-Bey-Abina et al., 2003). In response, the FDA as well as regulatory authorities in France, Germany, and Italy halted clinical trials investigating retroviral vectors in order for new guidelines relating to risk assessment and informed consent to be published (ESGT, 2003). Consensus at the European Society of Gene Therapy (ESGT) was that delays in the development of effective treatment be avoided and gene therapy clinical trials be resumed in a timely manner (ESGT, 2003). Serious adverse events underpinned the relatively lengthy period between the first in-human trial in 1990 and the first gene therapy approved in the Western world in 2012 (Ylä-Herttuala, 2012): Glybera, an adeno-associated virus-based gene therapy to treat the rare inherited disorder lipoprotein lipase deficiency. However, Glybera's approval has since been withdrawn due to its high cost, with treatment averaging at $1 million making it one of the world's most expensive therapies (Senior, 2017). As a potentially one-off curative treatment, high price tags are expected for gene therapies, particularly for rare diseases with small patient populations. Drug companies have further defended high costs citing the lifelong expenses of alternative treatments as well as payment plans and insurance covers available (Stein, 2019). Despite the withdrawal of Glybera, the number of clinical trials and approved therapies has since been steadily increasing (Ginn et al., 2018).

There are currently five gene therapies approved by the FDA and seven approved by the European Medicines Agency (EMA), all utilizing viral vectors (Table 1-5). While more than two thirds of gene therapy clinical trials in 2017 used viral vectors, ‘naked’ or plasmid DNA was the third most popular vector in development (Ginn et al., 2018). The majority of completed trials in 2017 were phase I or I/II, although the proportion of late-phase clinical trials has been increasing (Ginn et al., 2018). With more than a dozen near-term approvals and filings for approvals in 2019, the number of gene therapies approved across the US and Europe is anticipated to double within one to two years (ARM, 2020). Approximately three quarters of gene therapy trials are investigating its application in monogenic disorders and cancer (Ginn et al., 2018), mirroring the diseases for which gene therapies are currently approved (Table 1-5). Its applicability in other polygenic diseases, such as neurological, infectious, and cardiovascular disease, is also under investigation in clinical trials (Ginn et al., 2018). In addition to a growing understanding of the genetic basis of diseases, continuous development of non-viral and viral systems to improve the safety and efficacy of treatments underpins recent advances in the field. The rising potential of gene therapy is reflected by its considerable financing, which reached US$7.6 billion in 2019 (ARM, 2020). The substantial clinical benefit of gene therapy and its recent successes have also received considerable media attention, and public acceptability for somatic gene therapy has steadily been rising over the past ten years (Delhove et al., 2020). Despite these advancements, patient deaths in gene therapy clinical trials have still occurred recently, highlighting the risks of gene therapy persist (AACR, 2017, Holles and Conner, 2020). Nonetheless, authorities continue to voice their support; the FDA published six new guidelines relating to gene therapy manufacturing and clinical development at the start of 2020 (FDA, 2020). With the field expanding, developing safe and effective gene delivery systems remains cornerstone to make gene therapy a therapeutic reality for patients.

Table 1-5 Gene therapies approved by the FDA and EMA.

Name	Indications	Approval (year)	General description	Vector	Approach	Warnings
Imlygic (Talimogene laherparepvec)	Melanoma	EMA (’15) FDA (’15)	Genetically modified oncolytic viral therapy	HSV-1 vector encoding GM-CSF	*In vivo*	Herpetic infection; cellulitis at the injection site; impaired healing at the injection site; immune-mediated events; plasmacytoma at injection site; obstructive airway disorder
Strimvelis (Autologous CD34+ cells encoding ADA)	ADA-SCID	EMA (’16)	Genetically modified autologous CD34+ cells transduced to express ADA from HSC/HPC (CD34+)	Retroviral vector encoding ADA from HSC/HPC (CD34+)	*Ex vivo*	Leukemic transformation; serious infections; catheter-related events
Yescarta (axicabtagene ciloleucel)	Lymphoma	EMA (’17) FDA (’17)	CD19-directed genetically modified autologous T-cell immunotherapy	Retroviral vector encoding an anti-CD19 CAR	*Ex vivo*	Cytokine release syndrome*; neurologic toxicities*; hypersensitivity reactions; serious infections; prolonged cytopenias; febrile neutropenia; hypogammaglobulinemia; secondary malignancies; HBV reactivation; tumour lysis syndrome
Kymriah (Tisagenlecleucel)	Lymphoma	EMA (’18) FDA (’17)	CD19-directed genetically modified autologous T-cell immunotherapy	Lentiviral vector encoding an anti-CD19 CAR	*Ex vivo*	Cytokine release syndrome*; neurologic toxicities*; hypersensitivity reactions; serious infections; prolonged cytopenias; febrile neutropenia; hypogammaglobulinemia; secondary malignancies; tumour lysis syndrome
Luxturna (Voretigene neparvovec)	Inherited retinal dystrophy (biallelic RPE65 mutation)	EMA (’18) FDA (’17)	AAV vector-based gene therapy	rAAV2 vector encoding hRPE65	*In vivo*	Eye inflammation; permanent decline in visual acuity; retinal abnormalities; increased intraocular pressure; expansion of intraocular air bubbles; cataract; immunogenicity
Zolgensma (onasemnogene abeparvovec-xioi)	Spinal muscular atrophy (biallelic SMN1 mutation)	EMA (’20) FDA (’19)	AAV vector-based gene therapy	rAAV9 vector encoding SMN	*In vivo*	Acute serious liver injury*; thrombocytopenia; elevated troponin-i; immunogenicity; hepatic injury
Zynteglo (Autologous CD34+ cells encoding β A-T87Q-globin gene)	β-thalassaemia	EMA (‘19)	Genetically modified autologous CD34+ cells that contains HSCs transduced to express β A-T87Q-globin	Lentiviral vector encoding β A-T87Q-globin gene	*Ex vivo*	Risk of insertional oncogenesis; engraftment failure; delayed platelet engraftment

*black box warning (include full list of abbreviations). Table was created using EMA and FDA ‘Product Information’ reports. EMA, European Medicines Agency; FDA, Food and Drug Administration; ADA, adenosine deaminase; ADA-SCID, Adenosine deaminase severe combined immunodeficiency; HSV, herpes simplex virus; GM-CSF, granulocyte-macrophage colony-stimulating factor; HSC, haematopoietic stem cells; HPC, haematopoietic progenitor cells; CAR, chimeric antigen receptor; RPE65, retinal pigment epithelium-specific 65 kDa; AAV, adeno-associated virus; SMN1, survival motor neuron 1.

1.4 Ultrasound-mediated gene delivery (UMGD)

1.4.1 Ultrasound (US)

US is a biomedical imaging tool routinely used in a range of clinical applications for diagnostic purposes, with a safety record spanning decades (Torloni et al., 2009). As one of the most commonly used imaging modalities worldwide, its widespread availability and utilisation provides a basis for its acceptance by clinicians and patients alike. In physics, US refers to acoustic waves with a frequency higher than human hearing, i.e. above 20 kHz. For medical diagnostic applications, US waves typically lie in the frequency range of 1-20 MHz. Conventional diagnostic US broadly encompasses obstetric and neonatal scanning as well as adult and paediatric transcranial, abdominal, peripheral vascular, and ocular US. Alongside its diagnostic applications, US has developed as a therapeutic modality, which dates back to the 1950s where low frequencies were employed in physiotherapy for musculoskeletal disorders (Gam and Johannsen, 1995). Although current evidence questions the effectiveness of therapeutic US in physiotherapy (Ebadi et al., 2014, Van Den Bekerom et al., 2011), it has expanded to a range of applications, with therapeutic US now approved for cancer treatment, tissue ablation, lithotripsy, thrombus dissolution, and bone fracture healing, owing to the biological effects or 'bioeffects' of US (Miller et al., 2012).

In US imaging, an US probe or 'transducer' emits soundwaves which propagate through the human body. When these mechanical waves encounter a medium, they can either be reflected back to the transducer, scattered in other directions, absorbed by the medium, or transmitted on through the medium (Figure 1-11). Energy absorbed by the medium can lead to biological effects divided into thermal and non-thermal effects. Thermal effects arise from the absorption of energy and its conversion to heat, leading to an increase in temperature. Non-thermal or 'mechanical' effects are further subdivided into cavitational and non-cavitational effects. Cavitation refers to the activation of gas bodies in an US field and their expansion and contraction in response to pressure changes induced by US waves. Non-cavitational effects include acoustic radiation force, the force exerted by the momentum of the US waves, and acoustic streaming, the flow of liquid generated by radiation forces.

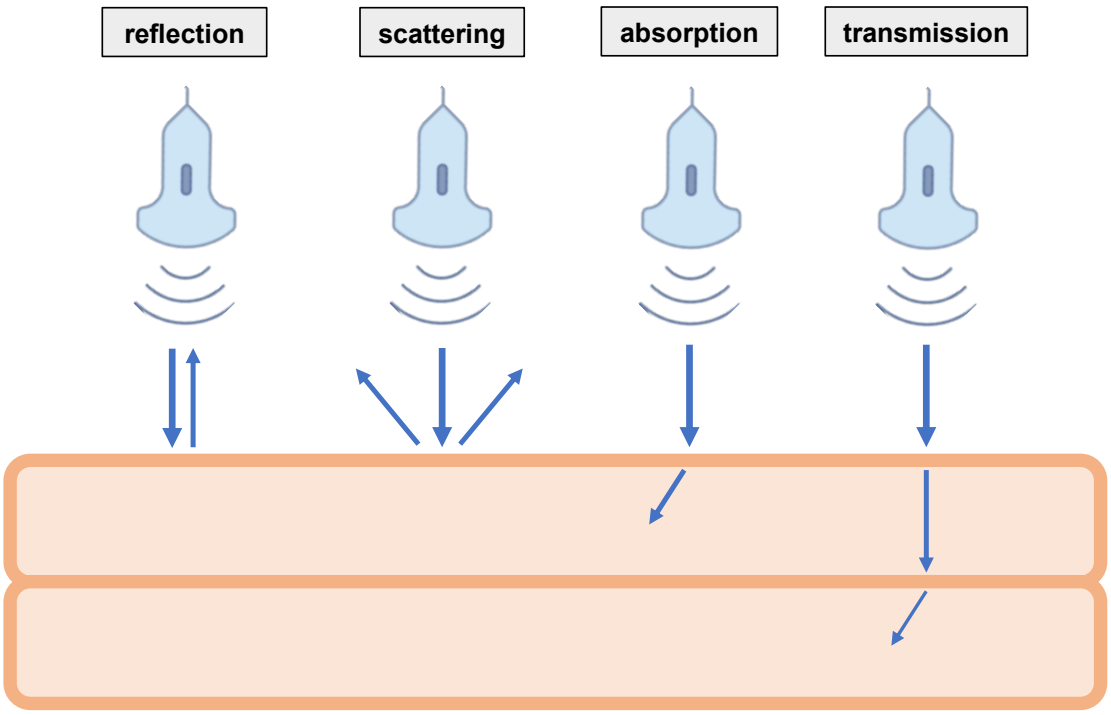

Figure 1-11 Diagram illustrating interaction of US with a medium.

In US imaging, a transducer emits soundwaves which can either be reflected back, scattered in other directions, absorbed by the medium, or transmitted through the medium (peach area).

Due to the potential safety risks associated with thermal and mechanical effects, conventional US machines display indices relating to these bioeffects, namely the thermal index (TI) and mechanical index (MI), respectively. The TI is a ratio of the acoustic power to the power required to increase the temperature by 1°C, a measure of relative risk of temperature rise. The MI is a ratio of the peak negative pressure derated by 0.3 dB/cm/MHz (to account for energy loss) to the square root of the frequency, a measure that indicates the relative potential for cavitation. For diagnostic US, safety standards are maintained by limits to the acoustic output of US machines (derated spatial peak temporal average intensity (I_{SPTA}) ≤720 mW/cm^2 and either MI ≤1.9 or derated spatial peak pulse average intensity (I_{SPPA}) ≤190 W/cm^2) as well as stringent guidelines relating to the TI, MI, and exposure time to promote the principle ‘as low as reasonably possible’ (FDA, 2019, BMUS, 2019). Although conventional diagnostic US machines can still be used for certain therapeutic purposes, novel US machines and probes have arisen alongside the growing field of therapeutic US (Song et al., 2012, Wong et al., 2019, Yonetsuji et al., 2013). In addition, conventional diagnostic US has undergone its own advancements, such as the development of contrast agents, which since their discovery have also emerged as therapeutic tools.

1.4.2 Microbubbles (MB)

The term ‘contrast echocardiography’ arose from the works of Dr Raymond Gramiak and Dr Pravin Shah, who reported in 1968 that ‘ultrasonic contrast injections’ of indocyanine green and saline produced enhanced echo signals during echocardiographic examinations (Gramiak and Shah, 1968), confirming observations described by Dr Claude Joyner at the First International Course on Diagnostic Ultrasound (Shah, 1993). In 1970, an *ex vivo* study investigating the mechanisms of the US contrast effect attributed the enhanced echo signals to the formation of miniature bubbles (Kremkau et al., 1970). Over a decade later, research into methods producing small, uniform, and stable MBs was underway to develop contrast agents that could be injected intravenously and pass through the pulmonary circulation to achieve non-invasive contrast echocardiography (Feinstein et al., 1984). Such investigations led to the approval of the first commercially available contrast agents: air-filled MBs composed of an albumin shell, Albunex, or polymer shell, Levovist and Echovist. Although safe and well-tolerated (Feinstein et al., 1990, Ries, 1997), all first-generation agents were eventually withdrawn, as the air-filled MBs were replaced with more stable MBs.

There are currently four commercially available MBs approved for diagnostic purposes (Table 1-6). MBs are gas-filled spheres encapsulated by a stabilising shell, typically consisting of lipids, albumin, or polymers and generally 0.5-10 μm in size (Sirsi and Borden, 2009). The core of ‘second generation agents’ comprise of a high molecular weight gas, either sulphur hexafluoride or perfluorocarbon, making them more resistant to pressure changes and less soluble in blood (Table 1-6). When exposed to US, MBs expand and contract due to changes in pressure as the mechanical sound waves propagate through a medium, which enhances their acoustic backscattering. MBs exhibit high echogenicity due to scattering from their cross-section and large impedance mismatch between the oscillating gas-filled bubbles and the surrounding fluid. This improves the signal to noise ratio, and MBs are used clinically in echocardiography and ultrasonography to assess blood flow characteristics and delineate tissue borders for improved diagnosis in CVD, cancer, and urinary tract conditions (Table 1-6). Alongside a growing understanding of the diagnostic value of MBs and their acoustic behaviour in an US field, preclinical and clinical research is investigating the therapeutic ability of MBs to facilitate drug and gene delivery.

Table 1-6 MBs currently approved worldwide.

Name	Indications	Approval	Shell	Gas (molecular formula)	Average size (µm)	Concentration (microbubbles/ml)
Luminity / Definity	Echocardiography	Australia Canada EU New Zealand South Korea Taiwan USA	Phospholipid	Perflutren (C_3F_8)	1.1-2.5	6.4×10^9
SonoVue / Lumason	Echocardiography Ultrasonography of cerebral, extracranial carotid, and peripheral arteries and portal veins Ultrasonography of liver and breast lesions Ultrasonography of excretory urinary tract	Canada China Brazil EU Iceland Israel Mexico Norway Russia South Korea Switzerland Taiwan USA	Phospholipid	Sulphur hexafluoride (SF_6)	1.5-2.5	$1.5\text{-}5.6 \times 10^8$
Optison	Echocardiography	EU Norway USA	Albumin	Perflutren (C_3F_8)	2.5-4.5	$5\text{-}8 \times 10^8$
Sonazoid	Ultrasonography of liver and breast lesions	China Japan Norway South Korea Taiwan	Phospholipid	Perflubutane (C_4F_{10})	2.6	1.2×10^9

Table was created using the ‘Global Contrast-Enhanced Ultrasound Map’ from icus-society.org and ‘Product Information’ reports.

1.4.3 Mechanisms of UMGD

At the turn of the 20th century, *in vitro* studies demonstrated the ability of US to stimulate plasmid DNA transfection in mammalian cells (Kim et al., 1996, Fechheimer et al., 1987). Simultaneously, lithotripsy shock waves were found to induce transfection in eukaryotic cells via increasing cell permeability attributed to acoustic cavitation (Lauer et al., 1997). Subsequent *in vitro* UMGD studies showed addition of Albunex MBs substantially increased transfection, providing evidence that acoustic cavitation and resulting sonoporation were the mechanisms underlying UMGD (Bao et al., 1997, Greenleaf et al., 1998).

Acoustic cavitation is the formation, growth, oscillation, and collapse of bubbles in an acoustic field. MBs are referred to as artificial cavitation nuclei as they expand and contract in an US field in response to pressure changes known as rarefaction and compression, respectively. Stable cavitation refers to the oscillation of bubbles around a resonant diameter, which has shown to exert pushing and pulling, microstreaming, and shear stress on adjacent cell membranes (Van Wamel et al., 2006, Nejad et al., 2016, Meng et al., 2019) (Figure 1-12A). Transient or 'inertial' cavitation occurs at higher intensities whereby bubbles rapidly expand during rarefaction and eventually collapse in the compression phase due to the inertia of the surrounding fluid, which has shown to produce shockwaves, shear stress, microjets, and free radicals (Helfield et al., 2016, Adhikari et al., 2015, Postema et al., 2004, Lawrie et al., 2000) (Figure 1-12B).

Stable and inertial cavitation underlie the transient formation of pores in cell membranes, a process known as sonoporation. Estimates of pore sizes range from several nanometres to micrometres (Yang et al., 2008, Kudo et al., 2009, Schlicher et al., 2006). Sonoporation pores display bidirectional transport (Van Wamel et al., 2006, Schlicher et al., 2006, Meijering et al., 2009, Fan et al., 2012) and reseal within seconds (Kudo et al., 2009, Van Wamel et al., 2006), attributed to the native wound healing response of cell membranes (Schlicher et al., 2006), Ca^{2+}-dependent and -independent mechanisms (Kudo et al., 2009, Fan et al., 2012), and lysosomal-exocytosis (Yang et al., 2008). Enhanced membrane permeabilization has been implicated as a key mechanism facilitating cellular uptake of exogenous agents of varying sizes and structures and has been shown

with nanospheres (Mehier-Humbert et al., 2005), fluorescent dyes (Schlicher et al., 2006), propidium iodide (Van Wamel et al., 2006), dextrans (Mehier-Humbert et al., 2005), proteins (Schlicher et al., 2006), and plasmid DNA (Duvshani-Eshet et al., 2006), highlighting a prominent role for cavitation in intracellular drug and gene delivery. Several other mechanisms arising from US and MB bioeffects implicated in the cellular delivery of foreign molecules include rearrangement of the cytoskeleton (Juffermans et al., 2009, Wang et al., 2018b), stimulation of endocytic pathways (Meijering et al., 2009), and disruption of the endothelial monolayer integrity (Juffermans et al., 2009), which have also been proposed to contribute to nuclear and intercellular transport. Although an understanding of the mechanisms governing UMGD remains incomplete, preclinical research underpins the potential of this delivery system as a strategy in gene therapy.

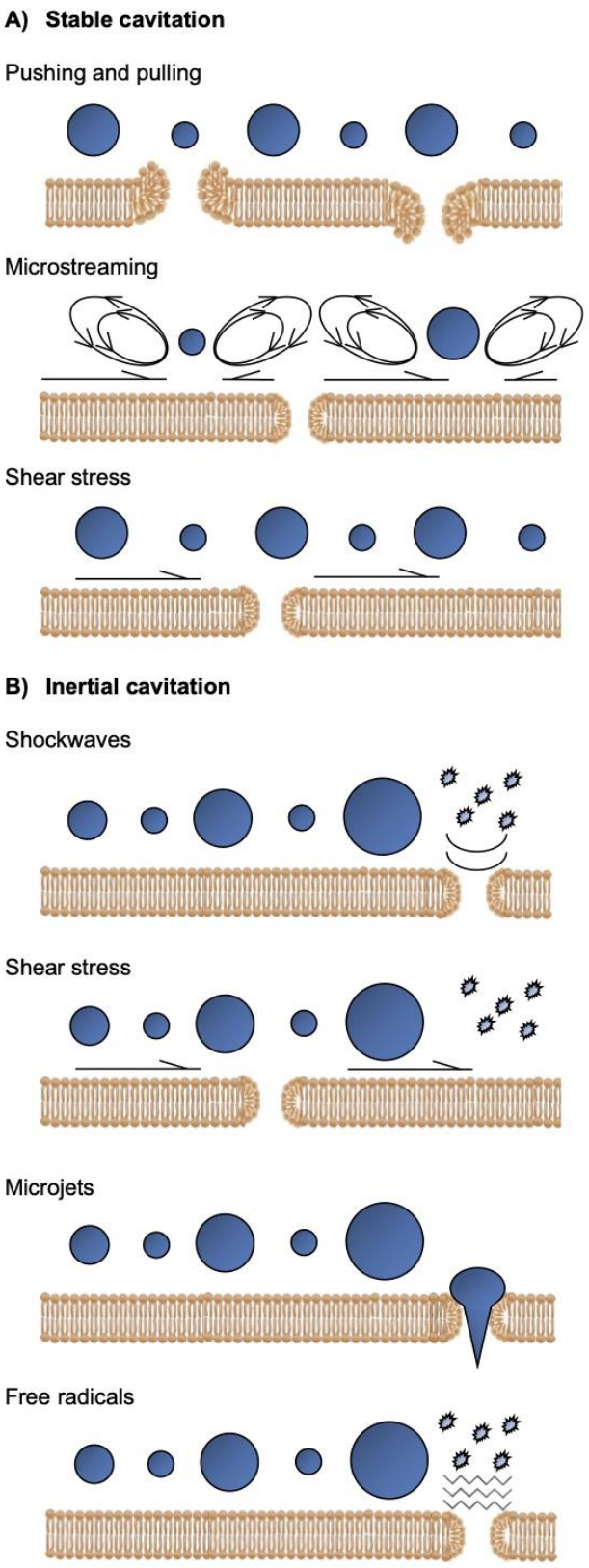

Figure 1-12 Diagram of proposed mechanisms of cell membrane sonoporation induced by (A) stable cavitation and (B) inertial cavitation.

MBs expand and contract in an US field due to rarefaction and compression of the medium through which US waves propagate. **(A)** Stable cavitation: MBs oscillate around a resonant diameter producing pulling/pushing mechanisms, shear stress, and microstreaming. **(B)** Inertial cavitation: MBs rapidly grow and then collapse during compression due to the inertial energy of surrounding fluid producing shock waves, shear stress, microjets, and sonochemical effects.

1.4.4 UMGD in development

Due to the safety risks associated with viral-based systems, research efforts have primarily focused on employing non-viral vectors in UMGD. Several *in vivo* studies have reported comparable transfer efficiencies between plasmid-based UMGD and other non-viral gene therapy methods, such as HVJ liposomes (Koike et al., 2005), lipofection (Pislaru et al., 2003), and electroporation (Sheyn et al., 2008). Although viral gene therapies have shown greater transfer efficiencies compared with non-viral UMGD, viral vectors exhibit less specificity due to transgene expression in the liver (Pislaru et al., 2003, Chen et al., 2003). Another advantage of UMGD when utilised in conjunction with non-viral vectors is a low risk of toxicity, which has consistently been demonstrated by a lack of adverse events in preclinical studies investigating different tissues, MBs, and US parameters (Newman and Bettinger, 2007). Several UMGD studies that reported abnormalities in functional, histological, and biochemical parameters found these were transient in nature (Guo et al., 2004, Tsunoda et al., 2005, Wang et al., 2014a). Other studies reporting local histological damage, such as inflammation, haemorrhage, and necrosis, found these side-effects were related to MB concentration (Koike et al., 2005), US exposure time (Ishida et al., 2016), and acoustic output (Ishida et al., 2016, Miao et al., 2005), which could be prevented by modulating these factors while still maintaining significant gene transfer. The growing potential of UMGD as a non-viral and non-invasive delivery system is further supported by application of the method to large animals. Proof-of-concept studies have demonstrated non-viral reporter gene transfer with minimal tissue damage in porcine and canine livers (Tran et al., 2019, Noble-Vranish et al., 2018, Noble et al., 2013) and hearts (Liu et al., 2015). Moreover, UMGD of therapeutic genes has been shown in the hearts of canine models of myocardial infarction (Yuan et al., 2012, Cui et al., 2017), in pancreatic islets of a baboon model of diabetes (Chen et al., 2014), and in the placenta of a baboon model of insufficient uterine artery remodelling (Babischkin et al., 2019). Nonetheless, proof-of-concept studies remain cornerstone experiments for demonstrating safety and specificity to support development of UMGD as an effective and clinically translatable gene therapy system.

1.5 Hypotheses and aims

1.5.1 Hypotheses

- UMGD stimulates tissue-specific gene transfer *in vivo*, representing a non-viral and non-invasive gene delivery system for targeting the placenta.

- Specific miRNAs are consistently dysregulated in placentas of patients with PE and show the same pattern of expression in a rat model of SPE.

- Dysregulated placental miRNAs in PE impact gene expression and functional properties of trophoblast cells, therefore representing potential therapeutic targets for gene therapy applications.

1.5.2 Aims

- To optimise an *in vivo* UMGD protocol to demonstrate tissue-specific gene transfer of a reporter gene in a surrogate organ in rodents.

- To apply the *in vivo* UMGD protocol to pregnant rodents to demonstrate placental-specific gene transfer of an expression vector.

- To identify dysregulated placental miRNAs that are consistently dysregulated in patients with PE as well as placental miRNAs differentially expressed in a rat model of SPE and compare their expression patterns.

- To Investigate the relationship between a candidate dysregulated placental miRNA and its predicted gene targets and functional effects *in vitro* in a trophoblast cell line.

Chapter 2 General materials and methods

This chapter details the general materials and methods utilised in subsequent results chapters. Any chapter-specific materials and methods and/or any adaptations to the general materials and methods are listed in the relevant results chapter.

2.1 General laboratory techniques

2.1.1 Luria-Bertani medium

For Luria-Bertani (LB) medium, 10 g tryptone, 5 g yeast extract, and 10 g of NaCl were dissolved in 950 mL dH_2O. For low-salt LB medium, 10 g tryptone, 5 g yeast extract, and 5 g of NaCl were dissolved in 950 mL dH_2O. The pH was adjusted to 8 with 1 M NaOH, and the volume was adjusted to 1 L with dH_2O. LB medium was sterilized by autoclaving.

2.1.2 Plasmid DNA purification

2.1.2.1 Transformation of plasmid DNA into competent bacteria

Plasmid DNA was transformed into MAX Efficiency™ DH5α™ Competent Cells (ThermoFisher, Paisley, UK). Competent cells were thawed on wet ice, and 50 µL were aliquoted into chilled 1.5 mL microcentrifuge tubes. Plasmid DNA (50 pg) was added to the competent cells, and the tubes were gently tapped to mix. The transformation mixture was incubated on ice for 30 min, heat-shocked for 45 s in a 42ºC water bath, and then placed on ice for 2 min. Room temperature S.O.C. Medium (450 µL) was added to the mixture, and the mixture was placed in a shaking incubator for 20 min at 37 ºC with shaking at 225 RPM. Transformed cells (100 µL) were spread on 90 mm plates containing Luria Agar (Formedium, Norfolk, UK) with 100 µg/mL ampicillin or Hygromycin B (Invivogen, San Diego, USA), and plates were incubated overnight at 37 ºC. The following morning, a single colony was used to inoculate a 10 mL overnight starter culture, from which a glycerol stock was prepared.

2.1.2.2 Glycerol stocks

Glycerol stocks of transformed bacterial culture were prepared as a long-term stock. To obtain 50% glycerol, 100% glycerol was diluted 1:1 with dH_2O and then sterilised by autoclaving. In a cryovial, 1 mL of overnight starter culture was added to 1 mL 50% glycerol and gently mixed by pipetting up and down. Glycerol stocks were stored at -80 ºC and replenished every 12 months.

2.1.2.3 Large-scale plasmid DNA purification by centrifugation

A single bacterial colony or swab from a glycerol stock of pVIVO2-GFP/LacZ was used to inoculate a 10 mL LB medium starter culture with 100 µg/mL Hygromycin B. Starter culture was incubated overnight at 37°C with shaking at 200 RPM. The following morning, starter culture was diluted 1:1000 into 1 L or 800 mL selective LB medium culture, which was incubated for 12 h at 37°C with shaking at 200 RPM. pVIVO2-GFP/LacZ was purified using QIAGEN Plasmid Mega Kit (QIAGEN, Hilden, Germany), according to the April 2012 QIAGEN Plasmid Purification Handbook. Bacterial cells in selective LB medium culture were harvested by centrifugation at 5000 RPM for 15 min at 4°C and supernatant was discarded. Bacterial cells were resuspended in 50 mL Buffer P1, containing 100 µg/mL RNase A and Lyse Blue diluted 1:1000. For alkaline lysis, 50 mL Buffer P2 was added and mixed by inverting the lysate 6 times, and the cell suspension was incubated at room temperature for 5 min. For precipitation of plasmid DNA, 50 mL prechilled Buffer P3 was added and mixed by inverting 6 times, and the cell suspension was incubated on ice for 30 min. To collect plasmid DNA, the suspension was centrifuged at 10000 RPM for 30 min at 4°C, and the supernatant was collected in a 250 mL polypropylene centrifuge tube. The supernatant was centrifuged at 10000 RPM for 15 min at 4°C, and the supernatant was collected in a clean 250 mL centrifuge tube. An optional 120 µL sample of cleared lysate was collected saved for an analytical gel to assess growth and lysis conditions. A QIAGEN-tip 2500 was equilibrated by adding 35 mL Buffer QBT to the column, which was allowed to empty by gravity flow. The supernatant was loaded onto the QIAGEN-tip 2500 and passed through the column by gravity flow. An optional 120 µL sample of the flow-through fraction was collected and saved for an analytical gel to assess efficiency of column loading. To remove any contaminants, the QIAGEN-tip 2500 was washed with 200 mL Buffer QC. Two optional 120 µL samples from the first and second half of the wash fractions were collected and saved for an analytical gel to assess plasmid DNA binding and removal of RNA. Plasmid DNA was eluted from the column by adding 35 mL Buffer QF to the QIAGEN-tip 2500. An optional 22 µL sample of the elute was collected and saved for an analytical gel to assess contamination. Eluted plasmid DNA was precipitated by adding 0.7 times the volume of room temperature isopropanol (Sigma Aldrich, Steinheim, Germany) and centrifuging at 14000 RPM

for 30 min at 4°C, and supernatant was discarded. The plasmid DNA pellet was washed with 7 mL room temperature 70% ETOH (Sigma Aldrich, Steinheim, Germany) and centrifuged at 14000 RPM for 10 min, and supernatant was discarded. The plasmid DNA pellet was air-dried for 10-20 min and resuspended in 320 µL nuclease free water (NFW). Plasmid DNA quality and concentration were measured using NanoDrop® ND-1000 Spectrophotometer (ThermoFisher, Paisley, UK), with an A260/A280 ratio of ~1.8 accepted as 'pure' DNA. Plasmid DNA concentration was adjusted to 4 µg/µL with NFW for *in vivo* use.

2.1.2.4 Large-scale plasmid DNA purification by filtration

A single bacterial colony or swab from a glycerol stock of luciferase plasmid vector (pGL3 or pGL4.13) was used to inoculate a 10 mL LB medium starter culture with 100 µg/mL ampicillin. Starter culture was incubated overnight at 37°C with shaking at 200 RPM. The following morning, starter culture was diluted 1:1000 into 1 L selective LB medium culture, which was incubated for 12 h at 37°C with shaking at 200 RPM.

pGL3 was purified using QIAfilter Plasmid Mega Kit (QIAGEN, Hilden, Germany), according to the April 2012 QIAGEN Plasmid Purification Handbook. Bacterial cells in selective LB medium culture were harvested by centrifugation at 5000 RPM for 15 min at 4°C and supernatant was discarded. Bacterial cells were resuspended in 50 mL Buffer P1, containing 100 µg/mL RNase A and Lyse Blue diluted 1:1000. For alkaline lysis, 50 mL Buffer P2 was added and mixed by inverting the lysate 6 times. The lysate was poured onto the QIAfilter Mega-Giga Catridge and incubated at room temperature for 10 min to allow a precipitate containing proteins, genomic DNA, and detergent to form. The lysate was then pulled through by a vacuum source. Buffer FWB2 (50 mL) was added to the QIAfilter Mega-Giga Catridge, and the precipitate was gently stirred with a sterile spatula. The remaining lysate was then pulled through by a vacuum source. An optional 120 µL sample of cleared lysate was collected saved for an analytical gel to assess growth and lysis conditions. A QIAGEN-tip 2500 was equilibrated by adding 35 mL Buffer QBT to the column, which was allowed to empty by gravity flow. The cleared lysate was loaded onto the QIAGEN-tip 2500 and passed through the column by gravity flow. An optional 120 µL sample of the flow-through fraction was collected and saved for an analytical gel to asses

efficiency of column loading. To remove any contaminants, the QIAGEN-tip 2500 was washed with 200 mL Buffer QC. An optional 120 µL sample of the wash fraction was collected and saved for an analytical gel to assess plasmid DNA binding and removal of RNA. Plasmid DNA was eluted from the column by adding 35 mL Buffer QF to the QIAGEN-tip 2500. An optional 22 µL sample of the elute was collected and saved for an analytical gel to assess contamination. Eluted plasmid DNA was precipitated by adding 0.7 times the volume of room temperature isopropanol (Sigma Aldrich, Steinheim, Germany) and centrifuging at 14000 RPM for 30 min at 4°C, and supernatant was discarded. The plasmid DNA pellet was washed with 7 mL room temperature 70% ETOH (Sigma Aldrich, Steinheim, Germany) and centrifuged at 14000 RPM for 10 min, and supernatant was discarded. The plasmid DNA pellet was air-dried for 10-20 min and resuspended in 320 µL NFW.

pGL4.13 was purified using Invitrogen™ PureLink™ HiPure Expi Plasmid Megaprep Kit (ThermoFisher, Vilnus, Lithuania), according to the Revision A.0 User Guide. Bacterial cells were resuspended in 50 mL Resuspension Buffer containing 100 µg/mL RNase A. For alkaline lysis, 50 mL Lysis Buffer was added and mixed by inverting the lysate 6 times, and the suspension was incubated for 5 min at room temperature. For precipitation of plasmid DNA, 50 mL Precipitation Buffer was added and mixed by inverting 6 times. The lysate was poured onto the Megaprep Lysate Filtration Cartridge and incubated at room temperature for 2 min to allow precipitate to float. The lysate was then pulled through by a vacuum source. Wash buffer (50 mL) was added to the Megaprep Lysate Filtration Cartridge, and the precipitate was gently stirred with a sterile spatula. The remaining lysate was then pulled through by a vacuum source. An optional 100 µL sample of cleared lysate was collected saved for an analytical gel to assess growth and lysis conditions. The Megaprep DNA Binding Cartridge was equilibrated by adding 100 mL Equilibration Buffer, which was pulled through by a vacuum source and discarded. The cleared lysate was loaded onto the Megaprep DNA Binding Cartridge, which was pulled through by a vacuum source. An optional 100 µL sample of the flow-through fraction was collected and saved for an analytical gel to assess efficiency of column loading. To remove any contaminants, the cartridge was washed twice with 175 mL wash buffer by pulling through the liquid with a vacuum source. An optional 100 µL sample of

the final wash fraction was collected and saved for an analytical gel to assess plasmid DNA binding and removal of RNA. The Megaprep DNA Binding Cartridge was attached to onto a clean, sterile Stericup Receiver flask (Merck, Dorset, UK). Plasmid DNA was eluted by adding 50 mL Elution Buffer and applying a soft vacuum (-200 to -300 mbar) for 30 s. After letting the cartridge stand for 1 min without agitation, the remaining plasmid DNA was eluted. An optional 100 µL sample of the elute was collected and saved for an analytical gel to assess contamination. Eluted plasmid DNA was precipitated by adding 0.7 times the volume of room temperature isopropanol (Sigma Aldrich, Steinheim, Germany) and centrifuging at 13000 RPM for 30 min at 4°C, and supernatant was discarded. The plasmid DNA pellet was washed with 20 mL room temperature 70% ETOH (Sigma Aldrich, Steinheim, Germany) and centrifuged at 13000 RPM for 10 min, and supernatant was discarded. The plasmid DNA pellet was air-dried for 10-20 min and resuspended in 320 µL 1X Tris-EDTA (TE) buffer.

2.1.2.5 Precipitation of samples from plasmid DNA purification

Samples from stages of the plasmid DNA purification procedure, including cleared lysates, flow-through fractions, wash fractions, and elutes, were collected to assess efficiency of the purification procedure. An equal volume of isopropanol (Sigma Aldrich, Steinheim, Germany) was added to samples. Samples were centrifuged for 30 min at 16 RPM at 4°C, and supernatant was discarded. Samples were washed with 500 µL of 70% ETOH (Sigma Aldrich, Steinheim, Germany) and centrifuged for 10 min at 16 RPM at 4°C, and supernatant was discarded. After air-drying for 10 min, samples were resuspended in 10 µL 1X TE buffer.

2.1.2.6 Restriction digest

Restriction digest of plasmid DNA was performed with XhoI (New England Biolabs, Dublin, Ireland) and BglII (New England Biolabs, Dublin, Ireland) restriction enzymes in a 30 µL reaction, using 250 ng of plasmid DNA. Reagents were incubated for 1 h and 30 min in a 37°C water bath, pulsed for several s, and incubated on ice prior to gel loading. Products were run on a 0.8% agarose gel at 110 mV. The reagents and volumes used in the reaction were as following:

Reagent	Volume (µL)
Plasmid DNA (500 ng/µL)	0.5
10X NE Buffer	3.0
XhoI (20000 U/mL)	2.0
NFW	24.5

Reagent	Volume (µL)
Plasmid DNA (500 ng/µL)	0.5
10X NE Buffer	3.0
BglII (10000 U/mL)	1.0
NFW	25.5

2.1.2.7 Plasmid DNA quality and concentration

Plasmid DNA quality and concentration were measured using NanoDrop® ND-1000 Spectrophotometer (ThermoFisher, Paisley, UK), with an A260/A280 ratio of ~1.8 accepted as 'pure' DNA. Plasmid DNA concentration was adjusted to 4 µg/µL with NFW or 1X TE when prepared for *in vivo* use.

2.1.3 Agarose gel electrophoresis

Visualisation and sizing of DNA/RNA molecules were performed on 0.8-1.5% agarose gels. Agarose (Invitrogen, Carlsbad, USA) was dissolved in 100 mL 1X Tris-Borate EDTA (TBE) by heating in microwave for 3-5 min and then left to cool for 15 min. Once the agarose was molten, 1.5 µL of 10 mg/mL ethidium bromide solution (Sigma, Dorset, UK) was added, and molten agarose was poured into a gel tray and left for 30 min to solidify with a well comb in place. Gels were placed in a BioRad electrophoresis tank (BioRad, Hampstead, UK) containing 1X TBE. Samples were loaded with 6X blue/orange loading dye (Promega, Madison, USA). 1 kb DNA ladder (Promega, Madison, USA) and 100 bp DNA ladder (New England Biolabs, Massachusetts, USA) were used to size samples. Gels were run at 110 mV (BioRad Powerpac 300, Hamsptead, UK) and visualized by transillumination with BioRad Molecular Imager (Chemidoc Imaging System, Hampstead, UK).

2.1.4 RNA extraction

Total RNA was extracted from tissue and cells using the miRNeasy Mini Kit (QIAGEN, Manchester, UK). Placental samples from the SPE rat model (50 mg) were homogenised in 700 µL QIAzol Lysis Reagent four times for 30 s at 25 kHz using Polytron PT2100 Benchtop Homogeniser (KINEMATICA, Luzern, Switzerland) with 3 mm dispersing aggregate. The dispersing aggregate was cleaned between each tissue sample by washing the aggregate three times in NFW for 30 s. All other tissue samples (50 mg) were homogenised in 700 µL QIAzol Lysis Reagent four times for 30 s at 25 kHz using TissueLyser (QIAGEN, Haan, Germany) with stainless steel beads. Cells were lysed directly in cell-culture dishes by adding 700 µL QIAzol Lysis Reagent. The lysate was transferred to a microcentrifuge tube and vortexed for 1 min. Tissue and cell homogenates were either stored at -80ºC, or RNA extractions were immediately performed.

Homogenates were placed at room temperature for 5 min. Chloroform (140 µL) was added and tubes were shaken vigorously for 15 s. Tubes were placed for a further 2-3 min at room temperature. Samples were centrifuged at 12000 x *g* for 15 min at 4ºC. All subsequent centrifuges were performed at 20ºC. The upper aqueous phase containing RNA (350 µL) was transferred to a tube containing 525 µL 100% ETOH. The sample was mixed thoroughly by pipetting up and down several times, and 700 µL was pipetted into a RNeasy Mini Spin Column in a 2 mL collection tube. Samples were centrifuged at 11000 x *g* for 15 s and flow-through was discarded; this was repeated using the remainder of the sample. An optional on-column DNase digestion was performed, or extractions were performed as following. Buffer RWT (700 µL) was added to the RNeasy Mini Spin Column to wash the column. Samples were centrifuged at 11000 x *g* for 15 s, and flow-through was discarded. Buffer RPE (500 µL) was added to the RNeasy Mini Spin Column to wash the column. Samples were centrifuged at 11000 x *g* for 15 s, and flow-through was discarded. Another 500 µL of Buffer RPE was added to dry the column, and samples were centrifuged at 11000 x *g* for 2 min. The RNeasy Mini Spin Column was placed in a new 2 mL collection tube and 40 µL of NFW was added. To elute the RNA, the samples were centrifuged at 11000 x *g* for 1 min. RNA yield was measured using NanoDrop® ND-1000 Spectrophotometer (ThermoFisher, Paisley, UK) as detailed in section 2.1.4.1. If the yield was >30 µg, a further 40 µL of NFW was added to the RNeasy Mini Spin Column. Samples

were centrifuged again at 11000 x *g* for 1 min to collect the elute in the same collection tube. Samples were stored at -80ºC until use.

2.1.4.1 Nucleic acid concentration and quality

RNA quality and concentration were measured using NanoDrop® ND-1000 Spectrophotometer (ThermoFisher, Paisley, UK), with an A260/A280 ratio of ~2.0 accepted as 'pure' RNA.

2.1.4.2 Agilent Bioanalyzer

RNA quality and concentration were measured by an external quality control service offered by Glasgow Polyomics using the Agilent 2100 Bioanalyzer. Samples were analysed using the Eukaryote Total RNA Nano assay, providing the concentration of RNA and an objective measurement of RNA quality known as the RNA integrity number (RIN). Following electrophoretic separation of RNA samples, RNA integrity was determined by analysing the entire electrophoretic trace and ratio of the 18S and 28S ribosomal RNA. The RIN scale ranges from 1 (degraded RNA) to 10 (intact RNA). All RNA samples with a RIN >8 were accepted.

2.2 SYBR and TaqMan RT-qPCR

2.2.1 Reverse transcription

Reverse transcription was performed for synthesis of cDNA, the first step in two-step RT-qPCR. TaqMan™ Reverse Transcription was performed for detection and quantification of mRNA expression with SYBR and TaqMan qPCR and TaqMan™ MicroRNA Reverse Transcription was performed for detection and quantification of miRNA expression with TaqMan qPCR.

2.2.1.1 TaqMan reverse transcription

cDNA synthesis for SYBR and TaqMan RT-qPCR was performed with Applied Biosystems™ TaqMan™ Reverse Transcription Reagents (ThermoFisher, Carlsbad, USA) by reverse transcription of RNA templates. Reverse transcription reactions were set-up as 20 µL reactions with 1000 ng of RNA template in 96-well PCR plates (Starlab, Milton Keynes, UK) on ice. Controls included no template

controls (NFW only and mastermix (MM) only) to monitor false positive results and no reverse transcriptase (RT) controls (no MultiScribe™ Reverse Transcriptase) to monitor genomic DNA contamination. Plates were covered with adhesive PCR plate seals (ThermoFisher, Paisley, UK) and centrifuged for 1 min at 1000 x *g*. Thermal cycling for reverse transcription was performed on MJ research Tetrad PTC-225 Thermal Cycler (MJ research, Ramsey, USA). The reagents used and reaction conditions were as following:

Template	Volume (µL) (SYBR)	Volume (µL) (TaqMan)
RNA up to 1000 ng		
NFW	adjust to 7.7	adjust to 9.6

Mastermix reagents	Volume (µL) (SYBR)	Volume (µL) (TaqMan)
10X RT Buffer	2.0	2.0
$MgCl_2$ (25 mM)	4.4	1.4
dNTPs (2.5 mM each)	4.0	4.0
Random Hexamers (50 µM)	1.0	1.0
RNase Inhibitor (20 U/µL)	0.4	1.0
MultiScribe™ Reverse Transcriptase (50 U/µL)	0.5	1.0

Thermocycling conditions

25°C for 10 min

48°C for 30 min (SYBR) and 37°C for 30 min (TaqMan)

95°C for 5 min

2.2.1.2 TaqMan miRNA reverse transcription

cDNA synthesis for detection and quantification of miRNA expression with TaqMan RT-qPCR was performed with Applied Biosystems™ TaqMan™ MicroRNA Reverse Transcription Reagents (ThermoFisher, Vilnius, Lithuania) by reverse transcription of RNA templates. Up to 10 ng of miRNA was reverse transcribed using 5X miRNA-specific stem-loop primers supplied with Applied Biosystems™ TaqMan™ MicroRNA Assays in a Tetrad PTC-225 Thermal Cycler (MJ research, Ramsey, USA). Reverse transcription reactions were set-up as 15 µL reactions in 96-well PCR plates (Starlab, Milton Keynes, UK) on ice. A no template control

was included for every mastermix with a 5X miRNA-specific stem-loop primer to monitor contamination. Plates were covered with adhesive PCR plate seals (ThermoFisher, Paisley, UK) and centrifuged for 1 min at 1000 x *g*. Thermal cycling for reverse transcription was performed on MJ research Tetrad PTC-225 Thermal Cycler (MJ research, Ramsey, USA). The reagents used and reaction conditions were as following:

Template	Volume (µL)
RNA up to 10 ng	
NFW	adjust to 5.00

Mastermix reagents	Volume (µL)
10X RT Buffer	1.50
100 mM dNTPs	0.15
RNase Inhibitor (20 U/ µL)	0.19
MultiScribe™ Reverse Transcriptase (50 U/ µL)	1.00
5X RT primer	3.00

Thermocycling conditions

16°C for 30 min

42°C for 30 min

85°C for 5 min

2.2.2 qPCR

2.2.2.1 SYBR qPCR for mRNA expression

Amplification of cDNA template was performed with *Power* SYBR™ Green PCR Master Mix (ThermoFisher, Warrington, UK). All PCR reactions were run in singleplex and used custom designed PCR primers (Eurofins Genomics, Ebersberg, Germany) to determine mRNA expression of the ß-actin housekeeping gene and gene of interest (GOI). All PCR reactions were set-up as 12.5 µL reactions in MicroAmp™ Optical 384-well reaction plates (ThermoFisher, Paisley, UK) on ice and were performed in triplicate. Controls included controls from the

cDNA plate and no-template controls (NFW only and MM only). Plates were covered with MicroAmp™ Optical Adhesive Film (ThermoFisher, Paisley, UK) and centrifuged for 1 min at 1000 x *g*. Thermal cycling for qRT-PCR was performed with QuantStudio 12K Flex Real-Time PCR System using standard SYBR qRT-PCR cycling conditions. A melt curve stage was performed to detect non-specific amplification. The reagents used and reaction conditions were as following:

Mastermix reagents	Volume (µL)
2X *Power* SYBR™ Green PCR Master Mix	6.35
Forward primer (500 nM)	0.50
Reverse primer (500 nM)	0.50
NFW	2.65
cDNA template	2.50

Thermocycling conditions
Hold stage:
50°C for 2 min
95°C for 10 min
PCR stage:
95°C for 15 s and 60°C for 1 min (40 cycles)
Melt curve stage:
95°C for 15 s
60°C for 1 min
95°C for 15 s

2.2.2.2 TaqMan qPCR for mRNA expression

Amplification of cDNA template was performed with TaqMan™ Universal Master Mix II, No UNG (ThermoFisher, Carlsbad, USA). All PCR reactions were run in duplex (VIC-labelled housekeeping and FAM-labelled GOI probe) and used Applied Biosystems™ 20X gene expression assays to determine mRNA expression. All PCR reactions were set-up as 5 µL reactions in MicroAmp™ Optical 384-well reaction plates (ThermoFisher, Paisley, UK) on ice and were performed in triplicate. Controls included controls from the cDNA plate and no-template controls (NFW only and MM only). Plates were covered with MicroAmp™ Optical Adhesive Film (ThermoFisher, Paisley, UK) and centrifuged for 1 min at 1000 x *g*.

Thermal cycling for TaqMan RT-qPCR was performed with QuantStudio 12K Flex Real-Time PCR System using standard TaqMan RT-qPCR thermal cycling conditions. The reagents used and reactions conditions were as following:

Mastermix reagents	Volume (µL)
2X TaqMan Universal Master Mix	2.00
20X GOI expression assay	0.25
20x housekeeper expression assay	0.25
cDNA template	2.00

2.2.2.3 TaqMan qPCR for miRNA expression

Amplification of cDNA template was performed with TaqMan™ Universal Master Mix II, No UNG (ThermoFisher, Carlsbad, USA). All PCR reactions were run in singleplex and used 20X TM probes supplied with Applied Biosystems™ TaqMan™ MicroRNA Assays. All PCR reactions were set-up as 10 µL reactions in MicroAmp™ Optical 384-well reaction plates (ThermoFisher, Paisley, UK) on ice and were performed in triplicate. Controls included controls from the cDNA plate and no-template controls (NFW only and MM only). Plates were covered with MicroAmp™ Optical Adhesive Film (ThermoFisher, Paisley, UK) and centrifuged for 1 min at 1000 x *g*. Thermal cycling for TaqMan qPCR was performed with QuantStudio 12K Flex Real-Time PCR System using standard TaqMan qPCR thermal cycling conditions. The reagents used and reactions conditions were as following:

Mastermix reagents	Volume (µL)
2X TaqMan Universal Master Mix	5.00
20X TM probe	0.50
NFW	3.84
cDNA template	0.66

2.2.3 Analysis of RT-qPCR

Gene expression was analysed using cycle threshold (Ct). Ct is the cycle number at which fluorescence from amplification of a PCR product crosses a threshold, indicating detection of fluorescence greater than background signal. Ct is therefore a relative measure of concentration of a PCR product. Ct values were

compared between samples and controls, after normalizing Ct values of a GOI to a housekeeping gene. Ct values from the GOI and housekeeping gene from samples and controls were extrapolated from the Real-Time PCR system and exported into Microsoft Excel for data analysis. For both samples and controls, the GOI was normalised to the housekeeping gene to obtain ΔCt as follows:

$$\Delta Ct = Ct_{(GOI)} - Ct_{(housekeeping)}$$

For each experiment performed in triplicate, the average ΔCt was calculated for samples and controls. For statistical analysis, the average ΔCt of samples was compared to controls.

2.3 *In vivo* procedures

All animal work was performed at the University of Glasgow in accordance with the United Kingdom Animals (Scientific Procedures) Act 1986, with all procedures approved by the Home Office under the Project Licence 70/9021 held by Dr Delyth Graham. All procedures were performed at the *in vivo* facility at the BHF Glasgow Cardiovascular Research Centre between 0900 and 1700 h i.e., during 'lights on' period. Stroke-prone spontaneously hypertensive (SHRSP) and Wistar Kyoto (WKY) rats used came from established inbred colonies at the University of Glasgow, maintained in-house since 1991 by strain-specific brother-sister mating. ICR (CD-1) outbred mice used were purchased from Envigo. All animals purchased externally were given a one-week acclimatisation period prior to any procedure. All rats and mice were housed in a temperature-controlled environment (21°C±3°C) and controlled 12-h light/dark conditions, with access to water and standard diet (rat and mouse No.1 maintenance diet, Special Diet Services). Rats and mice from the same strain and sex were housed together in individually ventilated cages with a maximum of five animals per cage. Corn cob bedding and sizzle nests were used as bedding. Non-aversive handling techniques were used when transferring animals between cages or equipment e.g., use of handling tubes. Animals were monitored daily for general welfare indicators, namely appearance, body functions (food and water intake) and behaviour (posture, social interaction and gait).

2.3.1 Plasmid DNA and MB suspension

UMGD studies utilised the commercially available contrast agent, SonoVue (Bracco International B.V., Amsterdam, Netherlands). A new kit of SonoVue, sulphur hexafluoride MBs stabilised by a phospholipid shell, was prepared immediately prior to commencing a UMGD study. The MB dispersion was prepared at double the concentration by discarding half the volume (2.5 mL) of NaCl 0.9% w/v (saline) solution. The remaining half was injected into the vial to reconstitute the lyophilised powder content by vigorously shaking the MB dispersion. A plasmid DNA and MB suspension was prepared on an individual basis for each animal. Prior to preparing the suspension for each animal, the MB dispersion was reconstituted by inverting the vial several times until cloudy. MB dispersion (500 µL) was collected with a 19 G needle (Terumo, Leuven, Belgium) in a 1 mL syringe and injected into a sterile microcentrifuge tube. The required volume of MB dispersion was then pipetted in a clean, sterile microcentrifuge tube. The required volume of 4 µg/µL plasmid DNA was added, making up the injectable plasmid DNA and MB suspension for one animal.

2.3.2 Anaesthetic procedure

All animals were anaesthetised prior to *in vivo* procedures in an induction chamber filled with 5% isoflurane and supplied with 1.5 L/min medical oxygen flow. Once anaesthesia was confirmed in animals by tail pinch, their nose and mouth were positioned in an anaesthetic mask. Animals were maintained on 1.5% isoflurane on a homeothermic mat, with adjustments made when required. At the end of all *in vivo* procedures, animals were monitored until they regained consciousness.

2.3.3 UMGD procedure

UMGD treatment animals underwent the same principal *in vivo* gene delivery procedure. For each UMGD study, protocol amendments and details of the animals and control animals are detailed in the methods section in the respective chapter.

2.3.3.1 Hair removal

For UMGD to the left kidney, rodents were placed in a supine position and hair was removed by shaving and depilatory cream across an area (~4 cm x 4.5 cm for rats or ~2 cm x 2.5 cm for mice) over the left upper quadrant below the ribcage, marking the area overlying the left kidney (Figure 2-1). An area of 1.5 cm x 2.5 cm over the left inguinal region was also shaved, marking the area overlying the left femoral vein (Figure 2-1). For UMGD to the heart, rodents were placed in a lateral recumbent position, and hair was removed by shaving and depilatory cream across an area of ~2 cm x 2.5 cm over the chest, marking the area overlying the heart (Figure 2-1). For UMGD to the placenta, mice were placed in a supine position, and hair was removed by shaving and depilatory cream across an area of ~4 cm x 4.5 cm over the left middle and lower quadrant and pubic region, marking the area overlying the left uterine horn (Figure 2-1). For UMGD to the heart and placenta, a glove filled with warm water was placed on the tail to dilate the tail vein.

2.3.3.2 UMGD treatment

The ACUSON Sequoia 512 ultrasound system (Siemens, Surrey, UK) and 15L8 linear array ultrasound transducer was used for all US scans. B-mode output was used for organ location, with an input frequency of 14 MHz, MI of 0.6, and focal depth of 10 mm. The transducer was placed on the shaved area overlying the target organ to obtain a longitudinal view of the left kidney, parasternal long axis view of the heart, or view of the foetoplacental unit (Figure 2-1). Once the organ was located and the appropriate view obtained, several images of the organ were taken using the image store function. The probe was then held in a fixed position, and output was set to harmonic imaging, with an input frequency of 7 MHz (H14 MHz), MI of 1.8, and focal depth of 10 mm. The output was either maintained (kept on) or frozen using the freeze function.

For UMGD to the left kidney in rats, a superficial incision was made to expose the left femoral vein prior to administer the plasmid DNA and MB suspension. In all UMGD studies, the plasmid DNA and MB suspension was stirred with a 25 G needle (Terumo, Leuven, Belgium) and drawn into a 1 mL syringe. For UMGD studies targeting the left kidney, the suspension was slowly administered over a

period of 5-60 s via the left femoral vein. For UMGD studies targeting the heart and placenta, the suspension was slowly administered over a period of 5-60 s via the tail vein. Once the suspension was fully administered, US was applied for a further 2 min utilising the harmonic imaging parameters set prior to the injection. The probe was then removed, and if a superficial incision was made it was sutured. Treatment animals were then recovered.

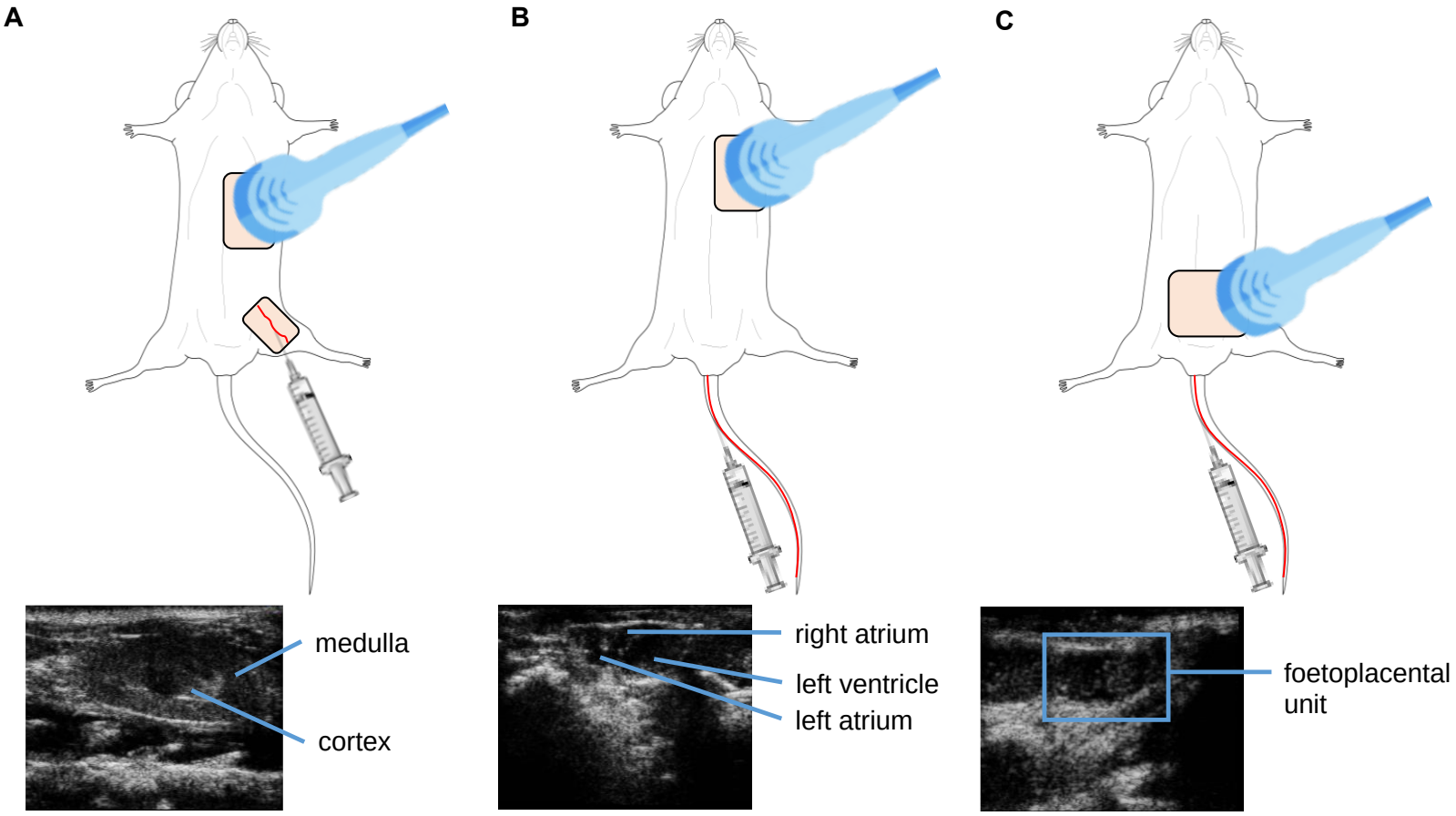

Figure 2-1 Diagram illustrating set-up of UMGD treatment to target organs and representative US images once appropriate view was obtained.

(A) Set-up of UMGD treatment target the left kidney (longitudinal view) with plasmid DNA and MB delivery via the left femoral artery. **(B)** Set-up of UMGD treatment to target the heart (parasternal long axis view) with plasmid DNA and MB delivery via the tail vein. **(C)** Set-up of UMGD treatment to target the placenta (view of the foetoplacental unit) with plasmid DNA and MB delivery via the tail vein.

2.3.3.3 Negative and positive control animals

Control animals from the same species as UMGD treatment animals were used in each study, and procedures were carried out on the same day as UMGD treatment animals. Control animals were anesthetised prior to any procedures as detailed in section 2.3.2. Negative control animals underwent the same hair removal procedure as detailed in section 2.3.3.1 and UMGD treatment as detailed in section 2.3.3.2 as treatment animals except, in place of the plasmid DNA and MB suspension, 1X phosphate buffered saline (PBS) (Gibco™, ThermoFisher, Paisley, UK) or a PBS and MB suspension was administered. For positive control animals, an area overlying the left gracilis muscle was shaved, and plasmid DNA or a plasmid DNA and MB suspension was administered into the gracilis muscle by multiple intramuscular (IM) injections.

2.3.4 Euthanasia

All animals were euthanised 3 d after UMGD procedures. Animals were anaesthetised as detailed in section 2.3.2. prior to euthanasia. Once anaesthesia was confirmed by tail pinch, animals were placed in a supine position with their nose and mouth positioned in an anaesthetic mask. Animals were maintained on 5% isoflurane while euthanised by exsanguination. Midline and quarterline thoracic incisions were made, followed by a blunt dissection at the sternum and transverse cuts along the bottom of the ribcage to open the thoracic cavity. Longitudinal cuts up the ribcage were made to expose the heart. In rats, perfusion was carried out with heparinised saline (5000 IU/mL) from the aortic arch, and the right atrium was cut to allow drainage to ensure rats were dead prior to continuing with tissue harvest. In mice, once the heart was exposed, the right atrium was cut to ensure mice were dead prior to harvesting tissue.

2.3.5 Tissue harvest

Tissues were dissected, cleaned and fixed in 10% (v/v) neutral buffered formalin (CellPath, Powys, UK), embedded in optimum cutting temperature (OCT) compound (VWR international, Leuven, Belgium), and/or snap frozen in liquid nitrogen. When required for multiple types of tissue processing, tissues were cut into pieces as following. Kidneys and hearts were cut longitudinally when two tissue pieces were required or longitudinally and transversely when three pieces

were required. The full gracilis muscle was dissected as far as possible and cut transversely when two pieces were required or transversely and longitudinally when three pieces were required. For the liver, a section from the left lateral lobe and right medial lobe were cut when two pieces were required and an additional section from the right lateral lobe was cut when three pieces were required. For the lungs, random sections from the right and left lungs were cut and for the spleen, random sections were cut. When tissue was only snap frozen, whole tissue samples of the heart (or separated atria and ventricles), left kidney, right kidney, skeletal muscle (gracilis muscle), liver, lungs, spleen, placenta, and foetuses were collected.

2.4 Histology

2.4.1 Formalin-fixed paraffin-embedded tissue processing

Tissues were fixed in 10% (v/v) neutral buffered formalin for 24 h. Tissues were washed three times for 10 min in 1X PBS and placed in 70% ETOH prior to tissue processing. Tissues were processed through a series of alcohol gradients to Histo-Clear (Fisher Scientific, Loughborough, UK) to paraffin wax in a Citadel 1000 processor (ThermoFisher, Loughborough, UK) in the following conditions:

Processing conditions
70% alcohol for 30 min
95% alcohol for 30 min
100% alcohol for 30 min (2x)
100% alcohol for 45 min (2x
100% alcohol for 60 min
Histo-Clear for 30 min (5x)
Paraffin wax for 30 min (2x)
Paraffin wax for 45 min (2x)

Tissues were then embedded in paraffin wax, with kidney sections positioned longitudinally, and tissue blocks were stored at 4ºC overnight prior to sectioning. Paraffin tissue blocks were sectioned at 5 µm using the Leica RM2235 Microtome (Leica biosystems, Milton Keynes, UK). Sections were mounted onto silane coated slides (Smith Scientific, Edenbridge UK), and dried in a 50ºC oven

overnight. Prior to staining, tissue sections were dewaxed and then rehydrated by placing slides through a series of alcohol gradients followed by a final wash as following:

Rehydration
Histo-Clear for 5 min (3x)
100% alcohol for 5 min (2x)
90% alcohol for 5 min
70% alcohol for 5 min
50% alcohol for 5 min
dH_2O for 5 min

2.4.2 Frozen tissue processing

Tissue embedded in OCT was transferred onto a tissue holder, which was placed on a freezing temperature bar in the microtome cryostat (Leica, Milton Keynes, UK). Frozen blocks were cryosectioned at 10 µm and mounted onto silane treated slides (Smith Scientific, Edenbridge UK). Sections were allowed to air dry for 3-5 h and stored at -20ºC.

2.5 Luminescence and colorimetric assays

2.5.1 Protein extraction

Mortar and pestle were used for tissue disruption, and tissue was homogenised in 1:20 (w/v) tissue protein extraction reagent (ThermoFisher, Loughborough, UK). Samples were homogenised either by gentle agitation on a shaker on ice for 30 min or by bead milling four times for 30 s at 30 kHz with the TissueLyser (QIAGEN, Haan, Germany) followed by three freeze-thaw cycles. Samples were centrifuged at 10000 x *g* for 5 min, and supernatant was collected.

2.5.2 Protein assay

Protein concentration of tissue samples was measured using the Pierce BCA protein assay (ThermoFisher, Loughborough, UK). Protein standards of bovine serum albumin (BSA) (ThermoFisher, Loughborough, UK) were prepared at concentrations ranging from 25-2000 µg/mL by dilution in 1X PBS. 1X PBS (0

µg/mL BSA) was used as a blank. Samples were diluted between 1:5 to 1:20 with 1X PBS to place values within the range of the standard curve. Samples and controls (25 µL) were pipetted into a clear flat bottom 96-well plate (Greiner, Dorset, UK) in duplicate or triplicate. Working reagent was prepared with BCA Reagent A and BCA Reagent B at a ratio of 50:1, of which 200 µL was added to each reaction well. The plate was incubated for 30 min at 37°C. Absorbance was measured at 562 nm with PerkinElmir 2030 plate reader (Perkin Elmer, Singapore, Singapore). The blank absorbance value was subtracted from all readings, and a standard curve was constructed from the known standard concentrations. Protein concentrations of samples were extrapolated from the standard curve.

2.5.3 Luciferase assay

Luciferase activity was measured using the luciferase assay reporter system (Promega, Southampton, UK). Luciferase assays were set-up on a white flat bottom 96-well plate (Greiner, Dorset, UK). Room temperature luciferase assay reagent (100 µL) (Promega, Southampton, UK) and 20 µL of sample supernatant or TPER (blank) were added to each well. Luciferase activity was measured in counts per second (CPS) for a period of 10 s using the PerkinElmir 2030 plate reader (Perkin Elmer, Singapore, Singapore). The blank absorbance value was subtracted from all readings prior to normalising luciferase activity to protein content.

2.6 Literature review

2.6.1 Literature search

Literature searches were conducted using PubMed database. Truncation searching was performed by assigning the wildcard character (*) to each term to capture entries that contain terms with the same word stem. Abstracts were initially screened to identify full-text research articles available in English. Thereafter, abstracts and/or full-text articles were screened for eligibility and/or relevance. For all studies included in the literature reviews, the full text was assessed for eligibility and/or relevance.

2.7 Statistical analysis

GraphPad Prism 9 was used to analyse data sets. Luciferase activity data are shown as mean counts per second (CPS)/µg of protein ± standard deviation (SD) or standard error of mean (SEM). Luciferase activity data were analysed by Friedman's test followed by Dunn's post-hoc multiple comparisons test. TaqMan data are shown as mean ΔCt ± SEM. TaqMan data were analysed using ΔCt values and groups were compared by unpaired t-test (with Welch's correction as appropriate) when comparing two groups or one-way ANOVA followed by Tukey's post-hoc multiple comparisons test when comparing three or more groups. Parametric tests were used since ΔCt values have shown to be normally distributed (Guo et al., 2010). Clinical characteristics are presented as mean ± standard deviation (SD) or median (range). All normally distributed variables were compared by unpaired t-test (with Welch's correction as appropriate) and non-normally/discrete variables were compared by Mann-Whitney U test. MTT assay data were expressed as median cell viability % (IQR). This was calculated from absorbance ratios of treatment values normalised to 'cells only' values set to 100% and analysed by Kruskal-Wallis test followed by Dunn's post-hoc multiple comparisons test. For statistical tests, $p<0.05$ was considered significant.

Chapter 3 Optimisation of an *in vivo* UMGD protocol in rodents

3.1 Introduction

Gene therapy represents a promising form of treatment for pregnancy-related disorders with an underlying genetic basis, such as FGR and PE. Recent developments in gene therapy for FGR pave the way for translational research. However, new gene delivery methods remain essential to extending research to other disorders, including PE. EVERREST marks the first-in-human trial to administer placental gene therapy during pregnancy (Spencer et al., 2017). Currently underway, the landmark study is evaluating the safety and efficacy of adenoviral delivery of a VEGF isoform, VEGF-$D^{\Delta N \Delta C}$, to uterine arteries as a therapy for severe early-onset FGR. Preclinical studies in guinea pig and sheep models of FGR demonstrated therapeutic benefit following a single administration of adenoviral VEGF (Ad-VEGF), evidenced by increased foetal weight and growth pre- and postnatally (Carr et al., 2014, Swanson et al., 2016, Carr et al., 2016). Assessment of histological, biochemical, and haematological parameters supported its safety profile, and evaluation of maternal and foetal tissue demonstrated limited off-target expression (Swanson et al., 2016). In accordance with regulatory requirements for transitioning the research into clinical trials, a study utilising *in vitro* and *ex vivo* human placental model systems showed placental integrity and function were largely maintained following Ad-VEGF-$D^{\Delta N \Delta C}$ infusion on the maternal side (Desforges et al., 2018). With all legal and ethical requirements meeting regulatory standards, the clinical trial was approved. Nonetheless, possible safety and efficacy issues associated with the adenoviral vector and its delivery method underpin the need for non-viral and non-invasive gene delivery systems targeting the placenta.

Local delivery of adenoviral vectors remains essential to mitigating potentially harmful systemic off-target effects. The *ex vivo* placental perfusion study found low levels of viral vector transfer across the placenta, demonstrating the risk of foetal gene transfer (Desforges et al., 2018). The majority of preclinical studies reported Ad-VEGF was not detected in any maternal or foetal tissue besides maternal uterine arteries (David et al., 2008, Mehta et al., 2012, Mehta et al.,

2014). Conversely, one of the final preclinical studies preceding the clinical trial detected the vector in a maternal ovary, highlighting the risk of off-target expression (Swanson et al., 2016). A phase II clinical trial utilising the same first-generation replication-deficient adenovirus demonstrated intracoronary delivery was safe and well tolerated in patients with coronary heart disease (Hedman et al., 2003). However, temporary fever and elevations in C-reactive protein (CRP) and lactate dehydrogenase (LDH) levels, markers of inflammation and cell injury respectively, were seen in several patients administered the gene therapy, potentially indicative of systemic inflammatory reactions. Similarly, a minor rise in LDH release was observed in the aforementioned *ex vivo* placental perfusion study, leading to an approximate 25-fold lower dose administered to patients in the EVERREST trial (Desforges et al., 2018). In a more recent phase I/IIa clinical trial in refractory angina patients, local intramyocardial delivery of Ad-VEGF-$D^{\Delta N \Delta C}$ was also safe and well tolerated (Hartikainen et al., 2017). Although transient changes were noted in plasma CRP, haemoglobin, and thrombin, there were no significant differences in adverse events and clinical parameters of safety from 14 d until 1-year follow-up. Preclinical and clinical studies employing the adenoviral vector support limited safety issues. A risk of off-target expression however still persists, a particular concern when targeting the placenta as both maternal and foetal safety must be considered.

In attempt to address maternal and foetal risks, preventative measures have been taken to ensure localised gene transfer. Preclinical studies optimised the gene delivery protocol to ensure gene transfer was restricted to the uterine arteries through reconstitution of the virus in pluronic gel in guinea pigs (Mehta et al., 2016) and occlusion of uterine arteries following laparotomy surgery in sheep (Carr et al., 2015). In the ongoing clinical trial, balloon occlusion catheters are being used for intravascular delivery of the virus to uterine arteries, which may interrupt uterine blood flow for up to 5 min (Desforges et al., 2018). This method is employed in clinical practice for controlling intraoperative bleeding in several pregnancy conditions, including abnormal placentation (Peng et al., 2019, Sun et al., 2018), elective caesarean section (Fuller et al., 2006), and uterine arteriovenous fistula (Yamamoto et al., 2015). Multiple studies have reported a lack of benefit and complications arising from balloon catheter placement (Bodner et al., 2006, Salim et al., 2015, Shrivastava

et al., 2007), and its routine use is therefore not recommended (ACOG, 2020). Less invasive and non-viral strategies for targeting the placenta therefore remain critical to extend research to other pregnancy disorders arising from abnormal placental development, such as PE.

UMGD in conjunction with a plasmid vector represents a non-viral and non-invasive method of gene transfer. Research into targeting the placenta remains limited, with a single *in vivo* UMGD study published to date (Babischkin et al., 2019). The study demonstrated therapeutic benefit of delivering VEGF to uterine arteries to restore remodelling capabilities (Babischkin et al., 2019). However, tissue-specific expression was not examined, a critical step in demonstrating the clinical translatability of UMGD to the placenta.

This chapter encompasses optimisation studies to develop an *in vivo* protocol for UMGD of a reporter gene to a more easily accessible organ in rodents, which could then be applied to the placenta. Rodents were chosen as suitable models to re-establish a previous successful method which targeted the heart in mice (Browning et al., 2011). Furthermore, with future investigations into targeting the placenta planned in rats due to availability of a rat model of PE (Morgan et al., 2018), rodents were selected for optimisation studies. Targeting rodent placentas with UMGD presents a unique challenge due to their relatively large litter size corresponding to a large number of placentas. Although the left and right uterine horns can help distinguish foetuses positioned along each horn, identifying a specific foetus and/or placenta *in utero* remains difficult. Optimisation studies were therefore conducted in non-pregnant rodents, utilising the kidney and heart as surrogate organs, which akin to the placenta are highly vascularised. In initial studies, the kidney was selected since the location of the organ is similar to that of the placenta and since the paired organ provides a comparable target and control in the same animal under same experimental conditions. Subsequently, the heart was targeted in optimisation studies to more closely recapitulate a previous UMGD study demonstrating tissue-specific gene transfer (Browning et al., 2011).

3.2 Hypothesis and aim

3.2.1 Hypothesis

UMGD stimulates targeted gene transfer with a non-viral vector *in vivo*.

3.2.2 Aim

- To conduct optimisation studies in rodents to develop an *in vivo* UMGD protocol for delivering a reporter gene to a surrogate organ.

3.3 Methods

All animal work was performed in accordance with the United Kingdom Animals (Scientific Procedures) Act 1986 under the authority of Home Office Licence 70/9021. All animals were housed and maintained as detailed in section 2.3. UMGD optimisation studies were conducted in adult SHRSP and WKY rats and adult female CD-1 mice, utilising the left kidney and subsequently heart as target surrogate organs. The strain, sex, age, and weight of every animal and the total n-number of animals in each study is listed in Table 3-1. An n=3 was selected for the treatment group to minimise the number of animals used for initial research into the feasibility of the technique. An n=1 for the negative and positive control groups was chosen as the minimum number required to interpret the results from the treatment group. All animals were included in the study analysis. Formal randomisation and blinding were not performed; the order of experimental groups was decided prior to experiments, (negative control, UMGD, and then positive control group) to avoid contamination in negative control animals. No a prior criteria were used when randomly selecting animals from the cage. Rodents were sacrificed 3 d after UMGD, and target and non-target organs were either fixed or frozen for evaluation of reporter gene transfer by analysis of histology, gene expression, and/or enzymatic activity.

3.3.1 Plasmid DNA preparation for *in vivo* use

3.3.1.1 Plasmid DNA purification

Plasmid DNA was transformed into competent MAX Efficiency™ DH5α™ Competent Cells as detailed in section 2.1.2.1. Glycerol stocks were prepared as a long-term stock as detailed in section 2.1.2.2. pVIVO2-GFP/LacZ was purified by centrifugation using the QIAGEN Plasmid Mega Kit (QIAGEN, Hilden, Germany) as detailed in section 2.1.2.3. A starter culture was initially diluted 1:1000 into 1 L selective LB medium culture. In subsequent experiments, starter culture was diluted 1:1000 into 800 mL selective LB medium culture. pGL3 was purified by filtration using the QIAfilter Plasmid Mega Kit (QIAGEN, Hilden, Germany) as detailed in section 2.1.2.4. pGL4.13 was purified by filtration using the Invitrogen™ PureLink™ HiPure Expi Plasmid Megaprep Kit (ThermoFisher, Vilnus,

Lithuania) as detailed in section 2.1.2.4. Plasmid DNA with an A260/A280 ratio of ~1.8 was accepted as 'pure' DNA as detailed in section 2.1.2.7.

3.3.1.2 Analytical gel of samples from plasmid DNA purification

Samples from stages of the plasmid DNA purification were precipitated as detailed in section 2.1.2.5. Samples were run on a 1% agarose gel as detailed in section 2.1.3 to assess efficiency of the purification procedure, namely: growth and lysis conditions, efficiency of column loading, plasmid DNA binding, removal of RNA, and contamination. Purified plasmid DNA was run on the same gel to confirm isolation of plasmid DNA, lack of contamination in the final product, and conformation of the plasmid. If contamination was suspected, restriction digest was performed as detailed in section 2.1.2.6. Only plasmid DNA considered 'pure' and confirmed as uncontaminated was used for *in vivo* procedures.

3.3.2 Plasmid DNA and MB suspension

The plasmid DNA and MB suspension was prepared on an individual basis for each animal in UMGD studies as detailed in section 2.3.1. The volume of plasmid DNA and MBs administered is listed in Table 3-1.

3.3.3 UMGD studies

3.3.3.1 UMGD

UMGD was conducted as detailed in section 2.3.3. For each UMGD study, details of the type of plasmid; target organ; probe hold/output; animal strain, sex, age, weight, treatment, and n-numbers; injection site; and volumes administered are listed in Table 3-1.

3.3.3.2 Negative and positive control animals

In the first study, a kidney obtained from a control SHRSP rat (sacrificed as part of an unrelated study due to a surplus of requirements) was used as a negative control. In subsequent studies, negative control animals underwent a similar procedure as UMGD treatment animals as detailed in section 2.3.3.3, with modifications listed in Table 3-1. Positive control animals underwent the same procedure as detailed in section 2.3.3.3, with modifications listed in Table 3-1.

Table 3-1 Full details of UMGD studies.

Study	Plasmid	Target organ	Probe hold / output	Strain (total n)	Sex (F/M)	Age (wk)	Weight (g)	Treatment (n)	Injection site	Plasmid volume (µL)	MB volume (µL)	PBS volume (µL)
1	pVIVO2	left kidney	stationary / frozen	SHRSP (4)	F	14	155-174	UMGD (3)	left femoral vein	20	60	-
					M	20	-	NC (1)	-	-	-	-
2	pVIVO2	left kidney	stationary / frozen	WKY (5)	F	17-19	195-201	UMGD (3)	left femoral vein	45	135	-
					F	17	214	NC (1)	left femoral vein	-	-	200
					F	17	211	PC (1)	gracilis muscle	50	150	-
3	pGL4.13	left kidney	sweeping / on	WKY (5)	F	13	193-196	UMGD (3)	left femoral vein	125	375	-
					F	13	172	NC (1)	left femoral vein	-	-	500
					F	13	186	PC (1)	gracilis muscle	200	-	-
4	pGL3	left kidney	sweeping / on	CD-1 (5)	F	6-8	25-32	UMGD (3)	left femoral vein	50	150	-
					F	6-8	30	NC (1)	left femoral vein	-	-	200
					F	6-8	28	PC (1)	gracilis muscle	50	-	-
5	pGL3	heart	stationary / on	CD-1 (5)	F	6-8	31- 35	UMGD (3)	tail vein	50	150	-
					F	6-8	33	NC (1)	tail vein	-	-	200
					F	6-8	29	PC (1)	gracilis muscle	50	-	-
6	pGL3	heart	stationary / on	CD-1 (5)	F	6-8	32- 45	UMGD (3)	tail vein	50	150	-
					F	6-8	39	NC (1)	tail vein	-	40	160
					F	6-8	40	PC (1)	gracilis muscle	17	33	-

All values (strain, sex, weight, and treatment parameters) for animals were collected and/or noted prior to treatment. SHRSP, stroke-prone spontaneously hypertensive rats; WKY, Wistar Kyoto; F, female; M, male; wk, weeks; UMGD, ultrasound-mediated gene delivery; NC, negative control, PC, positive control; MB, microbubble; PBS, phosphate-buffered saline.

3.3.3.3 Sacrifice and tissue processing

Animals were euthanised 3 d after UMGD procedures as detailed in section 2.3.4. Tissues were harvested and processed as detailed in section 2.3.5.

3.3.4 RNA extraction and quality control

RNA was extracted from tissue samples as detailed in section 2.1.4. Rat tissue was homogenised using Polytron PT2100 Benchtop Homogeniser (KINEMATICA, Luzern, Switzerland) and mouse tissue was homogenised using TissueLyser (QIAGEN, Haan, Germany). An optional on-column DNase digestion was performed. Buffer RWT (350 µL) was added to the RNeasy Mini Spin Column to wash the column. Samples were centrifuged at 11000 x *g* for 15 s, and flow-through was discarded. DNase I incubation mix (10 µL DNase I stock solution and 70 µL Buffer RDD) was added to the RNeasy Mini Spin Column and placed at room temperature for 15 or 30 min. Buffer RWT (350 µL) was added to the RNeasy Mini Spin Column to wash the column. Samples were centrifuged at 11000 x *g* for 15 s, and flow-through was discarded. The RNA extraction protocol was then followed as detailed in section 2.1.4. RNA quality and concentration were assessed as detailed in section 2.1.4.1.

3.3.5 SYBR and TaqMan RT-qPCR

SYBR RT-qPCR was performed as detailed in section 2.2, using custom designed primers (LGP1, LGFP2, and LacZ) listed in Table 3-2. TaqMan RT-qPCR was performed as detailed in section 2.2, using the TaqMan® Gene Expression Assay for Actb (assay ID Mm01205647_g1) and Luc (assay ID Mr03987587_mr) and custom TaqMan® Gene Expression Assay for Luc2 (Table 3-2). Data were analysed as detailed in section 2.2.3, with Ct values normalised to housekeeper (ß-actin).

Table 3-2 Custom designed primers for SYBR and TaqMan RT-qPCR

Primer (gene)	Forward Primer (5' to 3')	Reverse Primer (5' to 3')
LGFP1 (LGFP)	CACTATCTCCGCACTCAATC	CTGCTGCTGTCACAAACTC
LGFP2 (LGFP)	GACCCTAATGAGAAAAGAGACC	CATCCATTCCCAGAGTAATTCC
LacZ (LacZ)	CTCTCAATGGAGAGTGGAGG	ATGCATCTGCCAGTTGCTGG
Luc2 (LUC2)	GCGCAGCTTGCAAGACTATAAG	TTGTCGATGAGAGTGCTCTTAGC

3.3.6 PCR purification

SYBR RT-qPCR products were purified for sequencing using the QIAquick® PCR purification Kit (QIAGEN, Hilden, Germany). Five volumes of Buffer PB were added to 1 volume of PCR product. The sample was added to a QIAquick column and centrifuged for 60 s at 17900 x *g*, and flow-through was discarded. Buffer PE (750 µL) was added to the QIAquick column and centrifuged for 60 s at 17900 x *g*, and flow through was discarded. Residual wash buffer was removed by centrifuging the QIAquick column for another 60 s at 17900 x *g*. To elute purified PCR product, 30 µL of NFW was added to the QIAquick column and centrifuged for 60 s at 17900 x *g*.

3.3.7 Sequencing

Sequencing of SYBR RT-qPCR products was outsourced to GATC Biotech. Sequences were analyzed using CLC Sequence Viewer. Sequences were aligned to known template sequences of primer pairs, LGFP1 and LGFP2.

3.3.8 Fluorescence immunohistochemistry

Tissue sections were dewaxed and rehydrated as detailed in 2.4.1. Sections were subject to antigen retrieval by incubating slides in heated citrate buffer (pH 6) for 20 min. Sections were blocked with 100 µL blocking agent (Tris-buffered saline and 0.05% Tween20 (TBST) (Sigma, Darmstadt, Germany) with 15% goat serum (Vector Laboratories Ltd., Peterborough, UK)) for 1 h. Sections were incubated with 100 µL primary antibody (1:100 (study 1) dilution of mouse anti-GFP antibody [STJ97030] (St John's Laboratory, London, UK), 1:100 (study 1) and in 1:500 (study 2) dilution of rabbit anti-GFP antibody [ab6556] (Abcam, Cambridge, UK) and 1:300 (study 2) dilution of rabbit IgG fraction to ß-galactosidase (ß-gal) [ICN559762] (Fisher Scientific, Loughborough, UK)) or a negative IgG control (mouse IgG (Agilent Dako, Glostrup, Denmark) or rabbit IgG (ThermoFisher, Loughborough, UK) respectively) for 1 h at room temperature or overnight at 4°C. After washing three times with TBST, sections were incubated in 100 µL of secondary antibody (1:500 dilution of goat anti-mouse (H+L) highly cross-adsorbed Alexa Fluor 555 (ThermoFisher, Paisley, UK) or 1:500 dilution of goat anti-rabbit (H+L) highly cross-adsorbed Alexa Fluor 555 (ThermoFisher, Paisley, UK)). Sections were washed three times in TBS, mounted with ProLong

Diamond Antifade Mountant (ThermoFisher, Paisley, UK), sealed with coverslips (Smith Scientific, Edenbridge, UK), and allowed to cure overnight at room temperature. In study 2, sections were treated with Sudan Black B 0.1% for 5 min at room temperature prior to mounting. Fluorescence microscopy was performed with AxioObserver Z1 (Zeiss, Cambridge, UK), and images were analysed using Zen Pro software with display setting parameters kept constant. Images of kidney cross-sections were taken at 4X magnification and kidney sections were taken at 20X magnification. Medullary and cortical regions were distinguished by absence or presence of renal corpuscles, respectively. All fluorescence images were manipulated to the same level (brightness: +40% and contrast: -40%).

3.3.9 X-gal staining

Frozen OCT tissue blocks were cryosectioned at 10 µm, mounted onto silane treated slides (Smith Scientific, Edenbridge UK), and allowed to dry for 3-5 h as detailed in 2.4.2. Sections were fixed in 0.2% glutaraldehyde for 10 min at 4°C. Slides were washed three times for 5 min with LacZ wash buffer (1.5 mL 1M $MgCl_2$, 7.5 mL 1% NaDC, 7.5 mL 2% Nonidet-P40, and 733.5 mL 1X PBS). Slides were incubated in LacZ stain (72 mL LacZ wash buffer, 3 mL 25 mg/mL X-Gal, 0.159 g K-ferrocyanide, and 0.123 g k-ferricyanide) at 37°C overnight and washed twice with 1X PBS. Slides were dehydrated through a gradient of ETOH concentrations to Histo-Clear and mounted with cover slips. Images were taken with Olympus BX41 Microscope (Olympus, Essex, UK) at 20X magnification.

3.3.10 Luciferase activity

Luciferase activity was measured as detailed in section 2.5.3 and normalised to protein content, which was extracted by gentle agitation as detailed in section 2.5.1 and measured as detailed in section 2.5.2

3.3.11 Statistical analysis

GraphPad Prism 9 was used to summarise the data using descriptive statistics. Luciferase activity data are shown as mean CPS/µg of protein ± SD.

3.4 Results

3.4.1 UMGD optimisation studies delivering pVIVO2-GFP/LacZ to the left kidney in rats

3.4.1.1 Purification of pVIVO2-GFP/LacZ

The pVIVO2-GFP/LacZ plasmid, a 9620 bp dual reporter vector, was selected for initial *in vivo* UMGD optimisation studies targeting the left kidney as a surrogate organ. To assess efficiency of purification and pVIVO2-GFP/LacZ plasmid conformation, samples from stages of the purification procedure were run on an agarose gel. A band above 10000 bp (lane L) demonstrates denatured proteins, bacterial chromosomal DNA, and cell debris were removed, and the cleared lysate was enriched for plasmid DNA (Figure 3-1). A band above 10000 bp (lane F) indicates plasmid DNA was present in the flow-through fraction, and the column was overloaded (Figure 3-1). No band/s in the final wash fraction (lane W2) shows plasmid DNA was bound to the column and degraded RNA was removed (Figure 3-1). In the elute (lane E), a single band above 10000 bp demonstrates plasmid DNA was purified from *E. coli* and present in an open-circular conformation (Figure 3-1).

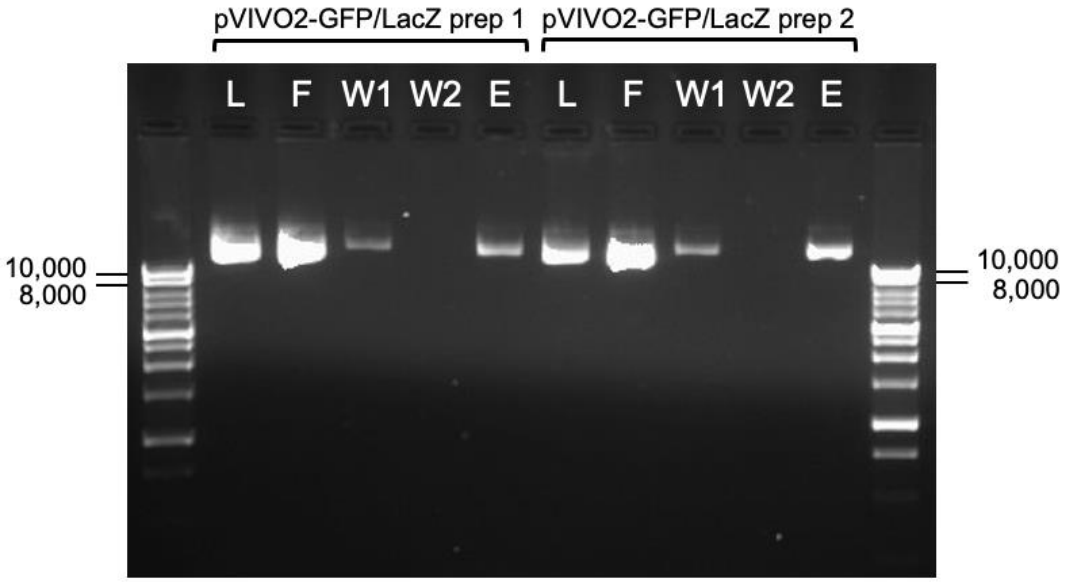

Figure 3-1 Representative agarose gel image of samples from stages of purification of pVIVO2-GFP/LacZ plasmid mega preps.

pVIVO2-GFP/LacZ plasmid was isolated from *E. coli* mega preps during which samples were collected to assess the stages of the purification procedure and confirm isolation of plasmid DNA. Up to 10 µL of the sample or 250 ng of DNA was loaded per lane and sized on a 1% agarose gel, using a 1 kb DNA ladder; sizes indicated in bp. Lane L: cleared lysate, lane F: flow-through fraction, lanes W1 and W2: wash fractions, lane E: elute.

3.4.1.2 *In vivo* UMGD of pVIVO2-GFP/LacZ to the left kidney in rats

Two *in vivo* UMGD optimisation studies targeting the left kidney in rats utilised the pVIVO2-GFP/LacZ plasmid. Specifically designed for *in vivo* use, the plasmid encodes two chemically synthesised reporter genes, LGFP and LacZ-ΔCpG, each with CpG motifs removed and their own promoter and polyadenylation signals to promote sustained expression (Invivogen, 2016).

3.4.1.2.1 Study 1

Fluorescence IHC and X-Gal staining were used to assess gene transfer by detection of protein expression of GFP and LacZ, respectively. Examination of GFP with IHC, using a mouse anti-GFP primary antibody, showed fluorescence in both the left and right kidneys of all three UMGD treatment rats (Figure 3-2). Fluorescence was observed in the medullary region in the left and right kidneys of UMGD treatment rats and a negative control rat (Figure 3-3), indicating non-specific antibody binding. Evaluation of GFP in the medullary and cortical regions of the left and right kidneys of UMGD treatment rats following incubation with a rabbit anti-GFP primary antibody showed low levels of fluorescence similar to incubation with an IgG control, providing evidence of a lack of gene transfer (Figure 3-4). Higher levels of fluorescence by qualitative assessment were seen in the medullary and cortical regions in the kidney of a negative control rat (Figure 3-5) compared to kidneys from UMGD treatment rats (Figure 3-4), further indicating failure of GFP transfer to the left kidney. X-Gal staining revealed presence of ß-gal (evidenced by blue staining) in the medulla and cortex in both the left and right kidneys of a UMGD treatment rat, representing detection of endogenous LacZ expression rather than LacZ gene transfer (Figure 3-6). There was no evidence of ß-gal in negative control organs: heart, liver, and skeletal muscle (Figure 3-6).

In this study, MBs were reconstituted for 20 min rather than 20 s due to human error. In all future studies, MBs were reconstituted for 20 s as described in the 'Summary of Product Characteristics'(EMA, 2008b). In addition, 40% of the intended plasmid DNA and MB dose (previously published dose successfully used in mice (Browning et al., 2011)) was administered due to loss of volume from unaccounted for dead space in the syringe. In all future studies, 100 µL dead space volume was accounted for when preparing the plasmid DNA and MBs.

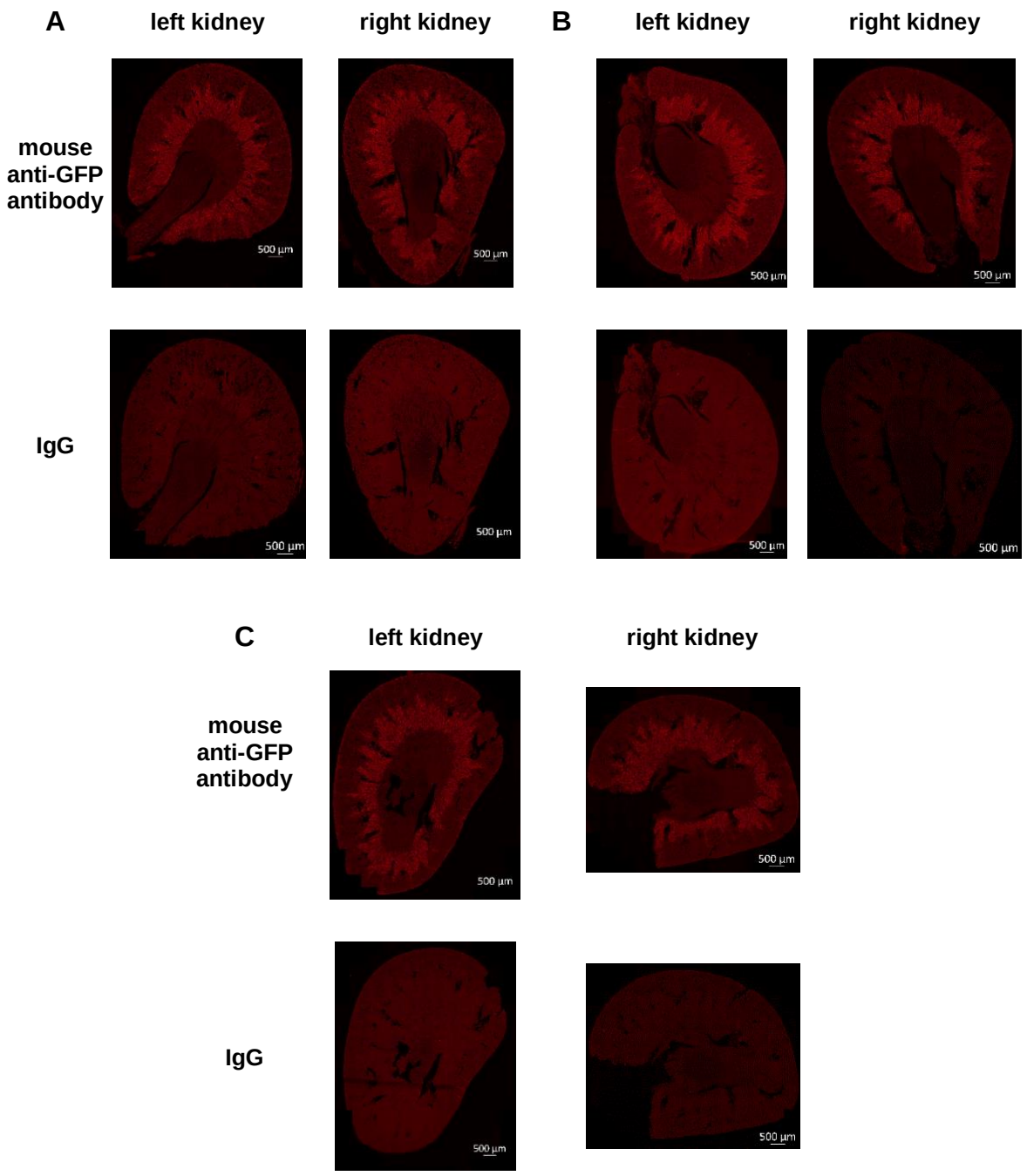

Figure 3-2 Representative images of visualisation of GFP with fluorescence IHC (mouse anti-GFP primary antibody) in cross-sections of left and right kidneys from UMGD treatment rats from study 1.

(A) UMGD treatment rat 1, **(B)** UMGD treatment rat 2, and **(C)** UMGD treatment rat 3 kidneys were incubated with mouse anti-GFP primary antibody (top panels) or mouse IgG (bottom panels) and goat anti-mouse Alexa Flour 555 secondary antibody to visualise GFP in the left kidneys (left panel) and right kidneys (right panel). All images were taken at 4x magnification. Scale bar represents 500 µm.

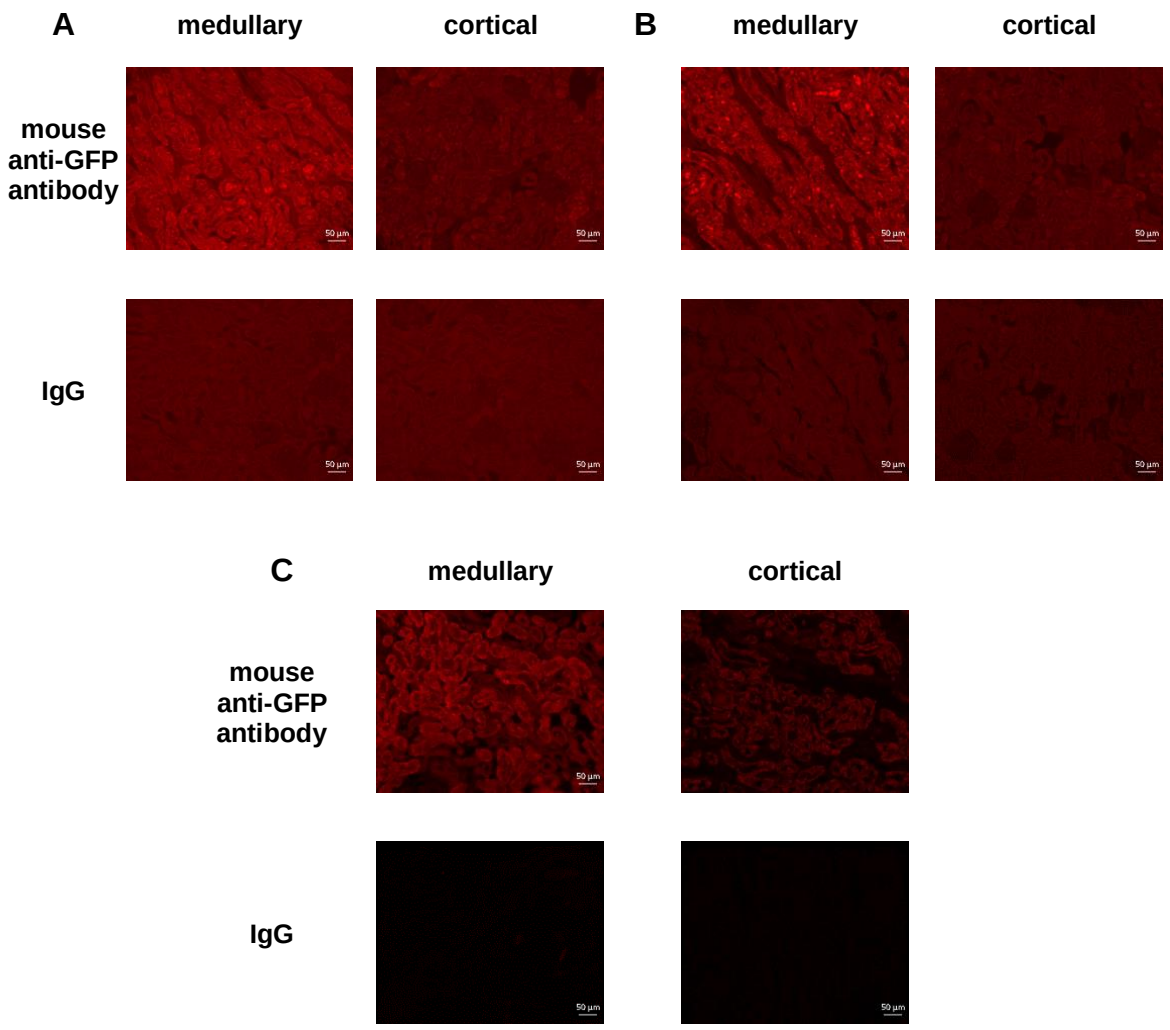

Figure 3-3 Representative images of visualisation of GFP with fluorescence IHC (mouse anti-GFP primary antibody) in medullary and cortical regions of kidneys from a UMGD treatment rat and the negative control rat from study 1.

(A) Left kidney of UMGD treatment rat, **(B)** right kidney of UMGD treatment rat, and **(C)** kidney of negative control rat were incubated with mouse anti-GFP primary antibody (top panels) or mouse IgG (bottom panels) and goat anti-mouse Alexa Flour 555 secondary antibody to visualise GFP. Representative images were taken from the medullary (left panel) and cortical (right panel) regions of the kidneys. All images were taken at 20x magnification. Scale bar represents 50 µm.

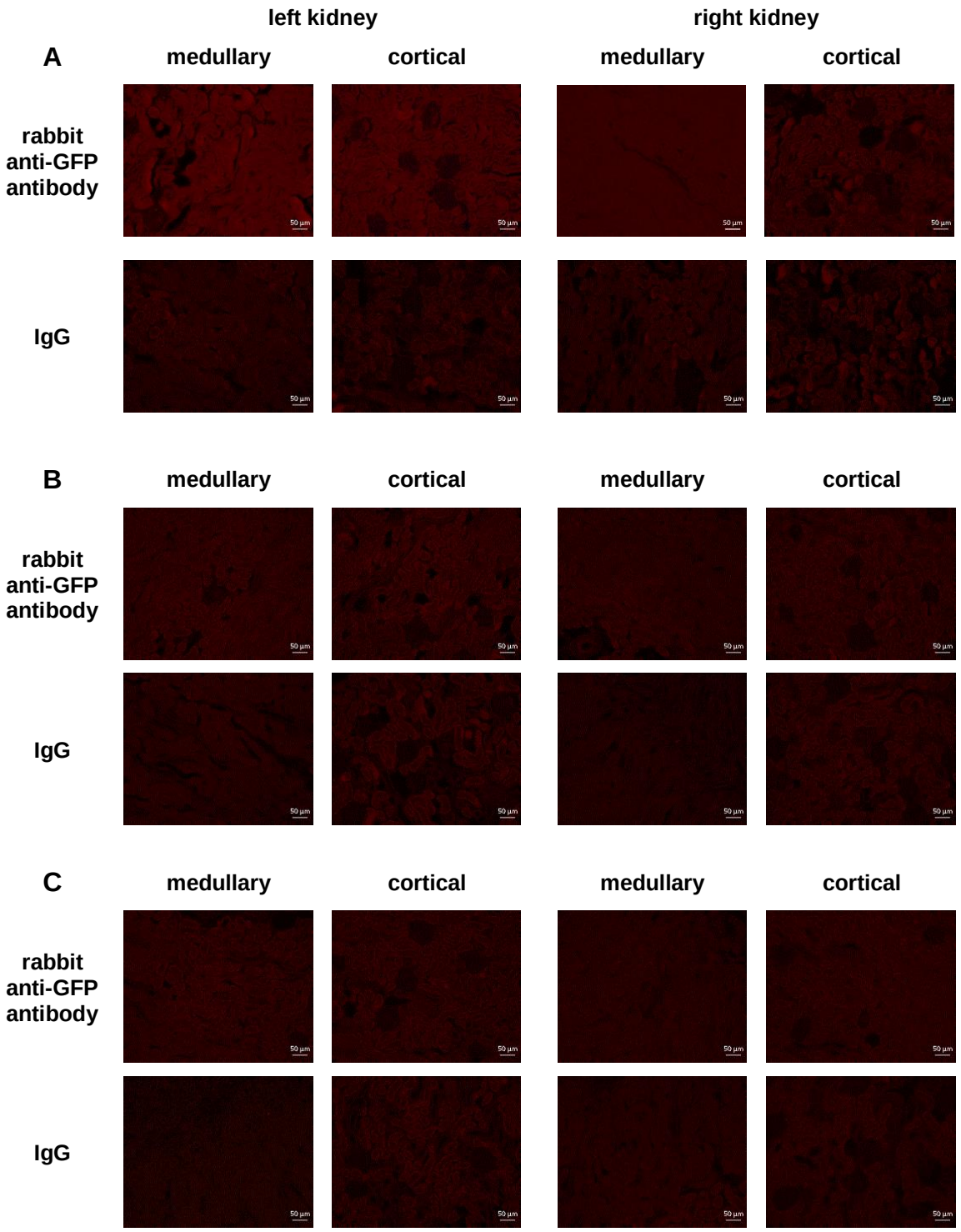

Figure 3-4 Representative images of visualisation of GFP with fluorescence IHC (rabbit anti-GFP primary antibody) in medullary and cortical regions of left and right kidneys from UMGD treatment rats from study 1.

(A) UMGD treatment rat 1, **(B)** UMGD treatment rat 2, and **(C)** UMGD treatment rat 3 kidneys were incubated with rabbit anti-GFP primary antibody (top panels) or rabbit IgG (bottom panels) and goat anti-rabbit Alexa Flour 555 secondary antibody to visualise GFP in the medullary and cortical regions of the left kidneys (left panel) and right kidneys (right panel). All images were taken at 20x magnification. Scale bar represents 50 µm.

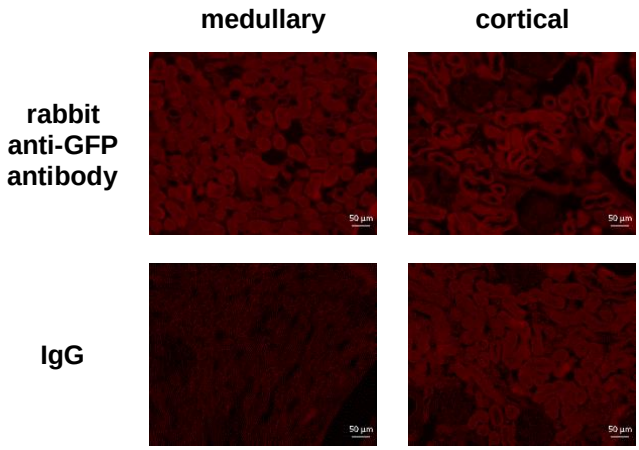

Figure 3-5 Representative images of visualisation of GFP with fluorescence IHC (rabbit anti-GFP primary antibody) in medullary and cortical regions of a kidney from the negative control rat from study 1.

Kidney sections were incubated with rabbit anti-GFP primary antibody (top panels) or rabbit IgG (bottom panels) and goat anti-rabbit Alexa Flour 555 secondary antibody to visualise GFP in the medullary (left panel) and cortical (right panel) regions. All images were taken at 20x magnification. Scale bar represents 50 µm.

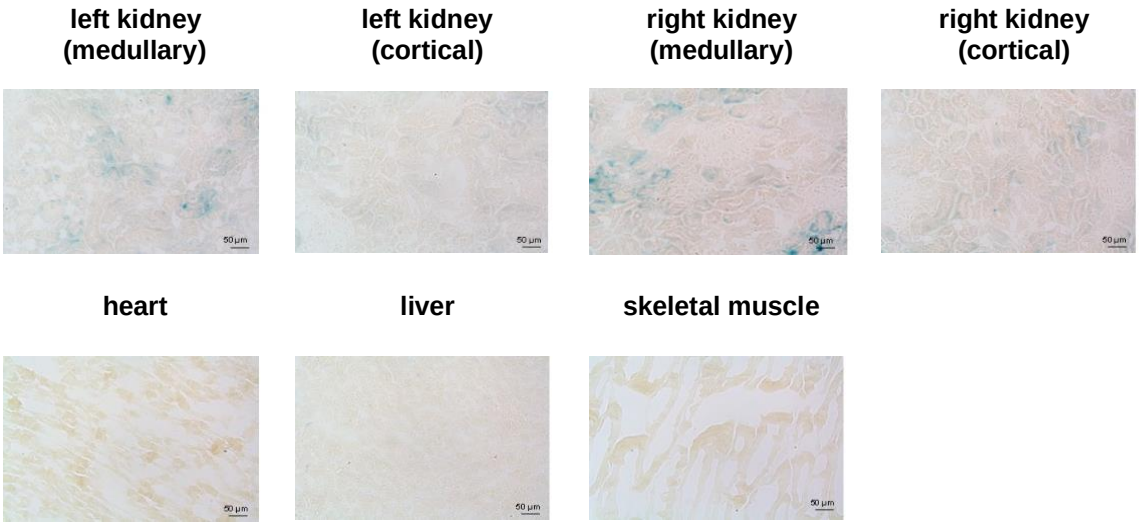

Figure 3-6 Representative images of visualisation of LacZ by X-Gal staining of β-gal in tissues from a UMGD treatment rat from study 1.

Tissue sections were incubated with X-Gal stain overnight. All images were taken at 20x magnification. Scale bar represents 50 µm.

3.4.1.2.2 Study 2

Although loss of volume from dead space was accounted for, 90% of the intended plasmid DNA and MB dose (previously published dose successfully used in mice (Browning et al., 2011)) was administered due to loss of volume unaccounted for by air bubble removal. Fluorescence IHC was used to examine GFP and LacZ protein expression and SYBR qPCR was used to examine GFP mRNA expression.

Evaluation of GFP in the medullary and cortical regions of the left and right kidneys of UMGD treatment rats following incubation with a rabbit anti-GFP primary antibody revealed low levels of fluorescence similar to incubation with an IgG control, providing evidence of unsuccessful GFP gene transfer (Figure 3-7). Non-targeted negative control kidneys from the positive control rat and negative control rat showed no detection of GFP (Figure 3-8). Unsuccessful gene transfer was further supported by lack of fluorescence in left and right kidneys of a UMGD treatment rat and control rats following addition of Sudan Black B to the IHC protocol to quench tissue auto fluorescence (Figure 3-9). Evaluation of LacZ gene transfer by examining ß-gal protein expression with IHC using a rabbit anti-ß-gal primary antibody showed similar levels of fluorescence with IgG controls and between both kidneys in a UMGD treatment rat and the negative control rat (Figure 3-10), suggesting lack of gene transfer.

Two custom GFP primer pairs were designed to detect mRNA expression of LGFP, a chemically synthesised allele of GFP expressed by the plasmid. Amplification with LGFP1 and LGFP2 showed detection of GFP in the right and left kidney of all three UMGD treatment rats (Appendix Table 8-1). LGFP1 was not detected in the kidneys of the negative control rat and plasmid only sample, while LGFP2 was detected in both the left and right kidney of the negative control rat and plasmid only sample (Appendix Table 8-1), indicating detection of contamination. The housekeeper ß-actin was stably expressed across both kidneys from all rats (Appendix Table 8-2).

SYBR qPCR products were sized on an agarose gel. No clear bands were visible in samples amplified with the LGFP1 primer pair, where the expected fragment size was 88 bp (Figure 3-11). Faint bands ~100 bp were visible in samples amplified with the LGFP2 primer pair, matching the expected fragment size of 76 bp (Figure 3-11). SYBR qPCR product sequences aligned to the LGFP1 and

LGFP2 template sequences (Figure 3-12). This demonstrates presence of GFP in SYBR qPCR products from the right kidney of a UMGD treatment rat and the left kidney of the negative control rat, providing evidence of contamination during tissue processing.

Given the issues with analysing reporter gene expression of pVIVO2-GFP/LacZ, future *in vivo* UMGD studies employed luciferase plasmid vectors, routinely used in UMGD studies (Browning et al., 2011, Browning et al., 2012, Shen et al., 2008, Song et al., 2011). Also, in all future studies, loss of volume from the plasmid DNA and MB suspension arising from both dead space and removal of air bubbles was taken into consideration.

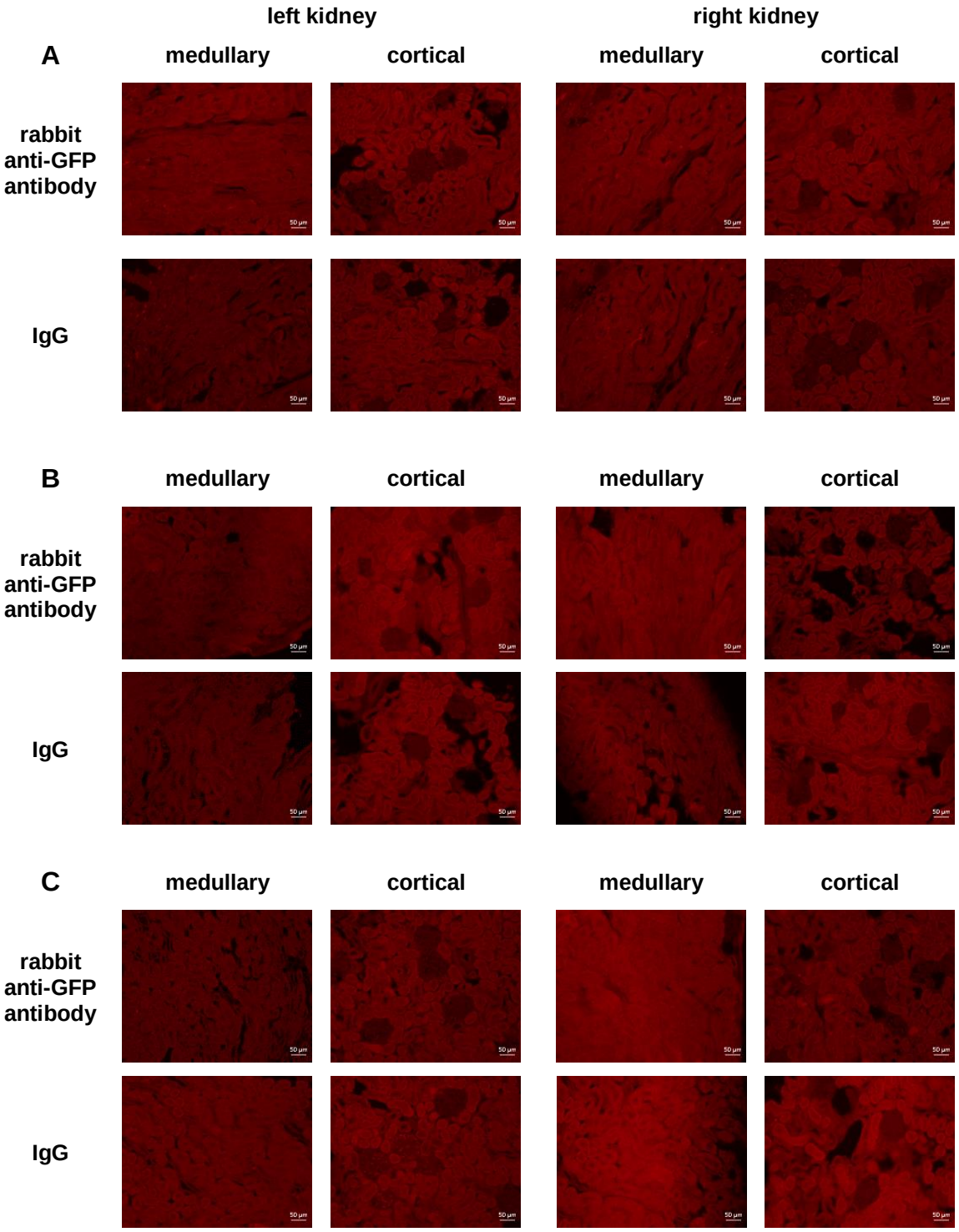

Figure 3-7 Representative images of visualisation of GFP with fluorescence IHC (rabbit anti-GFP primary antibody) in medullary and cortical regions of left and right kidneys from UMGD treatment rats from study 2.

(A) UMGD treatment rat 1, **(B)** UMGD treatment rat 2, and **(C)** UMGD treatment rat 3 kidneys were incubated with rabbit anti-GFP primary antibody (top panels) or rabbit IgG (bottom panels) and goat anti-rabbit Alexa Flour 555 secondary antibody to visualise GFP in the medullary and cortical regions of the left kidneys (left panel) and right kidneys (right panel). All images were taken at 20x magnification. Scale bars represent 50 µm.

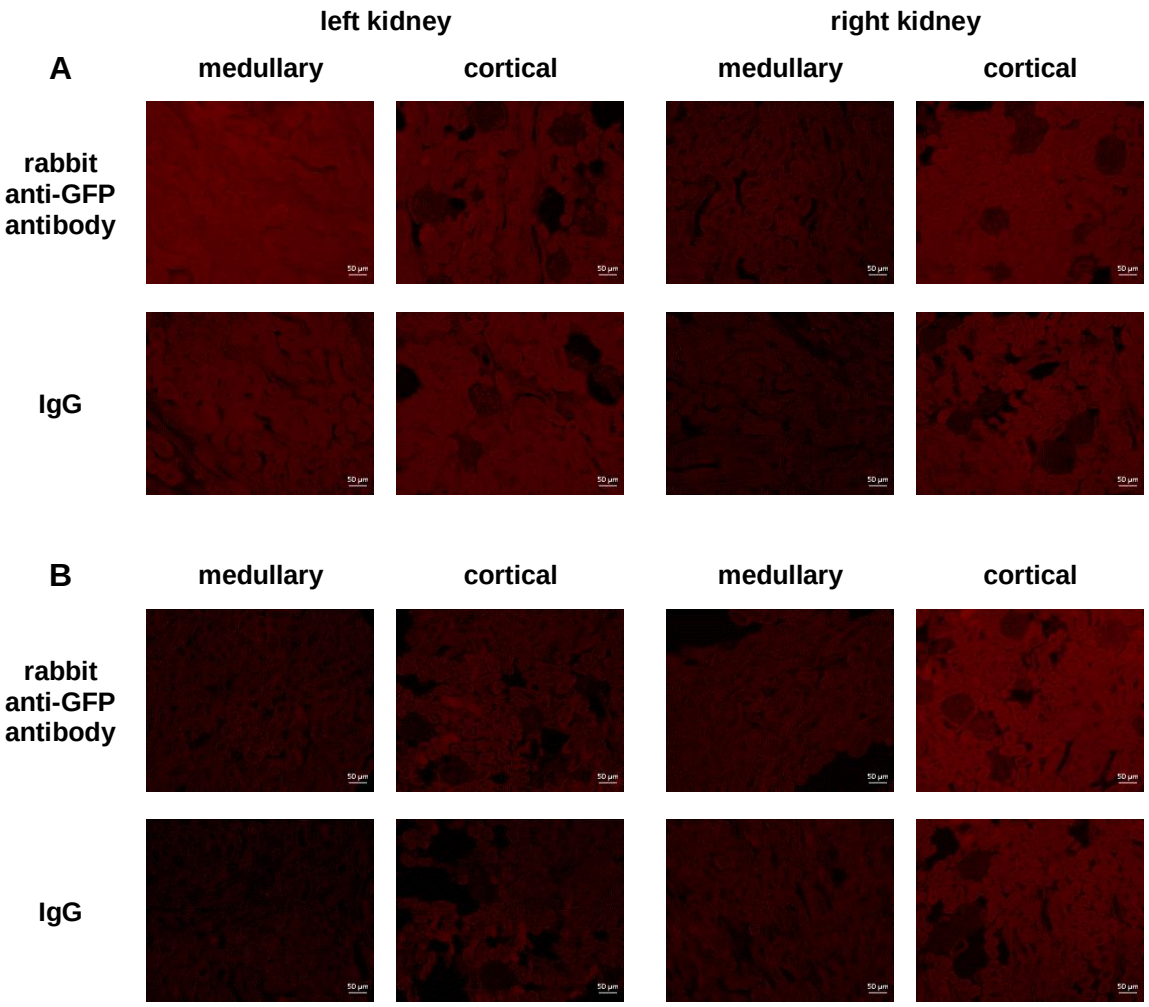

Figure 3-8 Representative images of visualisation of GFP with fluorescence IHC (rabbit anti-GFP primary antibody) in medullary and cortical regions of left and right kidneys from control rats from study 2.

(A) Negative control rat and **(B)** positive control rat kidneys were incubated with rabbit anti-GFP primary antibody (top panels) or rabbit IgG (bottom panels) and goat anti-rabbit Alexa Flour 555 secondary antibody to visualise GFP in the medullary and cortical regions of the left kidneys (left panel) and right kidneys (right panel). All images were taken at 20x magnification. Scale bars represent 50 µm.

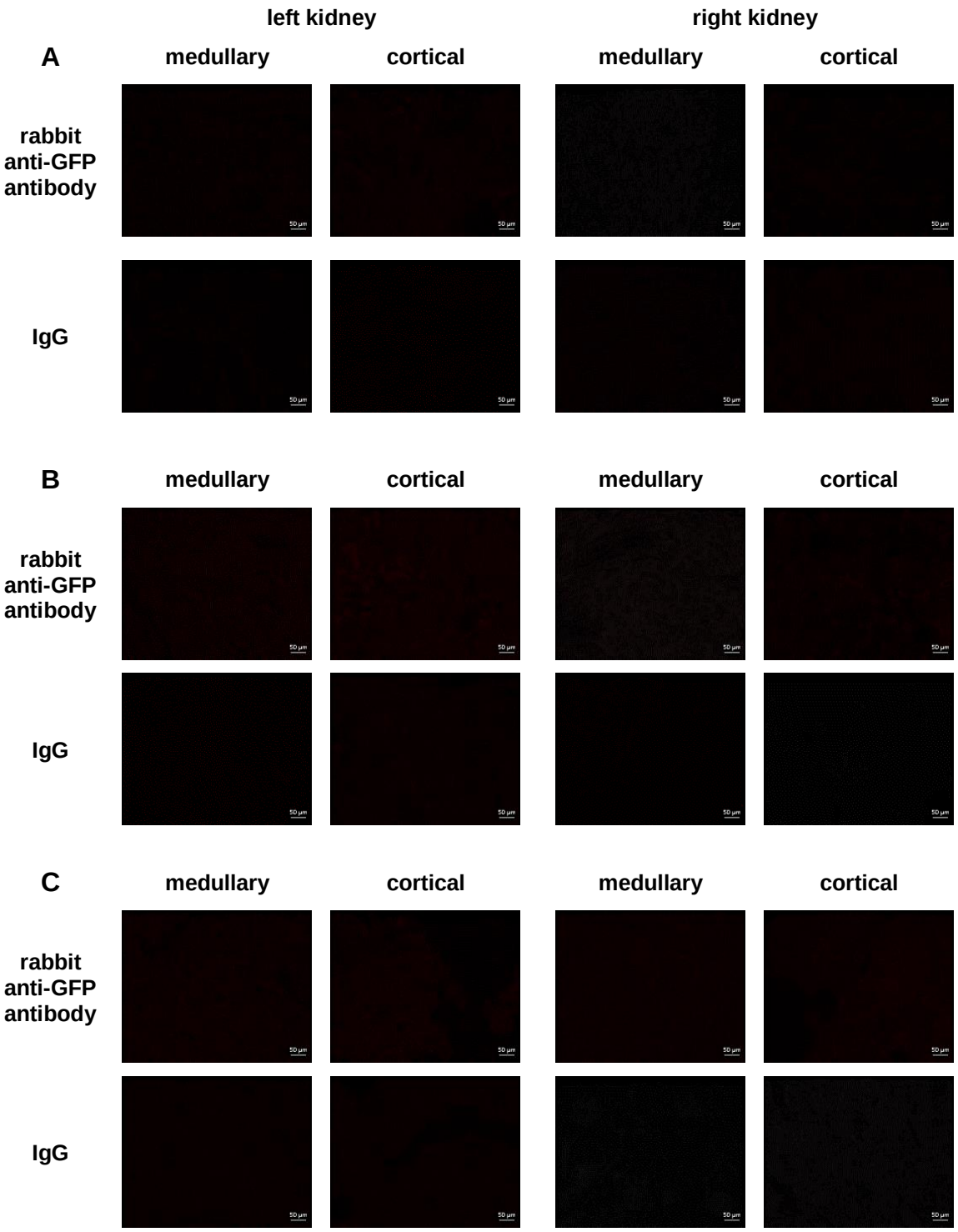

Figure 3-9 Representative images of visualisation of GFP with fluorescence IHC (rabbit anti-GFP primary antibody and 0.1% Sudan Black B) in medullary and cortical regions of left and right kidneys from UMGD treatment rats from study 2.

(A) UMGD treatment rat, **(B)** negative control rat, and (**C)** positive control rat kidneys were incubated with rabbit anti-GFP primary antibody (top panels) or rabbit IgG (bottom panels) and goat anti-rabbit Alexa Flour 555 secondary antibody followed by Sudan Black B treatment to visualise GFP in the medullary and cortical regions of the left kidneys (left panel) and right kidneys (right panel). All images were taken at 20x magnification. Scale bars represent 50 µm.

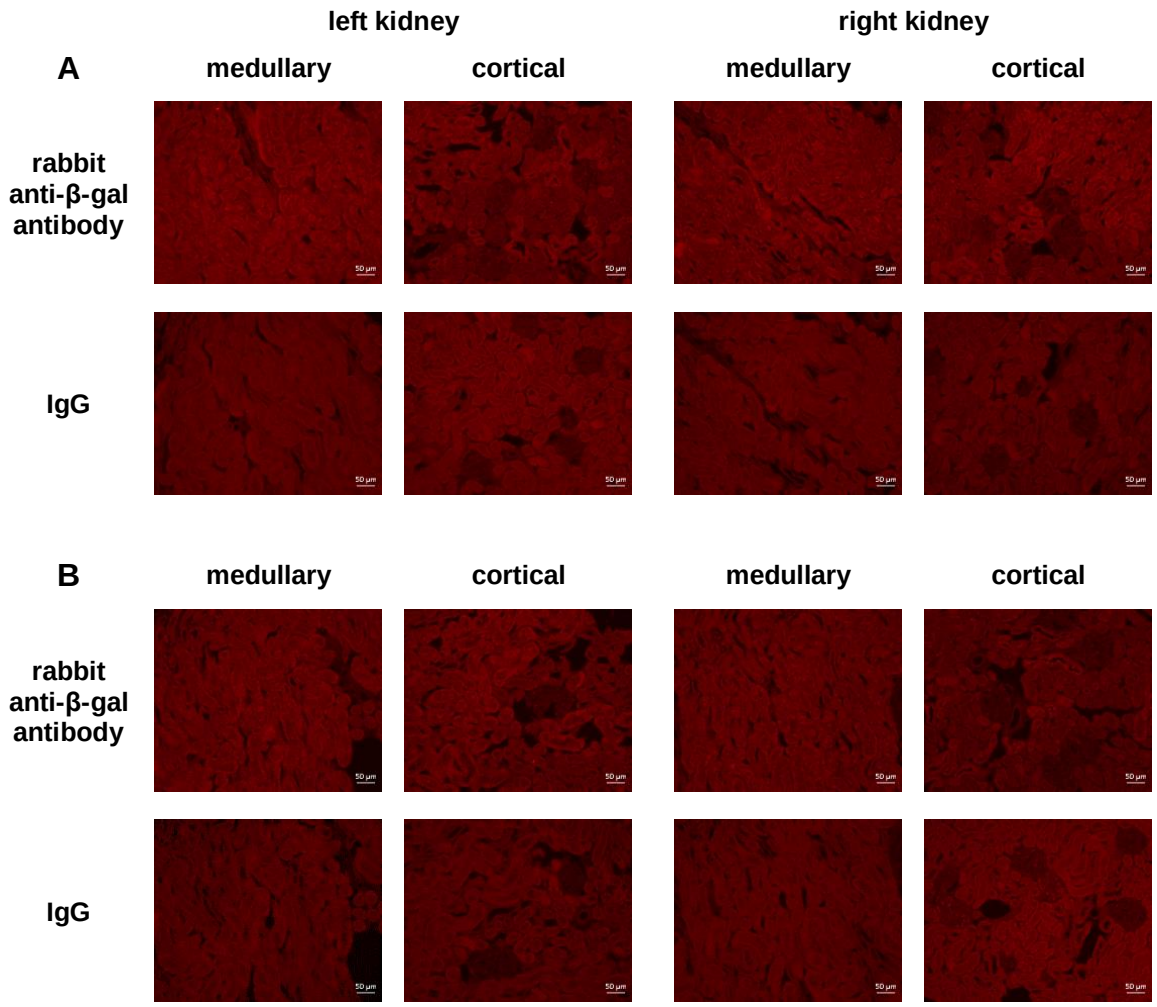

Figure 3-10 Representative images from visualisation of β-gal (LacZ) with fluorescence IHC (rabbit anti-β-gal primary antibody) in medullary and cortical regions of left and right kidneys from a UMGD treatment rat and the negative control rat from study 2.

(A) UMGD treatment rat and **(B)** negative control rat kidneys were incubated with rabbit anti-β-gal primary antibody (top panels) or rabbit IgG (bottom panels) and goat anti-rabbit Alexa Flour 555 secondary antibody to visualise β-gal (LacZ) in the medullary and cortical regions of the left kidneys (left panel) and right kidneys (right panel). All images were taken at 20x magnification. Scale bars represent 50 µm.

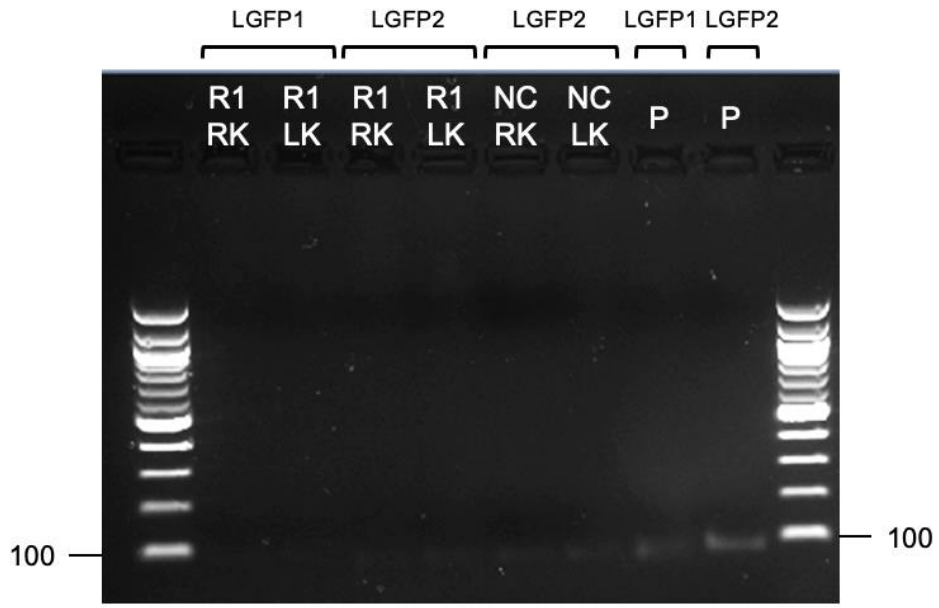

Figure 3-11 SYBR RT-qPCR products amplified with LGFP1 and LGFP2 primer pairs visualised on an agarose gel.

cDNA from SYBR RT-qPCR products of samples amplified with LGFP1 and LGFP2 was loaded at 100 ng per lane and sized on a 1.5% agarose gel, using a 100 bp DNA ladder; sizes indicated in bp. Samples from UMGD treatment rat 1 (R1) right kidney (RK) and left kidney (LK) amplified with LGFP1 (lane 1 and 2) and LGFP2 (lane 3 and 4), the negative control rat (NC) right kidney (RK) and left kidney (LK) amplified with LGFP2 (lane 5 and 6), and pVIVO2-GFP/LacZ plasmid (P) amplified with LGFP1 (lane 7) and LGFP2 (lane 8).

Figure 3-12 Chromatogram of sequences of SYBR RT-qPCR products aligned to LGFP1 and LGFP2 template sequences.

After PCR purification, SYBR RT-qPCR products were sequenced by GATC Biotech and aligned to LGFP1 and LGFP2 template sequence using CLC Sequence Viewer. Highlighted in yellow: LGFP1 and sequences of the forward and reverse primer and highlighted in green: LGFP2 and sequence of the forward primer. Blue arrows indicate orientation of primers. Samples from UMGD treatment rat 1 right kidney amplified with LGFP1 and LGFP2 and the negative control rat left kidney amplified with LGFP2.

3.4.2 UMGD optimisation studies delivering luciferase plasmids to the left kidney in rats and mice

3.4.2.1 Purification of pGL4.13

pGL4.13, a 4641 bp vector expressing *luc2* (modified Photinus Pyralis luciferase gene) was selected for *in vivo* UMGD targeting of the left kidney in rats. In order to assess the efficiency of the purification of pGL4.13 and plasmid conformation of isolated pGL4.13, samples from stages of the purification procedure and the final plasmid product were run on an agarose gel. In the cleared lysate (lane L), a band ~5000 bp indicates plasmid DNA was enriched in the lysate (Figure 3-13). No bands in the flow-through fraction (lane F) and final wash fraction (lane W2) demonstrates plasmid DNA efficiently bound to the column and degraded RNA was removed (Figure 3-13). Finally, presence of a band ~5000 bp in the elute (lane E) and plasmid only samples (lane P1 and P2) shows supercoiled plasmid DNA was purified (Figure 3-13).

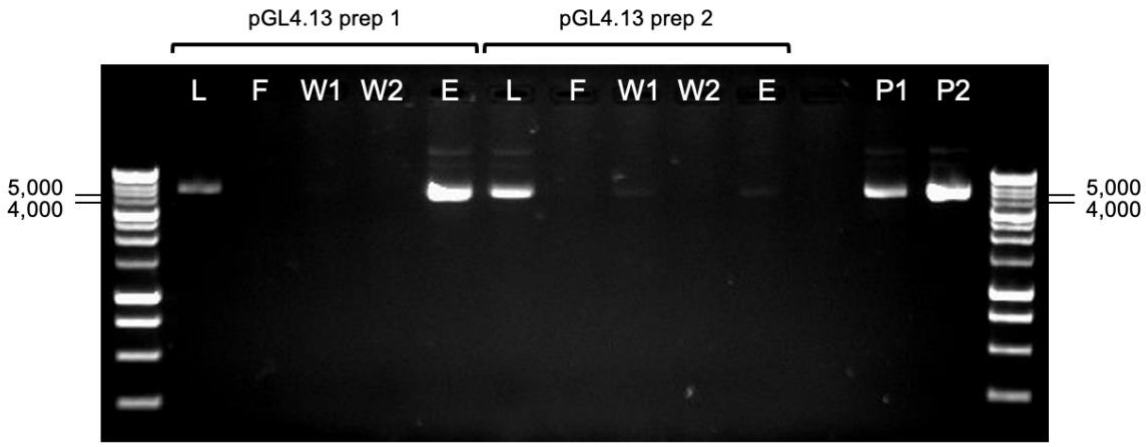

Figure 3-13 Representative agarose gel image of samples from stages of purification of pGL4.13 plasmid mega preps.

pGL4.13 plasmid was isolated from *E. coli* mega preps during which samples were collected to assess the stages of the purification procedure and confirm isolation of plasmid DNA. Up to 10 µL of the sample or 250 ng of DNA was loaded per lane and sized on a 1% agarose gel, using a 1 kb DNA ladder; sizes indicated in bp. Lane L: cleared lysate, lane F: flow-through fraction, lanes W1 and W2: wash fractions, lane E: elute, lane P1: pGL3 plasmid from prep1, lane P2: pGL3 plasmid from prep 2.

3.4.2.2 *In vivo* UMGD of pGL4.13 to the left kidney in rats

3.4.2.2.1 Study 3

In the previous UMGD studies, volumes of plasmid DNA and MBs administered were based on doses previously administered to mice (Browning et al., 2011). In this study, to account for a ~6-fold greater total blood volume in rats compared with mice (JHU, 2020), the plasmid DNA and MB suspension volume was increased by 2.5-fold, restricted by the maximum 500 µL volume of an IV bolus dose in rats. Luciferase and protein assays were used to examine luciferase activity and TaqMan qPCR was used to assess luciferase mRNA expression.

Luciferase activity greater than background activity was not detected in the target left kidney of any of the three UMGD treatment rats, indicating lack of luciferase gene transfer to the target organ (Figure 3-14). Luciferase activity was detected in the skeletal muscle of the positive control rat (156.39±22.38 CPS/µg of protein), demonstrating naked pGL4.13 plasmid delivery to skeletal muscle by IM injection (Figure 3-14).

Evaluation of luciferase mRNA expression with TaqMan qPCR was not possible. Although luciferase Ct values were undetermined in multiple negative controls (NFW and MM controls), luciferase was detected in the no RT negative control (Appendix Table 8-3). Ct values of ß-actin in the same no RT wells were undetermined (Appendix Table 8-3), suggesting plasmid DNA contamination. RNA extraction was repeated with prolonged DNase treatment to promote digestion of plasmid DNA and remove contamination. Luciferase was still detected across all negative controls while ß-actin was undetected (Appendix Table 8-4), suggesting plasmid DNA contamination from a source external to the samples. Due to contamination issues with custom qPCR probes, the pGL3 plasmid was selected for subsequent studies since the standard TaqMan® Gene Expression Assay for luciferase maps to *luc*+, the modified luciferase gene encoded by the vector, permitting evaluation of reporter gene mRNA expression.

Given the volume restrictions of an intravenous (IV) bolus dose in rats, all subsequent *in vivo* UMGD studies were conducted in mice in order to administer the same doses of plasmid DNA and MBs which had been shown to be successful in a previous published study in mice (Browning et al., 2011).

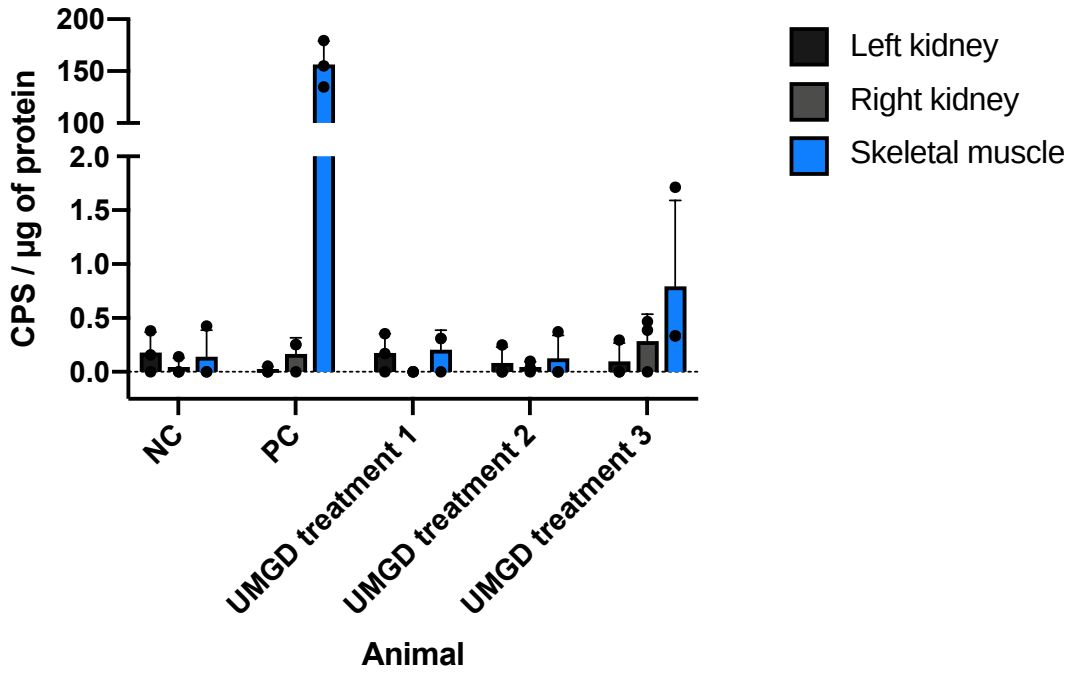

Figure 3-14 Luciferase activity in left and right kidneys and skeletal muscle of three UMGD treatment rats and the positive and negative control rats from study 3.

Luciferase activity in tissues from UMGD treatment and control rats three days after *in vivo* gene delivery experiment. UMGD treatment rats were administered an IV injection of pGL4.13 and MB suspension followed by 2 min of US exposure to the left kidney. The positive control rat received an IM injection of pGL4.13 and MB suspension. The negative control rat received an IV injection of PBS followed by 2 min of US exposure to the left kidney. Luciferase activity was measured in counts per second (CPS) and normalised to protein content. Data are shown as mean CPS/µg of protein±SD, n=1 tissue sample run in triplicate.

3.4.2.3 Purification of pGL3

pGL3, a 5256 bp vector expressing a modified Photinus Pyralis luciferase gene *luc*+, was selected for *in vivo* UMGD targeting the left kidney in mice. To assess efficiency of purification and isolated pGL3 plasmid conformation, samples from stages of the purification procedure and the final plasmid product were run on an agarose gel. Although no bands are visible in the cleared lysate (lane L), flow-through fraction (lane F), and wash fraction (lane W), two distinct bands in the elute (lane E) and final plasmid samples (lane P1 and P2) provide evidence that pGL3 was isolated (Figure 3-15). The lower band ~6000 bp suggests linear plasmid DNA was purified (Figure 3-15). To determine whether the upper band present above the DNA ladder represented bacterial chromosomal DNA contamination or open-circular plasmid DNA detection (Figure 3-15), restriction digest was performed. Digestion of pGL3 plasmid prep 1 with a single restriction enzyme, XhoI or BglII, produced a band ~6000 bp, indicating presence of linearised pGL3 plasmid rather than bacterial chromosomal DNA contamination (Figure 3-16). pGL3 plasmid prep 2 did not digest to completion (Figure 3-16). Presence of multiple bands and a light smear suggested potential chromosomal DNA contamination (Figure 3-16), and the prep was therefore discarded.

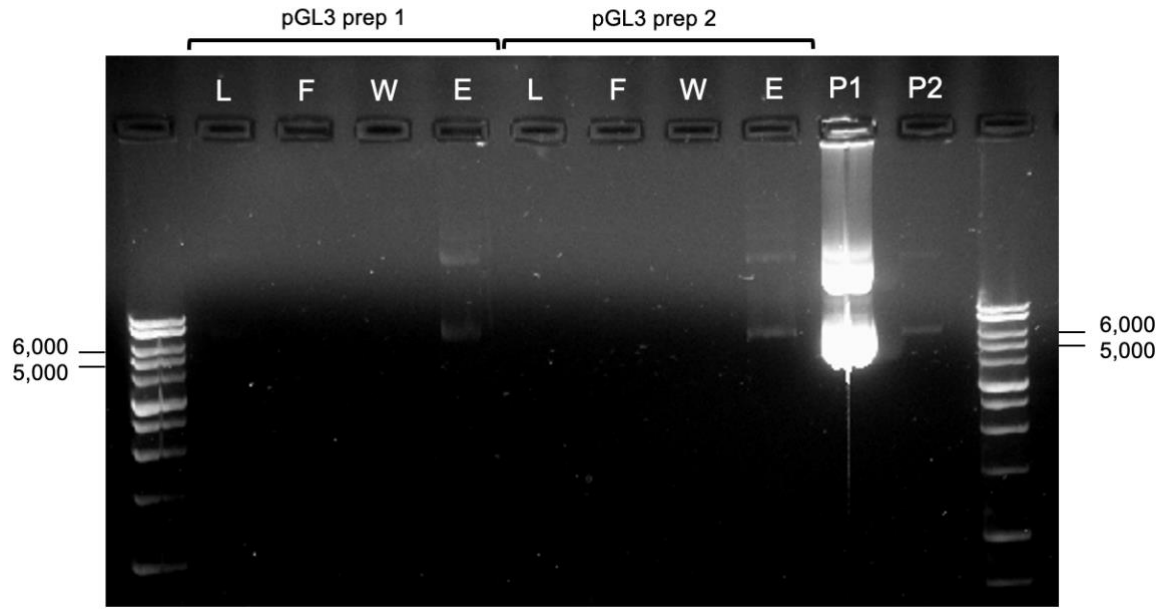

Figure 3-15 Representative agarose gel image of samples from stages of purification of pGL3 plasmid mega preps.

pGL3 plasmid was isolated from *E. coli* mega preps during which samples were collected to assess the stages of the purification procedure and confirm isolation of plasmid DNA. Up to 10 µL of the sample or 250 ng of DNA was loaded per lane and sized on a 1% agarose gel, using a 1 kb DNA ladder; sizes indicated in bp. Lane L: cleared lysate, lane F: flow-through fraction, lane W: wash fraction, lane E: elute, lane P1: pGL3 plasmid from prep1, lane P2: pGL3 plasmid from prep 2.

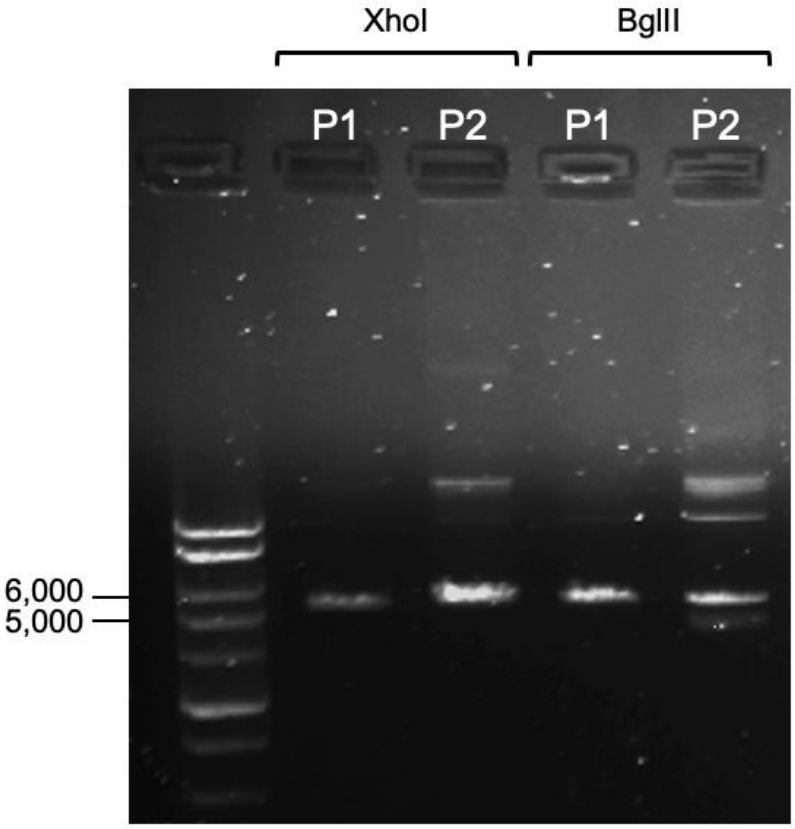

Figure 3-16 Restriction digest of pGL3 plasmid preps with XhoI and BglII restriction enzymes.

Single digested pGL3 plasmid DNA from two separate plasmid mega preps. DNA was loaded at 250 ng per lane and sized on a 0.8% agarose gel, using a 1kb DNA ladder; sizes indicated in bp Lane P1: prep 1 digested plasmid DNA and lane p2: prep 2 digested plasmid DNA.

3.4.2.4 *In vivo* UMGD of pGL3 to the left kidney in mice

3.4.2.4.1 Study 4

In contrast to all previous *in vivo* UMGD studies in this chapter, this study was conducted in mice, using the same doses of plasmid DNA and MBs administered to mice in a past study (Browning et al., 2011). Gene transfer of luciferase was assessed by measuring luciferase activity with luciferase and protein assays and mRNA expression with TaqMan qPCR.

A low level of luciferase activity was detected in the target left kidney of UMGD treatment mouse 1 (1.07±0.53 CPS/μg of protein), higher than background luciferase activity in the negative control mouse left kidney (0.19±0.18 CPS/μg of protein) and right kidney (0.74±0.71 CPS/μg of protein), suggesting low levels of gene transfer (Figure 3-17). The highest level of luciferase activity was seen in the skeletal muscle of the positive control mouse (241.39±10.56 CPS/μg of protein) (Figure 3-17).

Evaluation of luciferase mRNA expression with TaqMan qPCR showed luciferase Ct values were undetermined across all samples (Appendix Table 8-5). This suggests low levels of luciferase activity in the target left kidney of a treatment mouse may have reflected detection of background activity rather than gene transfer. ß-actin was stably expressed, and both luciferase and ß-actin were undetected in all negative controls (Appendix Table 8-6).

Given the lack of gene transfer when targeting the left kidney, it was decided that subsequent studies would utilise the heart as a surrogate organ. The heart was selected since this was the organ successfully targeted in the past study (Browning et al., 2011) which formed the basis of the *in vivo* protocols developed for UMGD studies in this chapter.

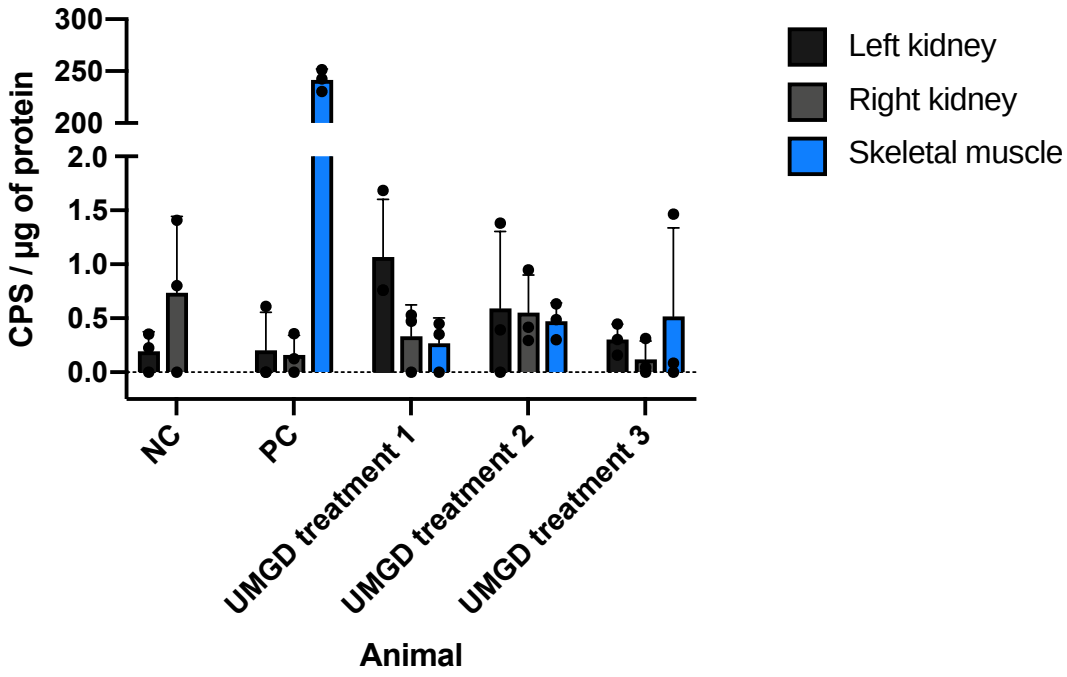

Figure 3-17 Luciferase activity in left and right kidneys and skeletal muscle of three UMGD treatment mice and the positive and negative control mice from study 4.

Luciferase activity in tissues from UMGD treatment and control mice three days after *in vivo* gene delivery experiment. UMGD treatment mice were administered an IV injection of pGL3 and MB suspension followed by 2 min of US exposure to the left kidney. The positive control mouse received an IM injection of pGL3. The negative control mouse received an IV injection of PBS followed by 2 min of US exposure to the left kidney. Luciferase activity was measured in counts per second (CPS) and normalised to protein content. Data are shown as mean CPS/µg of protein±SD, n=1 tissue sample run in triplicate.

3.4.3 UMGD optimisation studies delivering luciferase plasmids to mouse hearts

3.4.3.1 *In vivo* UMGD of pGL3 to mouse hearts

The same UMGD protocol previously established in mice (Browning et al., 2011) was utilised in the following two studies (Study 5 and Study 6) in terms of target organ, injection site, and dose of plasmid DNA and MBs. However, pGL3 was utilised in place of pGL4.13 to permit evaluation of luciferase mRNA expression with a standard TaqMan® Gene Expression Assay. Gene transfer of luciferase was also assessed by luciferase and protein assays which measure luciferase activity.

3.4.3.1.1 Study 5

Evaluation of luciferase mRNA expression with TaqMan qPCR was not possible due to background noise. Although the ß-actin housekeeper was stably expressed across samples and Ct values were undetermined in negative controls (Appendix Table 8-8), luciferase detected in the heart samples from the three UMGD treatment mice and skeletal muscle of the positive control mouse was comparable to non-target tissue (Appendix Table 8-7). TaqMan qPCR was subsequently run in singleplex and duplex to assess if primer interactions may have contributed to noise, but similar results were obtained (Appendix Table 8-9). In all future *in vivo* UMGD studies, evaluation of gene transfer at the mRNA level was not conducted.

Low levels of luciferase activity were detected in the heart of UMGD treatment mouse 1 (2.56±1.95 CPS/µg of protein), mouse 2 (0.66±0.73 CPS/µg of protein), and mouse 3 (2.05±2.08 CPS/µg of protein), compared to background luciferase activity in the heart of the positive control mouse (0.56±0.85 CPS/µg of protein) and negative control mouse (0.53±0.57 CPS/µg of protein) (Figure 3-18). Highest luciferase activity was detected in the skeletal muscle of the positive control mouse (21.2±5.90 CPS/µg of protein) (Figure 3-18). However, luciferase activity in the skeletal muscle of treatment mouse 1 (1.86±1.05 CPS/µg of protein) and mouse 3 (1.42±0.36 CPS/µg of protein) was higher than background activity in the skeletal muscle of the negative control mouse (0.57±0.70 CPS/µg of protein) (Figure 3-18), suggesting low levels detected in the hearts of UMGD treatment mice perhaps reflecting background luciferase activity rather than providing evidence of gene transfer.

Due to the large variation in expression levels between samples from a single tissue, tissue samples (representing technical replicates) were analysed ungrouped i.e., the mean and SD of individual tissue samples were summarised rather than the mean and SD of tissue samples when grouped. Analysis of heart tissue samples ungrouped revealed samples one and two of UMGD treatment mouse 1 (4.37±1.05 and 2.81±0.34 CPS/µg of protein, respectively) and sample three of UMGD treatment mouse 3 (4.45±0.29 CPS/µg of protein) had luciferase activity higher than background levels in the heart samples of the negative control mouse, with highest background activity in heart sample one of the negative control mouse (1.19±0.52 CPS/µg of protein) (Figure 3-19A), suggesting a low level of gene transfer in several heart samples. Heart tissue samples one and two of UMGD treatment mouse 1 and sample three of UMGD treatment mouse 3 also had luciferase activity higher than the non-targeted skeletal muscle of these UMGD mice, with highest background activity in skeletal muscle sample one of UMGD treatment mouse 1 and 3 (2.65±0.82 and 1.72±0.78 CPS/µg of protein, respectively) (Figure 3-19B), further suggesting a low level of gene transfer in these heart tissue samples. Due to large variations between heart tissue samples and gene transfer potentially detected in only several samples, hearts were dissected into atria and ventricles when analysing the tissue in subsequent experiments.

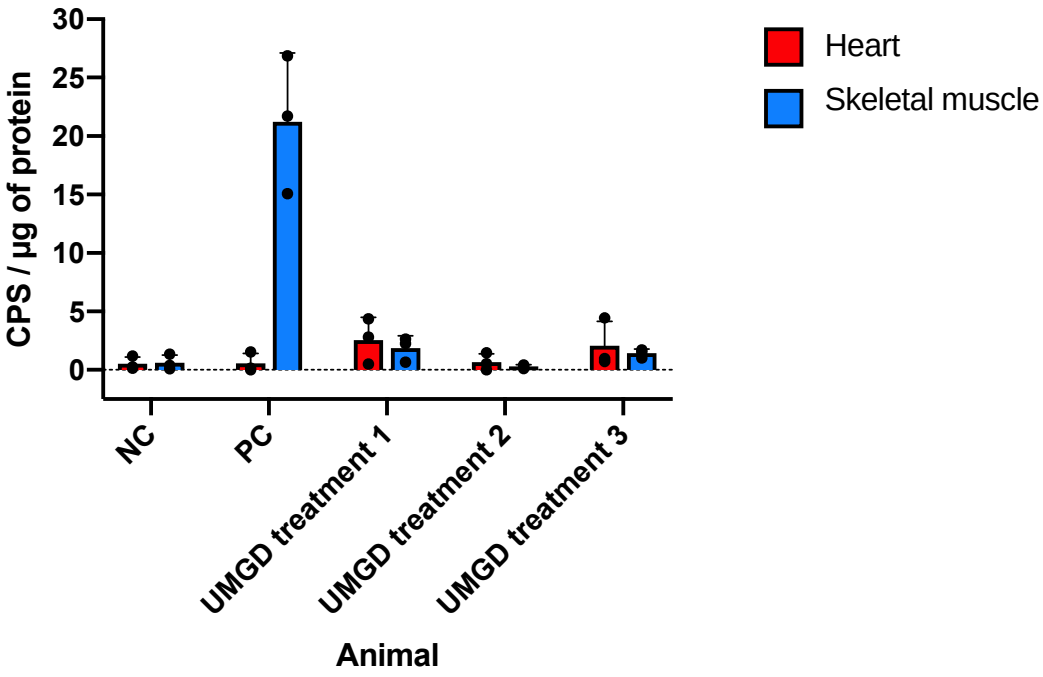

Figure 3-18 Luciferase activity in hearts and skeletal muscle of three UMGD treatment mice and the positive and negative control mice from study 5.

Luciferase activity in tissues from UMGD treatment and control mice three days after *in vivo* gene delivery experiment. UMGD treatment mice were administered an IV injection of pGL3 and MB suspension followed by 2 min of US exposure to the heart. The positive control mouse received an IM injection of pGL3. The negative control mouse received an IV injection of PBS followed by 2 min of US exposure to the heart. Luciferase activity was measured in counts per second (CPS) and normalised to protein content. Data are shown as mean CPS/µg of protein±SD, n=3 tissue samples run in triplicate.

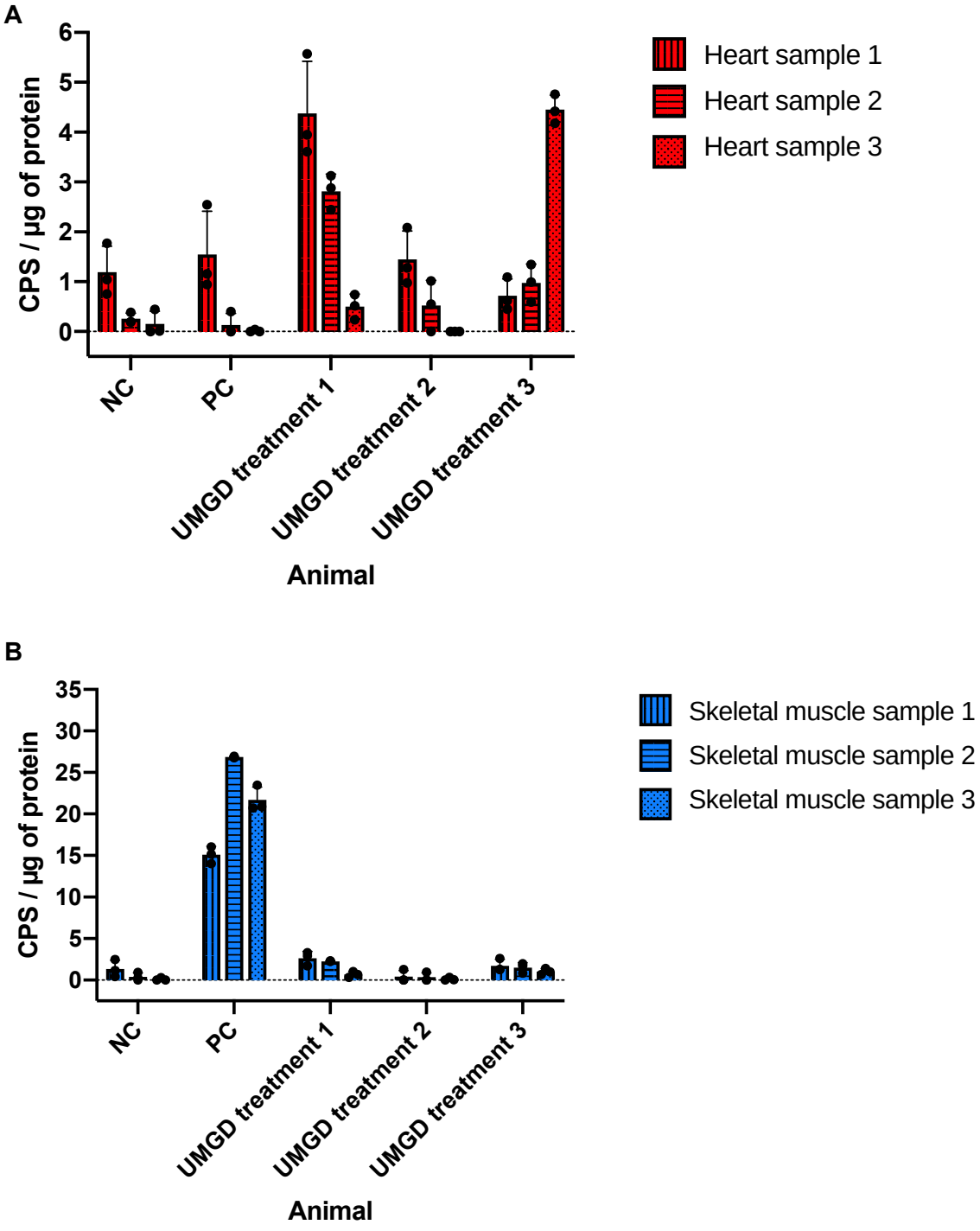

Figure 3-19 Luciferase activity in ungrouped samples of hearts and skeletal muscle of three UMGD treatment mice and the positive and negative control mice from study 5.

(A) Heart and **(B)** skeletal muscle samples ungrouped from UMGD treatment and control mice three days after *in vivo* gene delivery experiment. UMGD treatment mice were administered an IV injection of pGL3 and MB suspension followed by 2 min of US exposure to the heart. The positive control mouse received an IM injection of pGL3. The negative control mouse received an IV injection of PBS followed by 2 min of US exposure to the heart. Luciferase activity was measured in counts per second (CPS) and normalised to protein content. Data are shown as mean CPS/µg of protein±SD, n=1 tissue sample run in triplicate.

3.4.3.1.2 Study 6

A high level of luciferase activity was evident in the atria of UMGD treatment mouse 2 (14.6±19.5 CPS/µg of protein), greater than luciferase activity in the skeletal muscle of the positive control mouse (6.17±4.51 CPS/µg of protein) and background activity in the atria of the negative control mouse (7.77±2.79 CPS/µg) (Figure 3-20), providing evidence of gene transfer. Luciferase activity in the ventricles of UMGD treatment mouse 1 (1.04±0.20 CPS/µg of protein) and mouse 3 (6.43±5.84 CPS/µg of protein) was higher than background activity in the ventricles (0.49±0.05 CPS/µg of protein) but lower than background activity the atria (7.77±2.79 CPS/µg) of the negative control mouse (Figure 3-20), suggesting detection of background luciferase activity rather than gene transfer. Low levels of luciferase activity were detected in the skeletal muscle of treatment mouse 1 (1.03±0.13 CPS/µg of protein), higher than background luciferase in the negative control mouse skeletal muscle (0.88±0.13 CPS/µg of protein) but notably lower than luciferase activity in the positive control mouse skeletal muscle (6.17±4.51 CPS/µg of protein) (Figure 3-20).

Due to large variability in the atria, ventricles, and skeletal muscle, tissue samples (representing technical replicates) were analysed ungrouped. Analysis of ventricle samples ungrouped, showed that luciferase activity in sample two of UMGD treatment mouse 3 (19.9±0.66 CPS/µg of protein) was higher than any of atria or ventricle samples of the negative control mouse (Figure 3-21A), providing evidence of gene transfer. Analysis of atria samples ungrouped showed that sample three of UMGD treatment mouse 2 (55.2±28.2 CPS/µg of protein) had more than 3-fold higher luciferase activity than any of the four atria samples of the negative control mouse (5.48±0.70, 6.10±1.44, 14.4±1.14, and 5.05±4.33 CPS/µg of protein), suggesting gene transfer (Figure 3-21B). The remaining atria samples from UMGD treatment mouse 2 showed lower luciferase activity than any of the atria samples from the negative control mouse (Figure 3-21B).

With evidence of gene transfer to the heart, the subsequent proof-of-concept study employed the *in vivo* UMGD protocol used in these studies. However, despite analysing the ventricles and atria separately, variability within the tissue was still evident. Hence, the tissue protein extraction protocol was optimised for the proof-of-concept study.

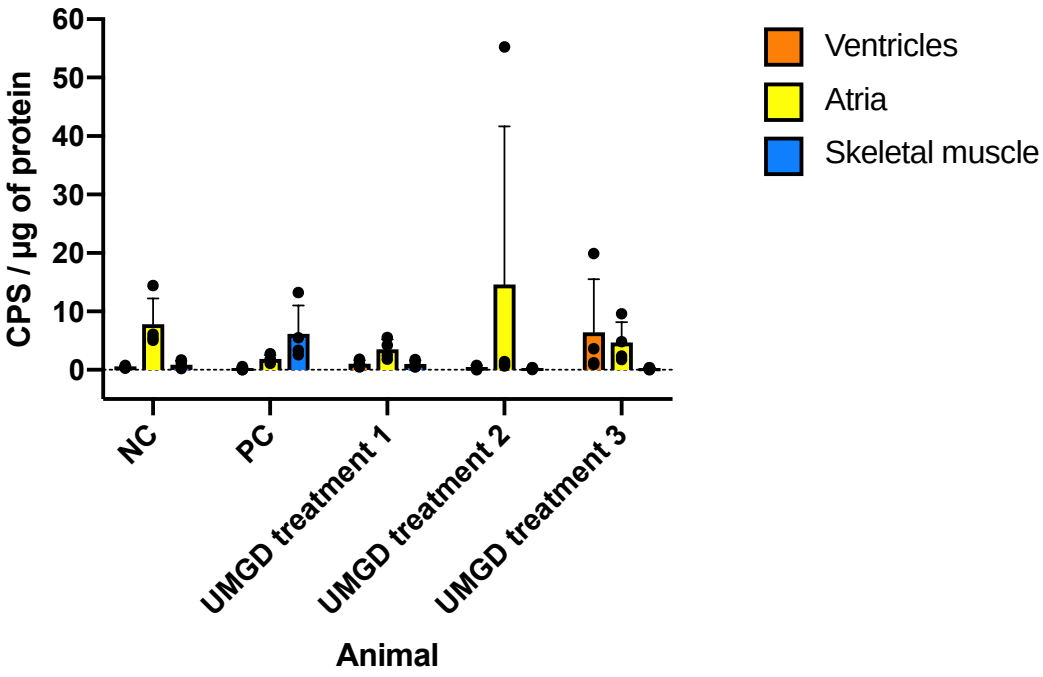

Figure 3-20 Luciferase activity in ventricles, atria, and skeletal muscle of three UMGD treatment mice and the positive and negative control mice from study 6.

Luciferase activity in tissues from UMGD treatment and control mice three days after *in vivo* gene delivery experiment. UMGD treatment mice were administered an IV injection of pGL3 and MB suspension followed by 2 min of US exposure to the heart. The positive control mouse received an IM injection of pGL3 and MB suspension. The negative control mouse received an IV injection of PBS and MBs followed by 2 min of US exposure to the heart. Luciferase activity was measured in counts per second (CPS) and normalised to protein content. Data are shown as mean CPS/µg of protein±SD, n=1 tissue sample run in triplicate.

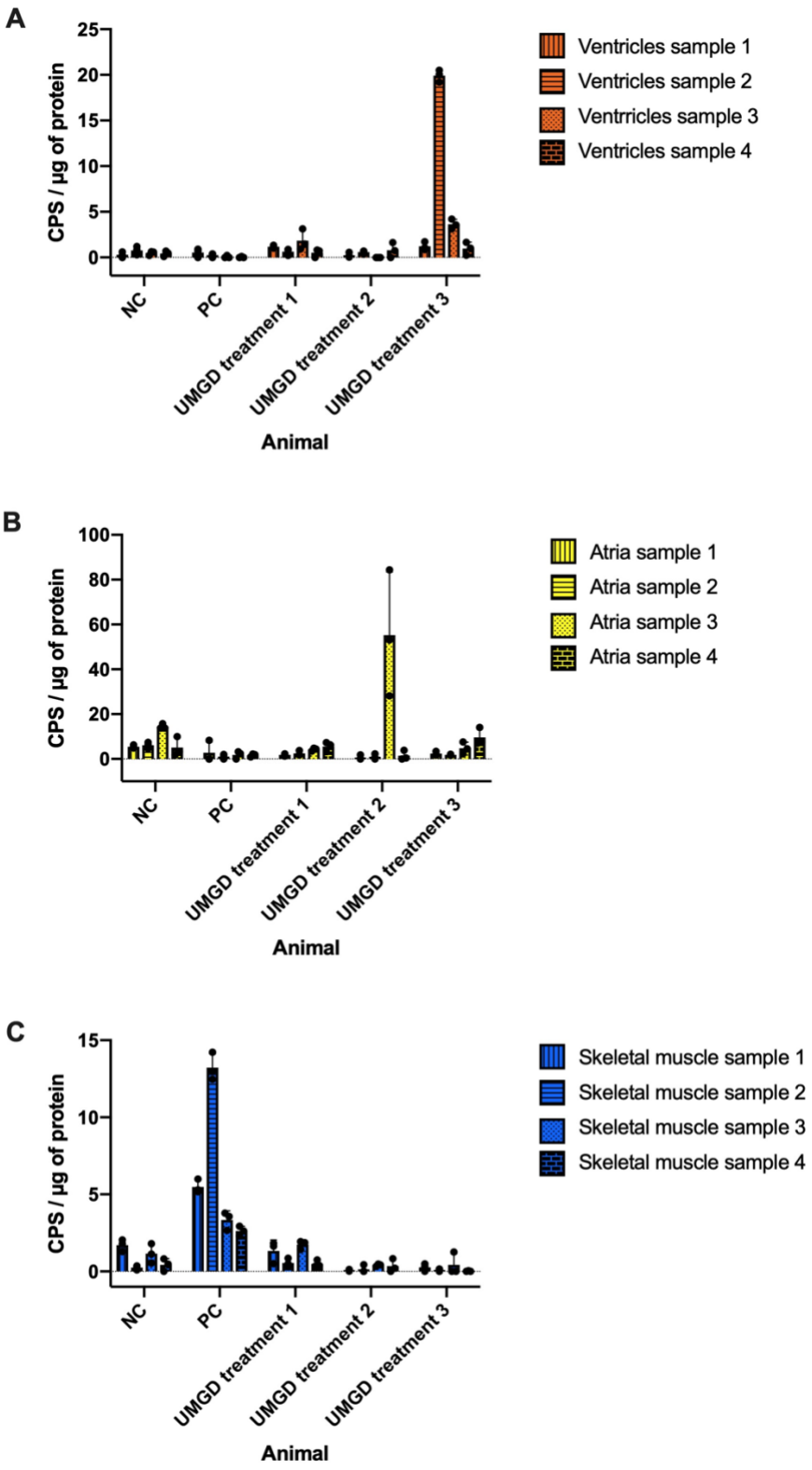

Figure 3-21 Luciferase activity in ungrouped samples of ventricles, atria, and skeletal muscle of three UMGD treatment mice and the positive and negative control mice from study 6.

(A) Ventricles, **(B)** atria, and **(C)** skeletal muscle samples ungrouped from UMGD treatment and control mice three days after *in vivo* gene delivery experiment. UMGD treatment mice were administered an IV injection of pGL3 and MB suspension followed by 2 min of US exposure to the heart. The positive control mouse received an IM injection of pGL3 and MB suspension. The negative control mouse received an IV injection of PBS and MBs followed by 2 min of US exposure to the heart. Luciferase activity was measured in counts per second (CPS) and normalised to protein content. Data are shown as mean CPS/µg of protein±SD, n=1 tissue sample run in triplicate.

3.5 Discussion

In this chapter, optimisation studies led to development of an *in vivo* UMGD protocol demonstrating evidence of luciferase gene transfer to mouse hearts, which can be subsequently utilised to demonstrate proof-of-concept. These optimisation studies provided unique insights into specific aspects that can be amended in future UMGD studies to further enhance gene transfer.

UMGD optimisation studies utilising pVIVO2-GFP/LacZ failed to provide evidence of gene transfer. Despite being designed for *in vivo* use, several features of the plasmid hindered its utility and may have contributed to a lack of gene transfer. pVIVO2-GFP/LacZ was consistently purified in an open-circular conformation, indicating damage to the plasmid (Schleef and Schmidt, 2004). If damage occurred within transcriptional units, this may have reduced its efficiency. In addition, its relatively large size compared to luciferase reporter vectors may have hindered its ability to enter cells. Previous *in vitro* studies investigating UMGD mechanisms show pore size plays a role in cellular uptake of plasmid DNA (Fan et al., 2013) and other molecules (Mehier-Humbert et al., 2005), with larger molecules showing poorer uptake. In terms of analysing reporter gene expression, consistent contamination in RT-qPCR experiments hindered use of the method to evaluate mRNA expression. Fluorescence IHC to examine protein expression also presented several limitations, with non-specific antibody binding and tissue autofluorescence producing high background signals. Skeletal muscle was selected as a positive control due to ease of and past experience with IM delivery of plasmid DNA; however, its use as a positive control hindered evaluation of different antibodies, antibody dilutions, and blocking conditions since IHC requires organ specific optimisation. Furthermore, evaluating gene transfer in tissue sections reduced the likelihood of detecting reporter genes since only a planar section of the kidney was targeted. This was due to stationary positioning of the 15L8 linear array probe, which emits a planar beam profile. Finally, endogenous LacZ in rat kidneys (Bolon, 2008) potentially masked evidence of gene transfer. These optimisation studies highlight the importance of considering the size of the plasmid and types of reporter genes and their required analysis for future UMGD studies.

UMGD optimisation study 3 employing the pGL4.13 plasmid to target the left kidney in rats also failed to demonstrate gene transfer. This may have arisen partially due to the footprint size of the 15L8 probe. A past study in canines reported significantly greater gene transfection with a planar unfocused transducer with a beam diameter of 52 mm compared to a focused transducer with a 13 mm diameter (Noble et al., 2013). Although a sweeping motion was performed to target a larger area as described in previous studies (Song et al., 2011, Tran et al., 2019), the size of the 15L8 probe and its beam profile may not be sufficient to trigger UMGD in rat organs compared to smaller mouse organs when utilising similar parameters (Browning et al., 2011). Unfocused transducers can exhibit larger US fields than focused transducers, in turn corresponding with greater UMGD treatment areas when held stationary. Nonetheless, studies comparing unfocused and focused transducers keeping US, plasmid DNA, and MB conditions closely matched have found no significant difference in gene transfer levels (Song et al., 2011, Tran et al., 2019). Moreover, large animal studies have demonstrated successful gene transfer utilising commercial US probes with focused transducers (Babischkin et al., 2019, Bez et al., 2018). Hence, the 15L8 probe may induce UMGD in rats but this requires adapting protocol parameters. Another factor that may have contributed to a lack of gene transfer was the dose administered, which was lower than the dose previously administered to mice (Browning et al., 2011). Due to the volume restrictions of an IV bolus dose, translating the protocol between species may therefore not only require optimising the dose but also administration method.

UMGD optimisation study 4 targeting the left kidney in mice showed evidence of gene transfer at low levels close to background in contrast to the distinctly higher levels in mouse hearts seen in a previously published study on which the protocol was based (Browning et al., 2011). Several key differences in the protocol may have contributed to low levels observed, including targeting the kidney rather than the heart. SonoVue is a transpulmonary contrast agent rapidly cleared through the lungs. In humans administered the maximum clinical dose, more than 80% of SonoVue was exhaled within 2 min (EMA, 2008b), and, in rats administered SonoVue via the femoral vein, non-enhanced imaging was observed after 70 s (Liu et al., 2013). Thus, UMGD to the kidney may be less efficient than delivery to the heart due to involvement of the pulmonary first-pass effect with

venous administration of the plasmid and MB suspension. This is further corroborated by findings from a previous study that examined different administration routes for UMGD to the kidney reporting significantly greater gene transfer when administering plasmid and MBs via the renal artery in comparison with the tail vein (Chen et al., 2012a). In UMGD studies, improved transfection efficiencies with arterial rather than venous administration have further been shown in the heart (Liu et al., 2015) and skeletal muscle (Christiansen et al., 2003), indicating arterial administration is potentially a superior method in terms of gene transfer efficiency. However, arterial administration has shown to cause more tissue damage in part arising from entrapment of larger MBs not cleared by the pulmonary circulation in arterioles and capillary networks (Lindner et al., 2002). In addition, cannulation of mouse and rat arteries normally requires temporary inhibition of blood flow and is therefore more invasive. With non-invasive venous administration therefore persisting as the preferred route of administration, future studies should account for loss of MB dose due to the first-pass effect.

There was evidence of transfer of the luciferase reporter gene with UMGD to mouse hearts, reflecting gene transfer seen in previous studies utilising similar protocol parameters (Browning et al., 2011, Browning et al., 2012). Although transfer levels were higher than the levels observed in UMGD optimisation studies targeting the kidney, large variability was evident in gene transfer levels. A key source of variability was the administration route, namely the tail vein injections. Although the tail was warmed prior to injections, IV placement was challenging, particularly given the relatively large size of needle gauge employed. A 25 G needle was utilised based on a previous study showing a 25 G needle significantly improved gene transfer compared to needles with a larger gauge (i.e. smaller internal diameter) due to a lower pressure gradient and less shear stress in needles with a larger diameter (Browning et al., 2011). In addition, viscosity of the suspension due to the plasmid concentration often caused the vein to collapse resulting in blanching of the tail. When multiple attempts were required, this led to loss of volume and visible alteration in MB characteristics due to the additional time required to administer the suspension. Challenges with tail vein injections hindered the reproducibility of the technique, supported by evidence of gene transfer seen in two of the three

UMGD treatment mice in this study. In turn, for the proof-of-concept study, only animals in which a full volume was administered without requiring multiple attempts were included.

In this chapter, although optimisation studies largely produced negative results, they were important for the progression to a proof-of-concept study. Initial optimisation studies allowed issues to be identified and logical modifications to be made to the protocol. The *in vivo* protocol developed in this chapter was applied to a minimum of n=3 UMGD treatment animals to demonstrate proof-of-concept in the following chapter.

Chapter 4 UMGD to mouse hearts and placenta

4.1 Introduction

Safe and effective delivery systems targeting the placenta remain central to the development of placental gene therapy for pregnancy-related disorders. Despite the translational progress of adenoviral-mediated delivery of VEGF for the treatment of FGR (Spencer et al., 2017), its invasive nature and safety concerns highlight the need for alternative strategies. Investigations by other research groups seeking to target the placenta with adenoviral vectors also highlight the safety issues associated with viral vectors. In pregnant rabbits, intraplacental injection of Ad-LacZ led to high transgene expression in the labyrinth zone of the placenta without histological changes (Keswani et al., 2015). While there was no evidence of gene transfer in the heart, ovary, or lung, off-target gene transfer was detected in the liver and spleen (Keswani et al., 2015). In the same study, although adenoviral insulin-like growth factor-1 (IGF-1) therapy restored foetal weight in a rabbit model of placental insufficiency, administration of the vector required invasive laparotomy surgery (Keswani et al., 2015). A separate group investigated distribution of a mutant adenoviral vector containing the Arg-Gly-Asp (RGD) peptide sequence (Ad-RGD), a sequence shown to promote cell entry (Mizuguchi et al., 2001), following tail vein administration in pregnant C57BL/6J mice (Katayama et al., 2011). In comparison to the WT vector, Ad-RGD induced significant and sustained transgene expression in the placenta (Katayama et al., 2011). Ad-RGD transduced foetal placental cells, and no transgene expression was found in the embryo. However, off-target gene transfer was evident in the liver, spleen, kidney, lung, heart, and colon of pregnant mothers (Katayama et al., 2011). While the high transfer efficiency of adenoviral vectors underpins their common use in preclinical investigations, the concern for off-target expression supports the development of non-viral strategies for targeting the placenta.

Two *in vivo* studies have investigated intraplacental injections of non-viral vectors as a strategy for placental gene therapy. It has been postulated that intraplacental injections could be safely conducted in humans with US guidance (Krishnan and David, 2017). In comparison with viral vectors, where intraplacental administration can induce foetal gene transfer (Woo et al., 1997, Türkay et al., 1999), studies have shown naked plasmid DNA does not cross the placenta unless delivered as part of a complex (Gaensler et al., 1999, Efremov

et al., 2010). In contrast, a study in a mouse model of surgically induced FGR showed complexes consisting of a polymer and plasmid DNA expressing human IGF-1 under the control of trophoblast-specific promoters (Cyp19a or PLAC1) achieved targeted placenta delivery (Ellah et al., 2015). IGF-1 appeared to be localised to the placenta, with no expression detected in control placentas from the opposite uterine horn as well as foetal liver samples, although other maternal tissue was not evaluated (Ellah et al., 2015). Furthermore, there was no evidence of inflammation or immune infiltration with intraplacental delivery of PLAC1-hIGF-1 complexes, which promoted a significant increase in pup birthweight similar to that of healthy controls (Ellah et al., 2015). A study in L-NAME induced PE-like rats showed intraplacental injection of agomir-126 caused a significant increase in miR-126 expression in treatment rats compared with non-treated PE rats (Yan et al., 2014). Expression of the miRNA in non-targeted tissue and foetuses was not evaluated, making it unknown whether placenta-specific and in turn foetal gene transfer occurs with intraplacental delivery of chemically modified oligonucleotides. Nonetheless, miR-126 treatment led to significantly greater foetal and placental weights, placental microvessel density, and proportion of live pups (Yan et al., 2014). However, blood pressure was not significantly influenced, and urinary protein data were not shown, indicating maternal complications were not resolved. While this study highlights the potential of modulating placental miRNAs as a gene therapy strategy in PE, further investigations are warranted due to lack of a therapeutic benefit in the mother. Overall, the risk of foetal gene transfer and invasive nature of intraplacental injections limits the utility of this technique for clinical translation. A non-invasive and non-viral delivery system which specifically targets the placenta would be the ideal method.

To address the need for placental-specific delivery, King et al. evaluated the ability of tumour-homing peptides (CGKRK or CRGDKGPDC) to target the placenta (King et al., 2016). FAM-labelled peptides administered via the tail vein to pregnant BALB/c mice accumulated in the labyrinth and decidual spiral arteries (King et al., 2016). Although the peptides were not seen in the heart, brain, liver, spleen, or lungs of dams, they were detected in the kidney (King et al., 2016). Liposomes were subsequently decorated with the peptides and administered via the tail vein to pregnant C57BL/6J mice (King et al., 2016).

Peptide-decorated liposomes were seen in the labyrinth and spiral arteries as well as maternal clearance organs (liver, spleen, and kidney) but notably absent from the maternal brain, heart, and lung as well as foetal tissue (King et al., 2016). In a subsequent study, the therapeutic potential of placental homing peptide-miRNA inhibitor conjugates was evaluated (Beards et al., 2017). First, an unconjugated scramble miRNA inhibitor was administered intravenously to pregnant C57BL/6J mice; the inhibitor was present in the placenta (labyrinth, junctional zone, and decidua) and in maternal tissue (heart, liver, kidney, and uterus) but absent from foetal organs (Beards et al., 2017). It had no significant effect on median foetal or placental weights, foetal-placental weight ratio, litter size, and the number of resorptions, suggesting it was well-tolerated (Beards et al., 2017). A miR-145 inhibitor and miR-675 inhibitor were then separately conjugated to a CGKRK peptide and administered intravenously to pregnant C57BL/6J mice; miR-145 and miR-675 have previously shown to alter trophoblast properties *in vitro* and found to be dysregulated in patients with PE and FGR (Gao et al., 2012, Hromadnikova et al., 2015a, Farrokhnia et al., 2014). While the miR-675 inhibitor conjugate significantly reduced placental miR-675 expression and significantly increased median placental weight compared to controls, the miR-145 inhibitor conjugate had no significant effect on placental miR-145 expression and median placental weight (Beards et al., 2017). Both conjugates had no significant effect on litter size or foetal resorptions, suggesting they were well-tolerated in the pregnant mice (Beards et al., 2017). However, off-target expression seen with the peptide-decorated liposomes and unconjugated scramble miRNA inhibitor demonstrates the difficulty in achieving targeted placental delivery with non-invasive gene therapy strategies.

UMGD in conjunction with a plasmid vector represents a non-viral and non-invasive method for targeted gene transfer. To date, a single published study has employed UMGD for targeting the placenta, with investigations conducted in a baboon model of impaired uterine artery remodelling to assess the role of VEGF in mediating the process (Babischkin et al., 2019). At multiple time points throughout gestation, cationic MBs conjugated to a plasmid encoding a VEGF isoform and GFP were administered for 10 min via a saphenous vein infusion during which the placental basal plate was exposed to US via a 2-6 MHz 6C2 transducer (B-mode output, 5-second burst pulses, and 1.9 MI) (Babischkin et al.,

2019). UMGD restored VEGF levels in EVTs (distal anchoring villi, cytotrophoblastic shell, and uterine arteries) and normalised the extent of remodelling in uterine arteries to that seen in healthy pregnant baboons (Babischkin et al., 2019). While the study demonstrates VEGF plays a key role in regulating trophoblast invasion and uterine artery remodelling in a non-human primate pregnancy, non-targeted maternal and foetal tissue were not analysed for transgene expression. Site-specific gene transfer with UMGD therefore remains essential for ensuring safety in the clinical translation of this research. In this chapter, a proof-of-concept study was conducted in non-pregnant mice utilising the heart as a surrogate organ to demonstrate tissue-specific gene transfer. The *in vivo* UMGD protocol developed in Chapter 3 (study 6) was utilised for the proof-of-concept heart study; however, pGL4.13 was used in place of pGL3 since pGL4 vectors harbour a synthetically engineered luciferase gene, *luc2*, that displays greater luciferase expression compared to pGL3 vectors (Promega, 2015). Subsequently, the UMGD protocol was applied to target the placenta of pregnant mice.

4.2 Hypothesis and aims

4.2.1 Hypothesis

UMGD induces tissue-specific gene transfer *in vivo*, representing a potentially non-viral and non-invasive gene delivery system for targeting the placenta.

4.2.2 Aims

- To show the *in vivo* UMGD protocol induces tissue-specific gene transfer of a reporter gene in a surrogate organ in a proof-of-concept study through hypothesis testing.

- To apply the *in vivo* UMGD protocol to pregnant rodents in an exploratory study to demonstrate placental-specific gene transfer of an expression vector.

4.3 Methods

All animal work was performed in accordance with the United Kingdom Animals (Scientific Procedures) Act 1986 under the authority of Home Office Licence 70/9021. All animals were housed and maintained as detailed in section 2.3. The proof-of-concept UMGD study was conducted in CD-1 mice targeting the heart. The UMGD protocol was then applied to pregnant CD-1 mice to target the placenta. Virgin CD-1 females were mated with C57BL/6J stud males, with two females housed with one male per cage for 3 d. Females were examined for coital plug and also examined by US on gestational day (GD) 12.5-14.5 to confirm pregnancy. The number of mice recruited and those excluded and included in the proof-of-concept heart study and placenta study are shown in Figure 4-1 and Figure 4-2, respectively. Only mice in which the full volume of injection suspension was administered without requiring multiple attempts were included in the study analysis. A minimum of n=3 was selected for the treatment group in the proof-of-concept heart study to enable inferential analysis for hypothesis testing. A minimum of n=1 was selected for the treatment group in the placenta study due to the exploratory nature of the research; however, n=12 females were time mated to account for lack of breeding. Non-pregnant mice were excluded from the placenta study, and in turn, used in the proof-of-concept heart study (Figure 4-1 and Figure 4-2). An n=1 for the negative control and positive control groups was chosen in both studies as this represents the minimum number required to interpret the results from the treatment groups in each study. Formal randomisation and blinding were not performed; the order of experimental groups was decided prior to experiments, (negative control, UMGD, and then positive control group) to avoid contamination in negative control animals. No a prior criteria were used when randomly selecting animals from the cage. Mice were sacrificed 3 d after UMGD (GD 15.5-17.5), and target and non-target organs were snap frozen for evaluation of reporter gene transfer by analysis of enzymatic activity.

4.3.1 Plasmid DNA preparation for *in vivo* use

4.3.1.1 Plasmid DNA purification

Plasmid DNA was transformed into competent MAX Efficiency™ DH5α™ Competent Cells as detailed in section 2.1.2.1. Glycerol stocks were prepared as a long-term stock as detailed in section 2.1.2.2. pGL4.13 was purified by filtration using the Invitrogen™ PureLink™ HiPure Expi Plasmid Megaprep Kit (ThermoFisher, Vilnus, Lithuania) as detailed in section Plasmid DNA with an A260/A280 ratio of ~1.8 was accepted as 'pure' DNA as detailed in section 2.1.2.7.

4.3.1.2 Analytical gel of samples from plasmid DNA purification

Samples from stages of the plasmid DNA purification were precipitated as detailed in section 2.1.2.5. Samples were run on a 1% agarose gel as detailed in section 2.1.3 to assess efficiency of the purification procedure, specifically: growth and lysis conditions, efficiency of column loading, plasmid DNA binding, removal of RNA, and contamination. Purified plasmid DNA was run on the same analytical gel to confirm isolation of plasmid DNA, lack of contamination in the final product, and conformation of the plasmid. Only plasmid DNA considered 'pure' and confirmed as uncontaminated was used for subsequent *in vivo* procedures.

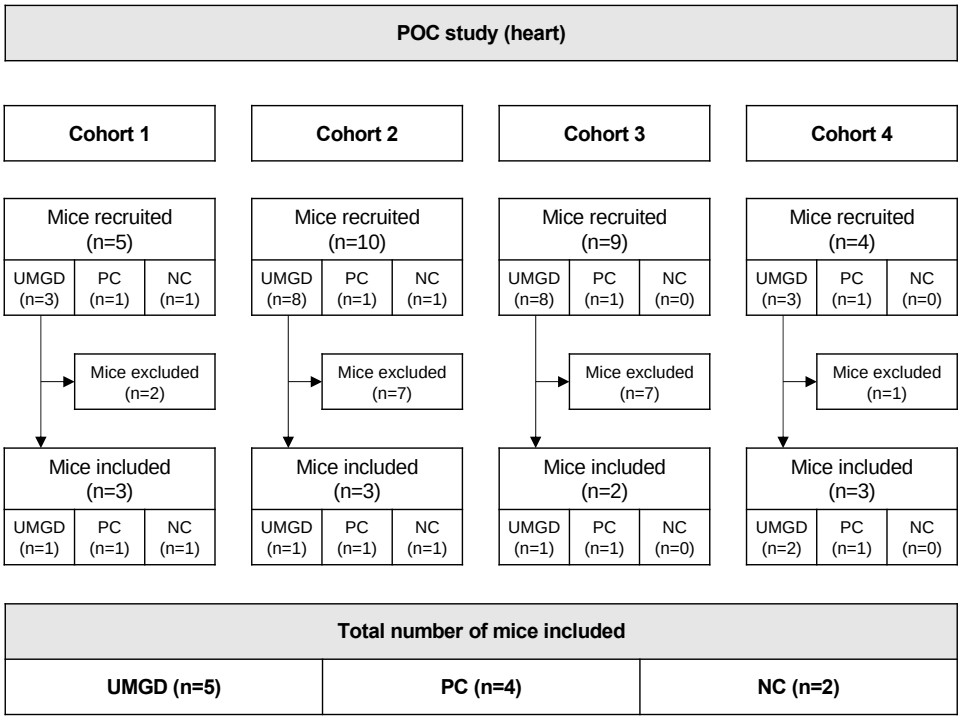

Figure 4-1 Flow diagram illustrating number of mice recruited, excluded, and included in each experiment for the UMGD proof-of-concept study targeting mouse hearts.

Mice in each cohort underwent procedures on the same day, but procedures between cohorts were performed on separate days. Mice were excluded if the tail vein injection was unsuccessful or required multiple attempts. POC, proof-of-concept; UMGD, ultrasound-mediated gene delivery; PC, positive control; NC, negative control.

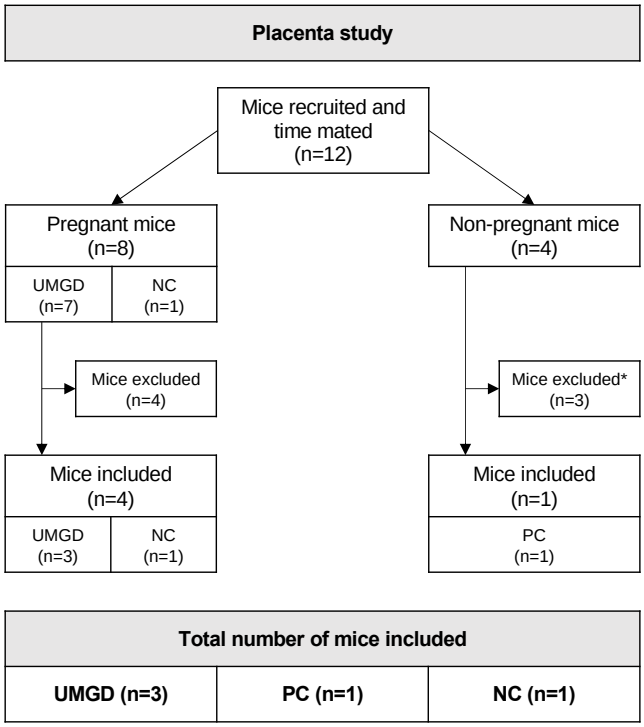

Figure 4-2 Flow diagram illustrating number of mice recruited, excluded, and included in the UMGD study targeting the placenta.

Pregnant mice were excluded if the tail vein injection was unsuccessful. *Non-pregnant mice were excluded to use in experiment 4 for the UMGD proof-of-concept study in the heart. POC, proof-of-concept; UMGD, ultrasound-mediated gene delivery; PC, positive control; NC, negative control.

4.3.2 Plasmid DNA and MB suspension

The plasmid DNA and MB suspension was prepared on an individual basis for each animal in UMGD studies as detailed in section 2.3.1. The volume of plasmid DNA and MBs administered is listed in Table 4-1.

4.3.3 UMGD studies

4.3.3.1 UMGD

UMGD was conducted as detailed in section 2.3.3. For each UMGD study, details of the type of plasmid; target organ; probe hold/output; animal strain, sex, age, weight, and treatment; total and group n-numbers of animals; injection site; and volumes administered are listed in Table 4-1.

4.3.3.2 Negative and positive control animals

For all studies, negative control animals underwent a similar procedure as UMGD treatment animals as detailed in section 2.3.3.3, with all modifications listed in Table 4-1. Positive control animals underwent the same procedure as detailed in section 2.3.3.3, with all modifications listed in Table 4-1.

4.3.3.3 Sacrifice and tissue processing

Animals were euthanised 3 d after UMGD procedures as detailed in section 2.3.4. Tissues were harvested and processed as detailed in section 2.3.5. The position and number of foetoplacental units in each uterine horn was recorded as shown in Figure 4-3.

Table 4-1 Full details of UMGD studies.

Study	Plasmid	Target organ	Probe hold / output	Strain (total n)	Sex (F/M)	Age (wks)	Weight (g)	Treatment (n)	Injection site	Plasmid volume (µL)	MB volume (µL)	PBS volume (µL)
POC heart	pGL4.13	heart	stationary / on	CD-1 (11)	F	6-8	25-33	UMGD (5)	tail vein	50	150	-
					F	6-8	28, 30	NC (2)	tail vein	-	-	200
					F	6-8	26-32	PC (4)	gracilis muscle	50	-	-
Placenta	pGL4.13	placenta	stationary / on	CD-1 (5)	F	6-8	37-49	UMGD (3)	tail vein	50	150	-
					F	6-8	49	NC (1)	tail vein	-	-	200
					F	6-8	29	PC (1)	gracilis muscle	50	-	-

All values (strain, sex, weight, and treatment parameters) for animals were collected and/or noted prior to treatment. POC, proof-of-concept; F, female; M, male; wks, weeks; UMGD, ultrasound-mediated gene delivery; NC, negative control, PC, positive control; MB, microbubble; PBS, phosphate-buffered saline.

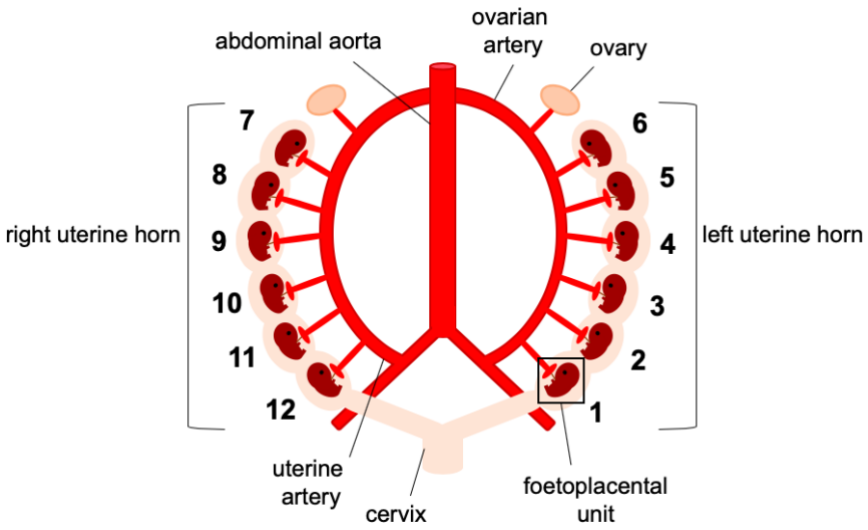

Figure 4-3 Diagram to show an example of the numbering system of foetoplacental units in the uterine horns.

Foetoplacental units (indicated by the black box) were numbered according to their positioning along the uterine horns. Foetuses were separated from their placentas, and whole tissue was snap frozen.

4.3.4 RNA extraction and quality control

RNA was extracted from tissue samples as detailed in section 2.1.4. Mouse tissue was homogenised using TissueLyser (QIAGEN, Haan, Germany). RNA quality and concentration were assessed as detailed in section 2.1.4.1.

4.3.5 Luciferase activity

Luciferase activity was measured as detailed in section 2.5.3 and normalised to protein content, which was extracted by bead-milling as detailed in section 2.5.1 and measured as detailed in section 2.5.2.

4.3.6 Statistical analysis

GraphPad Prism 9 was used to analyse all data sets. Luciferase activity data are shown as mean CPS/µg of protein ± SEM. Luciferase activity data in tissue from UMGD treatment mice were analysed by Friedman's test followed by Dunn's post-hoc multiple comparisons. For all statistical tests, $p<0.05$ was considered significant.

4.4 Results

4.4.1 UMGD proof-of-concept study delivering luciferase plasmid to mouse hearts

4.4.1.1 Purification of pGL4.13

pGL4.13, a 4641 bp vector expressing *luc2* (modified Photinus Pyralis luciferase gene) was selected to demonstrate proof-of-concept since pGL4 vectors harbour a synthetically engineered luciferase gene, *luc2*, that displays greater luciferase expression compared to pGL3 vectors (Promega, 2015). In order to assess efficiency of the purification of pGL4.13 and plasmid conformation of isolated pGL4.13, samples from stages of the purification procedure and the final plasmid product were run on an agarose gel. In the cleared lysate (lane L) and elute (lane E), a band ~6000 bp indicates plasmid DNA was enriched in the samples (Figure 4-4). No bands in the flow-through fraction (lane F) and wash fraction (lane W) demonstrates plasmid DNA was bound to the column and degraded RNA was removed (Figure 4-4). Finally, a band ~5000 bp and faint band above the DNA ladder in the plasmid only samples (lane P1 and P2) shows plasmid DNA was purified in an open-circular and supercoiled conformation (Figure 4-4).

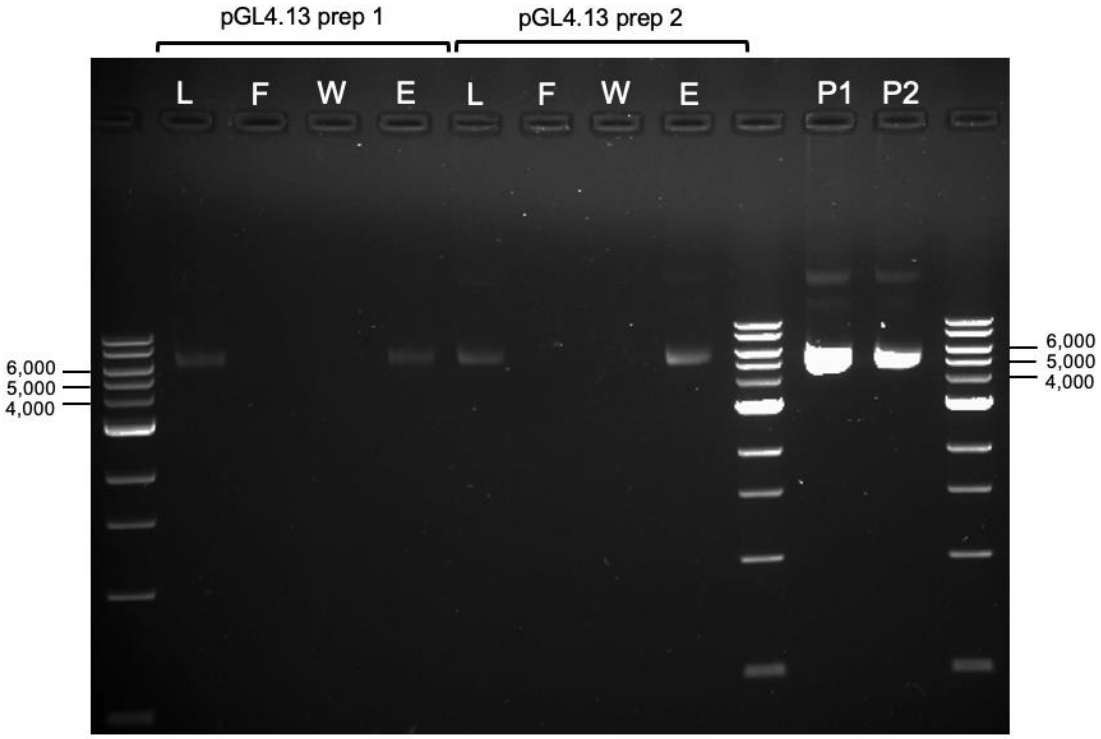

Figure 4-4 Representative agarose gel image of samples from stages of purification of pGL4.13 plasmid mega preps.

pGL4.13 plasmid was isolated from *E. coli* mega preps during which samples were collected to assess the stages of the purification procedure and confirm isolation of plasmid DNA. Up to 10 µL of the sample or 250 ng of DNA was loaded per lane and sized on a 1% agarose gel, using a 1 kb DNA ladder; sizes indicated in bp. Lane L: cleared lysate, lane F: flow-through fraction, lane W: wash fraction, lane E: elute, lane P1: pGL4.13 plasmid from prep1, lane P2: pGL4.13 plasmid from prep 2.

4.4.1.2 *In vivo* UMGD of pGL4.13 to mouse hearts

The UMGD protocol established in the previous chapter (Chapter 3) was utilised to demonstrate proof-of-concept UMGD of pGL4.13 to mouse hearts.

Luciferase activity in the ventricles and atria of UMGD treatment mice (12.28±17.04 and 1.11±1.42 CPS/µg of protein, respectively) was higher than background luciferase activity in the ventricles, atria, skeletal muscle, left kidney, right kidney, liver, lungs, and spleen of the negative control mouse (0.17±0.17, 0.92±0.80, 0.64±0.21, 0.04±0.04, 0.00±0.01, 0.04±0.06, 0.07±0.06, and 0.00±0.00 CPS/µg of protein, respectively) (Figure 4-5A), suggesting UMGD of pGL4.13 to the heart. Luciferase activity was highest in the skeletal muscle of the positive control mouse (382.26±632.70 CPS/µg of protein) (Figure 4-5A). In UMGD treatment mice, luciferase activity was significantly greater in the ventricles (12.28±17.04 CPS/µg of protein, $p<0.01$) compared to the non-target organs liver, lungs, and spleen (0.05±0.07, 0.05±0.1, and 0.01±0.03 CPS/µg of protein, respectively) (Figure 4-5B), providing evidence of tissue specific UMGD of pGL4.13 to mouse hearts. There was no significant difference between any other tissue of the UMGD treatment mice.

With this proof-of-concept study demonstrating tissue-specific UMGD in mice, the *in vivo* protocol was applied to targeting the placenta in pregnant mice.

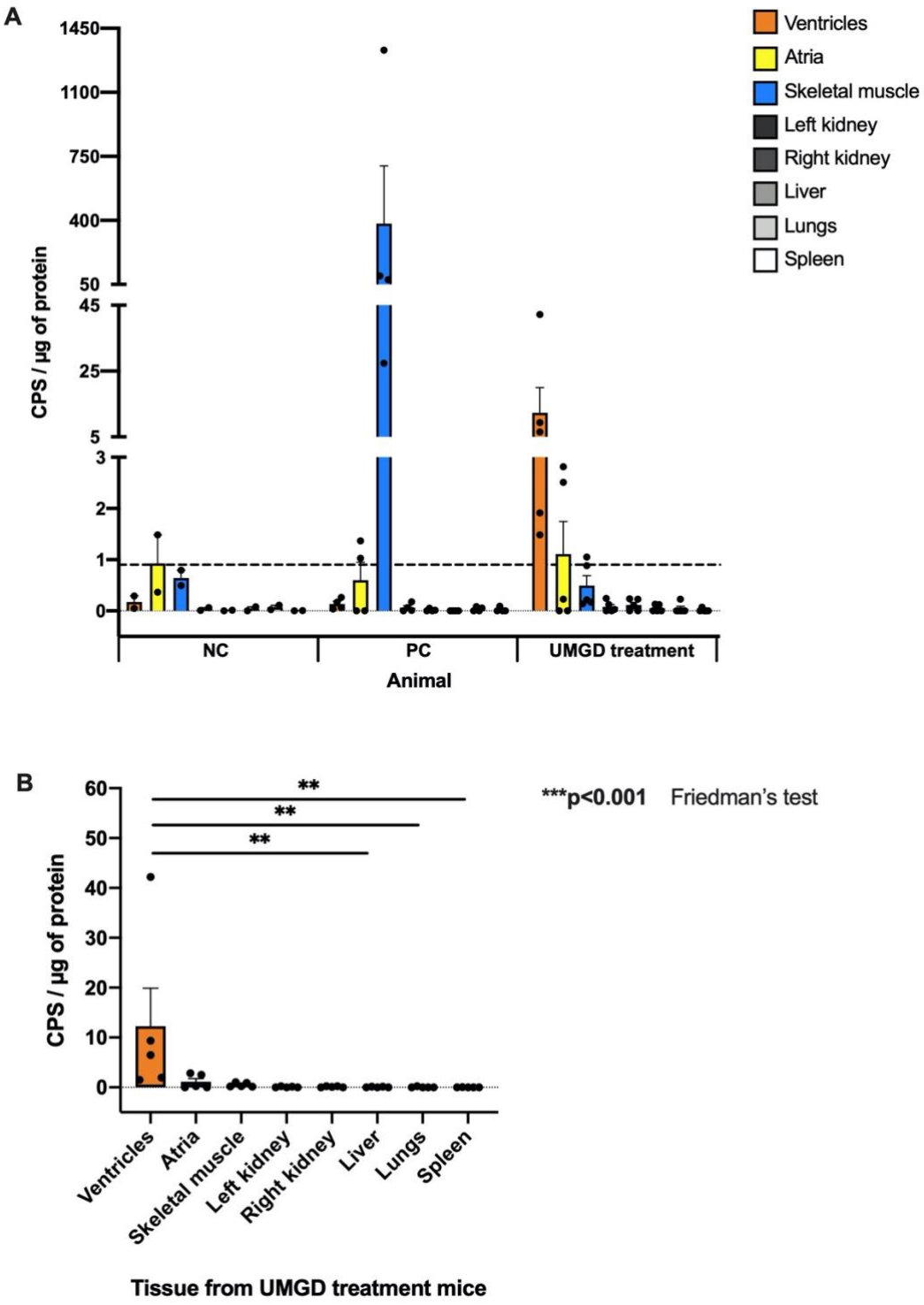

Figure 4-5 Luciferase activity in ventricles, atria, skeletal muscle, and other non-target organs of UMGD treatment mice and positive and negative control mice.

Luciferase activity in tissues from **(A)** UMGD treatment and control mice and **(B)** only UMGD treatment mice three days after *in vivo* gene delivery experiment. UMGD treatment mice were administered an IV injection of pGL4.13 and MB suspension followed by 2 min of US exposure to the heart. The positive control mice received an IM injection of pGL4.13. The negative control mice received an IV injection of PBS followed by 2 min of US exposure to the heart. Line at y=0.92 designates highest mean value from negative control mice tissue, indicating values below are background luciferase activity. Luciferase activity was measured in counts per second (CPS) and normalised to protein content. Data are shown as mean CPS/µg of protein±SEM, n=2 negative control mice, n=4 positive control mice, and n=5 UMGD treatment mice. **p<0.01 and ***p<0.001, n=5 UMGD treatment mice, analysed by Friedman's test followed by Dunn's post-hoc multiple comparisons test.

4.4.2 UMGD of pGL4.13 to the placenta in pregnant mice

The *in vivo* UMGD protocol utilised in the previous proof-of-concept study demonstrating tissue-specific gene transfer of pGL4.13 to mouse hearts was applied to pregnant mice to target the placenta. The total number of foetoplacental units in the targeted left uterine horn and non-targeted right uterine horn as well as the number of resorptions is shown in Table 4-2. In turn, in UMGD treatment mouse 1, 2, and 3, a total of 6, 7, and 7 placentas were potentially targeted.

Low levels of luciferase activity were detected in placenta 1 from UMGD treatment mice 1, 2, and 3 (0.80±0.18, 0.50±0.22, and 0.59±0.04 CPS/µg of protein, respectively), which were higher than the highest background activity detected in placenta 1 from the negative control mouse (0.29±0.14 CPS/µg of protein) (Figure 4-6), providing evidence of gene transfer to the placenta. However, only two samples from placenta 1 from UMGD treatment mouse 1 (1.12 and 0.76 CPS/µg of protein) and one sample from placenta 1 from UMGD treatment mouse 2 (0.92 CPS/µg of protein) were higher than the highest background activity detected in a placenta sample (placenta 2) from the negative control mouse (0.72 CPS/µg of protein) (Figure 4-6). In all other placentas from the UMGD treatment mice, luciferase activity was lower than the background activity in placenta 1 from the negative control mouse (Figure 4-6). Highest luciferase activity was detected in skeletal muscle from the positive control mouse (99.19±1.34 CPS/µg of protein) (Figure 4-6).

Table 4-2 Pregnancy outcomes in mice included in the UMGD study targeting placentas in the left uterine horn.

Mouse	Number of foetoplacental units		Number of resorptions
	left uterine horn	right uterine horn	
UMGD treatment mouse 1	6	4	0
UMGD treatment mouse 2	7	3	1*
UMGD treatment mouse 3	7	6	0
Negative control mouse	7	6	0
Positive control mouse	N/A	N/A	N/A

*resorption occurred in the right uterine horn. UMGD, ultrasound-mediated gene delivery; N/A, not applicable.

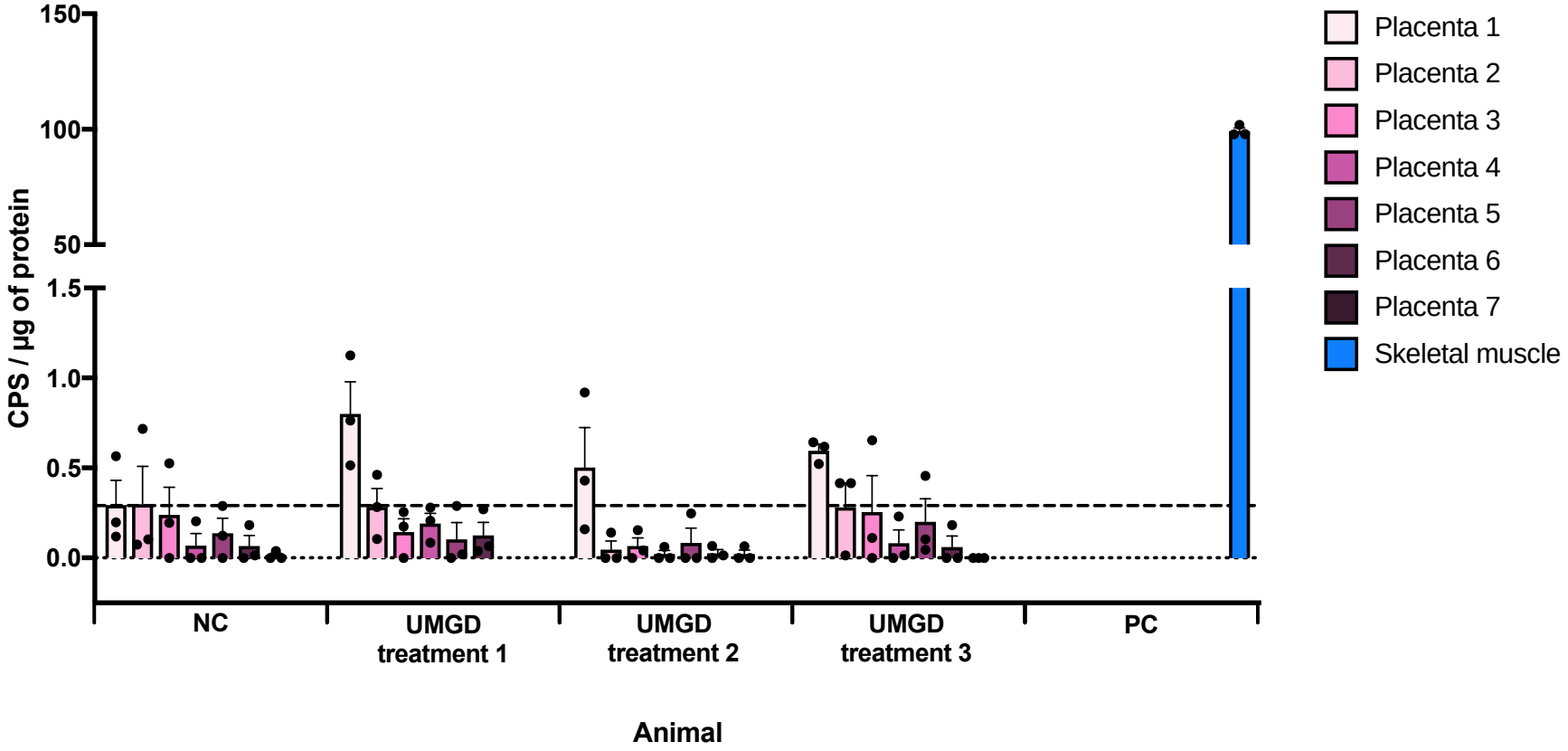

Figure 4-6 Luciferase activity in the placenta of UMGD treatment mice and the negative control mouse and in skeletal muscle of the positive control mouse.

Luciferase activity in tissues from UMGD treatment and control mice three days after *in vivo* gene delivery experiment. UMGD treatment mice were administered an IV injection of pGL4.13 and MB suspension followed by 2 min of US exposure to placenta in the left uterine horn. The positive control mouse received an IM injection of pGL4.13. The negative control mouse received an IV injection of PBS followed by 2 min of US exposure to placenta in the left uterine horn. Luciferase activity was not measured in skeletal muscle from the UMGD treatment mice and negative control mouse. A non-pregnant mouse was used as a positive control, so no placental tissue was available to measure. Line at y=0.29 designates highest mean value from negative control mice tissue, indicating values below are background luciferase activity. Luciferase activity was measured in counts per second (CPS) and normalised to protein content. Data are shown as mean CPS/µg of protein±SEM, n=3 tissue samples run in triplicate.

4.5 Discussion

UMGD may act as a non-viral and non-invasive method for targeting the placenta, representing a potentially new form of treatment for disorders arising from abnormal placental development, such as PE. In this chapter, an *in vivo* UMGD protocol was developed, demonstrating proof-of-concept of tissue-specific gene transfer of a luciferase plasmid to mouse hearts. When applied to pregnant mice to target the placenta, low levels of gene transfer were evident. Although expression in non-target tissue was not evaluated due to time constraints, this study provides a basic protocol for future UMGD studies seeking to target the placenta.

Tissue-specific gene transfer was demonstrated in the proof-of-concept UMGD study targeting mouse hearts. Transfer levels were higher than UMGD optimisation studies in the previous chapter (Chapter 3), demonstrating the importance of administering the full volume of the plasmid DNA and MB suspension in a single attempt. Due to small n-numbers, significance testing was not performed comparing tissue from the negative control mice with UMGD treatment mice. However, statistical analysis of target and non-target tissue from the UMGD treatment mice showed significantly greater luciferase activity was evident in the ventricles compared to some non-target organs (liver, lungs, and spleen), providing evidence of targeted gene transfer to the heart. Although there was a trend towards greater luciferase activity in the ventricles compared with the remaining non-target organs (skeletal muscle, left kidney, and right kidney), this was non-significant. Large variability was evident between both biological and technical replicates. Time constraints however meant that additional animals could not be included. In addition to biological variability arising from small n-numbers, several other sources likely contributed to variability in reporter gene activity as discussed in the following section.

In the proof-of-concept study targeting the heart, higher reporter gene activity was seen in the ventricles compared with the atria. This was expected since the left ventricle makes up the majority of the parasternal long axis view, with only a portion of the right atrium and left atrium in view. This degree of spatial targeting is supported by previous UMGD studies evaluating gene transfer across the heart. In a UMGD study in pigs seeking to target the left ventricular anterior

wall, positioning the probe in a parasternal long axis view and mid short axis view led to significantly increased transgene expression in the left ventricular anterior versus posterior wall (Schlegel et al., 2016). A study in rats found keeping the probe stationary (parasternal short axis view) or in motion (cranio-caudal direction) led to differing efficiencies between the anterior and posterior ventricles, apex, and atria, with lowest levels in the atria (Geis et al., 2009). In the proof-of-concept study, despite dividing the heart into atrial and ventricular samples to account for varying transfer levels across regions, high variability was still evident within samples. Moreover, adapting the tissue protein extraction protocol with the intent of achieving greater uniformity between samples from the same tissue did not reduce variability within samples. This highlights several factors that may be optimised in future experiments. Firstly, dividing tissue into further sections may help reduce variability in luciferase readings. Human technical variability in US imaging also likely contributed to differences in treatment area targeted. Rigs or platforms to position and control transducers may help reduce human variability but are more relevant to studies in which spatial specificity is crucial. The probe was held stationary in the proof-of-concept study to minimise the risk of misaligning the transducer focal point with the heart due to the beating motion of the heart. However, previous studies show performing a sweeping motion with the probe across the target organ leads to more uniform gene transfer across a larger region (Shen et al., 2008, Geis et al., 2009). This may represent a suitable strategy in stationary organs or to reduce variability if specificity is not a priority, particularly in larger organs or animals where there is a reduced risk of misaligning the probe beam with the target organ. Finally, whole animal bioluminescence could be used as an alternative to evaluate luciferase activity in intact target and non-target organs.

Gene transfer levels in the heart were lower compared with positive control levels in skeletal muscle following IM delivery of plasmid DNA. A previous UMGD study in rats similarly found IM injection of naked plasmid DNA into hindlimb skeletal muscle resulted in higher gene transfer levels than IV UMGD to the heart when using the same dose of plasmid DNA (Christiansen et al., 2003). Despite the apparent advantage of greater gene transfer seen with IM delivery of naked plasmid DNA, UMGD has consistently shown to induce significantly greater gene transfer than injection of naked plasmid DNA when targeting the same organ,

including in skeletal muscle (Wang et al., 2005), the liver (Shen et al., 2008), and the heart (Kondo et al., 2004). Comparing gene transfer levels between delivery methods to different organs rather than the same organ may therefore not accurately reflect transfer efficiency. Nonetheless, the positive control provided means of ascertaining that signals represented reporter gene transfer rather than an artefact and confirmed that the reporter gene was active and measurable.

In the study targeting the placenta, there was evidence of low levels of gene transfer, with mean luciferase activity higher in a single placenta in each UMGD treatment mice than the highest mean background luciferase activity detected in a placenta from the negative control mouse. However, only three experimental samples of placentas from UMGD treatment mice were higher than the highest background activity detected in an experimental placenta sample from the negative control mouse. These findings highlight gene transfer was inconsistent between samples and that reproducibility remains an issue with this technique. In addition to the factors previously discussed in the heart that likely contributed to variability and the strategies that could be adopted to reduce technical and biological variability, several factors may have contributed to a lack of reproducibility in the placenta and findings from the placenta offer insight into parameters that could be optimised in future UMGD studies to enhance gene transfer as discussed in the following section.

For every pregnant mouse subject to UMGD treatment, low levels of gene transfer were evident in the placenta positioned closest to the cervix on the targeted left uterine horn. In rodents, evidence suggests arteries supplying the placenta exhibit bidirectional inflow, in that they simultaneously receive blood from ovarian and uterine arteries, with the common iliac arteries at the cervical end acting as the predominant source (Raz et al., 2012, Ko et al., 2018). This physiological mechanism offers an explanation for evidence of gene transfer restricted to the placentas located closest to the cervix. However, these results may instead reflect coincidental targeting of the placenta located in this position in all treatment mice. Identifying the placenta targeted by UMGD remains difficult due to the inability to identify the positioning of placentas along a uterine horn *in utero* and the presence of multiple placentas on the US

display during imaging. Although irrelevant to nulliparous animals, this has important implications for preclinical UMGD studies targeting the placenta in litter-bearing animals. Additional studies are therefore required to further investigate whether gene transfer to the placenta positioned closest to the cervix occurred as a result of physiological or experimental factors. Micro-ultrasound is a type of US that operates at higher frequencies and therefore has higher a resolution than conventional diagnostic US. Studies in mice have shown micro-ultrasound can be used to examine embryonic and placental development due to its ability to identify specific foetoplacental units *in utero* (Foster et al., 2002, Mu et al., 2008). Hence, the system could be used to further investigate gene transfer to the placenta closest to the cervix, although this would require access to specialised US equipment.

Low levels close to background in the placenta of pregnant mice subject to UMGD, similar to those seen when targeting the kidney in optimisation studies (Chapter 3), highlight the need for future studies to adjust plasmid DNA and MB doses to account for the first pass-effect. Studies have shown greater gene delivery with increasing concentrations of a variety of MBs (Song et al., 2011, Panje et al., 2012, Shapiro et al., 2016), although highest efficiency was noted at sub-maximal concentrations. A larger number of MBs increases the probability of cavitation-induced mechanisms required for gene transfer, but transfer could be limited by the availability of plasmid. Another proposed mechanism for optimal gene transfer seen with sub-maximal MB concentrations is that cellular damage arising from higher MB concentrations limits gene transfer, supported by *in vitro* (Zhou et al., 2012, Nomikou et al., 2012, Rahim et al., 2006) and *in vivo* studies (Koike et al., 2005). Potential safety issues arising from higher MB concentrations and volume restrictions of injections may limit the ability to adjust the MB dose to account for the first-pass effect. Optimisation of other parameters may therefore be required to improve gene transfer efficiency. Previous UMGD studies have shown plasmid dose-related increases in gene delivery (Pislaru et al., 2003, Panje et al., 2012, Shapiro et al., 2016). Similar to MB concentration, greatest gene delivery was evident at sub-maximal plasmid doses, suggesting involvement of other factors limiting gene transfer efficiency. While raising plasmid DNA concentration increases the amount of genetic material available for gene transfer, it remains to be seen whether further

elevations would correspond with greater gene transfer. Moreover, it is important to consider that obtaining the required volume of plasmid DNA at higher concentrations may be technically challenging and the resulting more viscous plasmid DNA suspensions may further complicate tail vein injections.

In support of cavitation exerting a dominant influence over gene transfer levels, an *in vivo* study evaluating UMGD parameters for targeting cardiac tissue found significantly greater gene transfer at a higher MI and lower frequency (Chen et al., 2003). Furthermore, multiple *in vivo* studies targeting different organs and utilising different plasmids, MBs, and US parameters show a proportional relationship between peak negative pressure (PNP) and gene transfer (Miao et al., 2005, Song et al., 2011, Xie et al., 2012), with increases in acoustic pressure determining the extent of tissue damage. In the current study, an MI of 1.8 and frequency of 7 MHz were utilised corresponding to a PNP of 4.76 MPa. These settings were selected to enhance cavitation-related bioeffects compared to those achieved with 6 MHz and 1.6 MI, parameters utilised by the previous study on which the protocol was based (Browning et al., 2011). The parameters selected therefore represent the upper limits of the probe, with 1.9 the MI limit of diagnostic US systems. Future studies could further increase the MI from 1.8 to 1.9 by setting the probe output to contrast pulsed sequencing (Anderson et al., 2010, Steinl et al., 2016). In support, *in vivo* studies examining acoustic output have shown triggered US produces significantly greater gene transfer compared to continuous wave output (Chen et al., 2003, Pislaru et al., 2003). This is assumed to arise from replenishment of MBs between pulsing intervals. However, optimising output parameters to further stimulate cavitation increases the risk of tissue damage. UMGD studies evaluating differing acoustic pressures showed tissue damage arising at levels greater than 2 MPa (Miao et al., 2005, Song et al., 2011, Xie et al., 2012), notably lower than the PNP of 4.76 MPa utilised in the current study. Although safety assessments were not conducted, measurements provided by clinical US machines often display overestimated parameter values as a safety measure. Experimental validation of the US output of the 15L8 probe with a hydrophone and water bath set-up found that at H14 MHz (7 MHz output) the measured MI was 0.71 and MPa was 1.73, notably lower than the value displayed on the US machine (MI of 1.8) (Alete, 2008). Hence, optimising the MI, frequency, and/or PNP to increase the likelihood of cavitation

may not lead to the expected tissue damage based on the values displayed on the US machine, although this requires evaluation with safety assessments. Other parameters that have been examined *in vivo*, including duty cycle (Chen et al., 2011), pulse duration (Miao et al., 2005, Shen et al., 2008), and pulse length (Shen et al., 2008), were found to have no significant effect on gene transfer. Multiple studies also report extending treatment time beyond 2 min has no significant effect on transfer efficiency (Koike et al., 2005, Shen et al., 2008, Chen et al., 2011, Shapiro et al., 2016). This coincides with the short half-life of naked plasmid DNA and MBs under 10 min. Studies show trends towards higher intensities promoting gene transfer, but this parameter is not amenable on clinical diagnostic US machines (Chen et al., 2011, Sonoda et al., 2006, Liu et al., 2015). An alternative to adjusting output settings of the 15L8 probe is to evaluate other clinical transducers. Given the consistent use of frequencies ~1 MHz, a probe with lower frequencies may be desirable.

Another fundamental change that could be made is the type of MB employed. A UMGD study targeting skeletal muscle following IM plasmid DNA and MB administration found significantly greater gene transfer with SonoVue compared with Optison or Levovist (Wang et al., 2005). In contrast, a UMGD study targeting the heart following systemic administration of the plasmid DNA and MB suspension found Optison and Sonazoid induced significantly greater gene transfer (Alter et al., 2009). Further investigations found that the increased stability, rather than differences in the size and shell, account for the improved results with Optison and Sonazoid (Alter et al., 2009). Other studies have shown that MB size and shell composition significantly influence gene transfer (Liao et al., 2014, Browning et al., 2012). This highlights the uncertainty as to which MB most efficiently mediates gene delivery, likely dependent on multiple factors, including US parameters, target organ, and method of administration. Nonetheless, the negatively charged phospholipid shell of SonoVue does not bind negatively charged plasmid DNA, making the plasmid susceptible to degradation by nucleases in the blood. In turn, loading plasmid DNA into or onto MBs has shown to improve transfer efficiency. Multiple studies have shown greater gene transfer with positively charged cationic versus neutral MBs (Panje et al., 2012, Wang et al., 2012a) and MB-DNA complexes versus MBs alone (Chen et al., 2011, Burke et al., 2012). Introducing targeting moieties onto MBs has also shown to

enhance gene transfer (Xie et al., 2012). With SonoVue selected due to its availability and ease of preparation, future studies should take into consideration the convenience and feasibility of using other types of MBs.

Targeting the placenta with UMGD remains a potential form of non-viral and non-invasive gene therapy for disorders characterised by placental dysfunction. Although low levels of placental gene transfer were observed, plasmid DNA and/or MB volume and US parameters (MI or frequency) could be optimised in the protocol. Further changes including the type of probe and MB employed could also be incorporated. While this chapter provides a protocol for UMGD to the placenta, evaluation of safety parameters and demonstration of site-specific gene transfer through examination of non-target organs with the technique is still warranted for development of UMGD as a safe and effective method for targeting the placenta.

Chapter 5 Literature review of differentially expressed miRNAs in patients with PE and evaluation of candidate miRNAs in a rat model of superimposed PE (SPE)

5.1 Introduction

Since the discovery that placental miRNAs are dysregulated in patients with PE (Pineles et al., 2007), preclinical and clinical studies have sought to elucidate the role of placental miRNAs in the pathology of PE. In 2016, a systematic review of 24 expression profiling studies, of which 19 were conducted in placental tissue, identified 241 unique miRNAs differentially expressed in patients with PE (Sheikh et al., 2016). MiR-223, miR-210, and miR-126 were amongst the top 10 most frequently detected differentially expressed miRNAs in the placenta (Sheikh et al., 2016). Through examination of candidate and preclinical studies, the review found the miRNAs were implicated in key pathological processes of PE, namely immunity, ischaemia/hypoxia, and angiogenesis/vasculogenesis, respectively (Sheikh et al., 2016). Despite these studies providing evidence for a pathological role of these miRNAs in PE, a caveat lies in their reported direction of expression. Clinical studies show conflicting findings as to whether the miRNAs are up- or downregulated in preeclamptic placentas (Frazier et al., 2020). Besides methodological factors, these conflicting findings may be attributed to various biological factors, with placental miRNA expression found to differ between PE subtypes (Lykoudi et al., 2018, Weedon-Fekjær et al., 2014), presenting symptoms (Pineles et al., 2007, Awamleh et al., 2019), gestational age (Hromadnikova et al., 2015a, Anton et al., 2015, Yang et al., 2019b), and placental layers (Zhang et al., 2015a, Xu et al., 2014a).

Identifying a placental miRNA signature characteristic of PE or a subset of patients remains essential to identifying miRNAs that represent a clinically relevant therapeutic target. As PE is a disease almost exclusive to humans, clinical studies provide information essential to our understanding of placental miRNAs in PE. Animal models on the other hand provide a means of exploring the role and therapeutic potential of miRNAs in PE. Despite the unique insights and translational research that animal models offer, a limited number of studies have investigated placental miRNAs in animal models of PE (Kopriva et al., 2013, Yan et al., 2014, Yang et al., 2016a, Wang et al., 2020c).

Our research group previously established a novel model of SPE using Ang II at 500 ng/kg/min or 1000 ng/kg/min infusion from GD 10.5 in pregnant SHRSP rats (Morgan et al., 2018). On top of pre-existing hypertension, the 1000 ng/kg/min

treatment group displayed significantly elevated systolic and diastolic blood pressure compared to vehicle controls (Morgan et al., 2018). The albumin:creatinine ratio was also significantly increased in SPE rats compared to pre-Ang II levels and vehicle controls (Morgan et al., 2018). These findings highlight the animal model mirrors the clinical manifestations of a rise in blood pressure and new-onset proteinuria often characteristic of SPE in patients (Giannubilo et al., 2006, Townsend et al., 2016). SPE can also be diagnosed in the absence of a rise in blood pressure or new-onset proteinuria if maternal organ dysfunction develops (Brown et al., 2018). In SPE rats, histological examination of kidneys revealed morphological abnormalities, with evidence of Bowman capsule defects and reductions in the space between the visceral and parietal layers (Morgan et al., 2018). SPE rats treated with 1000 ng/kg/min also showed significant reductions in foetal and placental weight and uterine artery diameter and cross-sectional area, reflecting perinatal and maternal features seen in patients with SPE (Giannubilo et al., 2006). By exhibiting the haemodynamic and urinary profiles as well as multiorgan dysfunction of SPE in patients, our novel rat model of SPE provides a means of studying the role of placental miRNAs in a subtype of PE.

This chapter initially conducted a literature review to collate evidence from patient studies and identify clinically relevant miRNAs of potential interest for therapeutic targeting. Subsequently, the expression of candidate miRNAs was evaluated in our rat model of SPE, marking the first study to investigate placental miRNAs in an animal model of a PE subtype. To explore the biological factors that may contribute to differences in the reported direction of miRNA expression in clinical studies, miRNA expression was evaluated in whole placental tissue as well as individual placental layers. Examining placental miRNA expression in preclinical models is crucial to driving forward research investigating the therapeutic potential of targeting placental miRNAs.

5.2 Hypotheses and aims

5.2.1 Hypotheses

- Specific miRNAs are consistently dysregulated in placentas of patients with PE.

- Similar patterns of differentially regulated miRNAs are observed in the placenta of a preclinical model of PE when compared to human data in the literature.

5.2.2 Aims

- To identify significantly differentially expressed miRNAs detected by three or more miRNA expression profiling studies conducted in third trimester placentas of patients with PE through a literature review.

- To select candidate miRNAs for evaluation in a rat model of SPE through a literature review.

- To examine the expression of candidate miRNAs in whole placental tissue and individual placental layers of a rat model of SPE.

5.3 Methods

5.3.1 Literature review of miRNA expression profiling studies

5.3.1.1 Database search

A literature search was conducted using PubMed database for records published between the period January 1990 to March 2018 with the following search terms: (pre-eclamp OR preeclamp) AND (miR OR microRNA) (Figure 5-1). The search strategy was to identify miRNA expression profiling studies investigating differentially expressed miRNAs in third trimester placentas of patients with PE compared to normotensive controls without PE. The overall aim was to identify significantly differentially expressed placental miRNAs detected by three or more miRNA expression profiling studies.

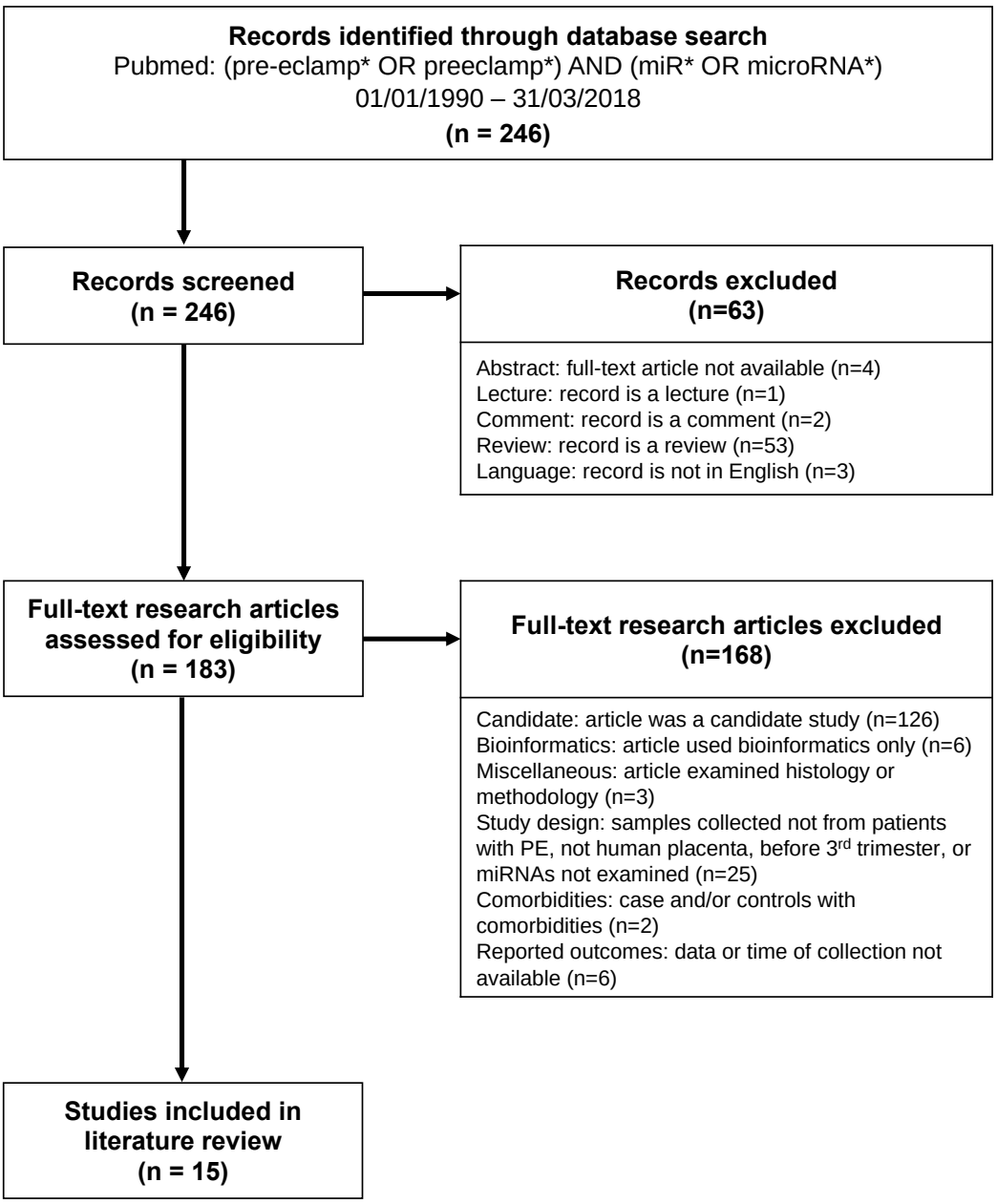

Figure 5-1 Flow diagram of number of records identified and screened, full-text articles excluded, and studies included in the literature review.

The search strategy was to identify miRNA expression profiling studies investigating differentially expressed miRNAs in third trimester placentas of patients with PE compared to normotensive controls without PE.

5.3.1.2 Study selection

Records were initially screened by screening abstracts to identify full-text research articles available in English. Thereafter, abstracts or full texts were assessed for eligibility according to the study selection criteria:

1. The study has conducted a miRNA expression profiling experiment (i.e. microarray or sequencing) to investigate differentially expressed placental miRNAs in patients with PE.

2. The study has examined third trimester placentas, with the time of tissue collection stated, comparing individuals diagnosed with PE to normotensive controls.

3. The study has provided data of some or all miRNAs detected as significantly differentially expressed by the miRNA expression profiling experiment.

For all studies included in the literature review, the full text was assessed for eligibility. Studies were included regardless of the type of PE investigated (i.e. diagnosed, mild, severe, EO, LO, and/or superimposed).

5.3.1.3 Data collection

From the studies included in the literature review, data were collected of all miRNAs reported as significantly differentially expressed between cases and controls, with significance defined by the study (e.g. p-value and fold change). Further information collected included type of study (i.e. microarray and/or sequencing), type of PE (i.e. diagnosed, mild, severe, EO, LO, and/or superimposed), sample size, type of delivery (preterm or term), and sampling area within the placenta.

5.3.1.4 Data analysis

Data of significantly differentially expressed placental miRNAs from individual studies was collated to identify miRNAs detected by three or more miRNA expression profiling studies.

5.3.2 Literature review for selection of candidate miRNAs

A literature review was conducted of the miRNAs identified as significantly differentially expressed in three or more miRNA expression profiling studies in third trimester placentas of patients with PE in order to select candidate miRNAs for evaluation in a rat model of SPE.

5.3.2.1 Criteria for candidate miRNAs

MiRNAs detected by three or more miRNA expression profiling studies were selected as candidates if they met all of the following three criteria:

1. Presence of a rat ortholog identical to the human miRNA sequence.

2. *In vitro* evidence supporting a role for the miRNA in the pathology of PE.

3. Validation of the miRNA in a fully and/or partially independent cohort.

5.3.2.2 MiRBase sequence alignment

The mature human miRNA sequence was imputed into the miRBase search engine. From the sequence search results, presence of a rat ortholog was identified by searching for the species-specific three-letter prefix for rats 'rno'. If present, 'align' was selected for the given rat miRNA ID, and sequence alignment between the human and rat miRNA was evaluated for full identicality.

5.3.2.3 Literature search

A literature search was conducted to identify studies providing *in vitro* evidence supporting a role for the miRNA in the pathology of PE and/or evidence of validation of the miRNA in an independent cohort. PubMed database was searched using the following terms: (mir-*x* OR hsa-mir-*x* oR microRNA *x* OR mir *x*) AND (preeclamp* OR pre-eclamp*) – with *x* designating the respective miRNA under enquiry. Abstracts were initially screened for relevance, after which selected full-text articles were assessed for *in vitro* and/or validation evidence. MiRNA expression profiling studies identified by the previous literature search (detailed in section 5.3.1.2) were also assessed for *in vitro* and/or validation evidence.

5.3.3 Evaluation of candidate miRNAs in a rat model of SPE

5.3.3.1 SPE rat model placental tissue

Placental tissue was obtained from a rat model of SPE previously established by our group (Morgan et al., 2018). In brief, the model was established as follows: once pregnancy was confirmed, 12-week-old SHRSP rats were randomly assigned to 0.9% saline vehicle (control) or Ang II at 1000 ng/kg/min (SPE) via ALZET® 2002 osmotic minipumps (Charles River, Kent, UK) implanted subcutaneously on GD 10.5. Dams were euthanised on GD 18.5 for collection of placental tissue. From each litter, whole placentas were excised, of which several were dissected into individual placental layers (decidua (dec), junctional zone (jx), and labyrinth (lab)), snap frozen in liquid nitrogen, and stored at -80°C (Figure 5-2). Whole placentas from n=4 SPE rats and n=4 control rats (total n= 8 rats) and individual placental layers from n=3 SPE rats and n=4 control rats (total n=7 rats) were available for evaluation of miRNA expression and included in the study analysis.

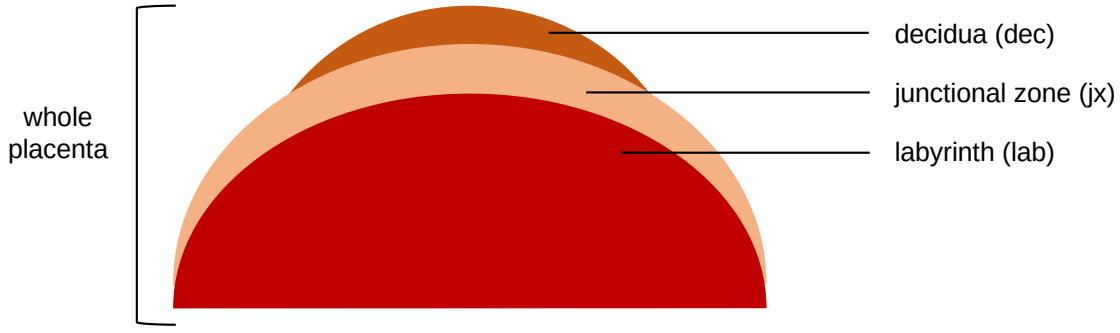

Figure 5-2 Diagram illustrating a cross-section of rat placental tissue showing the location and size of the placental layers.

Whole placental tissue and individual placental layers (decidua (dec), junctional zone (jx), and labyrinth (lab)) from the rat model of SPE were available for investigation. Dec, decidua; jx, junctional zone; lab, labyrinth.

5.3.3.2 RNA extraction and quality control

Total RNA was extracted from 50 mg of placental tissue using the miRNeasy Mini Kit (QIAGEN, Manchester, UK) as detailed in section 2.1.4. Once tissues were homogenised in QIAzol, RNA extractions were immediately carried out or tissues were stored at -80°C until RNA extractions were performed. RNA extracted from whole placental tissue was analysed using the Agilent BioAnalyzer 2100 as detailed in section 2.1.4.2. RNA extracted from individual placental layers was analysed using NanoDrop® ND-1000 Spectrophotometer as detailed in section 2.1.4.1. All tissues passed the respective quality control checks.

5.3.3.3 Evaluation of candidate miRNAs with TaqMan RT-qPCR

TaqMan RT-qPCR was performed as detailed in section 2.2 using the primers listed in Table 5-1. Data were analysed as detailed in section 2.2.3, with Ct values normalised to housekeeper (U87).

Table 5-1 Primer sequences of Applied Biosystems™ TaqMan™ microRNA Assays.

Assay name	Assay ID	Mature miRNA sequence
Hsa-miR-210	000512	CUGUGCGUGUGACAGCGGCUGA
Hsa-miR-223	000526	UGUCAGUUUGUCAAAUACCCC
Hsa-miR-195	000494	UAGCAGCACAGAAAUAUUGGC
Hsa-miR-16	000391	UAGCAGCACGUAAAUAUUGGCG
Hsa-miR-29b	000413	UAGCACCAUUUGAAAUCAGUGUU
Hsa-miR-30a-5p	000417	UGUAAACAUCCUCGACUGGAAG
Hsa-miR-181a	000480	AACAUUCAACGCUGUCGGUGAGU
Rno-miR-363	001355	AAUUGCACGGUAUCCAUCUGU
U87	001712	ACAATGATGACTTATGTTTTTGCCGTTTACCCAGCTGAG GGTTTCTTTGAAGAGAGAATCTTAAGACTGAGC

5.3.3.4 Statistical analysis

GraphPad Prism 9 was used to analyse all data sets. TaqMan data are shown as mean ΔCt ± SEM. TaqMan data were analysed using ΔCt values and the SPE model group (Ang II treated) and control group (vehicle treated) were compared by unpaired t-test (with Welch's correction as appropriate). For all statistical tests, $p<0.05$ was considered significant.

5.4 Results

5.4.1 Literature review of miRNA expression profiling studies

A total of fifteen studies were identified by the literature review which met the study selection criteria whereby data were presented showing significantly differentially expressed miRNAs in third trimester placentas of patients with PE compared to normotensive controls by conducting a miRNA expression profiling experiment (Table 5-2). The most common measure for defining statistical significance was inclusion of both a p-value and fold change cut-off, employed by a total of seven studies (Table 5-2). All subtypes of PE (i.e. mild, severe, EO, LO, and superimposed) were represented by at least one study; only one study involved patients with SPE (Table 5-2). Two of the fifteen studies had groups with sample sizes >20 (Table 5-2). In the majority of studies (eleven out of fifteen), preeclamptic pateints delivered preterm (Table 5-2). A significant difference in gestational age at delivery, and therefore at placental tissue collection, was noted in six studies (Table 5-2). The sampling area varied between studies, with sampling from maternal and/or foetal sites across the placenta, including the decidua, basal plate, placental villi, and chorionic plate (Table 5-2).

After collating the data from the fifteen miRNA expression profiling studies, a total of 22 significantly differentially expressed placental miRNAs were identified that were detected by three or more miRNA expression profiling studies in preeclamptic patients (Table 5-3). For ten of the miRNAs, studies concurred in the direction of miRNA expression, while for the remaining twelve miRNAs, studies were discordant in the direction of miRNA expression (Table 5-3).

Table 5-2 MiRNA expression profiling studies conducted in third trimester placentas of patients with PE included in the literature review.

Study	Type of study	Significance	Type of PE	Sample size (n)	Type of delivery	Sampling area
(Hu et al., 2009)	Microarray	p<0.05 and ≥2-FC	Severe LO	PE (n=4) control (n=4)	PE (term) control (term)	Chorionic tissue
(Mayor-Lynn et al., 2011)	Microarray	p<0.05 and >1.5-FC	Diagnosed	PE (n=7) control (n=6)	PE (preterm) control (term)	Placental villi
(Enquobahrie et al., 2011)	Microarray	p<0.05 and >1.5-FC	Diagnosed	PE (n=20) control (n=20)	PE (preterm)* control (term)	8 maternal and 8 foetal sites
(Wang et al., 2012b)	Microarray	p<0.05	Severe	PE (n=3) control (n=3)	PE (preterm) control (term)*	Placental villi
(Wang et al., 2012c)	Microarray	p<0.05	Severe	PE (n=5) control (n=5)	PE (term) control (term)	dMSCs
(Betoni et al., 2013)	Microarray	p<0.05	Diagnosed	PE (n=9) control (n=9)	PE (preterm) control (preterm)	Placenta
(Xu et al., 2014a)	Microarray	p<0.05	Severe	PE (n=14) control (n=33)	PE (preterm)* control (term)	Random sites from placental disc
(Weedon-Fekjær et al., 2014)	Sequencing	p<0.05 and FDR<0.01	EOPE and LOPE	EOPE (n=23) LOPE (n=26) control (n=23)	EOPE (preterm)* LOPE (term)* control (term)	Centrally located cotyledon
(Zhao et al., 2014)	Microarray	p<0.05 and >2-FC	Severe LO	PE (n=5) control (n=5)	PE (term) control (term)	dMSCs
(Zhang et al., 2015a)	Microarray	p<0.05 and >2-FC	Severe	PE (n=3) control (n=3)	PE (preterm)* control (term)	Basal plate
(Yang et al., 2015)	Sequencing	>1.2- or <-1.2-FC	Mild and severe	Mild (n=2) severe (n=2) control (n=1)	Mild (term) severe (preterm) control (n/a)	Placenta
(Zhou et al., 2016)	Sequencing	p≤0.01 and ≥1.5 or ≤0.66-FC	Diagnosed	PE (n=9) control (n=9)	PE (preterm)* control (term)	Chorionic plate along with central portion
(Vashukova et al., 2016)	Sequencing	p<0.01 and FDR<0.05	SPE	SPE (n=5) control (n=6)	PE (preterm) control (term)	8 maternal and 8 foetal sites
(Gunel et al., 2017)	Microarray	p<0.05 and >2-FC	Severe LO	PE (n=18) control (n=18)	PE (preterm)* control (term)	Placenta
(Lykoudi et al., 2018)	Microarray	p<0.05 and FDR≤0.05	EOPE and LOPE	EOPE (n=11) LOPE (n=5) control (n=8)	EOPE (preterm)* LOPE (preterm) control (preterm)	Central portion of the placenta

*statistically significant gestational age. FC, fold change; FDR, false discovery rate; PE, preeclampsia, EO, early onset; LO, late onset; SPE, superimposed PE, dMSCs, decidua-derived mesenchymal stem cells.

Table 5-3 MiRNAs significantly differentially expressed in three or more miRNA expression profiling studies in third trimester placentas of patients with PE.

miRNA	Studies reporting significant difference in miRNA expression		
	Up	**Down**	**Direction not reported**
210-3p	(Enquobahrie et al., 2011) (Betoni et al., 2013) (Xu et al., 2014a) (Weedon-Fekjær et al., 2014) (Zhang et al., 2015a) (Zhou et al., 2016) (Vashukova et al., 2016)	None	None
223-3p	None	(Betoni et al., 2013) (Xu et al., 2014a) (Weedon-Fekjær et al., 2014) (Zhao et al., 2014) (Vashukova et al., 2016)	None
16-5p	(Hu et al., 2009) (Wang et al., 2012c) (Zhao et al., 2014) (Zhang et al., 2015a)	None	None
193b-3p	(Betoni et al., 2013) (Xu et al., 2014a) (Zhou et al., 2016) (Vashukova et al., 2016)	None	None
31-5p	(Xu et al., 2014a) (Zhou et al., 2016) (Vashukova et al., 2016)	(Zhao et al., 2014)	None
584-5p	(Xu et al., 2014a)	(Enquobahrie et al., 2011) (Zhang et al., 2015a) (Zhou et al., 2016)	None
29b-3p	(Hu et al., 2009) (Wang et al., 2012c) (Zhao et al., 2014)	None	None
181a-5p	(Hu et al., 2009) (Xu et al., 2014a) (Zhang et al., 2015a)	None	None
524-3p	(Wang et al., 2012b) (Xu et al., 2014a) (Vashukova et al., 2016)	None	None
214-3p	None	(Hu et al., 2009) (Xu et al., 2014a) (Zhao et al., 2014)	None
363-3p	None	(Betoni et al., 2013) (Xu et al., 2014a) (Zhang et al., 2015a)	None
542-3p	None	(Betoni et al., 2013) (Xu et al., 2014a) (Lykoudi et al., 2018)	None
1-3p	(Zhang et al., 2015a)	(Enquobahrie et al., 2011) (Vashukova et al., 2016)	None
let-7f-5p	(Hu et al., 2009)	(Betoni et al., 2013) (Vashukova et al., 2016)	None
10b-5p	(Zhao et al., 2014) (Zhou et al., 2016)	None	(Wang et al., 2012c)
30a-5p	(Wang et al., 2012c) (Zhao et al., 2014)	(Lykoudi et al., 2018)	None
140-5p	(Zhao et al., 2014)	(Betoni et al., 2013)	(Wang et al., 2012c)
151-3p	(Xu et al., 2014a) (Zhou et al., 2016)	(Wang et al., 2012b)	None
192-5p	(Zhou et al., 2016)	(Wang et al., 2012b) (Betoni et al., 2013)	None
195-5p	(Hu et al., 2009)	(Xu et al., 2014a) (Vashukova et al., 2016)	None
224-5p	(Yang et al., 2015)	(Betoni et al., 2013) (Weedon-Fekjær et al., 2014)	None
301a-3p	(Zhao et al., 2014) (Yang et al., 2015)		(Wang et al., 2012c)

5.4.2 Literature review for selection of candidate miRNAs

Of the 22 miRNAs detected by three or more miRNA expression profiling studies, eight miRNAs met all three literature review criteria of presence of a conserved rat ortholog identical to the human sequence, *in vitro* evidence supporting a role for the miRNA in pathology of PE, and validation of the miRNA in a fully and/or partially independent cohort (Table 5-4). These miRNAs (miR-210-3p, miR-223-3p, miR-16-5p, miR-29b-3p, miR-181a-5p, miR-363-3p, miR-30a-5p, and miR-195-5p) were selected as candidates for evaluation in the placenta of a rat model of SPE.

Table 5-4 Selection of candidate miRNAs for evaluation in a rat model of SPE.

miRNA	Rat ortholog	Role in PE	Validated in independent cohort
210-3p	Yes (rno-miR-210-3p)	Yes[1,2,3,4]	Yes[3,21,22,23]
223-3p	Yes (rno-miR-223-3p)	Yes[5]	Yes[24]
16-5p	Yes (rno-miR-16-5p)	Yes[6,7,8]	Yes[25,26,27]
29b-3p	Yes (rno-miR-29b-3p)	Yes[9,10]	Yes[25,26,27]
181a-5p	Yes (rno-miR-181a-5p)	Yes[11,12,13]	Yes[27,28]
363-3p	Yes (rno-miR-363-3p	Yes[14]	Yes[29]
30a-5p	Yes (rno-miR-30a-5p)	Yes[15,16]	Yes[24,25,26]
195-5p	Yes (rno-miR-195-5p)	Yes[17,18,19]	Yes[24,27]
1-3p	Yes (rno-miR-1b)	No	No
31-5p	Yes (rno-miR-31a-5p)	No	No
214-3p	Yes (rno-miR-214-3p)	No	No
542-3p	Yes (rno-miR-542-3p)	No	No
let-7f-5p	Yes (rno-let-7f-5p)	No	No
140-5p	Yes (rno-miR-140-5p)	No	No
192-5p	Yes (rno-miR-192-5p)	No	No
301a-3p	Yes (rno-miR-301a-3p)	No	No
193b-3p	No	No	Yes[24,30]
584-5p	No	Yes[20]	Yes[20]
524-3p	No	No	Yes[24]
10b-5p	No	No	No
151a-3p	No	No	No
224-5p	No	No	No

(1) (Lee et al., 2011) (2) (Zhang et al., 2012) (3) (Luo et al., 2014) (4) (Luo et al., 2016) (5) (Meng et al., 2017) (6) (Wang et al., 2012c) (7) (Zhao et al., 2014) (8) (Zhu et al., 2016) (9) (Li et al., 2013) (10) (Gu et al., 2016) (11) (Wu et al., 2018) (12) (Liu et al., 2012) (13) (Zhang et al., 2015c) (14) (Thamotharan et al., 2017) (15) (Hu et al., 2015) (16) (Niu et al., 2018) (17) (Bai et al., 2012) (18) (Wu et al., 2016) (19) (Wang et al., 2018a) (20) (Jiang et al., 2015) (21) (Muralimanoharan et al., 2012) (22) (Lalevée et al., 2014) (23) (Adel et al., 2017) (24) (Xu et al., 2014a) (25) (Wang et al., 2012c) (26) (Zhao et al., 2014) (27) (Hu et al., 2009) (28) (Wang et al., 2018c) (29) (Zhang et al., 2015a) (30) (Zhou et al., 2016)

5.4.3 Evaluation of candidate miRNAs in a rat model of SPE

The expression of eight candidate miRNAs was evaluated by RT-qPCR to determine if they were significantly differentially expressed in a rat model of SPE compared to control rats. MiR-223-3p was significantly upregulated (3.26±0.12 vs 3.80±0.14 ΔCt, $p<0.05$) and miR-181a-5p was significantly downregulated (5.63±0.09 vs 5.32±0.05 ΔCt, $p<0.05$) in whole placental tissue of a rat model of SPE compared to controls (Figure 5-3A and B). MiR-210-3p was significantly downregulated in the decidual layer (1.43±0.03 vs 0.41±0.29 ΔCt, $p<0.05$) and significantly upregulated in the labyrinth layer (3.04±0.05 vs 3.60±0.12 ΔCt, $p<0.05$) of a rat model of SPE compared to controls (Figure 5-4C), while no significant difference was seen in whole placental tissue (Figure 5-3C). MiR-363-3p was significantly downregulated in the decidual layer (9.37±0.33 vs 8.06±0.24 ΔCt, $p<0.05$) and miR-195-5p was significantly upregulated in the decidual layer (1.14±0.03 vs 1.32±0.04 ΔCt, $p<0.05$) of a rat model of SPE compared to controls (Figure 5-4F and H), while no significant difference in miR-363-3p or miR-195-5p was seen in whole placental tissue (Figure 5-3F and H). The remaining candidate miRNAs (miR-16-5p, miR-29b-3p, and miR-30a-5p) were not significantly differentially expressed in whole placental tissue or individual placental layers of a rat model of SPE compared to controls (Figure 5-3D, E, and G and Figure 5-4D, E, and G).

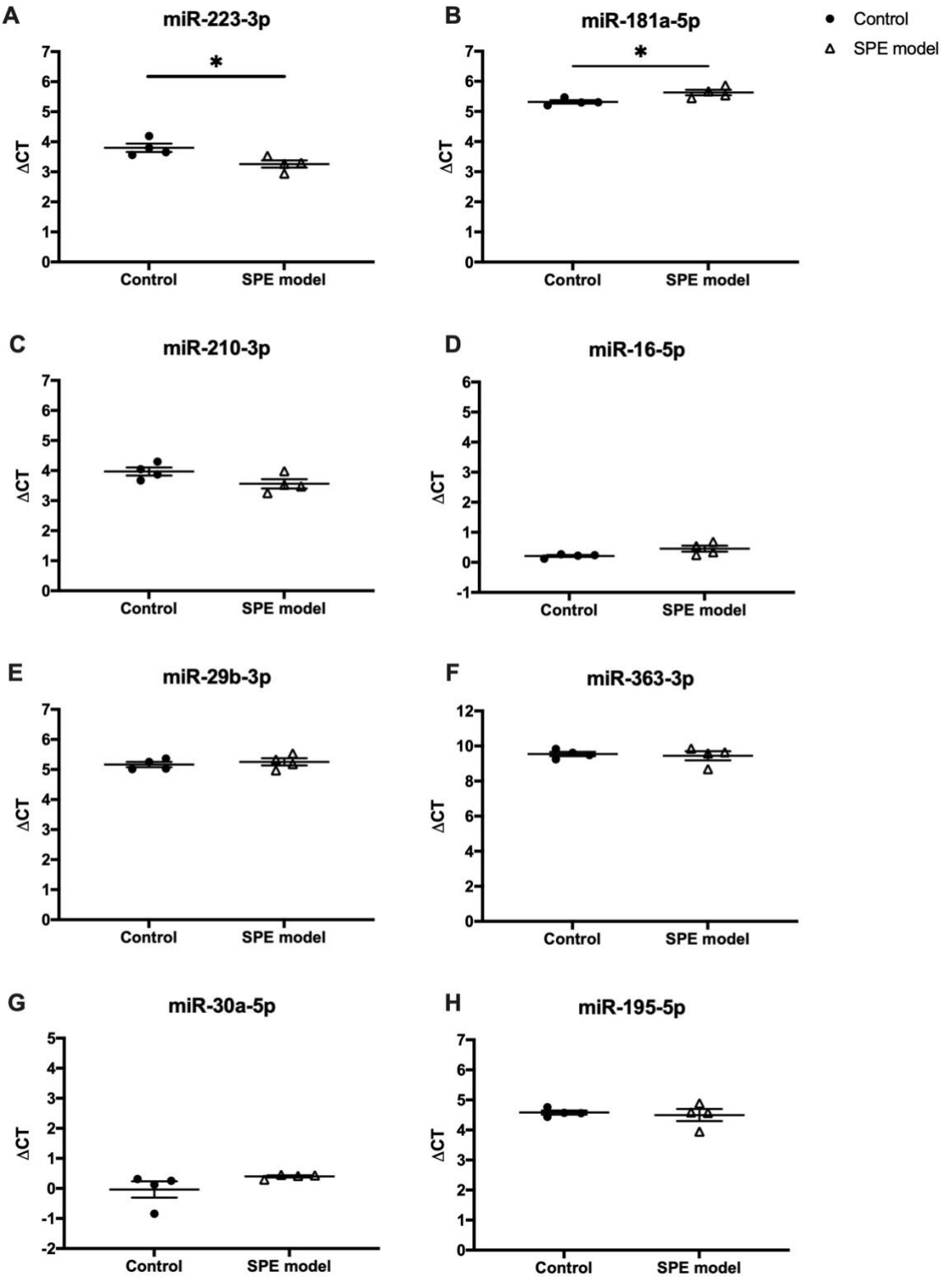

Figure 5-3 Evaluation of candidate miRNAs in whole placentas of a rat model of SPE by TaqMan RT-qPCR.

(A) MiR-223-3p was significantly upregulated in whole placental tissue of a rat model of SPE. **(B)** MiR-181a-5p was significantly downregulated in whole placental tissue of a rat model of SPE. **(C)** MiR-210-3p, **(D)** miR-16-5p, **(E)** miR-29b-3p, **(F)** miR-363-3p, **(G)** miR-30a-5p, and **(H)** miR-195-5p were not significantly differentially expressed in whole placental tissue of a rat model of SPE. Data are shown as mean ΔCt $\pm$ SEM. Ct values were normalised to housekeeper U87, *p<0.05, n=4 per group, analysed using ΔCt values by unpaired t-test or unpaired t-test with Welch's correction as appropriate.

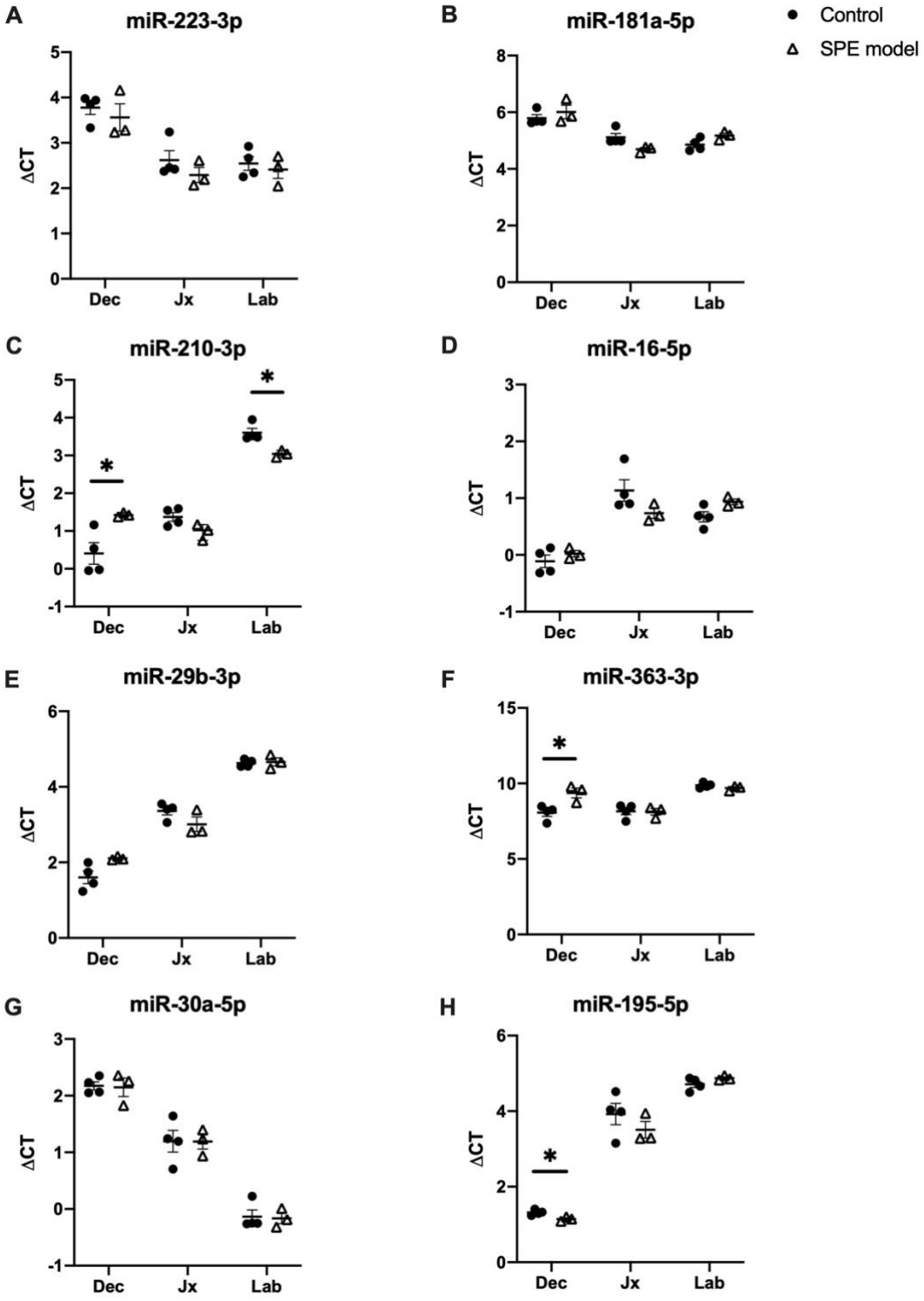

Figure 5-4 Evaluation of candidate miRNAs in individual placental layers (decidua, junctional zone, and labyrinth) of a rat model of SPE by TaqMan RT-qPCR.

(A) MiR-223-3p and **(B)** miR-181a-5p were not significantly differentially expressed in individual placental layers of a rat model of SPE. **(C)** MiR-210-3p was significantly downregulated in the decidua and significantly upregulated in the labyrinth of a rat model of SPE. **(D)** MiR-16-5p and **(E)** miR-29b-3p were not significantly differentially expressed in individual placental layers of a rat model of SPE. **(F)** MiR-363-3p was significantly downregulated in the decidua of a rat model of SPE. **(G)** MiR-30a-5p was not significantly differentially expressed in individual placental layers of a rat model of SPE. **(H)** MiR-195-5p was significantly upregulated in the decidua of a rat model of SPE. Data are shown as mean ΔCt ± SEM. Ct values were normalised to housekeeper U87, *p<0.05, n=3 in SPE group and n=4 in control group, analysed using ΔCt values by unpaired t-test or unpaired t-test with Welch's correction as appropriate. Dec, decidua; Jx, junctional zone; lab, labyrinth.

5.5 Discussion

In this chapter, a literature review identified placental miRNAs repeatedly detected as significantly differentially expressed by miRNA expression profiling studies in third trimester preeclamptic patients. Clinical studies were either in agreement or discordant in the direction of expression of the miRNAs in PE. Several candidate miRNAs were confirmed as significantly differentially expressed in whole placental tissue or individual placental layers of a rat model of SPE, providing novel evidence of dysregulation of miRNAs within placental layers in rats, a finding previously only shown in humans. Due to inconsistencies in the reported direction of expression of miRNAs, comparing findings from clinical and preclinical studies remains essential to elucidating the role of placental miRNAs in PE and their potential as therapeutic targets.

The incongruity between clinical studies in the direction of placental miRNA expression in PE may in part be attributed to methodological factors of expression profiling studies. Microarrays and sequencing offer the benefit of a hypothesis-free approach to quantitively profile miRNA content. However, sample preparation and processing as well as the sensitivity and specificity of a platform contribute to detection bias and, in turn, differences in reported miRNA expression levels (Willenbrock et al., 2009, Git et al., 2010). Features of miRNAs themselves can also impact their detection by profiling platforms due to the short length of miRNAs, sequence similarity between miRNA family members, and presence of miRNA isoforms (isomiRs) (Leshkowitz et al., 2013). A next generation sequencing study examining isomiRs in placental tissue from mild and severe PE patients reported differences in the types of isomiRs and their expression patterns between normal and disease samples as well as between PE subtypes (Guo et al., 2011). This further supports that isomiRs may contribute to differences in miRNAs detected and their reported direction of expression in preeclamptic patients. Another methodological factor that may account for a lack of replication between clinical studies is the utilisation of arbitrary fold change cut-offs in addition to p-values to designate significance. Although typically employed to identify miRNAs deemed biologically relevant, fold change cut-off values can exclude smaller RNA expression changes that are statistically significant by hypothesis testing. Various fold change threshold values utilised by studies in the literature review may contribute to differences

in miRNAs detected. Finally, expression profiling studies in the literature review had relatively small sample sizes and in turn lower statistical power to detect significant differences. Overall, studies with larger sample sizes are needed to add weighting to the findings. Despite the limitations of expression profiling studies, their unbiased approach compared to candidate studies highlights their utility in examining differentially expressed placental miRNAs in PE.

The inconsistencies between clinical studies in the literature review may also arise from biological factors, such as the type of PE examined. Studies in severe LOPE patients reported a significant upregulation of miR-let-7f-5p (Hu et al., 2009), miR-140-5p (Zhao et al., 2014), miR-192-5p (Zhou et al., 2016), and miR-195-5p (Hu et al., 2009), while studies in patients with diagnosed, superimposed, and severe PE found a significant downregulation of these miRNAs (Betoni et al., 2013, Vashukova et al., 2016, Wang et al., 2012b, Xu et al., 2014a). This suggests that a subset of miRNAs may show differential expression patterns unique to patients with severe LOPE. Similarly, a significant upregulation of miR-1-3p was identified in a study in patients with severe PE (Zhang et al., 2015a), while it was detected as downregulated by studies examining patients diagnosed with PE and SPE (Enquobahrie et al., 2011). Collating data from multiple expression profiling studies can therefore help to identify miRNAs that may show differential expression patterns between subtypes. In contrast, miR-584-5p and miR-151-3p were reported as both up- and downregulated in studies of patients with severe PE (Wang et al., 2012b, Xu et al., 2014a, Zhang et al., 2015a). This highlights certain placental miRNAs also exhibit differences in the direction of expression within a subtype of PE, supporting the involvement of other factors in governing placental miRNA expression.

Spatial and temporal regulation of placental miRNAs may also contribute to the diverging findings from clinical studies in the literature review. The study reporting a significant upregulation of miR-151-3p in patients with severe PE sampled random sites across the placenta (Xu et al., 2014a) in contrast to the study reporting a significant downregulation in severe PE patients which examined placental villous tissue free of decidua (Wang et al., 2012b). The former study reporting an increase in miR-151-3p went on to validate expression of the miRNA within placental layers, noting a significant decrease in the basal

plate and no significant difference in the chorionic plate (Xu et al., 2014a). Findings of an opposing direction of expression may therefore reflect layer-specific differences. Placental miRNAs have also shown to differ in expression across gestation between the trimesters (Morales-Prieto et al., 2012, Gu et al., 2013), with differences noted in PE patients as early as the first trimester (Singh et al., 2017). All studies included in the literature review examined third trimester placenta collected at the time of delivery, accounting for trimester-dependent changes. However, placental miRNA differences between term and preterm deliveries (Mayor-Lynn et al., 2011, Hromadnikova et al., 2017) as well as term and preterm PE (Anton et al., 2015, Yang et al., 2019b) indicate gestational age at delivery even within the third trimester may influence expression patterns. With significant differences in gestational age noted between PE and control groups as well as inclusion of both term and preterm deliveries, these factors may have further contributed to contrasting findings between clinical studies. In addition, other factors, including foetal weight (Awamleh et al., 2019, Pineles et al., 2007, Weedon-Fekjær et al., 2014), foetal sex (Muralimanoharan et al., 2015), maternal diet (Baker et al., 2017), pollutants (Li et al., 2015c), BMI (Tsamou et al., 2017), and smoking status (Maccani et al., 2010), have shown to alter placental miRNA expression. Despite the numerous variables potentially influencing placental miRNA expression, several miRNAs were consistently detected as significantly differentially expressed in the same direction of expression across multiple clinical studies. To gain further insight into factors such as PE subtype and placental region in regulating placental miRNAs, candidate miRNAs detected as significantly differentially expressed by multiple expression profiling studies were examined in a preclinical model of SPE.

MiR-223-3p was significantly upregulated in the rat model of SPE, while reported as significantly downregulated across expression profiling studies (Betoni et al., 2013, Xu et al., 2014a, Weedon-Fekjær et al., 2014, Zhao et al., 2014), including in a study of patients with SPE (Vashukova et al., 2016). Hence, upregulation in the rat model of SPE does not reflect miRNA changes distinct to SPE. These contrasting findings are also unlikely to reflect layer-specific differences since there was no significant difference in miR-223-3p expression within individual placental layers in the rat model of SPE. Furthermore, one

clinical study validated miR-223-3p as downregulated in both the chorionic and basal plate of PE patients (Xu et al., 2014a). The opposing findings may therefore reflect processes specific to the preclinical model. *In vitro*, miR-223-3p has shown to promote trophoblast survival, proliferation, and invasion by inhibiting signal transducer and activator of transcription 3 (STAT3) (Meng et al., 2017). Thus, lower miR-223-3p expression levels reported in PE patients may reflect loss of its physiological role in mediating trophoblast function in placental development, with studies reporting elevated expression and activation of STAT3 in placentas of PE patients (Meng et al., 2017, Xu et al., 2017). However, multiple studies have found reduced placental expression and activation of STAT3 in PE (Qu et al., 2018, Chen et al., 2018, Weber et al., 2012, Zhang et al., 2015d), suggesting other factors modulate STAT3. Additional *in vitro* studies examining functional properties and gene targets of miR-223-3p are required to gain a greater understanding of the role of the miRNA in trophoblasts. Furthermore, investigations into the role of miR-223-3p in other placental cell types remain to be conducted, with evidence suggesting miR-223-3p plays an important role in regulating immune cells and their responses. In bone marrow derived macrophages from miR-223-3p KO or WT mice, higher miR-223-3p expression shifted macrophage polarisation towards an anti-inflammatory M2 phenotype (Zhuang et al., 2012). In a separate study in mouse macrophages, downregulation of miR-223-3p in response to inflammatory stimuli activated STAT3 and, in turn, increased the production of pro-inflammatory cytokines (Chen et al., 2012b). With clinical studies repeatedly showing dysregulation of foetal and maternal macrophages in preeclamptic placentas and evidence of a shift towards an M1 phenotype in PE (Williams et al., 2009, Yang et al., 2017a, Milosevic-Stevanovic et al., 2016, Schonkeren et al., 2011, Ma et al., 2019), a reduction in miR-223-3p expression may correspond with loss of its anti-inflammatory properties. MiR-223-3p has also been identified as one of the miRNAs preferentially expressed in regulatory T cells (T reg cells) compared to naïve T cells (Cobb et al., 2006) and of the most substantially downregulated miRNAs in activated NK cells (Fehniger et al., 2010). Dysregulation of these cell types has been reported in preeclamptic placentas (Toldi et al., 2008, Milosevic-Stevanovic et al., 2016) and foetal and maternal macrophages, placental T reg cells, and uNK cells play a key role in inadequate spiral artery remodelling (reviewed by (Geldenhuys et al., 2018)). It remains to be explored whether miR-

223-3p expression may be altered in these cell types in PE, and in turn involved in mediating immune responses within the placenta in PE. Evaluation of miR-223-3p in different cell types as well as other animal models of PE may also provide insight into the cause of the contrasting increased expression in the SPE rat model, its role in the pathology of PE, and in turn its suitability as a therapeutic target. The consistent downregulation of miR-223-3p across clinical studies makes it a potential miRNA of interest to target therapeutically.

In the rat model of SPE, miR-181a-5p was significantly downregulated in whole placental tissue contrasting with the reported upregulation of miR-181a-5p in three expression profiling studies, conducted in patients with severe LOPE (Hu et al., 2009, Xu et al., 2014a) and severe PE (Zhang et al., 2015a). Candidate studies in patients with severe PE (Wang et al., 2018c) and diagnosed PE (Khaliq et al., 2018, Liu et al., 2012, Wu et al., 2018) have similarly found a significant upregulation of miR-181a-5p in third trimester placentas. Findings from the preclinical model may therefore suggest an increase in miR-181a-5p expression is unique to SPE. However, the expression profiling study in SPE patients did not detect miR-181a-5p as significantly differentially expressed, and miR-181a-5p expression has found to be increased in placentas complicated by gestational hypertension (Khaliq et al., 2018). Downregulation of miR-181a-5p in the rat model of SPE may therefore reflect a response to the Ang II infusion. In vascular smooth muscle cells derived from rat aorta, Ang II incubation inhibited miR-181a-5p expression by approximately 50% (Remus et al., 2013). In contrast, miR-181a-5p expression was not altered in HUVECs treated with Ang II (Lin et al., 2017). Whether circulating levels of Ang II in the rat model of SPE influenced miR-181-5p expression in certain placental cells remains unclear. However, miR-181a-5p has also been implicated in regulating the RAS in the kidney in neurogenic hypertension (Biancardi and Sharma, 2020) and in the placenta during pregnancy (Wang et al., 2018e), raising the possibility that a relationship between miR-181a-5p and Ang II exists. In kidneys of hypertensive patients, a decrease in miR-181a-5p and increase in renin was reported (Marques et al., 2011). In a mouse model of hypertension, targeted renal delivery of a miR-181a-5p mimic and bilateral renal denervation led to increased renal miR-181a-5p expression and decreased renal renin mRNA levels and blood pressure (overview by (Biancardi and Sharma, 2020)). Overexpression of miR-181a-5p in trophoblast

cells was associated with a reduction in renin mRNA and prorenin protein release (Wang et al., 2018e). These findings suggest miR-181a-5p in the kidney and placenta may exhibit the ability to suppress blood pressure via downregulating renin, a key enzyme of the RAS pathway. However, further experiments are required, and it remains speculative that elevated circulating levels of Ang II in the SPE rat model may contribute to downregulation of placental miR-181a-5p expression. *In vitro* studies show miR-181a-5p may be involved in modulating several aspects of placental development through a variety cell types. MiR-181a-5p has been shown to inhibit migration and invasion of trophoblasts in part by suppressing insulin-like growth factor 2 mRNA-binding protein 2, which exhibited significantly reduced protein levels in preeclamptic placentas (Wu et al., 2018), supporting the idea that an upregulation of miR-181a-5p may contribute to the pathological processes underlying PE. A separate *in vitro* study showed miR-181a-5p inhibited MSC proliferation and stimulated T cell proliferation and T cell IFN-γ production in co-cultures (Liu et al., 2012). In a latter *in vivo* study examining MSC-based therapy, the same group showed MSC proliferation and suppression of T cell proliferation were attributed to alleviating PE-like symptoms in a Th1 cell induced PE mouse model (Liu et al., 2014), suggesting overexpression of miR-181a-5p may modulate properties of MSCs that contribute to the development of PE. On the other hand, stimulating miR-181a-5p expression in human endometrial stromal cells promoted their decidualization via inhibiting Krüppel-like factor 12 (Zhang et al., 2015c), suggesting the miRNA may play an important physiological role in earlier stages of placental development. *In vitro* studies support a multifunctional role for the miRNA in different cell types, with its dysregulation in turn contributing to PE. Despite the conflicting results between the preclinical model of SPE and clinical studies, the consistently reported upregulation of miR-181a-5p in preeclamptic patients makes it an intriguing potential therapeutic target in PE.

MiR-210-3p exhibited a significant difference in expression in opposing directions in placental layers of the rat model of SPE. Although previous clinical studies have shown that a miRNA can be significantly differentially expressed in one placental layer and not another, no published study to date has reported an opposite direction of expression in different layers (i.e., upregulation in one layer and downregulation in another layer). This finding lends weight to the

concept that discrepancies between clinical studies may reflect layer-specific differences, although this novel finding in rats remains to be validated in human placental layers. Furthermore, an opposing direction of expression between placental layers may underpin a lack of significance in whole placental tissue, highlighting the importance of examining miRNAs within placental layers. The significant upregulation of miR-210-3p in the labyrinth of a rat model of SPE is in line with its consistently reported upregulation in expression profiling studies (Enquobahrie et al., 2011, Betoni et al., 2013, Xu et al., 2014a, Weedon-Fekjær et al., 2014, Zhang et al., 2015a, Zhou et al., 2016, Vashukova et al., 2016) and candidate studies (Muralimanoharan et al., 2012, Zhang et al., 2012, Lalevée et al., 2014, Luo et al., 2014, Wang et al., 2019a, Biro et al., 2019) in third trimester placentas from patients with PE. An increase in miR-210-3p has also been reported in blood samples from preeclamptic patients (Zhang et al., 2012, Ura et al., 2014, Xu et al., 2014a, Anton et al., 2013) as well as in pregnant women with chronic hypertension and gestational hypertension (Biró et al., 2017). A separate preclinical study also found significantly higher miR-210-3p expression in placentas of a poly I:C induced PE mouse model compared to WT controls (Kopriva et al., 2013). Finally, elevated levels of miR-210-3p have been reported in the uterine arteries of pregnant sheep residing at high altitude (Hu et al., 2017) and in human placentas from high-altitude pregnancies (Colleoni et al., 2013). These findings contribute to the growing body of evidence that an increase in placental miR-210-3p expression in PE may in part be driven by hypoxia, with hypoxia shown to induce miR-210-3p across primary cells and cell lines (Chan and Loscalzo, 2010), including HUVECS (Fasanaro et al., 2008), trophoblast cell lines (Ishibashi et al., 2012), primary trophoblasts (Zhang et al., 2012), and *ex vivo* uterine arteries (Hu et al., 2017). Studies reporting a significant downregulation of miR-210-3p in the placenta, namely in mild PE patients (Zhu et al., 2009) and pregnant mice exposed to moderate hypoxia levels (Krawczynski et al., 2016), suggest miR-210 expression may only be induced in more severe hypoxic conditions. An *in vitro* study showed miR-210-3p was only significantly increased in hypoxic conditions below 5% O_2, with no significant difference in cells exposed to 10% O_2, further supporting miR-210-3p may in part be regulated by a hypoxic gradient (Li et al., 2019). Evidence from *in vitro* studies in trophoblasts support an increase in miR-210-3p expression leading to pathological changes in the placenta, with its increased expression

shown to inhibit trophoblast invasion (Luo et al., 2016, Luo et al., 2014, Zhang et al., 2012, Anton et al., 2013, Wang et al., 2019a, Awamleh and Han, 2020, Li et al., 2019), migration (Zhang et al., 2012, Wang et al., 2019a, Awamleh and Han, 2020), proliferation (Li et al., 2019, Wang et al., 2019a), syncytialization (Wang et al., 2020b), tube-like formation (Wang et al., 2019a), and mitochondrial respiration (Muralimanoharan et al., 2015, Muralimanoharan et al., 2012, Anton et al., 2019). In contrast, in HUVECs, miR-210-3p has shown to stimulate formation of capillary-like structures, VEGF-mediated migration, and endothelial cell survival (Fasanaro et al., 2008). Hence, downregulation in the decidua in the SPE rat model may represent a loss of physiological function in other cell types. In addition, other factors, such as poly I:C (Kopriva et al., 2013) and TNF- α (Muralimanoharan et al., 2013, Luo et al., 2014) by stimulating nuclear factor-κB (NF-κB) have been shown to drive miR-210-3p expression, indicating hypoxia-independent mechanisms can regulate miR-210-3p expression. The causes and/or consequences of a significant downregulation of miR-210-3p in the decidua of the SPE rat model remain unknown but could reflect dysregulation in cell types other than trophoblasts or involvement of other mechanisms besides hypoxia regulating its expression as a protective mechanism. Of note, no published clinical study has yet validated miR-210-3p expression in the decidua of PE patients, which would provide insight into the potential layer- and/or cell specific expression of miR-210-3p. Further investigations in a variety of cell types and evaluation of hypoxia-independent stimuli could shed light on its role in the placenta and, in turn, PE. Given its consistently reported upregulation in PE, inhibiting miR-210-3p in the placenta represents a potential therapeutic strategy in PE.

There was no difference in miR-363-3p expression in whole placental tissue of the SPE rat model, but a significant downregulation was seen in the decidua. This is in agreement with the three expression profiling studies in patients diagnosed with PE (Betoni et al., 2013) and with severe PE (Xu et al., 2014a, Zhang et al., 2015a) as well as a candidate study in patients with severe PE (Zhu et al., 2009). An expression profiling study went on to validate miR-363-3p as downregulated in both the chorionic and basal plate (Zhang et al., 2015a). Altogether, evidence from studies to date suggests miR-363-3p is downregulated across the placenta in a range of PE subtypes. In contrast to its significant

differential expression in the SPE rat model, miR-363-3p was not detected as significantly differentially expressed in the expression profiling study conducted in SPE patients. Since a lack of significance may have arisen from methodological factors, additional studies are required to ascertain that miR-363-3p expression is decreased in SPE as supported by findings from the SPE rat model. In trophoblasts, nutrient restriction reduced miR-363-3p expression, which coincided with upregulation of its target genes sodium-coupled neutral amino acid transporters, SNAT1 and SNAT2 (Thamotharan et al., 2017). A previous study reported SNAT2 was downregulated in third trimester placentas from PE patients (Huang et al., 2018), while another study found no significant difference in the expression of the amino acid transporters in PE (Malina et al., 2005). Although investigations into the role of miR-363-3p in the placenta and PE remain limited, its consistent downregulation seen across preclinical and clinical studies highlight its potential as a therapeutic target in PE.

MiR-195-5p was significantly upregulated in the decidua of the SPE rat model, while no significant difference was seen in whole placental tissue. Although this is in agreement with an increase in expression reported by the expression profiling study examining chorionic tissue blocks in severe LOPE (Hu et al., 2009), the two other expression profiling studies reported a significant downregulation when sampling random sites across the placenta in both severe PE (Xu et al., 2014a) and SPE (Vashukova et al., 2016). Candidate studies similarly reported significant downregulation of miR-195-5p in third trimester placenta of severe LO (Gunel et al., 2020) and severe PE patients (Bai et al., 2012). In the profiling study conducted in SPE patients reporting a downregulation, decidual tissue was included when collecting samples from maternal sites. Hence, upregulation of miR-195-5p in the SPE rat model may reflect processes specific to the preclinical model rather than layer-specific changes. Evidence from *in vitro* studies suggests dysregulation of miR-195-5p in the placenta plays a role in PE via modulating genes that may contribute to the genetic basis of PE. In HUVECs, miR-195-5p overexpression inhibited endothelial cell invasion and tube formation via suppressing VEGFA (Zhao et al., 2017). Gene association studies have shown VEGFA polymorphisms (Hamid et al., 2020, Amosco et al., 2016) and haplotypes (Gannoun et al., 2017) are associated with PE. With VEGFA haplotypes either reducing or enhancing risk (Gannoun et al.,

2017), it remains unclear whether elevated placental miR-195-5p therefore represents a harmful or protective mechanism. In support of increased miR-195-5p mediating normal placental development, overexpression of miR-195-5p in trophoblasts promoted invasion via inhibiting activin A receptor type 2A (ACVR2A) (Bai et al., 2012) and activin A receptor type 2B (Wu et al., 2016), with susceptibility loci for PE identified within the ACVR2A gene in multiple populations (Roten et al., 2009, Ferreira et al., 2015, Amosco et al., 2019). In trophoblasts exposed to acute oxidative stress, miR-195-5p overexpression further stimulated apoptosis and reduced mitochondrial activity in part by inhibiting FAD-dependent oxidoreductase domain-containing 1 (FOXRED1) and pyruvate dehydrogenase phosphatase regulatory subunit (PDPR) (Wang et al., 2018a). However, chronic stimulation led to reduced miR-195-5p expression, coinciding with elevated levels of FOXRED1 and PDPR in placentas of preeclamptic patients (Wang et al., 2018a). Thus, evidence also suggests reduced placental miR-195-5p expression in PE may represent a defensive mechanism against oxidative stress. Overall, conflicting evidence regarding the direction of expression of placental miR-195-5p in PE likely mirrors its differential expression between cell types. Since miR-195-5p can target genes implicated in the genetic basis of PE in a range of cell types in the placenta, further preclinical and clinical studies should be conducted to gain a greater understanding of the role of miR-195-5p in the placenta in PE and its suitability as a therapeutic target.

Due to inconsistencies in the reported direction of expression of placental miRNAs in PE, collating and comparing evidence from preclinical and clinical studies remains essential to identify potential factors contributing to opposing findings. Evaluation of candidate miRNAs in the placenta of a rat model of SPE contributed to the growing body of evidence that placental miRNAs differ between PE subtypes and placental layers. The direction of expression of placental miRNAs in the preclinical model repeatedly contradicted findings from clinical studies, indicating SPE may exhibit a distinct miRNA expression profile. More clinical studies examining placental miRNAs exclusively in patients with SPE are therefore required since only one expression profiling study has been conducted to date. Furthermore, the novel finding of a miRNA expressed in opposite directions in different placental layers highlights the importance of

mapping miRNA expression across the placenta, as this has implications for targeting miRNAs therapeutically. Finally, while differing pathological processes between preclinical models and patients may account for differences in placental miRNA expression, identifying similarities is crucial for research seeking to target a placental miRNA therapeutically.

Chapter 6 Characterisation of miRNAs and predicted gene targets in the placentas of a rat model of SPE and patients with PE and in trophoblast cells

6.1 Introduction

Animal models are essential to studying pregnancy and its related disorders due to the ethical and practical limitations of conducting research in pregnant humans. Rodents in particular are commonly used in preclinical research due to the similarities between humans, rats, and mice in placental development, structure, and function (Rai and Cross, 2014, Georgiades et al., 2002). Moreover, genome-wide expression profiling studies in mouse and human placenta have revealed commonalities in molecular patterns across the placenta and gestation (Soncin et al., 2018, Cox et al., 2009). Genome-wide microarray profiling of first and third trimester human and mouse placenta detected 517 genes differentially expressed across gestation that were common to both species, representing 18% of mouse and 43% of human differentially expressed genes (Soncin et al., 2018). Furthermore, analysis of expression patterns revealed 129 genes were upregulated and 147 genes were downregulated in both species across gestation, while the remaining 231 showed differing patterns of expression between the species (Soncin et al., 2018). In a separate study, microarray expression analysis of human villous tree and mouse labyrinth samples detected 2869 transcripts unique to both species and 6609 transcripts common to both species, with over 70% of all detected transcripts correlating in expression between the human and mouse (Cox et al., 2009). Protein analysis of the same samples detected 6970 ortholog proteins of which 2519 were common to both species (Cox et al., 2009). Although these studies show species-specific patterns exist, they also highlight that humans and rodents display molecular similarities at both the transcriptional and posttranscriptional level in the placenta and across gestation.

MiRNA expression profiling studies in human primary trophoblasts and placental tissue demonstrate significant changes also occur in miRNA expression throughout pregnancy, implicating miRNAs as molecular regulators of placental development and function (Morales-Prieto et al., 2012, Gu et al., 2013). In turn, dozens of miRNA expression profiling studies in human placentas from pregnancy-related disorders, such as PE and FGR, show placental miRNAs are dysregulated in disease states (Sheikh et al., 2016, Chiofalo et al., 2017). However, only a handful of miRNA expression profiling studies have been conducted in pregnant rodents (Inoue et al., 2017, Inoue et al., 2020, Su et al.,

2020). Inoue et al. employed miRNA microarray profiling to examine expression of miRNAs from the rodent specific C2MC in the placenta of cluster deleted mice (Inoue et al., 2017). Knockdown of expression impaired placental development and frequently induced foetal lethality or defects (Inoue et al., 2017). Su et al. performed miRNA expression profiling on mouse placentas at embryonic day (E) 12.5, 13.5, 14.5, and 18.5, reporting significant differences in the expression of more than 50 miRNAs at E 18.5 (Su et al., 2020). Furthermore, Su et al. conducted miRNA expression profiling after administration of the immunostimulant, poly(I:C), reporting significant differences in several placental miRNAs (Su et al., 2020). Expression profiling studies make it possible to study global changes in expression in a hypothesis-free manner compared to the hypothesis-driven nature of candidate studies. The aforementioned profiling studies in pregnant rodents demonstrate that, like in humans, global changes in placental miRNA expression occur throughout pregnancy and in disease states. No published miRNA expression profiling study could be identified that examines placental miRNA expression in an animal model of PE. Collectively, this highlights the value of and need for miRNA expression profiling studies in animal models of PE. Elucidating the miRNA profile of animal models of PE allows for comparisons with human data, thereby providing insight into the role of placental miRNA in PE and their therapeutic potential.

In addition to examining placental miRNA expression, evaluating gene targets and the functional role of miRNAs in placental cell types are critical experiments to gain a greater understanding of the involvement of miRNAs in the placenta and in PE. A key example is miR-210-3p, the most frequently detected dysregulated miRNA in placentas of preeclamptic patients (Sheikh et al., 2016). A total of sixteen clinical studies have reported miR-210-3p is significantly upregulated in the placenta in PE, while one study in mild preeclamptic patients found it was significantly downregulated (Frazier et al., 2020). Numerous genes have been validated as miR-210-3p gene targets in trophoblasts through reporter construct assays, found to be significantly downregulated in preeclamptic placentas in which miR-210-3p was upregulated, and implicated in impaired trophoblast invasion, migration, iron metabolism, proliferation, and syncytialization, namely thrombospondin type I domain containing 7A (THSD7A), potassium channel modulatory factor 1 (KCMF1), ephrin-A3 (EFNA3), homeobox-

A9 (HOXA9), iron-sulphur cluster scaffold homolog (ISCU), cytoplasmic polyadenylation element-binding 2 (CPEB2), colony stimulating factor (CSF1), and integrin subunit alpha$_M$ (ITGAM), (Luo et al., 2016, Luo et al., 2014, Lee et al., 2011, Zhang et al., 2012, Wang et al., 2020b, Awamleh and Han, 2020). Dysregulation of miR-210-3p and its gene target ISCU has also shown to cause trophoblast mitochondrial dysfunction (Muralimanoharan et al., 2012, Anton et al., 2019). Collectively, these preclinical and clinical findings suggest increased expression of miR-210-3p may contribute to trophoblast dysfunction in PE. In poly I:C induced PE mice compared to WT mice, miR-210-3p expression was significantly upregulated and its predicted gene target STAT6 was significantly downregulated, a mediator that promotes the expression and differentiation of anti-inflammatory Th2 cytokines (Kopriva et al., 2013). STAT6 has previously shown to be downregulated in trophoblasts overexpressing miR-210-3p (Ahn et al., 2017) and in the placenta of preeclamptic patients (Su, 2016, Fan et al., 2016), suggesting miR-210-3p may also regulate the immune response of trophoblasts. These comparisons demonstrate the importance of examining evidence from patients, animal models, and *in vitro* studies, as each system enables investigations into different aspects of the role of placental miRNAs in health and disease.

In the previous chapter, significant differences were detected in candidate placental miRNAs in our rat model of SPE. Comparisons with published data from clinical studies revealed both differences and similarities between the rat model and preeclamptic patients. In this chapter, miRNA sequencing was performed to identify differentially expressed placental miRNAs in our SPE rat model in a hypothesis-free manner. Furthermore, the dysregulation of select miRNAs and predicted gene targets was examined by RT-qPCR in placental tissue from the rat model of SPE as well as preeclamptic patients to evaluate the clinical relevance of the findings. Evidence from placental tissue from the rat model of SPE and preeclamptic patients is in agreement with published data that miR-210-3p is upregulated in PE. In turn, the role of miR-210-3p was studied in trophoblasts *in-vitro* by knocking down and overexpressing the miRNA and evaluating its effects on previously unexplored predicted gene targets.

6.2 Hypotheses and aims

6.2.1 Hypotheses

- An altered placental miRNA transcriptome induces changes in placental gene expression in a rat model of SPE, with changes mirrored in the placentas of patients with PE.

- A placental miRNA dysregulated in PE affects predicted gene targets and the functional properties of trophoblast cells *in vitro*.

6.2.2 Aims

- Identify differentially expressed placental miRNAs in the placenta of a rat model of SPE using miRNA sequencing.

- Validate differentially expressed miRNAs in whole placentas and placental layers of a rat model of SPE and in placentas of patients with PE.

- Evaluate expression of predicted gene targets in placentas of a rat model of SPE and patients with PE.

- Investigate the relationship between a candidate placental miRNA, predicted gene targets, and functional effects *in vitro* in a trophoblast cell line.

6.3 Methods

6.3.1 SPE rat model placental tissue

Placental tissue was obtained from a rat model of SPE previously established by our group (Morgan et al., 2018), as described in section 5.3.3.1. In brief, the model was established as follows: once pregnancy was confirmed, 12-week-old SHRSP rats were randomly assigned to 0.9% saline vehicle (control) or Ang II at 1000 ng/kg/min (SPE) via ALZET® 2002 osmotic minipumps (Charles River, Kent, UK) implanted subcutaneously on GD 10.5. Dams were euthanised on GD 18.5 for collection of placental tissue. From each litter, whole placentas were excised, of which several were dissected into individual placental layers (decidua (dec), junctional zone (jx), and labyrinth (lab)), snap frozen in liquid nitrogen, and stored at -80°C. Whole placentas from n=4 SPE rats and n=4 control rats (total n= 8 rats) and individual placental layers from n=3 SPE rats and n=4 control rats (total n=7 rats) were available for evaluation of miRNA/gene expression and included in the study analysis.

6.3.2 RNA extraction and quality control

Total RNA was extracted from 50 mg of placental tissue using the miRNeasy Mini Kit (QIAGEN, Manchester, UK) as detailed in section 2.1.4. Once tissues were homogenised in QIAzol, RNA extractions were immediately carried out or tissues were stored at -80°C until RNA extractions were performed. RNA extracted from whole placental tissue was analysed using the Agilent BioAnalyzer 2100 as detailed in section 2.1.4.2. RNA extracted from individual placental layers was analysed using NanoDrop® ND-1000 Spectrophotometer as detailed in section 2.1.4.1. All tissues passed the respective quality control checks.

6.3.3 MiRNA library preparation, sequencing, and analysis

MiRNA library preparation and sequencing were performed by Glasgow Polyomics. MiRNA Sequencing libraries were prepared from total RNA using the QIAGEN QiaSeq miRNA Library Kit. Libraries were sequenced on the Illumina NextSeq™ 500 platform in 75 base, single end mode. Adapter and quality trimming of raw sequence reads was performed using the program CutAdapt. The quality of the reads before and after trimming were checked using the

program FastQC. The quality trimmed reads were aligned to the reference genome (GRCH38 release 79) using the program Bowtie (version 1.0.0). The number of reads aligning to known small RNAs, defined by a gff3 file for human (GRCH38 release 79) downloaded from miRBase, was obtained using bedtools. Mapped reads were input into DEseq2 for differential expression analysis to compare samples from the SPE model rat group and control rat group. A total of 827 reads mapped to known mature rat miRNAs listed in the miRBase database with a MIMAT accession number. The base mean, log2 fold change (z-scored), and p-value of <0.05 adjusted for a false discovery rate (FDR) <5% was determined for comparison of each mature miRNA. Principal component analysis (PCA) was performed by Glasgow Polyomics. The heatmap (including hierarchal analysis) and volcano plot were produced together with Simon Fisher, who designed the software PadPlot.

6.3.4 Literature review for selection of candidate miRNAs

The fifteen miRNA expression profiling studies identified in the literature review in the previous chapter (Table 5-2) were utilised in this chapter. In addition, four studies that had previously been excluded based on the time of placenta collection not being stated were included in this literature review (Table 6-1). These were included based on the assumption that placentas were collected at the time of delivery despite the study not explicitly stating this. The data from these four studies were collated with the data from the previously included fifteen studies (Table 5-2) to broaden the scope of miRNAs detected by expression profiling studies in placenta samples from preeclamptic patients. Candidate miRNAs were selected based on their direction of expression detected by miRNA sequencing in placentas of SPE model rats matching the direction of expression reported in expression profiling studies in placenta samples from preeclamptic patients.

Table 6-1 Additional miRNA expression profiling studies conducted in third trimester placentas of patients with PE included in the literature review.

Study	Type of study	Significance	Type of PE	Sample size (n)	Type of delivery	Sampling area
(Zhu et al., 2009)	Microarray	p<0.05 and >1.8-FC	Severe	PE (n=8) control (n=8)	PE and controls matched for gestational age at delivery	Placental villi
(Ishibashi et al., 2012)	Microarray and sequencing	p<0.05	EOPE, LOPE, and SPE	PE (n=8) control (n=10)	PE (term and preterm) control (term)	Placenta
(Choi et al., 2013)	Microarray	≥2-FC	Severe	PE (n=10) control (n=10)	PE (term) control (term)	Central portion of the placental disc
(Jiang et al., 2015)	Microarray	p<0.05 and >1.5-FC	Severe	PE (n=20) control (n=20)	PE (term) control (term)	8 maternal and 8 foetal sites

FC, fold change; PE, preeclampsia, EO, early onset; LO, late onset; SPE, superimposed PE, N/A, not available.

6.3.5 Validation of candidate miRNAs in placentas of a rat model of SPE by TaqMan RT-qPCR

TaqMan RT-qPCR was performed as detailed in section 2.2 using the primers listed in Table 6-2. Data were analysed as detailed in section 2.2.3, with Ct values normalised to housekeeper (U87).

Table 6-2 Primer sequences of Applied Biosystems™ TaqMan™ microRNA Assays.

Assay name	Assay ID	Mature miRNA sequence
Hsa-miR-210-3p	000512	CUGUGCGUGUGACAGCGGCUGA
Rno-miR-19b-3p	000396	UGUGCAAAUCCAUGCAAAACUGA
Hsa-miR-214-3p	002306	ACAGCAGGCACAGACAGGCAGU
Hsa-miR-145-5p	000467	GUCCAGUUUUCCCAGGAAUCCCUU
U87	001712	ACAATGATGACTTATGTTTTTGCCGTTTACCCAGCTGAG GGTTTCTTTGAAGAGAGAATCTTAAGACTGAGC

6.3.6 Study participants and placental tissue collection

Placental tissues were kindly gifted by a research group from University of Oxford. Placental tissues were obtained with written informed consent from women undergoing elective caesarean section without labour at John Radcliffe Hospital Maternity Centre in Oxford, UK between 2015-2019. Placental tissue was collected from patients with PE (n=6) and healthy pregnant women controls (n=4) approved by the Central Oxfordshire Research Ethics Committee C (REFS 07/H0607/74 & 07/H0606/148). PE was defined according to the ISSHP recommendation; new-onset hypertension (>140 mmHg systolic or >90 mmHg diastolic) and presence of one or more of the following: proteinuria (spot urine protein/creatinine >30 mg/mmol [0.3 mg/mg] or >300 mg/day or at least 1 g/L ['2 + '] on dipstick testing), other maternal organ dysfunction, and/or uteroplacental dysfunction (Tranquilli et al., 2014). Healthy pregnant women in the control group had no current or previous history of PE or other gestational hypertensive disorders and no foetal abnormalities. Tissue samples, approximately 8 mm in width, were collected within 10 min of delivery from between the middle section of the placenta and the umbilical cord, capturing

maternal and foetal portions of the placenta. Placentas were immediately snap frozen in liquid nitrogen and stored in -80°C until further analysis.

6.3.7 RNA extraction and quality control

After disrupting placental tissues with a mortar and pestle, total RNA was extracted from 50 mg of placental tissue using the miRNeasy Mini Kit (QIAGEN, Manchester, UK) as detailed in section 2.1.4. Once tissues were homogenised in QIAzol, RNA extractions were immediately carried out or tissues were stored at -80°C until RNA extractions were performed. RNA extracted was analysed using NanoDrop® ND-1000 Spectrophotometer as detailed in section 2.1.4.1. All tissues passed quality control.

6.3.8 Evaluation of candidate miRNAs in placentas of patients with PE by TaqMan RT-qPCR

TaqMan RT-qPCR was performed as detailed in section 2.2 using the primers listed in Table 6-3. Data were analysed as detailed in section 2.2.3, with Ct values normalised to housekeeper (RNU44).

Table 6-3 Primer sequences of Applied Biosystems™ TaqMan™ microRNA Assays.

Assay name	Assay ID	Mature miRNA sequence
Hsa-miR-210-3p	000512	CUGUGCGUGUGACAGCGGCUGA
Hsa-miR-19b-3p	000396	UGUGCAAAUCCAUGCAAAACUGA
Hsa-miR-214-3p	002306	ACAGCAGGCACAGACAGGCAGU
Hsa-miR-145-5p	000467	GUCCAGUUUUCCCAGGAAUCCCUU
RNU44	001094	CCTGGATGATGATAGCAAATGCTGACTGAACATGAAGGT CTTAATTAGCTCTAACTGACT

6.3.9 Gene target prediction

Gene target prediction of miR-210-3p was performed using two online software programs: TargetScan 7.2 (http://www.targetscan.org/vert_72/) and miRDB (http://www.mirdb.org). Gene target prediction of miR-210-3p was also performed using Ingenuity Pathway Analysis (IPA) software. IPA was utilised to identify predicted targets with high and moderate confidence. Predicted targets

were overlaid with genes implicated in PE as determined by the IPA database. Predicted gene targets were only considered as candidates if they had not yet been validated experimentally in trophoblast cells.

6.3.10 Evaluation of candidate gene targets by TaqMan RT-qPCR

TaqMan RT-qPCR was performed as detailed in section 2.2 using the primers listed in Table 6-4 for human placental samples and the primers listed in Table 6-5 for rat placental samples. Data were analysed as detailed in section 2.2.3, with Ct values normalised to housekeeper (RNU44 and U87).

Table 6-4 Human primer sequences of Applied Biosystems™ TaqMan™ Gene Expression Assays.

Gene name	Gene symbol	Assay ID	Fluorescent label
Brain-derived neurotrophic factor	BDNF	Hs02718934_s1	FAM
Fibroblast growth factor receptor-like 1	FGFRL1	Hs00222484_m1	FAM
NDUFA4, mitochondrial complex associated	NDUFA4	Hs00800172_s1	FAM
Solute carrier family 6 member 1	SLC6A1	Hs01104475_m1	FAM
β-2-microglobulin	B2M	Hs99999907_m1	VIC

Table 6-5 Rat primer sequences of Applied Biosystems™ TaqMan™ Gene Expression Assays.

Gene name	Gene symbol	Assay ID	Fluorescent label
Brain-derived neurotrophic factor	BDNF	Rn02531967_s1	FAM
Fibroblast growth factor receptor-like 1	FGFRL1	Rn01531250_g1	FAM
β-actin	ACTB	Rn00667869_m	VIC

6.3.11 Trophoblast cell culture

The human BeWo trophoblast cell line (ATCC, Middlesex, UK) was kindly gifted by Dr Dilys Freeman and Mrs Fiona Jordan (cells frozen down at -80ºC at passage 9). All cell culture work was carried out under sterile conditions in class II biological safety cabinets. Cells were maintained in complete media, DMEM/F-12 (Gibco™, ThermoFisher, Paisley, UK) supplemented with 10% foetal bovine serum

(FBS) (Gibco™, ThermoFisher, Paisley, UK) and 1% penicillin/streptomycin (Gibco™, ThermoFisher, Paisley, UK), in a humidified incubator with 5% CO_2 at 37°C.

6.3.11.1 Cell revival

Frozen down cells were thawed when required at 37ºC in a water bath and immediately transferred to a 10 mL universal containing 5 mL prewarmed complete media. The suspension was gently mixed by pipetting up and down several times and then centrifuged at 1200 RPM for 5 min. The supernatant was discarded, and the remaining cell pellet was resuspended in 1.5 mL of complete media. The cell suspension was added to a T25 flask containing 3.5 mL of prewarmed complete media and placed in the incubator for maintenance.

6.3.11.2 Cell maintenance

Cells were checked daily and media was changed every 24-72 h. Cells were passaged when they reached 70-80% confluency. Passaging was performed by removing media and washing the cells with 5 mL of 1X PBS. Cells were detached from the flask by adding 2 mL of 1X trypsin-EDTA (Sigma-Aldrich, Schnelldorf, Germany) and placing the flask in the incubator for 5 min. Cells were checked under the microscope to see if they had detached, and the flask was gently tapped until the cells were floating freely. To inactivate the trypsin, 6 mL of complete media was added to the flask. The total volume of cell suspension was transferred to a 10 mL universal and centrifuged at 1200 RPM for 5 min. The supernatant was discarded, and the remaining cell pellet was resuspended in complete media for subculturing at a 1:3 ratio or for cryopreservation. For cryopreservation, cells were resuspended in 95% complete media supplemented with 5% dimethyl sulfoxide (Fisher Scientific, Loughborough, UK) and aliquoted into cryovials (Alpha-laboratories, Hampshire, UK). The cryovials were placed in an isopropanol filled Mr. Frosty™ Freezing Container (ThermoFisher Scientific, Paisley, UK) overnight at -80ºC, and then transferred to a liquid nitrogen freezer for storage.

6.3.11.3 Cell counting

Cell counting was performed after trypsinisation prior to cryopreservation or for seeding cells at a desired density. Cells were counted using a Bright Line Haemocytometer (Sigma, Dorset, UK). The cell suspension (10 µL) was diluted 1:2 with 0.4% trypan blue (10 µL) (Sigma, Dorset, UK), and 10 µL of the solution was pipetted onto the haemocytometer underneath a coverslip. Using a light microscope, the number of viable cells in each of the corner quadrants was counted. Blue stained cells or cells touching the bottom or right-hand line of any quadrant were not counted. An average of the four quadrants was calculated and multiplied by 10^4 and corrected for by the dilution factor to obtain the number of cells per mL in the suspension.

6.3.11.4 Cell transfection

Cells were trypsinized and resuspended to obtain a seeding density of $1.5x10^5$ cells /mL and set aside in a 37ºC water bath prior to reverse transfection. Reverse transcription was performed on a 12-well plate using siPORT™ *NeoFX*™ Transfection Agent (Ambion, Loughborough, UK). SiPORT™ *NeoFX*™ Transfection Agent (3 µL or 1 µL) was diluted into Opti-MEM® medium to 50 µL and incubated for 10 min at room temperature. MirVana™ miRNA Mimic (miR-210-3p, assay ID MC10516), mirVana™ miRNA Inhibitor (has-miR-210-3p, assay ID MH10516), and mirVana™ miRNA Inhibitor Negative Control #1 (Ambion, Loughborough, UK) (3 µL) were diluted into Opti-MEM® medium to 50 µL. The diluted transfection reagent and diluted mirVana™ miRNA were mixed together at equal volumes and incubated at room temperature for 10 min. Transfection complexes were aliquoted at 100 µL per well. Cell suspensions of 900 µL containing $1.5x10^5$ cells were added to each well, and the plate was gently tilted back and forth to evenly distribute and mix the cell suspension with the transfection complexes. The cells were incubated for 24, 48, or 72 h until ready to assay.

6.3.11.5 RNA extraction and quality control

Total RNA was extracted from cells using the miRNeasy Mini Kit (QIAGEN, Manchester, UK) as detailed in section 2.1.4. Once cells were lysed by adding QIAzol, RNA extractions were immediately carried out or cell homogenates were stored at -80°C until RNA extractions were performed. RNA extracted was

analysed using NanoDrop® ND-1000 Spectrophotometer as detailed in section 2.1.4.1. All RNA extracted passed quality control.

6.3.11.6 Evaluation of miR-210-3p and predicted gene target expression by TaqMan RT-qPCR

TaqMan RT-qPCR was performed as detailed in section 2.2 using the primers listed in Table 6-4. Data were analysed as detailed in section 2.2.3, with Ct values normalised to housekeeper (RNU44).

6.3.11.7 MTT assay

Cell viability was measured with TACS® MTT Cell Proliferation Assay kit (R&D Systems, Abingdon, UK). Cells were washed with 1X PBS and transfection media was replaced with low serum (1% FBS) media. Cells were incubated with 100 µL MTT Reagent for 3 h at 37ºC. Detergent Reagent (1 mL) was added to each well, and cells were incubated overnight at room temperature. A 'no cells' control was used as a blank. Absorbance was measured at 560 nm using the PerkinElmir 2030 plate reader (Perkin Elmer, Singapore, Singapore). The blank absorbance value was subtracted from all readings prior to analysis.

6.3.12 Statistical analysis

For miRNA sequencing data, a p-adjusted value <0.05 was considered significant. GraphPad Prism 9 was used to analyse all other data sets. TaqMan data are shown as mean ∆Ct ± SEM and were analysed as follows: the SPE model group (Ang II) vs control group (vehicle) as well as patients with PE vs healthy controls were compared by unpaired t-test (with Welch's correction as appropriate); cells only, scramble, mimic and inhibitor groups were compared by one-way ANOVA followed by Tukey's post-hoc multiple comparisons test. Clinical characteristics are presented as mean ± SD or median (range). All normally distributed variables were compared by unpaired t-test (with Welch's correction as appropriate) and non-normally/discrete variables by Mann-Whitney U test. MTT assay data were expressed as median cell viability % (IQR). This was calculated from absorbance ratios of treatment values normalised to 'cells only' values set to 100% and analysed by Kruskal-Wallis test followed by Dunn's post-hoc multiple comparisons test. For statistical tests, $p<0.05$ was considered significant.

6.4 Results

6.4.1 RNA quality control

Rat placenta RNA quality and concentration were assessed prior to miRNA sequencing using the Agilent 2100 Bioanalyzer by analysing the electrophoretic trace. In the electrophoresis gel, bands at ~4000 and ~2000 nts across all placenta samples indicate detection of 28S and 18S ribosomal RNA, respectively (Figure 6-1A). Faint bands ~100 nts across all samples demonstrate detection of small RNA (Figure 6-1A). The electropherogram of a control sample shows clear distinct peaks of 28S and 18S ribosomal RNA at ~4000 and ~2000 nts, with low noise between the peaks, indicating extraction of intact RNA (Figure 6-1B). The electropherogram also shows a peak between 25-200 nts, indicating presence of small RNA such as miRNA (Figure 6-1B). The peak at 25 nts represents the DNA ladder (Figure 6-1B). The ratio of the 28S and 18S ribosomal RNA peaks determined the RIN. All RNA samples had a RIN greater than 8 (Table 6-6), indicating extraction of intact RNA suitable for miRNA sequencing.

6.4.2 Quality control of miRNA sequencing samples

A PCA plot was generated to visualise the variance between individual samples and groups based on their miRNA expression profiles. PCA clustering was observed between the control and SPE model group (PC1=46% variance and PC2=15% variance), indicating variation in the miRNA expression between samples was primarily due to treatment differences between control rats (vehicle) and SPE model rats (Ang II) (Figure 6-2). Samples in the SPE model group showed less variation than samples in the control group.

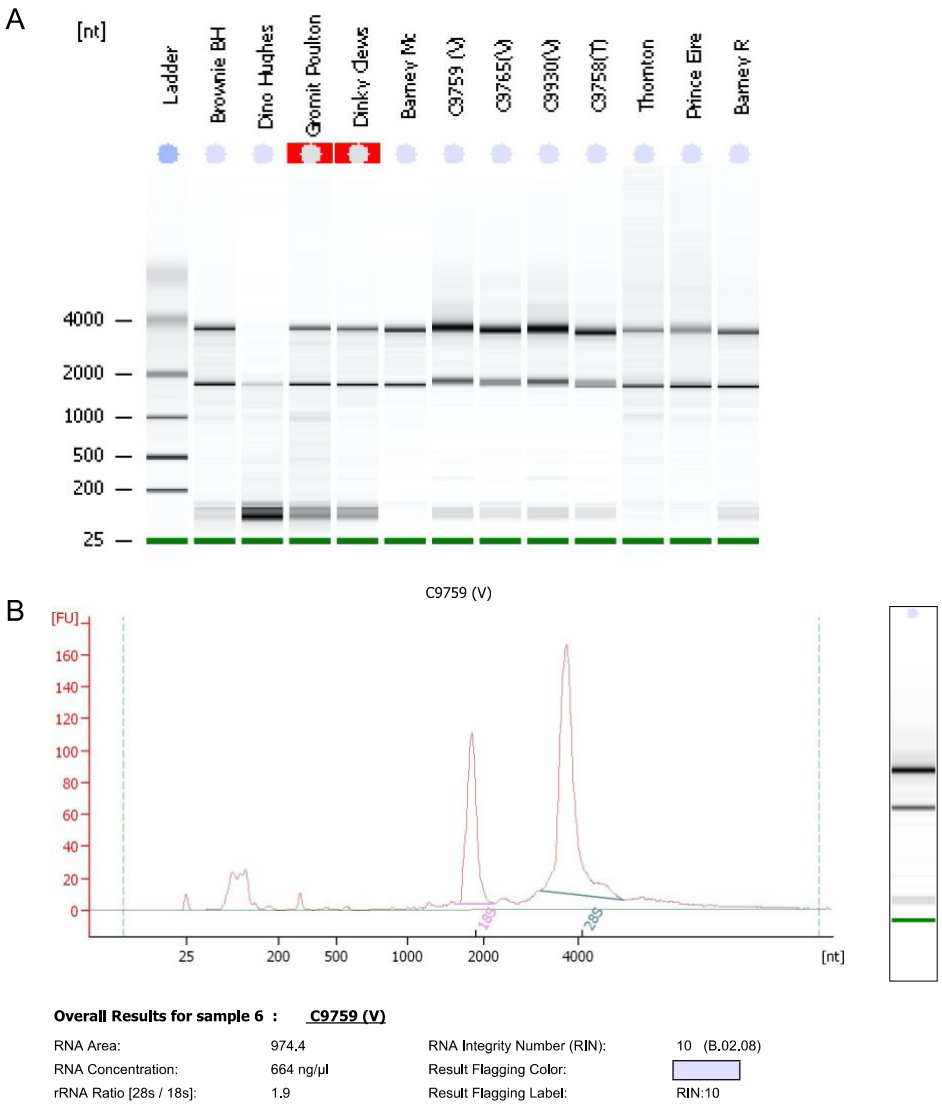

Figure 6-1 Representative image of Agilent 2100 Bioanalyzer results.

Representative results from Eukaryote Total RNA Nano assay run on whole placenta samples (C numbers) from control (vehicle-treated (V)) and SPE model (Ang II-treated (T)) SHRSP rats for assessment of RNA quality and concentration. **(A)** Electrophoresis run of the ladder, controls (Brownie BH, Dino Hughes, Gromit Poulton, Dinky Clews, Barney Mc, Prince Eire, and Barney R), and samples (C numbers). **(B)** Electropherogram for sample from control SHRSP rat (C9759) and overall results, including RNA concentration, rRNA Ratio (28S and 18S ribosomal RNA), and RIN.

Table 6-6 Agilent 2100 Bioanalyzer results of RNA quality (RIN) and concentration.

Animal	ID	RIN	Concentration (ng/µL)
Control	C9759	10.0	664
	C9765	9.5	420
	C9930	10.0	543
	C9767	10.0	452
SPE model	C9758	9.5	524
	C9872	10.0	514
	C9948	9.4	356
	C9955	9.4	382

RIN, research integrity number.

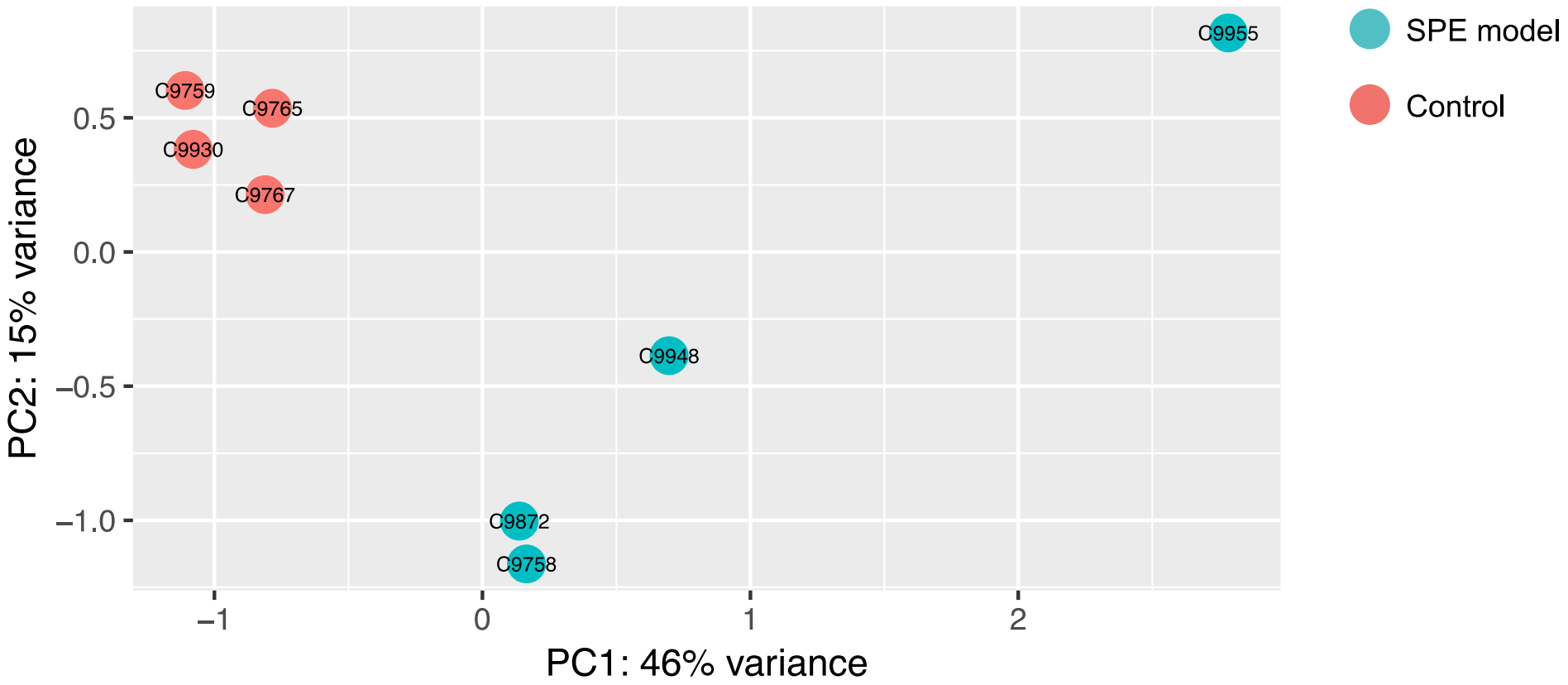

Figure 6-2 Principal component analysis plot of whole placental samples from control and SPE model rats.

PCA was performed to identify the variation between samples from the control and SPE model groups based on their miRNA expression data.

6.4.3 Summary of differentially expressed miRNAs by miRNA sequencing

In the placentas of SPE model rats, 56 miRNAs were significantly differentially expressed compared to control rats (adjusted p-value of<0.05) (Figure 6-3). Of these, 32 miRNAs were significantly upregulated and 24 miRNAs were significantly downregulated in the placentas of SPE model rats compared to control rats (adjusted p-value of<0.05) (Figure 6-3), which are listed in Table 6-7. Due to the relatively large number of significantly differentially expressed miRNAs detected by miRNA sequencing, a selection of candidate miRNAs was chosen to investigate further. Candidate miRNAs were selected based on their detection by miRNA expression profiling studies in placenta samples from preeclamptic patients.

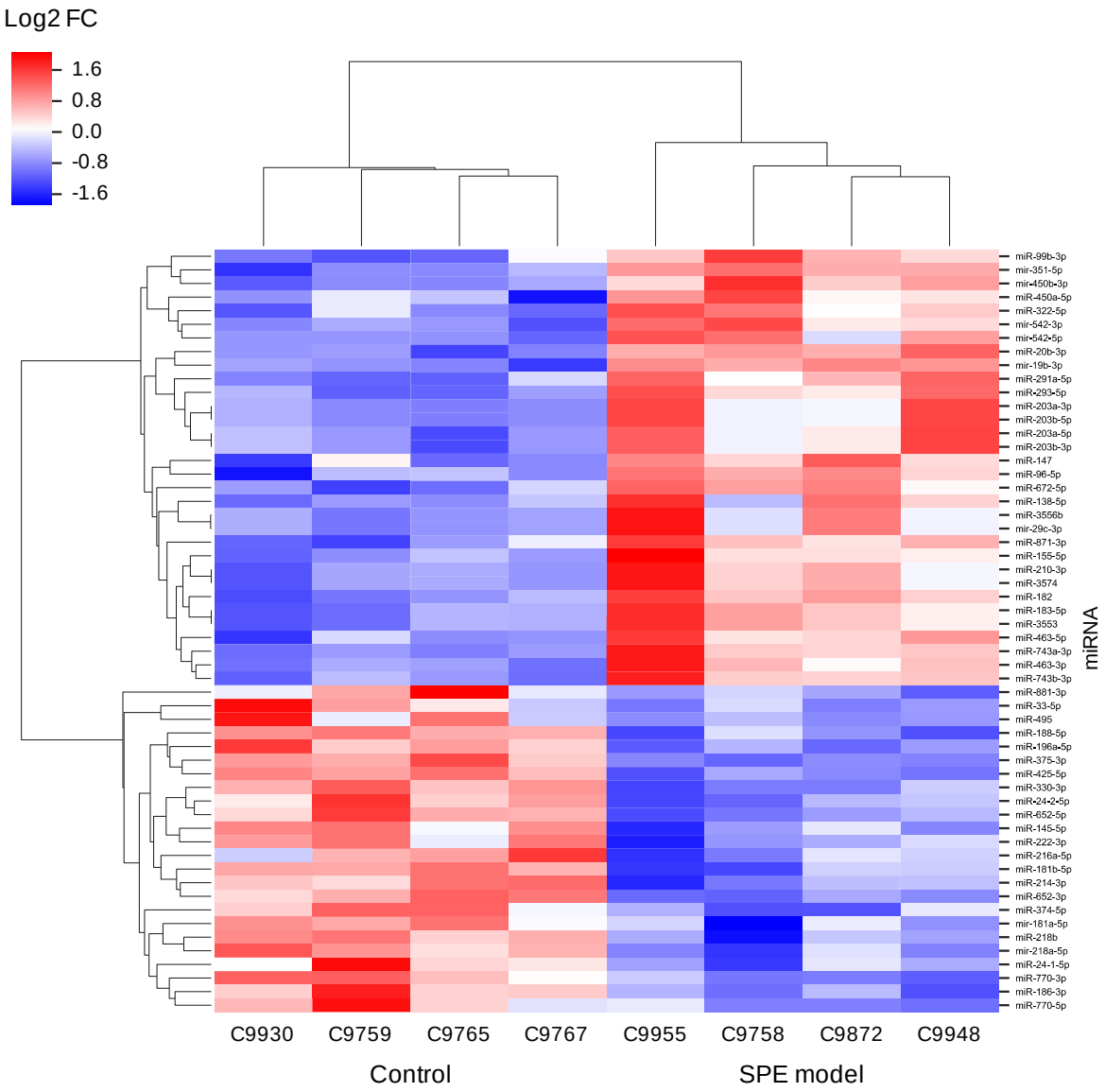

Figure 6-3 Heatmap of significantly differentially expressed miRNAs in placentas of SPE model rats compared to control rats as detected by miRNA sequencing.

Heatmap showing hierarchical cluster analysis of significantly differentially expressed miRNAs with expression presented as log2 fold change (z-scored) (adjusted p-value of <0.05). Red indicates upregulation and blue indicates downregulation in expression. Colour intensity is determined by log2 fold change. Each column represents a placenta sample from a single rat: control rats (C9930, C9759, C975, and C9767) and SPE model rats (C9955, C9758, C9872, and C9948). Dendrogram at the top of the heatmap represents hierarchical clustering of rats within and between groups, and dendrogram to the left of the heatmap represents hierarchical clustering within and between up- and downregulated miRNAs. FC, fold change.

Table 6-7 List of significantly differentially expressed miRNAs in placentas of SPE model rats compared to control rats as detected by miRNA sequencing.

Upregulated miRNAs				Downregulated miRNAs			
miRNA	**log2 FC**	**base mean**	**p-adjusted**	**miRNA**	**log2 FC**	**base mean**	**p-adjusted**
rno-miR-20b-3p	1.14	20.20	6.21E-03	rno-miR-652-5p	-1.46	47.93	3.90E-06
rno-miR-203a-3p	0.58	4287.63	1.89E-05	rno-miR-216a-5p	-0.99	22.78	4.48E-02
rno-miR-203b-5p	0.58	4287.63	1.89E-05	rno-miR-330-3p	-0.88	66.47	2.08E-04
rno-miR-210-3p	0.58	3024.11	1.89E-05	rno-miR-24-2-5p	-0.78	66.04	2.38E-03
rno-miR-3574	0.58	3024.11	1.89E-05	rno-miR-186-3p	-0.76	63.28	2.89E-03
rno-miR-138-5p	0.49	853.90	1.14E-03	rno-miR-24-1-5p	-0.63	65.60	3.35E-02
rno-miR-203a-5p	0.39	1353.45	9.55E-04	rno-miR-375-3p	-0.59	439.07	6.12E-08
rno-miR-203b-3p	0.39	1353.45	9.55E-04	rno-miR-652-3p	-0.46	431.25	2.33E-05
rno-mir-542-5p	0.37	22981.42	7.25E-05	rno-miR-214-3p	-0.45	352.06	9.24E-04
rno-mir-542-3p	0.36	264299.80	4.76E-05	rno-miR-770-5p	-0.44	274.99	6.78E-03
rno-miR-672-5p	0.35	926.81	9.24E-04	rno-miR-33-5p	-0.42	132.43	5.58E-02
rno-miR-147	0.34	544.48	6.37E-03	rno-miR-188-5p	-0.41	175.52	9.19E-03
rno-miR-155-5p	0.33	4335.52	2.38E-03	rno-miR-181b-5p	-0.40	286.37	6.21E-03
rno-miR-182	0.33	59057.97	4.76E-05	rno-miR-222-3p	-0.40	127.42	5.33E-02
rno-miR-3556b	0.31	4655.04	3.73E-03	rno-miR-196a-5p	-0.40	2287.91	1.89E-05
rno-mir-29c-3p	0.31	9259.60	6.21E-03	rno-miR-495	-0.38	744.40	9.19E-03
rno-miR-293-5p	0.31	72733.49	2.26E-04	rno-miR-770-3p	-0.37	443.10	2.01E-03
rno-mir-450b-3p	0.28	3831.14	7.33E-04	rno-miR-881-3p	-0.31	517.58	4.08E-02
rno-miR-322-5p	0.27	297923.00	2.89E-03	rno-miR-218b	-0.28	978.31	6.21E-03
rno-miR-291a-5p	0.27	3266.43	2.23E-03	rno-miR-425-5p	-0.26	6732.42	6.29E-05
rno-miR-463-5p	0.27	16596.91	2.95E-03	rno-miR-145-5p	-0.26	4483.38	6.21E-03
rno-miR-183-5p	0.26	37752.35	2.23E-03	rno-miR-374-5p	-0.23	3794.60	1.53E-02
rno-miR-3553	0.26	37752.35	2.23E-03	rno-mir-181a-5p	-0.23	1591.92	5.13E-02
rno-mir-19b-3p	0.26	25000.34	6.72E-05	rno-mir-218a-5p	-0.21	5580.29	9.19E-03
rno-miR-96-5p	0.25	25078.48	2.89E-03	rno-miR-652-5p	-1.46	47.93	3.90E-06
rno-mir-351-5p	0.24	59227.43	5.85E-04	rno-miR-216a-5p	-0.99	22.78	4.48E-02
rno-miR-743b-3p	0.23	18896.54	3.09E-03	rno-miR-330-3p	-0.88	66.47	2.08E-04
rno-miR-743a-3p	0.22	27050.93	3.29E-03				
rno-miR-450a-5p	0.21	21268.30	4.32E-02				
rno-miR-463-3p	0.21	15060.15	9.19E-03				
rno-miR-871-3p	0.19	9545.47	2.90E-02				
rno-miR-99b-3p	0.18	1762.04	5.58E-02				

MiRNAs are listed in descending order from largest log2 FC. FC, fold change.

6.4.4 Literature review for selection of candidate miRNAs

Of the 56 significantly differentially expressed miRNAs detected by miRNA sequencing, a total of eleven miRNAs were identified that were detected by miRNA expression profiling studies in placenta samples from preeclamptic patients (Table 6-8). The direction of expression of four miRNAs as detected by miRNA sequencing matched the direction of expression reported by the expression profiling studies in placentas of preeclamptic patients (Table 6-8). MiR-210-3p and miR-19b-3p were found to be upregulated and miR-214-3p and miR-145-5p were found to be downregulated in miRNA sequencing in placentas of the SPE rat model and in expression profiling studies in placentas of preeclamptic patients (Table 6-8). These candidates (miR-210-3p, miR-19b-3p, miR-214-3p, and miR-145-5p (Figure 6-4)) were selected for validation in whole placentas and individual placental layers in the rat model of SPE by TaqMan RT-qPCR.

Table 6-8 Selection of candidate miRNAs for validation in a rat model of SPE.

miRNA (direction of expression)	**Studies reporting significant difference in miRNA expression**		
	Up	**Down**	**Direction not reported**
210-3p (up)	(Enquobahrie et al., 2011) (Betoni et al., 2013) (Xu et al., 2014a) (Weedon-Fekjær et al., 2014) (Zhang et al., 2015a) (Vashukova et al., 2016) (Zhou et al., 2016)	None	None
214-3p (down)	None	(Hu et al., 2009) (Xu et al., 2014a) (Zhao et al., 2014)	None
19b-3p (up)	(Ishibashi et al., 2012) (Zhang et al., 2015a)	None	None
145-5p (down)	None	(Ishibashi et al., 2012)	
188-5p (down)	(Yang et al., 2015)	(Ishibashi et al., 2012)	None
182 (up)	(Zhang et al., 2015a)	(Jiang et al., 2015)	None
181a-5p (down)	(Hu et al., 2009) (Zhu et al., 2009) (Xu et al., 2014a) (Jiang et al., 2015) (Zhang et al., 2015a)	None	None
542-3p (up)	None	(Zhu et al., 2009) (Betoni et al., 2013) (Xu et al., 2014a) (Lykoudi et al., 2018)	None
495 (down)	(Ishibashi et al., 2012) (Zhao et al., 2014)	None	(Wang et al., 2012c)
542-5p (up)	None	(Ishibashi et al., 2012)	None
222-3p (down)	(Hu et al., 2009)	None	None

Selected candidate miRNAs are highlighted in bold.

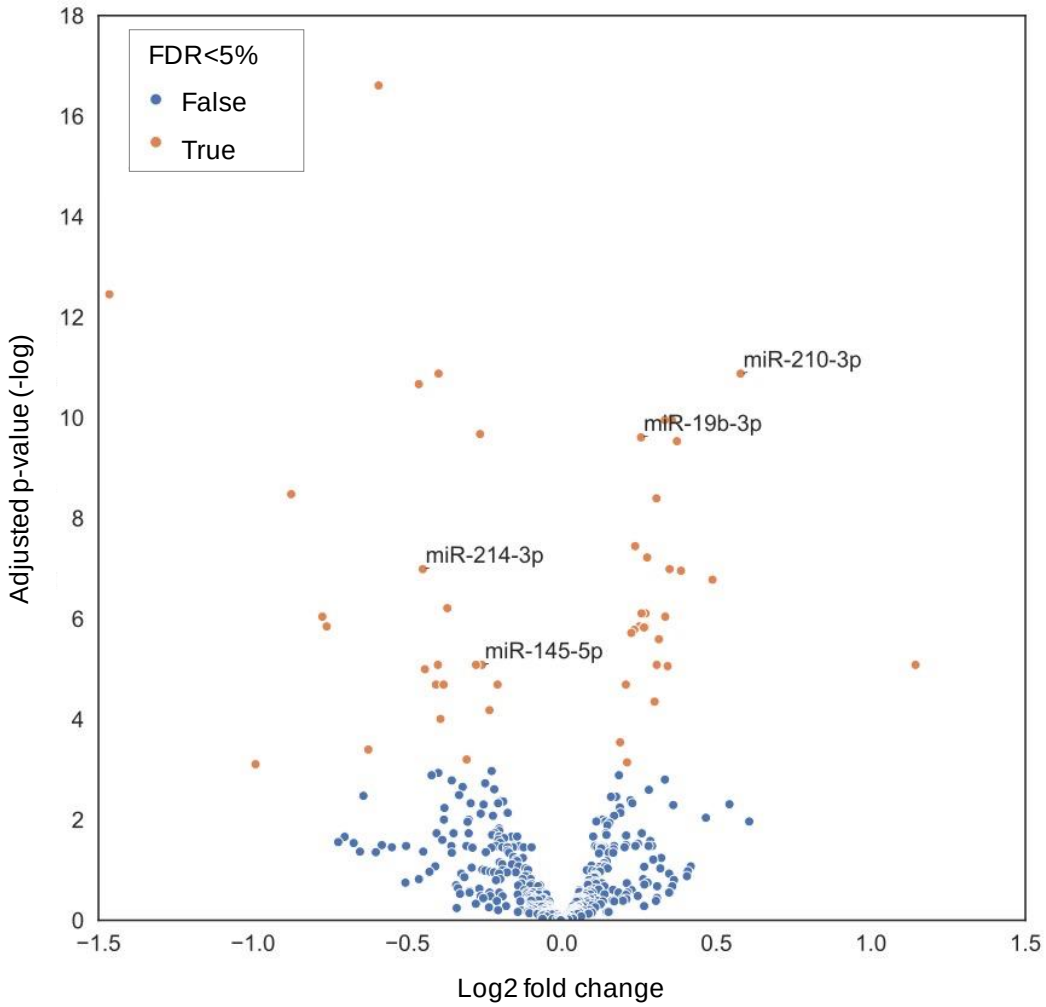

Figure 6-4 Volcano plot of miRNA expression in whole placenta samples of SPE models compared to controls as detected by miRNA sequencing.

Expression is presented as adjusted p-value (-log) plotted against log2 fold change, with positive fold change values indicating upregulation and negative values indicating downregulation of miRNAs in placentas of SPE model rats versus control rats. Orange denotes miRNAs significantly differentially expressed and blue denotes no significant difference in expression (p-value of <0.05 adjusted for false discovery rate (FDR)<5%).

6.4.5 Validation of candidate miRNAs in a rat model of SPE

The expression of four candidate miRNAs was evaluated by RT-qPCR in whole placentas and individual placental layers of SPE model rats compared to control rats to validate the findings from the miRNA sequencing experiment. None of the candidate miRNAs (miR-210-3p, miR-19b-3p, miR-214-3p, and miR-145-5p) were significantly differentially expressed in whole placentas of SPE model rats compared to controls (Figure 6-5). MiR-210-3p was significantly downregulated in the decidual layer (1.43±0.03 vs 0.41±0.29 ΔCt, $p<0.05$) and significantly upregulated in the labyrinth layer (3.04±0.05 vs 3.60±0.12 ΔCt, $p<0.05$) of SPE model rats compared to controls (Figure 6-6A) (as previously reported in Chapter 5 Figure 5-4). MiR-19b-3p was significantly downregulated in the decidual layer (2.69±0.13 vs 2.10±0.15 ΔCt, $p<0.05$) of SPE model rats compared to controls (Figure 6-6B). MiR-145-5p was significantly downregulated in the labyrinth layer (1.38±0.03 vs 1.26±0.02 ΔCt, $p<0.05$) of SPE model rats compared to controls (Figure 6-6D). There was no significant difference in miR-214-3p expression across any of the placental layers in SPE model rats compared to controls (Figure 6-6C).

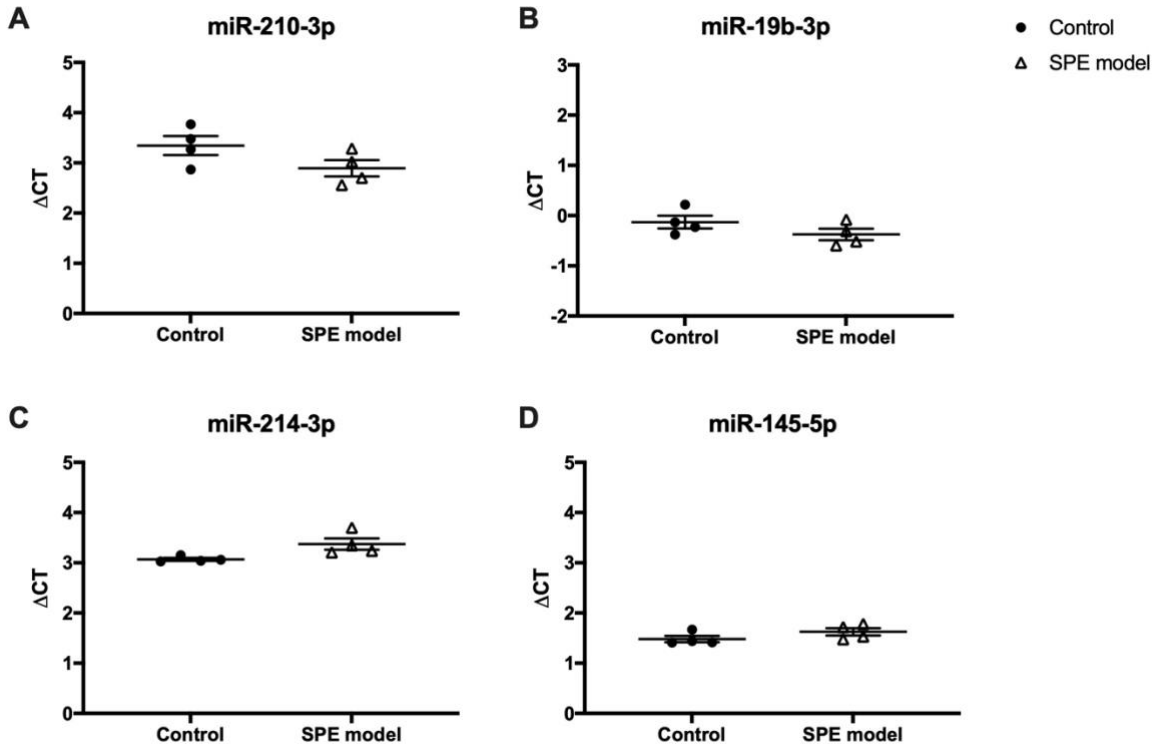

Figure 6-5 Evaluation of candidate miRNAs in whole placentas of a rat model of SPE by TaqMan RT-qPCR.

(A) MiR-210-3p, **(B)** miR-19b-3p, **(C)** miR-214-3p, and **(D)** miR-145-5p were not significantly differentially expressed in whole placental tissue of a rat model of SPE. Data are shown as mean ΔCt ± SEM. Ct values were normalised to housekeeper U87, n=4 per group, analysed using ΔCt values by unpaired t-test or unpaired t-test with Welch's correction as appropriate.

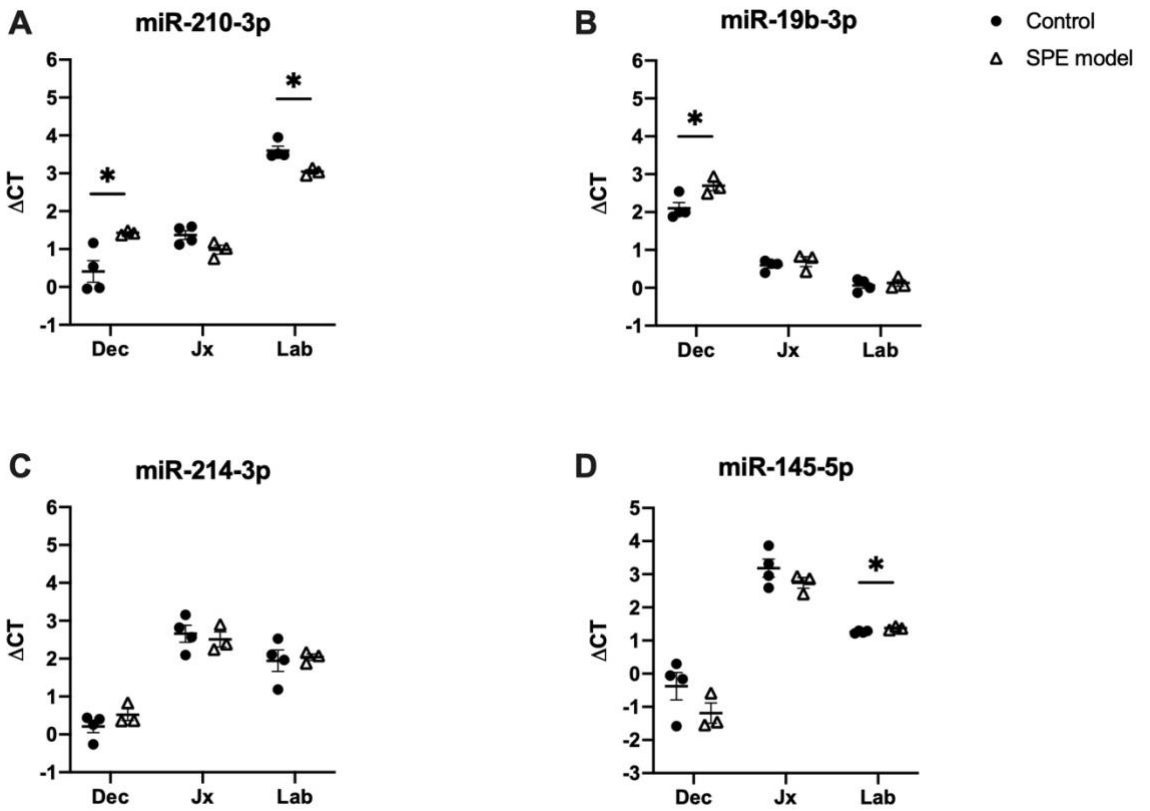

Figure 6-6 Evaluation of candidate miRNAs in individual placental layers (decidua, junctional zone, and labyrinth) of a rat model of SPE by TaqMan RT-qPCR.

(A) MiR-210-3p was significantly downregulated in the decidua and significantly upregulated in the labyrinth of a rat model of SPE (as previously reported in Chapter 5 Figure 5-4). **(B)** MiR-19b-3p was significantly downregulated in the decidua of a rat model of SPE. **(C)** MiR-214-3p was not significantly differentially expressed in individual placental layers of a rat model of SPE. **(D)** MiR-145-5p was significantly downregulated in the labyrinth of a rat model of SPE. Data are shown as mean ΔCt $\pm$ SEM. Ct values were normalised to housekeeper U87, *p<0.05, n=3 in SPE group and n=4 in control group, analysed using ΔCt values by unpaired t-test or unpaired t-test with Welch's correction as appropriate. Dec, decidua; Jx, junctional zone; Lab, labyrinth.

6.4.6 Candidate miRNAs in patients with PE

6.4.6.1 Clinical characteristics of study participants

The clinical characteristics of patients with PE (n=6) and healthy pregnant control women (n=4) are listed in Table 6-9. Patients with PE and healthy controls were matched in terms of maternal age, BMI, and parity (Table 6-9). However, patients with PE delivered at a significantly earlier gestational age compared to healthy controls ($p<0.05$), and infants of patients with PE were significantly lighter than infants of healthy controls ($p<0.05$) (Table 6-9). In line with the clinical symptoms of PE, patients with PE had significantly higher maximum systolic and diastolic blood pressure compared to healthy controls ($p<0.0001$), and significant proteinuria was detected in patients with PE compared to healthy controls ($p<0.01$) (Table 6-9).

6.4.6.2 Evaluation of candidate miRNAs in patients with PE

The expression of four candidate miRNAs was evaluated by RT-qPCR in placentas of patients with PE compared to healthy pregnant control women. In line with a significant upregulation in placentas of SPE model rats as detected by miRNA sequencing, miR-210-3p and miR-19b-3p were significantly upregulated in placentas of preeclamptic patients compared to controls (2.34±0.24 vs 4.03±0.24 ΔCt, $p<0.01$ and -0.26±0.16 vs 0.34±0.09 ΔCt, $p<0.05$, respectively) (Figure 6-7A and B). There was no significant difference in miR-214-3p and miR-145-5p expression in the placentas of preeclamptic patients compared to controls (Figure 6-7C and D).

Table 6-9 Clinical characteristics of pregnant healthy control women and women with PE.

Characteristic (units)	Control (n=4)	PE (n=6)
Maternal age (years)	35.3 ± 4.1	37.3 ± 4.1
Gestational age (weeks)	39.9 ± 1.2	35.7 ± 3.1*
Maximum[a] systolic blood pressure (mm Hg)	127.0 ± 8.7	176.0 ± 9.2 ****
Maximum[a] diastolic blood pressure (mm Hg)	69.0 ± 8.2	99.2 ± 3.1 ****
Maximum[a] protein (mg/dL)	ND/NAD	351.0 (41.0-786.0) **
Infant birth weight (g)	3868.8 ± 251.2	2271.0 ± 928.5 *
Body mass index at delivery (kg/m^2)	28.2 ± 6.0	25.5 ± 4.3
Parity (number of past pregnancies reaching viable gestation)	0.5 (0-1.0)	1.0 (1.0-1.0)

[a]maximum refers to maximum values recorded during pregnancy. Values are presented as mean ± SD or median (range), *p<0.05, **p<0.01, ****p<0.0001, unpaired t-test (with Welch's correction as appropriate) for age, blood pressure, weight, and body mass index and Mann-Whitney U test for protein and parity Mann-Whitney U test. PE, preeclampsia; ND, not detected; NAD, nothing abnormal detected.

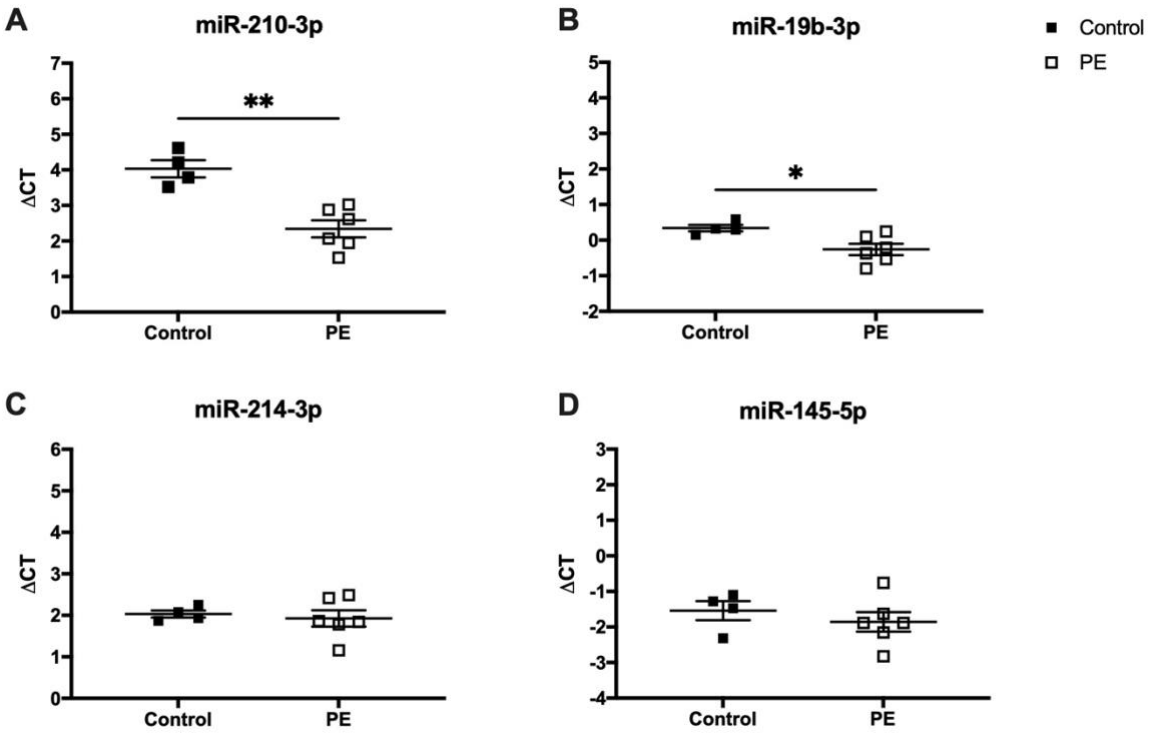

Figure 6-7 Evaluation of candidate miRNAs in placentas of patients with PE by TaqMan RT-qPCR.

(A) MiR-210-3p and **(B)** miR-19b-3p were significantly upregulated in placentas of patients with PE. **(C)** MiR-214-3p and **(D)** miR-145-5p were not significantly differentially expressed in placentas of patients with PE. Data are shown as mean ΔCt ± SEM. Ct values were normalised to housekeeper RNU44, *p<0.05 and **p<0.01, n=4 in healthy pregnant group and n=6 in PE group, analysed using ΔCt values by unpaired t-test.

6.4.7 Evaluation of predicted gene targets of miR-210-3p

6.4.7.1 Selection of candidate miR-210-3p predicted gene targets

TargetScan 7.2 and miRDB were utilised to identify predicted gene targets of miR-210-3p in humans. A total of 15 genes were predicted to be miR-210-3p targets in humans by both TargetScan and miRDB (Table 6-10). Although not predicted by TargetScan or miRDB to be a gene target in rats, fibroblast growth factor receptor-like 1 (FGFRL1) was selected as a candidate gene target since it has the greatest number of predicted conserved sites and has not yet been validated as a miR-210-3p gene target in trophoblast cells (Table 6-10). Brain-derived neurotrophic factor (BDNF) and NADH dehydrogenase (ubiquinone) 1 alpha subcomplex, 4, 9kDa (NDUFA4) were selected as candidate genes since they are predicted to be miR-210-3p targets in rats by both TargetScan and miRDB and have not yet been validated as miR-210-3p gene targets in trophoblast cells (Table 6-10).

In addition to TargetScan and miRDB, predicted gene targets of miR-210-3p were identified by IPA. The predicted gene targets of miR-210-3p were overlaid with the 707 genes IPA has listed as associated with PE. The overlap led to identification of a single gene, solute carrier family 6 member 1 (SLC6A1) (Figure 6-8). SLC6A1 was selected as the final candidate gene target to investigate further since it has also not yet been validated as a miR-210-3p gene target in trophoblast cells.

Table 6-10 Selection of candidate predicted gene targets of miR-210-3p in human and rat.

Predicted gene target in human	Number of conserved sites in human		Predicted gene target in rat		Validated target in trophoblast cells
	TargetScan	miRDB	TargetScan	miRDB	
FGFRL1	8	8	No	No	No
SCARA3	3	2	No	No	No
ELFN2	2	1	Yes	No	No
ISCU	1	1	Yes	Yes	Yes[1]
BDNF	1	1	Yes	Yes	No
NDUFA4	1	1	Yes	Yes	No
GPD1L	1	1	Yes	No	No
KMT2D	1	1	Yes	No	No
MID1IP1	1	1	Yes	No	No
KCMF1	1	1	No	No	Yes[2]
B4GALT5	1	1	No	No	No
DENND6A	1	1	No	No	No
DIMT1	1	1	No	No	No
E2F3	1	1	No	No	No
ST3GAL3	1	1	No	No	No

Selected candidate genes are highlighted in bold. (1) (Lee et al., 2011) and (2) (Luo et al., 2014). FGFRL1, fibroblast growth factor receptor-like 1; SCARA3, scavenger receptor class A member 3; ELFN2, extracellular leucine rich repeat and fibronectin type III domain containing 2; ISCU, iron-sulphur cluster assembly scaffold; BDNF, brain-derived neurotrophic factor; NDUFA4, NDUFA4, mitochondrial complex associated; GPDL1, glycerophosphodiesterase-like 1; KMT2D, lysine methyltransferase 2D; MID1IP1, MID1 interacting protein 1; KCMF1, potassium channel modulatory factor 1; B4GALT5, β-1,4-galactosyltransferase 5; DENND6A, DENN domain containing 6A; DIMT1, DIMT1 rRNA methyltransferase and ribosome maturation factor; E2F3, E2F transcription factor 3; ST3GAL3, ST3 β-galactoside alpha-2,3-sialyltransferase 3.

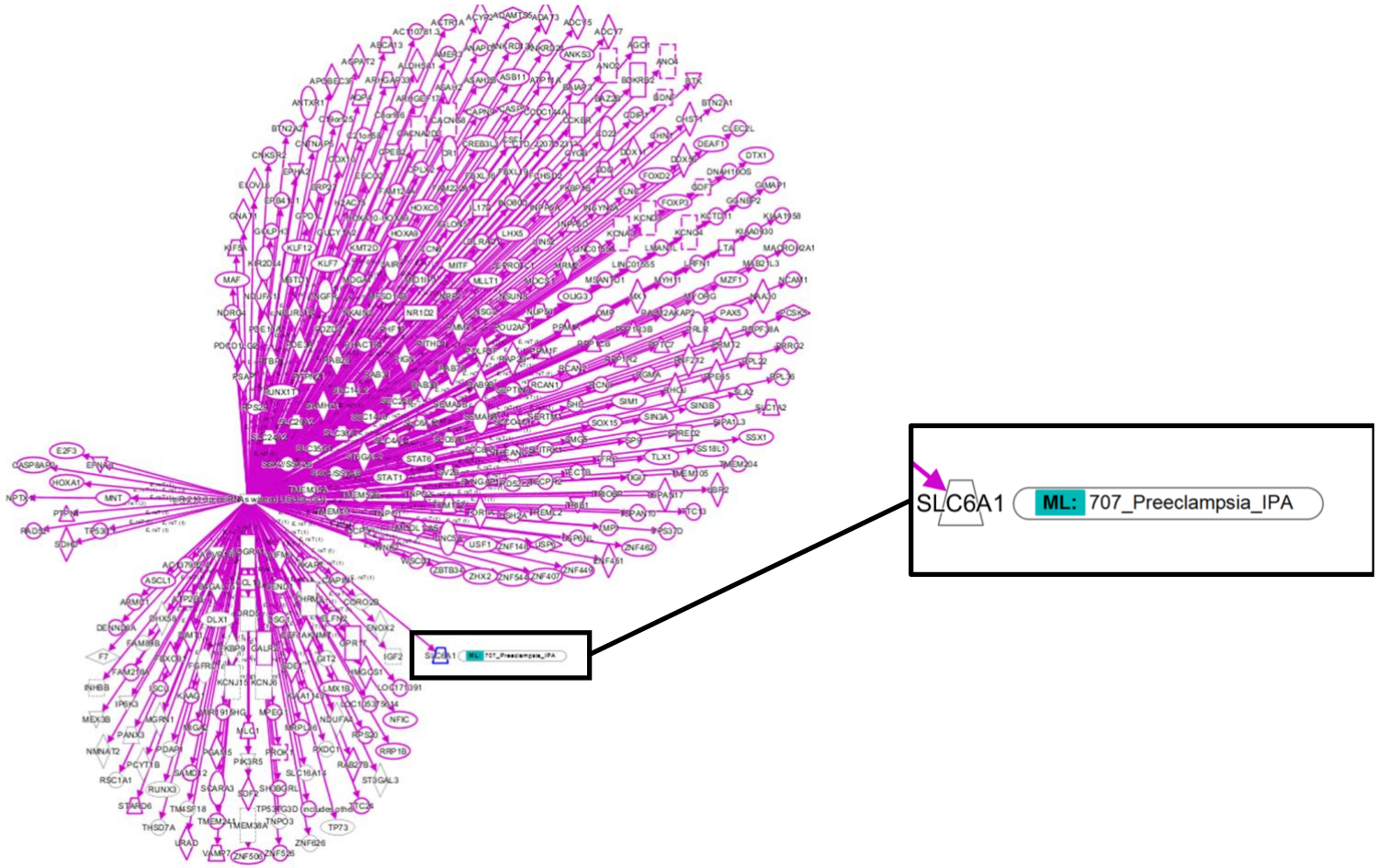

Figure 6-8 Predicted gene targets of miR-210-3p overlaid with 707 PE genes from IPA.

Overlay of predicted gene targets of miR-210-3p with 707 PE genes identifies a single gene: SLC6A1.

6.4.7.2 Evaluation of candidate miR-210-3p predicted gene targets in a rat model of SPE and patients with PE

The expression of four candidate genes (FGFRL1, BDNF, NDUFA4, and SLC6A1) was evaluated by RT-qPCR in placentas of patients with PE. FGFRL1 and BDNF were significantly downregulated in the placentas of preeclamptic patients compared to healthy pregnant controls (-10.56±0.30 vs -11.64±0.35 ΔCt, $p<0.05$ and -6.72±0.18 vs -8.08±0.21 ΔCt, $p<0.01$, respectively) (Figure 6-9A and B). NDUFA4 and SLC6A1 were not significantly differentially expressed in the placentas of preeclamptic patients compared to controls (Figure 6-9C and D).

The predicted gene targets FGFRL1 and BDNF that were significantly differentially expressed in patients with PE were subsequently evaluated in whole placentas of a rat model of SPE. FGFRL1 was significantly downregulated in SPE model rats compared to control rats (16.04±0.21 vs 15.28±0.18 ΔCt, $p<0.05$) (Figure 6-10A). BDNF was not detected in the placentas of SPE model and control rats (Figure 6-10B).

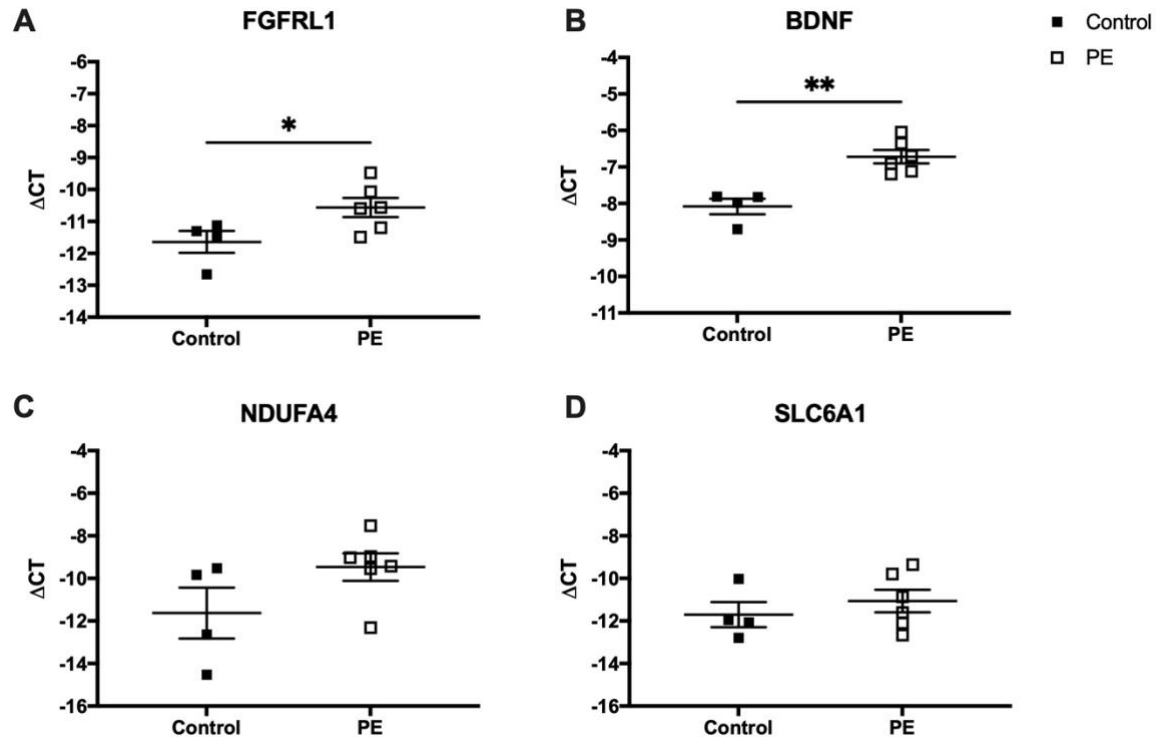

Figure 6-9 Evaluation of miR-210-3p predicted gene targets in placentas of patients with PE by TaqMan RT-qPCR.

(A) FGFRL1 and **(B)** BDNF were significantly downregulated in placentas of PE patients. **(C)** NDUFA4 and **(D)** SLC6A1 were not significantly differentially expressed in the placentas of PE patients. Data are shown as mean ΔCt ± SEM. Ct values were normalised to housekeeper B2M, *p<0.05 and **p<0.01, n=4 in healthy pregnant group and n=6 in PE group, analysed using ΔCt values by unpaired t-test.

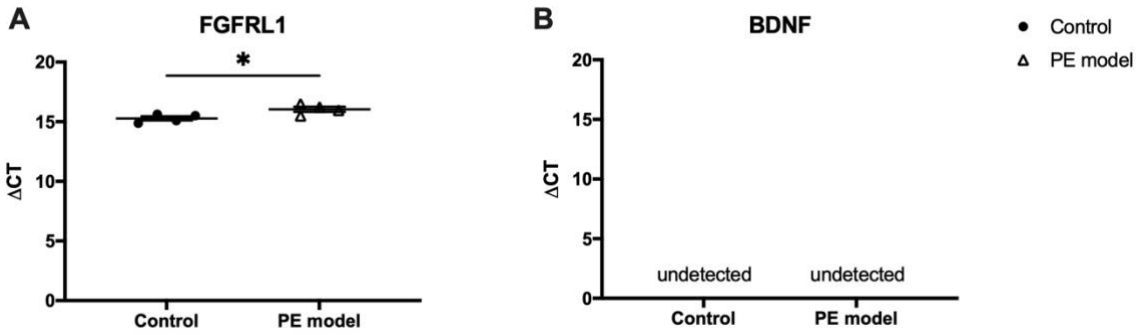

Figure 6-10 Evaluation of miR-210-3p predicted gene targets in whole placentas of a rat model of SPE by TaqMan RT-qPCR.

(A) FGFRL1 was significantly downregulated in whole placentas of a rat model of SPE. **(B)** BDNF was not detected in whole placentas of rats. Data are shown as mean ΔCt ± SEM. Ct values were normalised to housekeeper ACTB, n=4 per group, analysed using ΔCt values by unpaired t-test.

6.4.7.3 Evaluation of candidate miR-210-3p predicted gene targets in trophoblastic BeWo cells

Trophoblastic BeWo cells were transfected with a miR-210-3p mimic and miR-210-3p inhibitor to evaluate the effect of overexpressing and knocking down miR-210-3p on predicted gene targets: FGFRL1, BDNF, NDUFA4, and SLC6A1. In addition, BeWo cells were assayed for viability to determine if miR-210-3p overexpression and knockdown (and potentially dysregulation of predicted gene targets) influenced this property of trophoblast cells.

MiR-210-3p expression was significantly increased following transfection with a miR-210-3p mimic compared to untransfected cells (cells only) at 24 h (-6.63 ±0.09 vs 6.05±0.09 ΔCt, $p<0.0001$) and at 48 h (-7.26±0.04 vs 6.50±0.04 ΔCt, $p<0.0001$) (Figure 6-11A and C, respectively). MiR-210-3p expression was also significantly increased with the miR-210-3p mimic when compared to the negative control scramble ($p<0.0001$) and miR-210-3p inhibitor ($p<0.0001$) at both 24 and 48 h (Figure 6-11A and C). MiR-210-3p expression was significantly decreased following transfection with a miR-210-3p inhibitor compared to untransfected cells (cells only) at 24 h (7.59±0.22 vs 6.05±0.09 ΔCt, $p<0.0001$) and at 48 h (9.27±0.33 vs 6.50±0.04 ΔCt, $p<0.0001$) (Figure 6-11A and C, respectively). MiR-210-3p expression was also significantly decreased with the miR-210-3p inhibitor when compared to the negative control scramble ($p<0.0001$) and miR-210-3p mimic ($p<0.0001$) at both 24 and 48 h (Figure 6-11A and C, respectively).

Transfection of BeWo cells with miR-210-3p inhibitor led to a significant increase in cell viability compared to untransfected cells (cells only) at 24 h ($p<0.0001$) (Figure 6-11B) with no significant difference when compared to the negative control scramble and miR-210-3p mimic, suggesting transfection reagents were affecting cell viability. There was no significant difference in cell viability between transfection with the negative control scramble, miR-210-3p mimic, and miR-210-3p inhibitor at both 24 and 48 h (Figure 6-11B and D, respectively), further suggesting changes in miR-210-3p expression had no effect on cell viability. Due to the influence of transfection on cell viability, miRNA and gene target RT-qPCR data were reanalysed to compare mimic and inhibitor treatments with the negative control scramble rather than untransfected cells.

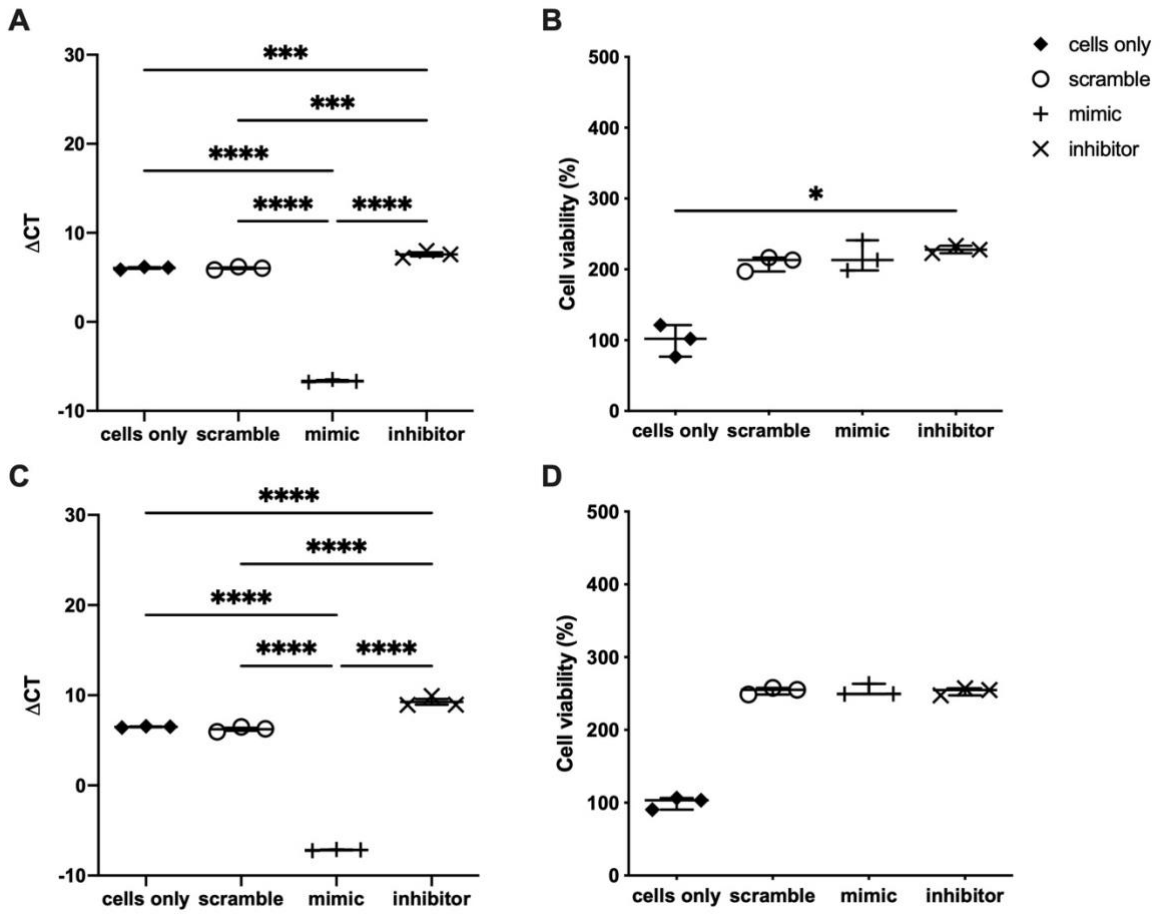

Figure 6-11 Evaluation of miR-210-3p expression by TaqMan RT-qPCR and cell viability by MTT assay in trophoblastic BeWo cells transfected with miR-210-3p mimic and inhibitor for (A) and (B) 24 hours and (C) and (D) 48 hours.

BeWo cells were transfected with 30 nM miRNA scramble/mimic/inhibitor and 3 µL siPORT™ NeoFX™ Transfection Agent for 24 and 48 hours and assayed for gene expression and cell viability. **(A)** MiR-210-3p was significantly increased after 24 hours with miR-210-3p mimic treatment compared to cells only, scramble, and miR-210-3p inhibitor treatment. MiR-210-3p was significantly decreased after 24 hours with miR-210-3p inhibitor treatment compared to cells only, scramble, and miR-210-3p mimic treatment. **(B)** Cell viability was significantly increased following 24-hour transfection with a scramble, mimic, and inhibitor compared to untransfected cells (cells only). **(C)** MiR-210-3p was significantly increased after 48 hours with miR-210-3p mimic treatment compared to cells only, scramble, and miR-210-3p inhibitor treatment. MiR-210-3p was significantly decreased after 48 hours with miR-210-3p inhibitor treatment compared to cells only, scramble, and miR-210-3p mimic treatment. **(D)** Cell viability was significantly increased following 48-hour transfection with a scramble, mimic, and inhibitor compared to untransfected cells (cells only). For **(A)** and **(C)**, data are shown as mean ΔCt ± SEM. Ct values were normalised to housekeeper RNU44, ***p<0.0001, n=3 technical replicates per group, analysed using ΔCt values by one-way ANOVA followed by Tukey's post-hoc multiple comparisons test. For **(B)** and **(D)**, data are shown as median (IQR). Values were expressed relative to untransfected cells only control (considered 100%), ****p<0.0001, n=3 technical replicates per group, analysed by analysed by Kruskal-Wallis test followed by Dunn's post-hoc multiple comparisons test.

6.4.7.3.1 MiR-210-3p and candidate predicted gene targets expression in BeWo cells transfected for 24 hours

After 24 h transfection, the miR-210-3p mimic led to a significant increase in miR-210-3p expression compared to the negative control scramble (-6.63±0.09 vs 6.02±0.10 ΔCt, $p<0.0001$) and miR-210-3p inhibitor (-6.63±0.09 vs 7.59±0.22 ΔCt, $p<0.0001$) (Figure 6-12A). The miR-210-3p inhibitor led to a significant decrease in miR-210-3p expression compared to the negative control scramble (7.59±0.22 vs 6.02±0.10 ΔCt, $p<0.0001$) and miR-210-3p mimic (7.59±0.22 vs -6.63±0.09 ΔCt, $p<0.0001$) (Figure 6-12A).

FGFRL1 was significantly downregulated following transfection with the miR-210-3p mimic compared to the negative control scramble (11.35±0.64 vs 9.44±0.15 ΔCt, $p<0.05$), while there was no significant difference in FGFRL1 expression following transfection with the miR-210-3p inhibitor (Figure 6-12B). BDNF was not significantly differentially expressed following transfection with the miR-210-3p mimic or inhibitor compared to the scramble (Figure 6-12C). NDUFA4 and SLC6A1 were not detected in BeWo cells following transfection with the negative control scramble, mimic, and inhibitor (Figure 6-12D and E).

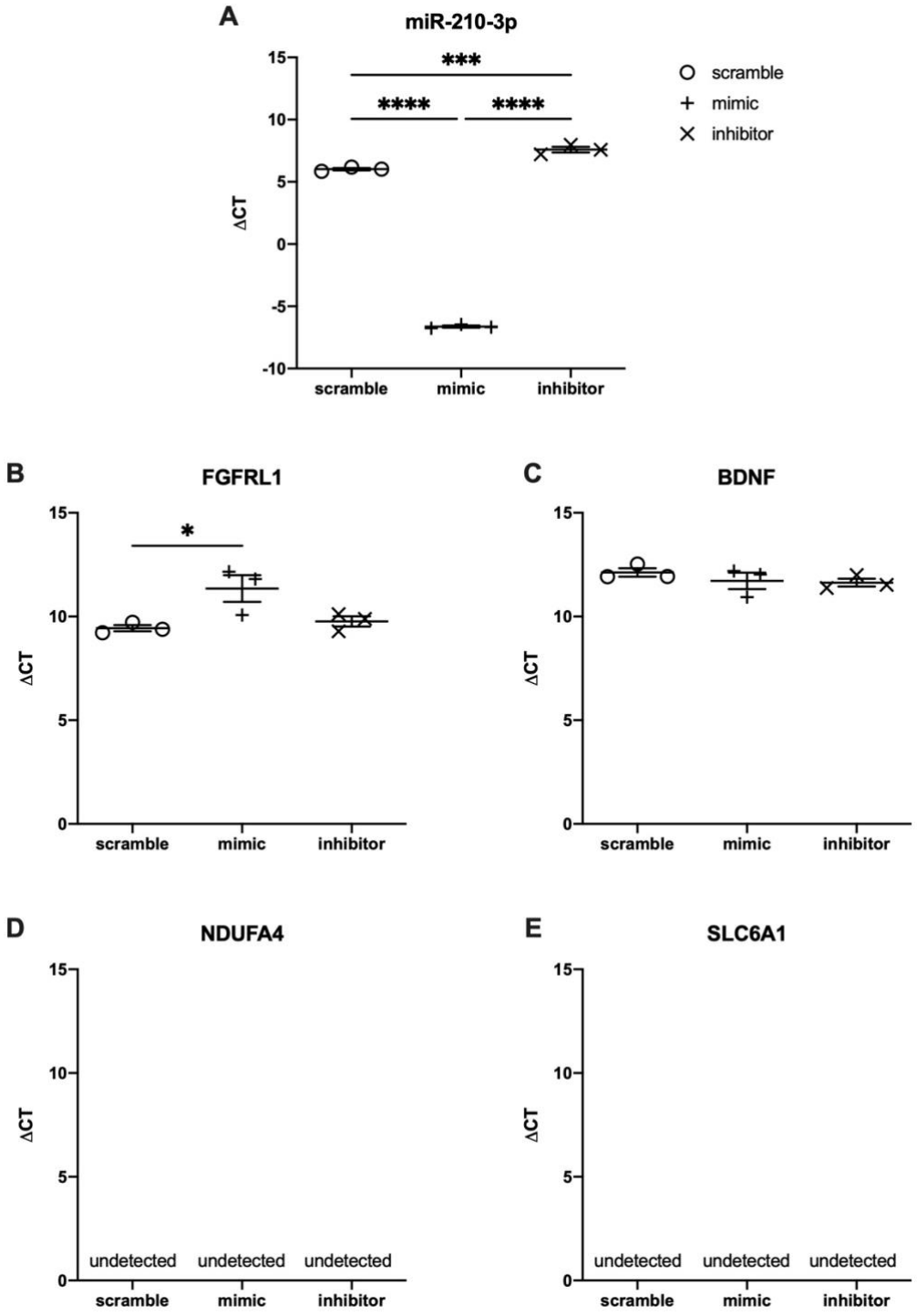

Figure 6-12 Evaluation by TaqMan RT-qPCR of miR-210-3p and predicted gene targets in trophoblastic BeWo cells transfected with miR-210-3p mimic and inhibitor for 24 hours.

BeWo cells were transfected with 30 nM miRNA scramble/mimic/inhibitor and 3 µL siPORT™ NeoFX™ Transfection Agent for 24 hours and assayed for gene expression. **(A)** MiR-210-3p was significantly increased after 24 hours with miR-210-3p mimic treatment compared to scramble and miR-210-3p inhibitor treatment. MiR-210-3p was significantly decreased after 24 hours with miR-210-3p inhibitor treatment compared to scramble and miR-210-3p mimic treatment. **(B)** FGFRL1 was significantly downregulated following miR-210-3p mimic treatment compared to scramble. **(C)** BDNF was not significantly differentially expressed following miR-210-3p mimic and inhibitor treatment compared to scramble. **(D)** NDUFA4 and **(E)** SLC6A1 were undetected in BeWo cells across all transfections. Data are shown as mean ΔCt ± SEM. Ct values were normalised to housekeeper RNU44 **(A)** and B2M **(B)** and **(C)**, *p<0.05 and ***p<0.0001, n=3 technical replicates per group, analysed using ΔCt values by one-way ANOVA followed by Tukey's post-hoc multiple comparisons test.

6.4.7.3.2 MiR-210-3p and candidate predicted gene targets expression in BeWo cells transfected for 48 hours

After 48 h transfection, the miR-210-3p mimic led to a significant increase in miR-210-3p expression compared to the negative control scramble (-7.16±0.04 vs 6.24±0.16 ΔCt, $p<0.0001$) and miR-210-3p inhibitor (-7.16±0.04 vs 9.27±0.33 ΔCt, $p<0.0001$) (Figure 6-13A). The miR-210-3p inhibitor led to a significant decrease in miR-210-3p expression compared to the negative control scramble (9.27±0.33 vs 6.24±0.16 ΔCt, $p<0.0001$) and miR-210-3p mimic (9.27±0.33 vs -7.16±0.04 ΔCt, $p<0.0001$) (Figure 6-13A).

FGFRL1 was significantly downregulated following transfection with the miR-210-3p mimic compared to the negative control scramble (11.58±0.43 vs 9.66±0.23 ΔCt, $p<0.05$) and miR-210-3p inhibitor (11.58±0.43 vs 9.61±0.46 ΔCt $p<0.05$) (Figure 6-13B). There was no significant difference in FGFRL1 expression between transfection with the negative control scramble and miR-210-3p inhibitor (Figure 6-13B). BDNF was not significantly differentially expressed following transfection with the miR-210-3p mimic or inhibitor compared to the scramble (Figure 6-13C). NDUFA4 and SLC6A1 were not detected in BeWo cells following transfection with the negative control scramble, mimic, and inhibitor (Figure 6-13D and E).

Due to the miR-210-3p mimic inducing supraphysiological overexpression of miR-210-3p, the transfection experiment was repeated with the lowest recommended volume of transfection agent (1 µL). MiR-210-3p mimic led to a significant increase in miR-210-3p expression compared to the negative control scramble (-3.73±0.12 vs 5.65±0.11 ΔCt, $p<0.0001$) and miR-210-3p inhibitor (-3.73±0.12 vs 6.98±0.06 ΔCt, $p<0.0001$) (Figure 6-14A). Transfection with 1 µL of transfection reagent still induced supraphysiological expression levels of miR-210-3p, but this was lower than with 3 µL of transfection reagent (-3.73 vs -7.16, respectively). While FGFRL1 was significantly reduced with the miR-210-3p mimic compared to the negative control scramble (4.56±0.01 vs 4.39±0.05 ΔCt, $p<0.05$), this was no longer significant when compared to the miR-210-3p inhibitor (Figure 6-14B). As was seen with 3 µL of transfection reagent, BDNF was not significantly differentially expressed (Figure 6-14C), and SLC6A1 was not detected (Figure 6-14E). However, NDUFA4 was detected following transfection

with 1 µL of transfection reagent with the negative control scramble, mimic, and inhibitor, although there was no significant difference between the treatments (Figure 6-14D). Additional 72 h transfections were run, but no significant difference in gene target expression was observed (data not shown).

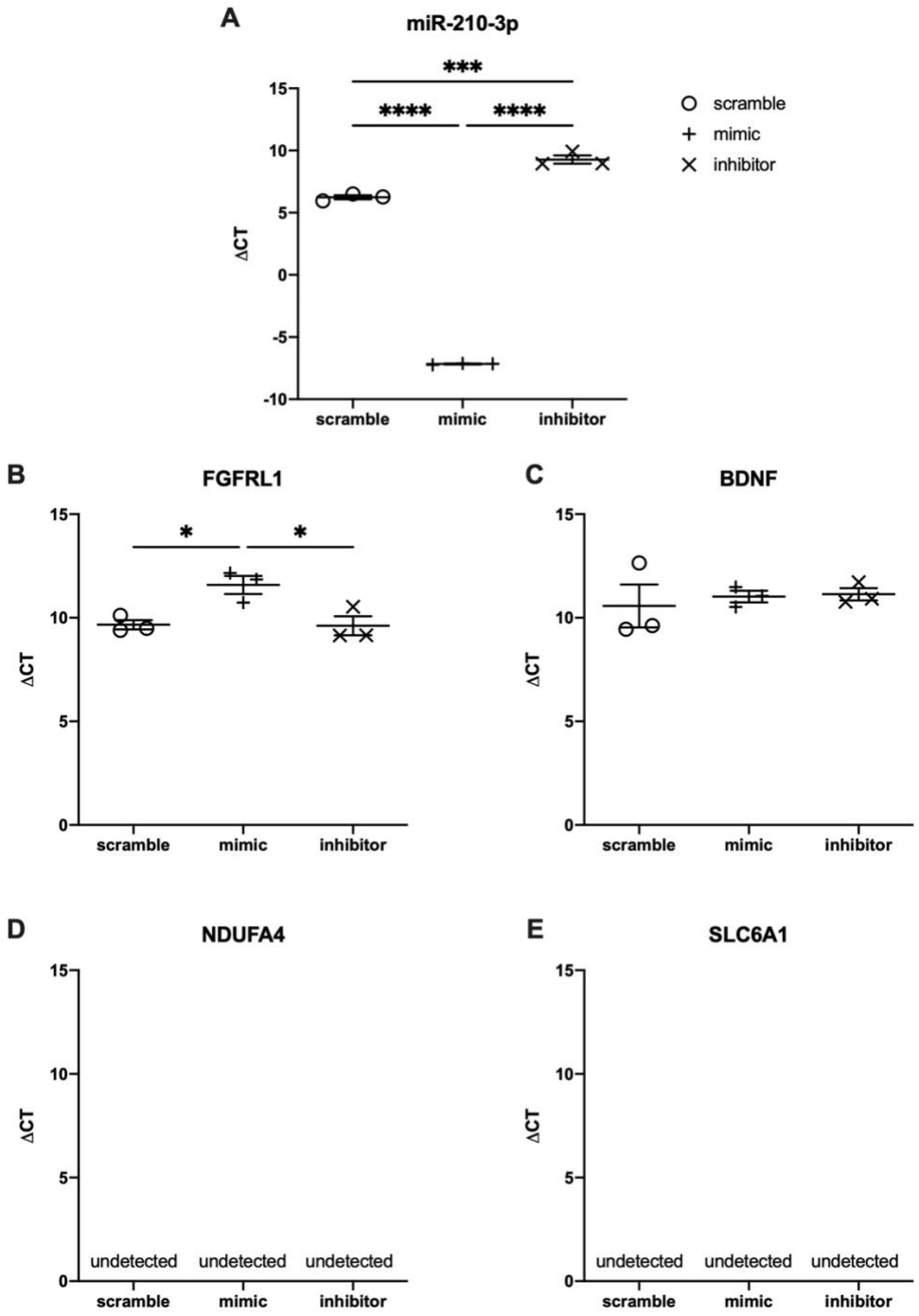

Figure 6-13 Evaluation by TaqMan RT-qPCR of miR-210-3p and predicted gene targets in trophoblastic BeWo cells transfected with miR-210-3p mimic and inhibitor for 48 hours.

BeWo cells were transfected with 30 nM miRNA scramble/mimic/inhibitor and 3 µL siPORT™ NeoFX™ Transfection Agent for 48 hours and assayed for gene expression. **(A)** MiR-210-3p was significantly increased after 48 hours with miR-210-3p mimic treatment compared to scramble and miR-210-3p inhibitor treatment. MiR-210-3p-3p was significantly decreased after 48 hours with miR-210-3p inhibitor treatment compared to scramble and miR-210-3p mimic treatment. **(B)** FGFRL1 was significantly downregulated following miR-210-3p mimic treatment compared to scramble and miR-210-3p inhibitor treatment. **(C)** BDNF was not significantly differentially expressed following miR-210-3p mimic and inhibitor treatment compared to scramble. **(D)** NDUFA4 and **(E)** SLC6A1 were undetected in BeWo cells across all transfections. Data are shown as mean ΔCt ± SEM. Ct values were normalised to housekeeper RNU44 **(A)** and B2M **(B)** and **(C)**, *p<0.05 and ***p<0.0001, n=3 technical replicates per group, analysed using ΔCt values by one-way ANOVA followed by Tukey's post-hoc multiple comparisons test.

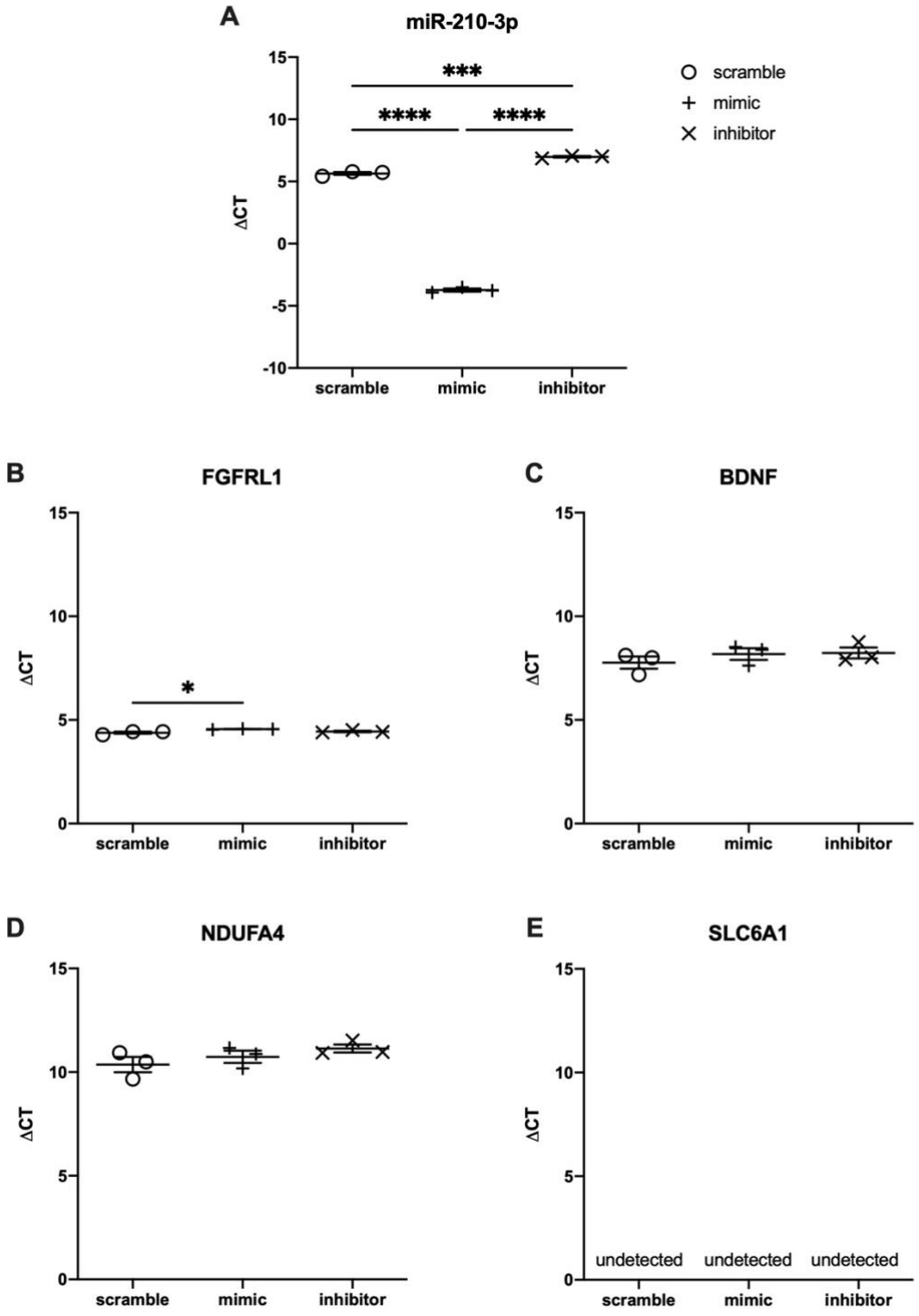

Figure 6-14 Evaluation by TaqMan RT-qPCR of miR-210-3p and predicted gene targets in trophoblastic BeWo cells transfected with miR-210-3p mimic and inhibitor for 48 hours.

BeWo cells were transfected with 30 nM miRNA scramble/mimic/inhibitor and 1 µL siPORT™ NeoFX™ Transfection Agent for 48 hours and assayed for gene expression. **(A)** MiR-210-3p was significantly increased after 24 hours with miR-210-3p mimic treatment compared to scramble and miR-210-3p inhibitor treatment. MiR-210-3p was significantly decreased after 24 hours with miR-210-3p inhibitor treatment compared to scramble and miR-210-3p mimic treatment. **(B)** FGFRL1 was significantly downregulated following miR-210-3p mimic treatment compared to scramble and miR-210-3p inhibitor treatment. **(C)** BDNF and **(D)** NDUFA4 were not significantly differentially expressed following miR-210-3p mimic and inhibitor treatment compared to scramble. **(E)** SLC6A1 were undetected in BeWo cells across all transfections. Data are shown as mean Ct ± SEM. Ct values were normalised to housekeeper RNU44 **(A)** and B2M **(B)**, **(C)**, and **(D)**, *p<0.05 and ***p<0.0001, n=3 technical replicates per group, analysed using ΔCt values by one-way ANOVA followed by Tukey's post-hoc multiple comparisons test.

6.5 Discussion

In this chapter, significantly differentially expressed placental miRNAs were identified in a rat model of SPE, representing the first study to conduct miRNA sequencing in the placenta of an animal model of PE. Furthermore, significant differences in the direction of expression of miRNAs (specifically, miR-210-3p, miR-19b-3p, and miR-145-5p) were found within placental layers of the SPE rat model, a finding previously only shown in human placentas. MiR-210-3p was shown to be significantly differentially expressed in the placentas of patients with PE. Expression of miR-210-3p and its predicted gene target, FGFRL1, demonstrated an inverse relationship in the placentas of the SPE rat model and preeclamptic patients as well as in placental trophoblast cells. This provides novel evidence of altered FGFRL1 expression in the placenta in PE, which may be linked to dysregulated placental miR-210-3p, adding to the existing literature that suggests miR-210-3p plays a pathological role in PE.

Comparing these findings with other PE animal models and clinical studies highlights the importance of investigating the role of placental miRNAs in subtypes of PE and in the different layers of the placenta. In a mouse model of PE, induced by activation of the maternal immune system with poly I:C, miR-210-3p was significantly upregulated in the placenta (Kopriva et al., 2013), corresponding with the increased expression detected by miRNA sequencing in our rat model of SPE and by RT-qPCR in patients with PE. An upregulation of placental miR-210-3p across PE subtypes is supported by the large number of clinical studies reporting increased miR-210-3p in the placentas of patients with mild (Adel et al., 2017), severe (Muralimanoharan et al., 2012), EO (Ishibashi et al., 2012), LO (Chen et al., 2019), diagnosed (Wang et al., 2019a), and SPE (Vashukova et al., 2016). In contrast, one study observed a significant downregulation of miR-210-3p in patients with mild PE (Zhu et al., 2009). It is unlikely this represents a miRNA signature specific to the mild PE subtype since another study in mild preeclamptic patients reported a significant increase in expression (Adel et al., 2017). Rather, a decrease in miR-210-3p expression may reflect differences in placental hypoxia and in turn underlying pathological processes. In a study of pregnant mice exposed to moderate hypoxia, a significant downregulation of placental miR-210-3p was noted (Krawczynski et al., 2016). Hence, miR-210-3p expression may only be induced in more severe

hypoxic conditions as previously discussed (Chapter 5 Discussion). However, hypoxia-independent stimuli also regulate placental miR-210-3p expression, supported by the significant downregulation of miR-210-3p observed in the maternal decidual layer as previously discussed (Chapter 5 Discussion). In further support of hypoxia-independent mechanisms driving miR-210-3p, the key mediator of the cellular response to hypoxia, HIF-1 α, was not significantly differentially expressed in any of the placental layers of this SPE model rat (Morgan et al., 2018). It should be noted though that expression levels of its isoform, HIF-2 α, were not measured, which has previously shown to drive miR-210-3p expression in trophoblasts *in vitro* (Lalevée et al., 2014). In terms of expression differences between layers, three clinical studies have shown elevated miR-210-3p levels in the basal plate (comprising of maternal and foetal tissue) (Luo et al., 2014, Xu et al., 2014a, Zhang et al., 2015a), and two of these found no significant difference in expression in the chorionic plate (comprising of foetal tissue) (Luo et al., 2014, Xu et al., 2014a). Investigating miR-210-3p expression between placental layers, and in particular the decidua of patients with SPE remains crucial, as it may provide insight into whether SPE shows a unique placental miR-210-3p signature.

In addition to the candidate miRNA miR-210-3p, expression profiling studies in the placentas of patients with PE reported dysregulation of the other candidates, miR-19b-3p (Ishibashi et al., 2012, Zhang et al., 2015b, Zhang et al., 2015a), miR-214-3p (Zhao et al., 2014, Xu et al., 2014a, Hu et al., 2009), and miR-145-5p (Ishibashi et al., 2012), with results matching the direction of expression seen in the miRNA sequencing conducted in rats with SPE. However, validation studies by RT-qPCR of these miRNAs in the placental layers of the SPE rat model produced conflicting results. Although a significant downregulation of miR-145-5p in the labyrinth matches the results from the miRNA sequencing experiment and clinical studies, a significant downregulation of miR-19b-3p in the decidua is in contrast to the increased expression observed in the miRNA sequencing experiments and in clinical studies. Furthermore, a number of significantly differentially expressed placental miRNAs detected by the miRNA sequencing experiment showed the opposite direction of expression as reported by sequencing or microarray experiments in patients with PE, including miR-181a-5p (Zhu et al., 2009, Jiang et al., 2015, Hu et al., 2009, Xu et al., 2014a,

Zhang et al., 2015a), miR-542-3p (Lykoudi et al., 2018, Xu et al., 2014a, Betoni et al., 2013, Zhu et al., 2009), and miR-222-3p (Hu et al., 2009), and in patients with SPE, namely miR-542-5p and miR-495 (Ishibashi et al., 2012). Finally, placental miRNAs (miR-126-3p (Yan et al., 2014), miR-148a/152 (Yang et al., 2016a), and miR-576-5p (Wang et al., 2020c)) previously investigated in other animal models of PE, specifically L-NAME-induced PE rats, were not detected by miRNA sequencing as significantly differentially expressed in our rat model of SPE. Collectively, these findings further highlight the importance of examining placental miRNA expression in individual layers both within animal models of PE and patients with PE.

Of the four candidate predicted gene targets of miR-210-3p, FGFRL1 and BDNF were significantly downregulated in the placentas of PE patients. FGFRL1 was also significantly downregulated in the placentas of SPE model rats, matching the upregulation of miR-210-3p seen in whole placental tissue from the SPE model rats as detected by miRNA sequencing and in the placentas of PE patients. FGFRL1 belongs to the fibroblast growth factor receptor (FGFR) family, which bind FGFs to regulate an array of cellular processes, including proliferation, differentiation, migration, and apoptosis (Trueb, 2011). Unlike other family members, FGFRL1 lacks an intracellular protein kinase domain required for signalling, contributing to evidence supporting its function as a decoy receptor (Trueb, 2011). Relatively few studies have investigated the role of FGFRs in the placenta. FGFRs are expressed in placental trophoblasts, macrophages, and blood vessel walls (Anteby et al., 2005) and have shown to regulate trophoblast characteristics (Baczyk et al., 2006). They have found to be dysregulated in trophoblasts in patients with PE (Loichinger et al., 2016) and upregulated in endothelial cells in patients with placental vascular disease (Wang et al., 2006). However, no study could be identified that has investigated FGFRL1 expression and/or function in the placenta. In the current study, overexpressing miR-210-3p in placental trophoblasts downregulated FGFRL1 expression levels, although this had no effect on trophoblast viability. Previous studies have shown increasing miR-210-3p, and in turn inhibiting FGFRL1, stimulates angiogenesis in endothelial cells (Cui et al., 2015) and cancer cells (Yang et al., 2016d), inhibits cancer cell proliferation (Yang et al., 2017b), and promotes (Liu et al., 2018d) or inhibits (Yang et al., 2017b) cell migration and invasion depending on cancer cell

type under study. Future studies may therefore seek to elucidate other trophoblast characteristics which may be altered, including migration and invasion, and the role of miR-210-3p and FGFRL1 in other placental cell types, such as macrophages.

BDNF belongs to a family of proteins known as neurotrophins, which play a key role in regulating differentiation, structure, and function of neurons (Hempstead, 2015). In pregnancy, evidence suggests BDNF supports placental growth and development by stimulating trophoblast cell growth and survival (Kawamura et al., 2009), protecting trophoblasts against oxidative stress (Fujita et al., 2011, Sahay et al., 2015), and potentially inducing angiogenesis (Sun et al., 2009) as well as promoting foetal growth and development via placental signalling (Mayeur et al., 2010, Kodomari et al., 2009). It has therefore been postulated that downregulation of placental BDNF may reflect pathological conditions while an upregulation may represent a protective role (Sahay et al., 2020). Previous studies in PE patients have reported lower levels of BDNF in placental cotyledons (D'souza et al., 2014) and the basal region of the placenta (Sahay et al., 2020) and higher levels in the central foetal region (Sahay et al., 2015), suggesting the role of BDNF differs across the placenta. In the current study, BDNF was significantly downregulated in the placentas of PE patients, which comprised of both maternal and foetal tissue. Although BDNF is a predicted target of miR-210-3p and an experimentally validated gene target in other cell types, overexpressing miR-210-3p in trophoblast cells had no significant effect on BDNF expression, indicating other factors influence BDNF expression to a greater extent in trophoblasts.

Investigating dysregulated placental miRNAs in a subtype of PE as well as within individual placental layers represents the major strength of the current study. However, a major limitation is that findings from an SPE rat model were evaluated in patients diagnosed with PE rather than patients with SPE. This was due to the limited availability of samples, which in turn accounts for the small sample size. Another limitation of the current study is that there were significant differences in foetal weight and gestational age at delivery between patients with PE and the healthy control group. These differences may have influenced miRNA and gene expression findings since placental miRNAs have

shown to differ depending on foetal weight (Awamleh et al., 2019, Pineles et al., 2007, Weedon-Fekjær et al., 2014) as well as between term and preterm deliveries (Mayor-Lynn et al., 2011, Hromadnikova et al., 2017) and term and preterm PE (Anton et al., 2015, Yang et al., 2019b). Controlling for preterm deliveries however is a double-edged sword. While controlling for the variable may account for its effects on placental miRNA expression, preterm deliveries are by definition not normal pregnancies and may therefore introduce other confounding effects when used as a control. Preclinical and clinical studies in PE subtypes remain cornerstone experiments for investigating the role of placental miRNAs in this heterogenous disorder.

Another weakness of this study was a lack of significance in miRNA expression in whole rat placentas when examined by RT-qPCR in comparison to miRNA sequencing. Selection of candidate miRNAs for validation was based on significance in miRNA sequencing and supporting literature from patients with PE rather than considering an arbitrary log2 fold change cut-off value. MiRNA expression levels have shown to exhibit a positive relationship with their activity (Kozomara et al., 2014), suggesting larger differences in miRNA expression may lead to greater changes in expression of target mRNA. This supports the use of a log2 fold change cut-off value in sequencing data in order to select candidate miRNAs for further investigation that are potentially more biologically relevant. However, other evidence suggests miRNA expression levels are a poor indicator of activity (Plotnikova et al., 2019, Kozomara et al., 2014). This underpinned the choice to select candidate miRNAs based on previous identification in patients, with the aim of validating clinically relevant miRNAs. As a result, candidate miRNAs exhibited log2 fold changes less than -0.5 and 1 in miRNA sequencing data. Hence, small changes in expression therefore arguably failed to reach significance when examined by RT-qPCR. In addition, a small sample size likely contributed to a lack of significance. Despite a small sample size, greater differences in expression were seen in individual placental layers, which reached significance with RT-qPCR. Finally, although the relationship between miR-210-3p and predicted gene targets FGFRL1, BDNF, NDUFA4, and SLC6A1 was explored *in-vitro*, in a preclinical PE model, and in patients with PE, validation with reporter constructs is required to confirm direct regulation of the miRNA and its gene targets. Nonetheless, the findings in this chapter provide novel evidence

and build on the growing number of studies that suggest miR-210-3p plays a key pathological role in PE by modulating gene expression and therefore represents a potential therapeutic target.

Chapter 7 General discussion

Gene therapy holds potential as a treatment strategy for PE, a complex disorder involving multiple genetic and environmental factors, with ineffective management. Although placental gene therapy for FGR has undergone considerable clinical progress, non-invasive and non-viral techniques that target the placenta are needed to address the safety concerns of the current gene therapy strategy for FGR. Furthermore, suitable targets for gene therapy for PE have yet to be found. This work sought to demonstrate that UMGD can achieve tissue-specific transfer of an expression vector in a non-invasive and non-viral manner and is therefore suitable for targeting placenta. Investigations into miRNA expression and predicted gene targets in placental tissue from a preclinical model of SPE as well as preeclamptic patients and in a trophoblast cell line sought to show miRNAs play a role in the pathology of PE by demonstrating their dysregulation and to identify potentially suitable therapeutic targets for gene therapy applications.

UMGD in conjunction with a plasmid vector represents a non-viral and non-invasive delivery system in gene therapy. Prior to this work, a single published study applied the technique to targeting the placenta *in vivo* (Babischkin et al., 2019). In the study, UMGD of VEGF to the placenta in a baboon model of impaired uterine artery remodelling restored EVT invasion of the uterine arteries (Babischkin et al., 2019). However, non-targeted tissues were not evaluated for gene transfer, an important preclinical measure to provide supporting evidence of safety of the technique. Furthermore, as mice are more practical and more frequently used as models of PE, establishment of a UMGD protocol for tissue-specific transfer of an expression vector that could be applied to mouse placentas was required. Following optimisation of an *in vivo* UMGD protocol in Chapter 3, a UMGD proof-of-concept study was conducted which demonstrated tissue-specific gene transfer of a luciferase plasmid to mouse hearts in Chapter 4. The protocol was then applied to mouse placentas, showing evidence of limited gene transfer. Non-target tissues were not evaluated for gene transfer due to time constraints, meaning this aspect of safety could not be confirmed in the study targeting the placenta. Placental-specific delivery of an expression vector with UMGD therefore remains to be demonstrated in order to support the

clinical translatability of this technique. Targeted delivery to the placenta evidenced by lack of gene transfer in non-target tissues is currently lacking in preclinical studies of gene therapy in pregnancy disorders. This is critical to the development of placental gene therapy since the lives of both mother and foetus are at risk.

In addition to the non-viral, non-invasive, and targeted aspects of UMGD, several other factors contribute to the potential of UMGD as a strategy for placental gene therapy. Diagnostic US is routinely used in pregnancy, and its safety record spans decades, supporting clinical translation of UMGD (Torloni et al., 2009). MBs as US contrast agents are not currently indicated in obstetrics due to limited research into possible harmful effects and lack of knowledge of their ability to pass through the placenta (Sidhu et al., 2018). Nonetheless, several studies investigating the diagnostic utility of MBs in pregnant patients support their safe use in pregnancy (Ordén et al., 2000, Windrim et al., 2016, Xiong et al., 2016). A study reporting on safety parameters following administration of Levovist found no harmful foetal or maternal effects relating to birthweight, placental weight and morphology, prenatal haemorrhage, cord arterial and venous blood pH, and umbilical artery resistance index (Ordén et al., 2000). A significant increase was observed in the number of foetal heart rate accelerations, movements, and short-term variations in heart rate, although this was attributed to the maternal stress response to US (Ordén et al., 2000). Preclinical studies investigating the effects of MBs on placental permeability provide evidence that MBs do not cross the placental barrier (Hua et al., 2009, Arthuis et al., 2013). Pregnant rats were administered the tracer compound Evan's blue followed by a bolus dose of 1 mL/kg SonoVue and subject to intermittent or continuous US at an MI of 0.13, 1.0, or 1.4 for 5 min (Hua et al., 2009). Evaluation by naked eye and fluorescence microscopy revealed Evan's blue was detectable in the placenta but none in the foetus across all groups (Hua et al., 2009). Post-sacrifice examination of tissue with lanthanum, a stain that cannot penetrate through the cell membrane, showed lanthanum particles were present in the intercellular space between syncytiotrophoblasts but not cytotrophoblasts, suggesting MBs may affect placental cells but do not disrupt the placental barrier (Hua et al., 2009). Another study in pregnant rats administered Vevo MicroMarker® found MBs did not alter perfusion in the umbilical cord or foetus, providing indirect

evidence that MBs do not disrupt the placental barrier (Arthuis et al., 2013). Furthermore, histological analysis revealed no foetal or placental abnormalities, although it should be noted the study was conducted at a relatively low MI of 0.43 (Arthuis et al., 2013). Although only a handful of studies have investigated the safety of MBs in pregnancy at MIs below 1.4, they suggest safety risks are low and thereby support utilizing UMGD for targeting the placenta. Nonetheless, investigating the effect of UMGD on placental permeability is pertinent to establishing foetal gene transfer does not occur. Foetal gene transfer was not assessed in the published UMGD study targeting the placenta and also not examined in the UMGD placenta study in Chapter 4 due to time constraints. Even if low, the risk of foetal gene transfer with UMGD to the placenta needs to be evaluated due to the serious ethical implications of this occurring.

The low levels of placental gene transfer in Chapter 4 highlight important factors that must be addressed for UMGD to be considered an efficient placental delivery system, namely optimal MB, vector, and US conditions. The plasmid DNA:MB ratio can significantly influence transfer efficiency. However, as previously discussed in Chapter 3 and 4, injection volume restrictions, safe MB concentrations, and technical challenges limit the adjustments that can be made to the concentration and volume of plasmid DNA and MBs. Custom-made MBs that protect plasmid DNA from degradation or display targeting abilities are therefore commonly used to enhance transfer efficiency. Despite this apparent advantage, a major benefit of using commercially available MBs is the data available from preclinical safety assessments relating to pregnancy. Preclinical studies of SonoVue and Luminity revealed ‘no special hazard for humans based on conventional studies of genotoxicity, fertility, embryo/foetal development, parturition or post-natal development, and local tolerance’ (EMA, 2008b, EMA, 2009). In contrast, in pregnant rabbits exposed to Optison, maternal and embryo/foetal toxicity was observed (EMA, 2008a). In addition to the preclinical safety data, SonoVue was selected for this work due to its availability and ease of preparation. SonoVue and Luminity can be prepared within under 2 min, with the approved medicinal products manufactured to government safety and quality standards ensuring minimal batch variation. This highlights the convenience and clinical translatability of commercially available MBs is an important advantage to consider for their use in UMGD studies. Altering plasmid DNA characteristics

may therefore be an alternative strategy to improve transfer efficiency rather than employing custom made MBS. Polymers complexed with plasmid DNA with trophoblast-specific promoters (Cyp19a or PLAC1) have previously shown to exhibit targeted placental delivery, with no evidence of inflammation or immune infiltration seen following intraplacental delivery of PLAC1 complexes (Ellah et al., 2015). Plasmid DNA with placental-specific promoters could therefore be adopted by future UMGD studies. Adjusting plasmid DNA characteristics to improve transfer efficiency is further supported by the high doses of MBs used in preclinical studies. The work in Chapter 3 and 4 utilised SonoVue doses at approximately 150 times the approved clinical dose, so increasing MB concentration and volume in future studies should be avoided to improve clinical translatability. Finally, future work should seek to optimise US parameters since different output modes and frequencies will likely improve transfer efficiency as previously discussed.

For the work in Chapter 3 and 4, plasmid vectors carrying reporter genes were utilised since the aim of the UMGD studies was to demonstrate proof-of-concept. The overarching concept was to establish the technique for targeting placental miRNAs. In the future, this could be achieved using miRNA expression plasmids or agomirs/antagomirs in conjunction with UMGD. Several UMGD studies have delivered miRNA expression plasmids via peripheral IV injections to the kidney (Zhong et al., 2011), liver (Yang et al., 2013), and heart (Liu et al., 2015), and provided evidence of targeted delivery as well as therapeutic benefit. An alternative approach is to use agomirs/antagomirs since their longer half-life and smaller size compared with plasmid DNA could enhance transfer efficiency. However, off-target effects remain a prevailing concern (Beards et al., 2017, Krützfeldt et al., 2005). An *in vivo* study investigating UMGD of agomirs/antagomirs showed delivery of the compounds complexed to cationic MBs to mouse hind limbs following tail vein administration (Kwekkeboom et al., 2015). The effect on miRNA expression in the target as well as non-target organs was not fully assessed. Hence, further studies are required to determine if UMGD of agomirs/antagomirs can localise delivery and stimulate efficient transfer. Given previous studies showing targeted delivery with miRNA expression plasmids and the targeting ability of plasmids to the placenta, future work may benefit from focussing on plasmid DNA delivery rather than agomirs/antagomirs.

Although the UMGD protocol established in Chapter 4 requires optimisation, application of the technique to pregnant mice is important for preclinical development of the delivery system.

In Chapter 5, a literature review was conducted of published expression profiling studies in placentas of preeclamptic patients which identified 22 significantly differentially expressed placental miRNAs consistently detected as dysregulated after collating data from fifteen studies. These findings build on a previous systematic review from 2016 that examined profiling studies of differentially expressed miRNAs in PE in any sample type (tissue, fluids, or otherwise) (Sheikh et al., 2016). Sub analysis identified twelve miRNAs dysregulated in PE in profiling studies examining placental tissue (Sheikh et al., 2016). Since the previous systematic review was performed, an additional four profiling studies examining preeclamptic placental tissue have been conducted. In addition to including more recent publications, more stringent criteria were applied to the literature review in Chapter 5 (examination of placental tissue from the third trimester with time of collection stated) than the sub analysis of the systematic literature review. The current work focussed on placental tissue since one of the overarching aims of this thesis was to evaluate the therapeutic potential of dysregulated miRNAs in the placenta. Furthermore, the literature review focussed on third trimester placental tissue since the aim of Chapter 5 was to evaluate candidate miRNAs in third trimester placental tissue that was available from a rat model of SPE. As a result of including newly published studies and excluding more studies compared with the systematic review, only three miRNAs (miR-210-3p, miR-223-3p, and miR-181a-5p) overlapped between the published systematic review and literature review in Chapter 5 in terms of the dysregulated placental miRNAs detected by at least three profiling studies. Of note, more recent publications included in the literature review also detected miR-210-3p and miR-223-3p as differentially expressed and the reported direction of expression agreed with findings from studies conducted prior to 2016. This highlights how the work in Chapter 5 builds on existing literature and the importance of conducting the up-to-date literature review given the growing number of expression profiling studies being conducted in preeclamptic patients.

Of the 22 differentially expressed placental miRNAs identified by the literature review in Chapter 5, ten miRNAs were reported by studies as being dysregulated in the same direction of expression. Studies concurred despite differences in terms of the type of experiment performed, type of PE under study, gestational age at the time of delivery, and sampling area. This suggests that some dysregulated placental miRNAs may be uniformly differentially expressed across the placenta and common to preeclamptic patients in the third trimester regardless of disease presentation. However, no miRNA was detected as significantly differentially expressed by all profiling studies. MiR-210-3p and miR-223-3p were the most frequently detected miRNAs, detected by seven and five studies respectively, all of which agreed in the direction of expression. Lack of detection by other studies may be attributed to methodological and biological factors as previously discussed. All studies included in the literature review examined third trimester placenta samples to account for differences in placental miRNA expression between trimesters, which has previously been reported (Morales-Prieto et al., 2012, Gu et al., 2013). However, even within the third trimester, studies have shown significant differences in placental miRNA expression (Mayor-Lynn et al., 2011, Hromadnikova et al., 2017, Anton et al., 2015, Yang et al., 2019b). With several of the clinical studies included in the literature review noting significant differences in gestational age between PE and control groups as well as examining term and preterm deliveries, this may account for inconsistent findings between clinical studies. Validation and replication in larger independent cohorts and across the placenta is therefore required to confirm whether some miRNAs are differentially expressed across the placenta and amongst all preeclamptic subtypes. On the other hand, the literature review provided evidence of placental miRNA expression differing between types of PE, adding to the existing literature that shows differences between subtypes (Lykoudi et al., 2018, Weedon-Fekjær et al., 2014) as well as presenting symptoms (Pineles et al., 2007, Awamleh et al., 2019). Finally, the literature review highlighted that a single miRNA expression profiling study has been conducted in patients with SPE. Since SPE exhibits overlapping but also distinct molecular, pathological, and clinical features compared with PE (Stanek, 2018, Barbosa et al., 2015, Chang et al., 2011), further miRNA expression profiling studies in this subset of patients are warranted.

One criterion for selecting candidate miRNAs from the literature review in Chapter 5 was published *in vitro* studies providing supporting evidence of a role for the miRNA in the pathology of PE. This was chosen as one of the criteria so that evidence from clinical through to *in vitro* studies could be referred to when discussing the potential role and therapeutic value of the miRNA in PE. However, this meant that fourteen miRNAs which may potentially contribute to abnormal placental development in PE were not investigated further. MiR-214-3p and miR-542-3p may be of particular interest to investigate in future preclinical studies given the agreement between clinical studies of their direction of expression in PE and the existence of a rat ortholog. Of the eight candidate miRNAs selected, five were significantly differentially expressed in whole placental tissue or individual placental layers of a rat model of SPE. This provides novel evidence of dysregulation of miRNAs within placental layers in rats, a finding previously only shown in humans. RNA expression profiling studies in rat and human placenta have shown distinct gene expression patterns exist between zonal layers relating to the functional compartmentalization of the placenta (Shankar et al., 2012, Sood et al., 2006). Hence, layer-specific patterns in miRNA expression would be expected. Another study conducted laser microdissection followed by RNA profiling on trophoblast subpopulations (syncytiotrophoblasts, invasive cytotrophoblasts, and endovascular cytotrophoblasts) from patients with severe PE and women who had a preterm birth (Gormley et al., 2017). Genes were significantly differentially expressed between the patient groups in a cell-specific manner and related to pathways known to be dysregulated in PE, such as vascular development; immune functions; responses to VEGF, TGF-ß, and oxygen; and cellular movement (Gormley et al., 2017). Transcriptional analysis also found five miRNAs (miR-20b, miR-181a-1, miR-339, miR-520-e, and miR-561) that were significantly differentially expressed between the patient groups (Gormley et al., 2017). In addition to layer-specific differences, miRNAs therefore also likely show significant differences between placental cell types in animal models of PE, although this requires experimental evidence.

In Chapter 5, comparisons between placental miRNA expression in the SPE rat model with published clinical studies of preeclamptic patients identified several miRNAs potentially suitable as therapeutic targets in PE. MiR-223-3p and miR-181a-5p were significantly differentially expressed in the placentas of the SPE

rat model, although in the opposite direction to that reported by clinical studies from the literature review as well as other candidate studies. MiR-181a-5p was significantly upregulated in the rat model of SPE, while significantly downregulated in profiling and candidate studies in preeclamptic patients. Although miR-223-3p was significantly upregulated in the rat model of SPE, it was significantly downregulated across clinical profiling studies, including in the study of patients with SPE. This suggests the opposing finding may reflect processes specific to the preclinical model and highlights the limitations of animal models in recapitulating a 'human' disease. It should be noted though that comparisons were made between an animal model of a specific subtype of PE with data from patients encompassing all PE subtypes, in terms of severity, disease onset, and timing of delivery, all factors which may have influenced the findings of clinical studies. Profiling studies of preeclamptic patients were included in the literature review regardless of the type of PE under study since only a single profiling study has been performed in pateints with SPE. Despite these opposing findings between the animal model and patient data, the consistency amongst clinical studies in the reported direction of expression of miR-223-3p and miR-181a-5p underpin their potential as therapeutic targets. However, future studies would need to employ other animal models of PE to investigate this further. Although no significant difference was seen in whole placental tissue, miR-363-3p was significantly downregulated in the decidua of the SPE rat model and across profiling and candidate studies. The miRNA therefore represents another potential therapeutic candidate and targeting the miRNA in the placenta could be investigated further in the rat model of SPE. MiR-195-5p was significantly upregulated in the decidua of the SPE rat model, which is in agreement with a profiling study conducted in severe LOPE patients but in disagreement with studies in patients with severe PE and SPE. The inconsistency between clinical studies as well as with the rat model of SPE, suggest miR-195-5p expression likely differs between subtypes. Nonetheless, *in vitro* studies have demonstrated miR-195-5p modulates genes (VEGFA and ACVR2A) in which polymorphisms have been shown to be associated with PE risk. Further preclinical and clinical studies should therefore be conducted to gain a greater understanding of the role of the miRNA in PE. Finally, miR-210-3p was significantly downregulated in the decidua but upregulated in the labyrinth of the SPE rat model. This is the first work that could be identified that shows

miRNAs can be differentially expressed in the opposite direction in different placental layers. The upregulation of miR-210-3p in the labyrinth is in line with the sixteen human profiling studies and candidate studies that show miR-210-3p is increased in preeclamptic patients. The downregulation of miR-210-3p in the decidua is in line with one clinical study that found miR-210-3p was downregulated in patients with mild PE. As previously discussed, downregulation of miR-210-3p may relate to low levels of hypoxia, with preclinical and clinical evidence supporting miR-210-3p as the master 'hypoxamir'. Differences in the direction of miR-210-3p expression in placental layers may account for the lack of significance of miR-210-3p expression in whole placental tissue of the SPE rat model. The labyrinth encompasses the largest area and may therefore have underpinned the trend towards an increased expression of miR-210-3p in whole placental tissue. Downregulation of miR-210-3p in the decidua however may have reduced relative expression levels when the placenta was examined as a whole. Despite the differences between layers, miR-210-3p remains a therapeutic target of interest and targeting the miRNA could be investigated further in the rat model of SPE. It remains unclear what layer or cell of the placenta would or could be targeted with gene therapy strategies. However, inhibiting miR-210-3p across the placenta could provide insight into whether/how the role of miR-210-3p differs between layers and in turn the physiological implications of further blocking its effects in the decidua.

The work in Chapter 6 was the first to conduct miRNA expression profiling in the placenta of an animal model of PE, detecting a total of 56 differentially expressed miRNAs in the rat model of SPE compared to controls. A literature review was conducted to select candidate miRNAs for validation with RT-qPCR in whole placental tissue and individual placental layers of the SPE rat model as well as in placentas from preeclamptic patients. Four studies that had previously been excluded from the literature review in Chapter 5 (based on the time of placenta collection not being stated) were included in the literature review in Chapter 6. After consideration, it was decided that it was reasonable to assume that the placentas were collected at the time of delivery despite the time of collected not explicitly being stated. This highlights a limitation of the literature review in Chapter 5, namely that an additional four studies could have been included to broaden its scope. The literature review in Chapter 6 showed that,

of the 56 dysregulated miRNAs, eleven had previously been detected in expression profiling studies in preeclamptic patients. This means the majority of dysregulated placental miRNAs may be specific to the animal model or species. It should be noted though that only one clinical profiling study has been conducted in patients with SPE, suggesting that a lack of congruity with clinical data could be attributed to the subtype under study. These factors may contribute to the number of significantly differentially expressed placental miRNAs detected by the sequencing experiment in the rat model of SPE that showed the opposite direction of expression as reported by sequencing or microarray experiments in patients with PE, including miR-181a-5p, miR-542-3p, and miR-222-3p, and in patients with SPE, namely miR-542-5p and miR-495. Candidate miRNAs for further investigation were selected based on their direction of expression in the SPE model matching the direction of expression reported in clinical studies to support future studies seeking to target a placental miRNA in the rat model of SPE. None of the candidate miRNAs were validated by RT-qPCR in whole placental tissue, highlighting a major limitation of this work.

Rather than utilizing an arbitrary log2 fold change cut-off (most commonly >2 or 1.5), the selection of candidate miRNAs was based on significance in miRNA sequencing and potential clinical relevance. MiRNA expression levels have shown to exhibit a positive relationship with their activity (Kozomara et al., 2014), suggesting larger differences in miRNA expression may lead to greater changes in expression of target mRNA. This supports the use of a log2 fold change cut-off value in sequencing data in order to select candidate miRNAs for further investigation that are potentially more biologically relevant. However, other evidence suggests miRNA expression levels are a poor indicator of activity (Plotnikova et al., 2019, Kozomara et al., 2014). Since the aim was to evaluate clinically relevant miRNAs, candidate miRNAs were selected based on published literature from preeclamptic patients reporting dysregulation of the miRNA rather than a log2 fold change cut-off. In turn, the four candidate miRNAs had a fold change less than +/-0.6. Hence, the differences in expression may not have been large enough to confer significance when measured by RT-qPCR. Within placental layers, three of the four candidate miRNAs showed significant differences in expression. Although a significant downregulation of miR-145-5p in

the labyrinth matched the results from the sequencing experiment and clinical studies, a significant downregulation of miR-19b-3p in the decidua contrasted with the increased expression observed in the sequencing experiments and in clinical studies. These findings support the concept that miRNA expression in whole placental tissue is largely determined by expression in the labyrinth, likely due to its large surface area. Since only one clinical study has detected dysregulation of placental miR-145-5p expression and only two clinical studies for miR-19b-3p, further clinical studies are required to draw any inferences concerning their suitability as therapeutic targets. Finally, as previously discussed miR-210-3p was dysregulated in the labyrinth and decidua in the SPE rat model.

Validation of the candidate miRNAs in placentas from preeclamptic patients found miR-210-3p and miR-19b-3p were significantly upregulated by 3-fold and 1.5-fold respectively, concurring with the increased expression detected by the sequencing experiment in the SPE rat model. A drawback of these findings is that validation was performed in patients diagnosed with PE rather than patients with SPE, the subtype modelled in the rat. This was due to the limited availability of samples, which in turn underpins the small sample size. In the current work, validation was performed in n=4 healthy controls and n=6 preeclamptic patients. In addition, it is important to consider that significant differences in foetal weight and gestational age at delivery between patients with PE and healthy controls may have had an impact of miRNA and gene expression findings since these factors have previously shown to affect placental miRNA expression (Awamleh et al., 2019, Pineles et al., 2007, Weedon-Fekjær et al., 2014, Mayor-Lynn et al., 2011, Hromadnikova et al., 2017, Anton et al., 2015, Yang et al., 2019b). Nonetheless, as findings from the current work on the preclinical PE model and preeclamptic patients supported the existing literature that miR-210-3p is dysregulated in PE, this miRNA was selected for further investigations into predicted gene targets and *in vitro* characterisation.

Of the four predicted gene targets (FGFRL1, BDNF, NDUFA4, and SLC6A1), FGFRL1 and BDNF were significantly downregulated in placentas from preeclamptic patients. Examination of these two genes in the placentas of the rat model of SPE found only FGFRL1 was significantly downregulated and BDNF

was undetected. Evaluation of all four genes in trophoblasts following miR-210-3p overexpression found only FGFRL1 was significantly downregulated. NDUFA4 and SLC6A1 were either undetected or detected at high Ct values, suggesting they unlikely play a role in cytotrophoblasts. As they showed no significant difference in expression in preeclamptic patients compared to healthy controls, this also suggests they are unlikely to play a role in PE. Overexpressing or knocking down miR-210-3p expression also had no significant effect on BDNF expression, indicating other factors beside the miRNA regulate BDNF expression or that it is not a direct target. Evidence from the preeclamptic patients, preclinical model, and *in vitro* studies suggest that FGFRL1 is a target of miR-210-3p and upregulation of the miRNA in PE coincides with downregulation of the gene. However, reporter construct assays are required to validate FGFRL1 as a gene target of miR-210-3p. Furthermore, a major limitation of these findings is that protein expression of the predicted gene target was not assessed, a key piece of evidence required to confirm inhibition of the mRNA at the posttranscriptional level. Nonetheless, studies have shown miRNAs can degrade the mRNA of gene targets (Ruike et al., 2008). The current findings provide indirect evidence that FGFRL1 is dysregulated in PE due to increased miR-210-3p expression, but further studies are required to confirm this. MiR-210-3p overexpression and knockdown had no effect on cell viability. A previous study showed miR-210-3p overexpression inhibited invasion and promoted iron accumulation in Swan 71 but not BeWo trophoblasts (Lee et al., 2011). Swan 71 cells are a model of extravillous cytotrophoblasts while BeWo cells are a model of villous cytotrophoblasts. Another study found miR-210-3p overexpression inhibited syncytialization of BeWo cells (Wang et al., 2020a), suggesting that miR-210-3p may modulate differentiation rather than proliferation of villous cytotrophoblasts. Hence, miR-210-3p may regulate different properties in distinct subpopulations of trophoblasts. Finally, several clinical studies have reported dysregulation of miR-210-3p in placentas from patients with cases of FGR and SGA (Awamleh and Han, 2020, Lee et al., 2011, Awamleh et al., 2019). This provides further evidence that miR-210-3p may regulate trophoblasts since impaired trophoblast function is a pathological feature common to these pregnancy complications (Khong et al., 1986, Kaufmann et al., 2003).

The work from Chapter 5 and 6 provides preclinical and clinical evidence that contributes to the existing literature implicating dysregulation of placental miR-210-3p expression in the pathology of PE. The majority of evidence suggests an upregulation of miR-210-3p in the placenta leads to downregulation of target genes contributing to the pathological processes underlying PE, primarily by modulating the properties of trophoblasts. In turn, miR-210-3p represents a prominent therapeutic target of interest, and future studies in animal models of PE should seek to evaluate whether inhibiting placental miR-210-3p expression confers therapeutic benefit. Given the *in vitro* evidence of miR-210-3p regulating trophoblasts and the availability of plasmids with trophoblast specific promoters, targeted inhibition of miR-210-3p in trophoblasts remains an intriguing therapeutic strategy to be explored. Due to lack of availability of placental tissue, miR-210-3p expression was not evaluated in the placentas of the SPE rat model at an earlier time point. This should be considered for future studies since it would provide insight into whether miR-210-3p dysregulation is a cause or consequence of PE pathology. Of note, several profiling and candidate clinical studies found miR-210-3p was significantly differentially expressed in the blood of preeclamptic patients between 11 and 20 weeks of pregnancy (Ura et al., 2014, Xu et al., 2014a, Anton et al., 2013). This indicates dysregulation may occur prior to PE diagnosis and therefore that miR-210-3p may contribute to early pathological processes. Whether this dysregulation occurs in the placenta however remains to be shown, with animal models providing the unique opportunity to study this given the ethical constraints in humans. One clinical study reported that miR-423-5p expression in first trimester plasma samples could predict the development of EOPE at a sensitivity of 87.5% and specificity of 80% (Timofeeva et al., 2018). Furthermore, miR-423-5p was significantly differentially expressed in term placenta of EOPE patients (Timofeeva et al., 2018). Dysregulation of a circulating miRNA prior to the onset of PE corresponding with dysregulation of the miRNA in the placenta would represent an ideal scenario for therapeutic targeting in the placenta. Therapy could be administered prior to disease onset as a preventative treatment following a precision medicine approach. Biro et al. found exosomal and Ago-bound miR-210-3p was significantly increased in preeclamptic patients (Biró et al., 2017, Biro et al., 2019). *In vitro,* the group showed hypoxia stimulated intracellular, exosomal, and Ago-bound miR-210-3p expression (Biro et al., 2019), suggesting

trophoblasts contribute to the elevated circulating levels of miR-210-3p in patients with PE. Although validation of placental and circulating miRNA expression profiles in larger cohorts is still required, this thesis contributes to the growing body of evidence that miR-210-3p represents a particular miRNA of interest to target therapeutically in PE.

This thesis has provided information on a gene therapy technique for targeting the placenta as well as miRNAs dysregulated in the placenta in PE. The development of safe and effective delivery systems that target the placenta remains key to establishing placental gene therapy as a strategy for pregnancy disorders arising from abnormal placental development, such as PE. A growing number of studies suggest placental miRNAs play a key role in the pathology of PE, and one study has shown therapeutic benefit to the foetus after targeting placental miRNAs in animal model of PE. Identifying suitable placental miRNAs to target therefore remains essential to establishing gene therapy as a therapeutic strategy in PE. The work in this thesis has provided means to further investigate UMGD for targeting the placenta in pregnant mice, important animal models in pregnancy research. In addition, the work in this thesis has highlighted attributes of miRNAs that should be considered in future work seeking to evaluate the role of placental miRNAs in PE and/or target placental miRNAs as well as led to the identification of several miRNAs in the placenta that are potentially suitable therapeutic targets in PE.

Chapter 8 Appendix

8.1 RT-qPCR raw data

8.1.1 Study 2

Table 8-1 Raw data of SYBR RT-qPCR run with primers, LGFP1 and LGFP2, on left and right kidneys of the three UMGD treatment rats and a negative control rat.

LGFP1						
Sample	Well	Gene	Ct	Tm1	Tm2	Tm3
Treatment rat 1 right kidney	A1	LGFP1	32.754	78.385		
	B1	LGFP1	32.175	78.385		
	C1	LGFP1	33.429	78.385		
Treatment rat 1 left kidney	A3	LGFP1	31.305	78.253		
	B3	LGFP1	38.143	70.779		
	C3	LGFP1	32.625	78.253	72.877	
Treatment rat 2 right kidney	A5	LGFP1	32.776	78.253	74.188	
	B5	LGFP1	32.712	78.385		
	C5	LGFP1	37.617	73.795	78.909	87.695
Treatment rat 2 left kidney	A7	LGFP1	32.867	78.385		
	B7	LGFP1	37.609	72.877		
	C7	LGFP1	37.496	72.877	78.909	87.564
Treatment rat 3 right kidney	A9	LGFP1	35.497	72.746		
	B9	LGFP1	32.847	78.253		
	C9	LGFP1	32.876	78.253	65.402	
Treatment rat 3 left kidney	A11	LGFP1	38.874	70.516		
	B11	LGFP1	32.793	78.385		
	C11	LGFP1	Undetermined	61.074		
Negative control right kidney	A13	LGFP1	Undetermined	61.337		
	B13	LGFP1	35.844	73.139		
	C13	LGFP1	34.670	73.139		
Negative control left kidney	A15	LGFP1	38.428	78.909	70.516	87.433
	B15	LGFP1	37.527	73.139		
	C15	LGFP1	39.343	73.664	82.319	87.433
Plasmid	A24	LGFP1	Undetermined	78.516		
NFW	A17	LGFP1	Undetermined	61.337		
LGFP2						
Sample	Well	Gene	Ct	Tm1	Tm2	Tm3
Treatment rat 1 right kidney	E1	LGFP2	33.680	76.811		
	F1	LGFP2	32.395	76.811		
	G1	LGFP2	Undetermined	71.959		
Treatment rat 1 left kidney	E3	LGFP2	31.982	76.811		
	F3	LGFP2	Undetermined	61.337		
	G3	LGFP2	Undetermined	70.779		
Treatment rat 2 right kidney	E5	LGFP2	31.736	76.811		
	F5	LGFP2	32.213	76.942		
	G5	LGFP2	Undetermined	61.337		
Treatment rat 2 left kidney	E7	LGFP2	33.895	76.942		
	F7	LGFP2	Undetermined	61.205		
	G7	LGFP2	Undetermined	61.205		
Treatment rat 3 right kidney	E9	LGFP2	32.179	76.942		
	F9	LGFP2	33.866	76.942		
	G9	LGFP2	33.748	76.942		
Treatment rat 3 left kidney	E11	LGFP2	Undetermined	61.205		
	F11	LGFP2	37.244	72.352		
	G11	LGFP2	33.540	76.942		
Negative control right kidney	E13	LGFP2	33.496	76.942		
	F13	LGFP2	33.787	76.942		
	G13	LGFP2	Undetermined	61.074		
Negative control left kidney	E15	LGFP2	Undetermined	87.564	61.337	76.155
	F15	LGFP2	31.869	76.942		
	G15	LGFP2	Undetermined	61.337		
Plasmid	E24	LGFP2	4.311	77.073		
NFW	E17	LGFP2	Undetermined	61.468		

Highlighted in bold: multiple melting temperatures, outlier melting temperatures, or undetermined Ct values and in red: samples selected to run on a gel and for sequencing. TM, melting temperature; Ct, cycle threshold; NFW, nuclease free water.

Table 8-2 Raw data of SYBR RT-qPCR run with the β-actin housekeeper on left and right kidneys of the three UMGD treatment rats and a negative control rat.

β-actin								
Sample	Well	Gene	Ct	Ct mean	Ct SD	Tm1	Tm2	Tm3
Treatment rat 1 right kidney	I1	ACTB	19.896	19.928	0.034	77.073		
	J1	ACTB	19.963			76.942		
	K1	ACTB	19.925			77.073		
Treatment rat 1 left kidney	I3	ACTB	19.019	19.013	0.038	77.073		
	J3	ACTB	18.973			77.073		
	K3	ACTB	19.048			77.073		
Treatment rat 2 right kidney	I5	ACTB	18.637	18.872	0.205	77.204		
	J5	ACTB	18.962			77.073		
	K5	ACTB	19.016			77.073		
Treatment rat 2 left kidney	I7	ACTB	18.877	18.926	0.065	77.073		
	J7	ACTB	19.000			77.073		
	K7	ACTB	18.902			76.942		
Treatment rat 3 right kidney	I9	ACTB	19.790	19.562	0.263	77.204		
	J9	ACTB	19.275			77.073		
	K9	ACTB	19.621			77.073		
Treatment rat 3 left kidney	I11	ACTB	19.880	19.861	0.049	77.073		
	J11	ACTB	19.806			77.073		
	K11	ACTB	19.898			77.073		
Negative control right kidney	I13	ACTB	19.712	19.691	0.020	77.073		
	J13	ACTB	19.689			77.073		
	K13	ACTB	19.673			77.073		
Negative control left kidney	I15	ACTB	19.472	19.572	0.089	77.204		
	J15	ACTB	19.643			77.204		
	K15	ACTB	19.602			77.204		
			all samples	*19.428*	*0.427*			
Plasmid	I24	ACTB	34.682			73.532	79.303	
NFW	I17	ACTB	36.751			74.188		

Highlighted in bold: multiple melting temperatures or outlier melting temperatures. '*All samples'* designates Ct mean and SD of Ct means of all kidney samples. TM, melting temperature; Ct, cycle threshold; SD, standard deviation; NFW, nuclease free water; ACTB, β-actin.

8.1.2 Study 3

Table 8-3 Raw data of TaqMan RT-qPCR run with primers, Luc2 and β-actin, on controls.

Controls					
Sample	Well	Gene	Ct	Gene	Ct
MM	**B21**	**Luc2**	**Undetermined**	**ACTB**	**Undetermined**
	B22	**Luc2**	**Undetermined**	**ACTB**	**Undetermined**
	B23	**Luc2**	**Undetermined**	**ACTB**	**Undetermined**
NFW	**D21**	**Luc2**	**Undetermined**	**ACTB**	**Undetermined**
	D22	**Luc2**	**Undetermined**	**ACTB**	**Undetermined**
	D23	**Luc2**	**Undetermined**	**ACTB**	**Undetermined**
MM from cDNA plate	**H21**	**Luc2**	**Undetermined**	**ACTB**	**Undetermined**
	H22	**Luc2**	**Undetermined**	**ACTB**	**Undetermined**
	H23	**Luc2**	**Undetermined**	**ACTB**	**Undetermined**
NFW from cDNA plate	**J21**	**Luc2**	**Undetermined**	**ACTB**	**Undetermined**
	J22	**Luc2**	**Undetermined**	**ACTB**	**Undetermined**
	J23	**Luc2**	**Undetermined**	**ACTB**	**Undetermined**
MM and NFW from cDNA plate	**N21**	**Luc2**	**Undetermined**	**ACTB**	**Undetermined**
	N22	Luc2	33.964	**ACTB**	**Undetermined**
	N23	**Luc2**	**Undetermined**	**ACTB**	**Undetermined**
No RT	L21	Luc2	32.969	**ACTB**	**Undetermined**
	L22	Luc2	33.662	**ACTB**	**Undetermined**
	L23	Luc2	33.745	**ACTB**	**Undetermined**

Highlighted in bold: undetermined Ct values. Ct, cycle threshold; SD, standard deviation; MM, master mix; NFW, nuclease free water; RT, reverse transcriptase; ACTB, β-actin; Luc2, luciferase.

Table 8-4 Raw data of TaqMan RT-qPCR run with primers, Luc2 and β-actin, on controls.

Controls					
Sample	Well	Gene	Ct	Gene	Ct
MM	**I18**	**Luc2**	**35.451**	**ACTB**	**Undetermined**
	I19	Luc2	34.198	**ACTB**	**Undetermined**
	I20	**Luc2**	**35.329**	**ACTB**	**Undetermined**
NFW	L18	Luc2	21.969	**ACTB**	**Undetermined**
	L19	Luc2	8.780	**ACTB**	**Undetermined**
	L20	**Luc2**	**Undetermined**	ACTB	29.710
MM from cDNA plate	**I2**	**Luc2**	**Undetermined**	**ACTB**	**Undetermined**
	I3	Luc2	33.064	**ACTB**	**Undetermined**
	I4	Luc2	33.603	**ACTB**	**Undetermined**
NFW from cDNA plate	**L2**	**Luc2**	**37.580**	**ACTB**	**Undetermined**
	L3	**Luc2**	**39.991**	**ACTB**	**Undetermined**
	L4	**Luc2**	**Undetermined**	**ACTB**	**Undetermined**
No RT	**L10**	**Luc2**	**Undetermined**	**ACTB**	**Undetermined**
	L11	Luc2	32.942	**ACTB**	**Undetermined**
	L12	Luc2	34.692	**ACTB**	**Undetermined**

Highlighted in bold: undetermined Ct or >35 Ct values. Ct, cycle threshold; SD, standard deviation; MM, master mix; NFW, nuclease free water; RT, reverse transcriptase; ACTB, β-actin; Luc2, luciferase.

8.1.3 Study 4

Table 8-5 Raw data of TaqMan RT-qPCR run with primers, Luc and β-actin, on left and right kidneys and skeletal muscles of the three UMGD treatment rats and a positive control rat and negative control rat.

Left kidney

Sample	Well	Gene	Ct	Ct mean	Ct SD	Gene	Ct	Ct mean	Ct SD
Treatment rat 1 left kidney	D2	**Luc**	**Undetermined**	N/A	N/A	ACTB	19.862	19.566	0.260
	D3	**Luc**	**Undetermined**			ACTB	19.376		
	D4	**Luc**	**Undetermined**			ACTB	19.460		
Treatment rat 2 left kidney	D6	**Luc**	**Undetermined**	N/A	N/A	ACTB	18.736	18.815	0.170
	D7	**Luc**	**Undetermined**			ACTB	18.699		
	D8	**Luc**	**Undetermined**			ACTB	19.010		
Treatment rat 3 left kidney	D10	**Luc**	**Undetermined**	N/A	N/A	ACTB	19.783	19.843	0.054
	D11	**Luc**	**Undetermined**			ACTB	19.886		
	D12	**Luc**	**Undetermined**			ACTB	19.860		
Positive control left kidney	D14	**Luc**	**Undetermined**	N/A	N/A	ACTB	19.152	19.192	0.035
	D15	**Luc**	**Undetermined**			ACTB	19.206		
	D16	**Luc**	**Undetermined**			ACTB	19.218		
Negative control left kidney	D18	**Luc**	**Undetermined**	N/A	N/A	ACTB	19.584	19.704	0.106
	D19	**Luc**	**Undetermined**			ACTB	19.786		
	D20	**Luc**	**Undetermined**			ACTB	19.741		
							all samples	*19.424*	*0.418*

Right kidney

Sample	Well	Gene	Ct	Ct mean	Ct SD	Gene	Ct	Ct mean	Ct SD
Treatment rat 1 right kidney	B2	**Luc**	**Undetermined**	N/A	N/A	ACTB	19.528	19.384	0.165
	B3	**Luc**	**Undetermined**			ACTB	19.204		
	B4	**Luc**	**39.733**			ACTB	19.420		
Treatment rat 2 right kidney	B6	**Luc**	**Undetermined**	N/A	N/A	ACTB	20.023	19.889	0.229
	B7	**Luc**	**Undetermined**			ACTB	19.624		
	B8	**Luc**	**Undetermined**			ACTB	20.019		
Treatment rat 3 right kidney	B10	**Luc**	**Undetermined**	N/A	N/A	ACTB	19.803	19.917	0.100
	B11	**Luc**	**Undetermined**			ACTB	19.990		
	B12	**Luc**	**Undetermined**			ACTB	19.959		
Positive control right kidney	B14	**Luc**	**Undetermined**	N/A	N/A	ACTB	19.399	19.300	0.096
	B15	**Luc**	**Undetermined**			ACTB	19.292		
	B16	**Luc**	**Undetermined**			ACTB	19.208		
Negative control right kidney	B18	**Luc**	**Undetermined**	N/A	N/A	ACTB	19.084	19.169	0.076
	B19	**Luc**	**Undetermined**			ACTB	19.192		
	B20	**Luc**	**Undetermined**			ACTB	19.230		
							all samples	*19.532*	*0.348*

Skeletal muscle

Sample	Well	Gene	Ct	Ct mean	Ct SD	Gene	Ct	Ct mean	Ct SD
Treatment rat 1 skeletal muscle	F2	**Luc**	**Undetermined**	N/A	N/A	ACTB	22.621	22.670	0.216
	F3	**Luc**	**Undetermined**			ACTB	22.483		
	F4	**Luc**	**Undetermined**			ACTB	22.906		
Treatment rat 2 skeletal muscle	F6	**Luc**	**Undetermined**	N/A	N/A	ACTB	21.481	21.553	0.076
	F7	**Luc**	**Undetermined**			ACTB	21.545		
	F8	**Luc**	**Undetermined**			ACTB	21.632		
Treatment rat 3 skeletal muscle	F10	**Luc**	**Undetermined**	N/A	N/A	ACTB	21.979	22.167	0.292
	F11	**Luc**	**38.416**			ACTB	22.504		
	F12	**Luc**	**Undetermined**			ACTB	22.019		
Positive control skeletal muscle	F14	**Luc**	**Undetermined**	N/A	N/A	ACTB	16.483	16.665	0.184
	F15	**Luc**	**Undetermined**			ACTB	16.663		
	F16	**Luc**	**Undetermined**			ACTB	16.850		
Negative control skeletal muscle	F18	**Luc**	**Undetermined**	N/A	N/A	ACTB	21.248	21.181	0.081
	F19	**Luc**	**Undetermined**			ACTB	21.091		
	F20	**Luc**	**Undetermined**			ACTB	21.204		
							all samples	*20.847*	*2.406*

Highlighted in bold: undetermined CT or >35 Ct values. '*All samples'* designates Ct mean and SD of Ct means of all tissue samples. Ct, cycle threshold; SD, standard deviation; ACTB, β-actin; Luc, luciferase; N/A, not available.

Table 8-6 Raw data of TaqMan RT-qPCR run with primers, Luc and β-actin, on controls.

Controls					
Sample	Well	Gene	Ct	Gene	Ct
MM	**J2**	**Luc**	**Undetermined**	**ACTB**	**Undetermined**
	J3	**Luc**	**Undetermined**	**ACTB**	**Undetermined**
	J4	**Luc**	**37.922**	**ACTB**	**Undetermined**
NFW	**H2**	**Luc**	**Undetermined**	**ACTB**	**Undetermined**
	H3	**Luc**	**Undetermined**	**ACTB**	**Undetermined**
	H4	**Luc**	**Undetermined**	**ACTB**	**Undetermined**
MM from cDNA plate	**J6**	**Luc**	**Undetermined**	**ACTB**	**Undetermined**
	J7	**Luc**	**Undetermined**	**ACTB**	**Undetermined**
	J8	**Luc**	**Undetermined**	**ACTB**	**Undetermined**
NFW from cDNA plate	**H6**	**Luc**	**Undetermined**	**ACTB**	**Undetermined**
	H7	**Luc**	**Undetermined**	**ACTB**	**Undetermined**
	H8	**Luc**	**Undetermined**	**ACTB**	**Undetermined**
No RT	**H10**	**Luc**	**Undetermined**	**ACTB**	**Undetermined**
	H11	**Luc**	**Undetermined**	**ACTB**	**Undetermined**
	H12	**Luc**	**Undetermined**	**ACTB**	**Undetermined**

Highlighted in bold: undetermined Ct or >35 Ct values. Ct, cycle threshold; SD, standard deviation; MM, master mix; NFW, nuclease free water; RT, reverse transcriptase; ACTB, β-actin; Luc, luciferase.

8.1.4 Study 5

Table 8-7 Raw data of TaqMan RT-qPCR run with primers, Luc and β-actin, on heart and skeletal muscle of the three UMGD treatment mice, a positive controls mouse, a negative control mouse, and controls

Heart

Sample	Well	Gene	Ct	Ct mean	Ct SD	Gene	Ct	Ct mean	Ct SD
Treatment mouse 1 heart	B1	Luc	30.258	31.016	0.664	ACTB	15.999	15.858	0.124
	B2	Luc	31.299			ACTB	15.766		
	B3	Luc	31.492			ACTB	15.810		
Treatment mouse 2 heart	B5	Luc	31.945	32.402	0.398	ACTB	16.031	16.048	0.035
	B6	Luc	32.584			ACTB	16.088		
	B7	Luc	32.677			ACTB	16.024		
Treatment mouse 3 heart	B9	Luc	33.340	34.419	0.946	ACTB	14.887	14.932	0.099
	B10	Luc	34.816			ACTB	15.045		
	B11	**Luc**	**35.102**			ACTB	14.863		
Positive control heart	B13	Luc	33.106	33.758	0.605	ACTB	15.744	15.736	0.012
	B14	Luc	33.866			ACTB	15.722		
	B15	Luc	34.301			ACTB	15.742		
Negative control heart	B17	Luc	37.756	32.724	0.302	ACTB	16.161	16.207	0.059
	B18	Luc	32.407			ACTB	16.187		
	B19	Luc	33.009			ACTB	16.274		
							all samples	*15.756*	*0.494*

Skeletal muscle

Sample	Well	Gene	Ct	Ct mean	Ct SD	Gene	Ct	Ct mean	Ct SD
Treatment mouse 1 skeletal muscle	**F1**	**Luc**	**Undetermined**	39.266	0.464	ACTB	16.238	16.289	0.057
	F2	**Luc**	**38.938**			ACTB	16.280		
	F3	**Luc**	**39.594**			ACTB	16.350		
Treatment mouse 2 skeletal muscle	**F5**	**Luc**	**Undetermined**	N/A	N/A	ACTB	17.111	17.192	0.071
	F6	**Luc**	**39.236**			ACTB	17.230		
	F7	**Luc**	**Undetermined**			ACTB	17.236		
Treatment mouse 3 skeletal muscle	F9	Luc	30.258	31.067	0.706	ACTB	16.474	16.415	0.056
	F10	Luc	31.384			ACTB	16.363		
	F11	Luc	31.559			ACTB	16.407		
Positive control skeletal muscle	F13	Luc	28.783	28.885	0.275	ACTB	15.042	15.070	0.032
	F14	Luc	29.196			ACTB	15.105		
	F15	Luc	28.676			ACTB	15.064		
Negative control skeletal muscle	**F17**	**Luc**	**Undetermined**	N/A	N/A	ACTB	16.668	16.681	0.031
	F18	**Luc**	**Undetermined**			ACTB	16.716		
	F19	**Luc**	**Undetermined**			ACTB	16.659		
							all samples	*16.329*	*0.785*

Highlighted in bold: undetermined Ct or >35 Ct values. '*All samples'* designates Ct mean and SD of Ct means of all tissue samples. Ct, cycle threshold; SD, standard deviation; ACTB, β-actin; Luc, luciferase; N/A, not available.

Table 8-8 Raw data of TaqMan RT-qPCR run with primers, Luc2 and β-actin, on controls.

Controls									
Sample	Well	Gene	Ct	Ct mean	Ct SD	Gene	Ct	Ct mean	Ct SD
NFW	**B21**	**Luc**	**Undetermined**	N/A	N/A	**ACTB**	**Undetermined**	N/A	N/A
	B22	**Luc**	**Undetermined**			**ACTB**	**Undetermined**		
	B23	**Luc**	**Undetermined**			**ACTB**	**Undetermined**		
MM	**D21**	**Luc**	**Undetermined**	N/A	N/A	**ACTB**	**Undetermined**	N/A	N/A
	D22	**Luc**	**Undetermined**			**ACTB**	**Undetermined**		
	D23	**Luc**	**Undetermined**			**ACTB**	**Undetermined**		
NFW from cDNA plate	**H24**	**Luc**	**37.688**	N/A	N/A	**ACTB**	**Undetermined**	N/A	N/A
	I24	**Luc**	**Undetermined**			**ACTB**	**Undetermined**		
	J24	**Luc**	**Undetermined**			**ACTB**	**Undetermined**		
MM from cDNA plate	**K24**	**Luc**	**Undetermined**	N/A	N/A	**ACTB**	**Undetermined**	N/A	N/A
	L24	**Luc**	**Undetermined**			**ACTB**	**Undetermined**		
	M24	**Luc**	**Undetermined**			**ACTB**	**Undetermined**		
No RT (SM)	**K22**	**Luc**	**Undetermined**	N/A	N/A	**ACTB**	**Undetermined**	N/A	N/A
	L22	**Luc**	**Undetermined**			**ACTB**	**Undetermined**		
	M22	**Luc**	**Undetermined**			**ACTB**	**Undetermined**		
No RT (Heart)	**H22**	**Luc**	**Undetermined**	N/A	N/A	**ACTB**	**Undetermined**	N/A	N/A
	I22	**Luc**	**Undetermined**			**ACTB**	**Undetermined**		
	J22	**Luc**	**Undetermined**			**ACTB**	**Undetermined**		

Highlighted in bold: undetermined Ct or >35 Ct values. Ct, cycle threshold; SD, standard deviation; MM, master mix; NFW, nuclease free water; RT, reverse transcriptase; ACTB, β-actin; Luc, luciferase; SM, skeletal muscle; N/A, not available.

Table 8-9 Raw data of TaqMan RT-qPCR run with primers, Luc and β-actin, on tissue samples and controls.

Tissue (duplex)								
Sample	Gene	Ct	Ct mean	Ct SD	Gene	Ct	Ct mean	Ct SD
Treatment mouse 1 heart	Luc	30.953	31.041	0.160	ACTB	19.048	18.990	0.051
	Luc	31.226			ACTB	18.970		
	Luc	30.945			ACTB	18.953		
Positive control skeletal muscle	Luc	29.633	29.771	0.154	ACTB	18.776	18.822	0.049
	Luc	29.937			ACTB	18.873		
	Luc	29.744			ACTB	18.817		
Negative control skeletal muscle	Luc	32.300	32.029	0.235	ACTB	20.228	20.418	0.164
	Luc	31.881			ACTB	20.512		
	Luc	31.907			ACTB	20.513		
MM only	Luc	31.986	32.053	0.102	**ACTB**	**Undetermined**	N/A	N/A
	Luc	32.170			**ACTB**	**Undetermined**		
	Luc	32.002			**ACTB**	**Undetermined**		
Tissue (singleplex)								
Treatment mouse 1 heart	Luc	30.121	30.163	0.037	ACTB	18.790	18.566	0.211
	Luc	30.174			ACTB	18.536		
	Luc	30.193			ACTB	18.372		
Positive control skeletal muscle	Luc	29.258	29.222	0.080	ACTB	18.599	18.442	0.140
	Luc	29.278			ACTB	18.331		
	Luc	29.130			ACTB	18.396		
Negative control skeletal muscle	Luc	30.709	30.893	0.227	ACTB	19.973	20.555	0.512
	Luc	31.147			ACTB	20.937		
	Luc	30.822			ACTB	20.754		
MM only	Luc	30.951	30.858	0.167	**ACTB**	**Undetermined**	N/A	N/A
	Luc	30.958			**ACTB**	**Undetermined**		
	Luc	30.665			**ACTB**	**Undetermined**		

Highlighted in bold: undetermined Ct or >35 Ct values. Ct, cycle threshold; SD, standard deviation; MM, master mix; ACTB, β-actin; Luc, luciferase; N/A, not available.

List of references

Á Rogvi, R., Forman, J., Damm, P. & Greisen, G. 2012. Women born preterm or with inappropriate weight for gestational age are at risk of subsequent gestational diabetes and pre-eclampsia. *PLoS One,* 7**,** e34001.

AACR. 2017. JCAR015 in ALL: A Root-Cause Investigation. *Cancer Discovery* [Online]. Available: https://cancerdiscovery.AACRjournals.org/content/early/2017/12/04/2159-8290.CD-NB2017-169 [Accessed 2017-12-05].

Aardema, M., Oosterhof, H., Timmer, A., Van Rooy, I. & Aarnoudse, J. 2001. Uterine artery Doppler flow and uteroplacental vascular pathology in normal pregnancies and pregnancies complicated by pre-eclampsia and small for gestational age fetuses. *Placenta,* 22**,** 405-11.

Abalos, E., Cuesta, C., Carroli, G., Qureshi, Z., Widmer, M., Vogel, J., Souza, J. & Network, W. M. S. O. M. A. N. H. R. 2014. Pre-eclampsia, eclampsia and adverse maternal and perinatal outcomes: a secondary analysis of the World Health Organization Multicountry Survey on Maternal and Newborn Health. *BJOG,* 121**,** 14-24.

Abalos, E., Cuesta, C., Grosso, A. L., Chou, D. & Say, L. 2013. Global and regional estimates of preeclampsia and eclampsia: a systematic review. *Eur J Obstet Gynecol Reprod Biol,* 170**,** 1-7.

Abalos, E., Duley, L., Steyn, D. W. & Gialdini, C. 2018. Antihypertensive drug therapy for mild to moderate hypertension during pregnancy. *Cochrane Database Syst Rev,* 2018**,** CD002252.

Acanda, Y., Wang, C. & Levy, A. 2019. Gene Expression in Citrus Plant Cells Using Helios ® Gene Gun System for Particle Bombardment. *Methods Mol Biol,* 2015**,** 219-228.

ACOG 2013. Hypertension in pregnancy. Report of the American College of Obstetricians and Gynecologists' Task Force on Hypertension in Pregnancy. *Obstet Gynecol,* 122**,** 1122-31.

ACOG 2020. Placenta Accreta Spectrum. *Obstetric Care Consensus.*

Adel, S., Mansour, A., Louka, M., Matboli, M., Elmekkawi, S. F. & Swelam, N. 2017. Evaluation of MicroRNA-210 and Protein tyrosine phosphatase, non-receptor type 2 in Pre-eclampsia. *Gene,* 596**,** 105-109.

Adhikari, U., Goliaei, A. & Berkowitz, M. 2015. Mechanism of membrane poration by shock wave induced nanobubble collapse: a molecular dynamics study. *J Phys Chem B,* 119**,** 6225-34.

Aggarwal, P., Chandel, N., Jain, V. & Jha, V. 2012. The relationship between circulating endothelin-1, soluble fms-like tyrosine kinase-1 and soluble endoglin in preeclampsia. *J Hum Hypertens,* 26**,** 236-41.

Agrawal, S., Cerdeira, A., Redman, C. & Vatish, M. 2018. Meta-Analysis and Systematic Review to Assess the Role of Soluble FMS-Like Tyrosine Kinase-1 and Placenta Growth Factor Ratio in Prediction of Preeclampsia: The SaPPPhirE Study. *Hypertension,* 71**,** 306-316.

Ahn, S., Jeong, E., Min, J. W., Kim, E., Choi, S. S., Kim, C. J. & Lee, D. C. 2017. Identification of genes dysregulated by elevation of microRNA-210 levels in human trophoblasts cell line, Swan 71. *Am J Reprod Immunol,* 5**,** epub.

Ajroud-Driss, S., Christiansen, M., Allen, J. & Kessler, J. 2013. Phase 1/2 open-label dose-escalation study of plasmid DNA expressing two isoforms of

hepatocyte growth factor in patients with painful diabetic peripheral neuropathy. *Mol Ther,* 21**,** 1279-86.

Akolekar, R., Syngelaki, A., Sarquis, R., Zvanca, M. & Nicolaides, K. 2011. Prediction of early, intermediate and late pre-eclampsia from maternal factors, biophysical and biochemical markers at 11-13 weeks. *Prenat Diagn,* 31**,** 66-74.

Alete, J. A. 2008. *Safe, Site-specific Gene Delivery using Ultrasound and Microbubble Technology*. Doctor of Philosophy (PhD), Imperial College London.

Alexander, B., Kassab, S., Miller, M., Abram, S., Reckelhoff, J., Bennett, W. & Granger, J. 2001. Reduced uterine perfusion pressure during pregnancy in the rat is associated with increases in arterial pressure and changes in renal nitric oxide. *Hypertension,* 37**,** 1191-5.

Aliño, S., Crespo, A. & Dasí, F. 2003. Long-term therapeutic levels of human alpha-1 antitrypsin in plasma after hydrodynamic injection of nonviral DNA. *Gene Ther,* 10**,** 1672-9.

Almasi-Hashiani, A., Omani-Samani, R., Mohammadi, M., Amini, P., Navid, B., Alizadeh, A., Khedmati Morasae, E. & Maroufizadeh, S. 2019. Assisted reproductive technology and the risk of preeclampsia: an updated systematic review and meta-analysis. *BMC Pregnancy Childbirth,* 19**,** 149.

Alsnes, I., Vatten, L., Fraser, A., Bjørngaard, J., Rich-Edwards, J., Romundstad, P. & Åsvold, B. 2017. Hypertension in Pregnancy and Offspring Cardiovascular Risk in Young Adulthood: Prospective and Sibling Studies in the HUNT Study (Nord-Trøndelag Health Study) in Norway. *Hypertension,* 69**,** 591-598.

Alter, J., Sennoga, C., Lopes, D., Eckersley, R. & Wells, D. 2009. Microbubble Stability Is a Major Determinant of the Efficiency of Ultrasound and Microbubble Mediated in Vivo Gene Transfer. *Ultrasound in medicine & biology,* 35**,** 976-84.

Altman, D., Carroli, G., Duley, L., Farrell, B., Moodley, J., Neilson, J., Smith, D. & Group, M. T. C. 2002. Do women with pre-eclampsia, and their babies, benefit from magnesium sulphate? The Magpie Trial: a randomised placebo-controlled trial. *Lancet,* 359**,** 1877-90.

Alton, E., Armstrong, D. K., Ashby, D., Bayfield, K. J., Bilton, D., Bloomfield, E. V., Boyd, A. C., Brand, J., Buchan, R., Calcedo, R., Carvelli, P., Chan, M., Cheng, S. H., Collie, D. D. S., Cunningham, S., Davidson, H. E., Davies, G., Davies, J. C., Davies, L. A., Dewar, M. H., Doherty, A., Donovan, J., Dwyer, N. S., Elgmati, H. I., Featherstone, R. F., Gavino, J., Gea-Sorli, S., Geddes, D. M., Gibson, J. S. R., Gill, D. R., Greening, A. P., Griesenbach, U., Hansell, D. M., Harman, K., Higgins, T. E., Hodges, S. L., Hyde, S. C., Hyndman, L., Innes, J. A., Jacob, J., Jones, N., Keogh, B. F., Limberis, M. P., Lloyd-Evans, P., Maclean, A. W., Manvell, M. C., Mccormick, D., Mcgovern, M., Mclachlan, G., Meng, C., Montero, M. A., Milligan, H., Moyce, L. J., Murray, G. D., Nicholson, A. G., Osadolor, T., Parra-Leiton, J., Porteous, D. J., Pringle, I. A., Punch, E. K., Pytel, K. M., Quittner, A. L., Rivellini, G., Saunders, C. J., Scheule, R. K., Sheard, S., Simmonds, N. J., Smith, K., Smith, S. N., Soussi, N., Soussi, S., Spearing, E. J., Stevenson, B. J., Sumner-Jones, S. G., Turkkila, M., Ureta, R. P., Waller, M. D., Wasowicz, M. Y., Wilson, J. M. & Wolstenholme-Hogg, P. 2015. Repeated nebulisation of non-viral CFTR gene therapy in patients with cystic fibrosis: a randomised, double-blind, placebo-controlled, phase 2b trial. *Lancet Respir Med,* 3**,** 684-91.

Alvarez, R., Sill, M., Davidson, S., Muller, C., Bender, D., Debernardo, R., Behbakht, K. & Huh, W. 2014. A phase II trial of intraperitoneal EGEN-001, an IL-12 plasmid formulated with PEG-PEI-cholesterol lipopolymer in the treatment of

persistent or recurrent epithelial ovarian, fallopian tube or primary peritoneal cancer: a gynecologic oncology group study. *Gynecol Oncol,* 133**,** 433-8.

Amosco, M., Tavera, G., Villar, V., Naniong, J., David-Bustamante, L., Williams, S., Jose, P. & Palmes-Saloma, C. 2019. Non-additive Effects of ACVR2A in Preeclampsia in a Philippine Population. *BMC pregnancy and childbirth,* 19.

Amosco, M., Villar, V., Naniong, J., David-Bustamante, L., Jose, P. & Palmes-Saloma, C. 2016. VEGF-A and VEGFR1 SNPs Associate With Preeclampsia in a Philippine Population. *Clinical and experimental hypertension (New York, N.Y. : 1993),* 38.

Ancel, P., Goffinet, F. & Group, E.-W. 2015. Survival and morbidity of preterm children born at 22 through 34 weeks' gestation in France in 2011: results of the EPIPAGE-2 cohort study. *JAMA Pediatr,* 169**,** 230-8.

Anderson, C., Rychak, J., Backer, M., Backer, J., Ley, K. & Klibanov, A. 2010. scVEGF Microbubble Ultrasound Contrast Agents: A Novel Probe for Ultrasound Molecular Imaging of Tumor Angiogenesis. *Invest Radiol,* 45**,** 579-85.

Anderson, C., Urschitz, J., Khemmani, M., Owens, J., Moisyadi, S., Shohet, R. & Walton, C. 2013. Ultrasound directs a transposase system for durable hepatic gene delivery in mice. *Ultrasound Med Biol,* 39**,** 2351-61.

Anderson, N., Sadler, L., Stewart, A., Fyfe, E. & Mccowan, L. 2012. Ethnicity, body mass index and risk of pre-eclampsia in a multiethnic New Zealand population. *Aust N Z J Obstet Gynaecol,* 52**,** 552-8.

Anteby, E. Y., Natanson-Yaron, S., Hamani, Y., Sciaki, Y., Goldman-Wohl, D., Greenfield, C., Ariel, I. & Yagel, S. 2005. Fibroblast growth factor-10 and fibroblast growth factor receptors 1-4: expression and peptide localization in human decidua and placenta. *Eur J Obstet Gynecol Reprod Biol,* 119**,** 27-35.

Anton, L., Devine, A., Polyak, E., Olarerin-George, A., Brown, A. G., Falk, M. J. & Elovitz, M. A. 2019. HIF-1alpha Stabilization Increases miR-210 Eliciting First Trimester Extravillous Trophoblast Mitochondrial Dysfunction. *Front Physiol,* 10**,** 699.

Anton, L., Olarerin-George, A. O., Hogenesch, J. B. & Elovitz, M. A. 2015. Placental expression of miR-517a/b and miR-517c contributes to trophoblast dysfunction and preeclampsia. *PLoS One,* 10**,** e0122707.

Anton, L., Olarerin-George, A. O., Schwartz, N., Srinivas, S., Bastek, J., Hogenesch, J. B. & Elovitz, M. A. 2013. miR-210 inhibits trophoblast invasion and is a serum biomarker for preeclampsia. *Am J Pathol,* 183**,** 1437-1445.

Araki, M. & Ishii, T. 2014. International regulatory landscape and integration of corrective genome editing into in vitro fertilization. *Reprod Biol Endocrinol,* 12**,** 108.

ARM 2020. ARM Annual Report & Sector Year in Review: 2019. *In:* Medicine, A. F. R. (ed.) *Advancing Gene, Cell, & Tissue-Based Therapies.* 2019 ed. www.alliancerm.org.

Arngrimsson, R., Björnsson, S., Geirsson, R., Björnsson, H., Walker, J. & Snaedal, G. 1990. Genetic and familial predisposition to eclampsia and pre-eclampsia in a defined population. *Br J Obstet Gynaecol,* 97**,** 762-9.

Arroyo, J., Chevillet, J., Kroh, E., Ruf, I., Pritchard, C., Gibson, D., Mitchell, P., Bennett, C., Pogosova-Agadjanyan, E., Stirewalt, D., Tait, J. & Tewari, M. 2011. Argonaute2 complexes carry a population of circulating microRNAs independent of vesicles in human plasma. *Proc Natl Acad Sci U S A,* 108**,** 5003-8.

Arthuis, C., Novell, A., Escoffre, J., Patat, F., Bouakaz, A. & Perrotin, F. 2013. New insights into uteroplacental perfusion: quantitative analysis using Doppler and contrast-enhanced ultrasound imaging. *Placenta,* 34**,** 424-31.

Aune, D., Saugstad, O., Henriksen, T. & Tonstad, S. 2014. Physical activity and the risk of preeclampsia: a systematic review and meta-analysis. *Epidemiology,* 25**,** 331-43.

Awamleh, Z., Gloor, G. B. & Han, V. K. M. 2019. Placental microRNAs in pregnancies with early onset intrauterine growth restriction and preeclampsia: potential impact on gene expression and pathophysiology. *BMC Med Genomics,* 12**,** 91.

Awamleh, Z. & Han, V. K. M. 2020. Identification of miR-210-5p in human placentae from pregnancies complicated by preeclampsia and intrauterine growth restriction, and its potential role in the pregnancy complications. *Pregnancy Hypertens,* 19**,** 159-168.

Babischkin, J. S., Aberdeen, G. W., Lindner, J. R., Bonagura, T. W., Pepe, G. J. & Albrecht, E. D. 2019. Vascular Endothelial Growth Factor Delivery to Placental Basal Plate Promotes Uterine Artery Remodeling in the Primate. *Endocrinology,* 160**,** 1492-1505.

Baczyk, D., Dunk, C., Huppertz, B., Maxwell, C., Reister, F., Giannoulias, D. & Kingdom, J. C. 2006. Bi-potential behaviour of cytotrophoblasts in first trimester chorionic villi. *Placenta,* 27**,** 367-74.

Bai, Y., Yang, W., Yang, H. X., Liao, Q., Ye, G., Fu, G., Ji, L., Xu, P., Wang, H., Li, Y. X., Peng, C. & Wang, Y. L. 2012. Downregulated miR-195 detected in preeclamptic placenta affects trophoblast cell invasion via modulating ActRIIA expression. *PLoS One,* 7**,** e38875.

Bailey, B., Euser, A., Bol, K., Julian, C. & Moore, L. 2020. High-altitude residence alters blood-pressure course and increases hypertensive disorders of pregnancy. *J Matern Fetal Neonatal Med***,** 1-8.

Baker, B. C., Mackie, F. L., Lean, S. C., Greenwood, S. L., Heazell, A. E. P., Forbes, K. & Jones, R. L. 2017. Placental dysfunction is associated with altered microRNA expression in pregnant women with low folate status. *Mol Nutr Food Res,* 61.

Baker, D. E. 2020. DHHS-FDA Notice of Opportunity for Hearing; James M. Wilson. *Department of Health and Human Services.* FDA.

Banek, C., Bauer, A., Gingery, A. & Gilbert, J. 2012. Timing of ischemic insult alters fetal growth trajectory, maternal angiogenic balance, and markers of renal oxidative stress in the pregnant rat. *Am J Physiol Regul Integr Comp Physiol,* 303**,** R658-64.

Bao, S., Thrall, B. & Miller, D. 1997. Transfection of a Reporter Plasmid Into Cultured Cells by Sonoporation in Vitro. *Ultrasound Med Biol,* 23**,** 953-9.

Barad, O., Meiri, E., Avniel, A., Aharonov, R., Barzilai, A., Bentwich, I., Einav, U., Gilad, S., Hurban, P., Karov, Y., Lobenhofer, E., Sharon, E., Shiboleth, Y., Shtutman, M., Bentwich, Z. & Einat, P. 2004. MicroRNA expression detected by oligonucleotide microarrays: system establishment and expression profiling in human tissues. *Genome Res,* 14**,** 2486-94.

Barbosa, I., Silva, W., Cerqueira, G., Novo, N., Almeida, F. & Novo, J. 2015. Maternal and fetal outcome in women with hypertensive disorders of pregnancy: the impact of prenatal care. *Ther Adv Cardiovasc Dis,* 9**,** 140-6.

Bartel, D. P. 2009. MicroRNA Target Recognition and Regulatory Functions. *Cell,* 136**,** 215-33.

Beards, F., Jones, L. E., Charnock, J., Forbes, K. & Harris, L. K. 2017. Placental Homing Peptide-microRNA Inhibitor Conjugates for Targeted Enhancement of Intrinsic Placental Growth Signaling. *Theranostics,* 7**,** 2940-2955.

Belch, J., Hiatt, W., Baumgartner, I., Driver, I., Nikol, S., Norgren, L. & Van Belle, E. 2011. Effect of fibroblast growth factor NV1FGF on amputation and death: a randomised placebo-controlled trial of gene therapy in critical limb ischaemia. *Lancet,* 377**,** 1929-37.

Bellamy, L., Casas, J. P., Hingorani, A. D. & Williams, D. J. 2007. Pre-eclampsia and risk of cardiovascular disease and cancer in later life: systematic review and meta-analysis. *BMJ,* 335**,** 974.

Benhamed, M., Herbig, U., Ye, T., Dejean, A. & Bischof, O. 2012. Senescence is an Endogenous Trigger for microRNA-Directed Transcriptional Gene Silencing in Human Cells. *Nat Cell Biol,* 14**,** 266-75.

Bentwich, I., Avniel, A., Karov, Y., Aharonov, R., Gilad, S., Barad, O., Barzilai, A., Einat, P., Einav, U., Meiri, E., Sharon, E., Spector, Y. & Bentwich, Z. 2005. Identification of hundreds of conserved and nonconserved human microRNAs. *Nat Genet,* 37**,** 766-70.

Berks, D., Hoedjes, M., Raat, H., Duvekot, J., Steegers, E. & Habbema, J. 2013. Risk of cardiovascular disease after pre-eclampsia and the effect of lifestyle interventions: a literature-based study. *BJOG,* 120**,** 924-31.

Bernstein, E., Kim, S., Carmell, M., Murchison, E., Alcorn, H., Li, M., Mills, A., Elledge, S., Anderson, K. & Hannon, G. 2003. Dicer is essential for mouse development. *Nat Genet,* 35**,** 215-7.

Betoni, J. S., Derr, K., Pahl, M. C., Rogers, L., Muller, C. L., Packard, R. E., Carey, D. J., Kuivaniemi, H. & Tromp, G. 2013. MicroRNA analysis in placentas from patients with preeclampsia: comparison of new and published results. *Hypertens Pregnancy,* 32**,** 321-39.

Bez, M., Kremen, T., Tawackoli, W., Avalos, P., Sheyn, D., Shapiro, G., Giaconi, J., Ben David, S., Snedeker, J., Gazit, Z., Ferrara, K., Gazit, D. & Pelled, G. 2018. Ultrasound-Mediated Gene Delivery Enhances Tendon Allograft Integration in Mini-Pig Ligament Reconstruction. *Molecular therapy : the journal of the American Society of Gene Therapy,* 26**,** 1746-1755.

Bhatt, K., Wei, Q., Pabla, N., Dong, G., Mi, Q. S., Liang, M., Mei, C. & Dong, Z. 2015. MicroRNA-687 Induced by Hypoxia-Inducible Factor-1 Targets Phosphatase and Tensin Homolog in Renal Ischemia-Reperfusion Injury. *J Am Soc Nephrol,* 26**,** 1588-96.

Biancardi, V. & Sharma, N. 2020. Connecting sympathetic and renin-angiotensin system overdrive in neurogenic hypertension through miRNA-181a. *Hypertens Res,* Online ahead of print.

Bilano, V. L., Ota, E., Ganchimeg, T., Mori, R. & Souza, J. P. 2014. Risk Factors of Pre-Eclampsia/Eclampsia and Its Adverse Outcomes in Low- and Middle-Income Countries: A WHO Secondary Analysis. *PLoS One,* 9**,** e91198.

Biro, O., Fothi, A., Alasztics, B., Nagy, B., Orban, T. I. & Rigo, J., Jr. 2019. Circulating exosomal and Argonaute-bound microRNAs in preeclampsia. *Gene,* 692**,** 138-144.

Biró, O., Alasztics, B., Molvarec, A., Joó, J., Nagy, B. & Rigó, J. 2017. Various levels of circulating exosomal total-miRNA and miR-210 hypoxamiR in different forms of pregnancy hypertension. *Pregnancy Hypertens,* 10**,** 207-212.

Blaese, R., Culver, K., Miller, A., Carter, C., Fleisher, T., Clerici, M., Shearer, G., Chang, L., Chiang, Y., Tolstoshev, P., Greenblatt, J., Rosenberg, S., Klein, H., Berger, M., Mullen, C., Ramsey, W., Muul, L., Morgan, R. & Anderson, W. 1995. T Lymphocyte-Directed Gene Therapy for ADA- SCID: Initial Trial Results After 4 Years. *Science,* 270**,** 475-80.

BMUS 2019. BMUS Guidelines for the safe use of Diagnostic Ultrasound Equipment. The British Medical Ultrasound Society.

Bodner, L., Nosher, J., Gribbin, C., Siegel, R., Beale, S. & Scorza, W. 2006. Balloon-assisted occlusion of the internal iliac arteries in patients with placenta accreta/percreta. *Cardiovasc Intervent Radiol,* 29**,** 354-61.

Boeldt, D. & Bird, I. 2017. Vascular adaptation in pregnancy and endothelial dysfunction in preeclampsia. *J Endocrinol,* 232**,** R27-R44.

Bohnsack, M. T., Czaplinski, K. & Görlich, D. 2004. Exportin 5 is a RanGTP-dependent dsRNA-binding protein that mediates nuclear export of pre-miRNAs. *RNA,* 10**,** 185-91.

Bolon, B. 2008. Whole Mount Enzyme Histochemistry as a Rapid Screen at Necropsy for Expression of Beta-Galactosidase (LacZ)-bearing Transgenes: Considerations for Separating Specific LacZ Activity From Nonspecific (Endogenous) Galactosidase Activity. *Toxicologic pathology,* 36**,** 265-76.

Bramham, K., Al, B., Seed, P., Poston, L., Shennan, A. & Chappell, L. 2011. Adverse maternal and perinatal outcomes in women with previous preeclampsia: a prospective study. *Am J Obstet Gynecol,* 204**,** 512.e1-9.

Brkic, J., Dunk, C., O'brien, J., Fu, G., Nadeem, L., Wang, Y. L., Rosman, D., Salem, M., Shynlova, O., Yougbare, I., Ni, H., Lye, S. J. & Peng, C. 2018. MicroRNA-218-5p Promotes Endovascular Trophoblast Differentiation and Spiral Artery Remodeling. *Mol Ther,* 26**,** 2189-2205.

Brooks, S. A. & Fry, R. C. 2017. Cadmium inhibits placental trophoblast cell migration via miRNA regulation of the transforming growth factor beta (TGF-β) pathway. *Food Chem Toxicol,* 109**,** 721-6.

Brosens, I., Robertson, W. & Dixon, H. 1970. The role of the spiral arteries in the pathogenesis of pre-eclampsia. *J Pathol,* 101**,** vi.

Brosens, I., Robertson, W. & Dixon, H. 1972. The role of the spiral arteries in the pathogenesis of preeclampsia. *Obstet Gynecol Annu,* 1**,** 177-91.

Broughton, J. P., Lovci, M. T., Huang, J. L., Yeo, G. W. & Pasquinelli, A. E. 2016. Pairing Beyond the Seed Supports MicroRNA Targeting Specificity. *Mol Cell,* 64**,** 320-33.

Brown, M. A., Magee, L. A., Kenny, L. C., Karumanchi, S. A., Mccarthy, F. P., Saito, S., Hall, D. R., Warren, C. E., Adoyi, G. & Ishaku, S. 2018. Hypertensive Disorders of Pregnancy: ISSHP Classification, Diagnosis, and Management Recommendations for International Practice. *Hypertension,* 72**,** 24-43.

Browning, R., Mulvana, H., Tang, M., Hajnal, J., Wells, D. & Eckersley, R. 2012. Effect of Albumin and Dextrose Concentration on Ultrasound and Microbubble Mediated Gene Transfection in Vivo. *Ultrasound in medicine & biology,* 38**,** 1067-77.

Browning, R. J., Mulvana, H., Tang, M., Hajnal, J. V., Wells, D. J. & Eckersley, R. J. 2011. Influence of needle gauge on in vivo ultrasound and microbubble-mediated gene transfection. *Ultrasound Med Biol,* 37**,** 1531-7.

Buerli, T., Pellegrino, C., Baer, K., Lardi-Studler, B., Chudotvorova, I., Fritschy, J., Medina, I. & Fuhrer, C. 2007. Efficient transfection of DNA or shRNA vectors into neurons using magnetofection. *Nat Protoc,* 2**,** 3090-101.

Burke, C., Suk, J., Kim, A., Hsiang, Y., Klibanov, A., Hanes, J. & Price, R. 2012. Markedly Enhanced Skeletal Muscle Transfection Achieved by the Ultrasound-Targeted Delivery of Non-Viral Gene Nanocarriers With Microbubbles. *J Control Release,* 162**,** 414-21.

Burton, G., Yung, H., Cindrova-Davies, T. & Charnock-Jones, D. 2009. Placental endoplasmic reticulum stress and oxidative stress in the pathophysiology of unexplained intrauterine growth restriction and early onset preeclampsia. *Placenta,* 30**,** S43-8.

Burton, G. J., Redman, C. W., Roberts, J. M. & Moffett, A. 2019. Pre-eclampsia: pathophysiology and clinical implications. *Bmj,* 366**,** l2381.

Buurma, A., Turner, R., Driessen, J., Mooyaart, A., Schoones, J., Bruijn, J., Bloemenkamp, K., Dekkers, O. & Baelde, H. 2013. Genetic variants in pre-eclampsia: a meta-analysis. *Hum Reprod Update,* 19**,** 289-303.

Cantwell, R., Clutton-Brock, T., Cooper, G., Dawson, A., Drife, J., Garrod, D., Harper, A., Hulbert, D., Lucas, S., Mcclure, J., Millward-Sadler, H., Neilson, J., Nelson-Piercy, C., Norman, J., O'herlihy, C., Oates, M., Shakespeare, J., De Swiet, M., Williamson, C., Beale, V., Knight, M., Lennox, C., Miller, A., Parmar, D., Rogers, J. & Springett, A. 2011. Saving Mothers' Lives: Reviewing maternal deaths to make motherhood safer: 2006-2008. The Eighth Report of the Confidential Enquiries into Maternal Deaths in the United Kingdom. *BJOG,* 118**,** 1-203.

Carr, D. J., Mehta, V., Wallace, J. M. & David, A. L. 2015. VEGF Gene Transfer to the Utero-Placental Circulation of Pregnant Sheep to Enhance Fetal Growth. *Methods Mol Biol,* 1332**,** 197-204.

Carr, D. J., Wallace, J. M., Aitken, R. P., Milne, J. S., Martin, J. F., Zachary, I. C., Peebles, D. M. & David, A. L. 2016. Peri- and Postnatal Effects of Prenatal Adenoviral VEGF Gene Therapy in Growth-Restricted Sheep. *Biol Reprod,* 94**,** 142.

Carr, D. J., Wallace, J. M., Aitken, R. P., Milne, J. S., Mehta, V., Martin, J. F., Zachary, I. C., Peebles, D. M. & David, A. L. 2014. Uteroplacental adenovirus vascular endothelial growth factor gene therapy increases fetal growth velocity in growth-restricted sheep pregnancies. *Hum Gene Ther,* 25**,** 375-84.

Carreras-Badosa, G., Bonmatí, A., Ortega, F., Mercader, J., Guindo-Martínez, M., Torrents, D., Prats-Puig, A., Martinez-Calcerrada, J., De Zegher, F., Ibáñez, L., Fernandez-Real, J., Lopez-Bermejo, A. & Bassols, J. 2017. Dysregulation of Placental miRNA in Maternal Obesity Is Associated With Pre- and Postnatal Growth. *J Clin Endocrinol Metab,* 102**,** 2584-2594.

Carson, A., Mctiernan, C., Lavery, L., Hodnick, A., Grata, M., Leng, X., Wang, J., Chen, X., Modzelewski, R. & Villanueva, F. 2011. Gene therapy of carcinoma using ultrasound-targeted microbubble destruction. *Ultrasound Med Biol,* 37**,** 393-402.

Caughey, A., Stotland, N., Washington, A. & Escobar, G. 2005. Maternal ethnicity, paternal ethnicity, and parental ethnic discordance: predictors of preeclampsia. *Obstet Gynecol,* 106**,** 156-61.

Chakraborty, C., Sharma, A. R., Sharma, G., Doss, C. G. P. & Lee, S. S. 2017. Therapeutic miRNA and siRNA: Moving from Bench to Clinic as Next Generation Medicine. *Mol Ther Nucleic Acids,* 8**,** 132-143.

Chames, M., Livingston, J., Ivester, T., Barton, J. & Sibai, B. 2002. Late postpartum eclampsia: a preventable disease? *Am J Obstet Gynecol,* 186**,** 1174-7.

Chan, S. Y. & Loscalzo, J. 2010. MicroRNA-210: a unique and pleiotropic hypoxamir. *Cell Cycle,* 9**,** 1072-83.

Chan, Y. C., Banerjee, J., Choi, S. Y. & Sen, C. K. 2012. miR-210: the master hypoxamir. *Microcirculation,* 3**,** 215-23.

Chang, S., Chao, A., Peng, H., Chang, Y., Wang, C., Cheng, P., Lee, Y., Chao, A. & Wang, T. 2011. Analyses of placental gene expression in pregnancy-related hypertensive disorders. *Taiwan J Obstet Gynecol,* 50**,** 283-91.

Chappell, L. C., Brocklehurst, P., Green, M. E., Hunter, R., Hardy, P., Juszczak, E., Linsell, L., Chiocchia, V., Greenland, M., Placzek, A., Townend, J., Marlow, N., Sandall, J. & Shennan, A. 2019. Planned early delivery or expectant management for late preterm pre-eclampsia (PHOENIX): a randomised controlled trial. *Lancet,* 394**,** 1181-90.

Charenton, C. & Graille, M. 2018. mRNA decapping: finding the right structures. *Philos Trans R Soc Lond B Biol Sci,* 373**,** 20180164.

Chatterjee, P., Weaver, L. E., Doersch, K. M., Kopriva, S. E., Chiasson, V. L., Allen, S. J., Narayanan, A. M., Young, K. J., Jones, K. A., Kuehl, T. J. & Mitchell, B. M. 2012. Placental Toll-like receptor 3 and Toll-like receptor 7/8 activation contributes to preeclampsia in humans and mice. *PLoS One,* 7**,** e41884.

Cheloufi, S., Dos Santos, C. O., Chong, M. M. & Hannon, G. J. 2010. A dicer-independent miRNA biogenesis pathway that requires Ago catalysis. *Nature,* 465**,** 584-9.

Chelsey, L., Cosgrove, R. & Annitto, J. 1962. Pregnancies in the sisters and daughters of eclamptic women. *Obstet Gynecol,* 20**,** 39-46.

Chen, J., Ma, Q., Wu, H., Zhou, A., Chen, X., Peng, Y., Liu, F. & Cheng, M. 2012a. Enhancing Effect of Ultrasound-Mediated Microbubble Destruction on Gene Delivery Into Rat Kidney via Different Administration Routes. *Asian Pacific journal of tropical medicine,* 5**,** 561-5.

Chen, J., Zhao, L., Wang, D., Xu, Y., Gao, H., Tan, W. & Wang, C. 2019. Contribution of regulatory T cells to immune tolerance and association of microRNA210 and Foxp3 in preeclampsia. *Mol Med Rep,* 19**,** 1150-1158.

Chen, Q., Wang, H., Liu, Y., Song, Y., Lai, L., Han, Q., Cao, X. & Wang, Q. 2012b. Inducible microRNA-223 down-regulation promotes TLR-triggered IL-6 and IL-1beta production in macrophages by targeting STAT3. *PLoS One,* 7**,** e42971.

Chen, S., Bastarrachea, R., Roberts, B., Voruganti, V., Frost, P., Nava-Gonzalez, E., Arriaga-Cazares, H., Chen, J., Huang, P., Defronzo, R., Comuzzie, A. & Grayburn, P. 2014. Successful ß cells islet regeneration in streptozotocin-induced diabetic baboons using ultrasound-targeted microbubble gene therapy with cyclinD2/CDK4/GLP1. *Cell Cycle,* 13**,** 1145-51.

Chen, S., Ding, J., Bekeredjian, R., Yang, B., Shohet, R., Johnston, S., Hohmeier, H., Newgard, C. & Grayburn, P. 2006. Efficient gene delivery to pancreatic islets with ultrasonic microbubble destruction technology. *Proc Natl Acad Sci U S A,* 103**,** 8469-74.

Chen, S., Shohet, R., Bekeredjian, R., Frenkel, P. & Grayburn, P. 2003. Optimization of Ultrasound Parameters for Cardiac Gene Delivery of Adenoviral or Plasmid Deoxyribonucleic Acid by Ultrasound-Targeted Microbubble Destruction. *J Am Coll Cardiol,* 42**,** 301-8.

Chen, S., Zhao, G., Miao, H., Tang, R., Song, Y., Hu, Y., Wang, Z. & Hou, Y. 2015. MicroRNA-494 inhibits the growth and angiogenesis-regulating potential of mesenchymal stem cells. *FEBS Lett,* 589**,** 710-7.

Chen, X., Tong, C., Li, H., Peng, W., Li, R., Luo, X., Ge, H., Ran, Y., Li, Q., Liu, Y., Xiong, X., Bai, Y., Zhang, H., Baker, P. N., Liu, X. & Qi, H. 2018. Dysregulated Expression of RPS4Y1 (Ribosomal Protein S4, Y-Linked 1) Impairs STAT3 (Signal Transducer and Activator of Transcription 3) Signaling to Suppress Trophoblast Cell Migration and Invasion in Preeclampsia. *Hypertension,* 71**,** 481-490.

Chen, Z., Liang, K., Qiu, R. & Luo, L. 2011. Ultrasound- And Liposome Microbubble-Mediated Targeted Gene Transfer to Cardiomyocytes in Vivo Accompanied by Polyethylenimine. *J Ultrasound Med,* 30**,** 1247-58.

Chendrimada, T. P., Gregory, R. I., Kumaraswamy, E., Norman, J., Cooch, N., Nishikura, K. & Shiekhattar, R. 2005. TRBP recruits the Dicer complex to Ago2 for microRNA processing and gene silencing. *Nature,* 436**,** 740-4.

Cheng, W., Liu, T., Jiang, F., Liu, C., Zhao, X., Gao, Y., Wang, H. & Liu, Z. 2011. microRNA-155 regulates angiotensin II type 1 receptor expression in umbilical vein endothelial cells from severely pre-eclamptic pregnant women. *Int J Mol Med,* 27**,** 393-9.

Chesley, L., Annitto, J. & Cosgrove, R. 1968. The familial factor in toxemia of pregnancy. *Obstet Gynecol,* 32**,** 303-11.

Chesley, L. & Cooper, D. 1986. Genetics of hypertension in pregnancy: possible single gene control of pre-eclampsia and eclampsia in the descendants of eclamptic women. *Br J Obstet Gynaecol,* 93**,** Br J Obstet Gynaecol.

Chiofalo, B., Laganà, A. S., Vaiarelli, A., La Rosa, V. L., Rossetti, D., Palmara, V., Valenti, G., Rapisarda, A. M. C., Granese, R., Sapia, F., Triolo, O. & Vitale, S. G. 2017. Do miRNAs Play a Role in Fetal Growth Restriction? A Fresh Look to a Busy Corner. *Biomed Res Int,* 2017**,** 6073167.

Choi, S., Yun, J., Lee, O., Han, H., Yeo, M., Lee, M. & Suh, K. 2013. MicroRNA expression profiles in placenta with severe preeclampsia using a PNA-based microarray. *Placenta,* 34**,** 799-804.

Christiansen, J., French, B., Klibanov, A., Kaul, S. & Lindner, J. 2003. Targeted Tissue Transfection With Ultrasound Destruction of Plasmid-Bearing Cationic Microbubbles. *Ultrasound Med Biol,* 29**,** 1759-67.

Chuang, Y., Chou, A., Wu, P., Chiang, P., Yu, T., Yang, L., Yoshimura, N. & Chancellor, M. 2003. Gene therapy for bladder pain with gene gun particle encoding pro-opiomelanocortin cDNA. *J Urol,* 170**,** 2044-8.

Chung, E. S., Miller, L., Patel, A. N., Anderson, R. D., Mendelsohn, F. O., Traverse, J., Silver, K. H., Shin, J., Ewald, G., Farr, M. J., Anwaruddin, S., Plat, F., Fisher, S. J., Auwerter, A. T., Pastore, J. M., Aras, R. & Penn, M. S. 2015. Changes in ventricular remodelling and clinical status during the year following a single administration of stromal cell-derived factor-1 non-viral gene therapy in chronic ischaemic heart failure patients: the STOP-HF randomized Phase II trial. *Eur Heart J,* 36**,** 2228-38.

Cluver, C., Novikova, N., Koopmans, C. M. & West, H. M. 2017. Planned early delivery versus expectant management for hypertensive disorders from 34 weeks gestation to term. *Cochrane Database Syst Rev,* 2017**,** CD009273.

Cnattingius, S., Reilly, M., Pawitan, Y. & Lichtenstein, P. 2004. Maternal and fetal genetic factors account for most of familial aggregation of preeclampsia: a population-based Swedish cohort study. *Am J Med Genet A,* 130a**,** 365-71.

Cobb, B. S., Hertweck, A., Smith, J., O'connor, E., Graf, D., Cook, T., Smale, S. T., Sakaguchi, S., Livesey, F. J., Fisher, A. G. & Merkenschlager, M. 2006. A role for Dicer in immune regulation. *J Exp Med,* 203**,** 2519-27.

Colleoni, F., Padmanabhan, N., Yung, H. W., Watson, E. D., Cetin, I., Tissot Van Patot, M. C., Burton, G. J. & Murray, A. J. 2013. Suppression of mitochondrial electron transport chain function in the hypoxic human placenta: a role for miRNA-210 and protein synthesis inhibition. *PLoS One,* 8**,** e55194.

Conrad, K. P. 2004. Mechanisms of renal vasodilation and hyperfiltration during pregnancy. *J Soc Gynecol Investig,* 11**,** 438-48.

Cook, J., Bennett, P. R., Kim, S. H., Teoh, T. G., Sykes, L., Kindinger, L. M., Garrett, A., Binkhamis, R., Macintyre, D. A. & Terzidou, V. 2019. First Trimester Circulating MicroRNA Biomarkers Predictive of Subsequent Preterm Delivery and Cervical Shortening. *Sci Rep,* 9**,** 5861.

Cox, B., Kotlyar, M., Evangelou, A. I., Ignatchenko, V., Ignatchenko, A., Whiteley, K., Jurisica, I., Adamson, S. L., Rossant, J. & Kislinger, T. 2009. Comparative systems biology of human and mouse as a tool to guide the modeling of human placental pathology. *Mol Syst Biol,* 5**,** 279.

Cronqvist, T., Tannetta, D., Mörgelin, M., Belting, M., Sargent, I., Familari, M. & Hansson, S. R. 2017. Syncytiotrophoblast derived extracellular vesicles transfer functional placental miRNAs to primary human endothelial cells. *Sci Rep,* 7**,** 4558.

Cross, C. E., Tolba, M. F., Rondelli, C. M., Xu, M. & Abdel-Rahman, S. Z. 2015. Oxidative Stress Alters miRNA and Gene Expression Profiles in Villous First Trimester Trophoblasts. *Biomed Res Int,* 2015**,** 257090.

Cui, H., Seubert, B., Stahl, E., Dietz, H., Reuning, U., Moreno-Leon, L., Ilie, M., Hofman, P., Nagase, H., Mari, B. & Kruger, A. 2015. Tissue inhibitor of metalloproteinases-1 induces a pro-tumourigenic increase of miR-210 in lung adenocarcinoma cells and their exosomes. *Oncogene,* 34**,** 3640-50.

Cui, J., Deng, Q., Zhou, Q., Cao, S., Jiang, N., Wang, Y., Chen, J., Hu, B. & Tan, T. 2017. Enhancement of Angiogenesis by Ultrasound-Targeted Microbubble Destruction Combined with Nuclear Localization Signaling Peptides in Canine Myocardial Infarction. *Biomed Res Int,* 2017**,** 9390565.

D'souza, V., Patil, V., Pisal, H., Randhir, K., Joshi, A., Mehendale, S., Wagh, G., Gupte, S. & Joshi, S. 2014. Levels of brain derived neurotrophic factors across gestation in women with preeclampsia. *Int J Dev Neurosci,* 37**,** 36-40.

Dai, L., Chen, Y., Sun, W. & Liu, S. 2018. Association Between Hypertensive Disorders During Pregnancy and the Subsequent Risk of End-Stage Renal Disease: A Population-Based Follow-Up Study. *J Obstet Gynaecol Can,* 40**,** 1129-1138.

Dai, Y., Qiu, Z., Diao, Z., Shen, L., Xue, P., Sun, H. & Hu, Y. 2012. MicroRNA-155 inhibits proliferation and migration of human extravillous trophoblast derived HTR-8/SVneo cells via down-regulating cyclin D1. *Placenta,* 33**,** 824-9.

Daud, A., Deconti, R., Andrews, S., Urbas, P., Riker, A., Sondak, V., Munster, P., Sullivan, D., Ugen, K., Messina, J. & Heller, R. 2008. Phase I trial of interleukin-

12 plasmid electroporation in patients with metastatic melanoma. *J Clin Oncol,* 26**,** 5896-903.

Daud, A., Takamura, K. T., Diep, T., Heller, R. & Pierce 2015. Long-term overall survival from a phase I trial using intratumoral plasmid interleukin-12 with electroporation in patients with melanoma. *J Transl Med,* 13**,** O3.

David, A. L., Torondel, B., Zachary, I., Wigley, V., Abi-Nader, K., Mehta, V., Buckley, S. M., Cook, T., Boyd, M., Rodeck, C. H., Martin, J. & Peebles, D. M. 2008. Local delivery of VEGF adenovirus to the uterine artery increases vasorelaxation and uterine blood flow in the pregnant sheep. *Gene Ther,* 15**,** 1344-50.

Davis, E., Lazdam, M., Lewandowski, A., Worton, S., Kelly, B., Kenworthy, Y., Adwani, S., Wilkinson, A., Mccormick, K., Sargent, I., Redman, C. & Leeson, P. 2012. Cardiovascular risk factors in children and young adults born to preeclamptic pregnancies: a systematic review. *Pediatrics,* 129**,** e1552-61.

Davisson, R., Hoffmann, D., Butz, G., Aldape, G., Schlager, G., Merrill, D., Sethi, S., Weiss, R. & Bates, J. 2002. Discovery of a spontaneous genetic mouse model of preeclampsia. *Hypertension,* 39**,** 337-42.

De Rie, D., Abugessaisa, I., Alam, T., Arner, E., Arner, P., Ashoor, H., Åström, G., Babina, M., Bertin, N., Burroughs, A. M., Carlisle, A. J., Daub, C. O., Detmar, M., Deviatiiarov, R., Fort, A., Gebhard, C., Goldowitz, D., Guhl, S., Ha, T. J., Harshbarger, J., Hasegawa, A., Hashimoto, K., Herlyn, M., Heutink, P., Hitchens, K. J., Hon, C. C., Huang, E., Ishizu, Y., Kai, C., Kasukawa, T., Klinken, P., Lassmann, T., Lecellier, C. H., Lee, W., Lizio, M., Makeev, V., Mathelier, A., Medvedeva, Y. A., Mejhert, N., Mungall, C. J., Noma, S., Ohshima, M., Okada-Hatakeyama, M., Persson, H., Rizzu, P., Roudnicky, F., Sætrom, P., Sato, H., Severin, J., Shin, J. W., Swoboda, R. K., Tarui, H., Toyoda, H., Vitting-Seerup, K., Winteringham, L., Yamaguchi, Y., Yasuzawa, K., Yoneda, M., Yumoto, N., Zabierowski, S., Zhang, P. G., Wells, C. A., Summers, K. M., Kawaji, H., Sandelin, A., Rehli, M., Hayashizaki, Y., Carninci, P., Forrest, A. R. R. & De Hoon, M. J. L. 2017. An integrated expression atlas of miRNAs and their promoters in human and mouse. *Nat Biotechnol,* 35**,** 872-8.

Deev, R., Plaksa, I., Bozo, I., Mzhavanadze, N., Suchkov, I., Chervyakov, Y., Staroverov, I., Kalinin, R. & Isaev, A. 2018. Results of 5-year follow-up study in patients with peripheral artery disease treated with PL-VEGF165 for intermittent claudication. *Ther Adv Cardiovasc Dis,* 12**,** 237-246.

Delhove, J., Osenk, I., Prichard, I. & Donnelley, M. 2020. Public Acceptability of Gene Therapy and Gene Editing for Human Use: A Systematic Review. *Hum Gene Ther,* 31**,** 20-46.

Delorme-Axford, E., Donker, R. B., Mouillet, J. F., Chu, T., Bayer, A., Ouyang, Y., Wang, T., Stolz, D. B., Sarkar, S. N., Morelli, A. E., Sadovsky, Y. & Coyne, C. B. 2013. Human placental trophoblasts confer viral resistance to recipient cells. *Proc Natl Acad Sci U S A,* 110**,** 12048-53.

Dempsey, J., Williams, M., Luthy, D., Emanuel, I. & Shy, K. 2003. Weight at birth and subsequent risk of preeclampsia as an adult. *Am J Obstet Gynecol,* 189**,** 494-500.

Desforges, M., Rogue, A., Pearson, N., Rossi, C., Olearo, E., Forster, R., Lees, M., Sebire, N. J., Greenwood, S. L., Sibley, C. P., David, A. L. & Brownbill, P. 2018. In Vitro Human Placental Studies to Support Adenovirus-Mediated VEGF-D(DeltaNDeltaC) Maternal Gene Therapy for the Treatment of Severe Early-Onset Fetal Growth Restriction. *Hum Gene Ther Clin Dev,* 29**,** 10-23.

Devor, E., Santillan, D., Scroggins, S., Warrier, A. & Santillan, M. 2020. Trimester-specific plasma exosome microRNA expression profiles in preeclampsia. *J Matern Fetal Neonatal Med,* 33**,** 3116-3124.

Devulapally, R., Lee, T., Barghava-Shah, A., Sekar, T. V., Foygel, K., Bachawal, S. V., Willmann, J. K. & Paulmurugan, R. 2018. Ultrasound-guided delivery of thymidine kinase–nitroreductase dual therapeutic genes by PEGylated-PLGA/PIE nanoparticles for enhanced triple negative breast cancer therapy. *Nanomedicine (Lond),* 13**,** 1051-66.

Di Mascio, D., Saccone, G., Bellussi, F., Vitagliano, A. & Berghella, V. 2020. Type of paternal sperm exposure before pregnancy and the risk of preeclampsia: A systematic review. *Eur J Obstet Gynecol Reprod Biol,* 251**,** 246-253.

Dimcevski, G., Kotopoulis, S., Bjånes, T., Hoem, D., Schjøtt, J., Gjertsen, B., Biermann, M., Molven, A., Sorbye, H., Mccormack, E., Postema, M. & Gilja, O. 2016. A human clinical trial using ultrasound and microbubbles to enhance gemcitabine treatment of inoperable pancreatic cancer. *J Control Release,* 243**,** 172-181.

Ding, J., Huang, F., Wu, G., Han, T., Xu, F., Weng, D., Wu, C., Zhang, X., Yao, Y. & Zhu, X. 2015. MiR-519d-3p Suppresses Invasion and Migration of Trophoblast Cells via Targeting MMP-2. *PLoS One,* 10**,** e0120321.

Dokras, A., Hoffmann, D., Eastvold, J., Kienzle, M., Gruman, L., Kirby, P., Weiss, R. & Davisson, R. 2006. Severe feto-placental abnormalities precede the onset of hypertension and proteinuria in a mouse model of preeclampsia. *Biol Reprod,* 75**,** 899-907.

Donker, R., Mouillet, J., Chu, T., Hubel, C., Stolz, D., Morelli, A. & Sadovsky, Y. 2012. The expression profile of C19MC microRNAs in primary human trophoblast cells and exosomes. *Mol Hum Reprod,* 18**,** 417-24.

Duckitt, K. & Harrington, D. 2005. Risk factors for pre-eclampsia at antenatal booking: systematic review of controlled studies. *BMJ,* 330**,** 565.

Duley, L., Gulmezoglu, A. M., Henderson-Smart, D. J. & Chou, D. 2010. Magnesium sulphate and other anticonvulsants for women with pre-eclampsia. *Cochrane Database Syst Rev,* Cd000025.

Duley, L., Henderson-Smart, D. J., Meher, S. & King, J. F. 2007. Antiplatelet agents for preventing pre-eclampsia and its complications. *Cochrane Database Syst Rev,* Cd004659.

Duley, L., Meher, S. & Jones, L. 2013. Drugs for treatment of very high blood pressure during pregnancy. *Cochrane Database Syst Rev,* 2013**,** CD001449.

Duvshani-Eshet, M., Baruch, L., Kesselman, E., Shimoni, E. & Machluf, M. 2006. Therapeutic ultrasound-mediated DNA to cell and nucleus: bioeffects revealed by confocal and atomic force microscopy. *Gene Ther,* 13**,** 163-72.

D'onofrio, B. M., Class, Q. A., Rickert, M. E., Larsson, H., Långström, N. & Lichtenstein, P. 2013. Preterm birth and mortality and morbidity: A population-based quasi-experimental study. *JAMA Psychiatry,* 70.

Ebadi, S., Henschke, N., Ansari, N., Fallah, E. & Van Tulder, M. 2014. Therapeutic ultrasound for chronic low-back pain. *Cochrane Database Syst Rev,* CD009169.

Efremov, A., Buglaeva, A., Orlov, S., Burov, S., Ignatovich, I., Dizhe, E., Shavva, V. & Perevozchikov, A. 2010. [Transfer of genetic constructions through the transplacental barrier into mice embryos]. *Ontogenez,* 41**,** 94-100.

Ellah, N., Taylor, L., Troja, W., Owens, K., Ayres, N., Pauletti, G. & Jones, H. 2015. Development of Non-Viral, Trophoblast-Specific Gene Delivery for Placental Therapy. *PLoS One,* 10**,** e0140879.

EMA 2008a. Optison: EPAR - product information. www.ema.europa.eu: EMA.

EMA 2008b. SonoVue: EPAR - Product Information. *European public assessment report*. www.ema.europa.eu: European Medicines Agency.

EMA 2009. Luminity:EPAR - product information. www.ema.europa.eu: European Medicines Agency.

England, L. & Zhang, J. 2007. Smoking and risk of preeclampsia: a systematic review. *Front Biosci,* 12**,** 2471-83.

Enquobahrie, D. A., Abetew, D. F., Sorensen, T. K., Willoughby, D., Chidambaram, K. & Williams, M. A. 2011. Placental microRNA expression in pregnancies complicated by preeclampsia. *Am J Obstet Gynecol,* 2**,** e12-21.

ESGT 2003. French Gene Therapy Group Reports on the Adverse Event in a Clinical Trial of Gene Therapy for X-linked Severe Combined Immune Deficiency (X-SCID). Position Statement From the European Society of Gene Therapy. *J Gene Med,* 5**,** 82-4.

Eskandari, F., Rezaei, M., Mohammadpour-Gharehbagh, A., Teimoori, B., Yaghmaei, M., Narooei-Nejad, M. & Salimi, S. 2019. The association of pri-miRNA- 26a1 rs7372209 polymorphism and Preeclampsia susceptibility. *Clin Exp Hypertens,* 41**,** 268-273.

Eskandari, F., Teimoori, B., Rezaei, M., Mohammadpour-Gharehbagh, A., Narooei-Nejad, M., Mehrabani, M. & Salimi, S. 2018. Relationships between Dicer 1 polymorphism and expression levels in the etiopathogenesis of preeclampsia. *J Cell Biochem,* 119**,** 5563-5570.

Esteve-Valverde, E., Ferrer-Oliveras, R., Gil-Aliberas, N., Baraldès-Farré, A., Llurba, E. & Alijotas-Reig, J. 2018. Pravastatin for Preventing and Treating Preeclampsia: A Systematic Review. *Obstet Gynecol Surv,* 73**,** 40-55.

Fallen, S., Baxter, D., Wu, X., Kim, T., Shynlova, O., Lee, M. Y., Scherler, K., Lye, S., Hood, L. & Wang, K. 2018. Extracellular vesicle RNAs reflect placenta dysfunction and are a biomarker source for preterm labour. *J Cell Mol Med,* 22**,** 2760-73.

Fan, G. L., Wei, H. & Wu, R. 2016. Expressions of STAT4 and STAT6 in placenta and serum of patients with preeclampsia and the significance. *Maternal & Child Health Care China,* 6**,** 1264-1267.

Fan, Z., Chen, D. & Deng, C. 2013. Improving ultrasound gene transfection efficiency by controlling ultrasound excitation of microbubbles. *J Control Release,* 170**,** 401-13.

Fan, Z., Liu, H., Mayer, M. & Deng, C. 2012. Spatiotemporally controlled single cell sonoporation. *Proc Natl Acad Sci U S A,* 109**,** 16486-91.

Farrokhnia, F., Aplin, J. D., Westwood, M. & Forbes, K. 2014. MicroRNA regulation of mitogenic signaling networks in the human placenta. *J Biol Chem,* 289**,** 30404-16.

Fasanaro, P., D'alessandra, Y., Di Stefano, V., Melchionna, R., Romani, S., Pompilio, G., Capogrossi, M. C. & Martelli, F. 2008. MicroRNA-210 modulates endothelial cell response to hypoxia and inhibits the receptor tyrosine kinase ligand Ephrin-A3. *J Biol Chem,* 23**,** 15878-83.

FDA 2019. Marketing Clearance of Diagnostic Ultrasound Systems and Transducers | FDA. *In:* Administration, U. S. F. D. (ed.). www.FDA.gov: Center for Devices and Radiological Health.

FDA 2020. FDA Continues Strong Support of Innovation in Development of Gene Therapy Products. *In:* Administration, U. S. F. D. (ed.) *Guidances issued today provide regulatory clarity for product developers.* www.FDA.gov: U.S. Food & Drug Administration.

Fechheimer, M., Boylan, J. F., Parker, S., Sisken, J. E., Patel, G. L. & Zimmer, S. G. 1987. Transfection of mammalian cells with plasmid DNA by scrape loading and sonication loading. *Proc Natl Acad Sci U S A,* 84, 8463-7.

Fehniger, T. A., Wylie, T., Germino, E., Leong, J. W., Magrini, V. J., Koul, S., Keppel, C. R., Schneider, S. E., Koboldt, D. C., Sullivan, R. P., Heinz, M. E., Crosby, S. D., Nagarajan, R., Ramsingh, G., Link, D. C., Ley, T. J. & Mardis, E. R. 2010. Next-generation sequencing identifies the natural killer cell microRNA transcriptome. *Genome Res,* 20, 1590-604.

Feinstein, S., Cheirif, J., Ten Cate, F., Silverman, P., Heidenreich, P., Dick, C., Desir, R., Armstrong, W., Quinones, M. & Shah, P. 1990. Safety and efficacy of a new transpulmonary ultrasound contrast agent: initial multicenter clinical results. *J Am Coll Cardiol,* 16, 316-24.

Feinstein, S., Ten Cate, F., Zwehl, W., Ong, K., Maurer, G., Tei, C., Shah, P., Meerbaum, S. & Corday, E. 1984. Two-dimensional contrast echocardiography. I. In vitro development and quantitative analysis of echo contrast agents. *J Am Coll Cardiol,* 3, 14-20.

Fernandes, A. & Chari, D. 2016. Part I: Minicircle vector technology limits DNA size restrictions on ex vivo gene delivery using nanoparticle vectors: Overcoming a translational barrier in neural stem cell therapy. *J Control Release,* 238, 289-299.

Ferreira, L., Gomes, C., Araújo, A., Bezerra, P., Duggal, P. & Jeronimo, S. 2015. Association Between ACVR2A and Early-Onset Preeclampsia: Replication Study in a Northeastern Brazilian Population. *Placenta,* 36, 186-90.

Forbes, K., Farrokhnia, F., Aplin, J. D. & Westwood, M. 2012. Dicer-dependent miRNAs provide an endogenous restraint on cytotrophoblast proliferation. *Placenta,* 33, 581-5.

Foster, F., Zhang, M., Zhou, Y., Liu, G., Mehi, J., Cherin, E., Harasiewicz, K., Starkoski, B., Zan, L., Knapik, D. & Adamson, S. 2002. A new ultrasound instrument for in vivo microimaging of mice. *Ultrasound Med Biol,* 28, 1165-72.

Frazier, S., Mcbride, M. W., Mulvana, H. & Graham, D. 2020. From animal models to patients: the role of placental microRNAs, miR-210, miR-126, and miR-148a/152 in preeclampsia. *Clin Sci (Lond),* 134, 1001-25.

Friedman, R. C., Farh, K. K., Burge, C. B. & Bartel, D. P. 2009. Most mammalian mRNAs are conserved targets of microRNAs. *Genome Res,* 19, 92-105.

Friedmann, T. & Roblin, R. 1972. Gene Therapy for Human Genetic Disease? *Science,* 175, 949-55.

Fujita, K., Tatsumi, K., Kondoh, E., Chigusa, Y., Mogami, H., Fujii, T., Yura, S., Kakui, K. & Konishi, I. 2011. Differential expression and the anti-apoptotic effect of human placental neurotrophins and their receptors. *Placenta,* 32, 737-44.

Fuller, A., Carvalho, B., Brummel, C. & Riley, E. 2006. Epidural anesthesia for elective cesarean delivery with intraoperative arterial occlusion balloon catheter placement. *Anesth Analg,* 102, 585-7.

Furukawa, S., Kuroda, Y. & Sugiyama, A. 2014. A comparison of the histological structure of the placenta in experimental animals. *J Toxicol Pathol,* 27**,** 11-8.

Fushima, T., Sekimoto, A., Minato, T., Ito, T., Oe, Y., Kisu, K., Sato, E., Funamoto, K., Hayase, T., Kimura, Y., Ito, S., Sato, H. & Takahashi, N. 2016. Reduced Uterine Perfusion Pressure (RUPP) Model of Preeclampsia in Mice. *PLoS One,* 11**,** e0155426.

Gaensler, K., Tu, G., Bruch, S., Liggitt, D., Lipshutz, G., Metkus, A., Harrison, M., Heath, T. & Debs, R. 1999. Fetal gene transfer by transuterine injection of cationic liposome-DNA complexes. *Nat Biotechnol,* 17**,** 1188-92.

Galaviz-Hernandez, C., Arámbula-Meraz, E., Medina-Bastidas, D., Sosa-Macías, M., Lazalde-Ramos, B., Ortega-Chávez, M. & Hernandez-García, L. 2016. The paternal polymorphism rs5370 in the EDN1 gene decreases the risk of preeclampsia. *Pregnancy Hypertens,* 6**,** 327-332.

Gallo, A., Tandon, M., Alevizos, I. & Illei, G. G. 2012. The Majority of MicroRNAs Detectable in Serum and Saliva Is Concentrated in Exosomes. *PLoS One,* 7.

Gam, A. & Johannsen, F. 1995. Ultrasound therapy in musculoskeletal disorders: a meta-analysis. *Pain,* 63**,** 85-91.

Gan, L., Liu, Z., Wei, M., Chen, Y., Yang, X., Chen, L. & Xiao, X. 2017. MiR-210 and miR-155 as potential diagnostic markers for pre-eclampsia pregnancies. *Medicine (Baltimore),* 28**,** e7515.

Gannoun, B., Al-Madhi, S., Zitouni, H., Raguema, N., Meddeb, S., Hachena, F., Mahjoub, T. & Almawi, W. 2017. Vascular Endothelial Growth Factor Single Nucleotide Polymorphisms and Haplotypes in Pre-Eclampsia: A Case-Control Study. *Cytokine,* 97**,** 175-180.

Gao, W. L., Liu, M., Yang, Y., Yang, H., Liao, Q., Bai, Y., Li, Y. X., Li, D., Peng, C. & Wang, Y. L. 2012. The imprinted H19 gene regulates human placental trophoblast cell proliferation via encoding miR-675 that targets Nodal Modulator 1 (NOMO1). *RNA Biol,* 9**,** 1002-10.

Gao, Y., She, R., Wang, Q., Li, Y. & Zhang, H. 2018. Up-regulation of miR-299 suppressed the invasion and migration of HTR-8/SVneo trophoblast cells partly via targeting HDAC2 in pre-eclampsia. *Biomed Pharmacother,* 97**,** 1222-1228.

Geis, N., Mayer, C., Kroll, R., Hardt, S., Katus, H. & Bekeredjian, R. 2009. Spatial Distribution of Ultrasound Targeted Microbubble Destruction Increases Cardiac Transgene Expression but Not Capillary Permeability. *Ultrasound in medicine & biology,* 35**,** 1119-26.

Geldenhuys, J., Rossouw, T. M., Lombaard, H. A., Ehlers, M. M. & Kock, M. M. 2018. Disruption in the Regulation of Immune Responses in the Placental Subtype of Preeclampsia. *Front Immunol,* 9**,** 1659.

Georgiades, P., Ferguson-Smith, A. & Burton, G. 2002. Comparative developmental anatomy of the murine and human definitive placentae. *Placenta,* 23**,** 3-19.

Ghossein-Doha, C., Van Neer, J., Wissink, B., Breetveld, N., De Windt, L., Van Dijk, A., Van Der Vlugt, M., Janssen, M., Heidema, W., Scholten, R. & Spaanderman, M. 2017. Pre-eclampsia: an important risk factor for asymptomatic heart failure. *Ultrasound Obstet Gynecol,* 49**,** 143-149.

Giannakou, K., Evangelou, E. & Papatheodorou, S. 2018. Genetic and non-genetic risk factors for pre-eclampsia: umbrella review of systematic reviews and meta-analyses of observational studies. *Ultrasound Obstet Gynecol,* 51**,** 720-730.

Giannubilo, S., Dell'uomo, B. & Tranquilli, A. 2006. Perinatal outcomes, blood pressure patterns and risk assessment of superimposed preeclampsia in mild chronic hypertensive pregnancy. *Eur J Obstet Gynecol Reprod Biol,* 126**,** 63-7.

Gilani, S. I., Weissgerber, T. L., Garovic, V. D. & Jayachandran, M. 2016. Preeclampsia and Extracellular Vesicles. *Curr Hypertens Rep,* 18**,** 68.

Ginn, S., Amaya, A., Alexander, I., Edelstein, M. & Abedi, M. 2018. Gene Therapy Clinical Trials Worldwide to 2017: An Update. *J Gene Med,* 20**,** e3015.

Giordano, J. C., Parpinelli, M. A., Cecatti, J. G., Haddad, S. M., Costa, M. L., Surita, F. G., Pinto E Silva, J. L. & Sousa, M. H. 2014. The Burden of Eclampsia: Results from a Multicenter Study on Surveillance of Severe Maternal Morbidity in Brazil. *PLoS One,* 9**,** e97401.

Git, A., Dvinge, H., Salmon-Divon, M., Osborne, M., Kutter, C., Hadfield, J., Bertone, P. & Caldas, C. 2010. Systematic comparison of microarray profiling, real-time PCR, and next-generation sequencing technologies for measuring differential microRNA expression. *Rna,* 16**,** 991-1006.

Goldenberg, R., Mcclure, E., Macguire, E., Kamath, B. & Jobe, A. 2011. Lessons for low-income regions following the reduction in hypertension-related maternal mortality in high-income countries. *Int J Gynaecol Obstet,* 113**,** 91-5.

Gormley, M., Ona, K., Kapidzic, M., Garrido-Gomez, T., Zdravkovic, T. & Fisher, S. J. 2017. Preeclampsia: novel insights from global RNA profiling of trophoblast subpopulations. *Am J Obstet Gynecol,* 217**,** 200.e1-200.e17.

Gramiak, R. & Shah, P. 1968. Echocardiography of the aortic root. *Invest Radiol,* 3**,** 356-66.

Greaney, S., Algazi, A., Tsai, K., Takamura, K., Chen, L., Twitty, C., Zhang, L., Paciorek, A., Pierce, R., Le, M., Daud, A. & Fong, L. 2020. Intratumoral Plasmid IL12 Electroporation Therapy in Patients with Advanced Melanoma Induces Systemic and Intratumoral T-cell Responses. *Cancer Immunol Res,* 8**,** 246-254.

Greenleaf, W., Bolander, M., Sarkar, G., Goldring, M. & Greenleaf, J. 1998. Artificial Cavitation Nuclei Significantly Enhance Acoustically Induced Cell Transfection. *Ultrasound Med Biol,* 24**,** 587-95.

Grimes, S., Bombay, K., Lanes, A., Walker, M. & Corsi, D. J. 2019. Potential biological therapies for severe preeclampsia: a systematic review and meta-analysis. *BMC Pregnancy Childbirth,* 19**,** 163.

Grimson, A., Farh, K. K. H., Johnston, W. K., Garrett-Engele, P., Lim, L. P. & Bartel, D. P. 2007. MicroRNA Targeting Specificity in Mammals: Determinants Beyond Seed Pairing. *Mol Cell,* 27**,** 91-105.

Grisch-Chan, H. M., Schlegel, A., Scherer, T., Allegri, G., Heidelberger, R., Tsikrika, P., Schmeer, M., Schleef, M., Harding, C. O., Häberle, J. & Thöny, B. 2017. Low-Dose Gene Therapy for Murine PKU Using Episomal Naked DNA Vectors Expressing PAH from Its Endogenous Liver Promoter. *Mol Ther Nucleic Acids,* 7**,** 339-49.

Grossman, P., Mendelsohn, F., Henry, T., Hermiller, J., Litt, M., Saucedo, J., Weiss, R., Kandzari, D., Kleiman, N., Anderson, R., Gottlieb, D., Karlsberg, R., Snell, J. & Rocha-Singh, K. 2007. Results from a phase II multicenter, double-blind placebo-controlled study of Del-1 (VLTS-589) for intermittent claudication in subjects with peripheral arterial disease. *Am Heart J,* 153**,** 874-80.

Gu, Y., Bian, Y., Xu, X., Wang, X., Zuo, C., Meng, J., Li, H., Zhao, S., Ning, Y., Cao, Y., Huang, T., Yan, J. & Chen, Z. 2016. Downregulation of miR-29a/b/c in

placenta accreta inhibits apoptosis of implantation site intermediate trophoblast cells by targeting MCL1. *Placenta,* 48**,** 13-19.

Gu, Y., Cui, S., Wang, Q., Liu, C., Jin, B., Guo, W., Liu, C., Chu, T., Shu, C., Zhang, F., Han, C. & Liu, Y. 2019. A Randomized, Double-Blind, Placebo-Controlled Phase II Study of Hepatocyte Growth Factor in the Treatment of Critical Limb Ischemia. *Mol Ther,* 27**,** 2158-2165.

Gu, Y., Sun, J., Groome, L. J. & Wang, Y. 2013. Differential miRNA expression profiles between the first and third trimester human placentas. *Am J Physiol Endocrinol Metab,* 304**,** E836-43.

Guha, T., Pichavant, C. & Calos, M. 2019. Plasmid-Mediated Gene Therapy in Mouse Models of Limb Girdle Muscular Dystrophy. *Mol Ther Methods Clin Dev,* 15**,** 294-304.

Guil, S. & Cáceres, J. 2007. The multifunctional RNA-binding protein hnRNP A1 is required for processing of miR-18a. *Nat Struct Mol Bio,* 14**,** 591-6.

Gunel, T., Hosseini, M., Gumusoglu, E., Kisakesen, H., Benian, A. & Aydinli, K. 2017. Expression profiling of maternal plasma and placenta microRNAs in preeclamptic pregnancies by microarray technology. *Placenta,* 52**,** 77-85.

Gunel, T., Kamali, N., Hosseini, M. K., Gumusoglu, E., Benian, A. & Aydinli, K. 2020. Regulatory effect of miR-195 in the placental dysfunction of preeclampsia. *J Matern Fetal Neonatal Med,* 33**,** 901-908.

Guo, D., Jiang, H., Chen, Y., Yang, J., Fu, Z., Li, J., Han, X., Wu, X., Xia, Y., Wang, X., Chen, L., Tang, Q. & Wu, W. 2018. Elevated microRNA-141-3p in placenta of non-diabetic macrosomia regulate trophoblast proliferation. *EBioMedicine,* 38**,** 154-61.

Guo, D., Li, X., Sun, P., Wang, Z., Chen, X., Chen, Q., Fan, L., Zhang, B., Shao, L. & Li, X. 2004. Ultrasound/microbubble enhances foreign gene expression in ECV304 cells and murine myocardium. *Acta Biochim Biophys Sin (Shanghai),* 36**,** 824-31.

Guo, H., Tague, L., Ray, R. & Tigyi, G. 2010. A two-step approach to qPCR experimental design and software for data analysis. *BMC Bioinformatics,* 11**,** 18.

Guo, L., Yang, Q., Lu, J., Li, H., Ge, Q., Gu, W., Bai, Y. & Lu, Z. 2011. A comprehensive survey of miRNA repertoire and 3' addition events in the placentas of patients with pre-eclampsia from high-throughput sequencing. *PLoS One,* 6**,** e21072.

Gysler, S. M., Mulla, M. J., Guerra, M., Brosens, J. J., Salmon, J. E., Chamley, L. W. & Abrahams, V. M. 2016. Antiphospholipid antibody-induced miR-146a-3p drives trophoblast interleukin-8 secretion through activation of Toll-like receptor 8. *Mol Hum Reprod,* 22**,** 465-74.

Gómez, O., Figueras, F., Fernández, S., Bennasar, M., Martínez, J., Puerto, B. & Gratacós, E. 2008. Reference ranges for uterine artery mean pulsatility index at 11-41 weeks of gestation. *Ultrasound Obstet Gynecol,* 32**,** 128-32.

Hacein-Bey-Abina, S., Garrigue, A., Wang, G., Soulier, J., Lim, A., Morillon, E., Clappier, E., Caccavelli, L., Delabesse, E., Beldjord, K., Asnafi, V., Macintyre, E., Dal Cortivo, L., Radford, I., Brousse, N., Sigaux, F., Moshous, D., Hauer, J., Borkhardt, A., Belohradsky, B., Wintergerst, U., Velez, M., Leiva, L., Sorensen, R., Wulffraat, N., Blanche, S., Bushman, F., Fischer, A. & Cavazzana-Calvo, M. 2008. Insertional Oncogenesis in 4 Patients After Retrovirus-Mediated Gene Therapy of SCID-X1. *J Clin Invest,* 118**,** 3132-42.

Hacein-Bey-Abina, S., Le, D. F., Carlier, F., Bouneaud, C., Hue, C., De Villartay, J., Thrasher, A., Wulffraat, N., Sorensen, R., Dupuis-Girod, S., Fischer, A., Davies, E., Kuis, W., Leiva, L. & Cavazzana-Calvo, M. 2002. Sustained Correction of X-linked Severe Combined Immunodeficiency by Ex Vivo Gene Therapy. *N Engl J Med,* 346**,** 1185-93.

Hacein-Bey-Abina, S., Von Kalle, C., Schmidt, M., Mccormack, M., Wulffraat, N., Leboulch, P., Lim, A., Osborne, C., Pawliuk, R., Morillon, E., Sorensen, R., Forster, A., Fraser, P., Cohen, J., De Saint Basile, G., Alexander, I., Wintergerst, U., Frebourg, T., Aurias, A., Stoppa-Lyonnet, D., Romana, S., Radford-Weiss, I., Gross, F., Valensi, F., Delabesse, E., Macintyre, E., Sigaux, F., Soulier, J., Leiva, L., Wissler, M., Prinz, C., Rabbitts, T., Le Deist, F., Fischer, A. & Cavazzana-Calvo, M. 2003. LMO2-associated Clonal T Cell Proliferation in Two Patients After Gene Therapy for SCID-X1. *Science,* 302**,** 415-9.

Hamid, H., Abdalla, S., Sidig, M., Adam, I. & Hamdan, H. 2020. Association of VEGFA and IL1β Gene Polymorphisms With Preeclampsia in Sudanese Women. *Molecular genetics & genomic medicine,* 8**,** e1119.

Han, J., Lee, Y., Yeom, K. H., Kim, Y. K., Jin, H. & Kim, V. N. 2004. The Drosha-DGCR8 complex in primary microRNA processing. *Genes Dev,* 18**,** 3016-27.

Harati-Sadegh, M., Kohan, L., Teimoori, B., Mehrabani, M. & Salimi, S. 2019. Analysis of polymorphisms, promoter methylation, and mRNA expression profile of maternal and placental P53 and P21 genes in preeclamptic and normotensive pregnant women. *J Biomed Sci,* 26**,** 92.

Harati-Sadegh, M., Kohan, L., Teimoori, B. & Salimi, S. 2018. The long non-coding RNA H19 rs217727 polymorphism is associated with PE susceptibility. *Journal of cellular biochemistryJ Cell Biochem,* 119**,** 5473-5480.

Harlap, S., Paltiel, O., Deutsch, L., Knaanie, A., Masalha, S., Tiram, E., Caplan, L., Malaspina, D. & Friedlander, Y. 2002. Paternal age and preeclampsia. *Epidemiology,* 13**,** 660-7.

Hartikainen, J., Hassinen, I., Hedman, A., Kivela, A., Saraste, A., Knuuti, J., Husso, M., Mussalo, H., Hedman, M., Rissanen, T. T., Toivanen, P., Heikura, T., Witztum, J. L., Tsimikas, S. & Yla-Herttuala, S. 2017. Adenoviral intramyocardial VEGF-DDeltaNDeltaC gene transfer increases myocardial perfusion reserve in refractory angina patients: a phase I/IIa study with 1-year follow-up. *Eur Heart J,* 38**,** 2547-2555.

Hausser, J., Syed, A. P., Bilen, B. & Zavolan, M. 2013. Analysis of CDS-located miRNA target sites suggests that they can effectively inhibit translation. *Genome Res,* 23**,** 604-15.

He, C., Shi, D., Wu, W., Ding, Y., Feng, D., Lu, B., Chen, H., Yao, J., Shen, Q., Lu, D. & Xue, J. 2004. Insulin expression in livers of diabetic mice mediated by hydrodynamics-based administration. *World J Gastroenterol,* 10**,** 567-72.

Hedman, M., Hartikainen, J., Syvanne, M., Stjernvall, J., Hedman, A., Kivela, A., Vanninen, E., Mussalo, H., Kauppila, E., Simula, S., Narvanen, O., Rantala, A., Peuhkurinen, K., Nieminen, M. S., Laakso, M. & Yla-Herttuala, S. 2003. Safety and feasibility of catheter-based local intracoronary vascular endothelial growth factor gene transfer in the prevention of postangioplasty and in-stent restenosis and in the treatment of chronic myocardial ischemia: phase II results of the Kuopio Angiogenesis Trial (KAT). *Circulation,* 107**,** 2677-83.

Hedman, M., Muona, K., Hedman, A., Kivelä, A., Syvänne, M., Eränen, J., Rantala, A., Stjernvall, J., Nieminen, M., Hartikainen, J. & Ylä-Herttuala, S.

2009. Eight-year safety follow-up of coronary artery disease patients after local intracoronary VEGF gene transfer. *Gene Ther,* 16**,** 629-34.

Helfield, B., Chen, X., Watkins, S. & Villanueva, F. 2016. Biophysical insight into mechanisms of sonoporation. *Proc Natl Acad Sci U S A,* 113**,** 9983-8.

Hempstead, B. L. 2015. Brain-Derived Neurotrophic Factor: Three Ligands, Many Actions. *Trans Am Clin Climatol Assoc,* 126**,** 9-19.

Henderson, J., Whitlock, E., O'conner, E., Senger, C., Thompson, J. & Rowland, M. 2014. Low-Dose Aspirin for the Prevention of Morbidity and Mortality From Preeclampsia: A Systematic Evidence Review for the U.S. Preventive Services Task Force [Internet]. *In:* Syntheses, U. S. P. S. T. F. E. (ed.). Rockville (MD): Agency for Healthcare Research and Quality (US).

Hiby, S., Walker, J., O'shaughnessy, K., Redman, C., Carrington, M., Trowsdale, J. & Moffett, A. 2004. Combinations of maternal KIR and fetal HLA-C genes influence the risk of preeclampsia and reproductive success. *J Exp Med,* 200**,** 957-65.

Higashijima, A., Miura, K., Mishima, H., Kinoshita, A., Jo, O., Abe, S., Hasegawa, Y., Miura, S., Yamasaki, K., Yoshida, A., Yoshiura, K. & Masuzaki, H. 2013. Characterization of placenta-specific microRNAs in fetal growth restriction pregnancy. *Prenat Diagn,* 33**,** 214-22.

Hill, L., Hilliard, D., York, T., Srinivas, S., Kusanovic, J., Gomez, R., Elovitz, M., Romero, R. & Strauss, J. 2011a. Fetal ERAP2 variation is associated with preeclampsia in African Americans in a case-control study. *BMC Med Genet,* 12**,** 64.

Hill, L., York, T., Kusanovic, J., Gomez, R., Eaves, L., Romero, R. & Strauss, J. 2011b. Epistasis between COMT and MTHFR in maternal-fetal dyads increases risk for preeclampsia. *PLoS One,* 6**,** e16681.

Holder, B., Tower, C., Jones, C., Aplin, J. & Abrahams, V. 2012. Heightened pro-inflammatory effect of preeclamptic placental microvesicles on peripheral blood immune cells in humans. *Biol Reprod,* 86**,** 103.

Holles, N. & Conner, E. 2020. Statement from Audentes – June 23rd, 2020. *In:* Therapeutics, A. (ed.). Audentes Therapeutics.

Holm, D., Dagnaes-Hansen, F., Simonsen, H., Gregersen, N., Bolund, L., Jensen, T. & Corydon, T. 2003. Expression of short-chain acyl-CoA dehydrogenase (SCAD) proteins in the liver of SCAD deficient mice after hydrodynamic gene transfer. *Mol Genet Metab,* 78**,** 250-8.

Holzbach, T., Vlaskou, D., Neshkova, I., Konerding, M., Wörtler, K., Mykhaylyk, O., Gänsbacher, B., Machens, H., Plank, C. & Giunta, R. 2010. Non-viral VEGF(165) gene therapy--magnetofection of acoustically active magnetic lipospheres ('magnetobubbles') increases tissue survival in an oversized skin flap model. *J Cell Mol Med,* 14**,** 587-99.

Hong, D., Kang, Y., Borad, M., Sachdev, J., Ejadi, S., Lim, H., Brenner, A., Park, K., Lee, J., Kim, T., Shin, S., Becerra, C., Falchook, G., Stoudemire, J., Martin, D., Kelnar, K., Peltier, H., Bonato, V., Bader, A., Smith, S., Kim, S., O'neill, V. & Beg, M. 2020. Phase 1 study of MRX34, a liposomal miR-34a mimic, in patients with advanced solid tumours. *Br J Cancer,* 122**,** 1630-1637.

Hong, F., Li, Y. & Xu, Y. 2014. Decreased placental miR-126 expression and vascular endothelial growth factor levels in patients with pre-eclampsia. *J Int Med Res,* 6**,** 1243-51.

Hopkins, S. K. C. C. C. A. J. 2016. *Therapeutic Vaccination for Patients With HPV16+ Cervical Intraepithelial Neoplasia (CIN2/3)* [Online]. www.ClinicalTrials..gov: National Institutes of Health. Available: https://clinicaltrials.gov/ct2/show/NCT00988559.

Howard, C., Forsberg, F., Minimo, C., Liu, J., Merton, D. & Claudio, P. 2006. Ultrasound guided site specific gene delivery system using adenoviral vectors and commercial ultrasound contrast agents. *J Cell Physiol,* 209**,** 413-21.

Hromadnikova, I., Dvorakova, L., Kotlabova, K. & Krofta, L. 2019. The Prediction of Gestational Hypertension, Preeclampsia and Fetal Growth Restriction via the First Trimester Screening of Plasma Exosomal C19MC microRNAs. *Int J Mol Sci,* 20**,** 2972.

Hromadnikova, I., Kotlabova, K., Hympanova, L. & Krofta, L. 2015a. Cardiovascular and Cerebrovascular Disease Associated microRNAs Are Dysregulated in Placental Tissues Affected with Gestational Hypertension, Preeclampsia and Intrauterine Growth Restriction. *PLoS One,* 10**,** e0138383.

Hromadnikova, I., Kotlabova, K., Ivankova, K. & Krofta, L. 2017. Expression profile of C19MC microRNAs in placental tissue of patients with preterm prelabor rupture of membranes and spontaneous preterm birth. *Mol Med Rep,* 16**,** 3849-3862.

Hromadnikova, I., Kotlabova, K., Ondrackova, M., Pirkova, P., Kestlerova, A., Novotna, V., Hympanova, L. & Krofta, L. 2015b. Expression profile of C19MC microRNAs in placental tissue in pregnancy-related complications. *DNA Cell Biol,* 34**,** 437-57.

Hu, E., Ding, L., Miao, H., Liu, F., Liu, D., Dou, H. & Hou, Y. 2015. MiR-30a attenuates immunosuppressive functions of IL-1beta-elicited mesenchymal stem cells via targeting TAB3. *FEBS Lett,* 589**,** 3899-907.

Hu, L., Han, J., Zheng, F., Ma, H., Chen, J., Jiang, Y. & Jiang, H. 2014. Early Second-Trimester Serum MicroRNAs as Potential Biomarker for Nondiabetic Macrosomia. *Biomed Res Int,* 2014**,** 394125.

Hu, X. Q., Dasgupta, C., Xiao, D., Huang, X., Yang, S. & Zhang, L. 2017. MicroRNA-210 Targets Ten-Eleven Translocation Methylcytosine Dioxygenase 1 and Suppresses Pregnancy-Mediated Adaptation of Large Conductance Ca2+-Activated K+ Channel Expression and Function in Ovine Uterine Arteries. *Hypertension***,** Epub.

Hu, X. Q. & Zhang, L. 2019. MicroRNAs in Uteroplacental Vascular Dysfunction. *Cells,* 8**,** 1344.

Hu, Y., Li, P., Hao, S., Liu, L., Zhao, J. & Hou, Y. 2009. Differential expression of microRNAs in the placentae of Chinese patients with severe pre-eclampsia. *Clin Chem Lab Med,* 8**,** 923-9.

Hua, X., Zhu, L., Li, R., Zhong, H., Xue, Y. & Chen, Z. 2009. Effects of diagnostic contrast-enhanced ultrasound on permeability of placental barrier: a primary study. *Placenta,* 30**,** 780-4.

Huang, L., Li, L., Chen, X., Zhang, H. & Shi, Z. 2016. MiR-103a targeting Piezo1 is involved in acute myocardial infarction through regulating endothelium function. *Cardiol J,* 23**,** 556-562.

Huang, Q., Ding, J., Gong, M., Wei, M., Zhao, Q. & Yang, J. 2019. Effect of miR-30e regulating NK cell activities on immune tolerance of maternal-fetal interface by targeting PRF1. *Biomed Pharmacother,* 109**,** 1478-1487.

Huang, X., Anderle, P., Hostettler, L., Baumann, M. U., Surbek, D. V., Ontsouka, E. C. & Albrecht, C. 2018. Identification of placental nutrient transporters associated with intrauterine growth restriction and pre-eclampsia. *BMC Genomics,* 19**,** 173.

Huppertz, B. 2008. Placental origins of preeclampsia: challenging the current hypothesis. *Hypertension,* 51**,** 970-5.

Hylenius, S., Andersen, A., Melbye, M. & Hviid, T. 2004. Association between HLA-G genotype and risk of pre-eclampsia: a case-control study using family triads. *Mol Hum Reprod,* 10**,** 237-46.

Hüttinger, C., Hirschberger, J., Jahnke, A., Köstlin, R., Brill, T., Plank, C., Küchenhoff, H., Krieger, S. & Schillinger, U. 2008. Neoadjuvant gene delivery of feline granulocyte-macrophage colony-stimulating factor using magnetofection for the treatment of feline fibrosarcomas: a phase I trial. *J Gene Med,* 10**,** 655-67.

Inoue, K., Hirose, M., Inoue, H., Hatanaka, Y., Honda, A., Hasegawa, A., Mochida, K. & Ogura, A. 2017. The Rodent-Specific MicroRNA Cluster within the Sfmbt2 Gene Is Imprinted and Essential for Placental Development. *Cell Rep,* 19**,** 949-956.

Inoue, K., Ogonuki, N., Kamimura, S., Inoue, H., Matoba, S., Hirose, M., Honda, A., Miura, K., Hada, M., Hasegawa, A., Watanabe, N., Dodo, Y., Mochida, K. & Ogura, A. 2020. Loss of H3K27me3 imprinting in the Sfmbt2 miRNA cluster causes enlargement of cloned mouse placentas. *Nat Commun,* 11.

Invivogen. 2016. *pVIVO-GFP/LacZ - Description* [Online]. www.invivogen.com. Available: https://www.invivogen.com/pvivo-gfplacz 2020].

Ishibashi, O., Ohkuchi, A., Ali, M. M., Kurashina, R., Luo, S. S., Ishikawa, T., Takizawa, T., Hirashima, C., Takahashi, K., Migita, M., Ishikawa, G., Yoneyama, K., Asakura, H., Izumi, A., Matsubara, S., Takeshita, T. & Takizawa, T. 2012. Hydroxysteroid (17-beta) dehydrogenase 1 is dysregulated by miR-210 and miR-518c that are aberrantly expressed in preeclamptic placentas: a novel marker for predicting preeclampsia. *Hypertension,* 59**,** 265-73.

Ishida, R., Kami, D., Kusaba, T., Kirita, Y., Kishida, T., Mazda, O., Adachi, T. & Gojo, S. 2016. Kidney-specific Sonoporation-mediated Gene Transfer. *Mol Ther,* 24**,** 125-34.

Ito, M., Sferruzzi-Perri, A. N., Edwards, C. A., Adalsteinsson, B. T., Allen, S. E., Loo, T. H., Kitazawa, M., Kaneko-Ishino, T., Ishino, F., Stewart, C. L. & Ferguson-Smith, A. C. 2015. A trans-homologue interaction between reciprocally imprinted miR-127 and Rtl1 regulates placenta development. *Development,* 142**,** 2425-30.

James, J., Saghian, R., Perwick, R. & Clark, A. 2018. Trophoblast plugs: impact on utero-placental haemodynamics and spiral artery remodelling. *Hum Reprod,* 33**,** 1430-1441.

Janssen, H. L. A., Reesink, H. W., Lawitz, E. J., Zeuzem, S., Rodriguez-Torres, M., Patel, K., Van Der Meer, A. J., Patick, A. K., Chen, A., Zhou, Y., Persson, R., King, B. D., Kauppinen, S., Levin, A. A. & Hodges, M. R. 2013. Treatment of HCV Infection by Targeting MicroRNA. *New England Journal of Medicine,* 368**,** 1685-1694.

Jauniaux, E., Watson, A., Hempstock, J., Bao, Y., Skepper, J. & Burton, G. 2000. Onset of maternal arterial blood flow and placental oxidative stress. A possible factor in human early pregnancy failure. *Am J Pathol,* 157**,** 2111-22.

JHU 2020. Species Specific Information. *In:* Committee, A. C. A. U. (ed.) *Procedures.*

Ji, L., Zhang, L., Li, Y., Guo, L., Cao, N., Bai, Z., Song, Y., Xu, Z., Zhang, J., Liu, C. & Ma, X. 2017. MiR-136 contributes to pre-eclampsia through its effects on apoptosis and angiogenesis of mesenchymal stem cells. *Placenta,* 50**,** 102-109.

Jian, G., David, S., Cheryl, S. & Stephanie, E. 2012. Maternal Ethnicity and Preeclampsia in New York City, 1995–2003. *Paediatr Perinat Epidemiol,* 26**,** 45-52.

Jiang, F., Li, J., Wu, G., Miao, Z., Lu, L., Ren, G. & Wang, X. 2015. Upregulation of microRNA335 and microRNA584 contributes to the pathogenesis of severe preeclampsia through downregulation of endothelial nitric oxide synthase. *Mol Med Rep,* 12**,** 5383-90.

Jiang, L., Long, A., Tan, L., Hong, M., Wu, J., Cai, L. & Li, Q. 2017. Elevated microRNA-520g in pre-eclampsia inhibits migration and invasion of trophoblasts. *Placenta,* 51**,** 70-75.

Jo, M., Shin, S., Jung, S., Kim, E., Song, J. & Hohng, S. 2015. Human Argonaute 2 Has Diverse Reaction Pathways on Target RNAs. *Mol Cell,* 59**,** 117-24.

Johnson, M. P., Brennecke, S. P., East, C. E., Göring, H. H. H., Kent, J. W., Dyer, T. D., Said, J. M., Roten, L. T., Iversen, A. C., Abraham, L. J., Heinonen, S., Kajantie, E., Kere, J., Kivinen, K., Pouta, A., Laivuori, H., Austgulen, R., Blangero, J. & Moses, E. K. 2012. Genome-Wide Association Scan Identifies a Risk Locus for Preeclampsia on 2q14, Near the Inhibin, Beta B Gene. *PLoS One,* 7**,** e33666.

Jonas, S. & Izaurralde, E. 2015. Towards a molecular understanding of microRNA-mediated gene silencing. *Nat Rev Genet,* 16**,** 421-33.

Juffermans, L., Van Dijk, A., Jongenelen, C., Drukarch, B., Reijerkerk, A., De Vries, H., Kamp, O. & Musters, R. 2009. Ultrasound and microbubble-induced intra- and intercellular bioeffects in primary endothelial cells. *Ultrasound Med Biol,* 35**,** 1917-27.

Kadyrov, M., Schmitz, C., Black, S., Kaufmann, P. & Huppertz, B. 2003. Pre-eclampsia and maternal anaemia display reduced apoptosis and opposite invasive phenotypes of extravillous trophoblast. *Placenta,* 24**,** 540-8.

Kanasaki, K., Palmsten, K., Sugimoto, H., Ahmad, S., Hamano, Y., Xie, L., Parry, S., Augustin, H., Gattone, V., Folkman, J., Strauss, J. & Kalluri, R. 2008. Deficiency in catechol-O-methyltransferase and 2-methoxyoestradiol is associated with pre-eclampsia. *Nature,* 453**,** 1117-21.

Kane, S. C., Da Silva Costa, F. & Brennecke, S. 2014. First Trimester Biomarkers in the Prediction of Later Pregnancy Complications. *Biomed Res Int,* 2014**,** 807196.

Karumanchi, S., Stillman, I. & Lindheimer, M. 2009. Chapter 6 – Angiogenesis and Preeclampsia. *Chesley's Hypertensive Disorders in Pregnancy (Fourth Edition)***,** 113-132.

Katayama, K., Furuki, R., Yokoyama, H., Kaneko, M., Tachibana, M., Yoshida, I., Nagase, H., Tanaka, K., Sakurai, F., Mizuguchi, H., Nakagawa, S. & Nakanishi, T. 2011. Enhanced in vivo gene transfer into the placenta using RGD fiber-mutant adenovirus vector. *Biomaterials,* 32**,** 4185-93.

Kaufmann, P., Black, S. & Huppertz, B. 2003. Endovascular trophoblast invasion: implications for the pathogenesis of intrauterine growth retardation and preeclampsia. *Biol Reprod,* 69**,** 1-7.

Kawahara, Y. & Mieda-Sato, A. 2012. TDP-43 promotes microRNA biogenesis as a component of the Drosha and Dicer complexes. *Proc Natl Acad Sci U S A,* 109**,** 3347-52.

Kawamura, K., Kawamura, N., Sato, W., Fukuda, J., Kumagai, J. & Tanaka, T. 2009. Brain-derived neurotrophic factor promotes implantation and subsequent placental development by stimulating trophoblast cell growth and survival. *Endocrinology,* 150**,** 3774-82.

Kayem, G., Kurinczuk, J., Spark, P., Brocklehurst, P., Knight, M. & System, U. O. S. 2011. Maternal and obstetric factors associated with delayed postpartum eclampsia: a national study population. *Acta Obstet Gynecol Scand,* 90**,** 1017-23.

Keswani, S., Balaji, S., Katz, A., King, A., Omar, K., Habli, M., Klanke, C. & Crombleholme, T. 2015. Intraplacental gene therapy with Ad-IGF-1 corrects naturally occurring rabbit model of intrauterine growth restriction. *Hum Gene Ther,* 26**,** 172-82.

Keyes, L., Armaza, J., Niermeyer, S., Vargas, E., Young, D. & Moore, L. 2003. Intrauterine growth restriction, preeclampsia, and intrauterine mortality at high altitude in Bolivia. *Pediatr Res,* 54**,** 20-5.

Khalil, A., Syngelaki, A., Maiz, N., Zinevich, Y. & Nicolaides, K. 2013. Maternal age and adverse pregnancy outcome: a cohort study. *Ultrasound Obstet Gynecol,* 42**,** 634-43.

Khaliq, O. P., Murugesan, S., Moodley, J. & Mackraj, I. 2018. Differential expression of miRNAs are associated with the insulin signaling pathway in preeclampsia and gestational hypertension. *Clin Exp Hypertens,* 40**,** 744-751.

Khong, T., De Wolf, F., Robertson, W. & Brosens, I. 1986. Inadequate maternal vascular response to placentation in pregnancies complicated by pre-eclampsia and by small-for-gestational age infants. *Br J Obstet Gynaecol,* 93**,** 1049-59.

Khorsandi, S., Bachellier, P., Weber, J., Greget, M., Jaeck, D., Zacharoulis, D., Rountas, C., Helmy, S., Helmy, A., Al-Waracky, M., Salama, H., Jiao, L., Nicholls, J., Davies, A., Levicar, N., Jensen, S. & Habib, N. 2008. Minimally invasive and selective hydrodynamic gene therapy of liver segments in the pig and human. *Cancer Gene Ther,* 15**,** 225-30.

Khvorova, A., Reynolds, A. & Jayasena, S. 2003. Functional siRNAs and miRNAs exhibit strand bias. *Cell,* 115**,** 209-16.

Kikas, T., Inno, R., Ratnik, K., Rull, K. & Laan, M. 2020. C-allele of rs4769613 Near FLT1 Represents a High-Confidence Placental Risk Factor for Preeclampsia. *Hypertension,* 76**,** 884-891.

Kim, H., Greenleaf, J., Kinnick, R., Bronk, J. & Bolander, M. 1996. Ultrasound-mediated Transfection of Mammalian Cells. *Hum Gene Ther,* 7**,** 1339-46.

Kim, J., Cheong, H., Lee, D., Shin, H. & Kim, Y. 2017. Genome-wide DNA methylation profiles of maternal peripheral blood and placentas: potential risk factors for preeclampsia and validation of GRK5. *Genes & Genomics,* 39**,** 197-206.

Kim, S., Lee, K. S., Choi, S., Kim, J., Lee, D. K., Park, M., Park, W., Kim, T. H., Hwang, J. Y., Won, M. H., Lee, H., Ryoo, S., Ha, K. S., Kwon, Y. G. & Kim, Y. M. 2018. NF-κB–responsive miRNA-31-5p elicits endothelial dysfunction associated

with preeclampsia via down-regulation of endothelial nitric-oxide synthase. *J Biol Chem,* 293**,** 18989-9000.

King, A., Ndifon, C., Lui, S., Widdows, K., Kotamraju, V. R., Agemy, L., Teesalu, T., Glazier, J. D., Cellesi, F., Tirelli, N., Aplin, J. D., Ruoslahti, E. & Harris, L. K. 2016. Tumor-homing peptides as tools for targeted delivery of payloads to the placenta. *Science advances,* 2**,** e1600349-e1600349.

Kitagawa, T., Iwazawa, T., Robbins, P., Lotze, M. & Tahara, H. 2003. Advantages and limitations of particle-mediated transfection (gene gun) in cancer immuno-gene therapy using IL-10, IL-12 or B7-1 in murine tumor models. *J Gene Med,* 5**,** 958-65.

Knight, M. & Ukoss 2007. Eclampsia in the United Kingdom 2005. *BJOG,* 114**,** 1072-8.

Ko, N., Mandalà, M., John, L., Gelinne, A. & Osol, G. 2018. Venoarterial Communication Mediates Arterial Wall Shear Stress-Induced Maternal Uterine Vascular Remodeling During Pregnancy. *Am J Physiol Heart Circ Physiol,* 315**,** H709-H717.

Kobayashi, Y., Kamimura, K., Abe, H., Yokoo, T., Ogawa, K., Shinagawa-Kobayashi, Y., Goto, R., R, I., Ohtsuka, M., Miura, H., Kanefuji, T., Suda, T., M, T., Aoyagi, Y., Zhang, G., Liu, D. & Terai, S. 2016. Effects of Fibrotic Tissue on Liver-targeted Hydrodynamic Gene Delivery. *Mol Ther Nucleic Acids,* 5**,** e359.

Kodomari, I., Wada, E., Nakamura, S. & Wada, K. 2009. Maternal supply of BDNF to mouse fetal brain through the placenta. *Neurochem Int,* 54**,** 95-8.

Koike, H., Tomita, N., Azuma, H., Taniyama, Y., Yamasaki, K., Kunugiza, Y., Tachibana, K., Ogihara, T. & Morishita, R. 2005. An Efficient Gene Transfer Method Mediated by Ultrasound and Microbubbles Into the Kidney. *J Gene Med,* 7**,** 108-16.

Kondo, I., Ohmori, K., Oshita, A., Takeuchi, H., Fuke, S., Shinomiya, K., Noma, T., Namba, T. & Kohno, M. 2004. Treatment of acute myocardial infarction by hepatocyte growth factor gene transfer: the first demonstration of myocardial transfer of a "functional" gene using ultrasonic microbubble destruction. *J Am Coll Cardiol,* 44**,** 644-53.

Kopriva, S. E., Chiasson, V. L., Mitchell, B. M. & Chatterjee, P. 2013. TLR3-induced placental miR-210 down-regulates the STAT6/interleukin-4 pathway. *PLoS One,* 8**,** e67760.

Kozomara, A., Hunt, S., Ninova, M., Griffiths-Jones, S. & Ronshaugen, M. 2014. Target repression induced by endogenous microRNAs: large differences, small effects. *PLoS One,* 9**,** e104286.

Krawczynski, K., Mishima, T., Huang, X. & Sadovskya, Y. 2016. Intact feto-placental growth in microRNA-210 deficient mice. *Placenta***,** 113-115.

Kremkau, F., Gramiak, R., Carstensen, E., Shah, P. & Kramer, D. 1970. Ultrasonic detection of cavitation at catheter tips. *Am J Roentgenol Radium Ther Nucl Med,* 110**,** 177-83.

Krishnan, T. & David, A. 2017. Placenta-directed gene therapy for fetal growth restriction. *Semin Fetal Neonatal Med,* 22**,** 415-422.

Krugner-Higby, L., Luck, M., Hartley, D., Crispen, H. M., Lubach, G. R. & Coe, C. L. 2009. High-risk pregnancy in rhesus monkeys (Macaca mulatta): a case of ectopic, abdominal pregnancy with birth of a live, term infant, and a case of gestational diabetes complicated by pre-eclampsia. *J Med Primatol,* 38**,** 252-6.

Krötz, F., Sohn, H., Gloe, T., Plank, C. & Pohl, U. 2003. Magnetofection potentiates gene delivery to cultured endothelial cells. *J Vasc Res,* 40**,** 425-34.

Krützfeldt, J., Rajewsky, N., Braich, R., Rajeev, K., Tuschl, T., Manoharan, M. & Stoffel, M. 2005. Silencing of microRNAs in vivo with 'antagomirs'. *Nature,* 438**,** 685-9.

Kudo, N., Okada, K. & Yamamoto, K. 2009. Sonoporation by single-shot pulsed ultrasound with microbubbles adjacent to cells. *Biophys J,* 96**,** 4866-76.

Kukuła, K., Urbanowicz, A., Kłopotowsk, I. M., Dąbrowski, M., Pręgowski, J., Kądziela, J., Chmielak, Z., Witkowski, A. & Rużyłło, W. 2019. Long-term follow-up and safety assessment of angiogenic gene therapy trial VIF-CAD: Transcatheter intramyocardial administration of a bicistronic plasmid expressing VEGF-A165/bFGF cDNA for the treatment of refractory coronary artery disease. *Am Heart J,* 215**,** 78-82.

Kumasawa, K., Ikawa, M., Kidoya, H., Hasuwa, H., Saito-Fujita, T., Morioka, Y., Takakura, N., Kimura, T. & Okabe, M. 2011. Pravastatin induces placental growth factor (PGF) and ameliorates preeclampsia in a mouse model. *Proc Natl Acad Sci USA,* 108**,** 1451-5.

Kumbhari, V., L, L., Piontek, K., Ishida, M., Fu, R., Khalil, B., Garrett, C., Liapi, E., Kalloo, A. & Selaru, F. 2018. Successful liver-directed gene delivery by ERCP-guided hydrodynamic injection (with videos). *Gastrointest Endosc,* 88**,** 755-763.

Kurki, T., Hiilesmaa, V., Raitasalo, R., Mattila, H. & Ylikorkala, O. 2000. Depression and anxiety in early pregnancy and risk for preeclampsia. *Obstet Gynecol,* 95**,** 487-90.

Kurzynska-Kokorniak, A., Koralewska, N., Pokornowska, M., Urbanowicz, A., Tworak, A., Mickiewicz, A. & Figlerowicz, M. 2015. The many faces of Dicer: the complexity of the mechanisms regulating Dicer gene expression and enzyme activities. *Nucleic Acids Res,* 43**,** 4365-80.

Kwak, P. & Tomari, Y. 2012. The N domain of Argonaute drives duplex unwinding during RISC assembly. *Nat Struct Mol Biol,* 19**,** 145-51.

Kwekkeboom, R., Lei, Z., Bogaards, S., Aiazian, E., Kamp, O., Paulus, W., Sluijter, J. & Musters, R. 2015. Ultrasound and microbubble-induced local delivery of MicroRNA-based therapeutics. *Ultrasound Med Biol,* 41**,** 163-76.

Laine, K., Murzakanova, G., Sole, K. B., Pay, A. D., Heradstveit, S. & Räisänen, S. 2019. Prevalence and risk of pre-eclampsia and gestational hypertension in twin pregnancies: a population-based register study. *BMJ Open,* 9**,** e029908.

Lalevée, S., Lapaire, O. & Bühler, M. 2014. miR455 is linked to hypoxia signaling and is deregulated in preeclampsia. *Cell Death Dis***,** e1408.

Lamarca, B., Parrish, M., Ray, L., Murphy, S., Roberts, L., Glover, P., Wallukat, G., Wenzel, K., Cockrell, K., Martin, J., Ryan, M. & Dechend, R. 2009. Hypertension in response to autoantibodies to the angiotensin II type I receptor (AT1-AA) in pregnant rats: role of endothelin-1. *Hypertension,* 54**,** 905-9.

Lan, H., Mu, W., Tomita, N., Huang, X., Li, J., Zhu, H., Morish, I. R. & Johnson, R. 2003. Inhibition of renal fibrosis by gene transfer of inducible Smad7 using ultrasound-microbubble system in rat UUO model. *J Am Soc Nephrol,* 14**,** 1535-48.

Lauer, U., Bürgelt, E., Squire, Z., Messmer, K., Hofschneider, P., Gregor, M. & Delius, M. 1997. Shock Wave Permeabilization as a New Gene Transfer Method. *Gene Ther,* 4**,** 710-5.

Lavie, O., Edelman, D., Levy, T., Fishman, A., Hubert, A., Segev, Y., Raveh, E., Gilon, M. & Hochberg, A. 2017. A phase 1/2a, dose-escalation, safety, pharmacokinetic, and preliminary efficacy study of intraperitoneal administration of BC-819 (H19-DTA) in subjects with recurrent ovarian/peritoneal cancer. *Arch Gynecol Obstet,* 295**,** 751-761.

Lawrie, A., Brisken, A., Francis, S., Cumberland, D., Crossman, D. & Newman, C. 2000. Microbubble-enhanced ultrasound for vascular gene delivery. *Gene Ther,* 7**,** 2023-7.

Lawrie, C., Gal, S., Dunlop, H., Pushkaran, B., Liggins, A., Pulford, K., Banham, A., Pezzella, F., Boultwood, J., Wainscoat, J., Hatton, C. & Harris, A. 2008. Detection of elevated levels of tumour-associated microRNAs in serum of patients with diffuse large B-cell lymphoma. *Br J Haematol,* 141**,** 672-5.

Lee, D. C., Romero, R., Kim, J. S., Tarca, A. L., Montenegro, D., Pineles, B. L., Kim, E., Lee, J., Kim, S. Y., Draghici, S., Mittal, P., Kusanovic, J. P., Chaiworapongsa, T., Hassan, S. S. & Kim, C. J. 2011. miR-210 targets iron-sulfur cluster scaffold homologue in human trophoblast cell lines: siderosis of interstitial trophoblasts as a novel pathology of preterm preeclampsia and small-for-gestational-age pregnancies. *Am J Pathol,* 179**,** 590-602.

Lee, M., Chea, K., Pyda, R., Chua, M. & Dominguez, I. 2017. Comparative Analysis of Non-viral Transfection Methods in Mouse Embryonic Fibroblast Cells. *J Biomol Tech,* 28**,** 67-74.

Lee, R., Feinbaum, R. & Ambros, V. 1993. The C. elegans heterochronic gene lin-4 encodes small RNAs with antisense complementarity to lin-14. *Cell,* 75**,** 843-54.

Lee, Y., Jeon, K., Lee, J., Kim, S. & Kim, V. 2002. MicroRNA maturation: stepwise processing and subcellular localization. *EMBO J,* 21**,** 4663-70.

Lee, Y., Kim, M., Han, J., Yeom, K. H., Lee, S., Baek, S. H. & Kim, V. N. 2004. MicroRNA genes are transcribed by RNA polymerase II. *EMBO J,* 23**,** 4051-60.

Lee, Y. & Magnus, P. 2018. Maternal and Paternal Height and the Risk of Preeclampsia. *Hypertension,* 71**,** 666-670.

Leitch, C., Cameron, A. & Walker, J. 1997. The changing pattern of eclampsia over a 60-year period. *Br J Obstet Gynaeco,* 104**,** 917-22.

Leshkowitz, D., Horn-Saban, S., Parmet, Y. & Feldmesser, E. 2013. Differences in microRNA detection levels are technology and sequence dependent. *Rna,* 19**,** 527-38.

Lewis, B. P., Burge, C. B. & Bartel, D. P. 2005. Conserved seed pairing, often flanked by adenosines, indicates that thousands of human genes are microRNA targets. *Cell,* 120**,** 15-20.

Li, D. & Wi, S. 2000. Changing paternity and the risk of preeclampsia/eclampsia in the subsequent pregnancy. *Am J Epidemiol,* 151**,** 57-62.

Li, J., Chen, L., Qiuqin, T., Wu, W., Hao, G., Lou, L., Jie, W., Hua, J., Hongjuan, D., Xia, Y., Chen, D., Hu, Y. & Wang, X. 2015a. The role, mechanism and potentially novel biomarker of microRNA-17-92 cluster in macrosomia. *Sci Rep,* 5**,** 17212.

Li, J., Song, L., Zhou, L., Wu, J., Sheng, C., Chen, H., Liu, Y., Gao, S. & Huang, W. 2015b. A MicroRNA Signature in Gestational Diabetes Mellitus Associated with Risk of Macrosomia. *Cell Physiol Biochem,* 37**,** 243-52.

Li, L., Huang, X., He, Z., Xiong, Y. & Fang, Q. 2019. miRNA-210-3p regulates trophoblast proliferation and invasiveness through fibroblast growth factor 1 in selective intrauterine growth restriction. *J Cell Mol Med,* 23**,** 4422-4433.

Li, P., Guo, W., Du, L., Zhao, J., Wang, Y., Liu, L., Hu, Y. & Hou, Y. 2013. microRNA-29b contributes to pre-eclampsia through its effects on apoptosis, invasion and angiogenesis of trophoblast cells. *Clin Sci (Lond),* 124**,** 27-40.

Li, Q., Kappil, M. A., Li, A., Dassanayake, P. S., Darrah, T. H., Friedman, A. E., Friedman, M., Lambertini, L., Landrigan, P., Stodgell, C. J., Xia, Y., Nanes, J. A., Aagaard, K. M., Schadt, E. E., Murray, J. C., Clark, E. B., Dole, N., Culhane, J., Swanson, J., Varner, M., Moye, J., Kasten, C., Miller, R. K. & Chen, J. 2015c. Exploring the associations between microRNA expression profiles and environmental pollutants in human placenta from the National Children's Study (NCS). *Epigenetics,* 10**,** 793-802.

Li, S. C., Chan, W. C., Hu, L. Y., Lai, C. H., Hsu, C. N. & Lin, W. C. 2010. Identification of homologous microRNAs in 56 animal genomes. *Genomics,* 96**,** 1-9.

Li, X., Li, C., Dong, X. & Gou, W. 2014. MicroRNA-155 inhibits migration of trophoblast cells and contributes to the pathogenesis of severe preeclampsia by regulating endothelial nitric oxide synthase. *Mol Med Rep,* 10**,** 550-4.

Li, X., Song, Y., Liu, D., Zhao, J., Xu, J., Ren, J., Hu, Y., Wang, Z., Hou, Y. & Zhao, G. 2017. MiR-495 Promotes Senescence of Mesenchymal Stem Cells by Targeting Bmi-1. *Cell Physiol Biochem,* 42**,** 780-796.

Liao, A., Hsieh, Y., Ho, H., Chen, H., Lin, Y., Shih, C., Chen, H., Kuo, C., Lu, Y. & Wang, C. 2014. Effects of microbubble size on ultrasound-mediated gene transfection in auditory cells. *Biomed Res Int,* 2014**,** 840852.

Lin, H., Pan, S., Meng, L., Zhou, C., Jiang, C., Ji, Z., Chi, J. & Guo, H. 2017. MicroRNA-384-mediated Herpud1 upregulation promotes angiotensin II-induced endothelial cell apoptosis. *Biochem Biophys Res Commun,* 488**,** 453-460.

Lin, L., Fan, Y., Gao, F., Jin, L., Li, D., Sun, W., Li, F., Qin, P., Shi, Q., Shi, X. & Du, L. 2018. UTMD-Promoted Co-Delivery of Gemcitabine and miR-21 Inhibitor by Dendrimer-Entrapped Gold Nanoparticles for Pancreatic Cancer Therapy. *Theranostics,* 8**,** 1923-1939.

Lindner, J., Song, J., Jayaweera, A., Sklenar, J. & Kaul, S. 2002. Microvascular Rheology of Definity Microbubbles After Intra-Arterial and Intravenous Administration. *Journal of the American Society of Echocardiography : official publication of the American Society of Echocardiography,* 15**,** 396-403.

Ling, H. 2016. Non-coding RNAs: Therapeutic Strategies and Delivery Systems. *Adv Exp Med Biol,* 937**,** 229-37.

Liu, E., Liu, Z., Zhou, Y., Chen, M., Wang, L. & Li, J. 2019a. MicroRNA-142-3p inhibits trophoblast cell migration and invasion by disrupting the TGF-β1/Smad3 signaling pathway. *Mol Med Rep,* 19**,** 3775-3782.

Liu, F., Wu, K., Wu, W., Chen, Y., Wu, H., Wang, H. & Zhang, W. 2018a. miR203 contributes to preeclampsia via inhibition of VEGFA expression. *Mol Med Rep,* 17**,** 5627-5634.

Liu, F., Wu, K., Wu, W., Chen, Y., Wu, H., Wang, H. & Zhang, W. 2018b. miR-203 contributes to pre-eclampsia via inhibition of VEGFA expression. *Mol Med Rep,* 17**,** 5627-34.

Liu, F., Zhu, J., Huang, Y., Guo, W., Rui, M., Xu, Y. & Hu, B. 2013. Contrast Imaging and Gene Delivery Through the Combined Use of Novel Cationic

Liposomal Microbubbles and Ultrasound in Rat Carotid Arteries. *Archives of medical science : AMS,* 9**,** 347-53.

Liu, J., Carmell, M., Rivas, F., Marsden, C., Thomson, J., Song, J., Hammond, S., Joshua-Tor, L. & Hannon, G. 2004. Argonaute2 is the catalytic engine of mammalian RNAi. *Science,* 305**,** 1437-41.

Liu, L., Wang, Y., Fan, H., Zhao, X., Liu, D., Hu, Y., Kidd, A. R., 3rd, Bao, J. & Hou, Y. 2012. MicroRNA-181a regulates local immune balance by inhibiting proliferation and immunosuppressive properties of mesenchymal stem cells. *Stem Cells,* 30**,** 1756-70.

Liu, L., Zhao, G., Fan, H., Zhao, X., Li, P., Wang, Z., Hu, Y. & Hou, Y. 2014. Mesenchymal stem cells ameliorate Th1-induced pre-eclampsia-like symptoms in mice via the suppression of TNF-alpha expression. *PLoS One,* 9**,** e88036.

Liu, R., Meng, Q., Shi, Y. & Xu, H. 2018c. Regulatory role of microRNA-320a in the proliferation, migration, invasion, and apoptosis of trophoblasts and endothelial cells by targeting estrogen-related receptor γ. *J Cell Physiol,* 234**,** 682-691.

Liu, X., Zhang, C., Wang, C., Sun, J., Wang, D., Zhao, Y. & Xu, X. 2018d. miR-210 promotes human osteosarcoma cell migration and invasion by targeting FGFRL1. *Oncol Lett,* 16**,** 2229-2236.

Liu, Y., Li, L., Su, Q., Liu, T., Ma, Z. & Yang, H. 2015. Ultrasound-Targeted Microbubble Destruction Enhances Gene Expression of microRNA-21 in Swine Heart via Intracoronary Delivery. *Echocardiography (Mount Kisco, N.Y.),* 32**,** 1407-16.

Liu, Z., Zhao, X., Shan, H., Gao, H. & Wang, P. 2019b. microRNA-520c-3p suppresses NLRP3 inflammasome activation and inflammatory cascade in preeclampsia by downregulating NLRP3. *Inflamm Res,* 68**,** 643-654.

Loichinger, M. H., Towner, D., Thompson, K. S., Ahn, H. J. & Bryant-Greenwood, G. D. 2016. Systemic and placental alpha-klotho: Effects of preeclampsia in the last trimester of gestation. *Placenta,* 41**,** 53-61.

Loudon, I. 2000. Maternal mortality in the past and its relevance to developing countries today. *Am J Clin Nutr,* 72**,** 241S-246S.

Lowe, S., Bowyer, L., Lust, K., Mcmahon, L., Morton, M., North, R., Paech, M., Said, J. & Zealand, S. O. O. M. O. A. A. N. 2015. The SOMANZ Guidelines for the Management of Hypertensive Disorders of Pregnancy 2014. *Aust N Z J Obstet Gynaecol,* 55**,** 11-6.

Lu, C., Chou, A., Wu, C., Yang, C., Chen, J., Wu, P., Lin, S., Muhammad, R. & Yang, L. 2002. Gene-gun particle with pro-opiomelanocortin cDNA produces analgesia against formalin-induced pain in rats. *Gene Ther,* 9**,** 1008-14.

Lu, C., Stewart, D. J., Lee, J. J., Ji, L., Ramesh, R., Jayachandran, G., Nunez, M. I., Wistuba, Ii, Erasmus, J. J., Hicks, M. E., Grimm, E. A., Reuben, J. M., Baladandayuthapani, V., Templeton, N. S., Mcmannis, J. D. & Roth, J. A. 2012. Phase I Clinical Trial of Systemically Administered TUSC2(FUS1)-Nanoparticles Mediating Functional Gene Transfer in Humans. *PLoS One,* 7**,** e34833.

Lu, T., Lu, W. & Zhao, L. 2017. MicroRNA-137 Affects Proliferation and Migration of Placenta Trophoblast Cells in Preeclampsia by Targeting ERRα. *Reprod Sci,* 24**,** 85-96.

Lucas, M. & Heller, R. 2003. IL-12 gene therapy using an electrically mediated nonviral approach reduces metastatic growth of melanoma. *DNA Cell Biol,* 22**,** 755-63.

Lumbers, E., Delforce, S., Arthurs, A. & Pringle, K. 2019. Causes and Consequences of the Dysregulated Maternal Renin-Angiotensin System in Preeclampsia. *Front Endocrinol (Lausanne),* 10**,** 563.

Lundstrom, K. 2018. Viral Vectors in Gene Therapy. *Diseases,* 6**,** 42.

Luo, L., Ye, G., Nadeem, L., Fu, G., Yang, B. B., Honarparvar, E., Dunk, C., Lye, S. & Peng, C. 2012. MicroRNA-378a-5p promotes trophoblast cell survival, migration and invasion by targeting Nodal. *J Cell Sci,* 125**,** 3124-32.

Luo, R., Shao, X., Xu, P., Liu, Y., Wang, Y., Zhao, Y., Liu, M., Ji, L., Li, Y. X., Chang, C., Qiao, J., Peng, C. & Wang, Y. L. 2014. MicroRNA-210 contributes to preeclampsia by downregulating potassium channel modulatory factor 1. *Hypertension,* 64**,** 839-45.

Luo, R., Wang, Y., Xu, P., Cao, G., Zhao, Y., Shao, X., Li, Y. X., Chang, C., Peng, C. & Wang, Y. L. 2016. Hypoxia-inducible miR-210 contributes to preeclampsia via targeting thrombospondin type I domain containing 7A. *Sci Rep,* 6**,** 19588.

Luo, Z., Julien, P., Wei, S., Audibert, F. & Fraser, W. 2018. Association of pre-eclampsia with SOD2 Ala16Val polymorphism among mother-father-infant triads. *Int J Gynaecol Obstet,* 142**,** 221-227.

Lv, Y., Lu, X., Li, C., Fan, Y., Ji, X., Long, W., Meng, L., Wu, L., Wang, L., Lv, M. & Ding, H. 2019. miR-145-5p promotes trophoblast cell growth and invasion by targeting FLT1. *Life Sci,* 239**,** 117008.

Lyall, F., Robson, S. & Bulmer, J. 2013. Spiral artery remodeling and trophoblast invasion in preeclampsia and fetal growth restriction: relationship to clinical outcome. *Hypertension,* 62**,** 1046-54.

Lykoudi, A., Kolialexi, A., Lambrou, G. I., Braoudaki, M., Siristatidis, C., Papaioanou, G. K., Tzetis, M., Mavrou, A. & Papantoniou, N. 2018. Dysregulated placental microRNAs in Early and Late onset Preeclampsia. *Placenta,* 61**,** 24-32.

Lytle, J. R., Yario, T. A. & Steitz, J. A. 2007. Target mRNAs are repressed as efficiently by microRNA-binding sites in the 5′ UTR as in the 3′ UTR. *Proc Natl Acad Sci U S A,* 104**,** 9667-72.

Ma, Y., Ye, Y., Zhang, J., Ruan, C. & Gao, P. 2019. Immune Imbalance Is Associated With the Development of Preeclampsia. *Medicine,* 98**,** e15080.

Maccani, M. A., Avissar-Whiting, M., Banister, C. E., Mcgonnigal, B., Padbury, J. F. & Marsit, C. J. 2010. Maternal cigarette smoking during pregnancy is associated with downregulation of miR-16, miR-21, and miR-146a in the placenta. *Epigenetics,* 5**,** 583-9.

Magee, L., Pels, A., Helewa, M., Rey, E., Von Dadelszen, P. & Group, C. H. D. O. P. H. W. 2014. Diagnosis, evaluation, and management of the hypertensive disorders of pregnancy. *Pregnancy Hypertens,* 4**,** 105-45.

Magnussen, E. B., Vatten, L. J., Lund-Nilsen, T. I., Salvesen, K., Smith, G. D. & Romundstad, P. R. 2007. Prepregnancy cardiovascular risk factors as predictors of pre-eclampsia: population based cohort study. *BMJ,* 335**,** 978.

Mahvi, D., Henry, M., Albertini, M., Weber, S., Meredith, K., Schalch, H., Rakhmilevich, A., Hank, J. & Sondel, P. 2007. Intratumoral injection of IL-12 plasmid DNA--results of a phase I/IB clinical trial. *Cancer Gene Ther,* 14**,** 717-23.

Malina, A., Daftary, A., Crombleholme, W., Markovic, N. & Roberts, J. 2005. Placental System A Transporter mRNA Is Not Different in Preeclampsia, Normal Pregnancy, or Pregnancies With Small-For-Gestational-Age Infants. *Hypertension in pregnancy,* 24.

Malnou, E. C., Umlauf, D., Mouysset, M. & Cavaille, J. 2018. Imprinted MicroRNA Gene Clusters in the Evolution, Development, and Functions of Mammalian Placenta. *Front Genet,* 9**,** 706.

Marques, F., Campain, A., Tomaszewski, M., Zukowska-Szczechowska, E., Yang, Y., Charchar, F. & Morris, B. 2011. Gene expression profiling reveals renin mRNA overexpression in human hypertensive kidneys and a role for microRNAs. *Hypertension,* 58**,** 1093-8.

Masuyama, H., Nakatsukasa, H., Takamoto, N. & Hiramatsu, Y. 2007. Correlation between soluble endoglin, vascular endothelial growth factor receptor-1, and adipocytokines in preeclampsia. *J Clin Endocrinol Metab,* 92**,** 2672-9.

Matijevic, R. & Johnston, T. 1999. In vivo assessment of failed trophoblastic invasion of the spiral arteries in pre-eclampsia. *Br J Obstet Gynaecol,* 106**,** 78-82.

Matranga, C., Tomari, Y., Shin, C., Bartel, D. & Zamore, P. 2005. Passenger-strand cleavage facilitates assembly of siRNA into Ago2-containing RNAi enzyme complexes. *Cell,* 123**,** 607-20.

Mayeur, S., Silhol, M., Moitrot, E., Barbaux, S., Breton, C., Gabory, A., Vaiman, D., Dutriez-Casteloot, I., Fajardy, I., Vambergue, A., Tapia-Arancibia, L., Bastide, B., Storme, L., Junien, C., Vieau, D. & Lesage, J. 2010. Placental BDNF/TrkB signaling system is modulated by fetal growth disturbances in rat and human. *Placenta,* 31**,** 785-91.

Maynard, S., Min, J., Merchan, J., Lim, K., Li, J., Mondal, S., Libermann, T., Morgan, J., Sellke, F., Stillman, I., Epstein, F., Sukhatme, V. & Karumanchi, S. 2003. Excess placental soluble fms-like tyrosine kinase 1 (sFlt1) may contribute to endothelial dysfunction, hypertension, and proteinuria in preeclampsia. *J Clin Invest,* 111**,** 649-58.

Mayor-Lynn, K., Toloubeydokhti, T., Cruz, A. C. & Chegini, N. 2011. Expression profile of microRNAs and mRNAs in human placentas from pregnancies complicated by preeclampsia and preterm labor. *Reprod Sci,* 18**,** 46-56.

MBRRACE-UK 2018. Saving Lives, Improving Mothers' Care - Lessons learned to inform maternity

care from the UK and Ireland Confidential Enquiries into Maternal Deaths and Morbidity 2014-16. Oxford: Oxford: National Perinatal Epidemiology Unit.

Mcdonald, S., Han, Z., Walsh, M., Gerstein, H. & Devereaux, P. 2010. Kidney disease after preeclampsia: a systematic review and meta-analysis. *Am J Kidney Dis,* 55**,** 1026-39.

Mcginnis, R., Steinthorsdottir, V., Williams, N. O., Thorleifsson, G., Shooter, S., Hjartardottir, S., Bumpstead, S., Stefansdottir, L., Hildyard, L., Sigurdsson, J. K., Kemp, J. P., Silva, G. B., Thomsen, L. C. V., Jaaskelainen, T., Kajantie, E., Chappell, S., Kalsheker, N., Moffett, A., Hiby, S., Lee, W. K., Padmanabhan, S., Simpson, N. A. B., Dolby, V. A., Staines-Urias, E., Engel, S. M., Haugan, A., Trogstad, L., Svyatova, G., Zakhidova, N., Najmutdinova, D., Dominiczak, A. F., Gjessing, H. K., Casas, J. P., Dudbridge, F., Walker, J. J., Pipkin, F. B., Thorsteinsdottir, U., Geirsson, R. T., Lawlor, D. A., Iversen, A. C., Magnus, P., Laivuori, H., Stefansson, K. & Morgan, L. 2017. Variants in the fetal genome near FLT1 are associated with risk of preeclampsia. *Nat Genet,* 49**,** 1255-1260.

Medeiros, L. A., Dennis, L. M., Gill, M. E., Houbaviy, H., Markoulaki, S., Fu, D., White, A. C., Kirak, O., Sharp, P. A., Page, D. C. & Jaenisch, R. 2011. Mir-290–295 deficiency in mice results in partially penetrant embryonic lethality and germ cell defects. *Proc Natl Acad Sci U S A,* 108**,** 14163-8.

Mehier-Humbert, S., Bettinger, T., Yan, F. & Guy, R. H. 2005. Plasma membrane poration induced by ultrasound exposure: implication for drug delivery. *J Control Release,* 104**,** 213-22.

Mehta, V., Abi-Nader, K. N., Peebles, D. M., Benjamin, E., Wigley, V., Torondel, B., Filippi, E., Shaw, S. W., Boyd, M., Martin, J., Zachary, I. & David, A. L. 2012. Long-term increase in uterine blood flow is achieved by local overexpression of VEGF-A(165) in the uterine arteries of pregnant sheep. *Gene Ther,* 19**,** 925-35.

Mehta, V., Abi-Nader, K. N., Shangaris, P., Shaw, S. W., Filippi, E., Benjamin, E., Boyd, M., Peebles, D. M., Martin, J., Zachary, I. & David, A. L. 2014. Local over-expression of VEGF-DDeltaNDeltaC in the uterine arteries of pregnant sheep results in long-term changes in uterine artery contractility and angiogenesis. *PLoS One,* 9**,** e100021.

Mehta, V., Ofir, K., Swanson, A., Kloczko, E., Boyd, M., Barker, H., Avdic-Belltheus, A., Martin, J., Zachary, I., Peebles, D. & David, A. L. 2016. Gene Targeting to the Uteroplacental Circulation of Pregnant Guinea Pigs. *Reprod Sci,* 23**,** 1087-95.

Meijering, B., Juffermans, L., Van Wamel, A., Henning, R., Zuhorn, I., Emmer, M., Versteilen, A., Paulus, W., Van Gilst, W., Kooiman, K., De Jong, N., Musters, R., Deelman, L. & Kamp, O. 2009. Ultrasound and microbubble-targeted delivery of macromolecules is regulated by induction of endocytosis and pore formation. *Circ Res,* 104**,** 679-87.

Meissner, J., Toporkiewicz, M., Czogalla, A., Matusewicz, L., Kuliczkowski, K. & Sikorski, A. 2015. Novel antisense therapeutics delivery systems: In vitro and in vivo studies of liposomes targeted with anti-CD20 antibody. *J Control Release,* 220**,** 515-528.

Meng, H., Xu, L., Jing, G., Qian, L. & Qi, M. 2017. MiR-223 promotes trophoblast cell survival and invasion by targeting STAT 3 in preeclampsia. *Int J Clin Exp Med,* 10**,** 6577-6585.

Meng, L., Liu, X., Wang, Y., Zhang, W., Zhou, W., Cai, F., Li, F., Wu, J., Xu, L., Niu, L. & Zheng, H. 2019. Sonoporation of Cells by a Parallel Stable Cavitation Microbubble Array. *Adv Sci (Weinh),* 6**,** 1900557.

Meyer, M. C., Brayden, J. E. & Mclaughlin, M. K. 1993. Characteristics of vascular smooth muscle in the maternal resistance circulation during pregnancy in the rat. *Am J Obstet Gynecol,* 169**,** 1510-6.

Meyer-Kovac, J., Kolbe, I., Ehrhardt, L., Leliavski, A., Husse, J., Salinas, G., Lingner, T., Tsang, A. H., Barclay, J. L. & Oster, H. 2017. Hepatic gene therapy rescues high-fat diet responses in circadian Clock mutant mice. *Mol Metab,* 6**,** 512-23.

Miao, C., Brayman, A., Loeb, K., Ye, P., Zhou, L., Mourad, P. & Crum, L. 2005. Ultrasound Enhances Gene Delivery of Human Factor IX Plasmid. *Hum Gene Ther,* 16**,** 893-905.

Miao, L., Yao, H., Li, C., Pu, M., Yao, X., Yang, H., Qi, X., Ren, J. & Wang, Y. 2016. A dual inhibition: microRNA-552 suppresses both transcription and translation of cytochrome P450 2E1. *Biochim Biophys Acta,* 1859**,** 650-62.

Miller, D., Smith, N., Bailey, M., Czarnota, G., Hynynen, K., Makin, I. & Medicine, B. C. O. T. A. I. O. U. I. 2012. Overview of therapeutic ultrasound applications and safety considerations. *J Ultrasound Med,* 31**,** 623-34.

Milosevic-Stevanovic, J., Krstic, M., Radovic-Janosevic, D., Popovic, J., Tasic, M. & Stojnev, S. 2016. Number of decidual natural killer cells & macrophages in pre-eclampsia. *Indian J Med Res,* 144**,** 823-830.

Mitchell, P. S., Parkin, R. K., Kroh, E. M., Fritz, B. R., Wyman, S. K., Pogosova-Agadjanyan, E. L., Peterson, A., Noteboom, J., O'briant, K. C., Allen, A., Lin, D. W., Urban, N., Drescher, C. W., Knudsen, B. S., Stirewalt, D. L., Gentleman, R., Vessella, R. L., Nelson, P. S., Martin, D. B. & Tewari, M. 2008. Circulating microRNAs as stable blood-based markers for cancer detection. *Proc Natl Acad Sci U S A,* 105, 10513-8.

Mizuguchi, H., Koizumi, N., Hosono, T., Utoguchi, N., Watanabe, Y., Kay, M. & Hayakawa, T. 2001. A simplified system for constructing recombinant adenoviral vectors containing heterologous peptides in the HI loop of their fiber knob. *Gene Ther,* 8, 730-5.

Moffett-King, A. 2002. Natural killer cells and pregnancy. *Nat Rev Immunol,* 2, 656-63.

Molnár, M., Sütö, T., Tóth, T. & Hertelendy, F. 1994. Prolonged blockade of nitric oxide synthesis in gravid rats produces sustained hypertension, proteinuria, thrombocytopenia, and intrauterine growth retardation. *Am J Obstet Gynecol,* 170, 1458-66.

Monteys, A. M., Spengler, R. M., Wan, J., Tecedor, L., Lennox, K. A., Xing, Y. & Davidson, B. L. 2010. Structure and activity of putative intronic miRNA promoters. *RNA,* 16, 495-505.

Montgomery, R. L., Hullinger, T. G., Semus, H. M., Dickinson, B. A., Seto, A. G., Lynch, J. M., Stack, C., Latimer, P. A., Olson, E. N. & Van Rooij, E. 2011. Therapeutic inhibition of miR-208a improves cardiac function and survival during heart failure. *Circulation,* 124, 1537-47.

Morales-Prieto, D. M., Chaiwangyen, W., Ospina-Prieto, S., Schneider, U., Herrmann, J., Gruhn, B. & Markert, U. R. 2012. MicroRNA expression profiles of trophoblastic cells. *Placenta,* 33, 725-34.

Morgan, H. L., Butler, E., Ritchie, S., Herse, F., Dechend, R., Beattie, E., Mcbride, M. W. & D, G. 2018. Modeling Superimposed Preeclampsia Using Ang II (Angiotensin II) Infusion in Pregnant Stroke-Prone Spontaneously Hypertensive Rats. *Hypertension,* 1, 208-218.

Mori, A., Nishi, H., Sasaki, T., Nagamitsu, Y., Kawaguchi, R., Okamoto, A., Kuroda, M. & Isaka, K. 2016. HLA-G expression is regulated by miR-365 in trophoblasts under hypoxic conditions. *Placenta,* 45, 37-41.

Mouillet, J. F., Chu, T., Nelson, D. M., Mishima, T. & Sadovsky, Y. 2010. MiR-205 silences MED1 in hypoxic primary human trophoblasts. *FASEB J,* 24, 2030-9.

Mu, J., Slevin, J., Qu, D., Mccormick, S. & Adamson, S. 2008. In vivo quantification of embryonic and placental growth during gestation in mice using micro-ultrasound. *Reprod Biol Endocrinol,* 6, 34.

Muralimanoharan, S., Guo, C., Myatt, L. & Maloyan, A. 2015. Sexual dimorphism in miR-210 expression and mitochondrial dysfunction in the placenta with maternal obesity. *Int J Obes (Lond),* 8, 1247-81.

Muralimanoharan, S., Maloyan, A., Mele, J., Guo, C., Myatt, L. G. & Myatt, L. 2012. MIR-210 modulates mitochondrial respiration in placenta with preeclampsia. *Placenta,* 33, 816-23.

Muralimanoharan, S., Maloyan, A. & Myatt, L. 2013. Evidence of sexual dimorphism in the placental function with severe preeclampsia. *Placenta,* 12, 1183-9.

Müller, O., Schinkel, S., Kleinschmidt, J., Katus, H. & Bekeredjian, R. 2008. Augmentation of AAV-mediated cardiac gene transfer after systemic administration in adult rats. *Gene Ther,* 15**,** 1558-65.

Nakagawa, K., Lim, E., Harvey, S., Miyamura, J. & Juarez, D. T. 2016. Racial/ethnic disparities in the association between preeclampsia risk factors and preeclampsia among women residing in Hawaii. *Matern Child Health J,* 20**,** 1814-24.

Nam, J. W., Rissland, O. S., Koppstein, D., Abreu-Goodger, C., Jan, C. H., Agarwal, V., Yildirim, M. A., Rodriguez, A. & Bartel, D. P. 2014. Global analyses of the effect of different cellular contexts on microRNA targeting. *Mol Cell,* 53**,** 1031-43.

Nayerossadat, N., T, M. & Ali, P. 2012. Viral and Nonviral Delivery Systems for Gene Delivery. *Adv Biomed Res,* 1**,** 27.

Nejad, S., Hosseini, H., Akiyama, H. & Tachibana, K. 2016. Reparable Cell Sonoporation in Suspension: Theranostic Potential of Microbubble. *Theranostics,* 6**,** 446-55.

Ness, R., Markovic, N., Harger, G. & Day, R. 2004. Barrier methods, length of preconception intercourse, and preeclampsia. *Hypertens Pregnancy,* 23**,** 227-35.

Ness, R. & Roberts, J. 1996. Heterogeneous causes constituting the single syndrome of preeclampsia: a hypothesis and its implications. *Am J Obstet Gynecol,* 175**,** 1365-70.

Newman, C. & Bettinger, T. 2007. Gene therapy progress and prospects: ultrasound for gene transfer. *Gene Ther,* 14**,** 465-75.

Newman, M. A. & Hammond, S. M. 2010. Emerging paradigms of regulated microRNA processing. *Genes Dev,* 24**,** 1086-92.

Newman, M. A., Thomson, J. M. & Hammond, S. M. 2008. Lin-28 interaction with the Let-7 precursor loop mediates regulated microRNA processing. *RNA,* 14**,** 1539-49.

Ngoc, N. T. N., Merialdi, M., Abdel-Aleem, H., Carroli, G., Purwar, M., Zavaleta, N., Campódonico, L., Ali, M. M., Hofmeyr, G. J., Mathai, M., Lincetto, O. & Villar, J. 2006. Causes of stillbirths and early neonatal deaths: data from 7993 pregnancies in six developing countries. *Bull World Health Organ,* 84**,** 699-705.

NICE 2019. Hypertension in pregnancy: diagnosis and management. *NICE guideline*. National Institute for Health and Care Excellence.

Nicol, F., Wong, M., Maclaughlin, F., Perrard, J., Wilson, E., Nordstrom, J. & Smith, L. 2002. Poly-L-glutamate, an anionic polymer, enhances transgene expression for plasmids delivered by intramuscular injection with in vivo electroporation. *Gene Ther,* 9**,** 1351-8.

Niu, Z. R., Han, T., Sun, X. L., Luan, L. X., Gou, W. L. & Zhu, X. M. 2018. MicroRNA-30a-3p is overexpressed in the placentas of patients with preeclampsia and affects trophoblast invasion and apoptosis by its effects on IGF-1. *Am J Obstet Gynecol,* 218**,** 249.e1-249.e12.

Noble, M., Kuhr, C., Graves, S., Loeb, K., Sun, S., Keilman, G., Morrison, K., Paun, M., Storb, R. & Miao, C. 2013. Ultrasound-targeted Microbubble Destruction-Mediated Gene Delivery Into Canine Livers. *Molecular therapy : the journal of the American Society of Gene Therapy,* 21**,** 1687-94.

Noble-Vranish, M., Song, S., Morrison, K., Tran, D., Sun, R., Loeb, K., Keilman, G. & Miao, C. 2018. Ultrasound-Mediated Gene Therapy in Swine Livers Using

Single-Element, Multi-lensed, High-Intensity Ultrasound Transducers. *Mol Ther Methods Clin Dev,* 10, 179-188.

Noguer-Dance, M., Abu-Amero, S., Al-Khtib, M., Lefèvre, A., Coullin, P., Moore, G. & Cavaillé, J. 2010. The primate-specific microRNA gene cluster (C19MC) is imprinted in the placenta. *Hum Mol Genet,* 19, 3566-82.

Nomikou, N., Tiwari, P., Trehan, T., Gulati, K. & Mchale, A. 2012. Studies on Neutral, Cationic and Biotinylated Cationic Microbubbles in Enhancing Ultrasound-Mediated Gene Delivery in Vitro and in Vivo. *Acta Biomater,* 8, 1273-80.

Nzelu, D., Dumitrascu-Biris, D., Hunt, K., Cordina, M. & Kametas, N. 2018. Pregnancy outcomes in women with previous gestational hypertension: A cohort study to guide counselling and management. *Pregnancy Hypertens,* 12, 194-200.

O'brien, J., Hayder, H., Zayed, Y. & Peng, C. 2018. Overview of MicroRNA Biogenesis, Mechanisms of Actions, and Circulation. *Front Endocrinol (Lausanne),* 9, 402.

Ogawa, K., Urayama, K. Y., Tanigaki, S., Sago, H., Sato, S., Saito, S. & Morisaki, N. 2017. Association between very advanced maternal age and adverse pregnancy outcomes: a cross sectional Japanese study. *BMC Pregnancy Childbirth,* 17, 349.

Olofsson, P., Laurini, R. & Marsál, K. 1993. A high uterine artery pulsatility index reflects a defective development of placental bed spiral arteries in pregnancies complicated by hypertension and fetal growth retardation. *Eur J Obstet Gynecol Reprod Biol,* 49, 161-8.

Ordén, M., Leinonen, M. & Kirkinen, P. 2000. Contrast-enhanced ultrasonography of uteroplacental circulation does not evoke harmful CTG changes or perinatal events. *Fetal Diagn Ther,* 15, 139-45.

Ørom, U., Nielsen, F. & Lund, A. 2008. MicroRNA-10a binds the 5'UTR of ribosomal protein mRNAs and enhances their translation. *Mol Cell,* 30, 460-71.

Ospina-Prieto, S., Chaiwangyen, W., Herrmann, J., Groten, T., Schleussner, E., Markert, U. & Morales-Prieto, D. 2016. MicroRNA-141 is upregulated in preeclamptic placentae and regulates trophoblast invasion and intercellular communication. *Transl Res,* 172, 61-72.

Ouyang, Y., Mouillet, J., Coyne, C. & Sadovsky, Y. 2014. Review: placenta-specific microRNAs in exosomes - good things come in nano-packages. *Placenta,* S69-73.

Paller, M. S. 1984. Mechanism of decreased pressor responsiveness to ANG II, NE, and vasopressin in pregnant rats. *Am J Physiol,* 247, H100-8.

Palmer, A. E., London, W. T., Sly, D. L. & Rice, J. M. 1979. Spontaneous preeclamptic toxemia of pregnancy in the patas monkey (Erythrocebus patas). *Lab Anim Sci,* 29, 102-6.

Palmer, K., Saglam, B., Whitehead, C., Stock, O., Lappas, M. & Tong, S. 2011. Severe early-onset preeclampsia is not associated with a change in placental catechol O-methyltransferase (COMT) expression. *Am J Pathol,* 178, 2484-8.

Palmer, S., Moore, L., Young, D., Cregger, B., Berman, J. & Zamudio, S. 1999. Altered blood pressure course during normal pregnancy and increased preeclampsia at high altitude (3100 meters) in Colorado. *Am J Obstet Gynecol,* 180, 1161-8.

Palmer, S., Zamudio, S., Coffin, C., Parker, S., Stamm, E. & Moore, L. 1992. Quantitative estimation of human uterine artery blood flow and pelvic blood flow redistribution in pregnancy. *Obstet Gynecol,* 80**,** 1000-6.

Panje, C., Wang, D., Pysz, M., Paulmurugan, R., Ren, Y., Tranquart, F., Tian, L. & Willmann, J. 2012. Ultrasound-mediated Gene Delivery With Cationic Versus Neutral Microbubbles: Effect of DNA and Microbubble Dose on in Vivo Transfection Efficiency. *Theranostics,* 2**,** 1078-91.

Park, H., Noh, E., Chung, H., Kang, M., Kim, E. & Park, S. 2012. Efficient generation of virus-free iPS cells using liposomal magnetofection. *PLoS One,* 7**,** e45812.

Peng, Z. H., Xiong, Z., Zhao, B. S., Zhang, G. B., Song, W., Tao, L. X. & Zhang, X. Z. 2019. Prophylactic abdominal aortic balloon occlusion: An effective method of controlling hemorrhage in patients with placenta previa or accreta. *Exp Ther Med,* 17**,** 1492-6.

Penn, M., Mendelsohn, F., Schaer, G., Sherman, W., Farr, M., Pastore, J., Rouy, D., Clemens, R., Aras, R. & Losordo, D. 2013. An open-label dose escalation study to evaluate the safety of administration of nonviral stromal cell-derived factor-1 plasmid to treat symptomatic ischemic heart failure. *Circ Res,* 112**,** 816-25.

Petry, C., Marcos, N., Pimentel, G., Hayes, M., Nodzenski, M., Scholtens, D., Hughes, I., Acerini, C., Ong, K., Lowe, W. & Dunger, D. 2016. Associations Between Fetal Imprinted Genes and Maternal Blood Pressure in Pregnancy. *Hypertension,* 68**,** 1459-1466.

Philippidis, A. 2016. Making History with the 1990 Gene Therapy Trial. *Genetic Engineering & Biotechnology News.* GEN.

Pickard, M., Adams, C. & Chari, D. 2017. Magnetic Nanoparticle-Mediated Gene Delivery to Two- and Three-Dimensional Neural Stem Cell Cultures: Magnet-Assisted Transfection and Multifection Approaches to Enhance Outcomes. *Curr Protoc Stem Cell Biol,* 40**,** 2D.19.1-2D.19.16.

Pijnenborg, R., Anthony, J., Davey, D., Rees, A., Tiltman, A., Vercruysse, L. & Van Assche, A. 1991. Placental bed spiral arteries in the hypertensive disorders of pregnancy. *Br J Obstet Gynaecol,* 98**,** 648-55.

Pijnenborg, R., Vercruysse, L. & Carter, A. 2011a. Deep trophoblast invasion and spiral artery remodelling in the placental bed of the lowland gorilla. *Placenta,* 32**,** 586-91.

Pijnenborg, R., Vercruysse, L. & Carter, A. M. 2011b. Deep trophoblast invasion and spiral artery remodelling in the placental bed of the chimpanzee. *Placenta,* 32**,** 400-8.

Pillay, P., Maharaj, N., Moodley, J. & Mackraj, I. 2016. Placental exosomes and pre-eclampsia: Maternal circulating levels in normal pregnancies and, early and late onset pre-eclamptic pregnancies. *Placenta,* 46**,** 18-25.

Pillay, P., Vatish, M., Duarte, R., Moodley, J. & Mackraj, I. 2019. Exosomal microRNA profiling in early and late onset preeclamptic pregnant women reflects pathophysiology. *Int J Nanomedicine,* 14**,** 5637-57.

Pineles, B. L., Romero, R., Montenegro, D., Tarca, A. L., Han, Y. M., Kim, Y. M., Draghici, S., Espinoza, J., Kusanovic, J. P., Mittal, P., Hassan, S. S. & Kim, C. J. 2007. Distinct subsets of microRNAs are expressed differentially in the human placentas of patients with preeclampsia. *American Journal of Obstetrics and Gynecology,* 196**,** 261.e1-261.e6.

Pislaru, S., Pislaru, C., Kinnick, R., Singh, R., Gulati, R., Greenleaf, J. & Simari, R. 2003. Optimization of Ultrasound-Mediated Gene Transfer: Comparison of Contrast Agents and Ultrasound Modalities. *Eur Heart J,* 24**,** 1690-8.

Plotnikova, O., Baranova, A. & Skoblov, M. 2019. Comprehensive Analysis of Human microRNA-mRNA Interactome. *Front Genet,* 10**,** 933.

Postema, M., Van Wamel, A., Lancée, C. & De Jong, N. 2004. Ultrasound-induced encapsulated microbubble phenomena. *Ultrasound Med Biol,* 30**,** 827-40.

Powe, C., Ecker, J., Rana, S., Wang, A., Ankers, E., Ye, J., Levine, R., Karumanchi, S. & Thadhani, R. 2011. Preeclampsia and the risk of large-for-gestational-age infants. *Am J Obstet Gynecol,* 204**,** 425.e1-6.

Powers, R., Jeyabalan, A., Clifton, R., Van Dorsten, P., Hauth, J., Klebanoff, M., Lindheimer, M., Sibai, B., Landon, M. & Miodovnik, M. 2010. Soluble fms-Like tyrosine kinase 1 (sFlt1), endoglin and placental growth factor (PlGF) in preeclampsia among high risk pregnancies. *PLoS One,* 5**,** e13263.

Promega. 2015. *pGL4 Luciferase Reporter Vectors Protocol* [Online]. www.promega.co.uk. Available: https://www.promega.co.uk/resources/protocols/technical-manuals/0/pgl4-luciferase-reporter-vectors-protocol/.

Purswani, J. M., Gala, P., Dwarkanath, P., Larkin, H. M., Kurpad, A. & Mehta, S. 2017. The role of vitamin D in pre-eclampsia: a systematic review. *BMC Pregnancy Childbirth,* 17**,** 231.

Qian, K., Hu, L., Chen, H., Li, H., Liu, N., Li, Y., Ai, J., Zhu, G., Tang, Z. & Zhang, H. 2009. Hsa-miR-222 is involved in differentiation of endometrial stromal cells in vitro. *Endocrinology,* 150**,** 4734-43.

Qiu, C., Coughlin, K., Frederick, I., Sorensen, T. & Williams, M. 2008. Dietary fiber intake in early pregnancy and risk of subsequent preeclampsia. *Am J Hypertens,* 21**,** 903-9.

Qiu, C., Sanchez, S., Lam, N., Garcia, P. & Ma, W. 2007. Associations of depression and depressive symptoms with preeclampsia: results from a Peruvian case-control study. *BMC Womens Health,* 7**,** 15.

Qu, H. M., Qu, L. P., Li, X. Y. & Pan, X. Z. 2018. Overexpressed HO-1 is associated with reduced STAT3 activation in preeclampsia placenta and inhibits STAT3 phosphorylation in placental JEG-3 cells under hypoxia. *Arch Med Sci,* 14**,** 597-607.

Rahim, A., Taylor, S., Bush, N., Ter Haar, G., Bamber, J. & Porter, C. 2006. Physical Parameters Affecting Ultrasound/Microbubble-Mediated Gene Delivery Efficiency in Vitro. *Ultrasound Med Biol,* 32**,** 1269-79.

Rai, A. & Cross, J. 2014. Development of the hemochorial maternal vascular spaces in the placenta through endothelial and vasculogenic mimicry. *Dev Biol,* 387**,** 131-41.

Rakhmilevich, A., Janssen, K., Hao, Z., Sondel, P. & Yang, N. 2000. Interleukin-12 gene therapy of a weakly immunogenic mouse mammary carcinoma results in reduction of spontaneous lung metastases via a T-cell-independent mechanism. *Cancer Gene Ther,* 7**,** 826-38.

Raper, S., Chirmule, N., Lee, F., Wivel, N., Bagg, A., Gao, G., Wilson, J. & Batshaw, M. 2003. Fatal Systemic Inflammatory Response Syndrome in a Ornithine Transcarbamylase Deficient Patient Following Adenoviral Gene Transfer. *Mol Genet Metab,* 80**,** 148-58.

Rasmussen, S. & Irgens, L. 2003. Fetal growth and body proportion in preeclampsia. *Obstet Gynecol,* 101, 575-83.

Raz, T., Avni, R., Addadi, Y., Cohen, Y., Jaffa, A., Hemmings, B., Garbow, J. & Neeman, M. 2012. The Hemodynamic Basis for Positional- And Inter-Fetal Dependent Effects in Dual Arterial Supply of Mouse Pregnancies. *PLoS One,* 7, e52273.

Redman, C. 1991. Current topic: pre-eclampsia and the placenta. *Placenta,* 12, 301-8.

Redman, C. 1992. 10 Immunological aspects of pre-eclampsia. 6, 601-615.

Redman, C., Tannetta, D., Dragovic, R., Gardiner, C., Southcombe, J., Collett, G. & Sargent, I. 2012. Review: Does size matter? Placental debris and the pathophysiology of pre-eclampsia. *Placenta,* S48-54.

Remus, E. W., Lyle, A. N., Weiss, D., Landàzuri, N., Weber, M., Searles, C. & Taylor, W. R. 2013. miR181a protects against angiotensin II-induced osteopontin expression in vascular smooth muscle cells. *Atherosclerosis,* 228, 168-74.

Ren, H., Zhou, L., Liu, M., Lu, W. & Gao, C. 2015. Peptide GE11-Polyethylene Glycol-Polyethylenimine for targeted gene delivery in laryngeal cancer. *Med Oncol,* 32, 185.

Rezaei, M., Mohammadpour-Gharehbagh, A., Narooei-Nejad, M., Teimoori, B., Mokhtari, M., Mehrabani, M., Yaghmaei, M., Najafi, D. & Salimi, S. 2019. The effect of the placental DROSHA rs10719 and rs6877842 polymorphisms on PE susceptibility and mRNA expression. *J Hum Hypertens,* 33, 552-558.

Ries, F. 1997. Clinical experience with echo-enhanced transcranial Doppler and duplex imaging. *J Neuroimaging,* 7.

Roberge, S., Bujold, E. & Nicolaides, K. 2018. Aspirin for the prevention of preterm and term preeclampsia: systematic review and metaanalysis. *Am J Obstet Gynecol,* 218, 287-293.e1.

Roberts, C., Algert, C., Morris, J., Ford, J. & Henderson-Smart, D. 2005. Hypertensive disorders in pregnancy: a population-based study. *Med J Aust,* 182, 332-5.

Roberts, J. & Redman, C. 1993. Pre-eclampsia: more than pregnancy-induced hypertension. *Lancet,* 341, 1447-51.

Roberts, V., Morgan, T., Bednarek, P., Morita, M., Burton, G., Lo, J. & Frias, A. 2017. Early first trimester uteroplacental flow and the progressive disintegration of spiral artery plugs: new insights from contrast-enhanced ultrasound and tissue histopathology. *Hum Reprod,* 32, 2382-2393.

Robillard, P., Hulsey, T., Alexander, G., Keenan, A., De Caunes, F. & Papiernik, E. 1993. Paternity patterns and risk of preeclampsia in the last pregnancy in multiparae. *J Reprod Immunol,* 24, 1-12.

Ropper, A. H., Gorson, K. C., Gooch, C. L., Weinberg, D. H., Pieczek, A., Ware, J. H., Kershen, J., Rogers, A., Simovic, D., Schratzberger, P., Kirchmair, R. & Losordo, D. 2009. VEGF Gene Transfer for Diabetic Polyneuropathy: A Randomized Double Blinded Trial. *Ann Neurol,* 65, 386-93.

Rosen, E. M., Muñoz, M. I., Mcelrath, T., Cantonwine, D. E. & Ferguson, K. K. 2018. Environmental contaminants and preeclampsia: A systematic literature review. *J Toxicol Environ Health B Crit Rev,* 21, 291-319.

Rosenberg, S., Aebersold, P., Cornetta, K., Kasid, A., Morgan, R., Moen, R., Karson, E., Lotze, M., Yang, J. & Topalian, S. 1990. Gene Transfer Into Humans--Immunotherapy of Patients With Advanced Melanoma, Using Tumor-Infiltrating

Lymphocytes Modified by Retroviral Gene Transduction. *N Engl J Med,* 323**,** 570-8.

Roten, L., Johnson, M., Forsmo, S., Fitzpatrick, E., Dyer, T., Brennecke, S., Blangero, J., Moses, E. & Austgulen, R. 2009. Association Between the Candidate Susceptibility Gene ACVR2A on Chromosome 2q22 and Pre-Eclampsia in a Large Norwegian Population-Based Study (The HUNT Study). *European journal of human genetics : EJHG,* 17.

Ruby, J. G., Jan, C. H. & Bartel, D. P. 2007. Intronic microRNA precursors that bypass Drosha processing. *Nature,* 448**,** 83-6.

Ruike, Y., Ichimura, A., Tsuchiya, S., Shimizu, K., Kunimoto, R., Okuno, Y. & Tsujimoto, G. 2008. Global correlation analysis for micro-RNA and mRNA expression profiles in human cell lines. *J Hum Genet,* 53**,** 515.

Saghian, R., Bogle, G., James, J. & Clark, A. 2019. Establishment of maternal blood supply to the placenta: insights into plugging, unplugging and trophoblast behaviour from an agent-based model. *Interface Focus,* 9**,** 20190019.

Sahay, A. S., Jadhav, A. T., Sundrani, D. P., Wagh, G. N. & Joshi, S. R. 2020. Differential Expression of Nerve Growth Factor (NGF) and Brain Derived Neurotrophic Factor (BDNF) in Different Regions of Normal and Preeclampsia Placentae. *Clin Exp Hypertens,* 42**,** 360-364.

Sahay, A. S., Sundrani, D. P., Wagh, G. N., Mehendale, S. S. & Joshi, S. R. 2015. Neurotrophin levels in different regions of the placenta and their association with birth outcome and blood pressure. *Placenta,* 36**,** 938-43.

Saito, S. & Sakai, M. 2003. Th1/Th2 balance in preeclampsia. *J Reprod Immunol,* 59**,** 161-73.

Salim, R., Chulski, A., Romano, S., Garmi, G., Rudin, M. & Shalev, E. 2015. Precesarean Prophylactic Balloon Catheters for Suspected Placenta Accreta: A Randomized Controlled Trial. *Obstet Gynecol,* 126**,** 1022-8.

Salimi, S., Eskandari, F., Rezaei, M., Narooei-Nejad, M., Teimoori, B., Yazdi, A. & Yaghmaei, M. 2019. The effect of miR-146a rs2910164 and miR-149 rs2292832 polymorphisms on preeclampsia susceptibility. *Mol Biol Rep,* 46**,** 4529-4536.

Salomon, C., Guanzon, D., Scholz-Romero, K., Longo, S., Correa, P., Illanes, S. & Rice, G. 2017. Placental Exosomes as Early Biomarker of Preeclampsia: Potential Role of Exosomal MicroRNAs Across Gestation. *J Clin Endocrinol Metab,* 102**,** 3182-3194.

Salonen Ros, H., Lichtenstein, P., Lipworth, L. & Cnattingius, S. 2000. Genetic effects on the liability of developing pre-eclampsia and gestational hypertension. *Am J Med Genet,* 91**,** 256-60.

Sandrim, V., Eleuterio, N., Pilan, E., Tanus-Santos, J., Fernandes, K. & Cavalli, R. 2016a. Plasma levels of increased miR-195-5p correlates with the sFLT-1 levels in preeclampsia. *Hypertens Pregnancy,* 35**,** 150-8.

Sandrim, V. C., Dias, M. C., Bovolato, A. C., Tanus-Santos, J. E., Deffune, E. & Cavalli, R. C. 2016b. Plasma from pre-eclamptic patients induces the expression of the anti-angiogenic miR-195-5p in endothelial cells. *J Cell Mol Med,* 20**,** 1198-200.

Sanghavi, M. & Rutherford, J. 2014. Cardiovascular physiology of pregnancy. *Circulation,* 130**,** 1003-8.

Sarker, S., Scholz-Romero, K., Perez, A., Illanes, S. E., Mitchell, M. D., Rice, G. E. & Salomon, C. 2014. Placenta-derived exosomes continuously increase in

maternal circulation over the first trimester of pregnancy. *J Transl Med,* 12**,** 204.

Sato, H., Hattori, S., Kawamoto, S., Kudoh, I., Hayashi, A., Yamamoto, I., Yoshinari, M., Minami, M. & Kanno, H. 2000. In vivo gene gun-mediated DNA delivery into rodent brain tissue. *Biochem Biophys Res Commun,* 270**,** 163-70.

Sawyer, G., Dong, X., Whitehorne, M., Grehan, A., Seddon, M., Shah, A., Zhang, X. & Fabre, J. 2007. Cardiovascular function following acute volume overload for hydrodynamic gene delivery to the liver. *Gene Ther,* 14**,** 1208-17.

Sawyer, G., Grehan, A., Dong, X., Whitehorne, M., Seddon, M., Shah, A., Zhang, X., Salehi, S. & Fabre, J. 2008. Low-volume hydrodynamic gene delivery to the rat liver via an isolated segment of the inferior vena cava: efficiency, cardiovascular response and intrahepatic vascular dynamics. *J Gene Med,* 10**,** 540-50.

Say, L., Chou, D., Gemmill, A., Tuncalp, O., Moller, A. B., Daniels, J., Gulmezoglu, A. M., Temmerman, M. & Alkema, L. 2014. Global causes of maternal death: a WHO systematic analysis. *Lancet Glob Health,* 2**,** e323-33.

Schleef, M. & Schmidt, T. 2004. Animal-free Production of Ccc-Supercoiled Plasmids for Research and Clinical Applications. *The journal of gene medicine,* 6**,** S45-53.

Schlegel, P., Huditz, R., Meinhardt, E., Rapti, K., Geis, N., Most, P., Katus, H., Müller, O., Bekeredjian, R. & Raake, P. 2016. Locally Targeted Cardiac Gene Delivery by AAV Microbubble Destruction in a Large Animal Model. *Hum Gene Ther Methods,* 27**,** 71-8.

Schlicher, R., Radhakrishna, H., Tolentino, T., Apkarian, R., Zarnitsyn, V. & Prausnitz, M. 2006. Mechanism of intracellular delivery by acoustic cavitation. *Ultrasound Med Biol,* 32**,** 915-24.

Schonkeren, D., Van Der Hoorn, M. L., Khedoe, P., Swings, G., Van Beelen, E., Claas, F., Van Kooten, C., De Heer, E. & Scherjon, S. 2011. Differential distribution and phenotype of decidual macrophages in preeclamptic versus control pregnancies. *Am J Pathol,* 178**,** 709-17.

Seligman, S., Buyon, J., Clancy, R., Young, B. & Abramson, S. 1994. The role of nitric oxide in the pathogenesis of preeclampsia. *Am J Obstet Gynecol,* 171**,** 944-8.

Senior, M. 2017. After Glybera's withdrawal, what's next for gene therapy? *Nature Biotechnology,* 35**,** 491-492.

Shah, P. 1993. Contrast echocardiography — a historical perspective. *Advances in Echo Imaging Using Contrast Enhancement*.

Shankar, K., Zhong, Y., Kang, P., Blackburn, M., Soares, M., Badger, T. & Gomez-Acevedo, H. 2012. RNA-seq analysis of the functional compartments within the rat placentation site. *Endocrinology,* 153**,** 1999-2011.

Shapiro, G., Wong, A., Bez, M., Yang, F., Tam, S., Even, L., Sheyn, D., Ben-David, S., Tawackoli, W., Pelled, G., Ferrara, K. & Gazit, D. 2016. Multiparameter Evaluation of in Vivo Gene Delivery Using Ultrasound-Guided, Microbubble-Enhanced Sonoporation. *J Control Release,* 223**,** 157-164.

Sheikh, A. M., Small, H. Y., Currie, G. & Delles, C. 2016. Systematic Review of Micro-RNA Expression in Pre-Eclampsia Identifies a Number of Common Pathways Associated with the Disease. *PLoS One,* 11**,** e0160808.

Shen, Z., Brayman, A., Chen, L. & Miao, C. 2008. Ultrasound With Microbubbles Enhances Gene Expression of Plasmid DNA in the Liver via Intraportal Delivery. *Gene therapy,* 15**,** 1147-55.

Shennan, A., Green, M. & Chappell, L. 2017. Maternal deaths in the UK: pre-eclampsia deaths are avoidable. *Lancet,* 389**,** 582-584.

Sheyn, D., Kimelman-Bleich, N., Pelled, G., Zilberman, Y., Gazit, D. & Gazit, Z. 2008. Ultrasound-based nonviral gene delivery induces bone formation in vivo. *Gene Ther,* 15**,** 257-66.

Shishehbor, M., Rundback, J., Bunte, M., Hammad, T., Miller, L., Patel, P., Sadanandan, S., Fitzgerald, M., Pastore, J., Kashyap, V. & Henry, T. 2019. SDF-1 plasmid treatment for patients with peripheral artery disease (STOP-PAD): Randomized, double-blind, placebo-controlled clinical trial. *Vasc Med,* 24**,** 200-207.

Sholook, M., Gilbert, J., Sedeek, M., Huang, M., Hester, R. & Granger, J. 2007. Systemic hemodynamic and regional blood flow changes in response to chronic reductions in uterine perfusion pressure in pregnant rats. *Am J Physiol Heart Circ Physiol,* 293**,** H2080-4.

Shrivastava, V., Nageotte, M., Major, C., Haydon, M. & Wing, D. 2007. Case-control comparison of cesarean hysterectomy with and without prophylactic placement of intravascular balloon catheters for placenta accreta. *Am J Obstet Gynecol,* 197**,** 402.e1-5.

Shu, W., Li, H., Gong, H., Zhang, M., Niu, X., Ma, Y., Zhang, X., Cai, W., Yang, G., Wei, M., Yang, N. & Li, Y. 2018. Evaluation of blood vessel injury, oxidative stress and circulating inflammatory factors in an L-NAME-induced preeclampsia-like rat model. *Exp Ther Med,* 16**,** 585-594.

Sibai, B., Ewell, M., Levine, R., Klebanoff, M., Esterlitz, J., Catalano, P., Goldenberg, R. & Joffe, G. 1997. Risk factors associated with preeclampsia in healthy nulliparous women. The Calcium for Preeclampsia Prevention (CPEP) Study Group. *Am J Obstet Gynecol,* 177**,** 1003-10.

Sibbald, B. 2001. Death but one unintended consequence of gene-therapy trial. *CMAJ,* 164**,** 1612.

Sidhu, P., Cantisani, V., Dietrich, C., Gilja, O., Saftoiu, A., Bartels, E., Bertolotto, M., Calliada, F., Clevert, D., Cosgrove, D., Deganello, A., D'onofrio, M., Drudi, F., Freeman, S., Harvey, C., Jenssen, C., Jung, E., Klauser, A., Lassau, N., Meloni, M., Leen, E., Nicolau, C., Nolsoe, C., Piscaglia, F., Prada, F., Prosch, H., Radzina, M., Savelli, L., Weskott, H. & Wijkstra, H. 2018. The EFSUMB Guidelines and Recommendations for the Clinical Practice of Contrast-Enhanced Ultrasound (CEUS) in Non-Hepatic Applications: Update 2017 (Long Version). *Ultraschall Med,* 39**,** e2-e44.

Siefker-Radtke, A., Zhang, X., Guo, C. C., Shen, Y., Pirollo, K. F., Sabir, S., Leung, C., Leong-Wu, C., Ling, C. M., Chang, E. H., Millikan, R. E. & Benedict, W. F. 2016. A Phase l Study of a Tumor-targeted Systemic Nanodelivery System, SGT-94, in Genitourinary Cancers. *Mol Ther,* 24**,** 1484-91.

Singh, K., Williams, J., 3rd, Brown, J., Wang, E. T., Lee, B., Gonzalez, T. L., Cui, J., Goodarzi, M. O. & Pisarska, M. D. 2017. Up-regulation of microRNA-202-3p in first trimester placenta of pregnancies destined to develop severe preeclampsia, a pilot study. *Pregnancy Hypertens,* 10**,** 7-9.

Sirohi, V., Gupta, K., Kapoor, R. & Dwivedi, A. 2019. MicroRNA-145 targets Smad1 in endometrial stromal cells and regulates decidualization in rat. *J Mol Med (Berl),* 97**,** 509-522.

Sirsi, S. & Borden, M. 2009. Microbubble Compositions, Properties and Biomedical Applications. *Bubble Sci Eng Technol,* 1**,** 3-17.

Skjærven, R., Vatten, L. J., Wilcox, A. J., Rønning, T., Irgens, L. M. & Lie, R. T. 2005. Recurrence of pre-eclampsia across generations: exploring fetal and maternal genetic components in a population based cohort. *BMJ,* 331**,** 877.

Smith, M., Waugh, J. & Nelson-Piercy, C. 2013. Management of postpartum hypertension. *Obstet Gynaecol,* 15**,** 45-50.

Smárason, A., Allman, K., Young, D. & Redman, C. 1997. Elevated levels of serum nitrate, a stable end product of nitric oxide, in women with pre-eclampsia. *Br J Obstet Gynaecol,* 104**,** 538-43.

Sohel, M. 2016. Extracellular/Circulating MicroRNAs: Release Mechanisms, Functions and Challenges *Achievements in the Life Sciences,* 10**,** 175-186.

Sohlberg, S., Stephansson, O., Cnattingius, S. & Wikström, A. 2012. Maternal body mass index, height, and risks of preeclampsia. *Am J Hypertens,* 25**,** 120-5.

Soncin, F., Khater, M., To, C., Pizzo, D., Farah, O., Wakeland, A., Arul Nambi Rajan, K., Nelson, K. K., Chang, C. W., Moretto-Zita, M., Natale, D. R., Laurent, L. C. & Parast, M. M. 2018. Comparative analysis of mouse and human placentae across gestation reveals species-specific regulators of placental development. *Development,* 145.

Sondergaard, M., Dagnaes-Hansen, F., Flyvbjerg, A. & Jensen, T. 2003. Normalization of growth in hypophysectomized mice using hydrodynamic transfer of the human growth hormone gene. *Am J Physiol Endocrinol Metab,* 285**,** E427-32.

Song, H., Yang, J., Lo, S., Wang, Y., Fan, W., Tang, X., Xue, J. & Wang, S. 2010. Gene transfer using self-assembled ternary complexes of cationic magnetic nanoparticles, plasmid DNA and cell-penetrating Tat peptide. *Biomaterials,* 31**,** 769-78.

Song, J., Pulkkinen, A., Huang, Y. & Hynynen, K. 2012. Investigation of standing wave formation in a human skull for a clinical prototype of a large-aperture, transcranial MR-guided Focused Ultrasound (MRgFUS) phased array: An experimental and simulation study. *IEEE Trans Biomed Eng,* 59**,** 435-44.

Song, S., Shen, Z., Chen, L., Brayman, A. & Miao, C. 2011. Explorations of High-Intensity Therapeutic Ultrasound and Microbubble-Mediated Gene Delivery in Mouse Liver. *Gene therapy,* 18**,** 1006-14.

Sonoda, S., Tachibana, K., Uchino, E., Okubo, A., Yamamoto, M., Sakoda, K., Hisatomi, T., Sonoda, K., Negishi, Y., Izumi, Y., Takao, S. & Sakamoto, T. 2006. Gene Transfer to Corneal Epithelium and Keratocytes Mediated by Ultrasound With Microbubbles. *Invest Ophthalmol Vis Sci,* 47**,** 558-64.

Sood, R., Zehnder, J. L., Druzin, M. L. & Brown, P. O. 2006. Gene expression patterns in human placenta. *Proc Natl Acad Sci U S A,* 103**,** 5478-83.

Soto-Sánchez, C., Martínez-Navarrete, G., Humphreys, L., Puras, G., Zarate, J., Pedraz, J. & Fernández, E. 2015. Enduring high-efficiency in vivo transfection of neurons with non-viral magnetoparticles in the rat visual cortex for optogenetic applications. *Nanomedicine,* 11**,** 835-4.

Spanggaard, I., Dahlstroem, K., Laessoee, L., Hansen, R., Johannesen, H., Hendel, H., Bouquet, C., Attali, P. & Gehl, J. 2017. Gene therapy for patients with advanced solid tumors: a phase I study using gene electrotransfer to muscle with the integrin inhibitor plasmid AMEP. *Acta Oncol,* 56**,** 909-916.

Spencer, R., Ambler, G., Brodszki, J., Diemert, A., Figueras, F., Gratacós, E., Hansson, S., Hecher, K., Huertas-Ceballos, A., Marlow, N., Marsál, K., Morsing, E., Peebles, D., Rossi, C., Sebire, N., Timms, J. & David, A. 2017. EVERREST prospective study: a 6-year prospective study to define the clinical and biological characteristics of pregnancies affected by severe early onset fetal growth restriction. *BMC Pregnancy Childbirth,* 17**,** 43.

Staff, A. C. 2019. The two-stage placental model of preeclampsia: An update. *J Reprod Immunol,* 134-135**,** 1-10.

Staines-Urias, E., Paez, M., Doyle, P., Dudbridge, F., Serrano, N., Ioannidis, J., Keating, B., Hingorani, A. & Casas, J. 2012. Genetic association studies in pre-eclampsia: systematic meta-analyses and field synopsis. *Int J Epidemiol,* 41**,** 1764-75.

Stanek, J. 2018. Placental pathology varies in hypertensive conditions of pregnancy. *Virchows Arch,* 472**,** 415-423.

Stanley, J., Andersson, I., Poudel, R., Rueda-Clausen, C., Sibley, C., Davidge, S. & Baker, P. 2012. Sildenafil citrate rescues fetal growth in the catechol-O-methyl transferase knockout mouse model. *Hypertension,* 59**,** 1021-8.

Stein, R. 2019. At $2.1 Million, New Gene Therapy Is The Most Expensive Drug Ever. *Health inc*. www.npr.org: NPR.

Steinl, D., Xu, L., Khanicheh, E., Ellertsdottir, E., Ochoa-Espinosa, A., Mitterhuber, M., Glatz, K., Kuster, G. & Kaufmann, B. 2016. Noninvasive Contrast-Enhanced Ultrasound Molecular Imaging Detects Myocardial Inflammatory Response in Autoimmune Myocarditis. *Circ Cardiovasc Imaging,* 9**,** e004720.

Stewart, D. J., Kutryk, M. J., Fitchett, D., Freeman, M., Camack, N., Su, Y., Siega, A. D., Bilodeau, L., Burton, J. R., Proulx, G. & Radhakrishnan, S. 2009. VEGF Gene Therapy Fails to Improve Perfusion of Ischemic Myocardium in Patients With Advanced Coronary Disease: Results of the NORTHERN Trial. *Mol Ther,* 17**,** 1109-15.

Stoll, B. J., Hansen, N. I., Bell, E. F., Walsh, M. C., Carlo, W. A., Shankaran, S., Laptook, A. R., Sánchez, P. J., Van Meurs, K. P., Wyckoff, M., Das, A., Hale, E. C., Ball, M. B., Newman, N. S., Schibler, K., Poindexter, B. B., Kennedy, K. A., Cotten, C. M., Watterberg, K. L., D'angio, C. T., Demauro, S. B., Truog, W. E., Devaskar, U. & Higgins, R. D. 2015. Trends in Care Practices, Morbidity, and Mortality of Extremely Preterm Neonates, 1993–2012. *JAMA,* 314**,** 1039-51.

Su, D. M. 2016. Correlation of STAT4 and STAT6 expression levels in preeclampsia placenta with sFlt-1 and ADMA generation as well as placental hypoxia. *Journal of Hainan Medical University,* 22**,** 50-53(4).

Su, H., Trombly, M. I., Chen, J. & Wang, X. 2009. Essential and overlapping functions for mammalian Argonautes in microRNA silencing. *Genes Dev,* 23**,** 304-17.

Su, Z., Frost, E., Lammert, C., Przanowska, R., Lukens, J. & Dutta, A. 2020. tRNA-derived fragments and microRNAs in the maternal-fetal interface of a mouse maternal-immune-activation autism model. *RNA Biol,* 17**,** 1183-1195.

Suda, T., Suda, K. & Liu, D. 2008. Computer-assisted hydrodynamic gene delivery. *Mol Ther,* 16**,** 1098-104.

Sufit, R., Ajroud-Driss, S., Casey, P. & Kessler, J. 2017. Open label study to assess the safety of VM202 in subjects with amyotrophic lateral sclerosis. *Amyotroph Lateral Scler Frontotemporal Degener,* 18**,** 269-278.

Sun, C., Hu, Y., Chu, Z., Huang, J. & Zhang, L. 2009. The effect of brain-derived neurotrophic factor on angiogenesis. *J Huazhong Univ Sci Technolog Med Sci,* 29**,** 139-43.

Sun, W., Burkholder, J., Sun, J., Culp, J., Turner, J., Lu, X., Pugh, T., Ershler, W. & Yang, N. 1995. In vivo cytokine gene transfer by gene gun reduces tumor growth in mice. *Proc Natl Acad Sci U S A,* 92**,** 2889-93.

Sun, W., Duan, S., Xin, G., Xiao, J., Hong, F., Hong, H., Wu, Y. & Xu, Y. 2018. Safety and efficacy of preoperative abdominal Aortic balloon occlusion in placenta increta and/or percreta. *J Surg Res,* 222**,** 75-84.

Swanson, A. & David, A. 2015. Animal models of fetal growth restriction: Considerations for translational medicine. *Placenta,* 36**,** 623-30.

Swanson, A. M., Rossi, C. A., Ofir, K., Mehta, V., Boyd, M., Barker, H., Ledwozyw, A., Vaughan, O., Martin, J., Zachary, I., Sebire, N., Peebles, D. M. & David, A. L. 2016. Maternal Therapy with Ad.VEGF-A165 Increases Fetal Weight at Term in a Guinea-Pig Model of Fetal Growth Restriction. *Hum Gene Ther,* 27**,** 997-1007.

Sweetman, D., Goljanek, K., Rathjen, T., Oustanina, S., Braun, T., Dalmay, T. & Münsterberg, A. 2008. Specific requirements of MRFs for the expression of muscle specific microRNAs, miR-1, miR-206 and miR-133. *Dev Biol,* 321**,** 491-9.

Takahashi, H., Ohkuchi, A., Kuwata, T., Usui, R., Baba, Y., Suzuki, H., Chaw, K. T., Matsubara, S., Saito, S. & Takizawa, T. 2017. Endogenous and exogenous miR-520c-3p modulates CD44-mediated extravillous trophoblast invasion. *Placenta,* 50**,** 25-31.

Tan, C., Ho, J., Chong, Y., Loganath, A., Chan, Y., Ravichandran, J., Lee, C. & Chong, S. 2008. Paternal contribution of HLA-G*0106 significantly increases risk for pre-eclampsia in multigravid pregnancies. *Mol Hum Reprod,* 14**,** 317-24.

Tang, L., Yang, M., Qin, L., Li, X., He, G., Liu, X. & Xu, W. 2020. Deficiency of DICER reduces the invasion ability of trophoblasts and impairs the pro-angiogenic effect of trophoblast-derived microvesicles. *J Cell Mol Med,* 24**,** 4915-30.

Tannetta, D., Collett, G., Vatish, M., Redman, C. & Sargent, I. 2017a. Syncytiotrophoblast extracellular vesicles – Circulating biopsies reflecting placental health. *Placenta,* 52**,** 134-8.

Tannetta, D., Masliukaite, I., Vatish, M., Redman, C. & Sargent, I. 2017b. Update of syncytiotrophoblast derived extracellular vesicles in normal pregnancy and preeclampsia. *J Reprod Immunol,* 119**,** 98-106.

Tenhola, S., Rahiala, E., Halonen, P., Vanninen, E. & Voutilainen, R. 2006. Maternal preeclampsia predicts elevated blood pressure in 12-year-old children: evaluation by ambulatory blood pressure monitoring. *Pediatr Res,* 59**,** 320-4.

Teune, M., Bakhuizen, S., Gyamfi, B., C, Opmeer, B., Van Kaam, A., Van Wassenaer, A., Morris, J. & Mol, B. 2011. A systematic review of severe morbidity in infants born late preterm. *Am J Obstet Gynecol,* 205**,** 374.e1-9.

Thaker, P. H., Brady, W. E., Lankes, H. A., Odunsi, K., Bradley, W. H., Moore, K. N., Muller, C. Y., Anwer, K., Schilder, R. J., Alvarez, R. D. & Fracasso, P. M. 2017. A phase I trial of intraperitoneal GEN-1, an IL-12 plasmid formulated with PEG-PEI-cholesterol lipopolymer, administered with pegylated liposomal doxorubicin in patients with recurrent or persistent epithelial ovarian, fallopian tube or primary peritoneal cancers: An NRG Oncology/Gynecologic Oncology Group study. *Gynecol Oncol,* 147**,** 283-90.

Thamotharan, S., Chu, A., Kempf, K., Janzen, C., Grogan, T., Elashoff, D. A. & Devaskar, S. U. 2017. Differential microRNA expression in human placentas of term intra-uterine growth restriction that regulates target genes mediating angiogenesis and amino acid transport. *PLoS One,* 12**,** e0176493.

Thilaganathan, B. & Kalafat, E. 2019. Cardiovascular System in Preeclampsia and Beyond. *Hypertension,* 73**,** 522-531.

Thornton, J. G. & Onwude, J. L. 1992. Convulsions in pregnancy in related gorillas. *Am J Obstet Gynecol,* 167**,** 240-1.

Thévenot, E., Jordão, J., O'reilly, M., Markham, K., Weng, Y., Foust, K., Kaspar, B., Hynynen, K. & Aubert, I. 2012. Targeted delivery of self-complementary adeno-associated virus serotype 9 to the brain, using magnetic resonance imaging-guided focused ultrasound. *Hum Gene Ther,* 23**,** 1144-55.

Timofeeva, A. V., Gusar, V. A., Kan, N. E., Prozorovskaya, K. N., Karapetyan, A. O., Bayev, O. R., Chagovets, V. V., Kliver, S. F., Iakovishina, D. Y., Frankevich, V. E. & Sukhikh, G. T. 2018. Identification of potential early biomarkers of preeclampsia. *Placenta,* 61**,** 61-71.

Tinsley, J. H., Chiasson, V. L., Mahajan, A., Young, K. J. & Mitchell, B. M. 2009. Toll-like receptor 3 activation during pregnancy elicits preeclampsia-like symptoms in rats. *Am J Hypertens,* 12**,** 1314-9.

Toldi, G., Svec, P., Vasarhelyi, B., Meszaros, G., Rigo, J., Tulassay, T. & Treszl, A. 2008. Decreased number of FoxP3+ regulatory T cells in preeclampsia. *Acta Obstet Gynecol Scand,* 87**,** 1229-33.

Torloni, M., Vedmedovska, N., Merialdi, M., Betrán, A., Allen, T., González, R., Platt, L. & Group, F. G. S. 2009. Safety of ultrasonography in pregnancy: WHO systematic review of the literature and meta-analysis. *Ultrasound Obstet Gynecol,* 33**,** 599-608.

Townsend, R., O'brien, P. & Khalil, A. 2016. Current best practice in the management of hypertensive disorders in pregnancy. *Integr Blood Press Control,* 9**,** 79-94.

Trabucchi, M., Briata, P., Garcia-Mayoral, M., Haase, A. D., Filipowicz, W., Ramos, A., Gherzi, R. & Rosenfeld, M. G. 2009. The RNA-binding Protein KSRP Promotes the Biogenesis of a Subset of miRNAs. *Nature,* 459**,** 1010-4.

Tran, D., Zhang, F., Morrison, K., Loeb, K., Harrang, J., Kajimoto, M., Chavez, F., Wu, L. & Miao, C. 2019. Transcutaneous Ultrasound-Mediated Nonviral Gene Delivery to the Liver in a Porcine Model. *Molecular therapy. Methods & clinical development,* 26**,** 275-284.

Tranquilli, A., Brown, M., Zeeman, G., Dekker, G. & Sibai, B. 2013. The definition of severe and early-onset preeclampsia. Statements from the International Society for the Study of Hypertension in Pregnancy (ISSHP). *Pregnancy Hypertens,* 3**,** 44-7.

Tranquilli, A. L., Dekker, G., Magee, L., Roberts, J., Sibai, B. M., Steyn, W., Zeeman, G. G. & Brown, M. A. 2014. The classification, diagnosis and management of the hypertensive disorders of pregnancy: A revised statement from the ISSHP. *Pregnancy Hypertens,* 4**,** 97-104.

Triche, E. W., Uzun, A., Dewan, A. T., Kurihara, I., Liu, J., Occhiogrosso, R., Shen, B., Parker, J. & Padbury, J. F. 2014. Bioinformatic approach to the genetics of preeclampsia. *Obstet Gynecol,* 123**,** 1155-61.

Trogstad, L., Eskild, A., Magnus, P., Samuelsen, S. & Nesheim, B. 2001. Changing paternity and time since last pregnancy; the impact on pre-eclampsia risk. A

study of 547 238 women with and without previous pre-eclampsia. *Int J Epidemiol,* 30**,** 1317-22.

Trueb, B. 2011. Biology of FGFRL1, the fifth fibroblast growth factor receptor. *Cell Mol Life Sci,* 68**,** 951-64.

Truesdell, S. S., Mortensen, R. D., Seo, M., Schroeder, J. C., Lee, J. H., Letonqueze, O. & Vasudevan, S. 2012. MicroRNA-mediated mRNA Translation Activation in Quiescent Cells and Oocytes Involves Recruitment of a Nuclear microRNP. *Sci Rep,* 2**,** 842.

Truong, G., Guanzon, D., Kinhal, V., Elfeky, O., Lai, A., Longo, S., Nuzhat, Z., Palma, C., Scholz-Romero, K., Menon, R., Mol, B. W., Rice, G. E. & Salomon, C. 2017. Oxygen tension regulates the miRNA profile and bioactivity of exosomes released from extravillous trophoblast cells – Liquid biopsies for monitoring complications of pregnancy. *PLoS One,* 12**,** e0174514.

Tsamou, M., Martens, D. S., Winckelmans, E., Madhloum, N., Cox, B., Gyselaers, W., Nawrot, T. S. & Vrijens, K. 2017. Mother's Pre-pregnancy BMI and Placental Candidate miRNAs: Findings from the ENVIRONAGE Birth Cohort. *Sci Rep,* 7**,** 5548.

Tsochandaridis, M., Nasca, L., Toga, C. & Levy-Mozziconacci, A. 2015. Circulating MicroRNAs as Clinical Biomarkers in the Predictions of Pregnancy Complications. *Biomed Res Int,* 2015**,** 294954.

Tsunoda, S., Mazda, O., Oda, Y., Iida, Y., Akabame, S., Kishida, T., Shin-Ya, M., Asada, H., Gojo, S., Imanishi, J., Matsubara, H. & Yoshikawa, T. 2005. Sonoporation using microbubble BR14 promotes pDNA/siRNA transduction to murine heart. *Biochem Biophys Res Commun,* 336**,** 118-27.

Turco, M. & Moffett, A. 2019. Development of the human placenta. *Development,* 146**,** dev163428.

Türkay, A., Saunders, T. & Kurachi, K. 1999. Intrauterine gene transfer: gestational stage-specific gene delivery in mice. *Gene Ther,* 6**,** 1685-94.

Ugen, K., Kutzler, M., Marrero, B., Westover, J., Coppola, D., Weiner, D. & Heller, R. 2006. Regression of subcutaneous B16 melanoma tumors after intratumoral delivery of an IL-15-expressing plasmid followed by in vivo electroporation. *Cancer Gene Ther,* 13**,** 969-74.

Umemura, K., Ishioka, S., Endo, T., Ezaka, Y., Takahashi, M. & Saito, T. 2013. Roles of microRNA-34a in the pathogenesis of placenta accreta. *J Obstet Gynaecol Res,* 39**,** 67-74.

Ura, B., Feriotto, G., Monasta, L., Bilel, S., Zweyer, M. & Celeghini, C. 2014. Potential role of circulating microRNAs as early markers of preeclampsia. *Taiwan J Obstet Gynecol,* 2**,** 232-4.

Van Den Bekerom, M., Van Der Windt, D., Ter Riet, G., Van Der Heijden, G. & Bouter, L. 2011. Therapeutic ultrasound for acute ankle sprains. *Cochrane Database Syst Rev,* 2011**,** CD001250.

Van Der Loo, J. & Wright, J. 2016. Progress and challenges in viral vector manufacturing. *Hum Mol Genet,* 25**,** R42-52.

Van Wamel, A., Kooiman, K., Harteveld, M., Emmer, M., Ten Cate, F., Versluis, M. & De Jong, N. 2006. Vibrating microbubbles poking individual cells: drug transfer into cells via sonoporation. *J Control Release,* 112**,** 149-55.

Vashukova, E. S., Glotov, A. S., Fedotov, P. V., Efimova, O. A., Pakin, V. S., Mozgovaya, E. V., Pendina, A. A., Tikhonov, A. V., Koltsova, A. S. & Baranov, V.

S. 2016. Placental microRNA expression in pregnancies complicated by superimposed preeclampsia on chronic hypertension. *Mol Med Rep,* 14**,** 22-32.

Vatten, L., Romundstad, P., Holmen, T., Hsieh, C., Trichopoulos, D. & Stuver, S. 2003. Intrauterine exposure to preeclampsia and adolescent blood pressure, body size, and age at menarche in female offspring. *Obstet Gynecol,* 101**,** 529-33.

Ventura, A., Young, A. G., Winslow, M. M., Lintault, L., Meissner, A., Erkeland, S. J., Newman, J., Bronson, R. T., Crowley, D., Stone, J. R., Jaenisch, R., Sharp, P. A. & Jacks, T. 2008. Targeted deletion reveals essential and overlapping functions of the miR-17~92 family of miRNA clusters. *Cell,* 132**,** 875-86.

Verwoerd, G., Hall, D., Grové, D., Maritz, J. & Odendaal, H. 2002. Primipaternity and duration of exposure to sperm antigens as risk factors for pre-eclampsia. *Int J Gynaecol Obstet,* 78**,** 121-6.

Vogel, J. P., Souza, J. P., Mori, R., Morisaki, N., Lumbiganon, P., Laopaiboon, M., Ortiz-Panozo, E., Hernandez, B., Perez-Cuevas, R., Roy, M., Mittal, S., Cecatti, J. G., Tuncalp, O. & Gulmezoglu, A. M. 2014. Maternal complications and perinatal mortality: findings of the World Health Organization Multicountry Survey on Maternal and Newborn Health. *Bjog,* 121 Suppl 1**,** 76-88.

Vousden, N., Lawley, E., Seed, P. T., Gidiri, M. F., Goudar, S., Sandall, J., Chappell, L. C. & Shennan, A. H. 2019. Incidence of eclampsia and related complications across 10 low- and middle-resource geographical regions: Secondary analysis of a cluster randomised controlled trial. *PLoS Med,* 16**,** e1002775.

Wang, D., Panje, C., Pysz, M., Paulmurugan, R., Rosenberg, J., Gambhir, S., Schneider, M. & Willmann, J. 2012a. Cationic versus neutral microbubbles for ultrasound-mediated gene delivery in cancer. *Radiology,* 264**,** 721-32.

Wang, D., Zhang, Z., O'loughlin, E., Wang, L., Fan, X., Lai, E. C. & Yi, R. 2013. MicroRNA-205 Controls Neonatal Expansion of Skin Stem Cells by Modulating the PI3K Pathway. *Nat Cell Biol,* 15**,** 1153-63.

Wang, H., Yang, L., Wu, J., Sun, L., Wu, J., Tian, H., Weisel, R. & Li, R. 2014a. Reduced ischemic injury after stroke in mice by angiogenic gene delivery via ultrasound-targeted microbubble destruction. *J Neuropathol Exp Neurol,* 73**,** 548-58.

Wang, H., Zhang, L., Guo, X., Bai, Y., Li, Y., Sha, J., Peng, C., Wang, Y. & Liu, M. 2018a. MiR-195 Modulates Oxidative Stress-Induced Apoptosis and Mitochondrial Energy Production in Human Trophoblasts via Flavin Adenine Dinucleotide-Dependent Oxidoreductase Domain-Containing Protein 1 and Pyruvate Dehydrogenase Phosphatase Regulatory Subunit. *J Hypertens,* 36.

Wang, H., Zhao, Y., Luo, R., Bian, X., Wang, Y., Shao, X., Li, Y. X., Liu, M. & Wang, Y. L. 2020a. A positive feedback self-regulatory loop between miR-210 and HIF-1alpha mediated by CPEB2 is involved in trophoblast syncytialization: implication of trophoblast malfunction in preeclampsia. *Biol Reprod,* 102**,** 560-570.

Wang, H., Zhao, Y., Luo, R., Bian, X., Wang, Y., Shao, X., Li, Y. X., Liu, M. & Wang, Y. L. 2020b. A positive feedback self-regulatory loop between miR-210 and HIF-1alpha mediated by CPEB2 is involved in trophoblast syncytialization: implication of trophoblast malfunction in preeclampsiadagger. *Biol Reprod,* 102**,** 560-570.

Wang, J., Knottnerus, A., Schuit, G., Norman, R., Chan, A. & Dekker, G. 2002. Surgically obtained sperm, and risk of gestational hypertension and pre-eclampsia. *Lancet,* 359**,** 673-4.

Wang, M., Zhang, Y., Cai, C., Tu, J., Guo, X. & Zhang, D. 2018b. Sonoporation-induced cell membrane permeabilization and cytoskeleton disassembly at varied acoustic and microbubble-cell parameters. *Sci Rep,* 8**,** 3885.

Wang, N., Feng, Y., Xu, J., Zou, J., Chen, M., He, Y., Liu, H., Xue, M. & Gu, Y. 2018c. miR-362-3p regulates cell proliferation, migration and invasion of trophoblastic cells under hypoxia through targeting Pax3. *Biomed Pharmacother,* 99**,** 462-468.

Wang, R., Liu, W., Liu, X., Liu, X., Tao, H., Wu, D., Zhao, Y. & Zou, L. 2019a. MicroRNA-210 regulates human trophoblast cell line HTR-8/SVneo function by attenuating Notch1 expression: Implications for the role of microRNA-210 in pre-eclampsia. *Mol Reprod Dev,* 86**,** 896-907.

Wang, S., Aurora, A. B., Johnson, B. A., Qi, X., Mcanally, J., Hill, J. A., Richardson, J. A., Bassel-Duby, R. & Olson, E. N. 2008. The endothelial-specific microRNA miR-126 governs vascular integrity and angiogenesis. *Dev Cell. 2008 Aug;15(2):261-71.,* 2**,** 261-71.

Wang, S., Wang, X., Weng, Z., Zhang, S., Ning, H. & Li, B. 2017. Expression and role of microRNA 18b and hypoxia inducible factor-1alpha in placental tissues of preeclampsia patients. *Exp Ther Med,* 14**,** 4554-4560.

Wang, W., Feng, L., Zhang, H., Hachy, S., Satohisa, S., Laurent, L. C., Parast, M., Zheng, J. & Chen, D. B. 2012b. Preeclampsia up-regulates angiogenesis-associated microRNA (i.e., miR-17, -20a, and -20b) that target ephrin-B2 and EPHB4 in human placenta. *J Clin Endocrinol Metab,* 97**,** E1051-9.

Wang, X., Athayde, N. & Trudinger, B. 2006. Egr-1 transcription activation exists in placental endothelium when vascular disease is present. *Bjog,* 113**,** 683-7.

Wang, X., Liang, H., Dong, B., Lu, Q. & Blomley, M. 2005. Gene Transfer With Microbubble Ultrasound and Plasmid DNA Into Skeletal Muscle of Mice: Comparison Between Commercially Available Microbubble Contrast Agents. *Radiology,* 237**,** 224-9.

Wang, X., Peng, S., Cui, K., Hou, F., Ding, J., Li, A., Wang, M. & Geng, L. 2020c. MicroRNA-576-5p enhances the invasion ability of trophoblast cells in preeclampsia by targeting TFAP2A. *Mol Genet Genomic Med,* 8**,** e1025.

Wang, X., Xu, X., Ma, Z., Huo, Y., Xiao, Z., Li, Y. & Wang, Y. 2011. Dynamic mechanisms for pre-miRNA binding and export by Exportin-5. *RNA,* 17**,** 1511-28.

Wang, Y., Dong, Q., Gu, Y. & Groome, L. J. 2016. Up-regulation of miR-203 expression induces endothelial inflammatory response: potential role in preeclampsia. *Am J Reprod Immunol,* 76**,** 482-90.

Wang, Y., Fan, H., Zhao, G., Liu, D., Du, L., Wang, Z., Hu, Y. & Hou, Y. 2012c. miR-16 inhibits the proliferation and angiogenesis-regulating potential of mesenchymal stem cells in severe pre-eclampsia. *Febs j,* 279**,** 4510-24.

Wang, Y., Li, Y., Yan, K., Shen, L., Yang, W., Gong, J. & Ding, K. 2018d. Clinical study of ultrasound and microbubbles for enhancing chemotherapeutic sensitivity of malignant tumors in digestive system. *Chin J Cancer Res,* 30**,** 553-563.

Wang, Y., Lumbers, E., Arthurs, A., Corbisier De Meaultsart, C., Mathe, A., Avery-Kiejda, K., Roberts, C., Pipkin, F., Marques, F., Morris, B. & Pringle, K.

2018e. Regulation of the human placental (pro)renin receptor-prorenin-angiotensin system by microRNAs. *Mol Hum Reprod,* 24**,** 453-464.

Wang, Y., Zhang, Y., Wang, H., Wang, J., Zhang, Y., Wang, Y., Pan, Z. & Luo, S. 2014b. Aberrantly up-regulated miR-20a in pre-eclampsic placenta compromised the proliferative and invasive behaviors of trophoblast cells by targeting forkhead box protein A1. *Int J Biol Sci,* 10**,** 973-82.

Wang, Z., Wang, P., Qin, Z., Xiu, X., Xu, D., Zhang, X. & Wang, Y. 2019b. MiRNA-548c-5p downregulates inflammatory response in preeclampsia via targeting PTPRO. *J Cell Physiol,* 234**,** 11149-11155.

Weber, J. A., Baxter, D. H., Zhang, S., Huang, D. Y., Huang, K. H., Lee, M. J., Galas, D. J. & Wang, K. 2010. The MicroRNA Spectrum in 12 Body Fluids. *Clin Chem,* 56**,** 1733-41.

Weber, M., Kuhn, C., Schulz, S., Schiessl, B., Schleussner, E., Jeschke, U., Markert, U. R. & Fitzgerald, J. S. 2012. Expression of signal transducer and activator of transcription 3 (STAT3) and its activated forms is negatively altered in trophoblast and decidual stroma cells derived from preeclampsia placentae. *Histopathology,* 60**,** 657-62.

Weedon-Fekjær, M. S., Sheng, Y., Sugulle, M., Johnsen, G. M., Herse, F., Redman, C. W., Lyle, R., Dechend, R. & Staff, A. C. 2014. Placental miR-1301 is dysregulated in early-onset preeclampsia and inversely correlated with maternal circulating leptin. *Placenta,* 9**,** 709-17.

Wei, J., Blenkiron, C., Tsai, P., James, J. L., Chen, Q., Stone, P. R. & Chamley, L. W. 2017. Placental trophoblast debris mediated feto-maternal signalling via small RNA delivery: implications for preeclampsia. *Sci Rep,* 7**,** 14681.

White, W., Sun, Z., Borowski, K., Brost, B., Davies, N., Rose, C. & Garovic, V. 2016. Preeclampsia/Eclampsia candidate genes show altered methylation in maternal leukocytes of preeclamptic women at the time of delivery. *Hypertens Pregnancy,* 35**,** 394-404.

Whitehead, C. L., Teh, W. T., Walker, S. P., Leung, C., Larmour, L. & Tong, S. 2013. Circulating MicroRNAs in Maternal Blood as Potential Biomarkers for Fetal Hypoxia In-Utero. *PLoS One,* 8.

Who 2012. Born too soon: the global action report on preterm birth. World Health Organization.

Willenbrock, H., Salomon, J., Sokilde, R., Barken, K. B., Hansen, T. N., Nielsen, F. C., Moller, S. & Litman, T. 2009. Quantitative miRNA expression analysis: comparing microarrays with next-generation sequencing. *Rna,* 15**,** 2028-34.

Williams, P. J. & Broughton Pipkin, F. 2011. The genetics of pre-eclampsia and other hypertensive disorders of pregnancy. *Best Pract Res Clin Obstet Gynaecol,* 25**,** 405-17.

Williams, P. J., Bulmer, J. N., Searle, R. F., Innes, B. A. & Robson, S. C. 2009. Altered decidual leucocyte populations in the placental bed in pre-eclampsia and foetal growth restriction: a comparison with late normal pregnancy. *Reproduction,* 138**,** 177-84.

Williams, Z., Ben-Dov, I. Z., Elias, R., Mihailovic, A., Brown, M., Rosenwaks, Z. & Tuschl, T. 2013. Comprehensive profiling of circulating microRNA via small RNA sequencing of cDNA libraries reveals biomarker potential and limitations. *Proc Natl Acad Sci U S A,* 110**,** 4255-60.

Windrim, R., Kingdom, J., Jang, H. & Burns, P. 2016. Contrast enhanced ultrasound (CEUS) in the prenatal evaluation of suspected invasive placenta percreta. *J Obstet Gynaecol Can,* 38**,** 975-978.

Wolschek, M., Thallinger, C., Kursa, M., Rössler, V., Allen, M., Lichtenberger, C., Kircheis, R., Lucas, T., Willheim, M., Reinisch, W., Gangl, A., Wagner, E. & Jansen, B. 2002. Specific systemic nonviral gene delivery to human hepatocellular carcinoma xenografts in SCID mice. *Hepatology,* 36**,** 1106-14.

Wong, A. Y., Kulandavelu, S., Whiteley, K. J., Qu, D., Langille, B. L. & Adamson, S. L. 2002. Maternal cardiovascular changes during pregnancy and postpartum in mice. *Am J Physiol Heart Circ Physiol,* 282**,** H918-25.

Wong, B., El-Jack, S., Newcombe, R., Glenie, T., Armstrong, G., Cicovic, A. & Khan, A. 2019. Shockwave Intravascular Lithotripsy of Calcified Coronary Lesions in ST-Elevation Myocardial Infarction: First-in-Man Experience. *J Invasive Cardiol,* 31**,** E73-E75.

Woo, Y., Raju, G., Swain, J., Richmond, M., Gardner, T. & Balice-Gordon, R. 1997. In utero cardiac gene transfer via intraplacental delivery of recombinant adenovirus. *Circulation,* 96**,** 3561-9.

Wu, H., Wang, H., Liu, M., Bai, Y., Li, Y. X., Ji, L., Peng, C., Yu, Y. & Wang, Y. L. 2016. MiR-195 participates in the placental disorder of preeclampsia via targeting activin receptor type-2B in trophoblastic cells. *J Hypertens,* 34**,** 1371-9.

Wu, L., Song, W.-Y., Xie, Y., Hu, L.-L., Hou, X.-M., Wang, R., Gao, Y., Zhang, J.-N., Zhang, L., Li, W.-W., Zhu, C., Gao, Z.-Y. & Sun, Y.-P. 2018. miR-181a-5p suppresses invasion and migration of HTR-8/SVneo cells by directly targeting IGF2BP2. *Cell Death & Disease,* 9**,** 1-14.

Wu, P., Haththotuwa, R., Kwok, C., Babu, A., Kotronias, R., Rushton, C., Zaman, A., Fryer, A., Kadam, U., Chew-Graham, C. & Mamas, M. 2017. Preeclampsia and Future Cardiovascular Health: A Systematic Review and Meta-Analysis. *Circ Cardiovasc Qual Outcomes,* 10**,** e003497.

Wu, S., Li, L., Wang, G., Shen, W., Xu, Y., Liu, Z., Zhuo, Z., Xia, H., Gao, Y. & Tan, K. 2014. Ultrasound-targeted stromal cell-derived factor-1-loaded microbubble destruction promotes mesenchymal stem cell homing to kidneys in diabetic nephropathy rats. *Int J Nanomedicine,* 9**,** 5639-51.

Wu, S., Sun, H. & Sun, B. 2020. MicroRNA-145 is involved in endothelial cell dysfunction and acts as a promising biomarker of acute coronary syndrome. *Eur J Med Res,* 25**,** 2.

Xiao, J., Tao, T., Yin, Y., Zhao, L., Yang, L. & Hu, L. 2017. miR-144 may regulate the proliferation, migration and invasion of trophoblastic cells through targeting PTEN in preeclampsia. *Biomed Pharmacother,* 94**,** 341-353.

Xie, A., Belcik, T., Qi, Y., Morgan, T., Champaneri, S., Taylor, S., Davidson, B., Zhao, Y., Klibanov, A., Kuliszewski, M., Leong-Poi, H., Ammi, A. & Lindner, J. 2012. Ultrasound-mediated Vascular Gene Transfection by Cavitation of Endothelial-Targeted Cationic Microbubbles. *JACC Cardiovasc Imaging,* 5**,** 1253-62.

Xie, M., Li, M., Vilborg, A., Lee, N., Shu, M. D., Yartseva, V., Šestan, N. & Steitz, J. A. 2013. Mammalian 5′-capped microRNA precursors that generate a single microRNA. *Cell,* 155**,** 1568-80.

Xiong, X., Demianczuk, N., Buekens, P. & Saunders, L. 2000. Association of preeclampsia with high birth weight for age. *Am J Obstet Gynecol,* 183**,** 148-55.

Xiong, X., Yan, P., Gao, C., Sun, Q. & Xu, F. 2016. The Value of Contrast-Enhanced Ultrasound in the Diagnosis of Cesarean Scar Pregnancy. *Biomed Res Int,* 2016**,** 4762785.

Xu, C., Li, X., Guo, P. & Wang, J. 2017. Hypoxia-Induced Activation of JAK/STAT3 Signaling Pathway Promotes Trophoblast Cell Viability and Angiogenesis in Preeclampsia. *Med Sci Monit,* 23**,** 4909-4917.

Xu, P., Zhao, Y., Liu, M., Wang, Y., Wang, H., Li, Y. X., Zhu, X., Yao, Y., Wang, H., Qiao, J., Ji, L. & Wang, Y. L. 2014a. Variations of microRNAs in human placentas and plasma from preeclamptic pregnancy. *Hypertension,* 63**,** 1276-84.

Xu, W., San Lucas, A., Wang, Z. & Liu, Y. 2014b. Identifying microRNA targets in different gene regions. *BMC Bioinformatics,* 15**,** S4.

Xue, F., Yang, J., Li, Q. & Zhou, H. 2019. Down-regulation of microRNA-34a-5p promotes trophoblast cell migration and invasion via targetting Smad4. *Biosci Rep,* 39.

Yamamoto, N., Koga, K., Akahane, M., Wada-Hiraike, O., Fujii, T. & Osuga, Y. 2015. Temporary balloon occlusion of the uterine arteries to control hemorrhage during hysterectomy in a case of uterine arteriovenous fistula. *J Obstet Gynaecol Res,* 41**,** 314-8.

Yan, T., Cui, K., Huang, X., Ding, S., Zheng, Y., Luo, Q., Liu, X. & Zou, L. 2014. Assessment of therapeutic efficacy of miR-126 with contrast-enhanced ultrasound in preeclampsia rats. *Placenta,* 35**,** 23-9.

Yan, T., Liu, Y., Cui, K., Hu, B., Wang, F. & Zou, L. 2013. MicroRNA-126 regulates EPCs function: implications for a role of miR-126 in preeclampsia. *J Cell Biochem,* 9**,** 2148-59.

Yang, A., Zhang, H., Sun, Y., Wang, Y., Yang, X., Yang, X., Zhang, H., Guo, W., Zhu, G., Tian, J., Jia, Y. & Jiang, Y. 2016a. Modulation of FABP4 hypomethylation by DNMT1 and its inverse interaction with miR-148a/152 in the placenta of preeclamptic rats and HTR-8 cells. *Placenta,* 46**,** 49-62.

Yang, C., Lim, W., Park, J., Park, S., You, S. & Song, G. 2019a. Anti-inflammatory effects of mesenchymal stem cell-derived exosomal microRNA-146a-5p and microRNA-548e-5p on human trophoblast cells. *Mol Hum Reprod,* 25**,** 755-771.

Yang, D., Gao, Y., Tan, K., Zuo, Z., Yang, W., Hua, X., Li, P., Zhang, Y. & Wang, G. 2013. Inhibition of hepatic fibrosis with artificial microRNA using ultrasound and cationic liposome-bearing microbubbles. *Gene Ther,* 20**,** 1140-8.

Yang, F., Gu, N., Chen, D., Xi, X., Zhang, D., Li, Y. & Wu, J. 2008. Experimental study on cell self-sealing during sonoporation. *J Control Release,* 131**,** 205-10.

Yang, H. L., Zhang, H. Z., Meng, F. R., Han, S. Y. & Zhang, M. 2019b. Differential expression of microRNA-411 and 376c is associated with hypertension in pregnancy. *Braz J Med Biol Res,* 52**,** e7546.

Yang, M., Chen, Y., Chen, L., Wang, K., Pan, T., Liu, X. & Xu, W. 2016b. miR-15b-AGO2 play a critical role in HTR8/SVneo invasion and in a model of angiogenesis defects related to inflammation. *Placenta,* 41**,** 62-73.

Yang, S., Li, H., Ge, Q., Guo, L. & Chen, F. 2015. Deregulated microRNA species in the plasma and placenta of patients with preeclampsia. *Mol Med Rep,* 1**,** 527-34.

Yang, S. W., Cho, E. H., Choi, S. Y., Lee, Y. K., Park, J. H., Kim, M. K., Park, J. Y., Choi, H. J., Lee, J. I., Ko, H. M., Park, S. H., Hwang, H. S. & Kang, Y. S. 2017a. DC-SIGN expression in Hofbauer cells may play an important role in

immune tolerance in fetal chorionic villi during the development of preeclampsia. *J Reprod Immunol,* 124**,** 30-37.

Yang, W., Wang, A., Zhao, C., Li, Q., Pan, Z., Han, X., Zhang, C., Wang, G., Ji, C., Jia, G., Ju, J., Gao, W., Yu, W., Liu, X., Chen, X., Feng, W., Gao, Z., Li, J. & Ren, C. 2016c. miR-125b Enhances IL-8 Production in Early-Onset Severe Preeclampsia by Targeting Sphingosine-1-Phosphate Lyase 1. *PLoS One,* 11**,** e0166940.

Yang, X. & Guo, F. 2019. miR3423p suppresses cell migration and invasion in preeclampsia by targeting plateletderived growth factor receptor alpha. *Mol Med Rep,* 20**,** 1772-1780.

Yang, X., Shi, L., Yi, C., Yang, Y., Chang, L. & Song, D. 2017b. MiR-210-3p inhibits the tumor growth and metastasis of bladder cancer via targeting fibroblast growth factor receptor-like 1. *Am J Cancer Res,* 7**,** 1738-1753.

Yang, Y., Li, H., Ma, Y., Zhu, X., Zhang, S. & Li, J. 2019c. MiR-221-3p is down-regulated in preeclampsia and affects trophoblast growth, invasion and migration partly via targeting thrombospondin 2. *Biomed Pharmacother,* 109**,** 127-134.

Yang, Y., Zhang, J., Xia, T., Li, G., Tian, T., Wang, M., Wang, R., Zhao, L., Lan, K. & Zhou, W. 2016d. MicroRNA-210 promotes cancer angiogenesis by targeting fibroblast growth factor receptor-like 1 in hepatocellular carcinoma. *Oncol Rep,* 36**,** 2553-2562.

Ye, X., Loeb, K., Stafford, D., Thompson, A. & Miao, C. 2003. Complete and sustained phenotypic correction of hemophilia B in mice following hepatic gene transfer of a high-expressing human factor IX plasmid. *J Thromb Haemost,* 1**,** 103-11.

Yin, Y., Liu, M. Y., H, Zhang, J. & Zhou, R. 2020. Circulating microRNAs as biomarkers for diagnosis and prediction of preeclampsia: A systematic review and meta-analysis. *European Journal of Obstetrics & Gynecology and Reproductive Biology,* 253**,** 121-132.

Ylä-Herttuala, S. 2012. Endgame: glybera finally recommended for approval as the first gene therapy drug in the European union. *Mol Ther,* 20**,** 1831-2.

Yoichi, S., Hirotaka, W., Kenji, N., Ryuichi, O., Masayo, K., Noriko, W., Toshiaki, H., Rika, S.-M., Takashi, K., Atsuo, O., Tsutomu, O., Minesuke, Y., Tomoko, K.-I. & Fumitoshi, I. 2008. Role of retrotransposon-derived imprinted gene, Rtl1 , in the feto-maternal interface of mouse placenta. *Nature Genetics,* 40**,** 243-248.

Yonetsuji, T., Ando, T., Wang, J., Fujiwara, K., Itani, K., Azuma, T., Yoshinaka, K., Sasaki, A., Takagi, S., Kobayashi, E., Liao, H., Matsumoto, Y. & Sakuma, I. 2013. A novel high intensity focused ultrasound robotic system for breast cancer treatment. *Med Image Comput Comput Assist Interv,* 16**,** 388-95.

Yuan, Q., Huang, J., Chu, B., Li, X., Li, X. & Si, L. 2012. A targeted high-efficiency angiogenesis strategy as therapy for myocardial infarction. *Life Sci,* 90**,** 695-702.

Yusuf, A., Kahane, A. & Ray, J. 2018. First and Second Trimester Serum sFlt-1/PlGF Ratio and Subsequent Preeclampsia: A Systematic Review. *J Obstet Gynaecol Can,* 40**,** 618-626.

Zamudio, S. 2007. High-altitude hypoxia and preeclampsia. *Front Biosci,* 12**,** 2967-77.

Zhang, C., Li, Q., Ren, N., Li, C., Wang, X., Xie, M., Gao, Z., Pan, Z., Zhao, C., Ren, C. & Yang, W. 2015a. Placental miR-106a ~ 363 cluster is dysregulated in preeclamptic placenta. *Placenta,* 36**,** 250-2.

Zhang, C., Li, Q., Ren, N., Li, C., Wang, X., Xie, M., Gao, Z., Pan, Z., Zhao, C., Ren, C. & Yang, W. 2015b. PPlacental miR-106a ~ 363 cluster is dysregulated in preeclamptic placenta. *Placenta,* 36**,** 250-2.

Zhang, G., Song, Y. & Liu, D. 2000. Long-term expression of human alpha1-antitrypsin gene in mouse liver achieved by intravenous administration of plasmid DNA using a hydrodynamics-based procedure. *Gene Ther,* 7**,** 1344-9.

Zhang, K., Zhang, X., Cai, Z., Zhou, J., Cao, R., Zhao, Y., Chen, Z., Wang, D., Ruan, W., Zhao, Q., Liu, G., Xue, Y., Qin, Y., Zhou, B., Wu, L., Nilsen, T., Zhou, Y. & Fu, X. D. 2018. A Novel Class of MicroRNA Recognition Elements That Function Only in Open Reading Frames. *Nat Struct Mol Biol,* 25**,** 1019-27.

Zhang, L., Wang, K., Wu, Q., Jin, L., Lu, H., Shi, Y., Liu, L., Yang, L. & Lv, L. 2019. Let-7 inhibits the migration and invasion of extravillous trophoblast cell via targeting MDM4. *Mol Cell Probes,* 45**,** 48-56.

Zhang, Q., Zhang, H., Jiang, Y., Xue, B., Diao, Z., Ding, L., Zhen, X., Sun, H., Yan, G. & Hu, Y. 2015c. MicroRNA-181a is involved in the regulation of human endometrial stromal cell decidualization by inhibiting Kruppel-like factor 12. *Reprod Biol Endocrinol,* 13**,** 23.

Zhang, Y., Diao, Z., Su, L., Sun, H., Li, R., Cui, H. & Hu, Y. 2010. MicroRNA-155 contributes to preeclampsia by down-regulating CYR61. *Am J Obstet Gynecol,* 202**,** 466.e1-7.

Zhang, Y., Fei, M., Xue, G., Zhou, Q., Jia, Y., Li, L., Xin, H. & Sun, S. 2012. Elevated levels of hypoxia-inducible microRNA-210 in pre-eclampsia: new insights into molecular mechanisms for the disease. *J Cell Mol Med,* 16**,** 249-59.

Zhang, Z., Yang, X., Zhang, L., Duan, Z., Jia, L., Wang, P., Shi, Y., Li, Y. & Gao, J. 2015d. Decreased expression and activation of Stat3 in severe preeclampsia. *J Mol Histol,* 46**,** 205-19.

Zhao, G., Miao, H., Li, X., Chen, S., Hu, Y., Wang, Z. & Hou, Y. 2016. TGF-beta3-induced miR-494 inhibits macrophage polarization via suppressing PGE2 secretion in mesenchymal stem cells. *FEBS Lett,* 590**,** 1602-13.

Zhao, G., Zhou, X., Chen, S., Miao, H., Fan, H., Wang, Z., Hu, Y. & Hou, Y. 2014. Differential expression of microRNAs in decidua-derived mesenchymal stem cells from patients with pre-eclampsia. *J Biomed Sci,* 21**,** 81.

Zhao, L., Bracken, M. B. & Dewan, A. T. 2013. Genome-wide association study of preeclampsia detects novel maternal single nucleotide polymorphisms and copy-number variants in subsets of the Hyperglycemia and Adverse Pregnancy Outcome (HAPO) study cohort. *Ann Hum Genet,* 77**,** 277-87.

Zhao, L., Triche, E. W., Walsh, K. M., Bracken, M. B., Saftlas, A. F., Hoh, J. & Dewan, A. T. 2012. Genome-wide association study identifies a maternal copy-number deletion in PSG11 enriched among preeclampsia patients. *BMC Pregnancy Childbirth,* 12**,** 61.

Zhao, W., Zhang, H. & Su, J. 2017. Downregulation of microRNA-195 Promotes Angiogenesis Induced by Cerebral Infarction via Targeting VEGFA. *Molecular medicine reports,* 16.

Zhao, Y., Ransom, J., Li, A., Vedantham, V., Von Drehle, M., Muth, A., Tsuchihashi, T., Mcmanus, M., Schwartz, R. & Srivastava, D. 2007. Dysregulation

of cardiogenesis, cardiac conduction, and cell cycle in mice lacking miRNA-1-2. *Cell,* 129**,** 303-17.

Zhong, X., Chung, A., Chen, H., Meng, X. & Lan, H. 2011. Smad3-mediated upregulation of miR-21 promotes renal fibrosis. *J Am Soc Nephrol,* 22**,** 1668-81.

Zhou, C., Zhang, Y., Irani, R., Zhang, H., Mi, T., Popek, E., Hicks, M., Ramin, S., Kellems, R. & Xia, Y. 2008. Angiotensin receptor agonistic autoantibodies induce pre-eclampsia in pregnant mice. *Nat Med,* 14**,** 855-62.

Zhou, C., Zou, Q. Y., Li, H., Wang, R. F., Liu, A. X., Magness, R. R. & Zheng, J. 2017. Preeclampsia Downregulates MicroRNAs in Fetal Endothelial Cells: Roles of miR-29a/c-3p in Endothelial Function. *J Clin Endocrinol Metab,* 102**,** 3470-3479.

Zhou, Q., Chen, J., Chen, Q., Wang, X., Deng, Q., Hu, B. & Guo, R. 2012. Optimization of Transfection Parameters for ultrasound/SonoVue Microbubble-Mediated hAng-1 Gene Delivery in Vitro. *Mol Med Rep,* 6**,** 1460-4.

Zhou, X., Li, Q., Xu, J., Zhang, X., Zhang, H., Xiang, Y., Fang, C., Wang, T., Xia, S., Zhang, Q., Xing, Q., He, L., Wang, L., Xu, M. & Zhao, X. 2016. The aberrantly expressed miR-193b-3p contributes to preeclampsia through regulating transforming growth factor-beta signaling. *Sci Rep,* 6**,** 19910.

Zhu, X. M., Han, T., Sargent, I. L., Yin, G. W. & Yao, Y. Q. 2009. Differential expression profile of microRNAs in human placentas from preeclamptic pregnancies vs normal pregnancies. *Am J Obstet Gynecol,* 200**,** 661.e1-7.

Zhu, X. M., Han, T., Wang, X. H., Li, Y. H., Yang, H. G., Luo, Y. N., Yin, G. W. & Yao, Y. Q. 2010. Overexpression of miR-152 leads to reduced expression of human leukocyte antigen-G and increased natural killer cell mediated cytolysis in JEG-3 cells. *Am J Obstet Gynecol,* 202**,** 592.e1-7.

Zhu, Y., Lu, H., Huo, Z., Ma, Z., Dang, J., Dang, W., Pan, L., Chen, J. & Zhong, H. 2016. MicroRNA-16 inhibits feto-maternal angiogenesis and causes recurrent spontaneous abortion by targeting vascular endothelial growth factor. *Sci Rep,* 6**,** 35536.

Zhuang, G., Meng, C., Guo, X., Cheruku, P. S., Shi, L., Xu, H., Li, H., Wang, G., Evans, A. R., Safe, S., Wu, C. & Zhou, B. 2012. A novel regulator of macrophage activation: miR-223 in obesity-associated adipose tissue inflammation. *Circulation,* 125**,** 2892-903.